5-2013

Stability Control of Triple Trailer Vehicles

Michael O'Neal Arant
Clemson University

STABILITY CONTROL OF TRIPLE TRAILER VEHICLES

A Dissertation
Presented to
the Graduate School of
Clemson University

In Partial Fulfillment
of the Requirements for the Degree
Doctor of Philosophy
Mechanical Engineering

---

by
Michael O'Neal Arant
May 2013

Accepted by:
Dr. Thomas R. Kurfess, Committee Co-Chair
Dr. David Bodde, Committee Co-Chair
Dr. E. Harry Law
Dr. Mohammed Daqaq
Dr. Imtiaz Haque

ABSTRACT

While vehicle stability control is a well-established technology in the passenger car realm, it is still an area of active research for commercial vehicles as indicated by the recent notice of proposed rulemaking on commercial vehicle stability by the National Highway Traffic Safety Administration (NHTSA, 2012). The reasons that commercial vehicle electronic stability control (ESC) development has lagged passenger vehicle ESC include the fact that the industry is generally slow to adopt new technologies and that commercial vehicles are far more complex requiring adaptation of existing technology. From the controller theory perspective, current commercial vehicle stability systems are generally passenger car based ESC systems that have been modified to manage additional brakes (axles). They do not monitor the entire vehicle nor do they manage the entire vehicle as a system.

This research introduces new and unique controller strategies that manage the vehicle as a distributed system with the goal of optimizing the stability of the vehicle system rather than optimizing the stability of each unit independently. This change required the development of new methods to model the complex multiple-unit vehicles as well as new methods to determine the operational state of each unit in the vehicle. The controller strategies implemented here also differ significantly from prior art in that they assess the vehicle's stability based on its current behavior and expected future behavior rather than relying on conventional reference vehicle model based error strategies.

The ESC methods developed and presented here are completely modular in nature. Their design is such that the addition (or removal) of units (dollies and trailers) is a simple matter of updating the number of degrees of freedom in the system and the number of controls the system has. Each vehicle unit has four degrees of freedom (side slip, yaw rate, roll rate, and roll) and each axle introduces a control input to the system. The ESC strategies are also relatively insensitive to vehicle parameter estimation (inertia, CG height, etc.) which are difficult to identify in practice and are required for conventional ESC strategies.

The ESC controllers developed here have proven to be very robust, managing large variations in load, loading arrangement, road surface friction, maneuver type, speed, etc. Analysis of the control responses showed that significant errors in the estimation of vehicle parameters did not affect the system performance significantly. Finally, the controllers demonstrated the much desired behavior of not activating prematurely or too aggressively which are significant issues with current ESC systems.

DEDICATION

Dedicated to my family: Coral, Elijah, Leah

ACKNOWLEDGMENTS

I would like to acknowledge the contributions of three members of my committee. First, I would like to thank Dr. Tom Kurfess who served as my primary advisor and provided support in assessing which direction to take this research and how to best demonstrate the potential of this work. Second, I would like to thank Dr. David Bodde who provided a much needed second perspective on how this research could affect the commercial vehicle market as well as advice on managing legal / regulatory aspects of this work. Third, I would like to thank Dr. Harry Law who advised on controller strategy and vehicle simulation techniques.

TABLE OF CONTENTS

LIST OF TABLES

LIST OF FIGURES

NOTATION

CG	Center of gravity for the vehicle or vehicle unit
α_i	Slip angle for axle i
a_i	Front axle to CG for unit i
b_i	Rear axle to CG for unit i
c_i	Fifth wheel to CG for unit i
d_i	Pintle hook to CG for unit i
e_i	Fifth wheel to roll axis for unit i
f_i	Pintle hook to roll axis for unit i
Z_i	CG to roll axis for unit i
h_r	roll axis height
ϕ_i	Roll of unit i
β_i	Side slip for unit i
ψ_i	Yaw for unit i
Ψ_i	Heading (velocity) for unit i
F_z	Vertical tire force
T	Track width
$C_{\alpha i}$	Axle i cornering stiffness
K_ϕ	Axle i suspension roll stiffness
$K_{\phi a}$	Axle i tire roll stiffness (roll stiffness about ground)
L_ϕ	Axle i suspension roll damping

ΔY Lateral CG shift

μ Ground friction

U_i Forward speed for unit i

F_{ij} Unit i to unit j coupling force (fifth wheel or pintle hook)

I_{izz} Unit i yaw moment of inertia

I_{ixz} Unit i yaw / roll product of inertia

I_{xxi} Unit i roll moment of inertia

A Linear time invariant state matrix

B Linear time invariant input matrix

C Linear time invariant output matrix

D Linear time invariant feed through matrix

M Linear time invariant mass matrix ($A = M^{-1} * K$)

K Linear time invariant mass stiffness ($A = M^{-1} * K$)

B_m Linear time invariant input component matrix ($B = M^{-1} * B_m$)

x State vector

y Output vector

P Final state cost

Q Increment state cost

R Increment control cost

J Quadratic cost function

U Control cost over finite time

B_w Gaussian process noise

v Gaussian measurement noise

CHAPTER ONE

INTRODUCTION

1.1 Motivation

While electric stability control (ESC) is now mandatory on all passenger cars in the US and Europe (NHTSA, 2007), it is still an emerging technology in the commercial vehicle segment as indicated by the recent proposed rulemaking notification by the National Highway Traffic Safety Administration (NHTSA, 2012). Commercial vehicle ESC implementation has also been complicated by the operational environment of the vehicles which differs from that of passenger cars. Instances of such issues include:

- Passenger cars have little mass variation in use. Commercial vehicle mass can change by 500% of curb weight.
- Passenger cars have fixed chassis parameters. Commercial vehicles generally swap trailers on a daily or shorter basis making it difficult to know anything about the construction of the towed units.
- Passenger cars are primarily sensitive to yaw divergence (even SUV type vehicles). Commercial vehicles can be either yaw or roll sensitive depending on load and driving circumstances.
- Passenger cars use hydraulic fluid for the brake system while commercial vehicle use compressed air. As air is highly compressible, this results in time delays in brake operation which can significantly affect system performance.

- Differing units (tractor or trailers) can have differing instabilities simultaneously and thus competing demands for stability intervention.

1.2 Problem Statement

Current ESC strategies, as implemented on passenger cars and some commercial tractors, manage the stability of just one vehicle unit (the car or the tractor). When adapting ESC to multiple unit vehicles, the current state of the art is to have the behavior of the first trailer inferred from its effects on the tractor. Multiple trailers are completely unobservable. Similarly, control actions on multiple unit vehicles are rather crude with the tractor ESC simply activating all trailer brakes in unison.

This type of control strategy does almost nothing to improve the stability of the trailers and is limited in its ability to improve the stability of the tractor. There have been many studies going back to MacAdam (MacAdam, 1982) indicating that it is difficult to effectively manage the stability of a multiple-unit vehicle without managing the entire vehicle as a system. Nevertheless, to date, the standard commercial vehicle ESC strategies are all single unit based.

1.3 Objectives

The primary objective of this work is to introduce and document new controller strategies that manage multiple-unit vehicles as distributed systems. That is the stability (yaw and roll) of the entire vehicle is addressed rather than the stability of a given unit in the vehicle. This is critically important as actions that stabilize one unit can de-stabilize an adjoining unit.

A secondary objective is to present a new method for modeling multiple unit vehicles using a modular approach. This approach can be implemented in code or hardware to quickly develop linearized models of any commercial vehicle. The approach also makes defining the control inputs (brakes on the vehicle) and their effect on the vehicle system a modular task as well.

1.4 Contribution

The proposed model development techniques result in accurate linear models of complex commercial vehicles that are easily scaled as units are added or removed. Additionally, the models require fewer states to capture the needed behavior of the vehicle and are less sensitive to parameter estimation errors.

The ESC algorithms developed and presented here are a significant improvement over the current state of the art. They are true system controllers which improve the stability of the vehicle system and they account for the interactions between units. Additionally, the model predictive controller and, to a lesser extent the set theory controller, have prediction capabilities to anticipate potential instability risks and react before the vehicle reaches a stability limitation.

1.5 Dissertation Overview

To make the presentation of the different aspects of this work easier to follow, this dissertation has been broken into six major sections:

- Background and fundamental knowledge
- Development of multiple-unit vehicle models

- Development of model predictive control strategies and controller performance
- Development of set theory (a.k.a. fuzzy logic) strategies and controller performance
- Analysis of relative merits of controllers
- Conclusions and summary

Chapter two (BACKGROUND) contains a significant amount of material on the history of commercial vehicle development (how we got to where we are) and stability control development (what the current tools are for managing vehicle instability). As it is important to justify why this subject is important to the broader world, there is also a significant discussion on accident statistics and the risks commercial vehicles are exposed to. Finally, as the controllers must know the state of the vehicle and apply corrective actions through the use of the brakes, there is a discussion on state estimation and tire / road interactions.

Chapter three (MODELING OF A TRIPLE TRUCK) covers the development of the linearized model for each unit of the vehicle. This includes defining the equations of motion and the unit to unit interactions. The assumptions on unit to unit interaction are very important as they define the system constraints and have a significant effect on the modeled dynamics.

Chapter four (LINEAR MODEL DEVELOPMENT AND EVALUATION) covers the modular assembly of the unit equations of motion into a linear time invariant (LTI) model. As will be shown, the assumptions made in chapter three (MODELING OF A TRIPLE TRUCK) affect the final vehicle system's behavior but the overall performance is quite good. The theory behind the approach is to make sure that the LTI model accurately reproduces the real vehicle for modes that are likely to be stability risks while allowing modes that are seldom, if ever, stability risks to deviate from the true vehicle.

Chapter five (OBSERVERS AND FILTERS) deals with the process and methods used to determine the true state of the dynamic system at any time as well as the estimation of vehicle parameters. To eliminate the need for accurate parameter assessments, the states of the vehicle are determined through direct measurement or the use of kinematic models and direct measurements. While the controllers employed here (MODEL PREDICTIVE CONTROL and FUZZY LOGIC CONTROL) are not as sensitive to parameter estimation as traditional controllers, it is useful to have a reasonable understanding of the vehicle system.

Chapter six (MODEL PREDICTIVE CONTROL) documents the theory and implementation of the first controller in this research. This is a rather unusual implementation of MPC which is why it is so effective and efficient. The downside to the method is that there are some situations that are not numerically solvable (infeasible conditions) which requires the algorithm switch to an alternate solution mode. Chapter six also documents the performance of the MPC controller as well as the robustness of the controller theory.

Chapter seven (FUZZY LOGIC CONTROL) documents the set theory controller development and its performance. Of particular interest here is the definition of the input and output membership functions as they produce natural dead bands around the nominal operational point of the vehicle (steady straight driving). This means that the controller does not activate the brakes until the system deviates significantly from a safe operational point. Also, the rule structure is used to define corrective actions that optimize the system as well as to introduce a limited predictive capability into the system.

Chapter eight (COMPARISON OF CONTROLLER PERFORMANCES) compares the two controller methods and comments on the trade-offs with the approaches. This section also includes several case studies to highlight the operation of the controllers and commentary on what the vehicle is doing and how the objectives of the controller were developed.

Chapter nine (CONCLUSIONS) summarizes the entire dissertation with the focus on the new methods developed and their potential implementation. There is also a discussion on potential improvements and what types of data would be needed for further evaluation.

While much effort has been extended to keep this dissertation as simple as possible, the subject matter is quite large and complex. To meet the goal of providing a concise summary of the work while capturing the relevant background, several portions of the research are only addressed in summary form in the main dissertation. In those cases, there are links to much more detailed documentation in the appendices.

CHAPTER TWO

BACKGROUND

Before describing the process and methods used to develop the multi-unit vehicle stability controllers presented in this work, it is necessary to understand how these vehicles are designed and operated. Unfortunately, the fields of commercial vehicle design, operation, stability, and control are far too complex to adequately address in a reasonable length background. As such, only a small introduction focused on a few key concepts will be given here. Should the reader desire more detailed information, Appendix A provides a much more thorough review of the background material that is applicable to this research.

2.1 Usage and Accident Statistics

The most obvious place to begin this discussion would be with the introduction of the need for commercial vehicle stability controllers and a description of what type of stability incidents commonly occur. To that end, a synopsis of the risks these vehicles face and statistical information on accidents is provided. Additional information on vehicle design (Appendix A.1), control actuation methods (Appendix A.3), and brake dynamics (Appendix A.5) are available for reference.

2.1.1. Commercial Vehicle Usage and Regulation

The commercial trucking industry transports approximately 70% of all freight in the US (Gerdes, 2002; Windsor, 2011) and this number is growing. The average tractor semitrailer also travels six times the miles per year as a typical passenger car (C. Chen & Tomizuka, 2000). Commercial vehicle usage (miles per year) is also increasing at approximately 3.5% per year compared to 2.5% for passenger car usage (Woodrooffe, Belzowski, Reece, & Sweatman, 2009). The obvious conclusion here is that the industry will only get larger with time with more trucks operating within the same infrastructure.

Regulation of the industry comes from a myriad of sources including the National Highway Traffic Safety Administration (NHTSA), Federal Motor Carrier Safety Administration (FMCSA), the American Association of State Highway and Transportation Officials (AASHTO), and many others. The regulations imposed by these agencies often times are focused on needs other than vehicle stability (see Appendix A.1.2 for more information). However, there has been recent interest in improving commercial vehicle stability (NHTSA, 2010; NHTSA, 2011; NHTSA, 2012) with the introduction of a proposal for mandatory commercial vehicle stability control (NHTSA, 2012) similar to the recent mandate for passenger car stability control (NHTSA, 2007). Thus this research is of significant value to our regulatory bodies as well as the commercial vehicle community. Additional regulatory information is available in Appendix A.1.2.

2.1.2. Commercial Vehicle Accidents

Unlike passenger cars which are generally dominated by yaw instability, commercial vehicles can be yaw or roll unstable – often simultaneously as can be observed in Figure 2-1.

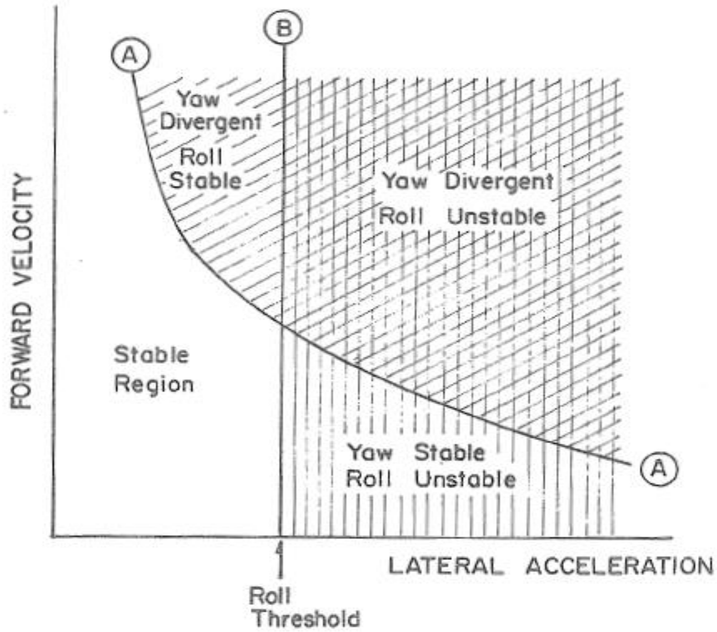

Figure 2-1: Yaw and Roll Stability Regimes (MacAdam, 1982)

This complex yaw and roll stability is also observed in accident statistics (Figure 2-2) which indicates both yaw and roll risks do exist.

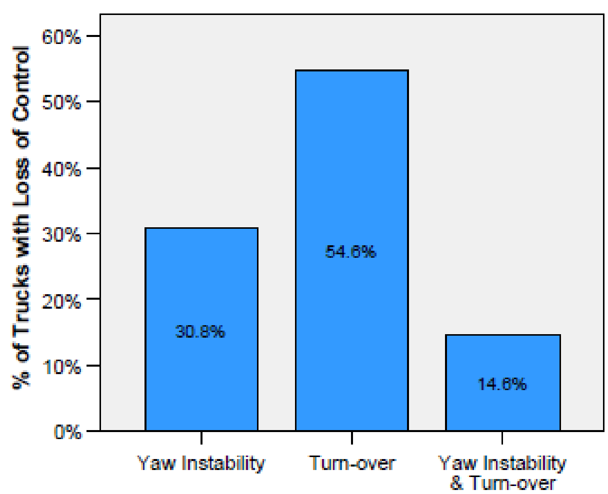

Figure 2-2: Commercial Vehicle Accident Type (Kharrazi & Thomson, 2008a)

Finally, the stability risks are not limited to poor road conditions (Figure 2-3) or particular maneuvers (Figure 2-4).

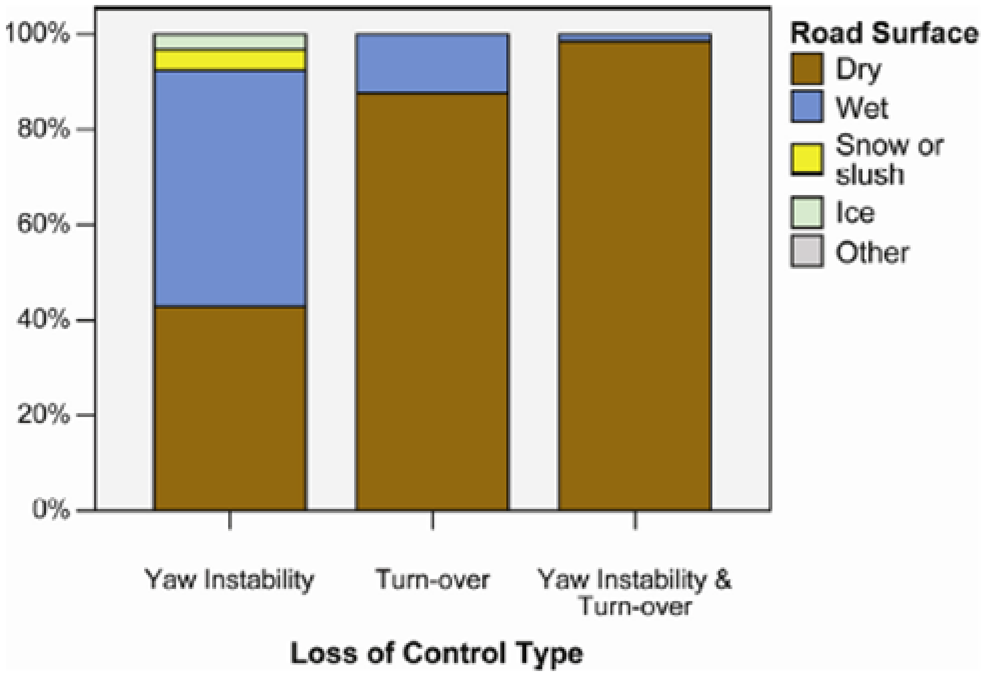

Figure 2-3: Road Surface Condition and Accident Type (Kharrazi & Thomson, 2008b)

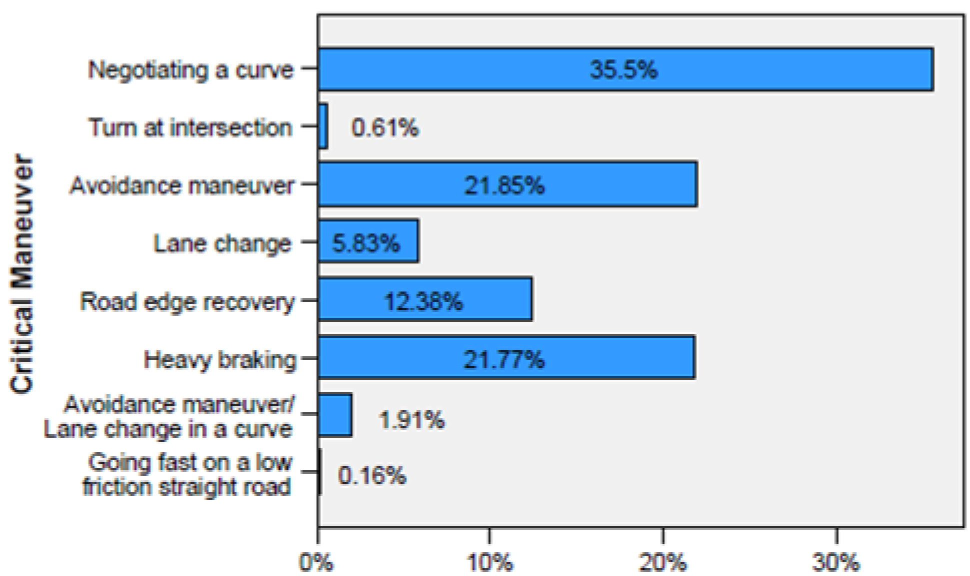

Figure 2-4: Yaw Instability Accident Type (Kharrazi & Thomson, 2008a)

Additional information on the stability and safety of commercial vehicles can be found in Appendix A.2.

2.2 Conventional Stability Control

The current state of the art in commercial vehicle stability control is single unit (the tractor) based with the trailer(s) un-monitored (Andersky & Conklin, 2008; NHTSA, 2012; Pape et al., 2007). Further, these systems cannot manage the trailer brakes independently as there is only one brake command line to the trailer(s). However, recent technology changes including electronic air brake systems (EBS) offer the potential to improve this situation (Freightliner LLC, 2007; NHTSA, 2009). More information on this topic is available in Appendix A.5.1. Note: nearly all electronic stability control (ESC) systems use the brakes as this has proven to be the most inexpensive and to offer the best compromise between controllability and driver intent (Manning & Crolla, 2007; Nantais, 2006).

2.2.1. Reference Models

Traditionally, vehicle stability controller design has been focused on controlling the error between the actual vehicle and an idealized reference vehicle (Figure 2-5).

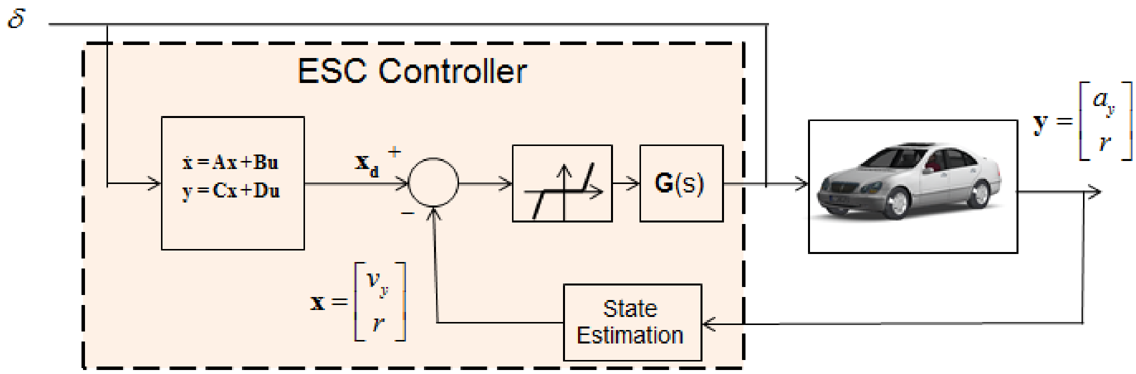

Figure 2-5: Traditional Error Based Controller (Limroth, 2009)

Generally, the controller structure implemented has been of a PI / PD / PID form (L. K. Chen & Shieh, 2011; Chih-Keng Chen, Trung-Kien Dao, & Hai-Ping Lin, 2010; Ghoneim et al., 2000; Limroth, 2009; S. Zhou, Guo, & Zhang, 2008) or LQR (Miege & Cebon, 2002; Tianjun, Changfu, Zheng, Tian, & Zheng, 2007; Tianjun & Zheng, 2008; Tianjun & Changfu, 2009; Tianjun & Changfu, 2009) form with a few cases of model predictive controller methods using a reference vehicle for output targets (Anwar, 2005; Bahaghighat, Kharrazi, Lidberg, Falcone, & Schofield, 2010; Falcone, Tseng, Borrelli, Asgari, & Hrovat, 2008). In all cases, the controller requires that the vehicle be simulated using a simplified model to obtain an estimate of the intended vehicle response that the actual vehicle should track.

2.2.2. Combined Yaw and Roll Stability

The need for the stability controller to manage both yaw and roll stability simultaneously has been noted by multiple authors (Ma & Peng, 1999; Woodrooffe, Blower, & Green, 2010; Wu, 2001). However, there is continued use of yaw and roll decoupled systems within the industry (B. Chen & Peng, 1999b). Also, research into multiple trailer vehicle systems (MacAdam et al., 2000) has shown that the vehicle needs to be treated as a system rather than a series of individual units. But, save for a few two unit (tractor and single trailer) development controllers, there are currently no electronic stability control (ESC) systems capable of meeting this need to evaluate the vehicle as a system. More details are available in Appendix A.2.4 and Appendix A.2.6.

2.2.3. Threat Indicators

To assess when the vehicle is approaching an instability point, numerous researchers have derived stability indicators based on lateral acceleration levels (Dahlberg & Stensson, 2006), lateral load transfer (Kamnik, Boettiger, & Hunt, 2003), kinetic energy (S. B. Choi, 2008), anticipated time to rollover (B. Chen & Peng, 1999b), and anticipated time to axle saturation (Limroth, 2009). As the reference model gives the "desired" lateral dynamic response, there are fewer lateral dynamic error assessments. Since there is no "desired" roll, the roll threat indicators are used to determine how close the vehicle is to roll instability. Appendix A.3.1 contains additional information on this point. Note: The research presented here does not use any stability metrics of this type.

2.3 Vehicle Measurement

In general, there are two classes of data needed to evaluate the stability of the vehicle. The first is the determination of the current dynamic state of the vehicle (state estimation). The second is the determination of the vehicle's properties (mass, inertia, CG location, etc.) (parameter estimation). Generally, the estimation of the states and parameters cannot be easily separated as the same source data is used to determine both.

This has led to the development of filtering approaches to get good estimates (Best, Gordon, & Dixon, 2000; Chang & Gordon, 2009; Limroth, 2009; Venhovens & Naab, 1999; Wenzel, Burnham, Blundell, & Williams, 2006; Yu, Güvenç, & Özgüner, 2008). Details on how these approaches work is available in Appendix A.6. Note: the controller strategies proposed here break this interdependence of state and parameter estimation.

2.3.1. State Estimation

There are three general methods to evaluate the states of the vehicle:

- Direct measurement using sensors.
- Measurement and kinematic model, often employing a Kalman filter (Appendix A.6.4).
- Measurement and a physical model – usually a filter (Kalman / recursive least squares) and physical model.

As it is historically difficult to separate the determination of the states and the determination of the system parameters, most researchers use some combination of a physical model and other data source (cases 5, 6, or 7 in Figure 2-6) (Bevly, Ryu, & Gerdes, 2006; Tin Leung, Whidborne James, Purdy, & Dunoyer, 2011). As the physical model is generated from the vehicle parameters, one can see how this introduces a feedback loop and makes determination of the true parameters and true states difficult. Appendix A.6.2 contains additional information on this point if needed.

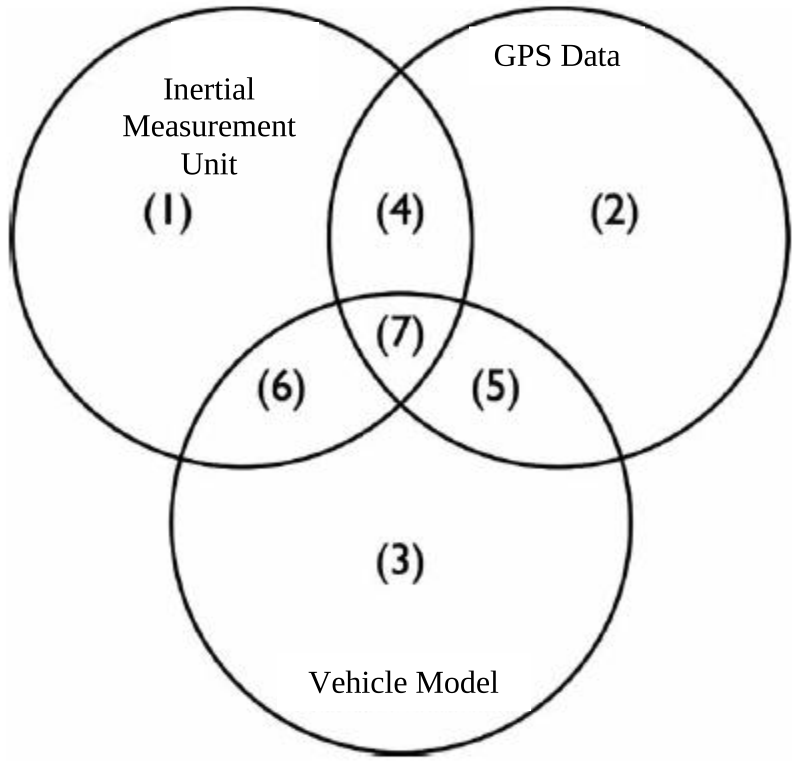

Figure 2-6: Vehicle State Estimation Methods (Tin Leung et al., 2011)

2.3.2. Parameter Estimation

Generally the vehicle parameters are either assumed (Park, Yoon, Kim, & Yi, 2008) or estimated by observing the vehicle's dynamic behavior and using an inverted form of the linearized model to estimate the vehicle parameters (Limroth, 2009; Shraim, Ouladsine, Fridman, & Romero, 2008; Tin Leung et al., 2011). However, it is very difficult to assume parameters such as mass, CG location, and cornering stiffness for commercial vehicles or to estimate these parameters due to unit to unit interactions (Andersky & Conklin, 2008; Brown, Schwarz, Moeckli, & Marshall, 2009; L. K. Chen & Shieh, 2011; Du & Zhang, 2008; Solmaz, Akar, & Shorten, 2006; J. Wang & Hsieh, 2009). This poses a major problem when there is a need for an accurate model of the vehicle for use in controller development. Appendix A.6.1 covers this topic in more detail.

CHAPTER THREE

MODELING OF A TRIPLE TRUCK

A commercial vehicle is a very complex piece of machinery with many nonlinear dynamic responses. As one of the control theories to be used required a linear time invariant (LTI) model, an effort was undertaken to reduce the vehicle system and generate a reliable LTI model. This linear model (a linear bicycle type model with roll) was derived by first modeling each unit of the vehicle (tractor, trailer, and dolly) and then managing the unit interactions by use of fifth wheel and pintle hook constraint forces. The following section describes the linear model development and justifies the assumptions made therein. Note: As the equations become quite large and there are numerous figures, some of the basic model formulation is located in Appendix C.

3.1. Generalized Motion of a Rigid Body

While a vehicle is certainly not a rigid object, having suspensions, bushings, and frame compliances, it was useful to treat the vehicle chassis as a rigid body as this made the dynamics analysis much simpler. This approach reduced the analysis of motion to a set of force and moment balances for each vehicle unit which was much easier to implement. In this case, there were six sets of force and moment equations for the tractor, trailers and dollies. The art in the process was in determining when the vehicle could be reasonably simplified and in defining the forces and moments acting on the vehicle and between the vehicle segments.

3.1.1. Basis of Rigid Chassis Assumptions

While a passenger car chassis is often many times stiffer than the suspensions attached to it, this is not always the case for commercial vehicles. Generally tractors have low torsional stiffness values (as low as 800 Nm/deg) (Arant et al. 2009) so that the vehicle can twist over uneven roads and maintain good tire contact with the road. Trailer stiffness values range from a few thousand to a few million N-m/deg depending on construction, trailer type, and length (Arant et al., 2009; Pape et al., 2008).

The manner in which most commercial vehicles are operated lent some justification to the rigid chassis assumption so long as the lateral acceleration levels are relatively low. At low lateral acceleration levels, the overturning moment is generally low and the resulting suspension moment reactions are also low. This helps to limit torsion in the chassis. Of course, as the lateral acceleration builds, this assumption breaks down. But, as the goal of the research here was to keep the vehicles operating at lower lateral acceleration levels, the rigid model approach was reasonable. Further justification for this assumption can also be found in Appendix A.4.

3.1.2. Rigid Body Motion and Basic Equations of Motion (EOM)

For readers who are not familiar with the process of developing linearized vehicle models, a brief introduction to the process of deriving equations of motion is in order. Generally, the process starts with the assumption that the vehicle is a single chassis that is in free space. That is all six degrees of freedom are present. Then tire forces (external forces) and Newtonian rules of mechanics are applied. Finally, the dynamic equations are simplified by dropping negligible terms and dynamic behaviors that are not of interest (longitudinal acceleration in this case). A detailed presentation of this process can be seen in Appendix C.3.

3.2. Simplifying Roll (Axle and Fifth Wheel)

The purpose of a vehicle's suspension is to isolate the chassis from the road and thus reduce loads transmitted to the sprung mass. However, the suspension also permits the chassis to roll relative to the axles during lateral handling maneuvers and this roll introduces an additional degree of freedom to the system for each axle in the vehicle unit. As the final linear model needed to be computationally quick, the removal of unnecessary degrees of freedom was deemed important. To that end, simplifications to the model that removed the axle to chassis roll degree of freedom were investigated.

While it is not often thought of as a "suspension" the fifth wheel also acts as a roll point for the chassis with a typical trailer rotating about the fifth wheel in the front and the suspension in the rear. In the case of a fifth wheel, the roll is between two sprung masses which are already included in the equations of motion so no additional terms are introduced. However, the fifth wheel does tie the units together which adds constraints (inter-unit forces and moments) to the analysis.

3.2.1. Fifth Wheel Constraint

While the fifth wheel connection between a trailer and the towing unit (tractor or dolly) constrains the relative linear motions, it does not provide much resistance to relative rotations. Obviously, a fifth wheel provides no yaw resistance as the fifth wheel's purpose is to permit relative yaw motions. Fifth wheels are also designed to rock forward and backward so that the trailer plate and the fifth wheel are co-planar at all times (the tractor / trailer plates do not have to be parallel to the ground). Finally, for reasons of unit to unit compatibility, ease of operation, design costs, and other factors, the fifth wheel connections also permit significant relative roll between the vehicle units as illustrated in the kinematic test below (Figure 3-1). The result is that the fifth wheel acts much like a ball joint when the vehicle is operating normally (Figure 3-2). This means that the two units are effectively decoupled in roll when the vehicle is in its linear range. Only when the unit to unit relative roll angles are large does the fifth wheel act as a roll coupling device of any significant magnitude. Note: the small moment generated about zero (Figure 3-2) is due to movement of the center of pressure between the trailer and the fifth wheel. The initial magnitude is thus highly dependent on the trailer load.

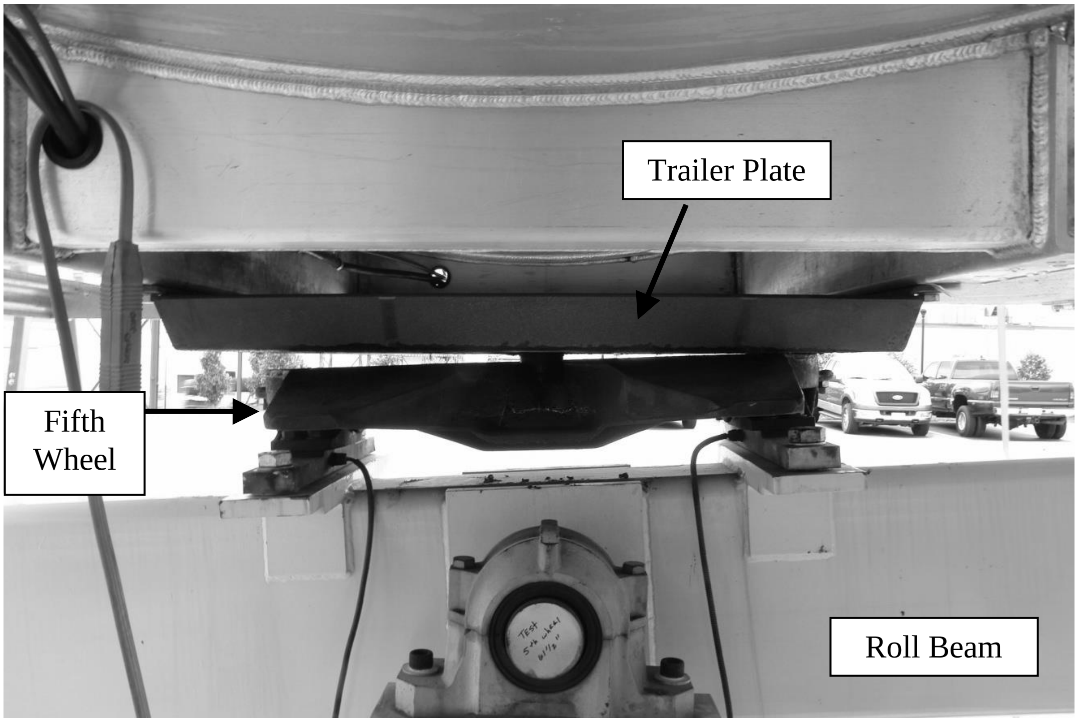

Figure 3-1 Actual Fifth Wheel Separation in Roll (Kinematic Test) (Arant, 2010)

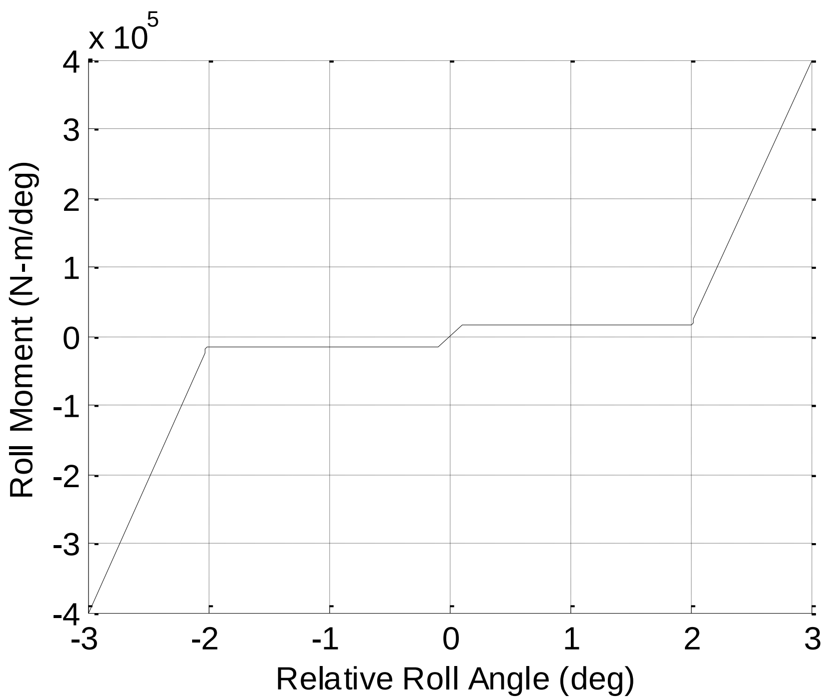

Figure 3-2: Typical Fifth Wheel Roll Moment (Arant, 2010)

Side note: The roll moment curve in Figure 3-2 is not only highly non-linear; it is highly dependent on the particular fifth wheel, trailer, and payload. The moment about the zero relative roll is a function of the payload (normal load) and the fifth wheel width. The "dead band" between the center of pressure moment and the engagement of the locking pawls is dependent on the pawl design, the pawl lash (wear), and the kingpin wear. The final stiffness is a function of the pawl design, and the locking mechanism. The resulting curve is a function of the design and wear of the two units and the current payload. Thus, even if it were useful to know the curve shape, it would be nearly impossible to predict the coupling behavior.

3.2.2. Sprung and Unspring Mass Rotation

As the suspension of a commercial vehicle is generally simple in construction with a solid axle and two springs, it can be easily broken into two parts: The sprung mass (Figure 3-3) and the axle (Figure 3-4). The relative deflections of the suspensions acting over the spring spacing width can also be modeled as a torsional moment with a roll center. The roll center is then positioned along the axis of the vehicle at the nominal height of the suspension. Equations 3-1 and 3-2 define the rotation of the sprung and unsprung components and their interactions for such a simplified suspension. Note: Z_s is the sprung mass CG height to roll center, h_r is the roll center height, and ϕ/ ϕ_a are the sprung and unsprung roll angles.

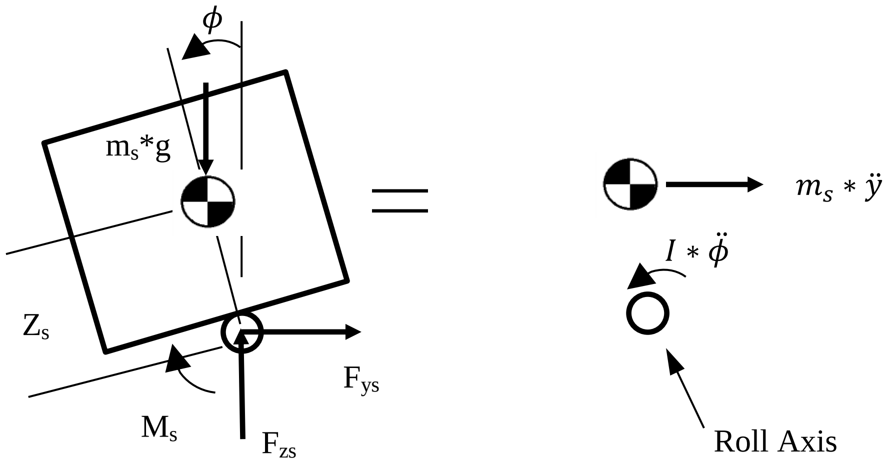

Figure 3-3: Chassis Free Body

$$-I*\ddot{\phi}+m_s*\ddot{y}*Z_s*\cos(\phi)=M_s-m_s*g*Z_s*\sin(\phi) \qquad \textbf{3-1}$$

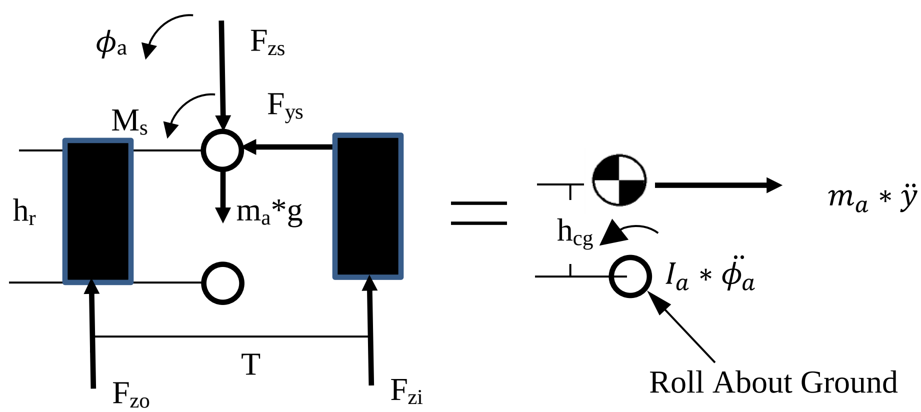

Figure 3-4: Axle Free Body

$$\begin{aligned}&-I_a*\ddot{\phi}_a+m_a*\ddot{y}*h_{cg}*\cos(\phi_a)=\\&F_{zo}*\frac{T}{2}-F_{zi}*\frac{T}{2}-F_{ys}*h_r*\cos(\phi_a)-M_s-m_a*g*h_r*\sin(\phi_a)\end{aligned} \qquad \textbf{3-2}$$

For a typical trailer, even an unloaded one, the sprung trailer mass is significantly more than the axle mass (Table 3-1). This fact, along with the fact that the trailer CG is significantly higher than the axle CG, means that the overturning moment seen at the ground is predominantly due to the sprung mass indicating that the unsprung mass can be neglected. Also, as the axle roll stiffness (generated from vertical tire stiffness) is generally 8 to 10 times the suspension roll stiffness (Table 3-2); the rotation about the roll center is generally much larger than the rotation about the ground.

Table 3-1: Sprung and Unsprung Component Mass

Component	Mass (kg)
Tractor Sprung Mass	7800
Front Axle	370
Rear Axle	600
Unloaded Trailer	6500
Trailer Axle	400

Table 3-2: Example Parameters for Lateral Displacement Test

Parameter	Description	Value	Parameter	Description	Value
Z_s (m)	Roll center to CG height	1	m_s (kg)	Sprung mass	6500
h_r (m)	Roll center height	1	m_a (kg)	Unsprung mass	400
K_ϕ (N-m /deg)	Suspension roll stiffness	1000	h_{cg} (m)	Unsprung mass height	0.7
$K_{\phi a}$ (N-m /deg)	Axle (tire) roll stiffness	8000	$\ddot{y}$ (m/s^2)	Lateral Acceleration	0.25

3.2.3. Combined Mass Rotation Model for Suspension

The above analysis of the roll behavior of a suspension (Equations 3-1and 3-2) indicates that the lateral offset of the sprung mass CG is a function of the sprung and unsprung roll (Equation 3-3) where the roll angles are defined in Equations 3-4 and 3-5. Based on the above observations, dropping the unsprung mass from the axle roll equation (3-5) would not significantly affect the predicted unsprung mass roll angle as m_s is on the order of 10 times the size of m_a for an unloaded vehicle and $Z_s + h_r$ is greater than h_a. However, the effect of the sprung mass overturning moment cannot be ignored. For this reason, it would appear that the axle roll must be accounted for in the model. Note: as the ground roll stiffness is generally on the order of 8 to 10 times the suspension roll stiffness and Z_s (CG to roll axis) is greater than h_r (roll axis height), the suspension roll angles are generally larger than the ground roll angles.

$$\Delta Y = Z_s * \sin(\phi) + h_r * \sin(\phi_a) \tag{3-3}$$

$$\phi = \frac{m_s * \ddot{y} * Z_s}{K_\phi} \tag{3-4}$$

$$\phi_a = \frac{m_s * \ddot{y} * (Z_s + h_r) + m_a * \ddot{y} * h_a}{K_{\phi a}} \approx \frac{m_s * \ddot{y} * (Z_s + h_r)}{K_{\phi a}} \tag{3-5}$$

As the modeling requirements here needed to both reduce the number of degrees of freedom in the model and maintain an accurate estimation of vehicle stability, the requirements presented above were not very appealing. While ignoring the axle rotation would make the linearized model more efficient (elimination of the unsprung motions) it would result in underestimations of actual CG motion. As the resulting error is a function of the roll stiffness, CG height, etc., there is some dispersion on the amplitude of this error. However, errors on the order to 30% are reasonable.

The compromise solution to efficiently estimate the lateral CG shift of the sprung mass started with the expansion of Equation 3-3 as shown in Equation 3-6. From there, small angle assumptions were made (Equation 3-7) and the unsprung mass was dropped (Equation 3-8). With the equation linearized, a series of algebraic transformations were then executed (Equations 3-9 through 3-11).

$$\Delta \mathrm{Y} = Z_s * sin\left(\frac{m_s * Z_s * \ddot{y}}{K_\phi}\right) + h_r * sin\left(\frac{(m_s * (Z_s + h_r) + m_a * h_{cg}) * \ddot{y}}{K_{\phi a}}\right) \quad \textbf{3-6}$$

$$\Delta \mathrm{Y} = Z_s * \left(\frac{m_s * Z_s * \ddot{y}}{K_\phi}\right) + h_r * \left(\frac{(m_s * (Z_s + h_r) + m_a * h_{cg}) * \ddot{y}}{K_{\phi a}}\right) \quad \textbf{3-7}$$

$$\Delta \mathrm{Y} = Z_s * \left(\frac{m_s * Z_s * \ddot{y}}{K_\phi}\right) + h_r * \left(\frac{m_s * (Z_s + h_r) * \ddot{y}}{K_{\phi a}}\right) \quad \textbf{3-8}$$

$$\frac{\Delta \mathrm{Y}}{\mathrm{Z_s}} = \left(\frac{m_s * Z_s * \ddot{y}}{K_\phi}\right) + \frac{h_r}{Z_s} * \left(\frac{m_s * (Z_s + h_r) * \ddot{y}}{K_{\phi a}}\right) \quad \textbf{3-9}$$

$$\frac{\Delta \mathrm{Y} * K_\phi}{\mathrm{Z_s}} = m_s * \ddot{y} * \left(Z_s + \frac{h_r}{Z_s} * \frac{(Z_s + h_r) * K_\phi}{K_{\phi a}}\right) \quad \textbf{3-10}$$

$$\frac{\Delta \mathrm{Y} * K_\phi}{\mathrm{Z_s} * m_s * \ddot{y}} = Z_s + \frac{h_r}{Z_s} * \frac{(Z_s + h_r) * K_\phi}{K_{\phi a}} \quad \textbf{3-11}$$

If the right hand side of Equation 3-11 is replaced with a new constant Z_{sa} as defined in Equation 3-12, then Equation 3-3 can be stated as Equation 3-13. Noting that this is very similar to the result of the small angle assumption transformation (Equation 3-6 to 3-7) implies that the system can be modeled as described in Equation 3-14.

$$\mathrm{Z_{sa}} = Z_s + \frac{h_r}{Z_s} * \frac{(Z_s + h_r) * K_\phi}{K_{\phi a}} \quad \textbf{3-12}$$

$$\Delta \mathrm{Y} \approx \mathrm{Z_{sa}} * \frac{\mathrm{Z_s} * m_s * \ddot{y}}{K_\phi} \quad \textbf{3-13}$$

$$\Delta \mathrm{Y} \approx \mathrm{Z_{sa}} * \sin\left(\frac{\mathrm{Z_s} * m_s * \ddot{y}}{K_\phi}\right) \quad \textbf{3-14}$$

The transformation above is an approximation of the original system where the combined suspension rotation and the axle rotation is replaced by only the suspension rotation but with the distance between the sprung mass CG and the roll center increased (effectively a lowering of the roll center) (Equation 3-14). The resulting estimate of the lateral displacement of the sprung mass CG is quite good as can be observed in Figure 3-5. Not surprisingly, the error decreases as the ratio of the sprung to unsprung mass increases (Figure 3-6). Figure 3-5 and Figure 3-6 were derived using a fixed lateral acceleration and fixed unsprung mass. They denote the anticipated increase in lateral CG offset with increased payload.

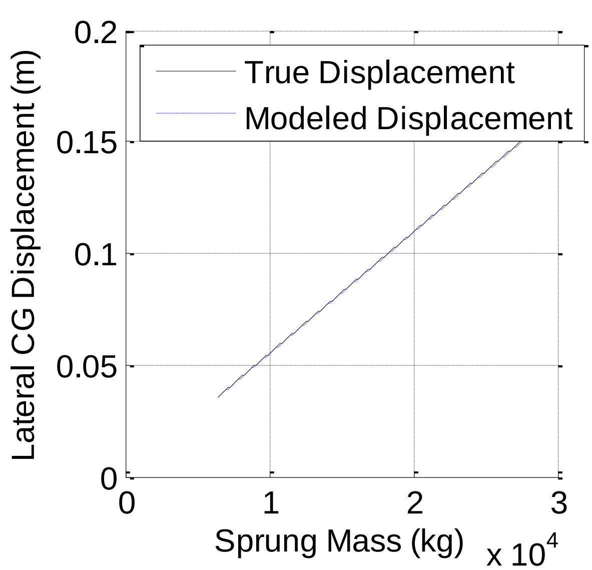

Figure 3-5: Sprung Mass CG Displacement for Fixed Lateral Acceleration and Fixed Unsprung Mass

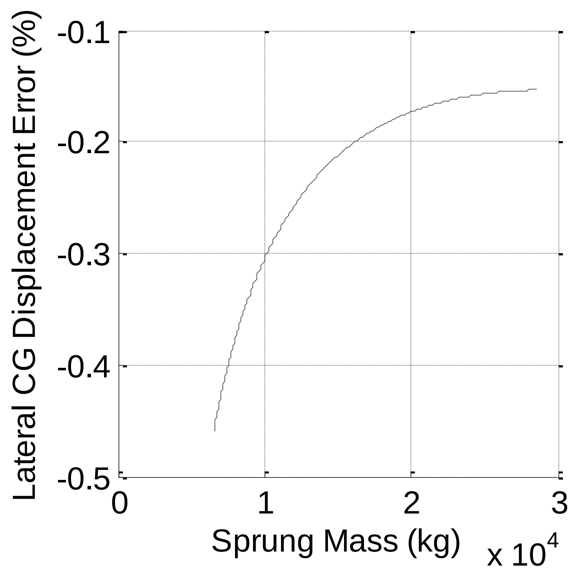

Figure 3-6: Sprung Mass CG Displacement Error for Fixed Lateral Acceleration and Fixed Unsprung Mass

3.3. Tire Modeling

Except for aerodynamic forces, which are not accounted for in this model, all reaction forces and moments applied to the vehicle are generated through the tires. As such, realistic tire models were needed. Since section A.5.2 provides a good review of tire modeling techniques, only a brief discussion on the implementation of the tire model is presented here. Note: the controllers were designed to limit side slip angles to approximately ± 5º which meant that aerodynamic side loading was minimal.

3.3.1. Tire Force Generation

As the linear model developed in this exercise was a simplified bicycle model with roll, the cornering stiffness values used in the analysis were defined on a per axle basis. Thus for multi-tire axles or tandems, the cornering stiffness was the sum of the individual tire cornering stiffness. While lateral load transfer does reduce the per-axle cornering stiffness (C_α) of a real vehicle (Figure A-67), this effect was ignored here. The justification for this simplification was that if the lateral load transfer was large enough to significantly affect the tire cornering stiffness, then the vehicle had already deviated significantly far from the linearized model assumptions rendering a C_α correction irrelevant.

The lateral force per axle was determined based on Equation 3-15 using the axle slip angle (addressed in Sections D.1.2 through D.1.4) and the per-axle cornering stiffness. While the full non-linear model incorporated tire relaxation length effects, the linearized model did not. The justification for this simplification was that tire relaxation length (a first order delay effect) has a much smaller time constant than the vehicle system for any reasonable forward speed.

$$F_y = C_\alpha * \alpha \qquad \textbf{3-15}$$

3.3.2. Traction Ellipse

The stability control method employed in this work was based upon the actuation of the vehicle's brakes. When the brakes are actuated and longitudinal forces develop, the lateral force a tire can develop for a given slip angle deteriorates (see section A.5.2 / Figure A-76). This longitudinal / lateral force relationship is often called a traction ellipse and is defined as shown in Equation 3-16. This simplified tire traction model was used in the controller where the initial longitudinal tractive force demand was taken to be the tractive demand at the preceding time step.

$$\left(\frac{F_y}{\mu * Fz}\right)^2 + \left(\frac{F_x}{\mu * Fz}\right)^2 = 1 \qquad \textbf{3-16}$$

3.4. Final Equations of Motion

Before a model predictive controller could be developed, it was necessary to convert the non-linear system into a linear time invariant (LTI) model. The task of generating the LTI model is addressed in Section 4; the final equations of motion for vehicle unit used in that process are presented here. While this is a well-documented process for single unit vehicles and conventional tractor / single trailer vehicles, it is less so for multiple unit vehicles (Goodarzi, Ghajar, Baghestani, & Esmailzadeh, 2009; Tianjun et al., 2007; Wu, 2001). The full model development, including free body diagrams, yaw and roll motions, and state variable selection, is available in Appendix D.1.

3.4.1. Vehicle States and Equations

For consistency and ease of use, all of the models developed in this work used the vehicle unit side slip (β), vehicle unit yaw rate$(\dot{\psi})$, vehicle unit roll rate $(\dot{\phi})$, and vehicle unit roll angle (ϕ) as the state variables. By using only rotations and rotational rates, it was easier to interpret the results as one naturally expects roll and side slip to be on the same order of magnitude and yaw rate to be significantly larger than rollrate. Appendix D.2.1 documents the state selection.

3.4.2. Tractor Equations of Motion

As the first unit in the vehicle, the tractor's state variables are $\beta_1, \dot{\psi}_1, \dot{\phi}_1,$ and ϕ_1. Equation 3-17 (Equation D-48) is the tractor lateral force equation, Equation 3-18 (Equation D-49) is the yaw moment equation, and Equation 3-19 (Equation D-50) is the roll moment equation. The development of these equations can be found in Appendix D.2.5. Note: U_i is the unit forward speed, Z_i is the CG height to roll center, $C_{\alpha i}$ is the tire cornering stiffness, a_i is the front axle to CG distance, b_i is the rear axle to CG distance, and M_i is the brake induced corrective moment for axle i.

$$m_1 * U_1 * (\dot{\beta}_1 + \dot{\psi}_1) - m_1 * Z_1 * \ddot{\phi}_1 = -(C_{\alpha f} + C_{\alpha r}) * \beta_1 - (a_1 * C_{\alpha f} - b_1 * C_{\alpha r}) * \frac{\dot{\psi}_1}{U_1} - F_{12} + C_{\alpha f} * \delta \qquad \textbf{3-17}$$

$$I_{1zz} * \ddot{\psi}_1 - I_{1xz} * \ddot{\phi}_1 + m_1 * Z_1 * U_1 * \dot{\phi}_1$$

$$= -\left(a_1 * C_{\alpha f} - b_1 * C_{\alpha r}\right) * \beta_1 - \frac{\left(a_1^2 * C_{\alpha f} + b_1^2 * C_{\alpha r}\right) * \dot{\psi}_1}{U_1} + c_{:} \quad \textbf{3-18}$$

$$* F_{12} + a_1 * C_{\alpha f} * \delta + \mathrm{M_f} + \mathrm{M_r}$$

$$(I_{1xx} + m_1 * Z_1^2) * \ddot{\phi}_1 - I_{1xz} * \ddot{\psi}_1$$

$$= m_1 * Z_1 * g * \phi_1 + m_1 * Z_1 * \mathrm{U}_1 * \left(\dot{\beta}_1 + \dot{\psi}_1\right) - \left(K_f + K_r\right) * \mathrm{\phi}_{:} \quad \textbf{3-19}$$

$$- \left(L_f + L_r\right) * \dot{\mathrm{\phi}}_1 + \mathrm{F}_{12} * \mathrm{f}_1$$

3.4.3. Trailer Equations of Motion

The trailer's state variables are $\beta_i, \dot{\psi}_i, \dot{\phi}_i$, and ϕ_i where i represents the trailer number. Equation 3-20 (Equation D-51) is the trailer lateral force equation, Equation 3-21 (Equation D-52) is the yaw moment equation, and Equation 3-22 (Equation D-53) is the roll moment equation. The development of these equations can be found in Appendix D.2.5

$$m_i * U_i * \left(\dot{\beta}_i + \dot{\psi}_i\right) - m_i * Z_i * \ddot{\phi}_i = F_{i-1i} - \beta_i * C_{\alpha i} + \frac{b_i * C_{\alpha i} * \dot{\psi}_i}{U_i} - F_{ii+1} \quad \textbf{3-20}$$

$$I_{izz} * \ddot{\psi}_i - I_{ixz} * \ddot{\phi}_i + m_i * Z_i * U_i * \dot{\phi}_i$$

$$= c_i * F_{i-1i} + b_i * C_{\alpha i} * \beta_i - \frac{b_i^2 * C_{\alpha i} * \dot{\psi}_i}{U_i} + d_i * F_{ii+1} + \mathrm{M_i} \quad \textbf{3-21}$$

$$(I_{ixx} + m_i * Z_i^2) * \ddot{\phi}_i - I_{ixz} * \ddot{\psi}_i$$

$$= m_i * Z_i * g * \phi_i + m_i * Z_i * \mathrm{U_i} * \left(\dot{\beta}_i + \dot{\psi}_i\right) - K_i * \mathrm{\phi_i} - L_i * \dot{\phi}_i \quad \textbf{3-22}$$

$$- \mathrm{F}_{i-1i} * \mathrm{f_i}$$

3.4.4. Dolly Equations of Motion

The dolly's state variables are $\beta_i, \dot{\psi}_i, \dot{\phi}_i$, and ϕ_i where i represents the dolly number. Equation 3-23 (Equation D-54) is the dolly lateral force equation, Equation 3-24 (Equation D-55) is the yaw moment equation, and Equation 3-25 (Equation D-56) is the roll moment equation. The development of these equations can be found in Appendix D.2.5.

$$m_i * U_i * (\dot{\beta}_i + \dot{\psi}_i) - m_i * Z_i * \ddot{\phi}_i = F_{i-1i} - \beta_i * C_{\alpha i} + \frac{b_i * C_{\alpha i} * \dot{\psi}_i}{U_i} - F_{ii+1} \quad \textbf{3-23}$$

$$I_{izz} * \ddot{\psi}_i - I_{ixz} * \ddot{\phi}_i + m_i * Z_i * U_i * \dot{\phi}_i$$
$$= d_i * F_{i-1i} + b_i * C_{\alpha i} * \beta_i - \frac{b_i^2 * C_{\alpha i} * \dot{\psi}_i}{U_i} + c_i * F_{ii+1} + \mathrm{M_i} \quad \textbf{3-24}$$

$$(I_{ixx} + m_i * Z_i^2) * \ddot{\phi}_i - I_{ixz} * \ddot{\psi}_i$$
$$= m_i * Z_i * g * \phi_i + m_i * Z_i * \mathrm{U_i} * (\dot{\beta}_i + \dot{\psi}_i) - K_i * \phi_\mathrm{i} - L_i * \dot{\phi}_i \quad \textbf{3-25}$$
$$+ \mathrm{F}_{ii+1} * \mathrm{f_i}$$

3.4.5. Hinge Constraint

As the vehicle units are joined by fifth wheels and pintle hooks, there are articulation points between each of the units. These points can be modeled as a pin joints which introduces a constraint equation (Equation 3-26 / D-18) for each joint. This equation will be used in the LTI system development in Section 4 to mathematically relate the unit to unit motions.

$$\dot{\beta}_{i+1} = \dot{\beta}_i - \frac{c_i * \ddot{\psi}_i}{\mathrm{U_i}} - \frac{c_{i+1} * \ddot{\psi}_{i+1}}{\mathrm{U_{i+1}}} + \dot{\psi}_i - \dot{\psi}_{i+1} \quad \textbf{3-26}$$

CHAPTER FOUR

LINEAR MODEL DEVELOPMENT AND EVALUATION

Section 3 culminated with presentation of the individual equations of motion (EOM) for each vehicle unit (EOM development documented in Appendix D.2). The obvious next step was to combine the units into a vehicle which is addressed in the first part of this chapter. However, it should be noted that the particular linear model developed was based on the A-type dolly (Figure A-7) configuration as it is the most common US configuration. There are other dolly types ("B" and "C" – Appendix F) which could be of interest as well. The advantage of using the "A" type dolly, in addition to the practical usage consideration, was that the "B" and "C" dolly types are mathematical simplifications of the "A" type dolly making the modeling work here more broadly appealing. Details on the dolly comparisons can be found in Appendix F.

4.1.State Space Formulation

When dealing with linearized models, it is usually most convenient to convert the equations of motion into state space formulation (Equation 4-1). This entails converting the EOMS (Equation 4-2) into a set of first order equations through variable substitution methods (Equations 4-3 through 4-6). Note: As the lateral force (Equations 3-17, 3-20, and 3-23) and yaw moment (Equations 3-18, 3-21, and 3-24) were already first order, this conversion was only necessary for the roll moment equations (Equations 3-19, 3-22, and 3-25). Thus there were two first order equations generated from each roll moment equation.

$$\dot{x} = A * x + B * u \tag{4-1}$$

$$M * \ddot{x} + C * \dot{x} + k * x = f \tag{4-2}$$

$$\ddot{x} = \dot{v} \tag{4-3}$$

$$M * \dot{v} + C * v + K * x = f \tag{4-4}$$

$$\begin{gathered} \dot{x} = v \\ \dot{v} = -M^{-1} * K * x - M^{-1} * C * v + M^{-1} * f \end{gathered} \tag{4-5}$$

$$\begin{bmatrix} \dot{x} \\ \dot{v} \end{bmatrix} = \begin{bmatrix} 0 & I \\ -M^{-1} * K & -M^{-1} * C \end{bmatrix} * \begin{bmatrix} x \\ v \end{bmatrix} + + \begin{bmatrix} 0 \\ M^{-1} \end{bmatrix} * f \tag{4-6}$$

However, in this case, it was not a trivial task to generate a complete set of first order equations that were compact and understandable. The easier solution was to divide each first order state equation into three parts as shown in Equation 4-8. This formulation separated each equation into a mass (or inertia) component (M), a stiffness component (K), and an input component (B_m). These matrices were generally much easier to develop and implement in code as the only necessary task was to separate the first order derivatives on the left and organize the states and the inputs on the right. With this method, the state space model could be developed once the system was in numerical form by dividing out the mass as shown in Equation 4-9.

$$\dot{x} = A * x + B * u \tag{4-7}$$

$$M * \dot{x} = K * x + B_m * u \tag{4-8}$$

$$\dot{x} = M^{-1} * K * x + M^{-1} * B_m * u \tag{4-9}$$

A simple example of how this method works is presented in Equations 4-10 through 4-12.

$$\dot{x} + 2 * \dot{y} = 3 * x - 5 * y + B1$$
$$\dot{y} = 5 * x - \dot{x} + B2 \qquad \textbf{4-10}$$

$$\begin{bmatrix} 1 & 2 \\ 1 & 1 \end{bmatrix} * \begin{bmatrix} \dot{x} \\ \dot{y} \end{bmatrix} = \begin{bmatrix} 3 & -5 \\ 5 & 0 \end{bmatrix} * \begin{bmatrix} x \\ y \end{bmatrix} + \begin{bmatrix} 1 & 0 \\ 0 & 1 \end{bmatrix} * \begin{bmatrix} B1 \\ B2 \end{bmatrix} \qquad \textbf{4-11}$$

$$\begin{bmatrix} \dot{x} \\ \dot{y} \end{bmatrix} = \begin{bmatrix} 7 & 5 \\ -2 & 5 \end{bmatrix} * \begin{bmatrix} x \\ y \end{bmatrix} + \begin{bmatrix} -1 & 2 \\ 1 & -1 \end{bmatrix} * \begin{bmatrix} B1 \\ B2 \end{bmatrix} \qquad \textbf{4-12}$$

4.2. Triple Truck (Tractor and Three Trailers)

Before beginning the mathematical assembly of the triple truck model, a process for systematically defining the units and their connections was developed (Table 4-1). The approach taken was to sequentially build the linear model just as one would build the actual vehicle.

Table 4-1: Vehicle Unit Numbering and Connection Type

Unit Number	Unit Description	Leading Connection	Trailing Connection
Unit 1	Tractor	None	Fifth Wheel
Unit 2	First Trailer	Fifth Wheel	Pintle Hook
Unit 3	First Dolly	Pintle Hook	Fifth Wheel
Unit 4	Second Trailer	Fifth Wheel	Pintle Hook
Unit 5	Second Dolly	Pintle Hook	Fifth Wheel
Unit 6	Third Trailer	Fifth Wheel	None

For the remainder of this work the individual units comprising this model will be referred to by their vehicle unit number. As noted in Section D.2, inter unit forces (internal forces) were denoted as F_{ij} where i represents the leading unit and j the following unit so all internal forces will be listed as F_{12}, F_{34}, etc. thereby denoting the two units which are connected by the coupling connection.

4.2.1. Combined Vehicle Equations

As the development of the final form of the equations of motion for each individual unit was covered in Section 3.4, this section will only deal with the assembly of the equations into a complete vehicle. The starting point for this is the restatement of the equations of motion for each vehicle unit. The cancelation of internal forces is addressed in Section 4.2.2. If the reader desires more detail on the expansion of the unit equations of motion to describe each unit individually, the process is defined in Appendix D.3.

4.2.2. Internal Force Cancelation and State Space Form

To cancel the internal forces between the successive units, the set of yaw moment equations were solved simultaneously. For the case here, there were three iterations of Equation 3-21 (Equations D-61, D-69, and D-77) for units 2, 4, and 6 and two iterations of Equation 3-24 (Equations D-65 and D-73,) for units 3 and 5. These were solved for the five unit to unit constraint forces (F_{12}, F_{23}, F_{34}, F_{45}, and F_{56}). The constraint forces were then substituted back into the remaining equations of motion. The yaw moment equation for the trailers and dollies was then replaced with the first order constraint equation (Equation 3-26) for each towed unit. The full vehicle state vector is shown in Equation 4-13. For space reasons, the full matrices are listed in Appendix G.

$$x = \begin{bmatrix} \beta_1, \dot{\psi}_1, \dot{\phi}_1, \phi_1, \beta_2, \dot{\psi}_2, \dot{\phi}_2, \phi_2, \beta_3, \dot{\psi}_3, \dot{\phi}_3, \phi_3, \ldots \\ \beta_4, \dot{\psi}_4, \dot{\phi}_4, \phi_4, \beta_5, \dot{\psi}_5, \dot{\phi}_5, \phi_5, \beta_6, \dot{\psi}_6, \dot{\phi}_6, \phi_6 \end{bmatrix}^T \qquad \textbf{4-13}$$

The resulting states of the system were a concatenation of the 4 states for each unit: side slip (β), yaw rate ($\dot{\psi}$), rollrate ($\dot{\phi}$), and roll (ϕ). For information on how the states were measured, please refer to Section 5.1.

4.2.3. A Note on Dolly Motion

As the dolly is decoupled in roll from the trailer (both fifth wheel and pintle hook are modeled as ball joints) and the dolly has a very low mass, it was not expected to experience significant roll moments. This observation will be proven in the model analysis (Section 4.3) and, as a result, one could argue that the model need not consider the dolly roll and roll rate. This is true and one could reduce the vehicle state space from 24 to 20 degrees of freedom (2 dollies) quite easily. The dolly roll information was left in the analysis here for the following reasons:

- Clarity of model assembly. It was deemed easier to follow the model construction if all units had the same degrees of freedom.
- Potential model extension. Should a new dolly type which does restrict relative roll be developed, the model could be used to simulate the full vehicle's dynamic performance.
- As will be shown in Section 4.6, the dollies are eventually removed from the final system altogether making the roll reduction a moot point.

4.3. Dynamic Simulation of Vehicle

After completion of the linear model in Section 4.2, a validation exercise was undertaken to ensure that the LTI model would serve as a good representative of the actual vehicle. To assess the model's quality and accuracy, three maneuvers were simulated (step steer, swept sine, and double lane change) in two load configurations (base vehicle and fully loaded). While there are an infinite number of loading scenarios for a three trailer vehicle, only two were assessed for reasons of practicality. However, these two cases represent the bounds of the usage range of the vehicle.

As physical vehicle testing was prohibitively expensive, a non-linear TruckSim® simulation was used as the reference vehicle. The linear model validation was made by extracting the steering input and dynamic vehicle responses from TruckSim®, applying the steering demands to the linear model, and comparing the linear model's responses to the TruckSim® simulation responses. To make the comparisons reasonable, the TruckSim® simulations were limited to maneuvers which kept the vehicle near the linear domain of operation.

4.3.1. Vehicle Parameters

The first task in the process of validating the model was to define the vehicle parameters. These were drawn from the TruckSim® model and are listed in Appendix E. The only linear model parameter with significant deviation from the reference model is the roll damping. Prior research by the author and others has shown that damper (shock absorber) viscous damping is not a major source of roll energy dissipation in trailers (LaClair et al., 2010). However, there is a good deal of hysteretic damping from the trailer arm bushings and pneumatic damping due to air movement between suspension air bags (common plumbing). As including hysteretic damping in the linear model would complicate it, the damping was modeled as viscous in nature. Since damping has little effect on the model (see Section 4.5), this was not a significant issue.

4.3.2. Step Input Response

The first validation made was the most basic test of the unloaded vehicle under near steady state conditions (transient behavior at step input and then steady state response with fixed steering). In this case a 180º step steer (6.75º road wheel steer) was applied to the model when driving at 40 km/h. The analysis shows that the linear model does a good job of predicting the behavior of the tractor and all trailers (Figure 4-1and Figure 4-2). Note that the non-linear model's drive torque (tractor) causes the side slip to deviate from the linear model prediction. Unit definitions are located in Table 4-1.

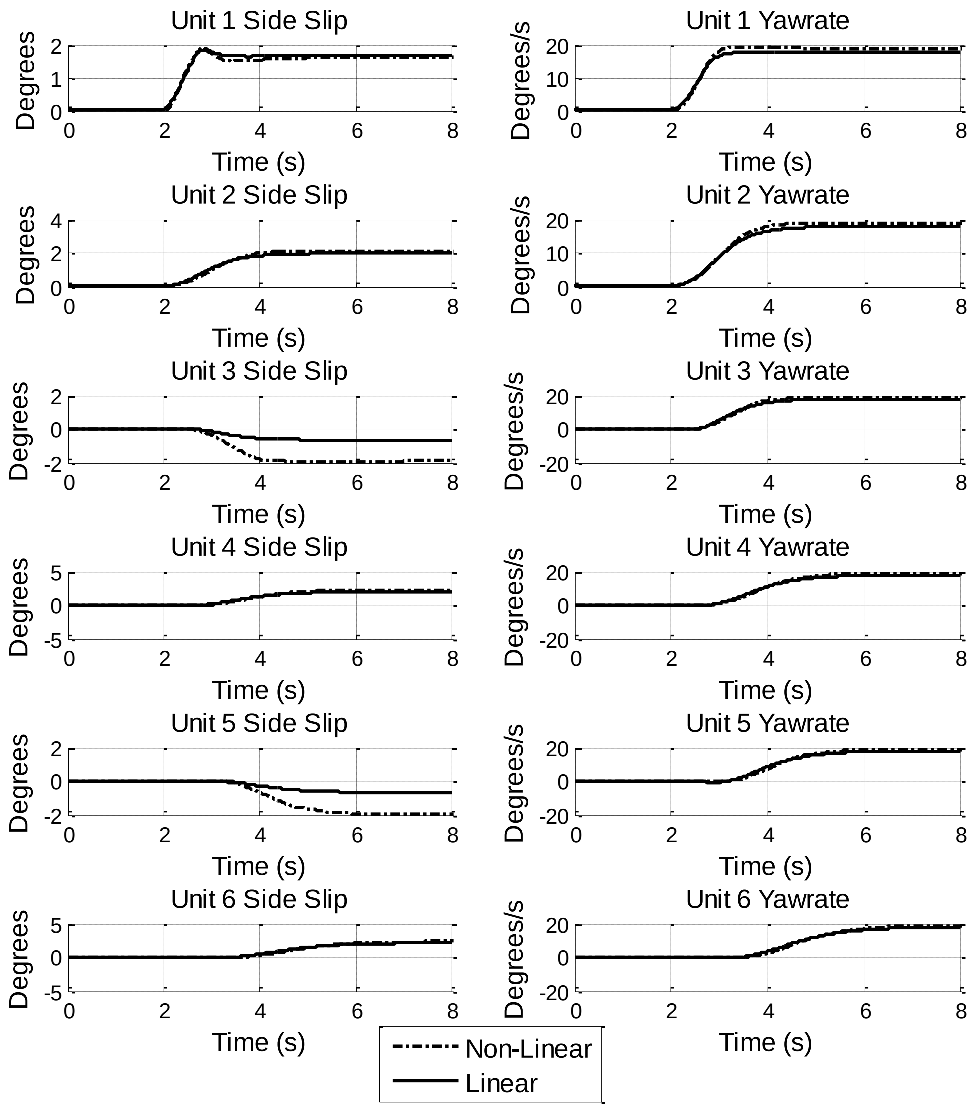

Figure 4-1: Unloaded Lane Change - Side Slip and Yaw Rate

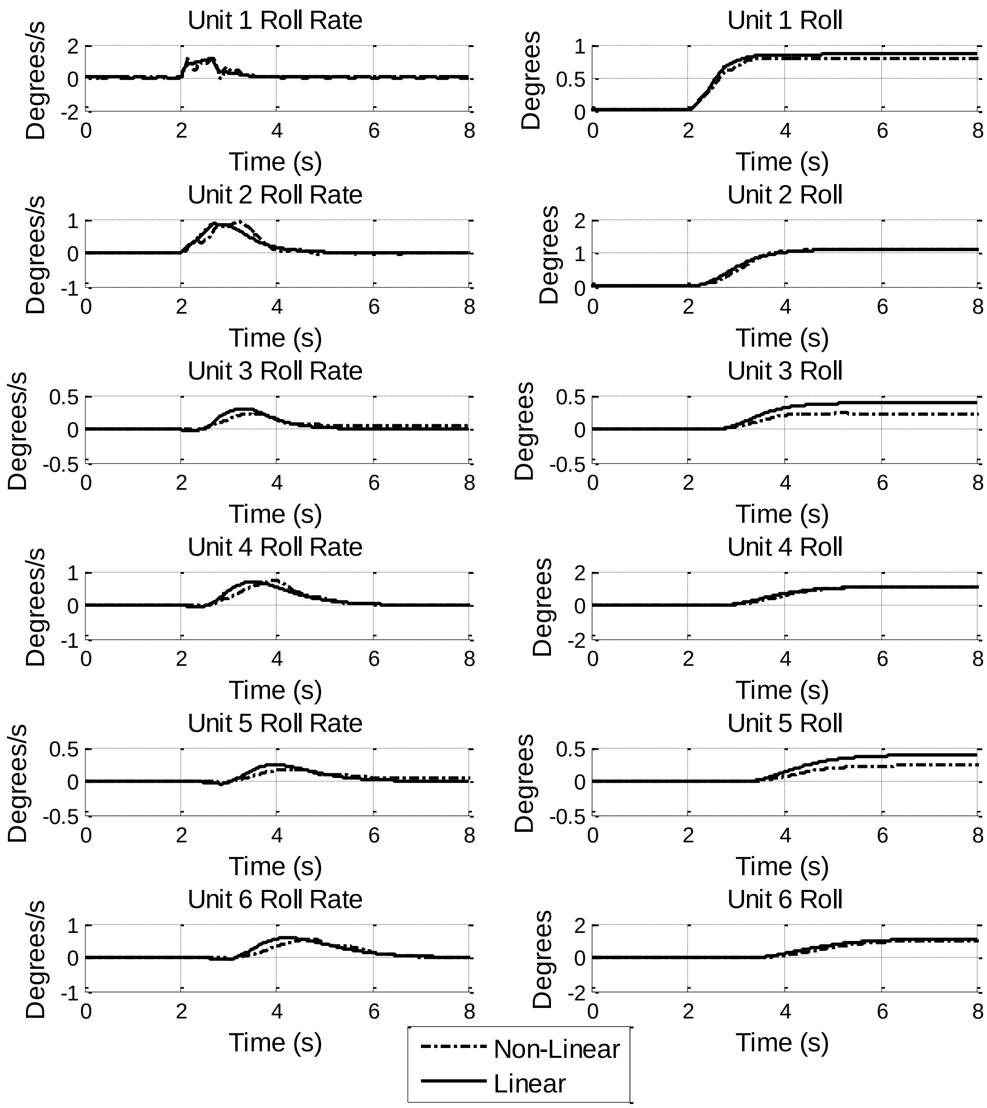

Figure 4-2: Unloaded Lane Change - Roll Rate and Roll

The less accurate reproduction of the dolly motions (units 3 and 5) was not deemed to pose a significant issue as the dollies generally do not pose a stability risk for the vehicle (see Section 4.5). They rarely see large roll angles (save for when the attached trailer rolls over) and their yaw behavior is almost entirely driven by the orientation of the attached trailers and the required tire lateral force development. For the dolly to experience a yaw related issue, one or both of the attached trailers would have to deviate significantly from their desired paths first which would be seen as an instability event itself. More on this topic is provided in Section 4.5.

4.3.3. Swept Sine Response

When the unloaded vehicle was simulated using a 0.1 to 10 Hz. swept sine at 60 km/h, the model reproduced the non-linear vehicle's performance quite well (Figure 4-3 and Figure 4-4). As the roll angles were relatively low (within the linear range of the vehicle), the linear model matched the actual vehicle quite well. For side slip and yaw rate, the model matched the tractor and trailer responses. Only for the dolly did the simulations deviate. However, as noted before, the dollies seldom poses a stability risk so the error is quite acceptable (see Section 4.5).

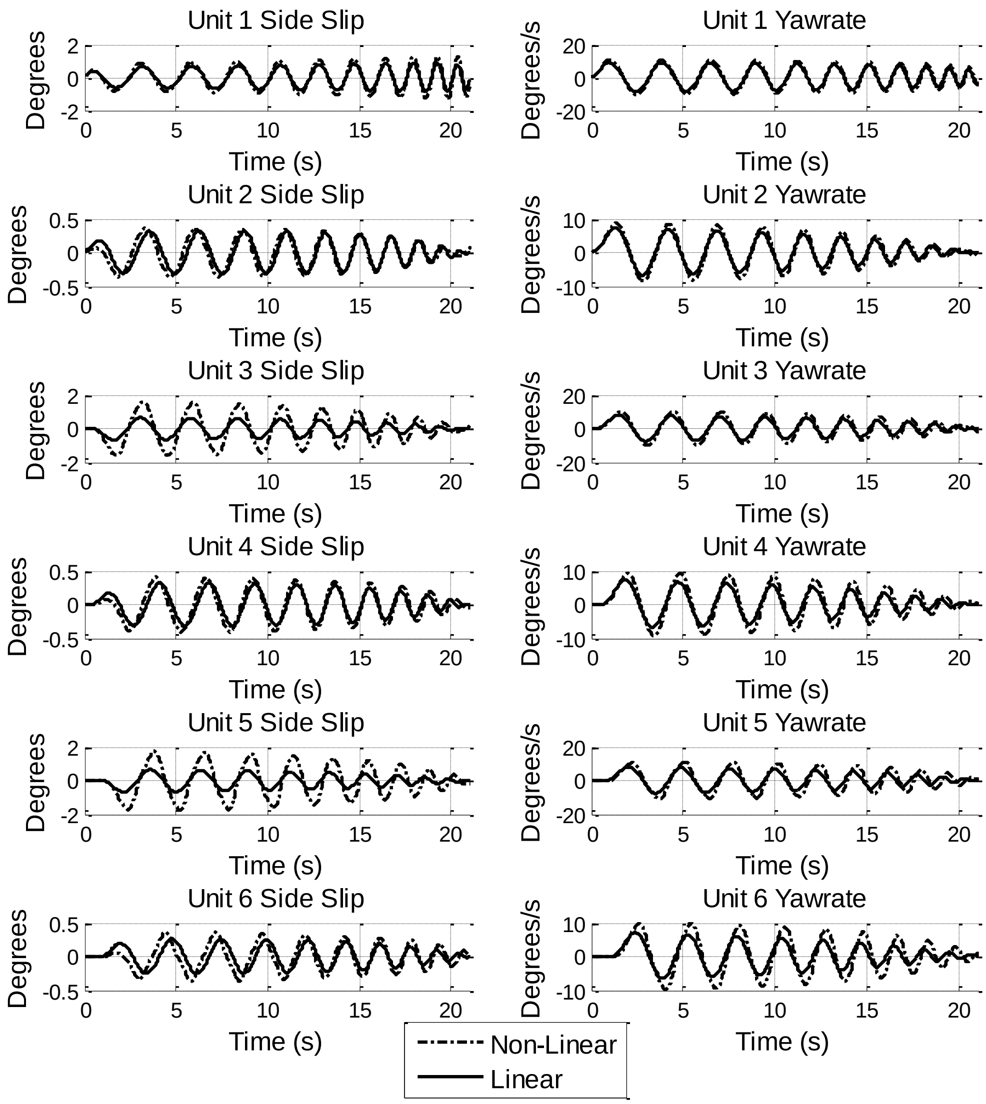

Figure 4-3: Unloaded Swept Sine - Side Slip and Yaw Rate

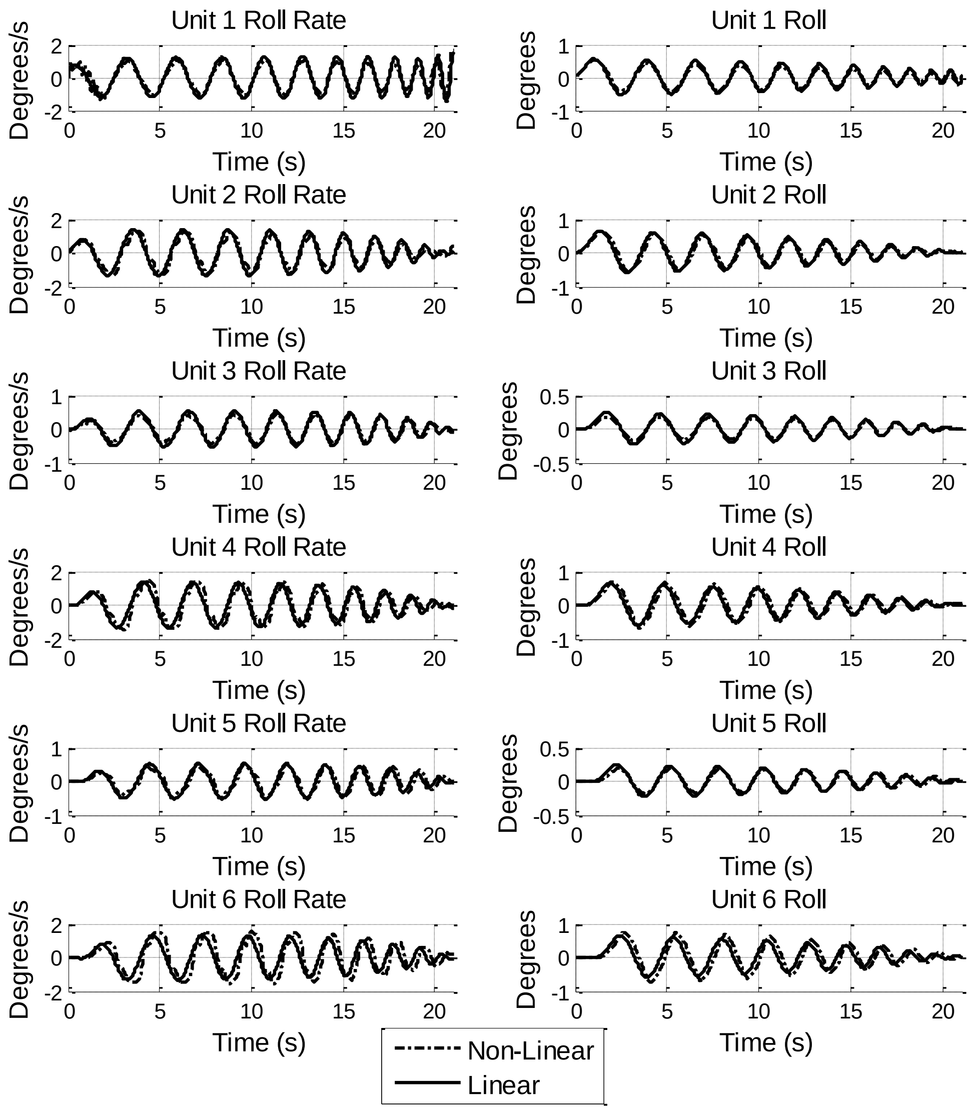

Figure 4-4: Unloaded Swept Sine - Roll rate and Roll

4.3.4. Double Lane Change Response

While the step steer and swept sine tests were the standard methods for evaluating the steady state and transient responses of the vehicle, neither are generally seen in the real world. As such, a double lane change at 70 km/h was included as well (Figure 4-5 and Figure 4-6). The lane shift was 3.5 meters and the first and last gates were 80 meters apart. The model reproduced the dynamic behavior of all of the units of interest (tractor and trailers) with reasonable accuracy.

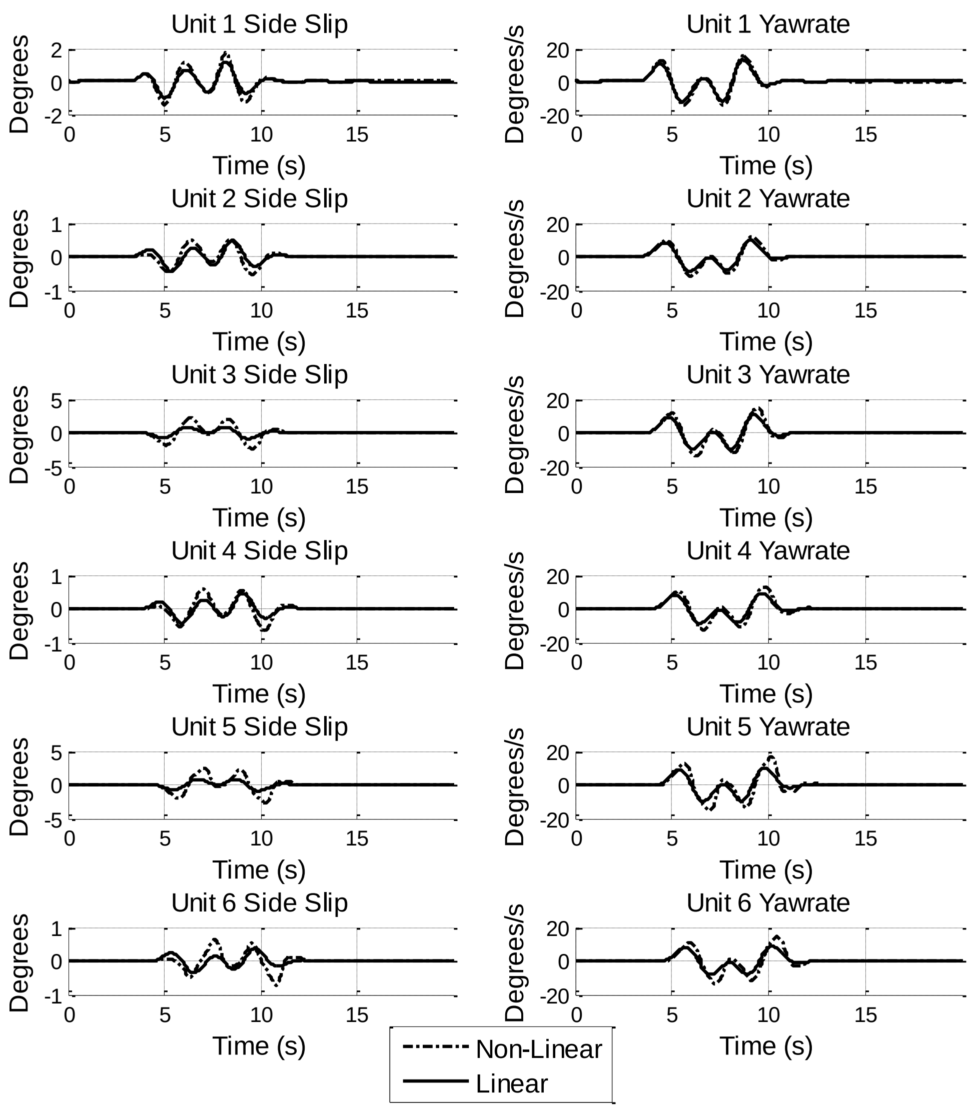

Figure 4-5: Unloaded Double Lane Change - Side Slip and Yaw Rate

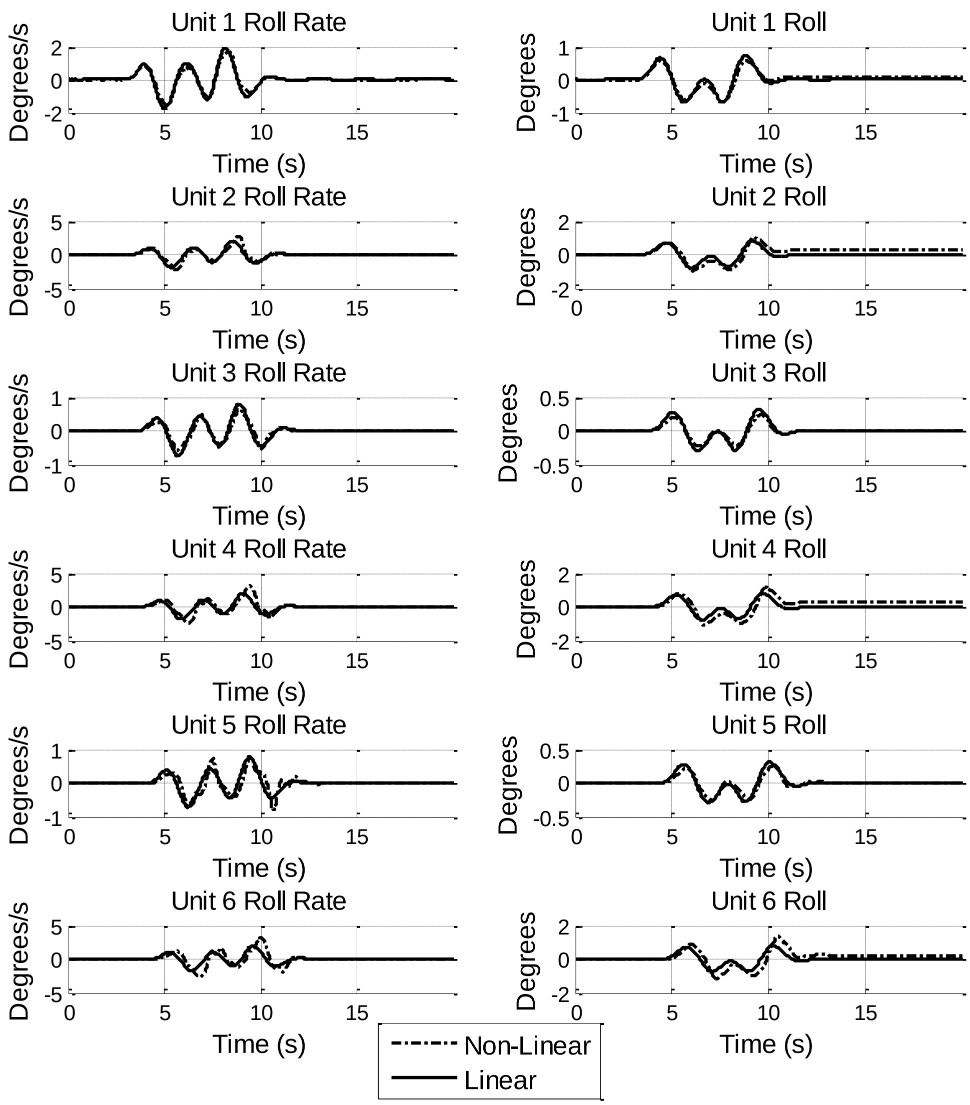

Figure 4-6: Unloaded Double Lane Change - Roll Rate and Roll

4.3.5. Rearward Amplification

In addition to providing validation that the model matched the reference vehicle, the simulation also reproduced the classical rear amplification phenomena seen in multi-unit vehicles such as this (Figure 4-7 and Figure 4-8) where following trailers experience larger dynamic responses than the leading units. In the roll behavior of the vehicle one can clearly see that each vehicle unit's roll is progressively larger than the preceding unit's (excluding dollies).

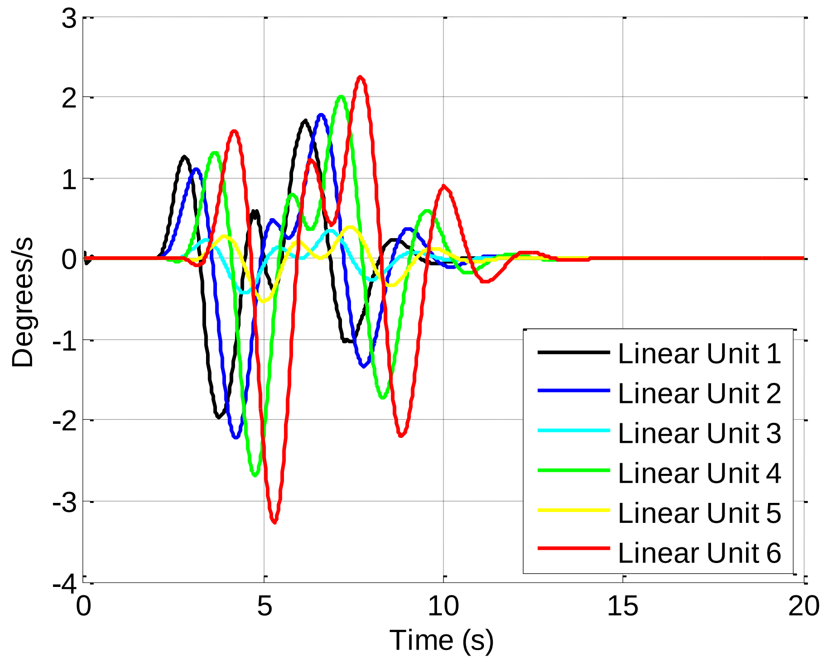

Figure 4-7: Double Lane Change Rear Amplification Roll Rate

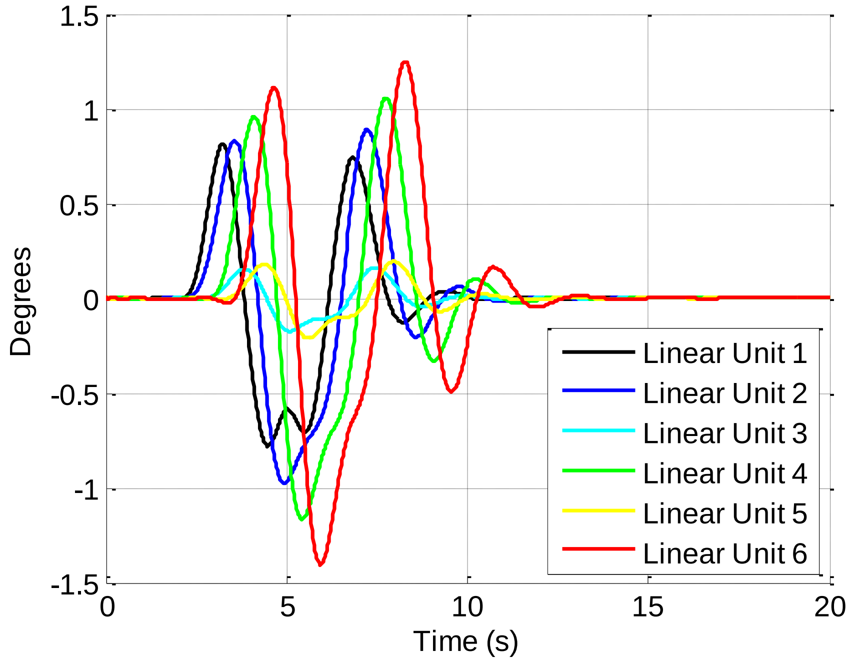

Figure 4-8: Double Lane Change Rear Amplification Roll

For clarity, the rear amplitude cases above were run at a slightly reduced speed as compared to the double lane change test (Section 4.3.4) to ensure that all units of the vehicle remained within the linear operational range.

4.4. Payload Adjustments

As commercial vehicles such as triple trucks are intended to be used to transport goods, it was deemed prudent to assess the linear model's performance when loaded. To that end, the three validation cases above were re-run with a loaded vehicle. Generally, the model reproduced the non-linear vehicle's behavior with a few exceptions as will be shown. Note: In each case where the linear model deviated from the reference, the deviation was such that it would not degrade the linear model's usefulness in evaluating the ultimate stability of the vehicle.

4.4.1. Step Steer

The dynamic response of the loaded vehicle to the step steer (Figure 4-9 and Figure 4-10) indicates that the linear model again closely matched the side slip and yaw rate of the reference vehicle. In roll, the linear model continued to match the reference vehicle as well save for the tractor and dollies. As previously noted, the dollies are not the primary stability risk so the error in the evaluation of the dolly states is not of significant concern. Generally, tractors do not pose a significant roll risk either, having relatively low centers of gravity. The deviation in tractor and dolly roll angle is due to the elimination of the fifth wheel roll moment (extremely non-linear fifth wheel roll stiffness).

The loaded step steer case again used a 180º hand wheel / 6.75 º road wheel input at a speed of 30 km/h. This is a rather aggressive maneuver akin to an emergency heading change at an intersection. In this case, the first trailer rolls significantly (5º) and runs through the lash in the fifth wheel. This introduced a roll moment to the tractor which caused the tractor roll angle to increase. But, as the linear model had no roll coupling between the tractor and first trailer, it did not capture this effect. Note: even with the non-linear roll coupling the tractor roll angle was less than half the trailer roll angles (trailer loading arrangements per industry norm).

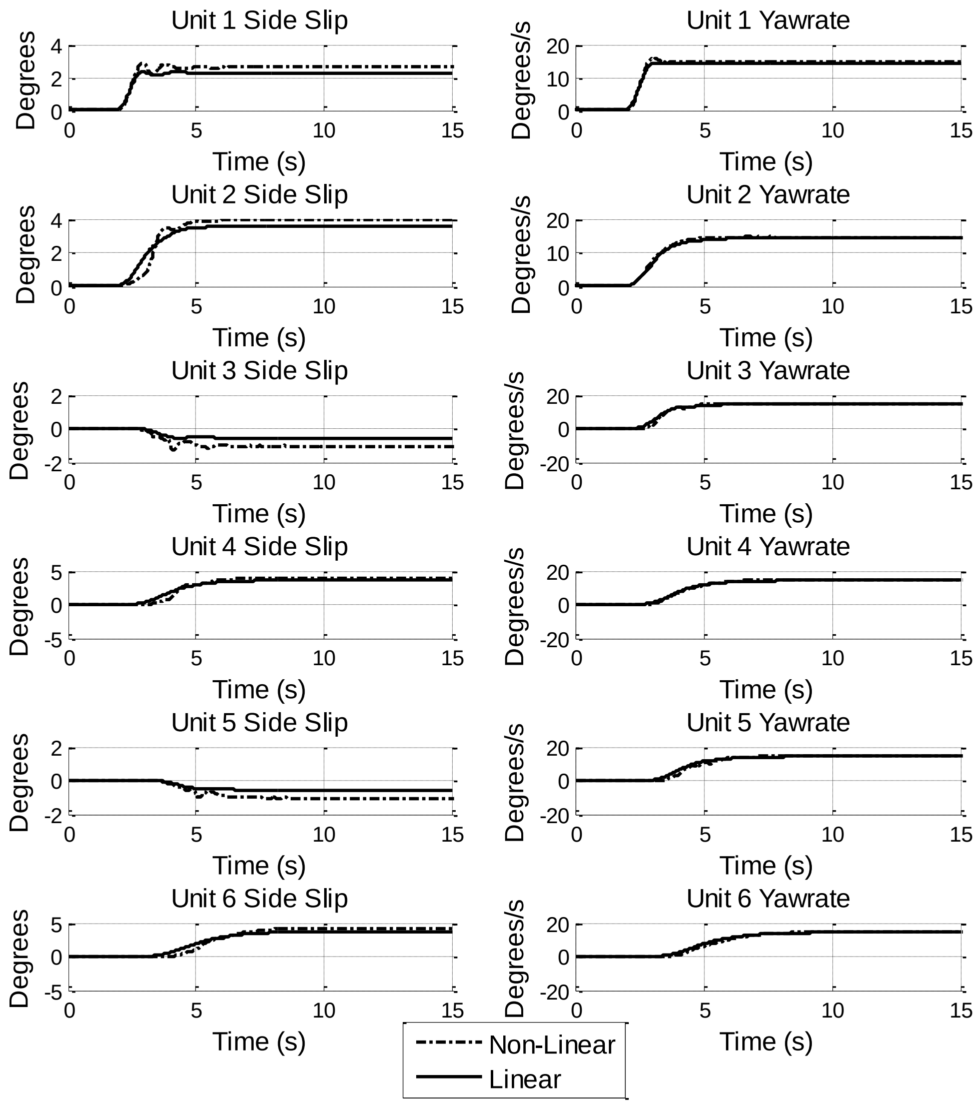

Figure 4-9: Loaded Step Steer - Side Slip and Yaw Rate

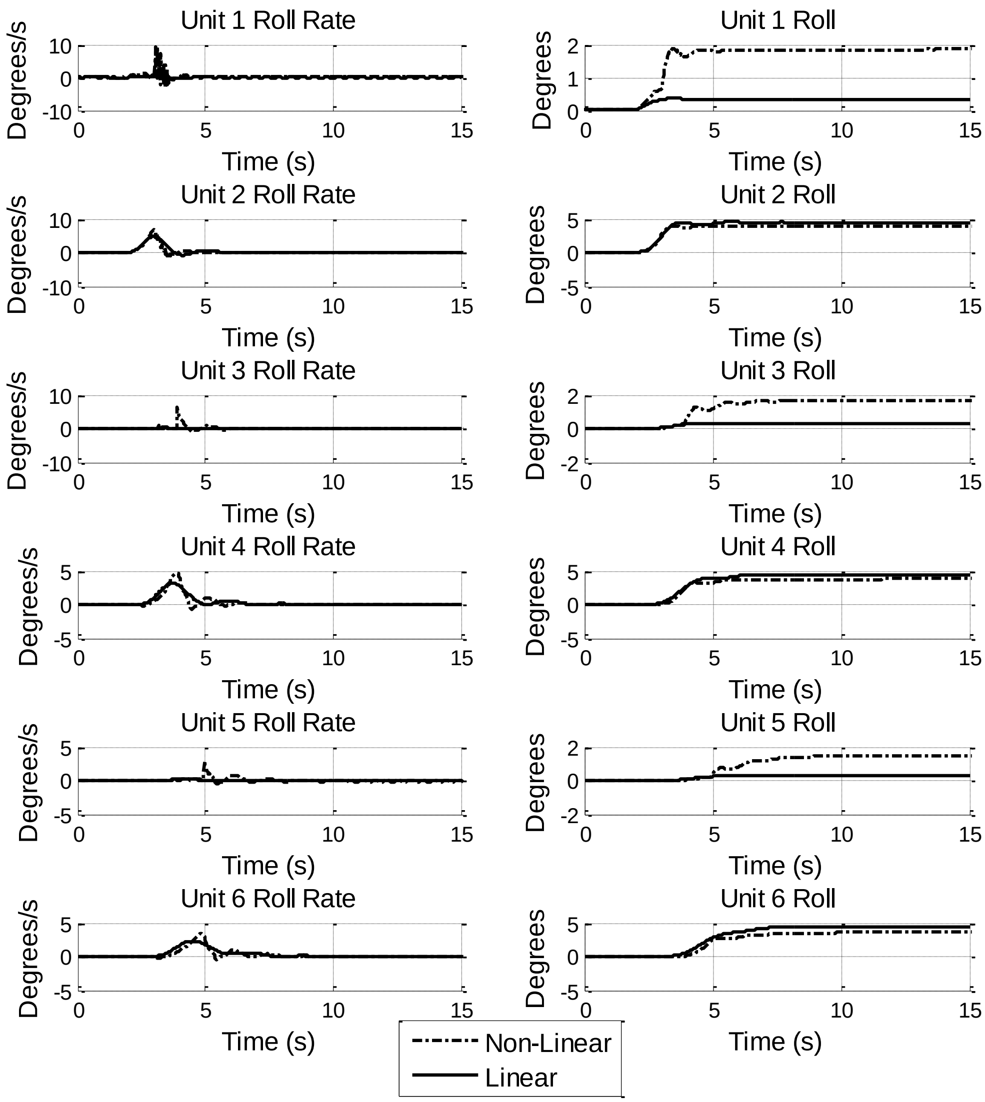

Figure 4-10: Loaded Step Steer - Roll Rate and Roll

While the failure to predict the tractor roll angle was technically an error, it is really not that significant an issue. In the real world, it is very seldom that a tractor will roll before the trailer(s) as the trailers generally see larger dynamic inputs (see Section 4.3.5), have higher CG heights (600 mm vs. 1,200 up to 2,000mm for the trailer), and have larger masses (and overturning moments). Given that the model did capture the trailer roll angles well, it should serve as an accurate indicator of the vehicle's stability even if the tractor roll is under predicted. Note: prior research by the author and others did produce cases where the tractor wheels lifted before the trailer wheels but those cases were the result of the front of the trailer rolling more than the rear of the trailer and then rolling the tractor (Pape et al., 2008). Again, the stability risk was the trailer as the tractor remained relatively stable until the trailer ran through the fifth wheel lash and rolled the tractor.

4.4.2. Swept Sine

When developing the loaded swept sine maneuver, it was quite difficult to define a test which operated in the linear range of the vehicle for the entire maneuver. The simulation used a frequency range from 0.1 to 10 Hz. at a speed of 30 km/h. While not perfect, the resulting model performance proved to be reasonably accurate.

The most significant deviation between the reference and the linear model's performance was in the side slip of the trailers (Figure 4-11) and the general attenuation of dynamic response at higher steering inputs (Figure 4-12). The rollrate attenuation was not deemed to be a significant issue as it mostly occurs for steering inputs above 5 Hz. which is higher than what a typical driver can achieve in an actual vehicle.

The trailer side slip phase lead, which was visible in this test due to the high payload load and transient maneuver, was partially attributed to the lack of tire relation length effects in the model and partially to trailer axle roll steer (Figure 4-13). The trailer side slip phase issue must be accepted as a limitation of the linearization of the vehicle.

However, the phasing does not affect the peak amplitudes which are more important in terms of predicting potential future instability. Note: the prediction covers a five second horizon and any bound violation within that horizon results in corrective action. The phasing is on a much smaller time scale.

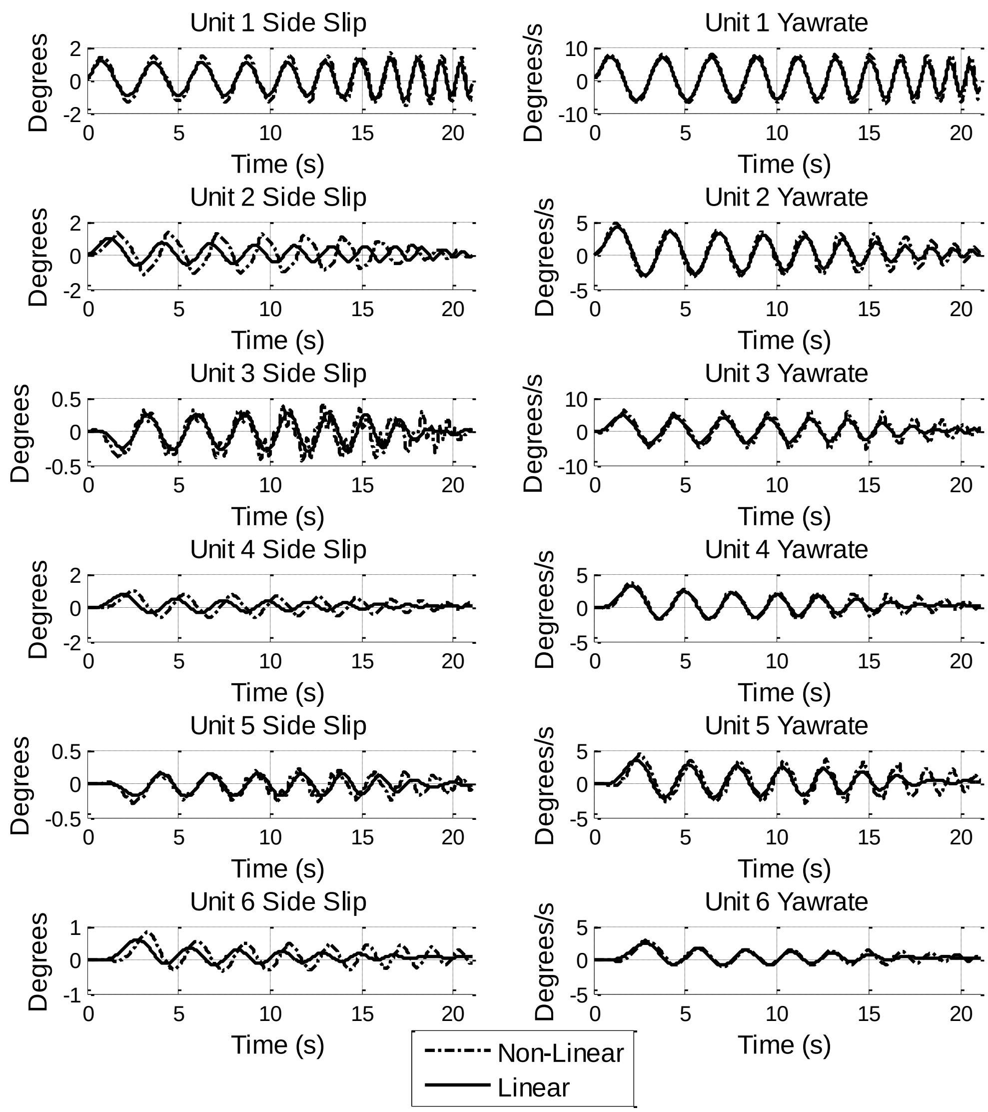

Figure 4-11: Loaded Swept Sine - Side Slip and Yaw Rate

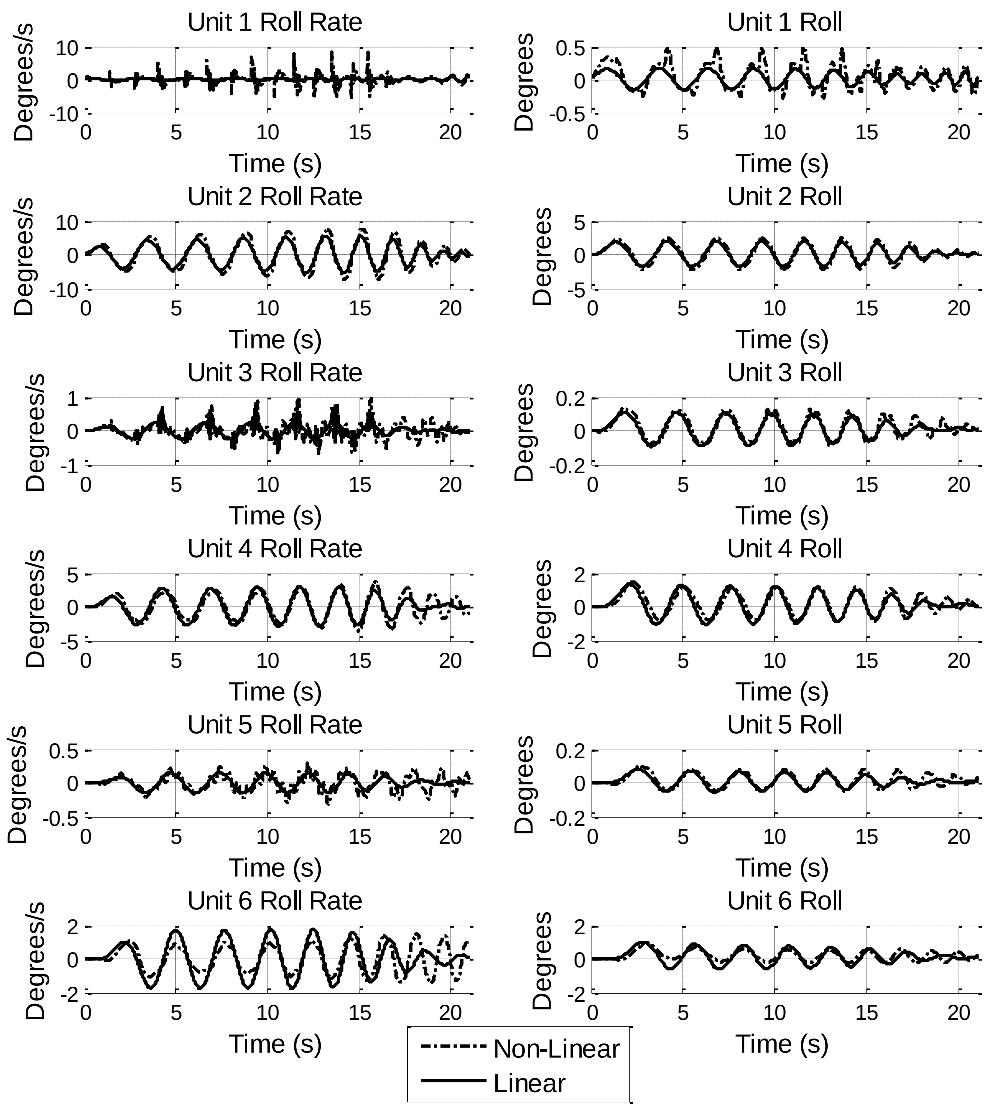

Figure 4-12: Loaded Swept Sine - Roll Rate and Roll

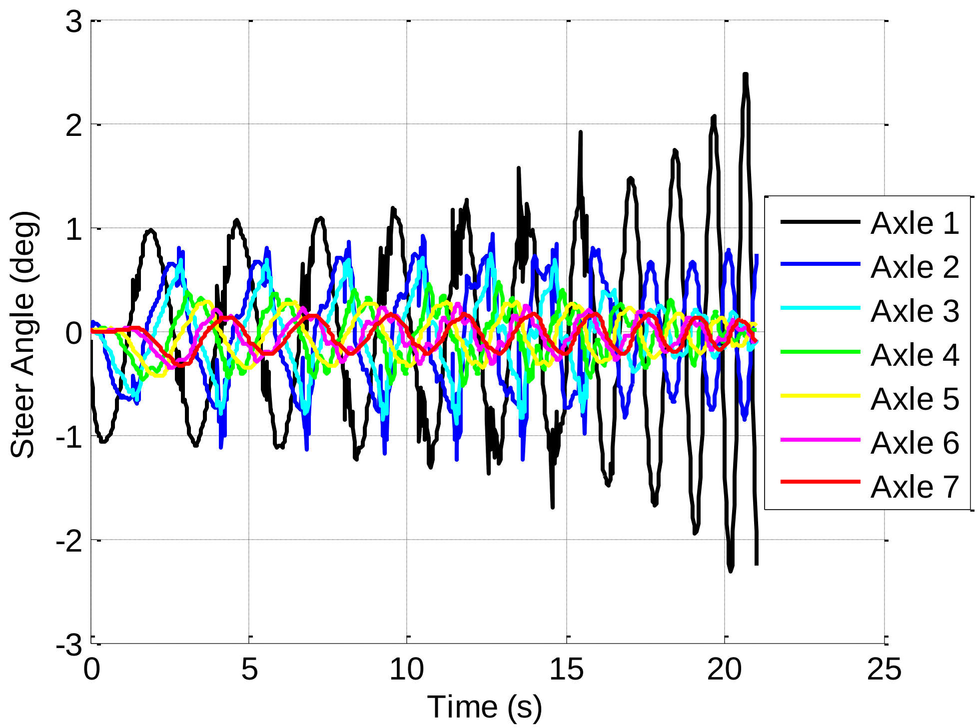

Figure 4-13: Reference Model Loaded Swept Sine Axle Steer

4.4.3. Double Lane Change

The final validation simulation was the loaded vehicle double lane change (Figure 4-14 and Figure 4-15) in which the linear model again matched the reference non-linear vehicle model well. The linear model again under predicted the roll of the tractor due to the removal of the tractor to first trailer coupling in roll (Section 4.4.1). The remaining states for the tractor and all three trailers were reproduced acceptably. Again, the dollies were not modeled as well, but are not of significant concern.

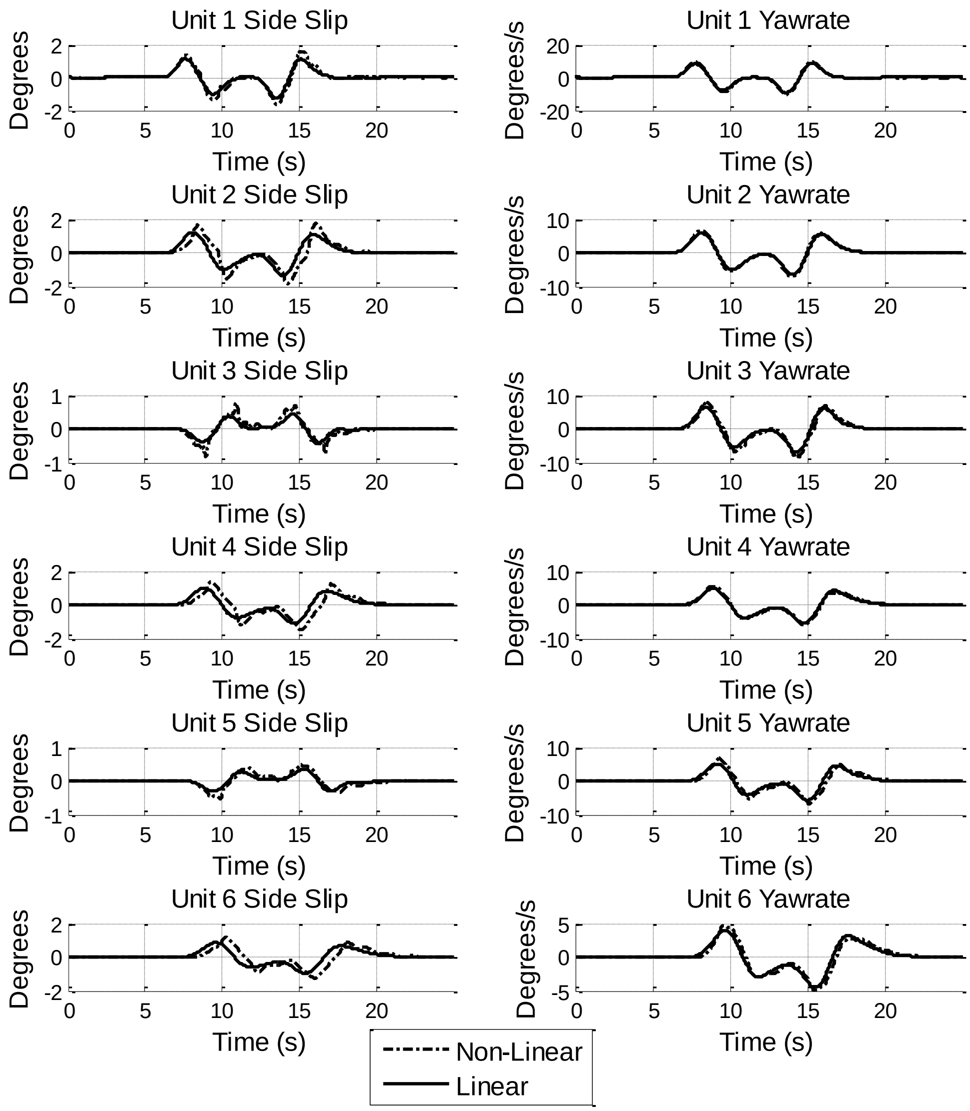

Figure 4-14: Loaded Double Lane Change - Side Slip and Yaw Rate

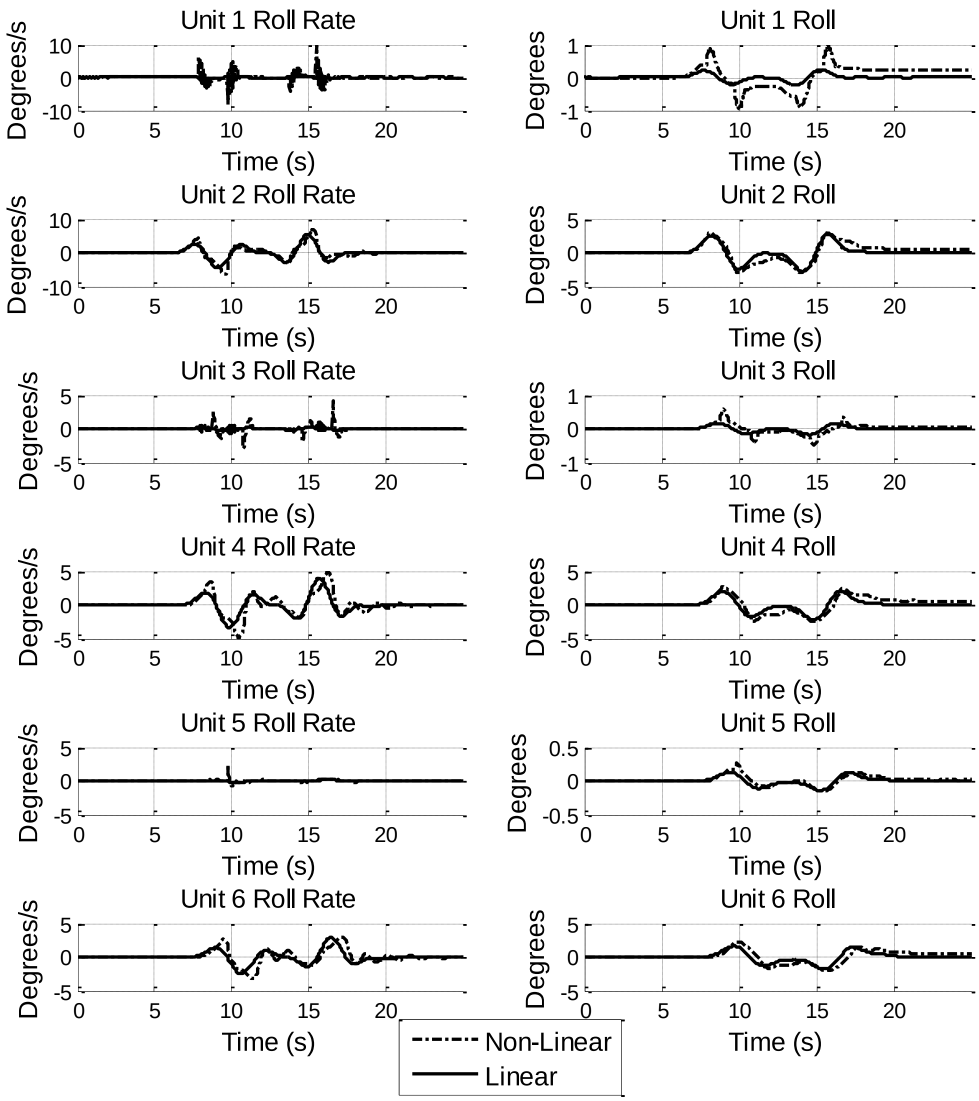

Figure 4-15: Loaded Double Lane Change - Roll Rate and Roll

4.5. Eigen Value Analysis

One of the useful properties of a linear model is the ability to quickly assess the overall stability of the system by examining its eigenvalues. Since the state space model is dependent on vehicle parameters that change with vehicle operation (speed, mass, inertia, roll stiffness, etc.) an analysis of the eigenvalues can shed light on the general stability of the vehicle in its current configuration. While all vehicle parameters affect the system stability, a few have larger effects and warrant a brief review.

4.5.1. Speed Dependency

It is well known that the stability of many vehicles decreases with speed (Ghoneim et al., 2000; Yi Feng-yan, Xie Mei-zhi, & Wei Chao-yi, 2010) and the vehicle presented here is no exception. Generally, the effect of speed on stability could be observed by evaluation of the eigenvalues symbolically. However, the linear vehicle here has 24 states which are dynamically interconnected such that symbolic analysis of the eigenvalues was infeasible as they are difficult to simplify or interpret. Given this situation, the approach used to assess speed dependency on stability incorporated a simpler vehicle for illustrative purposes and the use of a numerically based approach for the triple truck. Note: literature reference material on eigenvalue assessment of stability is all based on conventional single trailer vehicles (two units) while the reference vehicle here has six units. As a consequence, the vehicle here displayed more modes and incorporated some new dynamic behaviors as compared to prior work.

Before beginning the evaluation of the full vehicle, a simple yaw only tractor model was developed to demonstrate the effect of speed on lateral stability. In this case, the states were simply the tractor side slip and yaw rate (Equation 4-14). The resulting state space for the model is described in Equations 4-14 through 4-15. Evaluation of the system produced the eigenvalues shown in Equation 4-18. Note that the expansion of

Equation 4-17 (Equation 4-18) indicates that as the speed increases, the vehicle moves from over damped to under damped and the real part of the eigenvalues get smaller.

$$x = [\beta \quad \dot{\psi}]' \tag{4-14}$$

$$\dot{x} = \begin{bmatrix} -\frac{C_{af} + C_{ar}}{U_1 * m_1} & -\frac{m_1 * {U_1}^2 + C_{af} * a_1 - C_{ar} * b_1}{{U_1}^2 * m_1} \\ \frac{C_{ar} * b_1 - C_{af} * a_1}{I_{zz1}} & -\frac{C_{af} * {a_1}^2 + C_{ar} * {b_1}^2}{U_1 * I_{zz1}} \end{bmatrix} * x + B * u \tag{4-15}$$

$$0 = \det\left(\begin{bmatrix} -\frac{C_{af} + C_{ar}}{U_1 * m_1} & -\frac{m_1 * {U_1}^2 + C_{af} * a_1 - C_{ar} * b_1}{{U_1}^2 * m_1} \\ \frac{C_{ar} * b_1 - C_{af} * a_1}{I_{zz1}} & -\frac{C_{af} * {a_1}^2 + C_{ar} * b1^2}{U_1 * I_{zz1}} \end{bmatrix}\right) \tag{4-16}$$

$$0 = \frac{C_{af} * C_{ar} * b_1^2 + C_{ar} * C_{af} * a_1^2 + m_1 * U_1^2 * C_{ar} * b_1}{U_1^2 * m_1 * I_{zz1}} + \frac{-m_1 * U_1^2 * C_{af} * a_1 + 2 * C_{af} * a_1 * C_{ar} * b_1}{U_1^2 * m_1 * I_{zz1}} \tag{4-17}$$

$$Eig(A) = -\frac{1}{2} * \frac{C_{af} + C_{ar}}{U_1 * m_1} - \frac{1}{2} * \frac{C_{af} * a_1^2 + C_{ar} * b_1^2}{U_1 * I_{zz1}} \pm \frac{1}{2}\left(\frac{\left(C_{af} * a_1^2 + C_{ar} * b_1^2\right)^2}{U_1^2 * I_{zz1}^2} - 2 * \left(C_{af} * a_1^2 + C_{ar} * b_1^2\right) * \frac{C_{af} + C_{ar}}{U_1^2 * m_1 * I_{zz1}} + \frac{\left(C_{af} + C_{ar}\right)^2}{U_1^2 * m_1^2} - 4 * \left(C_{ar} * b_1 - C_{af} * a_1\right) * \frac{m_1 * U_1^2 + C_{af} * a_1 - C_{ar} * b_1}{U_1^2 * m_1 * I_{zz1}}\right)^{\frac{1}{2}} \tag{4-18}$$

If the tractor's parameters are substituted into Equation 4-19, the effect of vehicle speed is even more apparent (Figure 4-16).

$$Eig(A) = \frac{-398 \pm \sqrt{11630 - 51.9 * U_1^2}}{2 * \mathrm{U}_1} \quad \textbf{4-19}$$

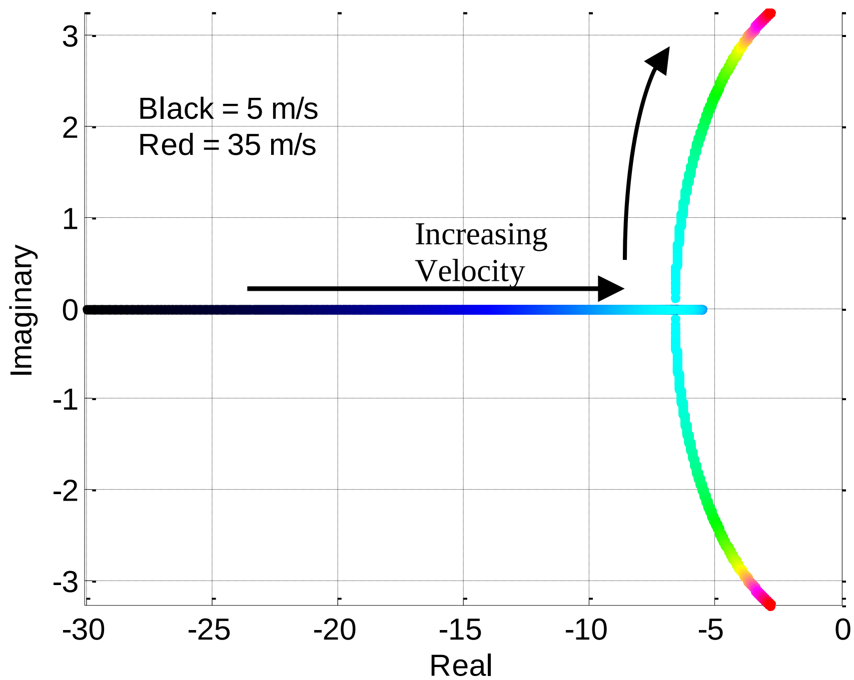

Figure 4-16: Tractor Only Yaw Only Eigenvalues vs. Speed

A similar analysis was done on a tractor and single trailer vehicle (Figure 4-17). Here the trailer becomes under damped at a lower speed than the tractor (note the darker blue color for the trailer eigenvalues when the trace leaves the real axis). The real parts of the trailer's eigenvalues also are reducing at a faster rate than the tractor's. This is predominately due to the lack of yaw damping at the fifth wheel so only the trailer axle (tires) provides any damping to the trailer. This is also in agreement with prior research into combination vehicle dynamics: "Vehicle speeds have a greater impact on the semitrailer, with the increasing of vehicle speeds, the system damping ratio decreases, therefore steering stability decreases significantly." (Yi Feng-yan et al., 2010)

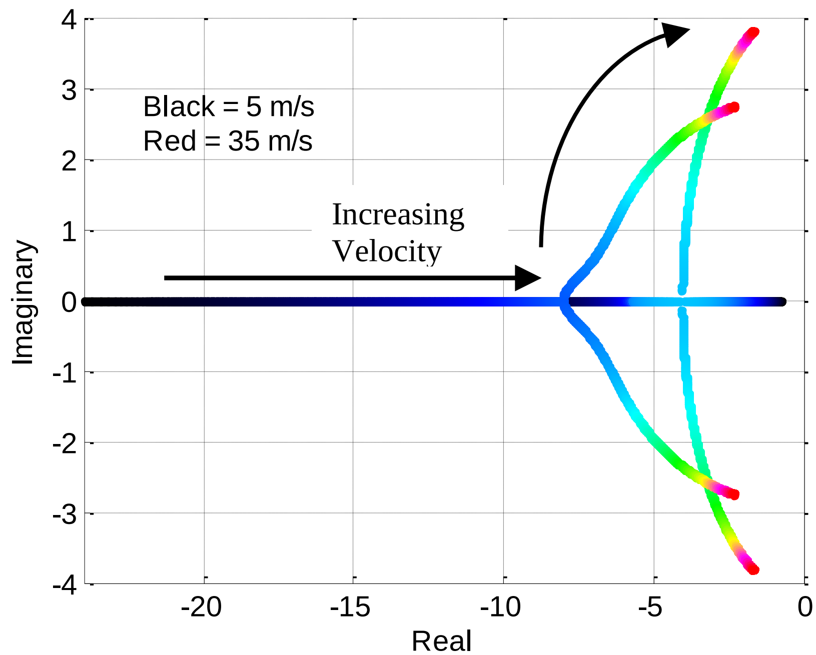

Figure 4-17: Tractor and Trailer Yaw Only Eigenvalues vs. Speed

Expanding the yaw analysis to the triple truck (six units without roll) clearly showed the effect of speed on the vehicle's yaw stability (Figure 4-18). Some of the more important observations included:

- The dollies had the largest frequencies and lowest damping. They also had the lowest under damped speed threshold which agreed with prior simplifications on dolly behavior (low inertia, orientation driven by adjacent trailers, etc.) (Section 4.3.2).

- The three eigenvalue sets with the smallest real parts were the three trailers. The key observation was that the trailers were the least stable components of the vehicle.
- The tractor was significantly more stable than the trailers as assumed in Section 4.2.2.

Note: The parameters used to generate the triple truck yaw response below and the triple truck yaw and roll response (Figure 4-19) use slightly different values for the fourth, fifth, and sixth unit's tire cornering stiffness. This was done solely to separate the response of the nearly identical units for visual purposes. The unmodified parameters produced curves that nearly overlaid making distinction of units 3 / 5 and 2 / 4 / 6 difficult.

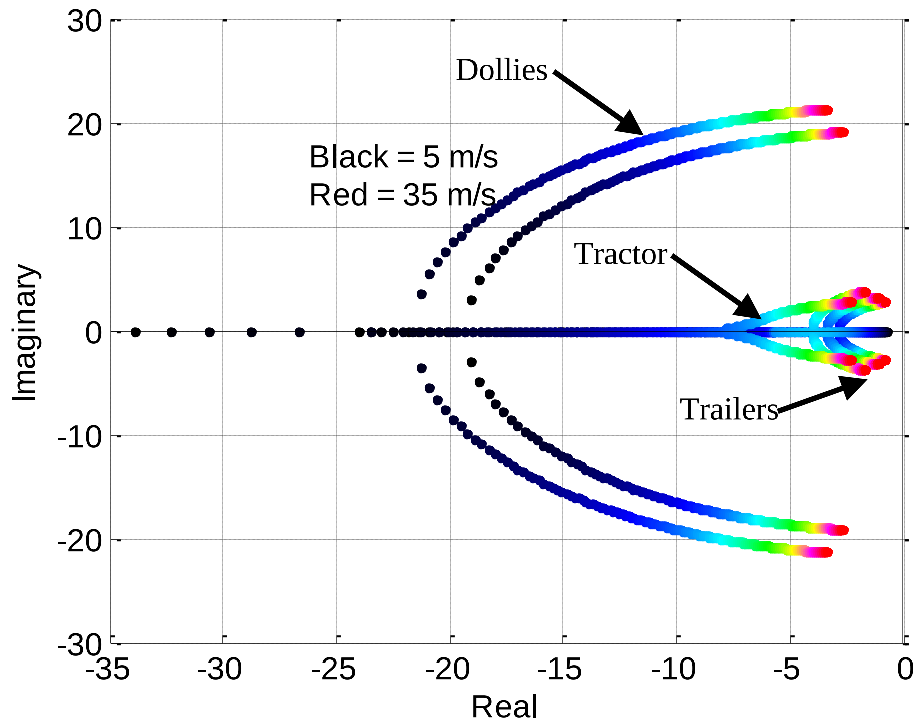

Figure 4-18: Triple Yaw Only Eigenvalues vs. Speed

Incorporating roll into the model did change the yaw dynamics of the triple truck to some extent but the trailers still remained the least stable followed by the tractor (Figure 4-19). Note the trailers had the smallest real portion eigenvalues in yaw and roll. Of particular interest was that the trailers were never over damped in roll and were under damped in yaw for speeds above 15 m/s (33 mile/hour). Also, the dollies were under damped in yaw for speeds above 9 m/s (20 mile/hour).

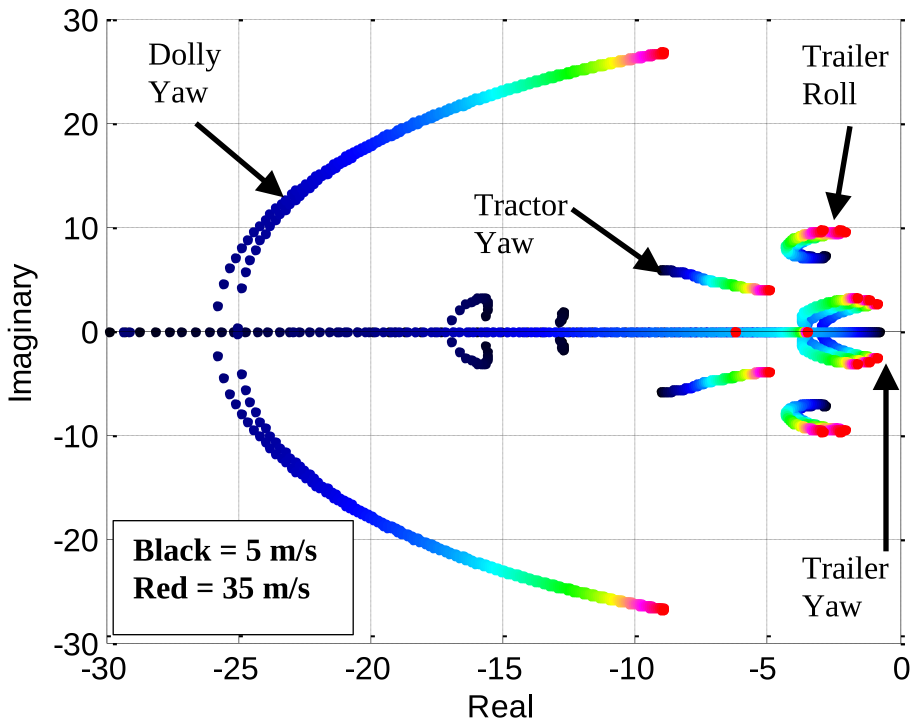

Figure 4-19: Unloaded Triple Vehicle Eigenvalues vs. Speed

In order to make the behavior of the trailers and the yaw response of the dollies easier to observe, the above figure had the real axis truncated at -30. The information not displayed was the roll behavior of the tractor and dollies. As these units were decoupled in roll from the remainder of the vehicle (Section 3.2.1), it was not a surprise that their real eigenvalue parts were highly negative. Finally, the trailer eigenvalues (Figure 4-19) agree with prior work by others (Figure 4-20) (Eisele & Peng, 2000). The tractor eigenvalues differ from the work by Eisele as that research included a roll moment connection between the tractor and trailer where this work has the trailers decoupled in roll.

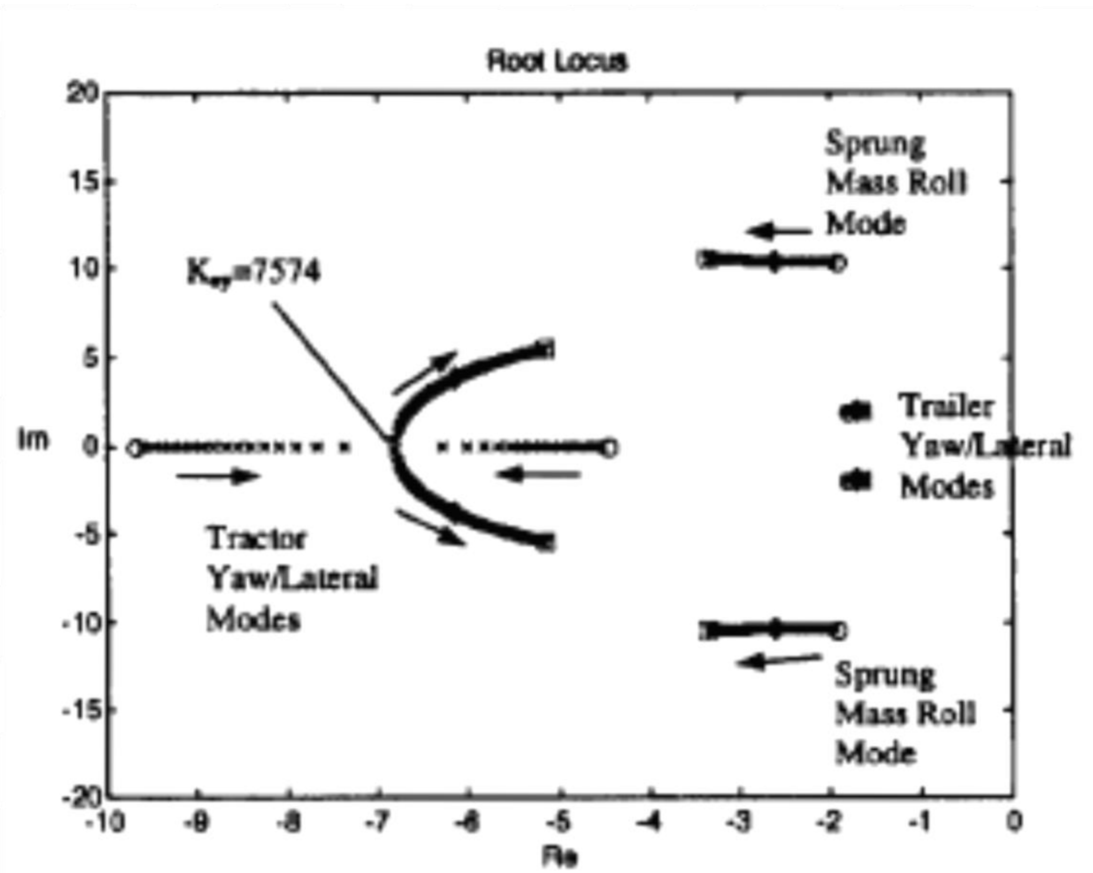

Figure 4-20: Tractor and Single Trailer Eigenvalues (Eisele & Peng, 2000)

4.5.2. Payload Dependency

In addition to speed sensitivity, the vehicle's behavior was also sensitive to the payload mass. As seen in Figure 4-21, the trailer's stability reduces with increased mass (in both yaw and roll). Additionally, the dolly yaw stability decreased with mass. In this case, roll stability of the dolly and tractor did not decrease due to the fact that both the pintle hitch and fifth wheel were decoupled in roll (see Section 3.2.1).

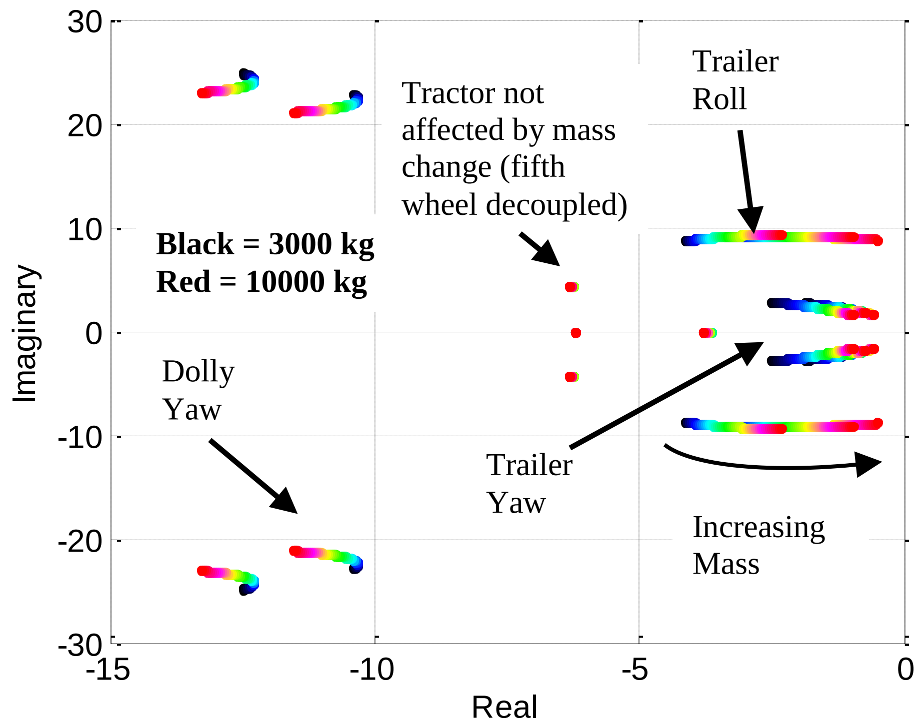

Figure 4-21: Triple Eigenvalue vs. Payload Mass

4.5.3. Time Constant

In addition to determining stability, the eigenvalue analysis was useful in defining how "fast" the system was. As the eigenvalues move further right, the system dynamics become slower to decay (Equation 4-20). The system eigenvalues were mostly affected by speed and load (Table 4-2) but other factors such as tire cornering stiffness, roll moment, etc. also contribute.

$$\tau = \frac{-1}{Real(\lambda)} \tag{4-20}$$

Table 4-2: LTI Eigenvalue Table

Speed (m/s)	Loaded	Slowest Eigenvalue	Time Constant (s)
10	N	2.5±0i	0.4
20	N	1.8±3.0i	0.6
30	N	1.0±3.4i	1.0
10	Y	1.2 ± 3.3i	0.83
20	Y	0.9±2.0i	1.1
30	Y	0.7±1.8i	1.4

Understanding the order of magnitude for the system time constant and how the time constant changed with load and speed was useful in the design of the model predictive controller in Section 6.

4.5.4. Eigenvalue Summary

Based on the stability analysis above, the linearized model appeared to be a suitable representation of the real vehicle. Thus it was deemed that the stability controllers could be developed around this linear model and then applied to the real vehicle. As will be shown in Section 6, the linear model need only predict the potential for instability which is a less demanding task than predicting the actual rollover or yaw instability point.

4.6. Model Reduction

While the above linear model of the vehicle was deemed accurate and could be used for control development purposes, there existed significant issues with the identification of the dolly states. In a real world usage condition, there would be no data on the state of the dollies as it is impractical / costly to equip the dollies with sensors. Further, it is difficult to estimate the dynamics of the dollies as they are much lighter and have smaller inertias than the trailers and therefore have little effect on the trailer dynamics. For these reasons, efforts were taken to remove the dollies from the dynamic system.

4.6.1. State Removal

Given that the dollies are not the stability risk for the system (Section 4.5), it was decided to drop them from the LTI system through the use of a steady state gain approach where the steady state values of the removed states are substituted into the dynamics of the reduced order system. This is a rather well established process (Garcia & Acha, 2008; Samar, Postlethwaite, & Gu, 1995; Varga, 1991) and works well when the states to be dropped are faster (reach steady state sooner) than the states to be kept.

4.6.2. Reduced Eigenvalue Analysis

Based on the reduction policy in Section 4.6.1, the LTI system order was reduced from 24 states to 16 states by dropping the dolly side slip (β), vehicle unit yaw rate$(\dot{\psi})$, vehicle unit roll rate $(\dot{\phi})$, and vehicle unit roll (ϕ) for both dollies. As the symbolic formulation of the LTI system was in an $A = M^{-1}*K$ form (Equation 4-8), the state reduction was executed once the system was in numerical form. This required the state reduction routine be executed at every time step, but it is quite fast and did not pose any significant issues.

As can be seen in Figure 4-22, the state reduction process kept all of the important (slower) eigenvalues. The trailer dynamics (the units with the largest stability risk) were almost completely unaffected. The states that were affected by the reduction belonged to the tractor and dollies which had already been identified as being stable. The effect of the state reduction on the dynamic behavior of the vehicle (Figure 4-23) was minimal (Figure 4-24). In this case the maneuver was a free response (zero steering input) with relatively large initial conditions. Again, Unit number definitions are presented in Table 4-1.

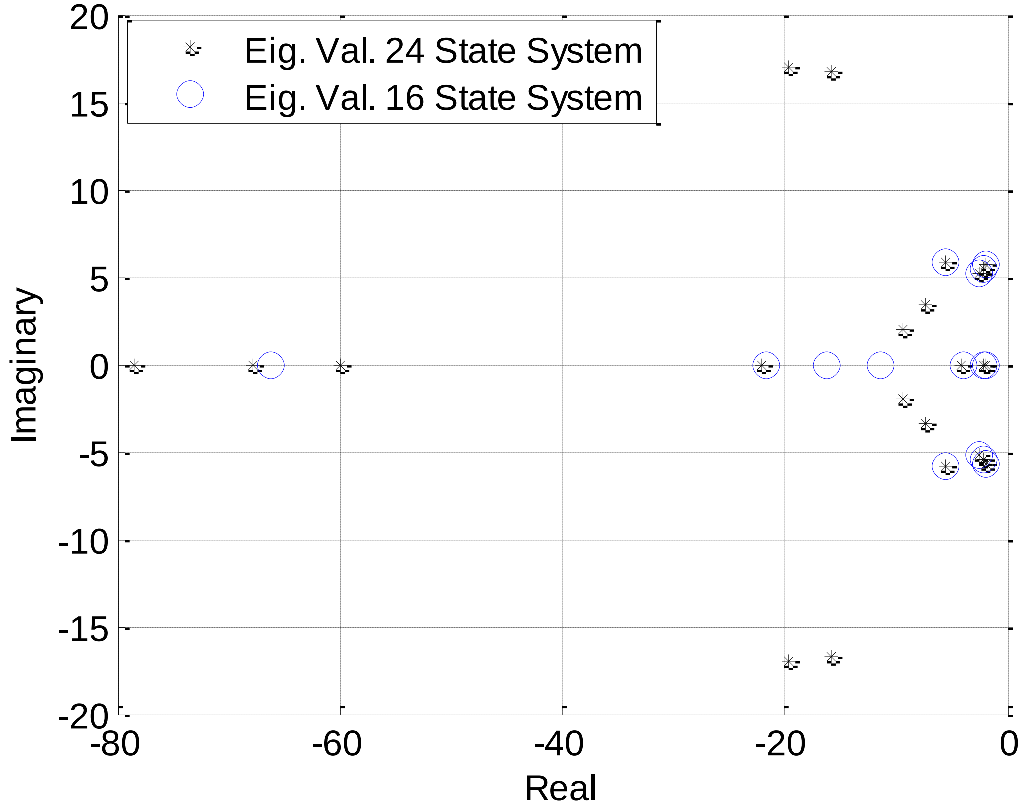

Figure 4-22: Pre and Post State Reduction Eigenvalues

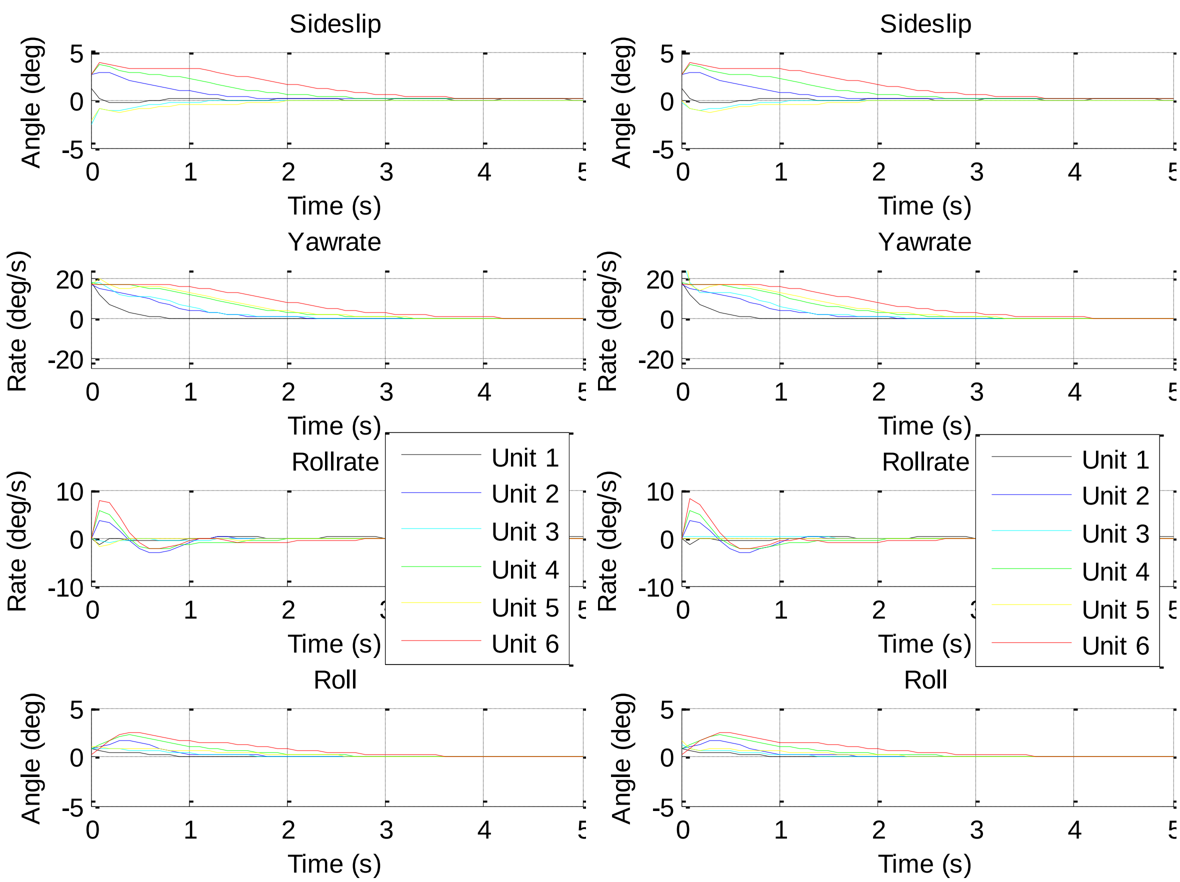

Figure 4-23: Full State (Left) and Reduced State (Right) Free Response at 40 kph

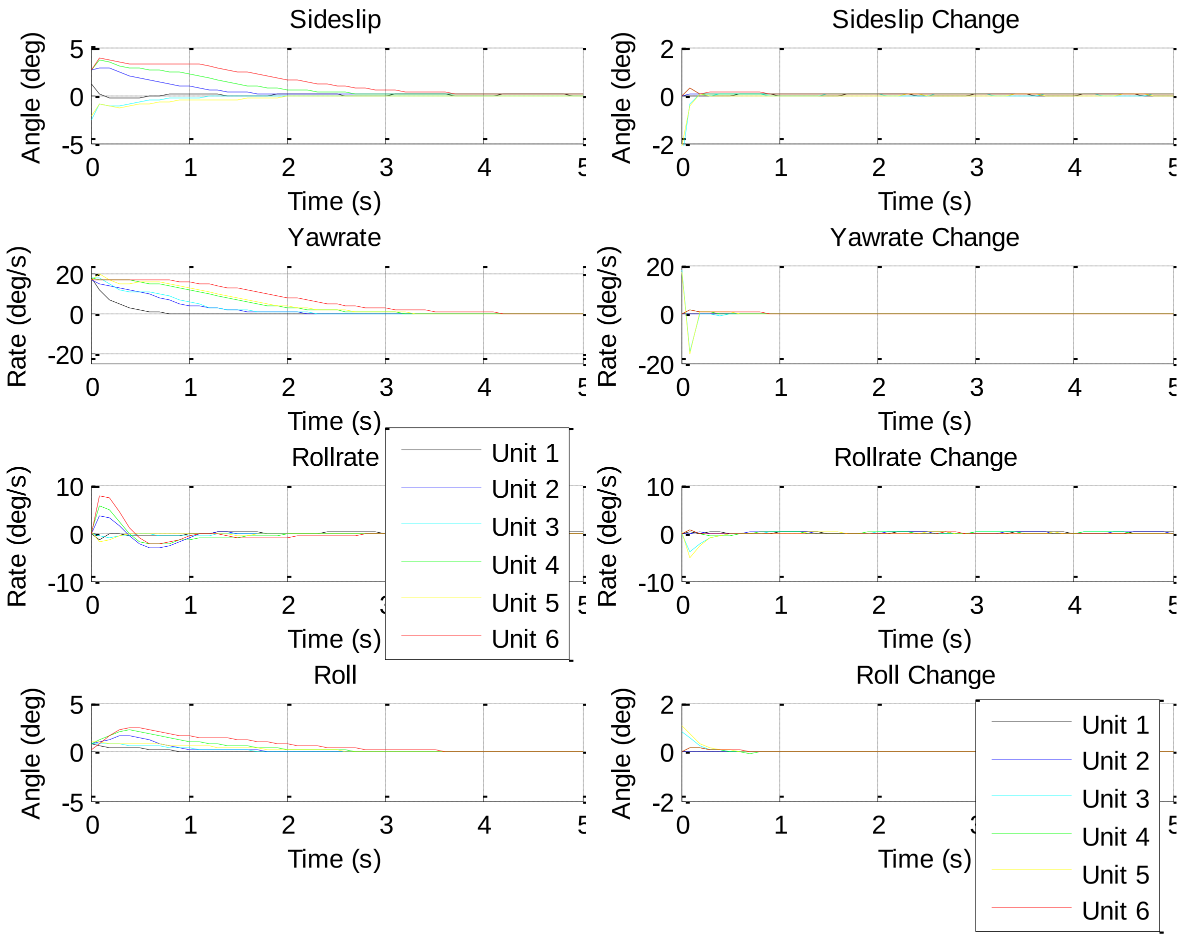

Figure 4-24: State Response (Left) and State Reduction Error (Right) Free Response at 40 kph

CHAPTER FIVE

OBSERVERS AND FILTERS

In order to evaluate the stability of the vehicle, one generally needs to know the current state of the vehicle and have some information on the vehicle system. The former requires information on the side slips, yaw rates, roll rates, and roll angles need for each vehicle unit. The latter requires information on the vehicles mass, CG location, etc. This section describes how this data is obtained.

5.1. State Estimation

As discussed in Section A.6.2 and shown in Figure A-82, there are two common sources of state measurements: Inertial units and GPS. As these cannot provide all the information needed to know the vehicle's states, they are usually combined with a physical model of the vehicle to estimate the remaining states. As one of the objectives of this work was to break the dependency between parameter estimation and state estimation (Section A.6.1), the approach used in this work derives all state estimates from direct measurement or through combining direct measurements using Kalman filtering approaches and kinematic models. Thus at no time is a state estimation derived using a physical model of the vehicle system[1].

[1] With the one exception of tire cornering stiffness which is in reality a ratio of slip angle and estimated forces. As the ratio is the desired objective, this is an acceptable option. This is addressed in Section 5.2.3.

5.1.1. Inertial Units, GPS, and Kalman Filters

The data used to evaluate the states of the vehicle come from sets of inertial measurement units (one unit per tractor or trailer) and dual antenna GPS units (one unit per tractor or trailer). These are combined using kinematic models and Kalman filtering techniques (Section A.6.4). Direct sensing of side slip and roll is not practical as the sensors are prohibitively expensive and do not perform well in all environmental situations (Deng & Zhang, 2006). For brevity, the full state development is listed in Appendix H and a brief overview is given here.

The inertial measurement units cost around $50 each and the GPS systems cost around $300 each (Bevly, 2004). However, all major fleets already have GPS on every vehicle unit for inventory tracking so the true GPS cost is just the upgrade cost to a two antenna system or about $75 each. The Kalman filtering process used in this work is a combination of techniques proposed by Ryu (Ryu & Gerdes, 2004) and Bevly (Bevly, 2004) with the data on sensor noise / bias / etc. from Ryu and Bevly as well (Bevly, 2004; Bevly et al., 2006; Ryu & Gerdes, 2004). To make sure that the important dynamics of the system are captured, the GPS needs to operate at 5 Hz. or greater (Bevly et al., 2006).

5.1.2. Collecting the States

In the modeling here, yaw rate and roll rate are directly measured while the side slip and roll are derived through the use of Kalman filters based on kinematic model calculations. As Kalman filters are a fairly well understood tool in vehicle modeling (Bennett & Norman, 2006; Bevly, 2004; Kalman, 1960; Venhovens & Naab, 1999;

Wenzel et al., 2006; Wenzel, Burnham, Blundell, & Williams, 2007), the description of how the filter works has been documented in Appendix H.1. The important thing to understand here is that the vehicle states are derived by integrating the inertial measurement unit (IMU) and using the two antenna global position system (GPS) to correct drift, bias, etc.

5.1.3. Effective Gaussian Noise

While the determination of the vehicle states was the primary objective of this effort, the approach did permit the estimation of some other useful parameters such as yaw, heading, and velocity. In fact, the approach used here for determining side slip is based on the ratio of lateral and longitudinal velocity (Equation 5-1) rather than the traditional GPS based side slip method where side slip is the difference between the vehicle velocity heading (Ψ) and yaw or heading angle (ψ) (Equation 5-2). Velocity heading is the angle (relative to true north) of the vehicle velocity vector. Heading angle is the angle (relative to true north) of the vehicle axis.

$$\beta = \tan^{-1}\left(\frac{V_y}{U}\right) \approx \frac{V_y}{U} \quad \textbf{5-1}$$

$$\beta = \Psi - \psi \quad \textbf{5-2}$$

The effective Gaussian sensor noise levels for each measurement after filtering are presented in Table 5-1. Details on the calculations are provided in Appendix H.3.

Table 5-1: Effective State Gaussian Levels

Measurement	Gaussian Noise (SI)	Gaussian Noise (Common)
Side slip	0.0005 rad	0.028 deg
Yaw rate	0.005 rad/s	0.28 deg/s
Rollrate	0.005 rad/s	0.28 deg/s
Roll	0.0005 rad	0.028 deg
Yaw	0.002 rad	0.11 deg
Ay	0.006 m/s^2	0.0006 g
Vx	0.005 m/s	0.018 km/h
Vy	0.005 m/s	0.018 km/h
Pitch	0.010 rad	0.57 deg
Grade	0.002 rad	0.11 deg

Finally, Figure 5-1 shows the relationship between GPS sampling frequency and effective Gaussian noise. Note that for sampling rates over 5 Hz., there is little benefit from the increased sampling rate while the system cost rises quickly. The flat lines past 40 Hz. are due to the fact that most commercial IMU systems operate around 40 Hz. making a faster GPS system irrelevant.

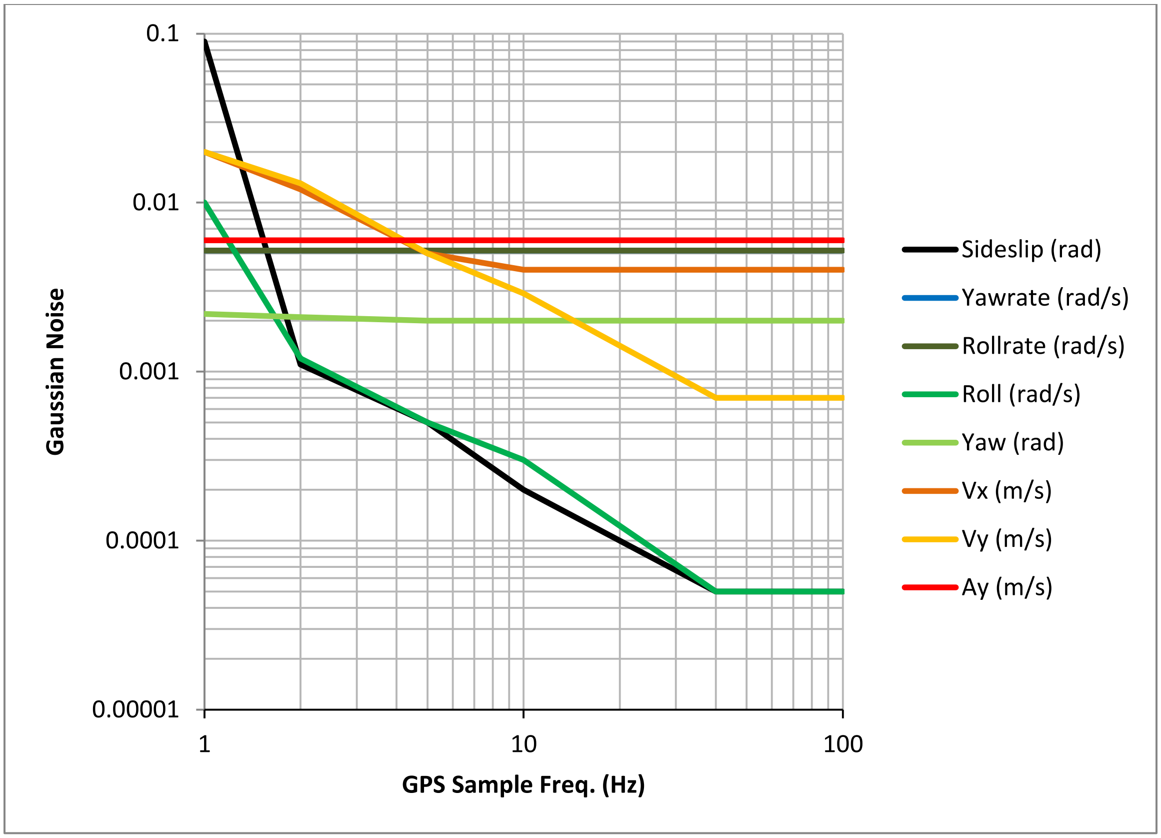

Figure 5-1: Gaussian Noise vs. GPS Update Rate

5.2. Parameter Estimation

Traditionally, solving for the vehicle parameters (mass, CG location, Inertia, etc.) has been difficult as the parameters are estimated from the measured states and the states are derived using the vehicle parameters (see Section 2.3). The work here breaks that compromise by directly measuring key parameters, estimating some from secondary measurements, and modifying the control strategy so that parameter errors are not so significant.

5.2.1. Measuring Sprung Mass Using Air Bags

Among the vehicle parameters, mass is one of the most significant and often difficult to measure for a commercial vehicle (Huh et al., 2007; Limroth, 2009; Nantais, 2006). Generally, mass has been estimated through comparing measured lateral acceleration with projected lateral force (estimated tire reaction forces). Errors in either tire property estimation or measurement of lateral acceleration can cause errors in the mass assessment.

The approach used here is quite different. All (or nearly all) modern commercial vehicles use air suspensions for all but the steer axle. Further, the steer axle load changes very little between a bob-tail (no trailer) and fully loaded configuration. Typical front axle load ranges are between 10,500 lb. and 11,500 lb. with 12,000 lb. being the maximum legal limit. For the remaining suspension, all one needs to know is the air bag surface area (standard sizing) and the internal air pressure to gage the vehicle mass. This approach also has the benefit of accurately determining the longitudinal CG locations as well.

The second useful property of this approach is that pressure sensors are very cheap (approximately $25) (Newmatics Inc., 2013) making it economically feasible to implement. The drawback is that the sensors are noisy and the air pressure varies with vertical motion of the sprung mass resulting in significant noise in the signal (Figure 5-2). However, the mass does not change with time so simple filters can be used such as the 3rd order 0.1 Hz. low pass Butterworth filter in Figure 5-3.

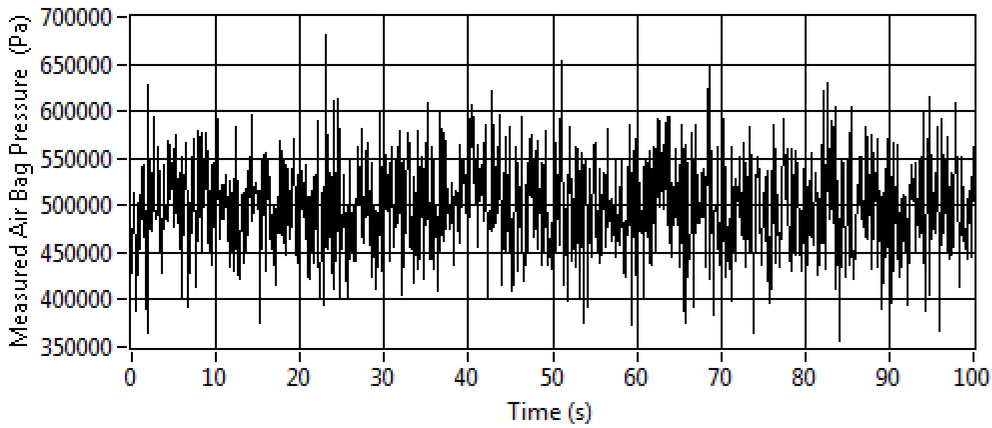

Figure 5-2: Typical Measured Air Pressure

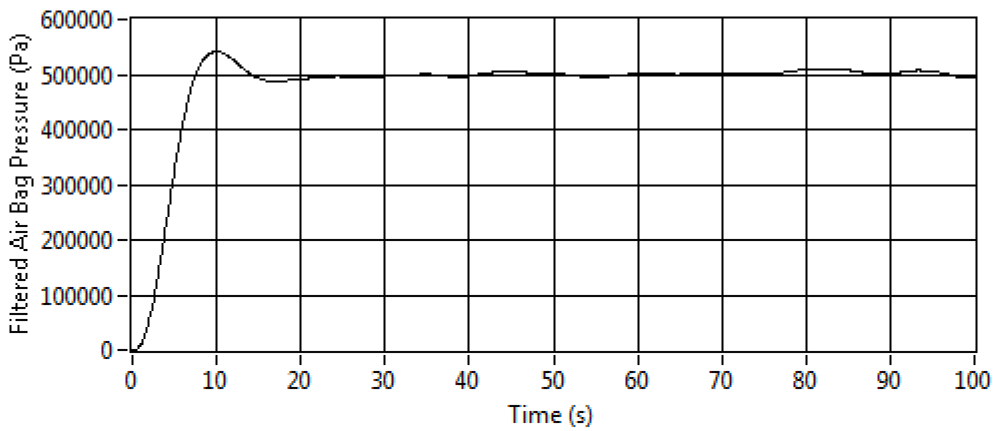

Figure 5-3: Filtered Air Pressure Data (0.1 Hz. Low Pass, 3rd Order)

5.2.2. Estimating Inertia, CG height

With a known mass and longitudinal CG location, the inertia can be estimated assuming a distribution of mass. This is not unrealistic as most shippers take care to equalize the load to improve transient dynamic behavior of the vehicles. In a similar manner, the CG height can be estimated assuming a uniform volume (DOT 13.5' maximum height limit) and DOT maximum loading. This approach biases the CG estimation higher than it might be in reality but a higher estimate causes the controller to intervene sooner with the result that any error in CG height estimation acts as a safety margin. Note: As will be shown in Section 6.2.1, the error in assuming that the braking forces do not affect the lateral cornering potential of the tires is much greater than the errors introduced by estimating the inertia and CG height making this approach quite reasonable.

5.2.3. Tire Cornering Stiffness

The only vehicle parameter not directly measured is tire cornering stiffness. Cornering stiffness (on a per-axle basis) is estimated by re-arranging the equations of motion (Equations 3-17 through 3-25) to solve for C_α given the measured lateral acceleration, measured mass, and estimated slip angles. Now the reader may note that it is not possible to directly measure the dolly slip angles like the steer axle is measured (via. CAN BUS - angular sensors on the steering column). However, through GPS it is possible to know the position, orientation, and heading of each trailer. From that the dolly angle can be determined and with it the slip angles. This can be accomplished two different ways. The first is to invert the entire linear time invariant vehicle model (Section 2.3.2) with the inputs being the states and the outputs being the cornering stiffness values (these are in the stiffness matrix – Section G.2). This approach requires the driver steering input, measured side slips, and articulation angles. The slip angles are defined in Equations D-2, D-3, and D-5. Alternately, once could simplify the vehicle to a series of individual units and use Equations D-2 and D-3 with simpler single unit EOM models (Equations D-6 and D-7). This approach, of course, results in lower accuracy in the cornering stiffness estimation, but it is usually good enough.

Now it is true that there is noise in the GPS data, accelerometer data, and mass estimate but the cornering stiffness does not change over time (at least it takes many days to evolve). Thus filtering techniques such as Kalman or recursive least squares can be used. The recursive least squares method seems to be the more efficient.

5.2.4. LTI Model Sensitivity to Parameter Estimation

To explain why the above estimations of CG height (Section 5.2.2) and inertia were not considered to be significant modeling issues, consider the following three eigenvalue studies. The first (Figure 5-4) is the effect of a ± 1 meter error in estimating the CG height of the trailers. Since a one meter error is quite large and well beyond anticipated errors in estimating CG height, this represents the absolute bounds of the CG height sensitivity. Note that as CG goes up, the trailer is less stable as expected.

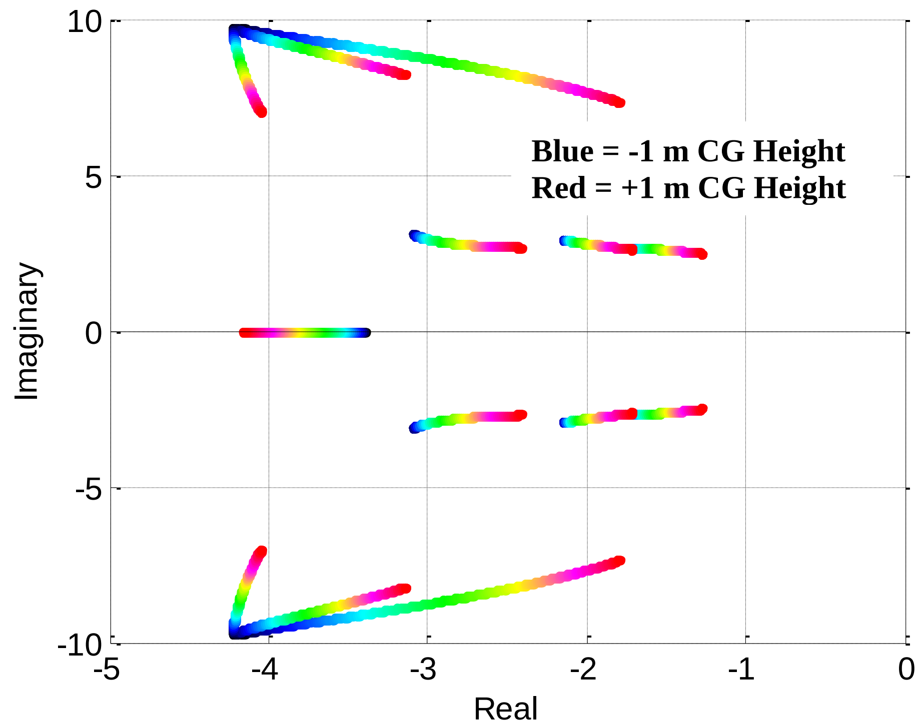

Figure 5-4: Trailer Eigenvalues vs. CG Height

Next, consider the effect of errors in measuring inertia (Figure 5-5). An inertia measurement error range from 50% to 200% is much larger than what would be expected to occur when the estimations are based on a relatively uniform loading but the actual loading differed. Remember, the longitudinal CG position is accurately captured.

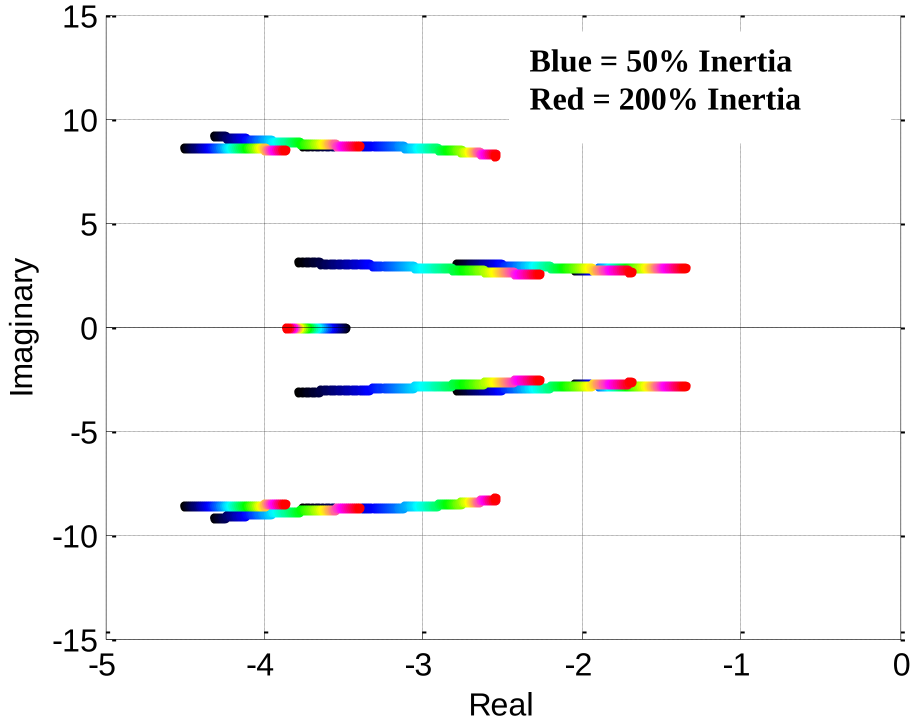

Figure 5-5: Trailer Eigenvalues vs. Trailer Inertia

Finally, consider Figure 5-6 which illustrates the effect of a ±50% error in estimating tire cornering stiffness. Now, as the MPC solver does not update the cornering stiffness over the horizon as the brakes are applied (see Section 6.2.1), a 50% error in estimating C_α is quite possible. In fact, the error might be even larger. The eigenvalues are more sensitive to a 50% change in C_α than for a 2 meter change in CG height or a 200% change in inertia. If the controller can manage with the errors in C_α, then it can manage the potential errors in CG and inertia.

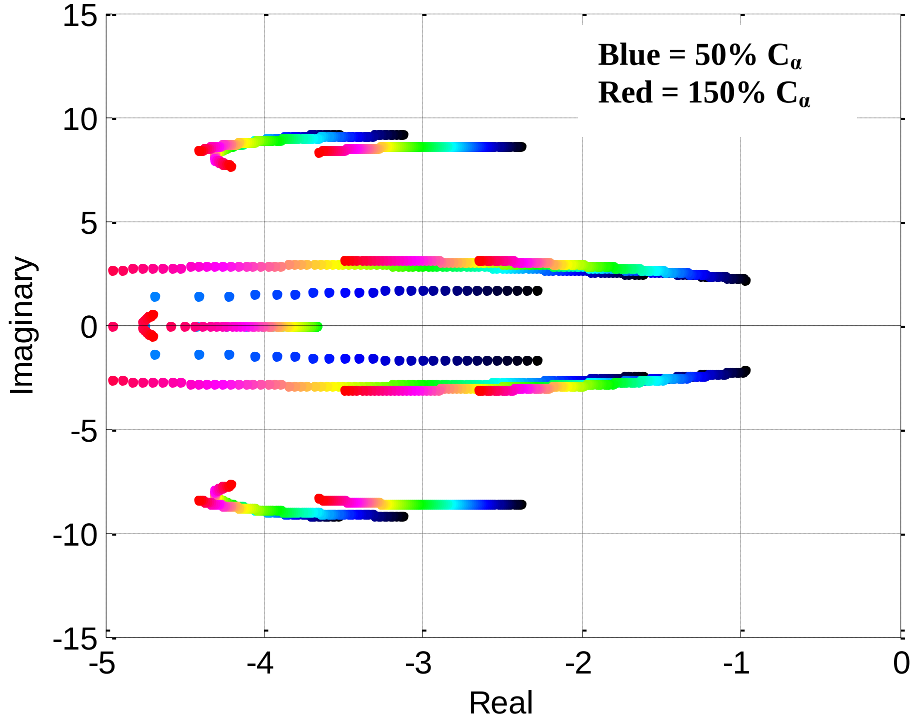

Figure 5-6: Trailer Eigenvalues vs. Cornering Stiffness

CHAPTER SIX

MODEL PREDICTIVE CONTROL

Traditional controller strategies focus on adjusting inputs to maintain desired outputs based on the system's current dynamic state using a reference model for error assessment. Model predictive control (MPC) focuses on predicting needed control actions in the future before output target errors grow. This predictive, or anticipatory, capability produces smoother and often less aggressive control inputs as the controller can see how control actions affect the system over time and act prior to the actual need.

Model predictive control (a.k.a. receding horizon control) is a relatively new controller strategy in vehicle controls. When MPC has been implemented for vehicle stability control, it has been used in conjunction with a reference vehicle model which defines the desired dynamic behavior of the vehicle (Anwar, 2005; Falcone et al., 2008; Lee & Yoo, 2009; H. Zhou & Liu, 2009). In this form, MPC offers the advantage of estimating future stability needs but still requires an accurate reference model of the vehicle system.

The work here introduces a new approach for implementing MPC for vehicle stability control. The method proposed here does not use a reference and thus does not demand the same level of accuracy on parameter estimation. Also, the proposed method can be evaluated with a much larger time step without losing fidelity which results in a more efficient solver (in terms of computational demand).

6.1. General Model Predictive Control Theory

Model predictive control is a control strategy where the controller attempts to manage the system's current operational point as well as predicting the future operational states of the system. It is mostly used in large complex systems such as power plants, chemical plants, refineries, etc. In many cases these plants have more outputs than controls and the systems are not decoupled (outputs are not independent of each other). The future state of the plant is predicted using a discrete linear time invariant (LTI) model of the system (Equations 6-1and 6-2) where u(k) is the optimized control input at each time step in the prediction.

$$x(k+1) = A * x(k) + B * u(k) \tag{6-1}$$

$$\mathrm{y(k)} = \mathrm{C} * \mathrm{x(k)} \tag{6-2}$$

Side note: A multiple unit commercial vehicle is not unlike the plants where MPC is traditionally used. It has more states than inputs and the states are coupled.

At each point in time, the controller simulates the behavior of the system over a series of time steps into the future minimizing the combined output cost and input cost (more on this in Section 6.1.2). The control demand at the initial time (u(0)) is extracted and applied to the real system. The process then repeats with the next time step of the physical system. It is important to note that the system time step (sampling rate of the plant) and the simulation time step (step size into the future for simulation purposes) do not have to be the same size. The ability to decouple the sampling and prediction sampling rates contributes significantly to the speed and robustness of this method.

6.1.1. Observable and Controllable

The MPC strategy requires the existence of a linear time invariant model of the plant for prediction of the future dynamics (see Sections 3 and 4). The LTI model can be updated at each simulation time step to more accurately reflect the current plant but it is fixed within the MPC prediction algorithm; i.e. the plant dynamics are fixed over the prediction horizon. While MPC can work with LTI systems with positive real eigenvalues (unstable systems), they are more difficult to solve. Also, unstable plants may not have feasible (obtainable) solutions such that no permissible control input can stabilize the system.

As the controller needs to "see" the system and "control" the system, the LTI model should be evaluated at every time step (measurement step) to insure that it is both controllable and observable. The details on how to determine if a system is controllable and observable can be found in Appendix I or in standard controls text books (Franklin & Powell, 1994; Ogata, 2002). Additionally, for this work, it was necessary to test if the system was stable (eigenvalues with negative real parts) as the control inputs were bounded. All three tests (observable, controllable, stable) were performed on the LTI model at each time step in the simulation.

6.1.2. Traditional Formulation

MPC consists of a discrete system model (Equation 6-3), an output (Equation 6-4), a cost function (Equation 6-5), and an inequality statement (Equation 6-6). The inequality can be omitted if there are no bounds on the outputs of the system. Note: the quadratic costs for the outputs (P, Q) and inputs (R) are user defined weights. P and Q must be positive semi-definite or positive definite, R must be positive definite.

$$x(k+1) = A * x(k) + B_u * u(k) \tag{6-3}$$

$$y(k) = C * x(k) + D * u(k) \tag{6-4}$$

$$J = y(N)' * P * y(N) + \sum_{k=0}^{N-1} y(k)' * Q * y(k) + u(k)' * R * u(k) \tag{6-5}$$

$$F * x(k) \leq b \tag{6-6}$$

As traditional MPC controllers use reference models to determine stability, the output cost in Equation 6-5 is generally re-written as the error in output (Equation 6-7).

$$\begin{aligned} J = {} & (y(N) - \hat{y}(N))' * P * (y(N) - \hat{y}(N)) \\ & + \sum_{k=0}^{N-1} (y(k) - \hat{y}(k))' * Q * (y(k) - \hat{y}(k)) + u(k)' * R * u(k) \end{aligned} \tag{6-7}$$

The process for building the MPC quadratic cost function is based on the observation that the future states are derived from the current states (Equation 6-8); i.e. the future dynamics are modeled by stacking the state model. X (Equation 6-9) is the state variables over the time interval and Φ is the staked state matrix (Equation 6-10). Γ is the input matrix for the full horizon (Equation 6-11). Ω and Ψ are the output and input cost matrices over the full horizon (Equation 6-12). These, in turn, are used to generate the interval quadratic cost (Equation 6-13) and linear input (Equation 6-14) for the cost function (Equation 6-21). The interval output constraint (Equation 6-15) and input constraint (Equation 6-16) are similarly combined (Equation 6-17). Finally, the interval inequality function is developed (Equations 6-18 through 6-20). The cost function for the system (Equation 6-21) is then a standard quadratic cost function that can be solved using quadratic solvers such as quadprog (MATLAB) subject to the inequality constraint (Equation 6-20).

$$x(1) = Ax(0) + Bu(0)$$

$$x(2) = Ax(1) + Bu(1) = A^2x(0) + ABu(0) + Bu(1) \tag{6-8}$$

$$x(N) = A^N x(0) + A^{N-1} * Bu(0) + \cdots + ABu(N-2) + Bu(N-1)$$

$$X = \Phi * x(0) + \Gamma * U \tag{6-9}$$

$$X = \begin{bmatrix} x(1) \\ \dots \\ x(N) \end{bmatrix}, \quad \Phi = \begin{bmatrix} A^1 \\ \dots \\ A^N \end{bmatrix} \tag{6-10}$$

$$\Gamma = \begin{bmatrix} B & 0 & \dots & 0 \\ AB & B & \dots & 0 \\ \dots & \dots & \dots & 0 \\ A^{N-1}B & A^{N-2}B & \dots & B \end{bmatrix}, \quad U = \begin{bmatrix} u(0) \\ \dots \\ u(N-1) \end{bmatrix} \tag{6-11}$$

$$\Omega = \begin{bmatrix} Q & 0 & \dots & 0 \\ 0 & Q & \dots & 0 \\ \dots & \dots & \dots & 0 \\ 0 & 0 & \dots & P \end{bmatrix}, \quad \Psi = \begin{bmatrix} R & 0 & \dots & 0 \\ 0 & R & \dots & 0 \\ \dots & \dots & \dots & 0 \\ 0 & 0 & \dots & R \end{bmatrix} \tag{6-12}$$

$$G = 2 * (\Psi + \Gamma' * \Omega * \Gamma) \tag{6-13}$$

$$F = 2 * \Gamma' * \Omega * \Phi \tag{6-14}$$

$$M_i = \begin{bmatrix} 0 \\ 0 \\ -C \\ C \end{bmatrix} \tag{6-15}$$

$$E_i = \begin{bmatrix} -I \\ I \\ 0 \\ 0 \end{bmatrix} \tag{6-16}$$

$$D = \begin{bmatrix} M_o \\ 0 \\ \dots \\ 0 \end{bmatrix}, \quad \mathrm{M} = \begin{bmatrix} 0 & 0 & \dots & 0 \\ 0 & M_1 & \dots & 0 \\ \dots & \dots & \dots & 0 \\ 0 & 0 & \dots & M_N \end{bmatrix}, \qquad \Sigma = \begin{bmatrix} E_0 & 0 & \dots & 0 \\ 0 & E_1 & \dots & 0 \\ \dots & \dots & \dots & 0 \\ 0 & 0 & \dots & E_{N-1} \end{bmatrix} \tag{6-17}$$

$$S = M * \Gamma + \Sigma \tag{6-18}$$

$$W = -(M * \Phi + D) \tag{6-19}$$

$$S * U \leq C + W * x(0) \tag{6-20}$$

$$J = \frac{1}{2} * U' * G * U + U' * F * x(0) \tag{6-21}$$

As quadratic costs are convex (assuming that the system is positive definite or positive semi-definite) there will exist a unique minimum. The resulting optimal cost has a linear structure (Equation 6-22).

$$U^{*} = -G^{-1} * F * x(0) \tag{6-22}$$

Every time the linear model is updated, the MPC model (Equations 6-9 through 6-21) have to be updated. But as this is simple linear algebra, it is quite fast. At each time step in the simulation, the quadratic solver is used to define the optimal control strategy over the projected horizon.

If the MPC controller is bounded, meaning either the outputs or inputs have limits to their permissible values, the bounds are incorporated in the quadratic solver as inequalities (Equation 6-6). The risk with using bounds is that there may not be a feasible (achievable) solution and the control demands necessary to maintain the output set points cannot be met given the limits on input ranges. This issue will be addressed in Section 6.1.4. For details on inequality bounds, see (Coleman & Li, 1996; Gould & Toint, 2004).

6.1.3. Inclusion of Feed Forward

In the research here there was an additional issue that needed addressing: the driver controlled the dominate input into the system. This meant that the state space model contained a feed forward component (Equation 6-23). As the MPC controller could not affect this input, it was not part of the controller cost function. To understand how the MPC controller worked with feed forward, consider the case of a stable (negative real eigenvalue) system with three outputs and three inputs (one being the feed forward input). This system is not meant to represent the vehicle or any other physical system. Its only use here is to simplify the explanation of how the controller works as the actual vehicle had 16 states and 8 inputs making it difficult to illustrate behaviors.

Reviewing the example system's open loop response with non-zero feed forward indicates that the system stabilizes in about 10 seconds (Figure 6-1). Note: As the linear model is not meant to represent any physical system, there are no units on the inputs and outputs. It is simply an illustrative tool. Also, the feed forward is listed in the input plot to make it clearer that there is an uncontrolled input into the system.

$$x(k+1) = A * x(k) + B_u * u(k) + B_\delta * \delta \tag{6-23}$$

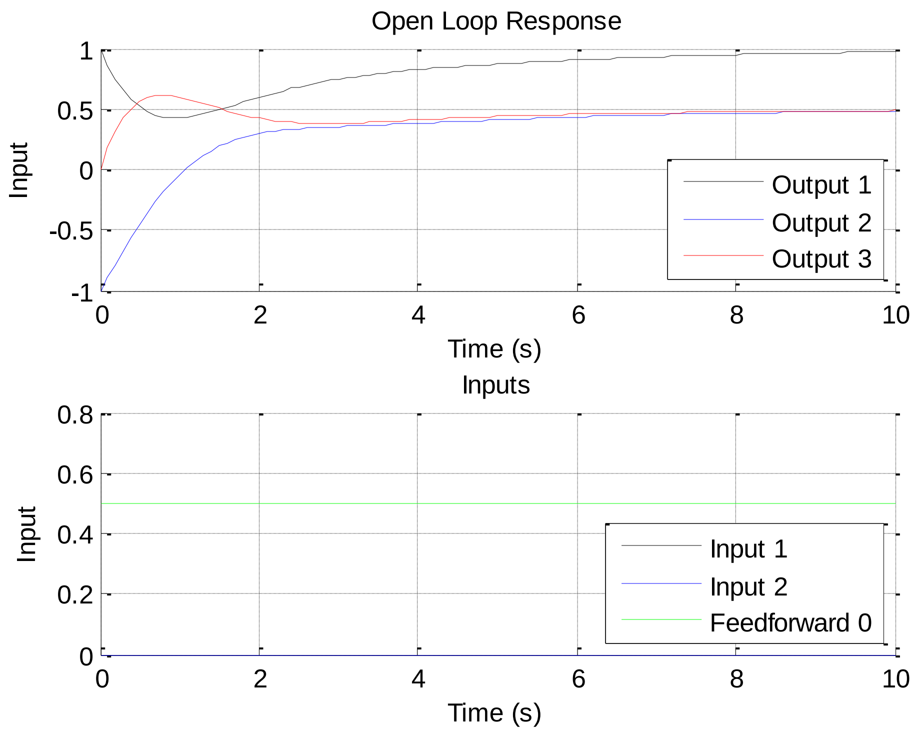

Figure 6-1: Open Loop Model with Feed Forward

A model predictive controller was then applied to the system with the three states as the outputs and the two available inputs as controls. In this illustration, the MPC solver was run with a step size of 0.1 seconds and a horizon of 11 steps. The total number of steps evaluated was 100 (10 seconds / 0.1 seconds per step). This meant that the MPC optimized the system 100 times with each optimization previewing 11 steps or 1.1 seconds into the future.

Note how the modified MPC algorithm kept the fixed feed forward (red input #3) in Figure 6-2 but used the free inputs (#1 and #2) to lower the outputs (the reference output was zero for all states). The MPC controller minimized the combined cost of the states deviating from zero and the inputs deviating from zero. Note: The particular outputs and inputs of the MPC controller were dependent on the weights (matrices P, Q, and R in Equation 6-7). Here, P, Q, and R were all identity. The objective was to show the model and controller behaviors.

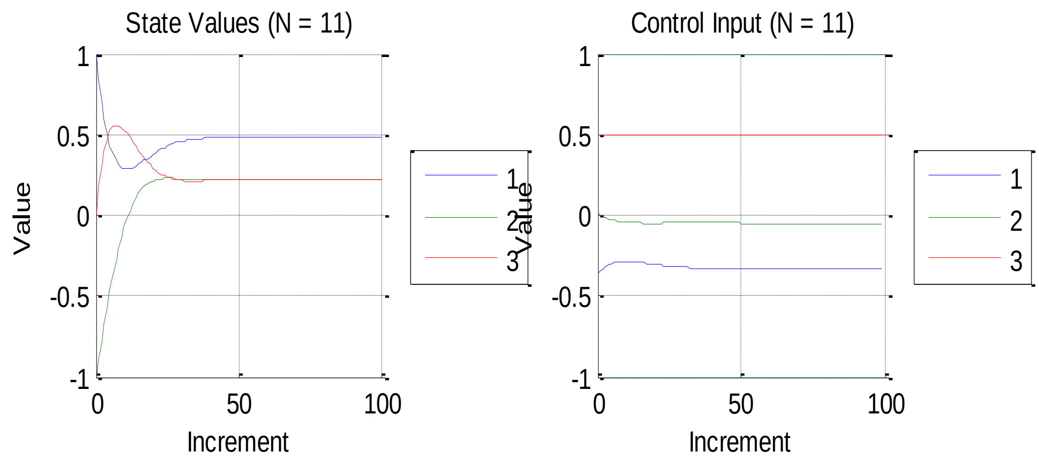

Figure 6-2: MPC Model with Feed Forward Term

6.1.4. New MPC Cost Formulation / Controller Theory

The stability control research presented here differs from prior work in that the proposed MPC cost function does not contain any information on outputs (Equation 6-24). Typically, a cost function like this would result in no control being applied (minimum control cost) and indeed, for most cases, there is no control demand. However, the output bounds still exist and the controller must activate to keep the system in bounds. Thus the controller is dormant until a stability risk (bound violation) is detected at which point it implements the minimum control action necessary to bring the vehicle back within bounds.

$$J = \sum_{k=0}^{N-1} u(k)' * R * u(k) \qquad \textbf{6-24}$$

If the bound restrictions on the outputs and inputs are such that a feasible solution is not achievable, the algorithm switches to a traditional cost formulation (Equation 6-7) with high output cost and low input cost (Q >> R). This drives the system toward a safe operational point as quickly as possible. The resulting "best achievable" outputs are then used as the updated bounds for the bound only MPC routine (Equation 6-24) and the model is re-evaluated. In this way the vehicle is returned to a safe operational point as quickly as physically possible.

To see how the bound only MPC works in practice, consider the same system used in Figure 6-1 but with initial conditions that violate the ±1 bounds on all outputs (Figure 6-3). Here the open loop stable system eventually decays such that all output are within ±1 but it takes some time for output 1 to drop below 1. Now contrast the free response system behavior (Figure 6-3) with the MPC controlled response in Figure 6-4. Note that the MPC has the maximum control input of -1 for the two inputs it manages at time = 0. This is because the system is violating a constraint and needs to be driven back into a safe region. As soon as all states are within the safe region (about 1 second), the controller turns off. The MPC only activates when an output is in violation of a bound – be that an initial condition violation or a projected future violation.

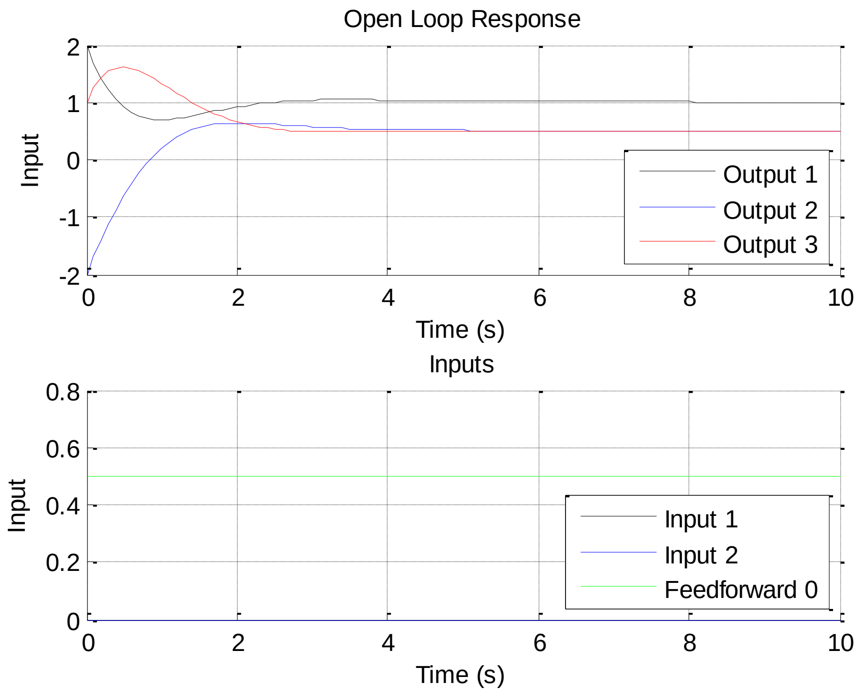

Figure 6-3: Large Initial Condition Free Response

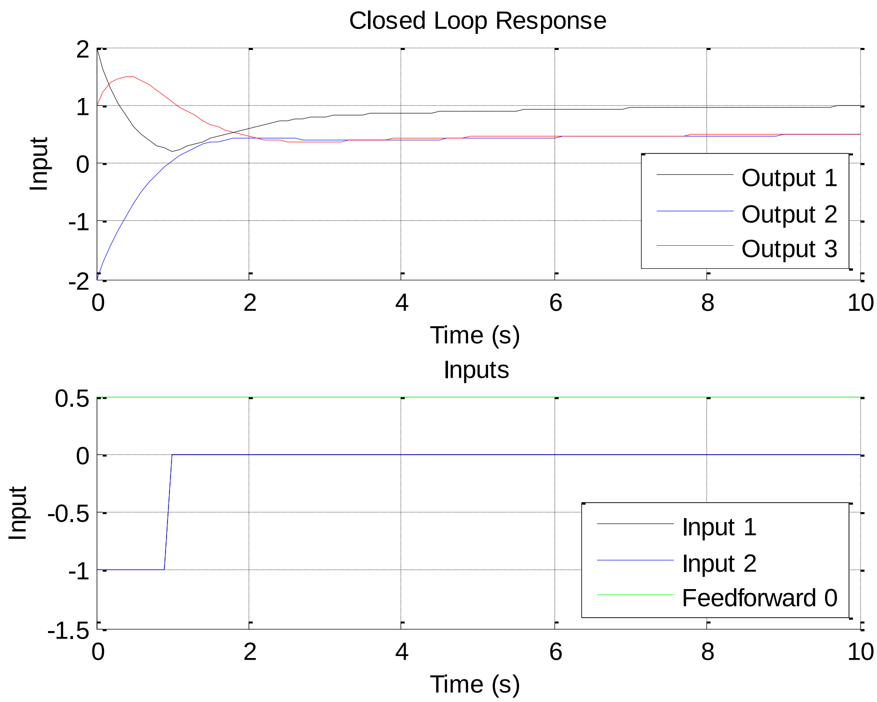

Figure 6-4: Large Initial Condition Bounded MPC Controller

While the above plots are useful for showing how the MPC corrects for bound errors, the controller's purpose is to prevent that type of issue (large initial conditions) from occurring. The strategy of the controller is to prevent the system from going out of bounds if a large feed forward is applied such as seen in Figure 6-5. Note that the MPC (Figure 6-6) initially has no response but as the system is driven out of bounds the MPC acts <u>before</u> the system ever reaches the bound limits. This is due to the predictive capabilities of MPC and is a part of what makes the controller so powerful and flexible.

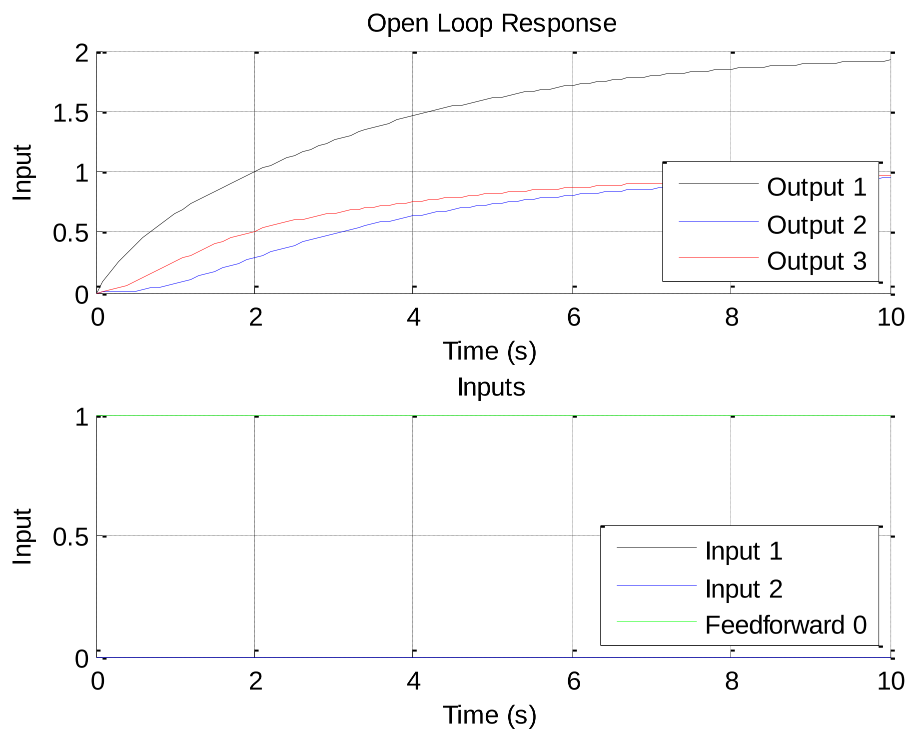

Figure 6-5: Large Feed Forward Open Loop

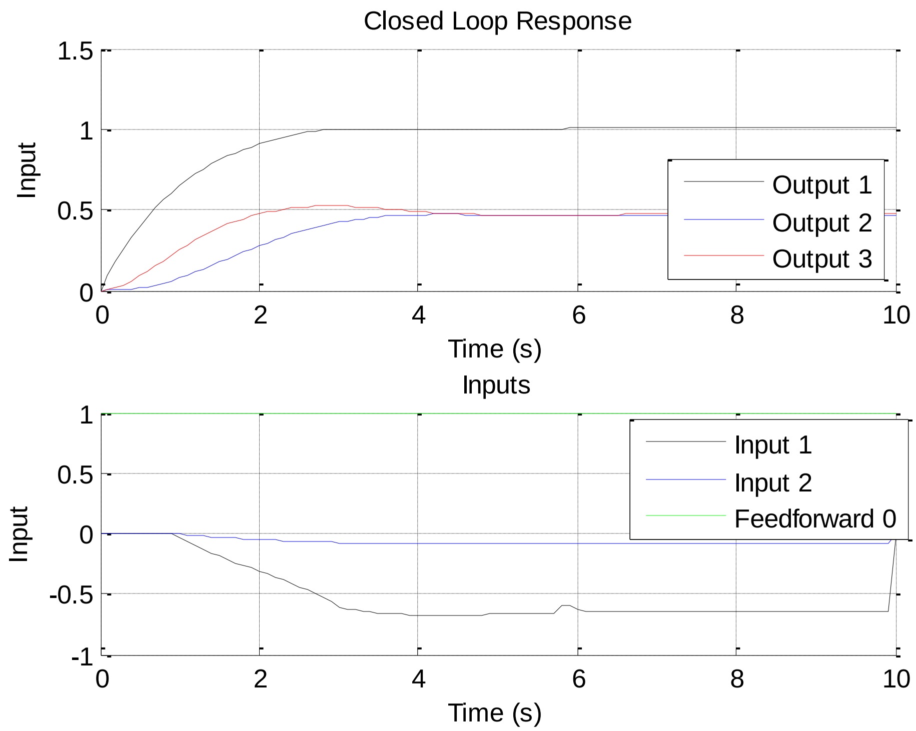

Figure 6-6: Large Feed Forward MPC Control

6.2. Model Predictive Control Implementation

The implementation of the MPC strategy for the vehicle was rather straight forward. First, the linear time invariant (LTI) model (Section 4.1) was updated with the current vehicle parameters. The LTI system was reduced to remove the dolly states (Section 4.6), and the MPC solver executed. The resulting control action at time zero (the current time step) was then converted into brake demands (MPC control variables were moments about the ground plane at each axle) and passed to a brake controller. The brake controller also managed the anti-lock brake system to ensure that wheel lock was avoided.

6.2.1. Vehicle Parameters in the Linear Time Invariant Model

As noted in Section 5.2.3, the only vehicle parameter needed for the LTI model that was not directly measured or estimated from measurements was the tire cornering stiffness. However, as errors in the estimation of this parameter were self-compensating, it was deemed acceptable to use the cornering stiffness estimation procedure outlined in Section 5.2.3. In Section 5.2.2 it was noted that CG height and inertia were estimated and not directly measured. At this point, the typical response would be to question how errors in basic vehicle parameters could affect the MPC predictive capability (see Section 5.2.4).

It turns out that errors in estimating CG height and inertia are not of concern as there is a much more significant error source, namely the evolution of tire cornering stiffness. To understand why this error exists, it is necessary to remember that the LTI model, which contains the tire cornering stiffness, is updated at every simulation time step. However, the LTI model is NOT updated within the MPC solver as it evaluates the predictive horizon.

Now the tire cornering stiffness is significantly affected by the brake activation (Section 3.3.2) thus each time the LTI model is updated, the cornering stiffness changes based on the current brake usage. But, the MPC control input is brake based so the cornering stiffness (and thus the LTI model) should change with predicted future brake usage. This, of course, is impossible as the LTI model inside the MPC solver is fixed (the core of the solver is a quadratic program using fixed matrices (Section 6.1.2)).

The result is that as the MPC controller predicts changes to the brake application, the LTI model it is using for the vehicle estimator degrades. This degradation can easily be more significant than the errors in the LTI model introduced from estimations of initial cornering stiffness, CG height, or inertia (see Section 5.2.4). The reason that the controller works so well is that the LTI errors are generally present in the far distant future (when more time has passed to change the brake demand) leaving the more critical current and near current brake demands less sensitive to the error.

6.2.2. Defining Feed Forward Input

As noted in Section 6.1.3, the inclusion of feed forward in a MPC model is generally a rather difficult objective. The MPC algorithm used here was specifically developed to manage both the feed forward and the removal of output costs. In implementing the controller, the elimination of the output cost was rather easy as Q and P in Equation 6-7 were set to zero. But the selection of the feed forward input was not as clear as this represented the driver's input at the steering wheel.

In this controller, the feed forward value was taken to be constant with the magnitude of the feed forward being the current road wheel steer angle. The justifications for this assumption were as follows:

- The MPC can adjust brake inputs much faster than a human can change the steering angle.
- We are most concerned with the corrective control response at time zero for which the steering input is correct.

- Relatively short horizons are used (5 seconds)
- We have no information on what the driver might do so predicting steering behavior is difficult.
- The model is updated every time step so we have a series of "fixed" steering inputs over time.

Admittedly, assuming that steering is constant is not ideal for all maneuvers (Figure 6-7 for example) but the controller is robust enough that the corrective actions do stabilize the vehicle. Note: see Section 9.3 for commentary on how the steering input estimation might be improved.

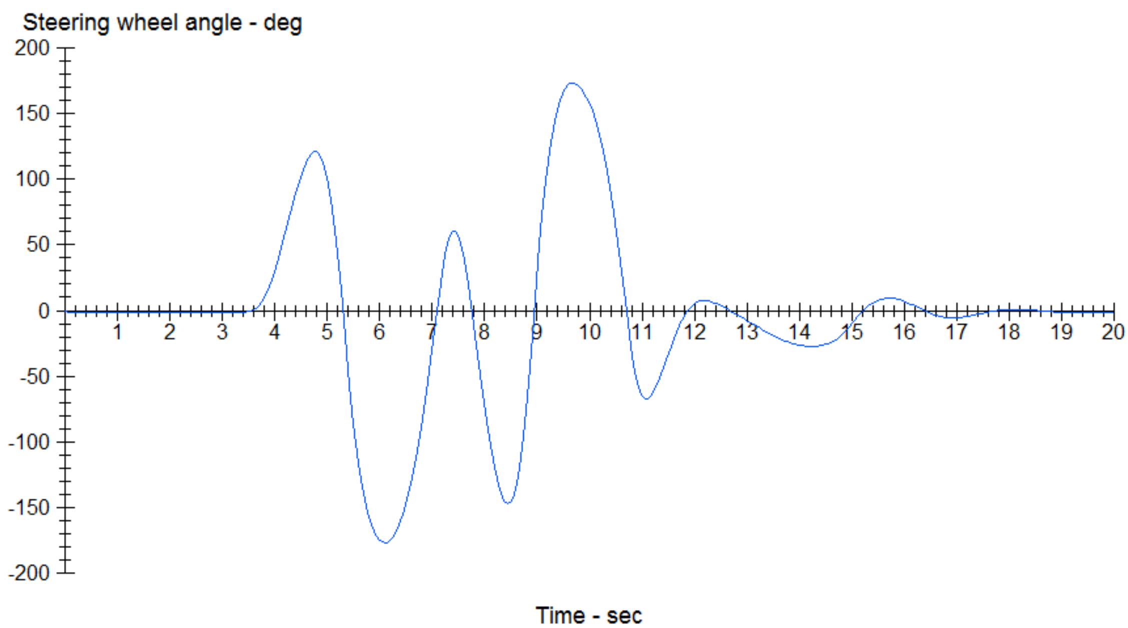

Figure 6-7: Steering Input for Double Lane Change

6.3. Simulation Results

To test the MPC controller, multiple maneuvers and events were evaluated. The following conditions were permutated to make the complete test suite:

- Load: Unloaded (all trailers), Loaded (all trailers), Last trailer loaded
- Maneuvers: Double lane change, Step steer, Ramp steer, Swept sine
- Road friction: mu = 0.85 (dry), 0.6 (wet), 0.25 (ice)

In all cases the MPC stability system performed well. As the number of case studies was far too great to present here, only a summary is presented. The remaining step steer and double lane change cases are documented in Appendix J.

6.3.1. Predictive Control – Anticipatory Brake Action

The most powerful feature of the MPC controller was its ability to anticipate probable instability. As an example, consider the loaded vehicle step steer on dry pavement. In this maneuver the uncorrected vehicle rolled over (starting with the second trailer – unit 4) (Figure 6-8). However, the MPC recognized the impending threat given the feed forward command and initial conditions and applied corrective moments to stabilize the system before any indication of instability was observed.

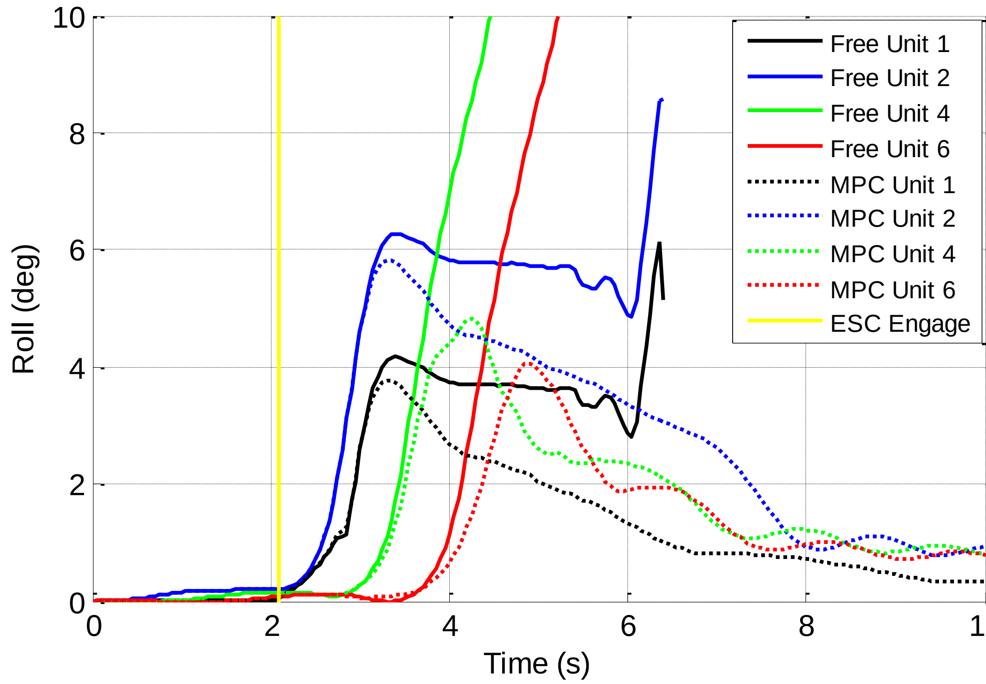

Figure 6-8: Roll Angle MPC Loaded Vehicle, Step Steer, mu = 0.85

Moreover, it can be seen in Figure 6-9 that the MPC activated the last axle's brakes at nearly the same time that the steer axle brakes were activated. The controller projected that the trailers would see the same destabilizing lateral acceleration in the near future and acted to stabilize them before the instability event occurred. The controller also recognized the risk far ahead of the actual event. Figure 6-10 illustrates the position of the vehicle at the initiation of the ESC response. Note that the vehicle is not yet turning much less posing an instability risk. Figure 6-8 underscores this fact as the ESC engagement (vertical yellow line) occurs before any significant roll develops in any of the vehicle units.

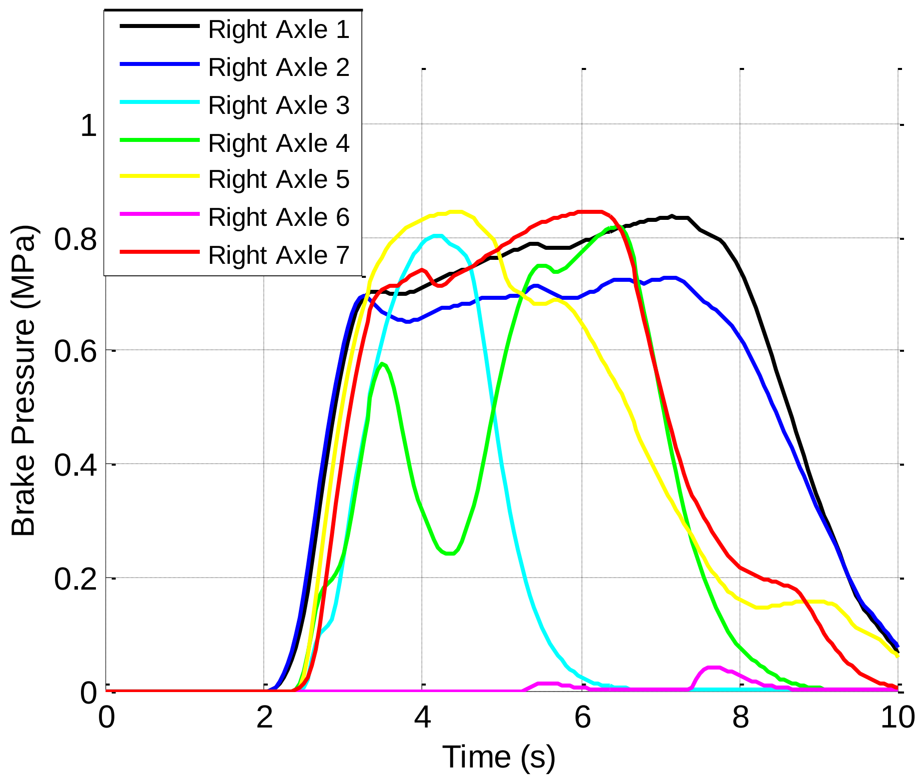

Figure 6-9: Right Side Brake Pressure, MPC, Loaded Vehicle, Step Steer, mu = 0.85

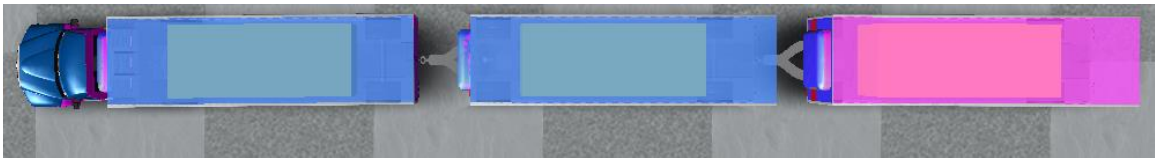

Figure 6-10: Illustration, MPC, Loaded Vehicle, Step Steer, mu = 0.85

6.3.2. Self-Correcting Actions – Systems Control Approach

While the anticipatory capability of the MPC controller permitted earlier intervention, the cost optimization strategy was capable of producing highly sophisticated control behaviors. This made the MPC strategy both proactive and highly adaptable to the particular operational environment. For instance, in the step steer case above (Figure 6-10) the controller activated the 6th axle's LEFT brake (Green arrow in Figure 6-11). This seemed counter intuitive as it would appear that this brake command would increase yaw rate / lateral acceleration and make rollover more likely. But a review of the larger dynamics showed that this input was actually helpful when the vehicle was managed as a system.

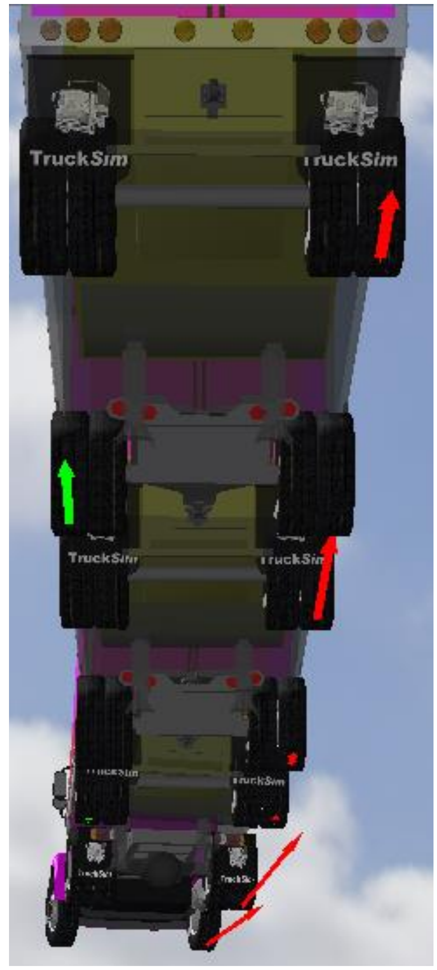

Figure 6-11: Brake Image MPC Loaded Vehicle, Step Steer, mu = 0.85

Figure 6-12 shows that left side brakes were modulated unlike the right side brakes (Figure 6-9) with only the last dolly seeing much left side control input initially. What was happening was that the controller recognized that the trailers were headed toward a roll instability event based on the steer input and initial conditions even though no trailers were seeing any risk indicators at the start of the maneuver. But activating only the right rear brake on the last trailer while it was still maintaining a straight ahead trajectory might have led to a jackknife of the vehicle. So the controller applied a moment to the last dolly to “steer” it and keep the trailer from jackknifing. I.e. the left dolly brake caused the dolly to rotate about the pintle hook and orient itself such that it was “steering” the last trailer connected to it. The controller maximized the stability of the system, not the stability of the individual units.

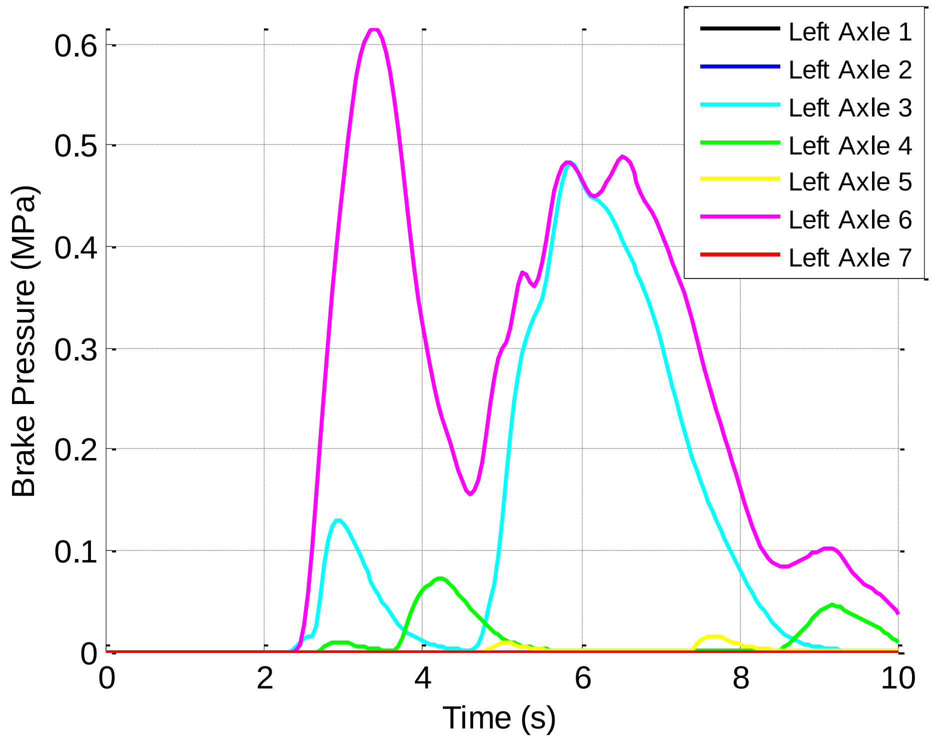

Figure 6-12: Left Side Brake Pressure, MPC, Loaded Vehicle, Step Steer, mu = 0.85

Finally, the predictive capability of the controller is seen in the reduction of peak lateral acceleration of each successive unit (Figure 6-13). The more time the controller had (further back the trailer was), the better the system was at stabilizing the unit. The noise seen in the first and second trailers was from brake modulation of the adjoining dollies.

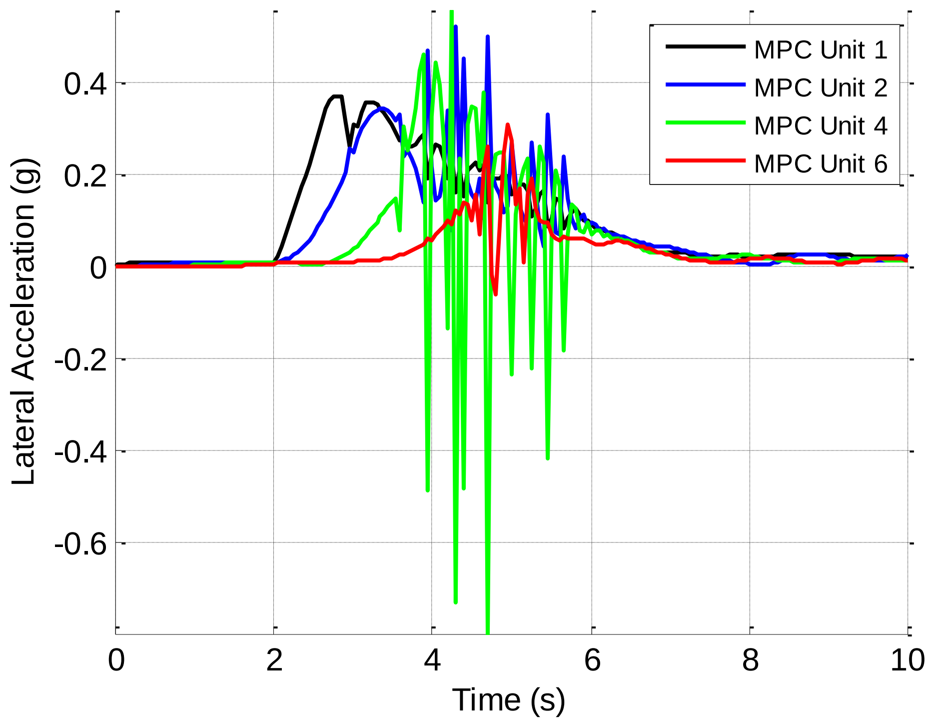

Figure 6-13: Unit Lateral Acceleration MPC Loaded Vehicle, Step Steer, mu = 0.85

6.3.3. Stabilizing "Un-Stabilizable" Events

There has not been extensive research into the stability control of multiple unit vehicles with the limited work being on active suspensions (Sampson, Jeppesen, & Cebon, 2000; Sampson, Jeppesen, & Cebon, 2006), lateral motions only (Winkler, Fancher, & MacAdam, 1983), or managing only single unit stability (MacAdam et al., 2000). Of this work, the material from MacAdams is most relevant where yaw and roll stability of multiple unit vehicles was assessed using individual unit controllers (MacAdam et al., 2000). The conclusion from that work was that the unit to unit interactions made overall vehicle system stability control more difficult. In fact, the researchers concluded that multiple unit control on ice was extremely difficult as corrective actions for one unit tended to destabilize adjoining units.

As the controller here was a system controller and not a unit controller it was able to stabilize any vehicle configuration (number of units, mass, etc.) for any maneuver on any surface, including ice. For example, consider the unloaded double lane change (the most difficult low mu maneuver) where the MPC system was able to prevent a jackknife (Figure 6-14) (Blue is uncontrolled vehicle and pink is the MPC vehicle). Figure 6-15 shows how the controller maintained the unit side slips within acceptable limits despite the extremely low traction limits and unit to unit interactions. Figure 6-16 and Figure 6-17 show the left to right modulation of the brake demands as the vehicle steered first left and then right. Note that as soon as the vehicle exited the maneuver and was stable, the controller released automatically.

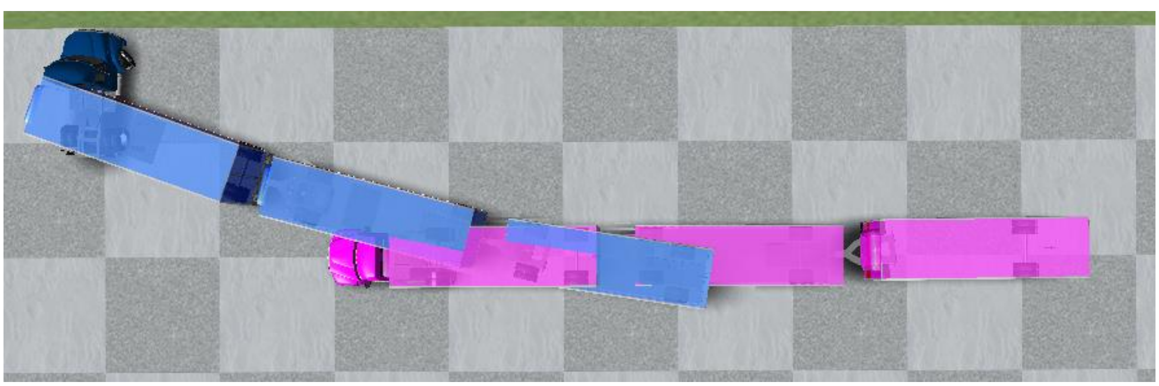

Figure 6-14: Illustration: MPC, Unloaded Vehicle, Double Lane Change, mu = 0.25

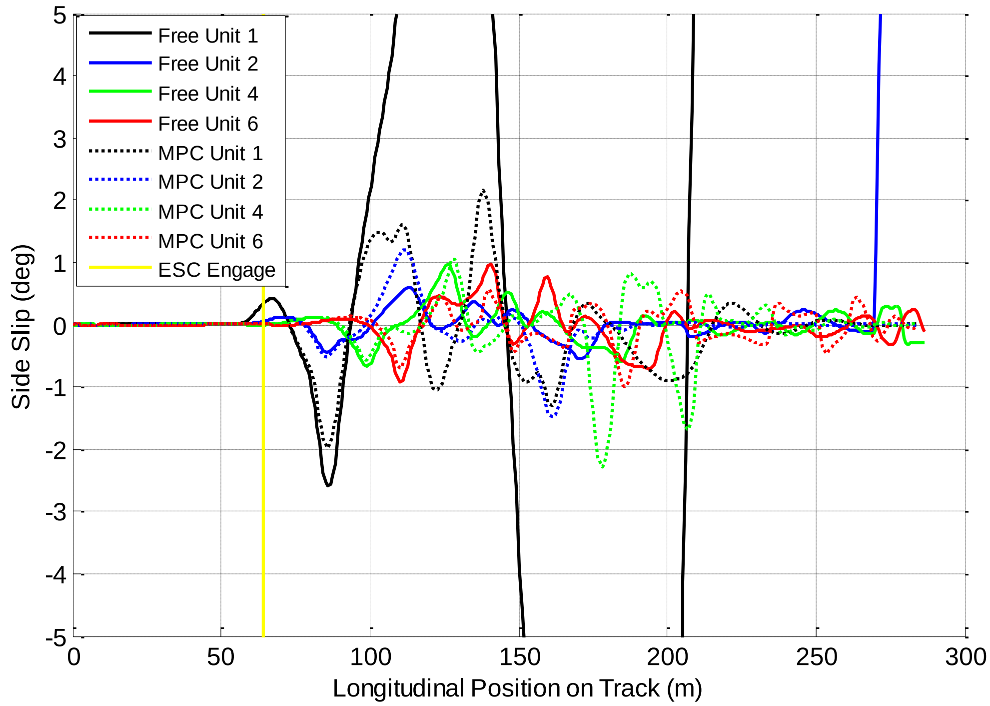

Figure 6-15: Side Slip, MPC, Unloaded Vehicle, Double Lane Change, mu = 0.25

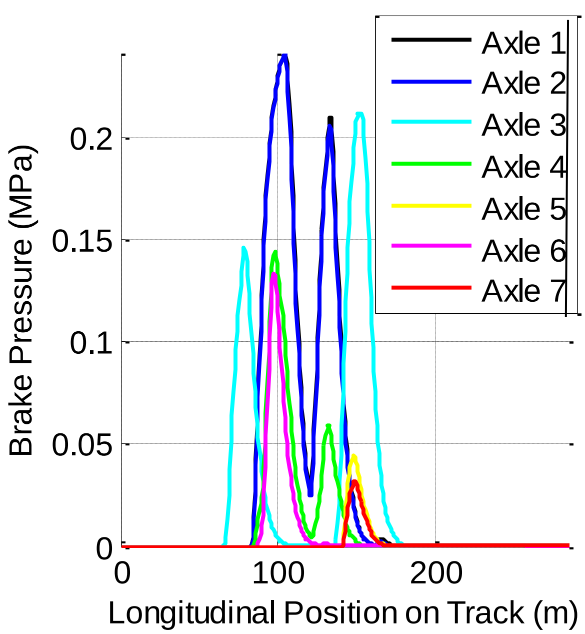

Figure 6-16: Left Brake, MPC, Unloaded Vehicle, Double Lane Change, mu = 0.25

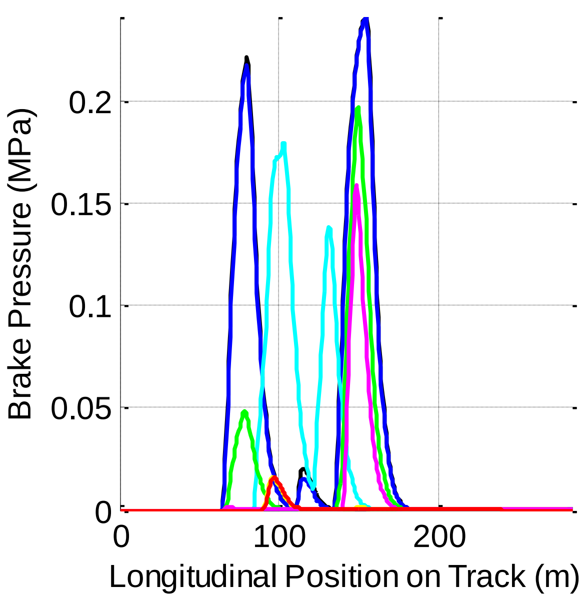

Figure 6-17: Right Brake, MPC, Unloaded Vehicle, Double Lane Change, mu = 0.25

6.3.4. Balancing Stability Modes

As shown in Section 6.3.2, the MPC strategy was capable of predicting when it might be destabilizing the system through over application of the brakes and compensate for the destabilizing demands. This capability arises from the fact that the MPC strategy was developed to minimize the vehicle system instability by minimizing the control cost for the system. For instance, take the dry (mu = 0.85) step steer for a loaded vehicle. Section 6.3.2 showed that the controller activated the trailer brakes at near peak pressure as soon as the vehicle began to enter the turn and held that pressure (Figure 6-9).

For the wet (mu = 0.6) case, the MPC does not hold full brake pressure to the trailers (Figure 6-18 and Figure 6-19). As the traction limit is lower for the wet condition, the trailers start to slide under heavy braking (Figure 6-20) and the controller predicted this side slip error and reduced the trailer braking. But the controller kept the tractor braking (it was stable) to reduce the lateral acceleration levels.

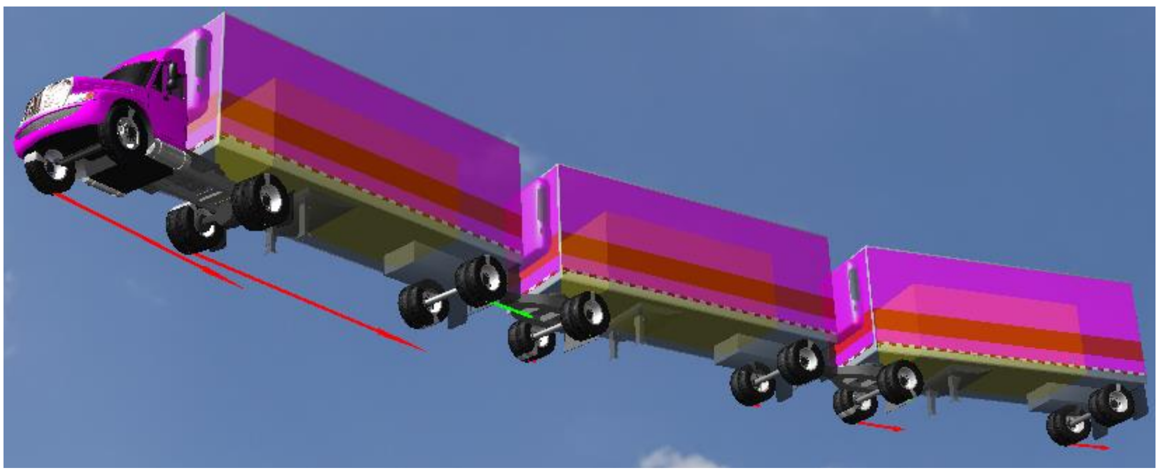

Figure 6-18: Illustration, MPC, Loaded Vehicle, Step Steer, mu = 0.6

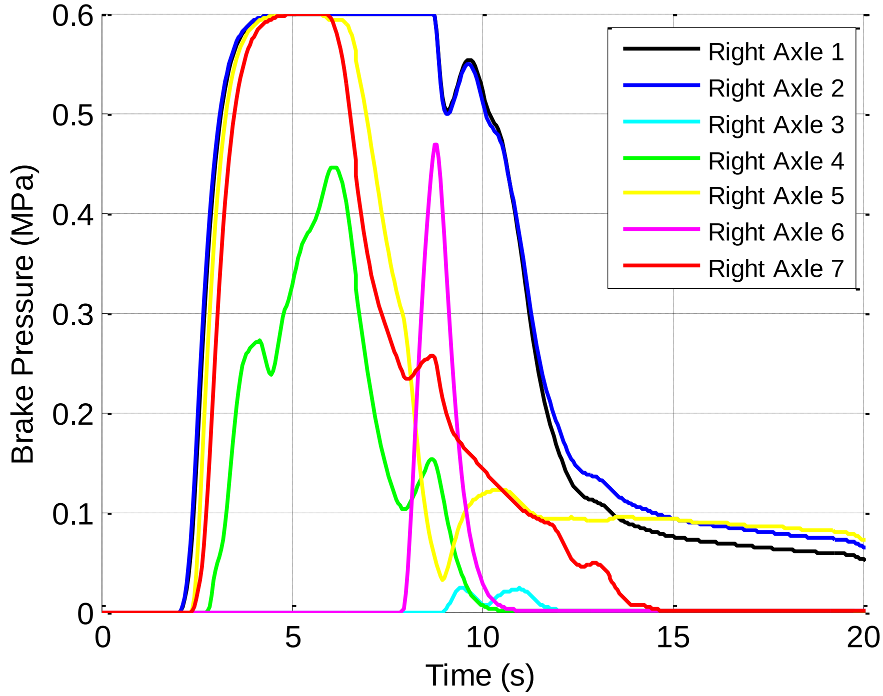

Figure 6-19: Right Brake Pressure, MPC, Loaded Vehicle, Step Steer, mu = 0.6

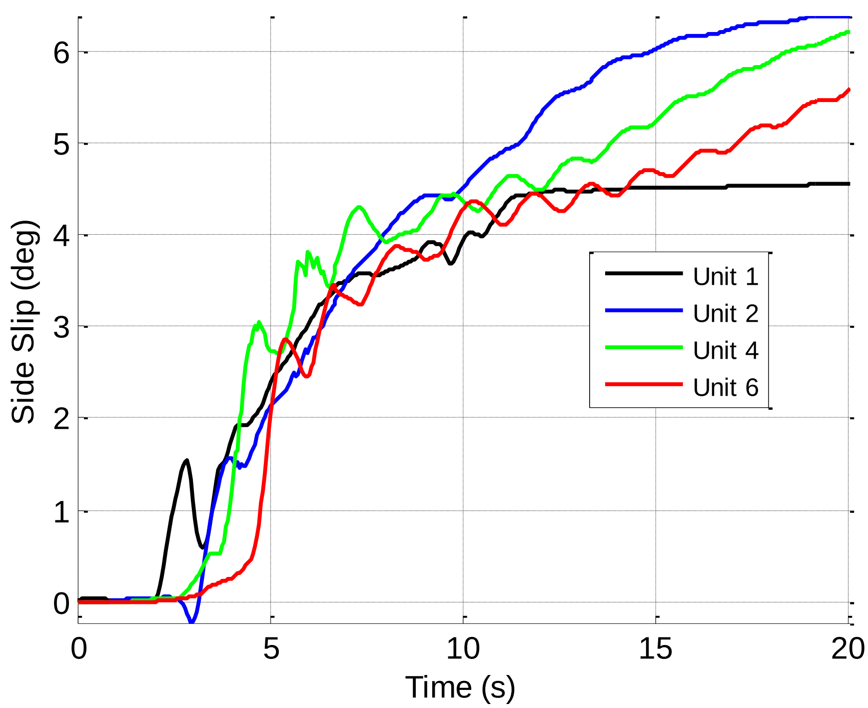

Figure 6-20: Side Slip, MPC, Loaded Vehicle, Step Steer, mu = 0.6

6.4. Bounds, Step Size, Horizon

There are essentially three "tuning" parameters for the model predictive controller as implemented here. The first is the selection of the bounds for the vehicle states. The second is the selection of the predictive model step size. The third is the selection of the horizon. These parameters are inter-dependent and cannot be optimized individually. However, their sensitivities could be evaluated and are presented here.

6.4.1. Bound Sensitivity

The current MPC bounds (Table 6-1) were selected by observing the stability of the uncontrolled vehicle over a range of loads and maneuvers. These bounds worked well in all of the simulations. However, to test the sensitivity of the controller to the bound selection, the simulations were run with a ± 25% change in the bound value.

Table 6-1: MPC Bounds

Measurement	Bound (SI)	Bound (Common)
Side slip	0.1 rad	5.7 deg
Yaw rate	0.3 rad/s	17 deg/s
Rollrate	0.05 rad/s	2.8 deg/s
Roll	0.03 rad	1.7 deg

For space consideration, only a couple of the bound sensitivity plots are shown here; however, the results presented are consistent with the general observations on boundary selection and system performance. Figure 6-21 shows the vehicle speed during a double lane change maneuver on ice. When the bound sizes were reduced (more aggressive control), the vehicle slowed more as expected. The oscillation in the low bound cases between 12 and 15 seconds was from the tractor's attempt to regain the set velocity and the effect of the resulting high torque demand on stability. Essentially the engine engaged, broke traction under acceleration (Axle 2), the controller intervened, and the process repeated. The higher the bounds (loose control), the smoother and faster the vehicle was until the bounds were so large that the controller could not intervene in time to maintain stability (125% case). In general a bound selection range of ±20% of the nominal values in Table 6-1 was quite acceptable.

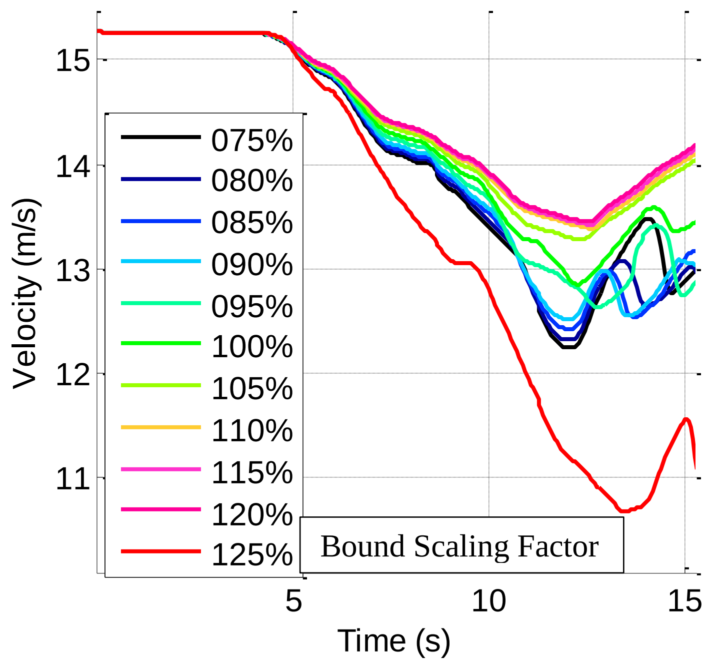

Figure 6-21: MPC Bound Sensitivity - Loaded Vehicle, Double Lane Change, mu = 0.25

Similar bound sensitivity was noted for the case of a loaded vehicle executing a step steer on wet asphalt (Figure 6-22). For tight bounds (75% to 85% of the nominal values in Table 6-1), the controller was a bit aggressive as can be seen in the oscillations of the side slip (system engaging and disengaging frequently). Larger bound intervals resulted in slightly more system overshoot. However, any of the bounds would have been acceptable for stability. The trade-off would be driver acceptance (intervention frequency) and system response time.

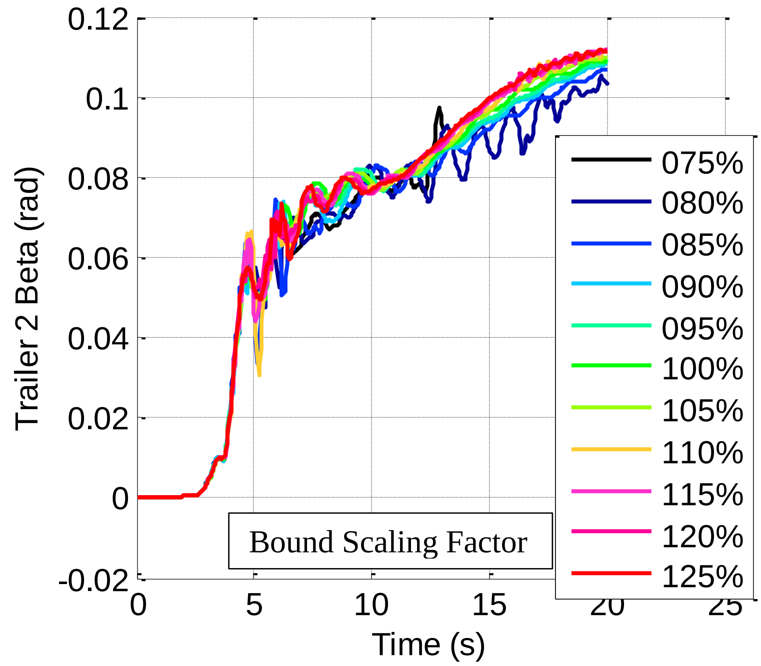

Figure 6-22: MPC Bound Sensitivity - Loaded Vehicle, Step Steer, mu = 0.6

6.4.2. Horizon Selection

As discussed in Section 4.5, the vehicle system's slowest eigenvalue ranged between -0.7 and -1.4 (real part) depending on load and speed. That placed the time constant in the range of 0.7 to 1.4 seconds (Section 4.5.3). The general rule of thumb is that the controller needs to see three time constants out for good performance. While one could use the LTI model to gage the time constant for each usage case, it would go against the desire to reduce the requirement for highly accurate vehicle parameter data needed to develop the LTI model. As MPC is a fast method the decision was made to fix the horizon at 5 seconds which would be sufficient for the slowest time constant case. Faster systems just got the benefit of a greater horizon.

6.4.3. Time Step Selection

To assess the sensitivity of the system to the MPC step size, the control response was evaluated for a 5 second horizon with different step sizes. In this case, the system time constant was 1.2 seconds. From Figure 6-23 one can observe that a step size greater than approximately ½ the time constant resulted in a stable prediction of required corrective action (other test cases produced similar results). As the controller's objective was to drive the system back into bounds as quickly as possible, short time steps generally resulted in larger control inputs (need to move the system in a shorter time frame). Shorter time steps also typically had larger variations in control demand between the first time step and the second time step (Figure 6-24) as the vehicle tended to overshoot and correct which was a consequence of the large control inputs.

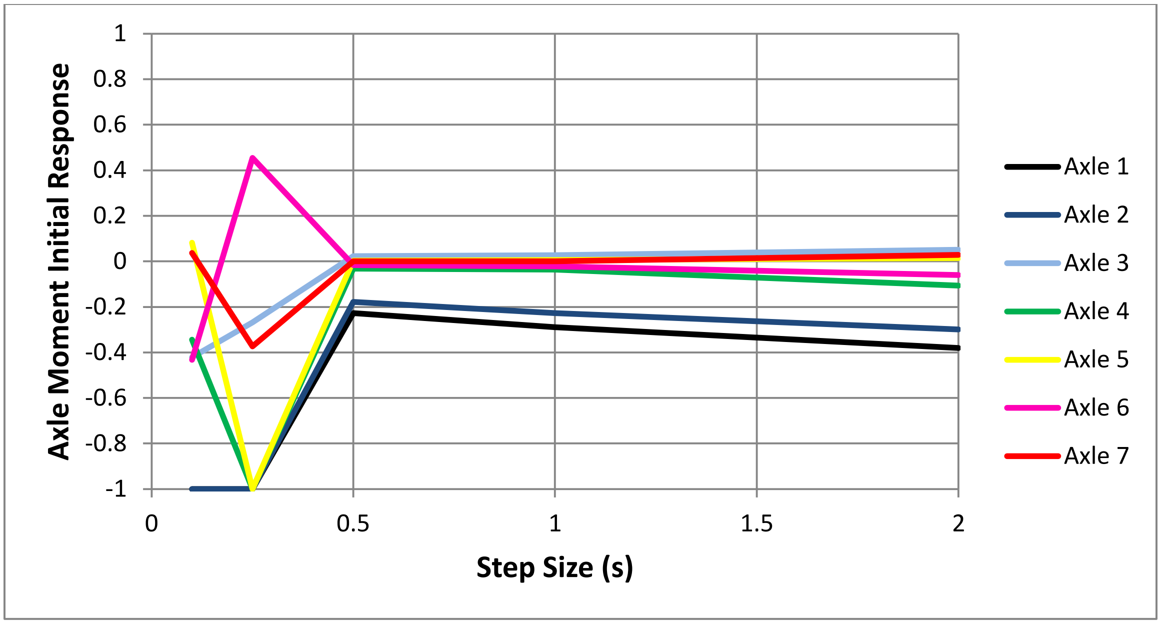

Figure 6-23: MPC Step Size Effect on Controller Demand (5s Horizon)

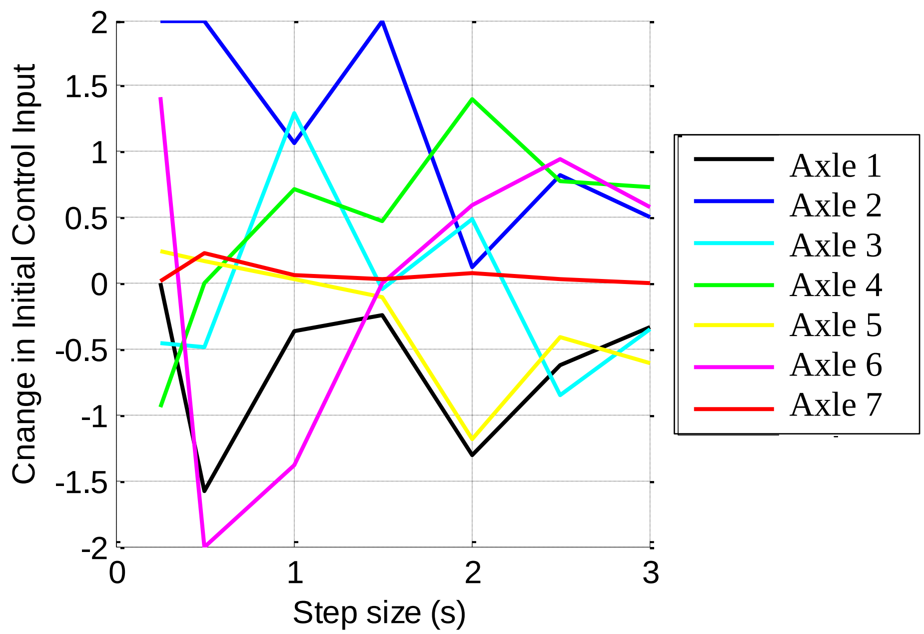

Figure 6-24: MPC Step Size Effect on Control Step Variation (N=1 to N=2)

As a major objective was to decouple the selection of the controller step size and horizon from the linear model (eigenvalue evaluation), the decision was made to fix the step size at 1 second and the horizon at 5 seconds. This resulted in a fast model (5 time steps to evaluate) while keeping the step size greater than ½ the largest observed system time constant and the horizon greater than three times the time constant for all velocity and loading arrangements. A larger time step was not selected as it was desired to have the step size approximately equal to the faster (unloaded and slower velocity) time constants.

6.4.4. Defining "Optimal" MPC Conditions

As noted before, the selection of the bounds, step size, and horizon were all interdependent. The controller proposed here has proven to be very robust and efficient regardless of the selection of bound, step size, or horizon (within reason). The largest limitation to tuning the controller parameters at present is the need for a broader database of vehicles and usage conditions.

6.5. Noise and Sample Rate

As the performance of the controller was also dependent on the quality of the state estimations and the update rate of the controller, it was deemed prudent to evaluate the sensitivity of the system to those parameters as well. As these two issues were largely decoupled (controller update rate and state estimation accuracy are very loosely related), they were treated independently.

6.5.1. State Estimation Noise

As discussed in Sections 5.1 and H.3, the effective noise in the state measurements was a function of the noise in the IMU and the GPS systems. However, the use of

Kalman filters significantly improved the quality of the state estimations providing the controller with usable data on the vehicle's performance. More information on this can be found in Section H.3.2 (sensor noise) and section H.3.3 (GPS update rate).

Nevertheless, the question remained as to how the measurement noise affected the controller's performance. As the MPC strategy here is not a classical feedback arrangement, traditional approaches to measure sensitivity were difficult to implement. As a result, the approach used was to evaluate the effect of noise on the performance of the system by observing the system's stability.

To begin, consider the open loop poles of the vehicle system during a double lane change (Figure 6-25) without the benefit of a stability controller. As the uncontrolled vehicle crashed, it was not surprising that the discrete open loop poles were outside the stability circle (in red). However, when the MPC was added, the resulting system response was stable for the entire event.

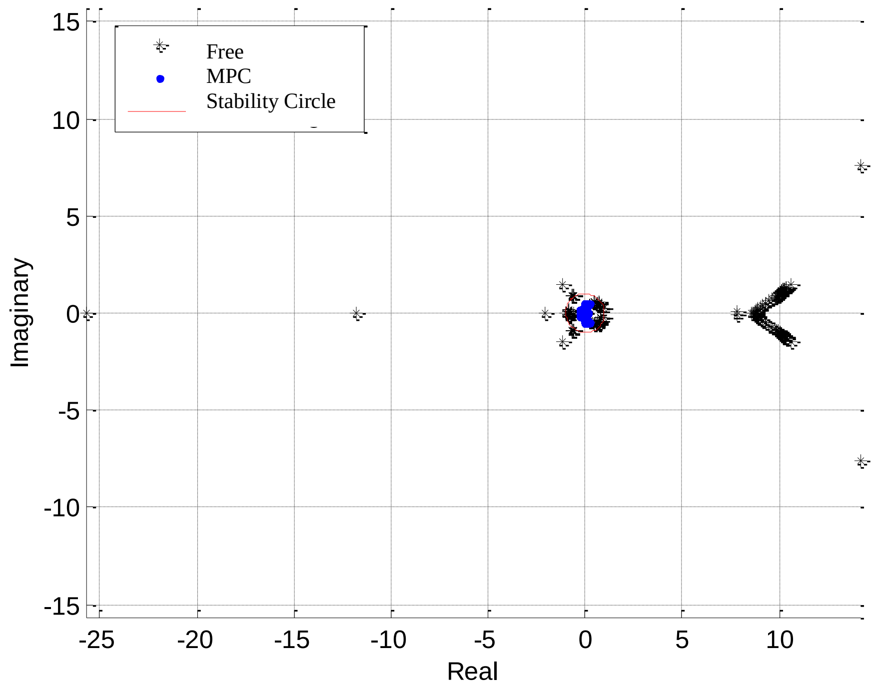

Figure 6-25: Discrete Eigenvalues, Loaded, Lane Change, mu = 0.6

As it was a bit hard to see the poles for the MPC system in Figure 6-25, the stable region was magnified as shown in Figure 6-26. To gage the sensitivity of the controller to state estimation noise, the Gaussian noise for all states was doubled and the simulation re-run. The resulting poles for the "noisy" system were impossible to distinguish from the original system (Figure 6-27). This was not surprising at all as the MPC strategy relies only on predicting the future instability and reacting to the predictions. Noise in the state estimations mostly affects the current state evaluation (current time step). As the projection time progressed, the effect of parameter errors (see Section 5.2) and the effect of brake demand (see Section 5.2.4) was more significant and these were constant in the analysis here. Note: For discrete systems, Eigen values within in the unit circle are stable; Eigen values outside the unit circler are unstable. All Eigen values for the controlled vehicle were within the unit circle.

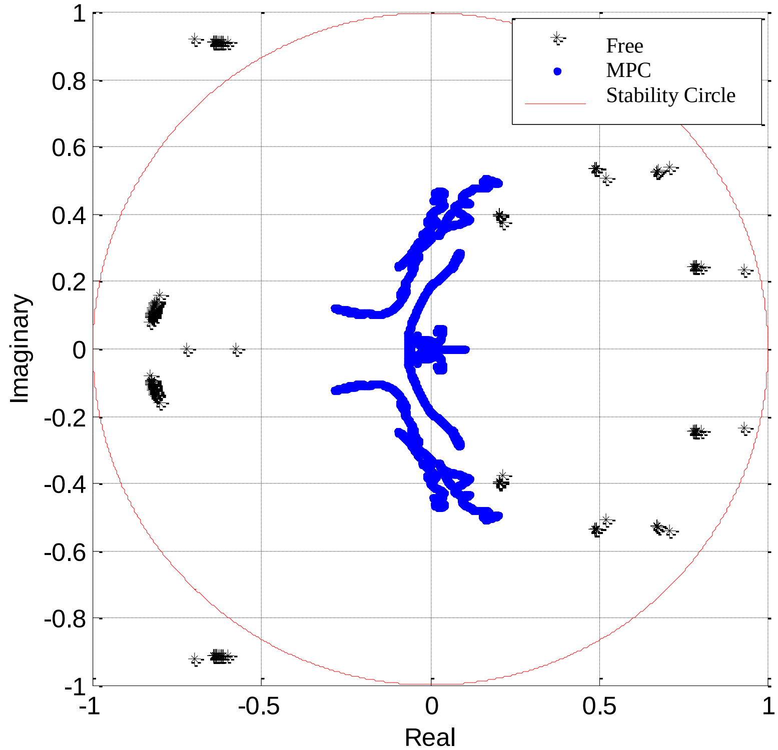

Figure 6-26: Discrete Eigenvalues, Loaded, Lane Change, mu = 0.6

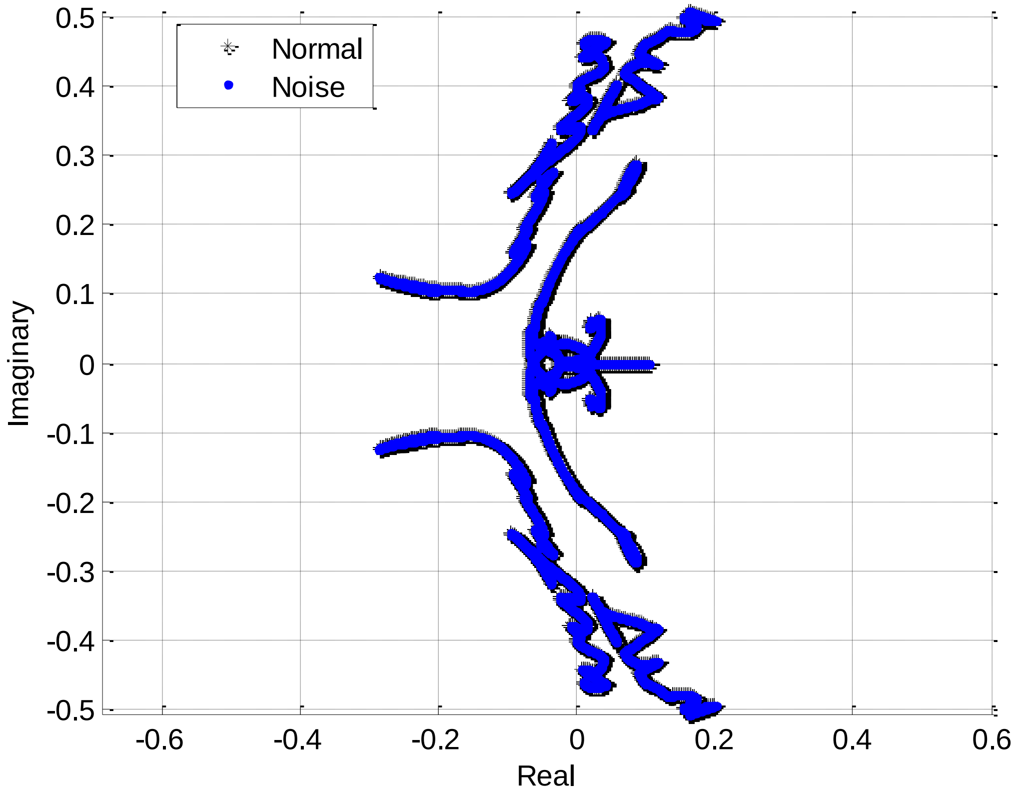

Figure 6-27: State Estimation Noise, Discrete Eigenvalues, Loaded, Lane Change, mu = 0.6

6.5.2. Controller Update Rate

The next question was how much of an effect the update rate of the controller had on the performance. This is different than the evaluation of the GPS update rate on state error discussed in Section H.3.3. This question centered on what was the effect of reducing the controller response frequency. The general expectation here was that any controller update rate that was significantly faster than the vehicle system's response time would be sufficient.

As it has already been shown that the trailers were the stability limit and the trailer modes had time constants on the order of 0.4 up to 1.4 seconds (depending on load and speed – Section 4.5), any controller system update rate faster than the critical modes should work well. To test this, a case study was run with the nominal controller update rate of 40 Hz. and a reduced controller update rate of 10 Hz. (Figure 6-28). As can be seen, the stability of the vehicle was not affected significantly. Subsequent analysis of the side slip (Figure 6-29) and roll (Figure 6-30) also showed little effect. Again, this was not surprising as the important modes of the vehicle were greater than 0.4 seconds and the two controllers were operating at 0.1 and 0.025 seconds respectively. Of course, a controller operating at 5 Hz. might not perform so well, but it would be unusual to see a controller with a cycle time that low.

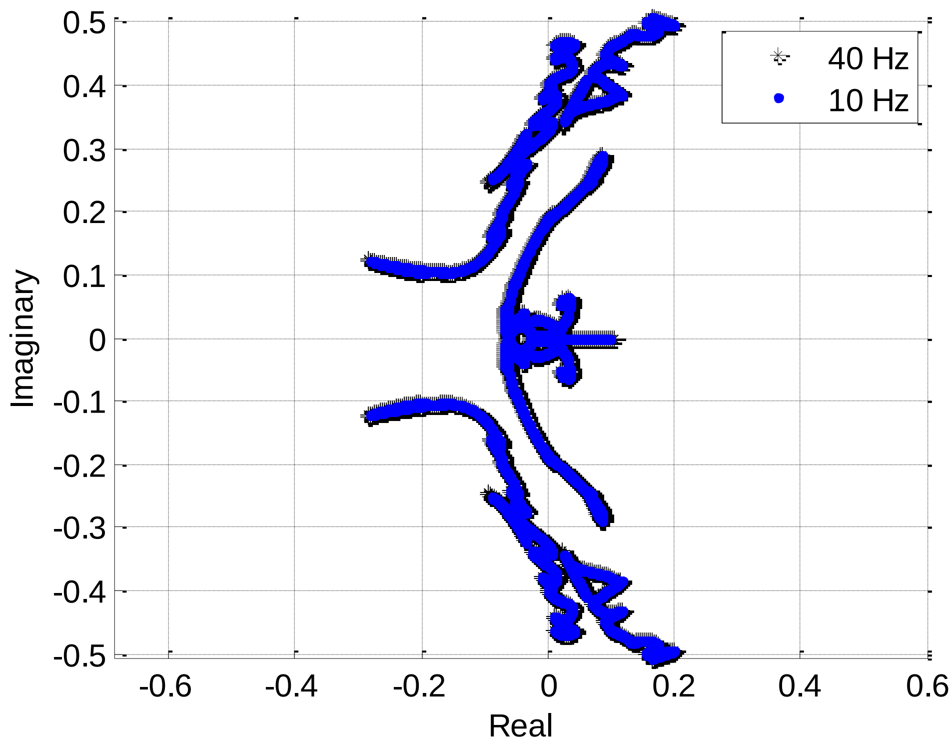

Figure 6-28: Discrete Eigenvalues, MPC Controller Update Rate, Loaded Vehicle, Double Lane Change, mu 0.6

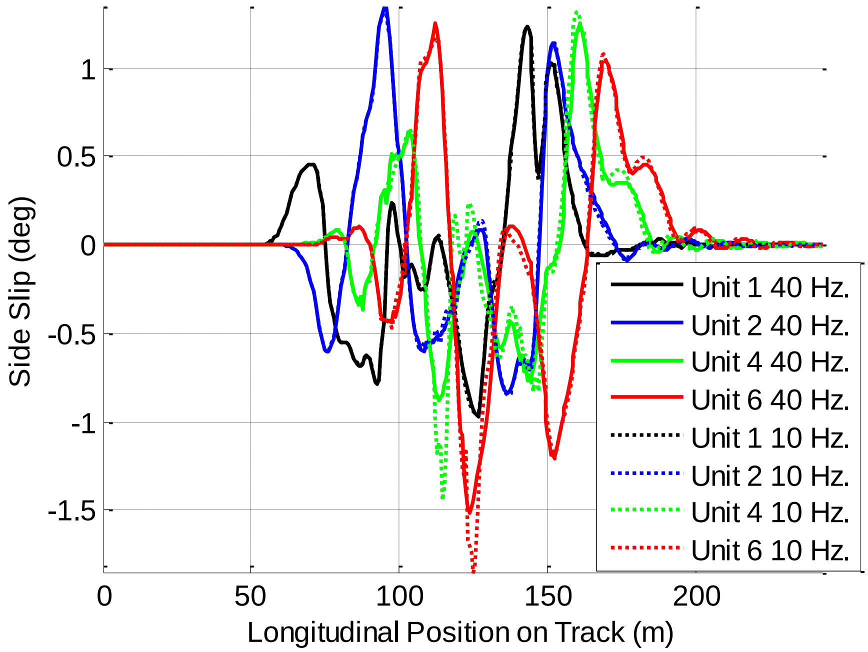

Figure 6-29: Side Slip, MPC Controller Update Rate, Loaded Vehicle, Double Lane Change, mu 0.6

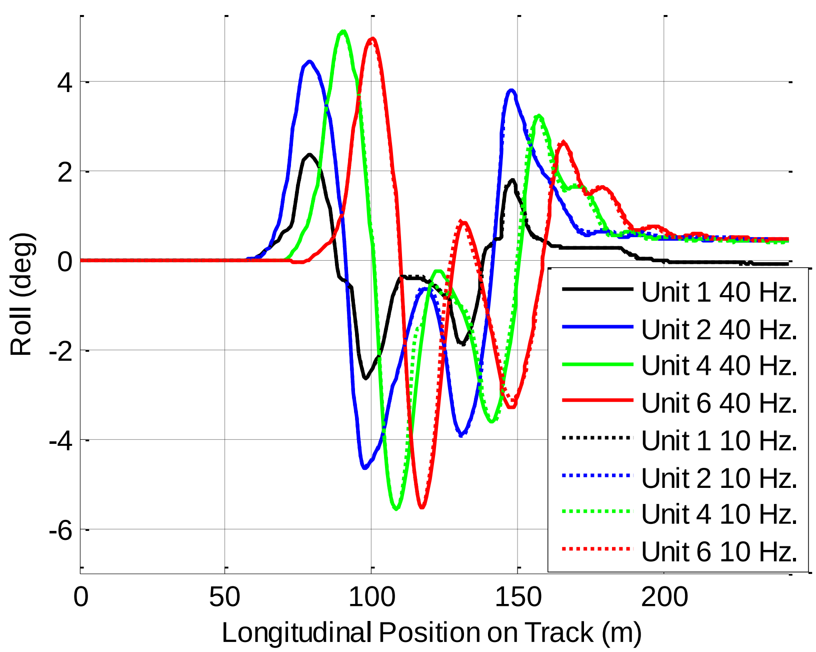

Figure 6-30: Roll, MPC Controller Update Rate, Loaded Vehicle, Double Lane Change, mu 0.6

6.6. A Comment on Anti-Lock Brakes

It turns out that one of the biggest influences on the performance of the controller was the anti-lock brake system (ABS). This was particularly true on low mu surfaces where it can be difficult to spin a heavy wheel that has been locked through aggressive braking (each wheel end has a mass of approximately 200 kg). While electronic air brakes (EBS)[2] do significantly reduce the brake time constant, the brakes are still air powered. The combination of compressible media and large / heavy brake shoes (Appendix A.5.1) results in response times that can be slower than desired. In this research, the brake time constant was taken to be 0.25 seconds. Note: Electric air disk brakes have already been developed and are used in Europe. Air disk brakes require much less air volume and could improve the system performance significantly.

To gage the sensitivity of the controller to brake time constant, several cases were run. Figure 6-31 shows the yaw rate response of a loaded vehicle on ice (mu = 0.25) in a double lane change. It is clear that all of the controller models were significantly better than the open loop vehicle (red). But it is also apparent that as the brake time constant grew (from black to yellow) the controller performance degraded. Now the current brake system (time constant of 0.25 seconds) is clearly better than no control, but a simple way to make the controller better would be to move to air disk brakes with smaller time constants.

---

[2] Electronic Air Brake Systems (EBS) retain the use of air to power the brake system (compressing the brake shoe against the drum – Section A.5) but replace the command to activate the brakes with an electronic signal. Thus the activation command has a much smaller delay than the current air pressure based system.

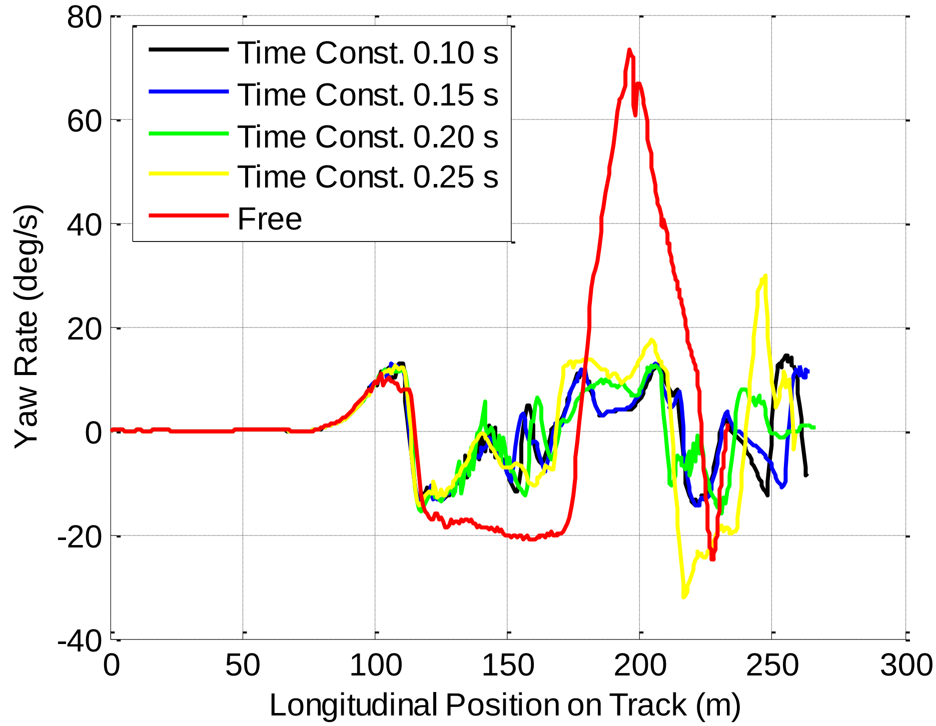

Figure 6-31: Trailer 3 Yaw Rate, MPC Brake Time Constant Effect, Loaded Vehicle, Lane Change, mu=0.25

CHAPTER SEVEN

FUZZY LOGIC CONTROL

7.1. Fuzzy Logic Controller Design

Fuzzy logic control is a term used to describe set theory as implemented in a dynamic system controller. The controller decision is based on whether an input is contained in a given membership function (and to what degree), what rules apply to that membership function, and what output membership functions apply to the rules (and to what degree). The term "Fuzzy" refers to the fact that an input parameter can be a member (or partial member) of more than one input membership function with more than one rule applying and more than one output membership (or partial membership) being active.

7.1.1. Fuzzy Logic Controller Development

The fuzzy logic controller developed here is unique in that it does not use a comparison between the actual vehicle and a reference model of the vehicle as is typically done (Boada, 2006; Xiao, Chen, Zhou, & Zu, 2011). The controller here looks solely at the states of the vehicle and takes advantage of the fact that the least stable units in the vehicle (the trailers) experience events after the tractor providing time to prepare for a potential trailer stability risk. To prevent over activation of the controller, the membership sets were designed such that natural deadbands existed eliminating the need to write special rules to suppress the controller when it was not needed.

The general controller idea is that inputs (unit states) are tested against input membership functions, the membership functions are acted on by rules defining corrective actions for observed instabilities, and the output actions filtered / combined by the output memberships to derive a final corrective action (Figure 7-1). Set combinations and rule development are generally performed using Boolean (and / or) logic. The result is a control action for each vehicle system input (in this case, seven control commands for the seven vehicle axles) driven by 12 vehicle state estimates (side slip, yaw rate, and roll for the tractor and each trailer).

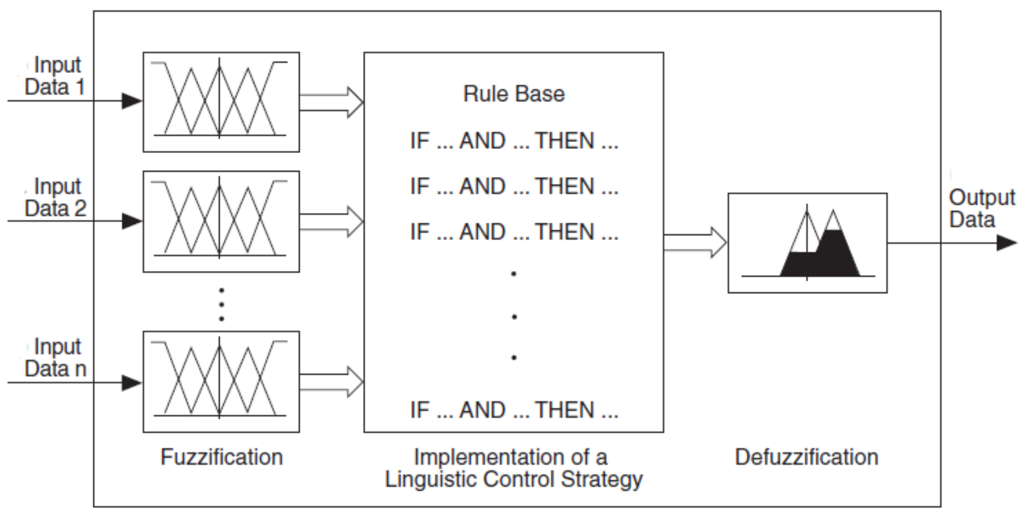

Figure 7-1: Fuzzy Logic Input / Output Schematic (National Instruments Corporation, 2009)

7.1.2. Input Memberships

All 12 inputs to the controller (side slip, yaw rate, and roll for the four vehicle units) were processed using the same input membership structure (Figure 7-2). The limits for each state are given in Table 7-1 where the bounds define the inner edges of the negative and positive domains and the limits define the outer edges of the memberships. The degree to which a given input was a member of a given set was determined by the set boundary. For instance, if the input for Figure 7-2 was 0.08, then the input would have a membership of 0.2 for center and a membership of 0.6 for positive. If the input was greater than 0.1, the only membership would be positive with a value of 1.

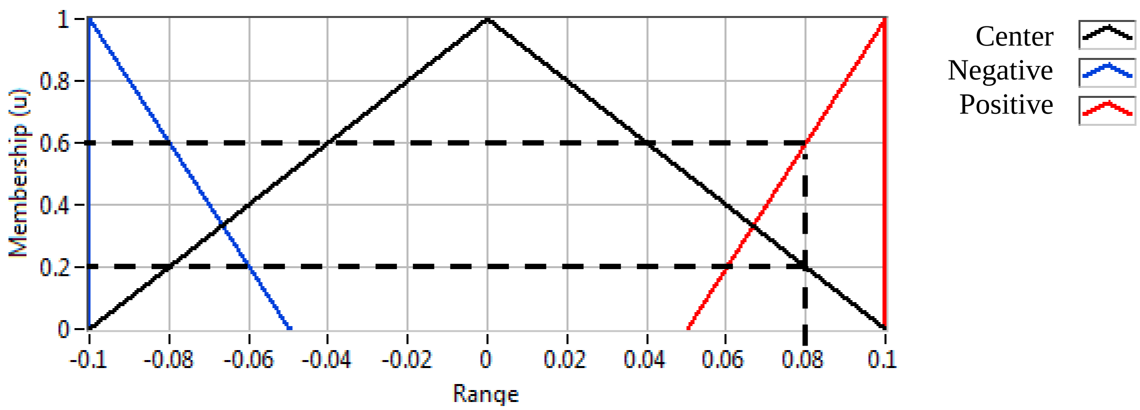

Figure 7-2: Fuzzy Logic Input Membership Structure

Table 7-1: Fuzzy Logic Bounds

Measurement	Bound (SI)	Limit(SI)	Bound (CES)	Limit (CES)
Side slip	0.075 rad	0.15 rad	4.3 deg	8.6 deg
Yaw rate	0.3 rad/s	0.6 rad/s	17 deg/s	34 deg/s
Roll	0.05 rad	0.075 rad	2.9 deg	4.3 deg

7.1.3. Rules and Their Interpretations

The rules simply related the inputs to the outputs using logic switching. For example, a rule may be stated as Equation 7-1 which means: If unit 1 side slip is positive, then apply a positive moment to axle 1

$$\text{If Beta1 is Positive then A1 is Positive} \tag{7-1}$$

Of course, this is a rather simple rule and they can get more complex with multiple input conditions (combinations using and / or statements) and multiple outputs (usually and statements). For example Equation 7-2 is interpreted as: If the tractor has a positive roll angle and the tractor and first trailer both have positive yaw rates (turning the same direction) or the tractor has a positive yaw rate and the first trailer has a minimal yaw rate, then apply a negative moment to axle 3. Basically, this is assuming that the trailer will be seeing the same roll threat as the tractor in the near future.

$$\begin{gathered}\text{If roll1 is Positive and yaw rate1 is Positive and} \\ \text{(yaw rate2 is Positive or yaw rate2 is Center)} \\ \text{then A3 is Negative A3}\end{gathered} \tag{7-2}$$

When multiple criteria were used in the if-then statement, the weight applied to the output was the minimum (AND) of the contributing membership criteria. For example, if the membership criteria in Equation 7-2 were 0.3 for the criteria "Positive roll1", 0.5 for the criteria "Positive yaw rate1", and 0.4 for the criteria "Positive yaw rate2" then the resulting weight would be 0.3. Details on the Fuzzy Logic controller can be found in Appendix K.

7.1.4. Output Memberships

There were seven fuzzy logic controller inputs to the vehicle system, labeled A1 through A7, representing the seven axle moments. Each axle moment input had the same membership function arrangement (Figure 7-3).

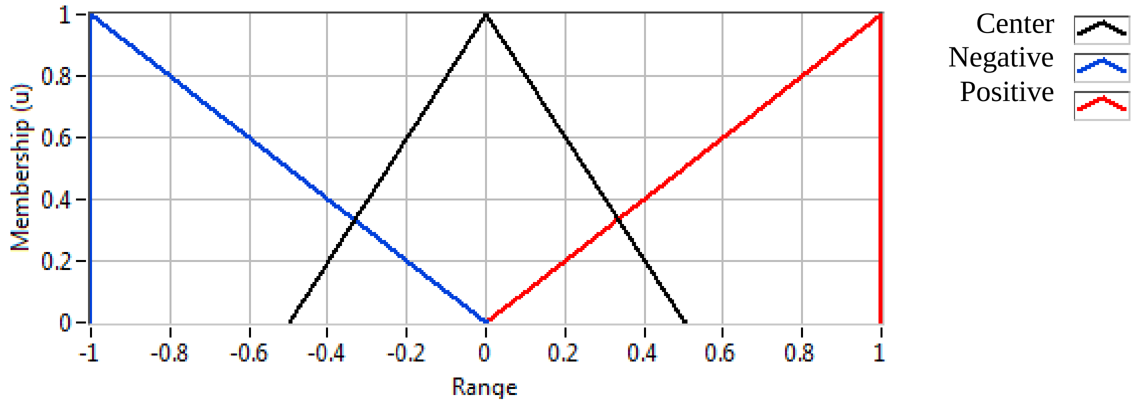

Figure 7-3: Fuzzy Logic Output Membership Structure

As it is quite possible for one rule to produce a Negative (or Positive) output and a second rule to produce a Center output for the same axle, some method was needed to determine the final control response to the vehicle axle. This was managed by applying the membership weights to each output set and then finding the centroid. For illustration, consider Figure 7-4 where "Negative" has a weight of 0.6 and "Center" has a weight of 0.4. The resulting output would then be the centroid location of the aggregate area which is around -0.4.

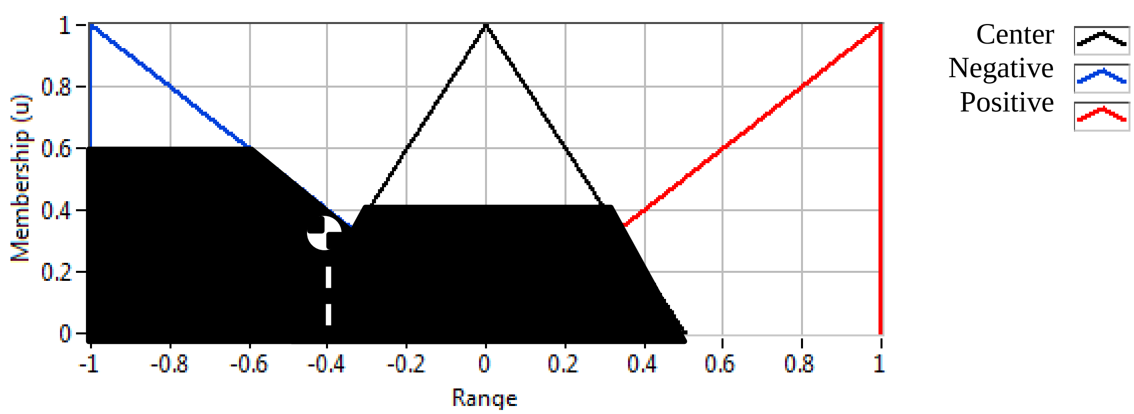

Figure 7-4: Fuzzy Logic Output Membership Structure

7.2. Controller Concept

There were three basic objectives that the fuzzy logic controller tried to meet. The first was to mimic the ability to look into the future and predict stability risks. The second was to "balance" the needs of the vehicle units for optimal system performance. The third was to smooth out the engagement of the ESC system so that the vehicle (and driver) did not experience multiple harsh activations of the system. The future stability assessment was accomplished through clever rule development and the observation that the trailers, which were the stability limitation, followed the tractor. The "balanced" response was obtained through rule selection and membership weighting. The smoothing of the ESC system was accomplished through selection of the input sets.

7.2.1. Natural Deadband

All inputs to the controller (vehicle states) had identical looking input membership functions (Figure 7-2) with significant gaps between the Negative and Positive responses. The rules were designed so that a Center input set did not produce a corrective action, thus effectively generating a range over which a given vehicle state would not produce a corrective response. As it is impossible to visualize all 12 degrees of freedom at one time, the effect is illustrated with a two degree of freedom example using unit 1 side slip (beta1) and unit 1 yaw rate (yaw rate1). Note that Figure 7-5 has a large flat zone with an output of zero and the flat zone is centered about the origin. As the origin indicates no side slip and no yaw rate, this means the vehicle is not turning and does not require corrective measures. The output for this illustration is axle 1 (steer) corrective moment demand. However, once the states exceed the input set bounds, a corrective output demand builds. Moreover, the corrective response grows more quickly if both states are violating their respective bounds.

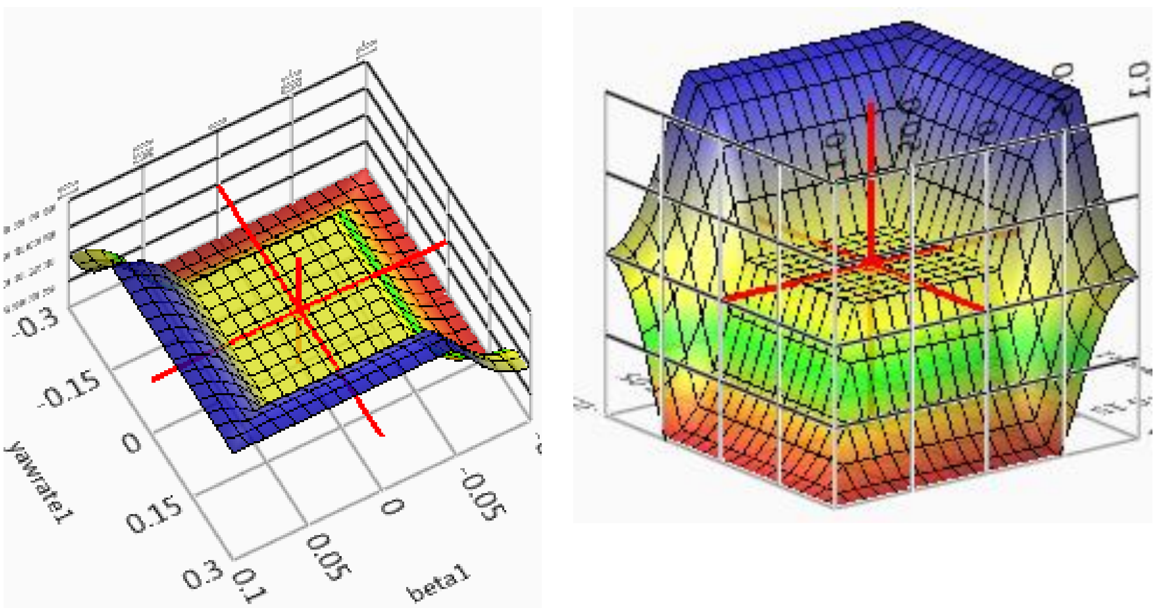

Figure 7-5: Fuzzy Logic Output Shape

7.2.2. "Predictive" Capabilities

As noted in the introduction, the controller mimics the ability to predict future instability by observing the current states of the leading units and projecting what is likely to happen to following units. I.e. rules were developed that could interpret particular behaviors of the leading units and generate appropriate corrective responses for the trailing units. This is not a true predictive capability like what was possible with MPC (Section 6.1) but it was good enough to improve overall system performance.

However, the quality of the predictive assessment is solely dependent on the skill of the individual developing the sets and rules.

7.2.3. “System” Control vs. Unit Control

A major benefit of the MPC controller was that it treated the vehicle system rather than the individual units (Section 6.1). While the fuzzy logic controller is not a “system” controller by design, it does function as a system controller via rule development. Each unit’s states are assessed and from the sets and rules, brake demands are determined. But any unit can make demands on any given axle. For instance, the tractor and lead trailer both make demands on the drive axle (second axle). Also, multiple units can be assessed in the same rule (Equation 7-2) to “see” the system’s performance. As all of the demands are combined and the final control requirement calculated using the centroid method (Section 7.1.4) the resulting response is a balance of the (potentially) competing unit demands. Of course, the effectiveness of the approach depends on how well the developer understands the vehicle system dynamics and brake activation / management when developing the rules and membership shapes.

As a final note, this controller is very easy to scale as the number of units change. All that is needed is to add additional states, outputs (brake demands), and rules. Moreover, the rules are largely replications of the existing rule set requiring only the addition of the axle outputs.

7.3. Controller Performance

In general, the fuzzy logic controller performed quite well over a very large range of loads, maneuvers, and road conditions. The controller generally intervened in time to avoid an instability event without being overly aggressive. However, the tuning of the controller was rather demanding as the set groupings, rule structure, and bound selection had to satisfy competing needs for a myriad of stability risks.

To provide some context as to the performance of the fuzzy logic controller, A few cases are reviewed here. Appendix K contains information on the fuzzy logic controller performance for all test cases and Section 8 will address direct comparison of the fuzzy logic and MPC controllers under various conditions.

7.3.1. Overview of Case Studies

The fuzzy logic controller was subjected to the exact same set of case studies as the model predictive controller (Section 6.3). Through testing it was observed that the fuzzy logic controller needed slightly tighter bounds on side slip and roll compared to MPC. This indicated that the fuzzy logic controller was a little slower to react which made sense given that the MPC controller could "see" further into the future. Section K contains the results of the test cases for reference.

The "slower" reaction was not a result of the rule selection but rather the deadband size. Simply put, the tractor had to roll enough to activate the rules and that took some time to occur. The fuzzy logic controller was "faster" with tighter bounds but then it tended to be overly aggressive and activate when not needed.

7.3.2. High mu Cases

To test the roll control capabilities of the fuzzy logic controller, the dry step steer case (mu = 0.85) was evaluated using a loaded vehicle (Figure 7-6). In the roll response one can clearly see that the controller did not activate until the tractor and first trailer had developed significant roll (2.9 seconds). However, once the controller activated it recognized that the second and third units were most likely headed for an instability event as well and activated the brakes on all units (Figure 7-7). Finally, as the roll correction produced some undesirable yaw deviations, particularly for unit 2 (trailer 1) (Figure 7-8); the left side brakes were applied to correct the vehicle's path (Figure 7-9). The yaw correction serves as a good illustration of how the controller tried to balance the system's needs through the combining of competing stability demands (Section 7.2.3). However, the quality of the system optimization is solely dependent on the selection of input / output sets and rules. Note: The uncontrolled vehicle in this case rolled over which is why the curves abruptly end.

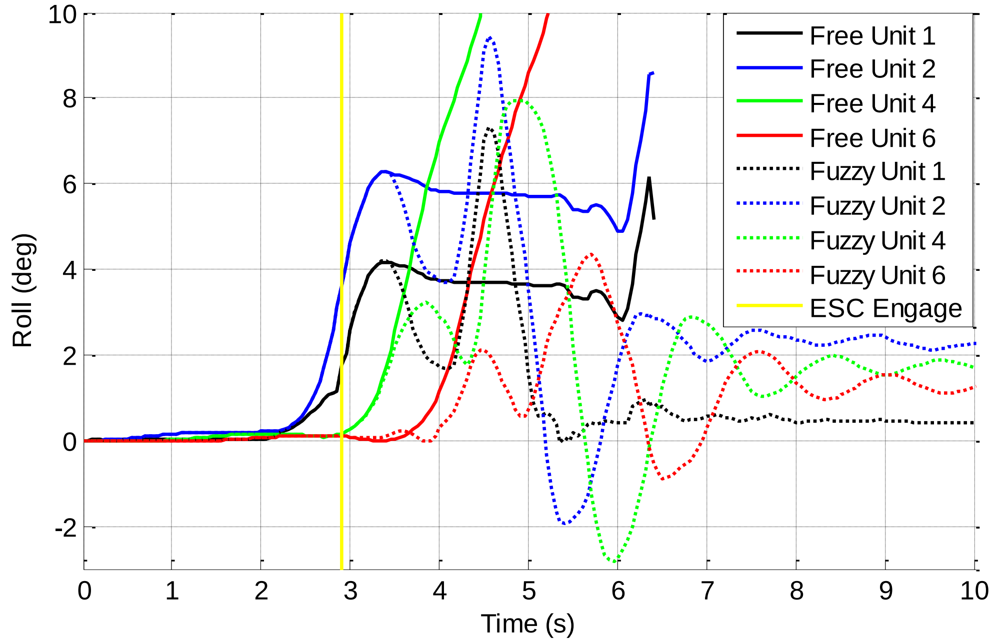

Figure 7-6: Roll Angle, Fuzzy, Loaded Vehicle, Step Steer, mu = 0.85

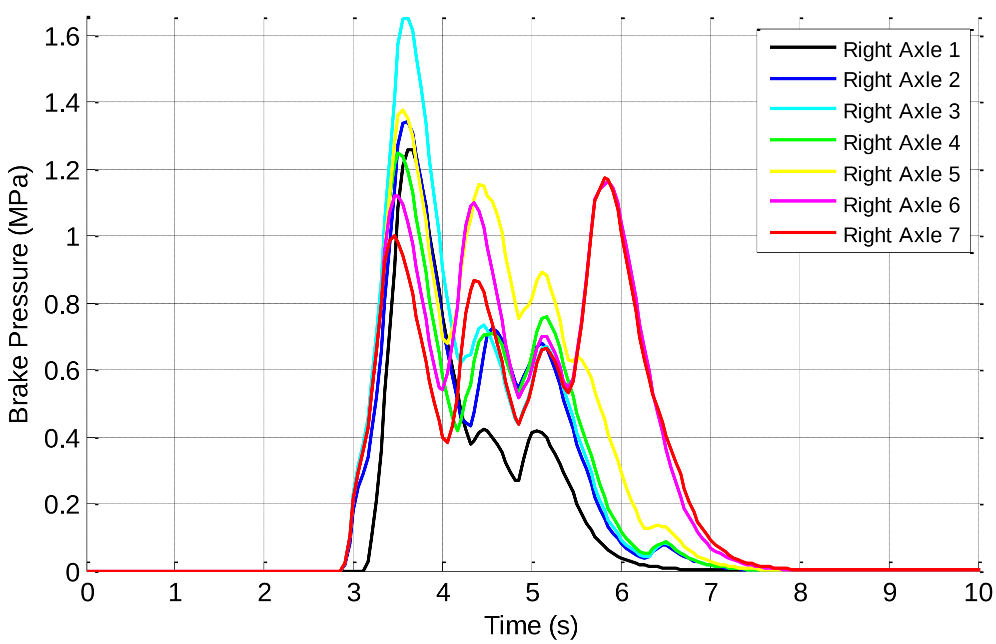

Figure 7-7: Right Side Brake Pressure, Fuzzy, Loaded Vehicle, Step Steer, mu = 0.85

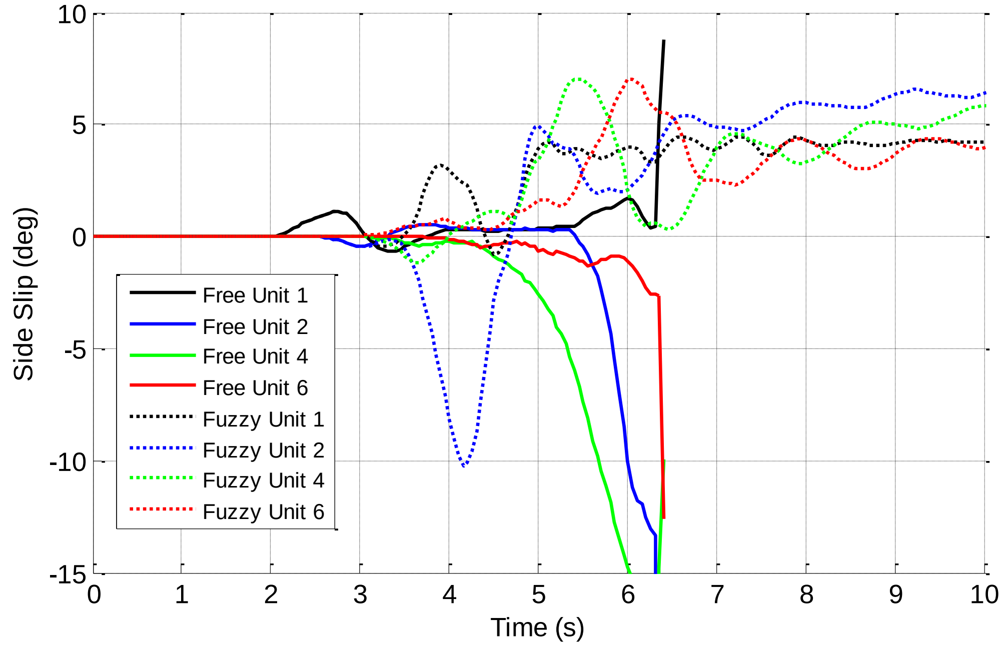

Figure 7-8: Side Slip, Fuzzy, Loaded Vehicle, Step Steer, mu = 0.85

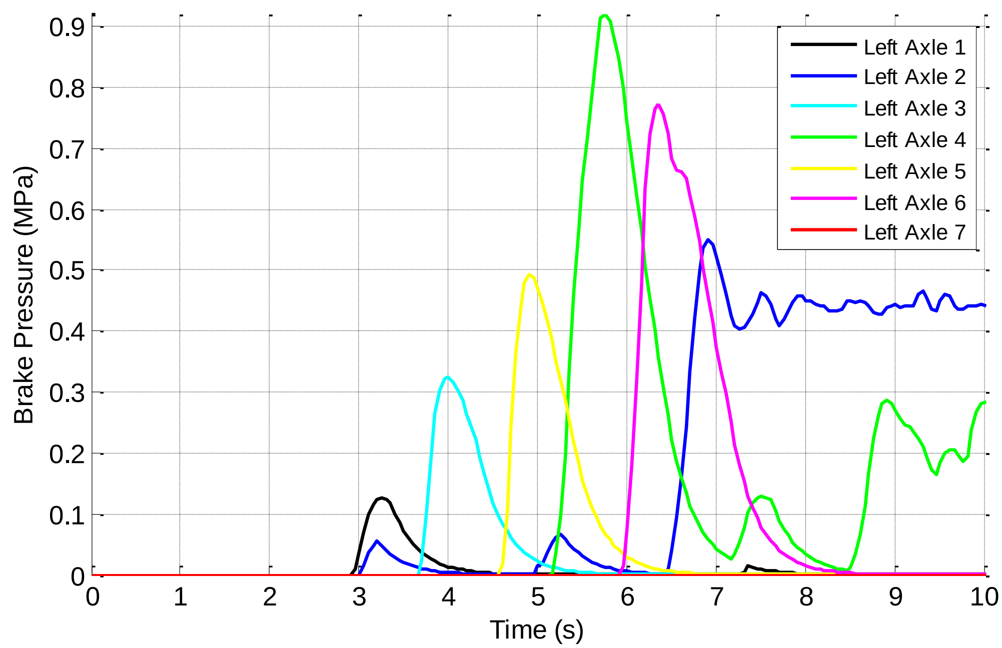

Figure 7-9: Left Side Brake Pressure, Fuzzy, Loaded Vehicle, Step Steer, mu = 0.85

7.3.3. Mid mu Case

When the above test maneuver was repeated on a wet track (mu = 0.6), the controller again intervened at 2.9 seconds (Figure 7-10 vs. Figure 7-6). The fuzzy logic controller does not have any information on road surface condition (it only sees the current states) so it cannot predict tire saturation effects. Thus, as the vehicle had not yet saturated its tires, the vehicle dynamics and controller performance were unchanged (relative to the mu = 0.85 case) up to this point. Consequently, the initial brake demand (Figure 7-11) was also similar to the dry case brake demand (Figure 7-7). However, once lateral saturation was reached, the controller adjusted to the vehicle's current dynamic state as can be seen in the brake modulation (Figure 7-12 vs. Figure 7-8). The controller managed the change in vehicle behavior through relative brake proportioning based on stability risks. Note: Saturation occurred around the 3.8 second mark.

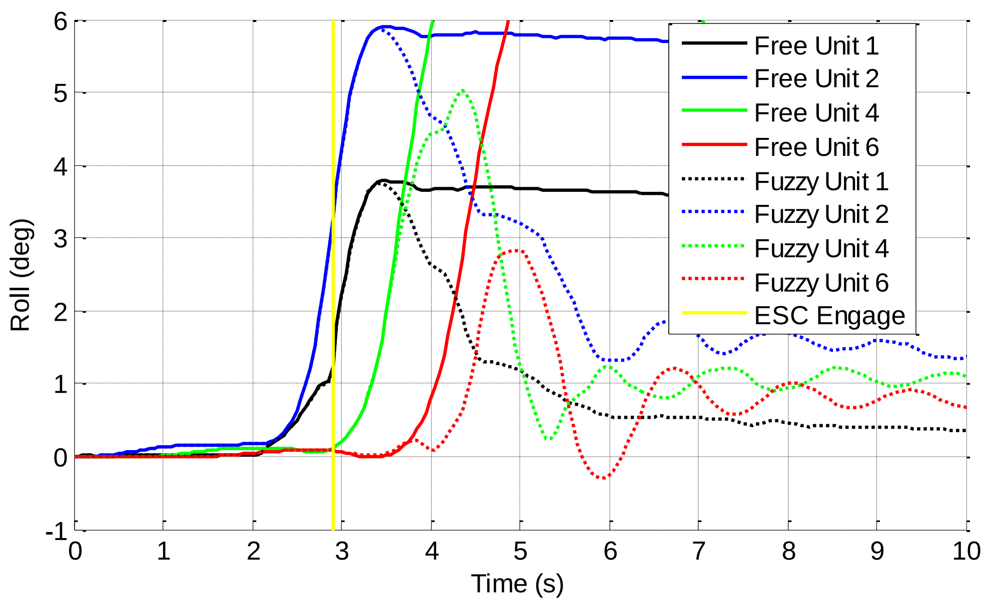

Figure 7-10: Roll, Fuzzy, Loaded Vehicle, Step Steer, mu=0.6

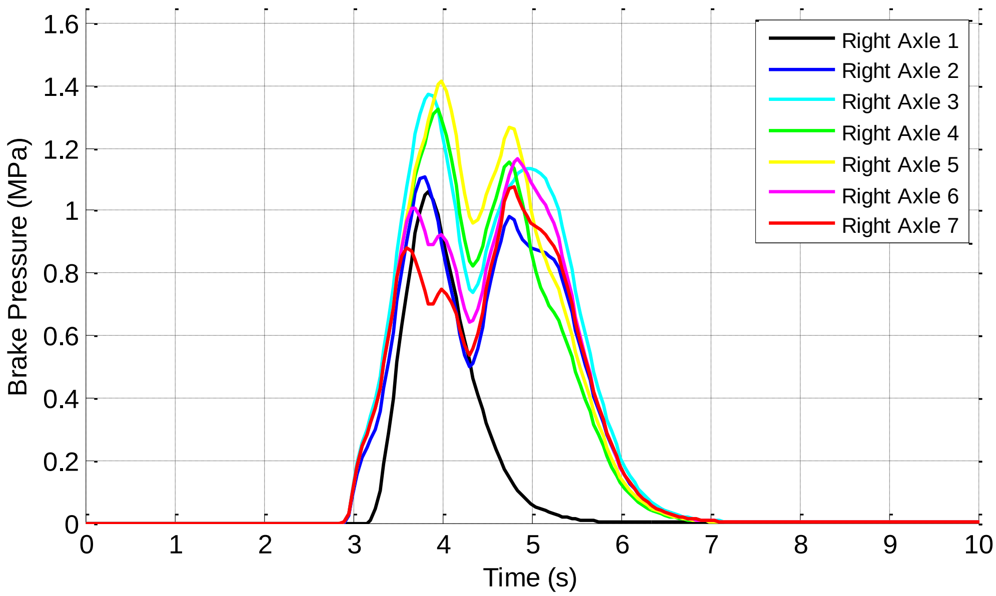

Figure 7-11: Right Brake Pressure, Fuzzy, Loaded Vehicle, Step Steer, mu=0.6

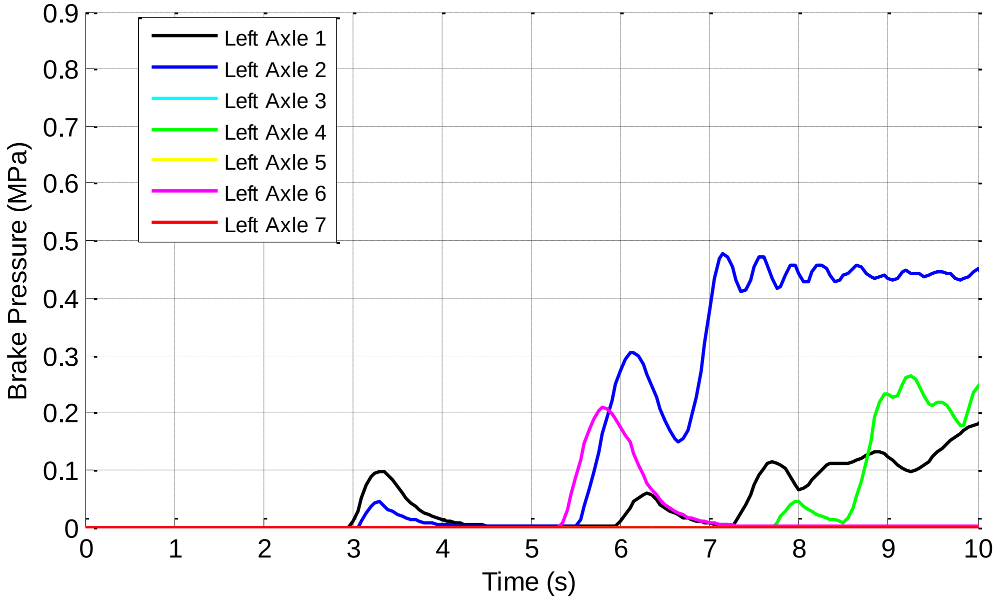

Figure 7-12: Left Brakes, Fuzzy, Loaded Vehicle, Step Steer, mu=0.6

7.3.4. Low mu Cases

Perhaps the most demanding case for a stability controller is the double lane change on ice. This maneuver has significant transients, reversals in trajectory, and very little traction available to stabilize the vehicle. These issues are why it has been deemed to be a nearly impossible problem by others in the past (Section 6.3.2). However, with careful development of the membership sets and rules, it was possible to create a fuzzy logic controller that stabilized the vehicle (see Section 7.2.3). Figure 7-13 shows the fuzzy logic vehicle (green) and the open loop vehicle (blue) at the end of the maneuver.

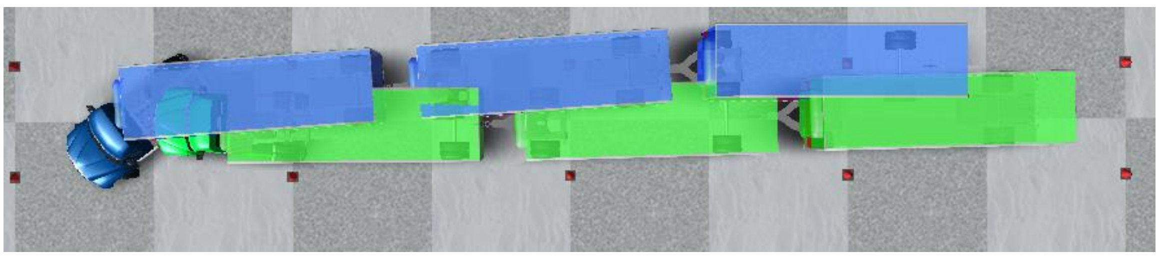

Figure 7-13: Fuzzy, Unloaded Vehicle, Double Lane Change, mu = 0.25

By reviewing the side slip angles (Figure 7-14); one can observe that the fuzzy logic controller did not prevent the tractor from experiencing large side slips. In fact the controlled tractor response is very nearly the same as the open loop vehicle until the vehicle is well within the second gate of the maneuver (125 meters into the event - Figure 7-15). This is a result of the controller not being able to anticipate what the tractor may experience. However, the controller does subsequently dampen the tractor's oscillation once it violates the set side slip bounds and triggers the controller. Note: The first ESC event occurred around 110 meters into the maneuver and the second occurred around 160 meters into the maneuver – both when the tractor side slip exceeded 4.3 degrees (Table 7-1).

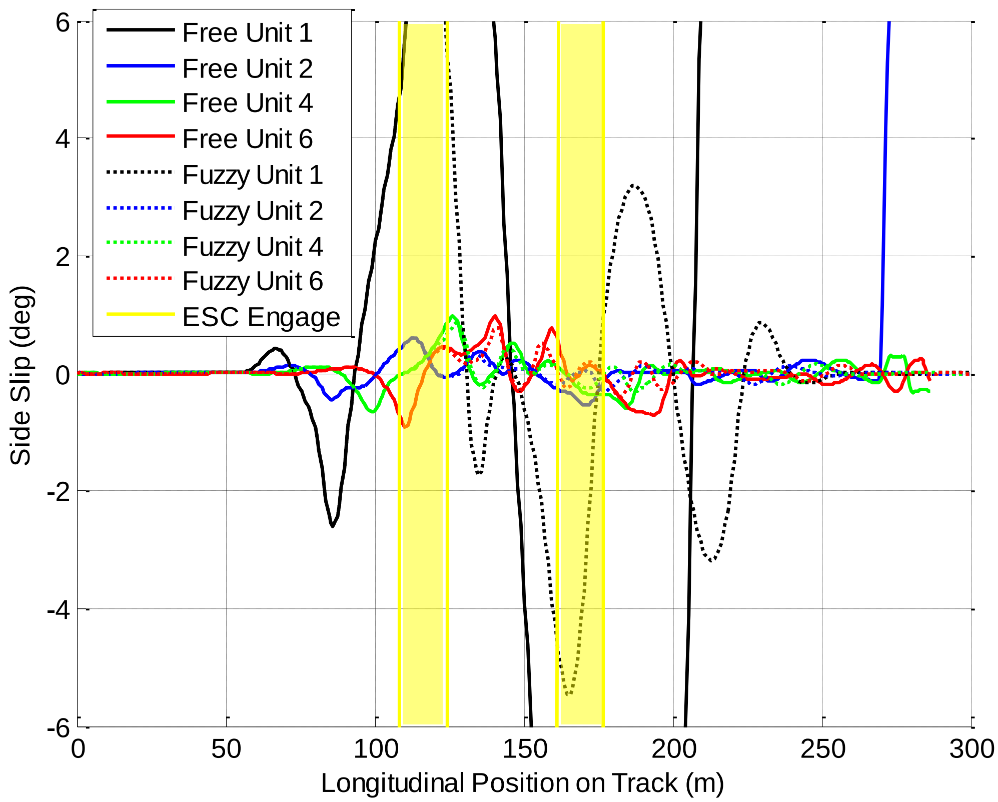

Figure 7-14: Side Slip, Fuzzy, Unloaded Vehicle, Double Lane Change, mu = 0.25

Figure 7-15 indicates that the large side slip deviations occurred when the driver was attempting to "straighten" the vehicle upon completion of a lateral position change. On a low mu surface, it is difficult to generate sufficient traction to counter the vehicle's inertia. For higher mu cases the lack of lateral control is not as great as there is more traction potential to exploit to drive the vehicle back to a safe operational point. Finally, the issues noted with brake time constants and their effects on controller quality (Section 6.6) apply to the fuzzy logic controller as well.

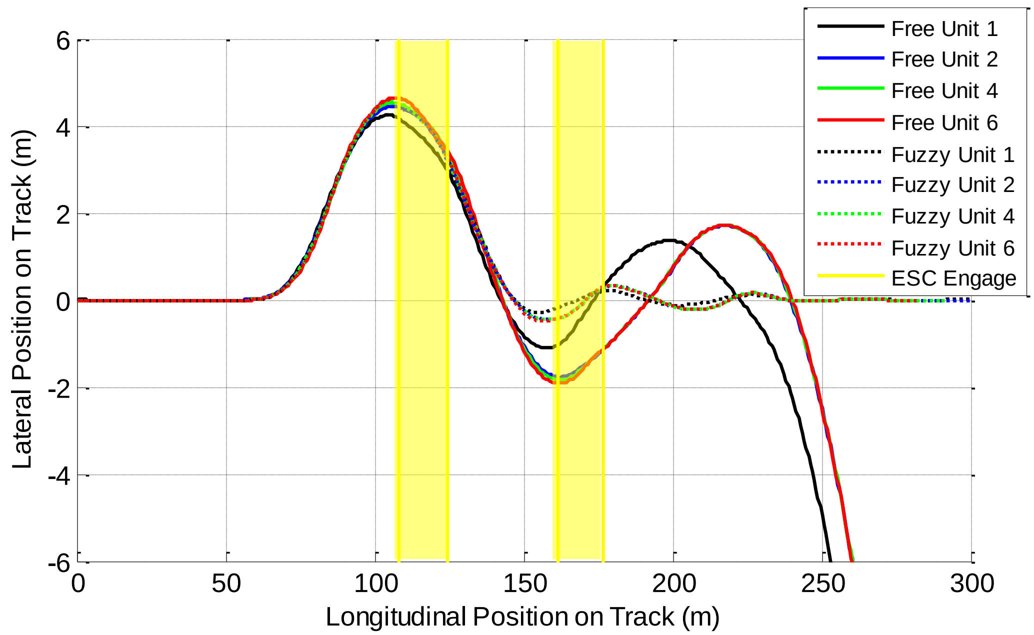

Figure 7-15: Vehicle Position, Fuzzy, Unloaded Vehicle, Double Lane Change, mu = 0.25

7.4. Bounds Sensitivity

As was the case with the MPC strategy, the fuzzy logic controller used bounds to define the safe operational range of the vehicle. Thus the same question on how sensitive the controller was to boundary selection was pertinent here as well. Figure 7-16 below shows the effect of bound size on the yaw rate of the tractor. Here it can be observed that a bound scaling of ±25% (increase / decrease of the boundary value by 25%) had little effect until the last part of the double lane change. As it seemed rather odd that the bound size would have had this effect, the vehicle speed was checked (Figure 7-17). Here it was observed that the tighter bounds resulted in the vehicle slowing dramatically. The “noise” for the 75% case in Figure 7-16 is actually the effect of drive torque induced yaw (tractor trying to maintain speed).

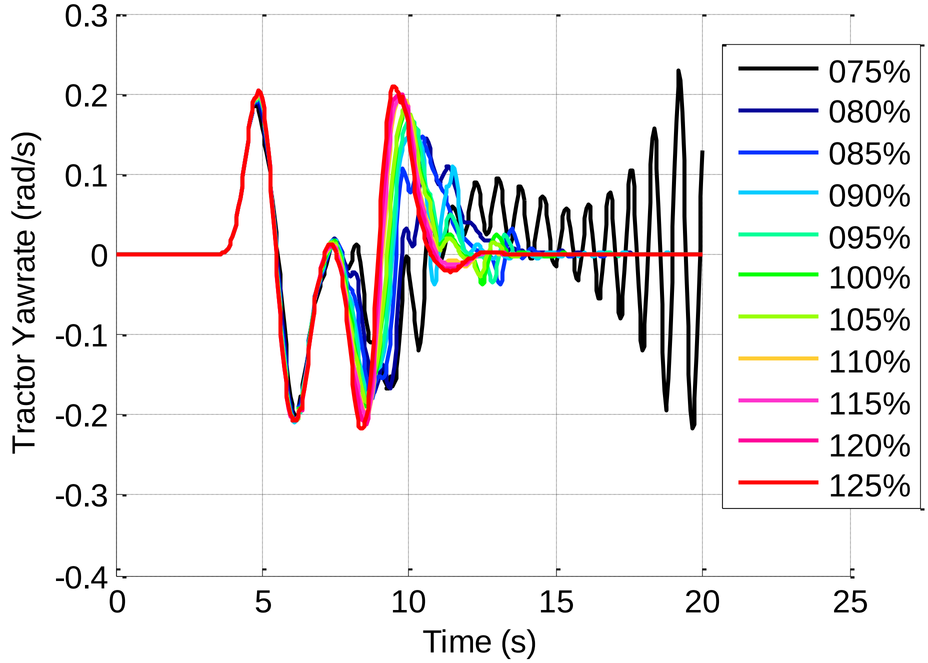

Figure 7-16: Fuzzy Logic Bound – Yaw Rate, Loaded Vehicle, Double Lane Change, mu = 0.85

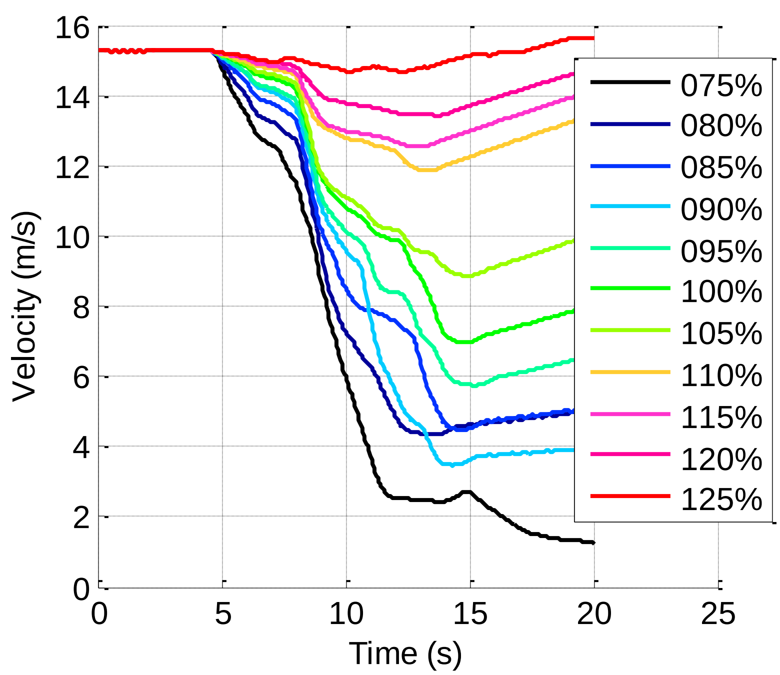

Figure 7-17: Fuzzy Logic Bound – Velocity, Loaded Vehicle, Double Lane Change, mu = 0.85

To make sure that the bound selection was not a particularly critical criterion for the controller, the second trailer side slip was evaluated (Figure 7-18). The controller performance is relatively robust with respect to the bound selection until the vehicle speed drops so low that the tractor begins to yaw heavily due to high torque and traction limitations. This causes the trailer to jerk laterally resulting in side slip errors. Note: similar investigations with other maneuvers showed similar limitations as well. The controller was reasonably insensitive to (reasonable) bound selections so long as the controller did not drastically alter the vehicle's speed.

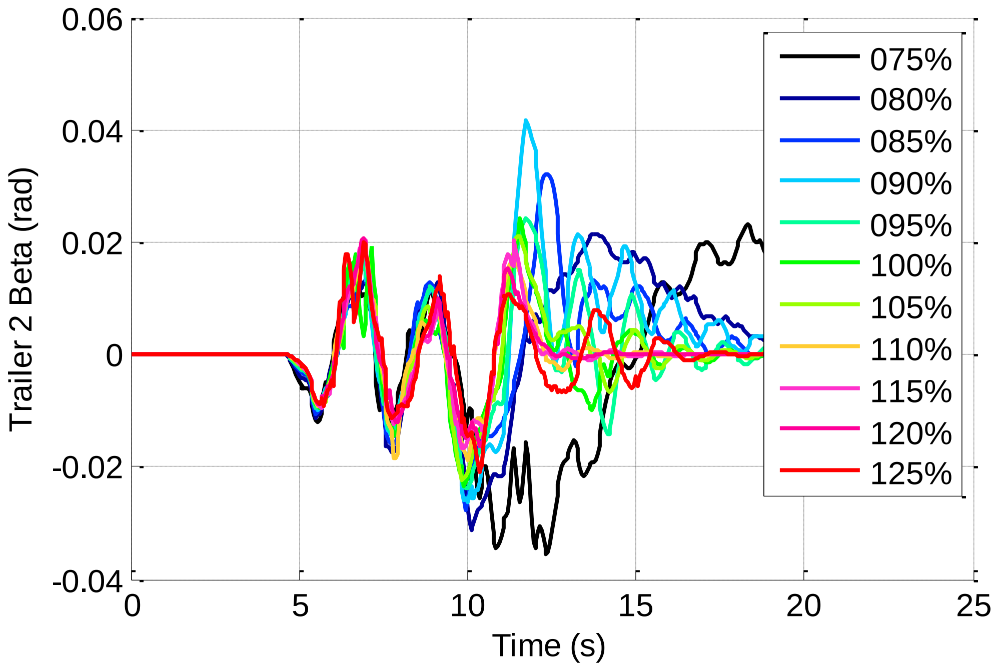

Figure 7-18: Fuzzy Logic Bound – Side Slip, Loaded Vehicle, Double Lane Change, mu = 0.85

7.5. Summary

The fuzzy logic controller was successful in improving the vehicle system's stability in every case it was tested. However, to reach that goal, significant tuning of the input sets and rules was necessary. This tuning was often times not particularly intuitive as the trade-offs were not always obvious. Had the vehicle system been decoupled, the design of the controller would have been much easier; but then a sophisticated controller like this would probably not have been needed as unit only controllers would have performed quite well in that environment. This is important as the controller's effectiveness in balancing competing stability needs and predicting what needs may arise was solely dependent on the quality of the set definitions and rules. It cannot derive new rules or set memberships as needed.

CHAPTER EIGHT

COMPARISON OF CONTROLLER PERFORMANCES

Since two different controllers were developed in this work, it seemed reasonable to compare their performances under differing circumstances. The objective of this comparison was not necessarily to determine which one was "better" but to use the comparison to gage where each strategy's strengths were. As the full analysis of the model predictive controller is available in Appendix J and the full analysis of the fuzzy logic controller is available in Appendix K, this section deals with a few highlights on each strategy.

8.1. General Theory

One of the development goals for both of the controllers was to break the traditional link to a reference model (linear model describing the "desired" vehicle behavior). This was accomplished by switching the control from reference following to boundary avoidance. To do this, the controllers needed some method to predict when stability risks might occur as reacting only to the current state with hard boundaries would produce abrupt control behaviors.

8.1.1. Model Predictive Control

The MPC approach tackled the need to predict future stability risks in a very elegant way. The ability to step the linear model forward in time and optimize the control approach for a finite horizon meant that accurate estimations of (near) future behavior could be made quickly. The optimization of the finite time also produced smoother brake activations as the controller could intervene with a smaller and less aggressive response before an instability event occurred.

8.1.2. Fuzzy Logic

While the fuzzy logic controller could not predict the future stability of the entire vehicle, it did have a limited ability to react before a trailer instability event occurred. As noted in Section 4.5, the trailers were the least stable parts of the system and the trailers saw events after the tractor. So by observing the behavior of the tractor and trailers and the use of rules which compared the dynamic states of the tractor and trailers the controller could anticipate the risks to the trailers and apply corrections before the trailers were at risk.

8.1.3. Predictive Case Study

Perhaps the worst case maneuver for combined yaw and roll stability is the dry double lane change with two unloaded trailers followed by a loaded trailer. The last trailer is subjected to the rear amplification effect (Section 4.4.3) and the last trailer is far more sensitive to rollover due to its higher CG. Figure 8-1 shows how both controllers reduced the roll of the last trailer. However, the MPC controller had a more significant reduction, including a reduction in roll at the first left hand turn (100 m station). The reason that the MPC had such a significant reduction in third trailer roll was that it applied a brake demand sooner (Figure 8-2) while the fuzzy logic waited until later before applying a “panic” full brake correction (Figure 8-3).

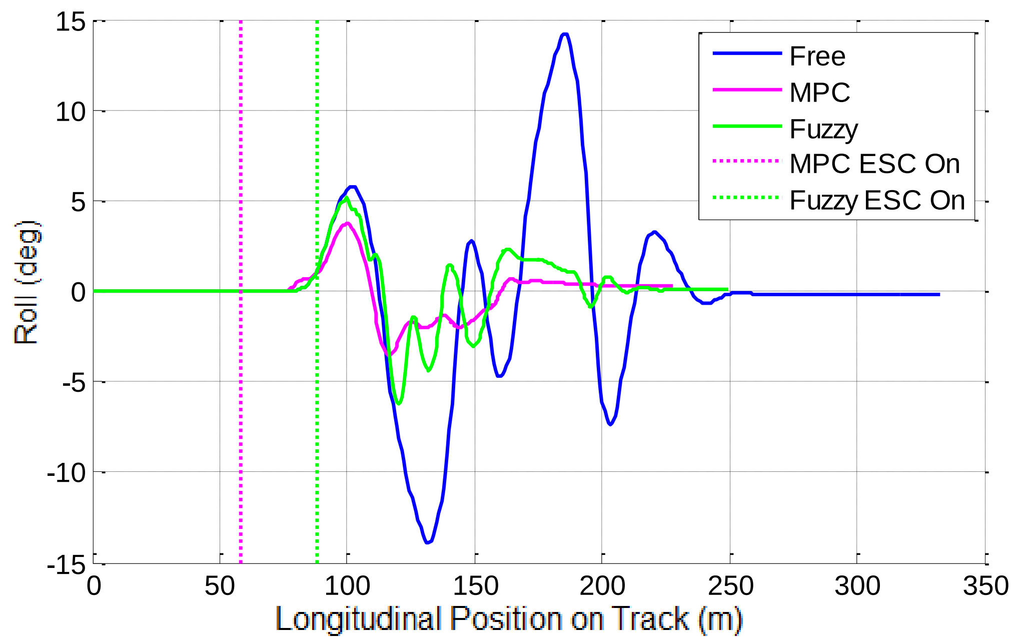

Figure 8-1: Roll Angle, Lane Change, Unloaded-Unloaded-Loaded, mu 0.85

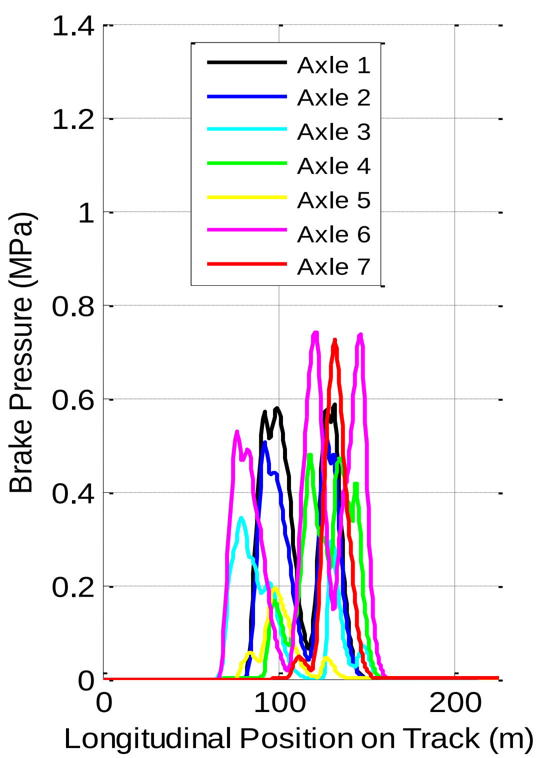

Figure 8-2: MPC Brake Demand, Lane Change, Unloaded-Unloaded-Loaded, mu 0.85

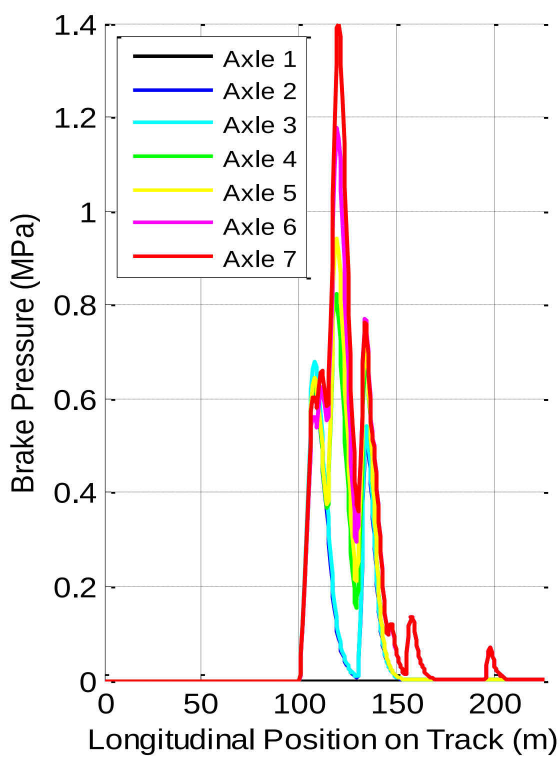

Figure 8-3: Fuzzy Brake Demand, Lane Change, Unloaded-Unloaded-Loaded, mu 0.85

In addition to the poorer roll performance, the consequence of the fuzzy logic's "panic" braking was the loss of lateral force at axle 5 and the resultant increase in side slip of the second trailer (Figure 8-4). Note: Trailer 3 did not show the same side slip as it had not yet reached the left turn. Now it might be possible to reduce the resultant side slip seen in this case through better rule development, but attempts to do so resulted in other negative consequences such as slower response times and smaller corrective moments.

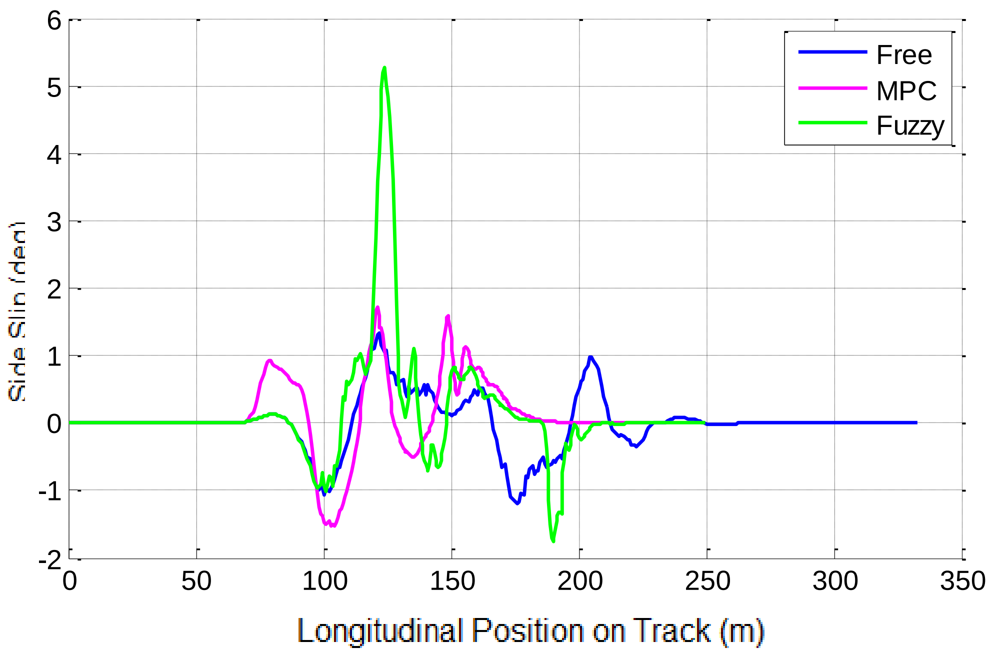

Figure 8-4: Trailer 2 Side Slip, Lane Change, Unloaded-Unloaded-Loaded, mu 0.85

The MPC controller was able to better gage the vehicle system threat as it had a linear model (with the correct loading arrangement) to predict future behavior. The fuzzy logic controller only knew the roll behavior of the tractor and leading trailers (which had typical lower roll angles) to predict what the last trailer would do (Figure 8-1). One could argue that the fuzzy logic controller should be able to predict that the last trailer would be more susceptible to roll instability based on a time history of the vehicle dynamics up to this point; but in practice, this resulted in over application of the brakes as the roll behavior is non-linear due to the fifth wheel arrangement (see Section 3.2.1).

8.2. Head-to-Head Cases

As a follow-up to the predictive case study, a series of head-to-head studies were investigated. The six case studies were selected as they either represented a particularly difficult control problem or highlighted some aspect of one of the controllers. More information on the controller responses is available in Appendix J (MPC) and Appendix K (fuzzy logic).

8.2.1. Unloaded Vehicle Ramp Steer on Ice

A ramp steer maneuver is a test where the vehicle is given a fixed steering rate while traveling at a fixed (or at least initially fixed) speed. Depending on the need of the test, the input can be slow or quick. In this case, the vehicle was traveling at 40 km/h on ice and the steer input was 6 degrees / second at the steering wheel (0.24 degrees / second road wheel). This is a steady state test and it shows how the controllers deal with slowly encroaching stability risks.

The primary objective of the controllers in this case was to keep the vehicle from yaw divergence (ice road). Due to its predictive capability, the MPC activated first (Figure 8-5) but both controllers had the same initial side slip angles (Figure 8-6). However, the MPC system could “see” that it was headed to a jackknife due to the large steering demand at the end of the maneuver while the fuzzy logic system could only see the current states which did not indicate such a threat. As a result, the MPC kept applying brakes until the vehicle stopped while the fuzzy logic jackknifed (Figure 8-7). While this is admittedly a rather obtuse situation (the driver would never do this), it is useful for showing the value of the predictive part of the MPC.

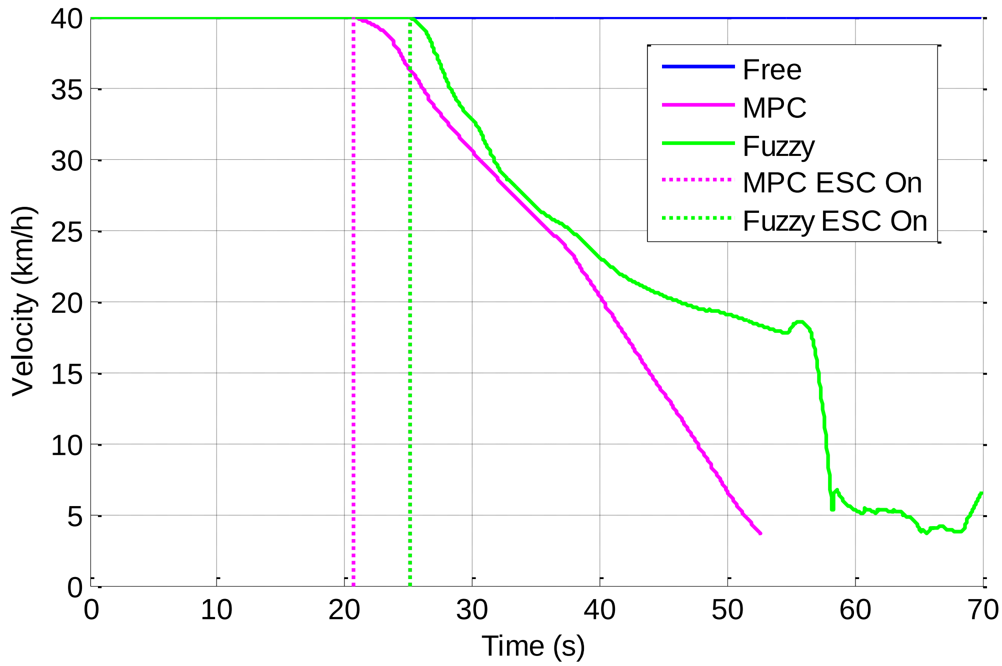

Figure 8-5: Velocity, MPC - Fuzzy Comparison, Unloaded Ramp Steer, mu = 0.25

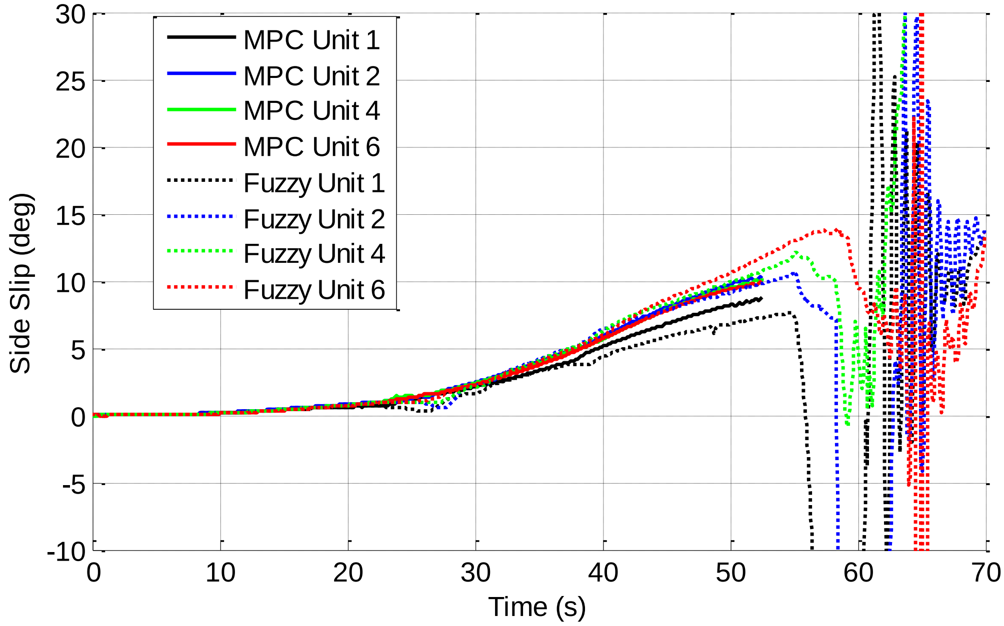

Figure 8-6: Side Slip, MPC - Fuzzy Comparison, Unloaded Ramp Steer, mu = 0.25

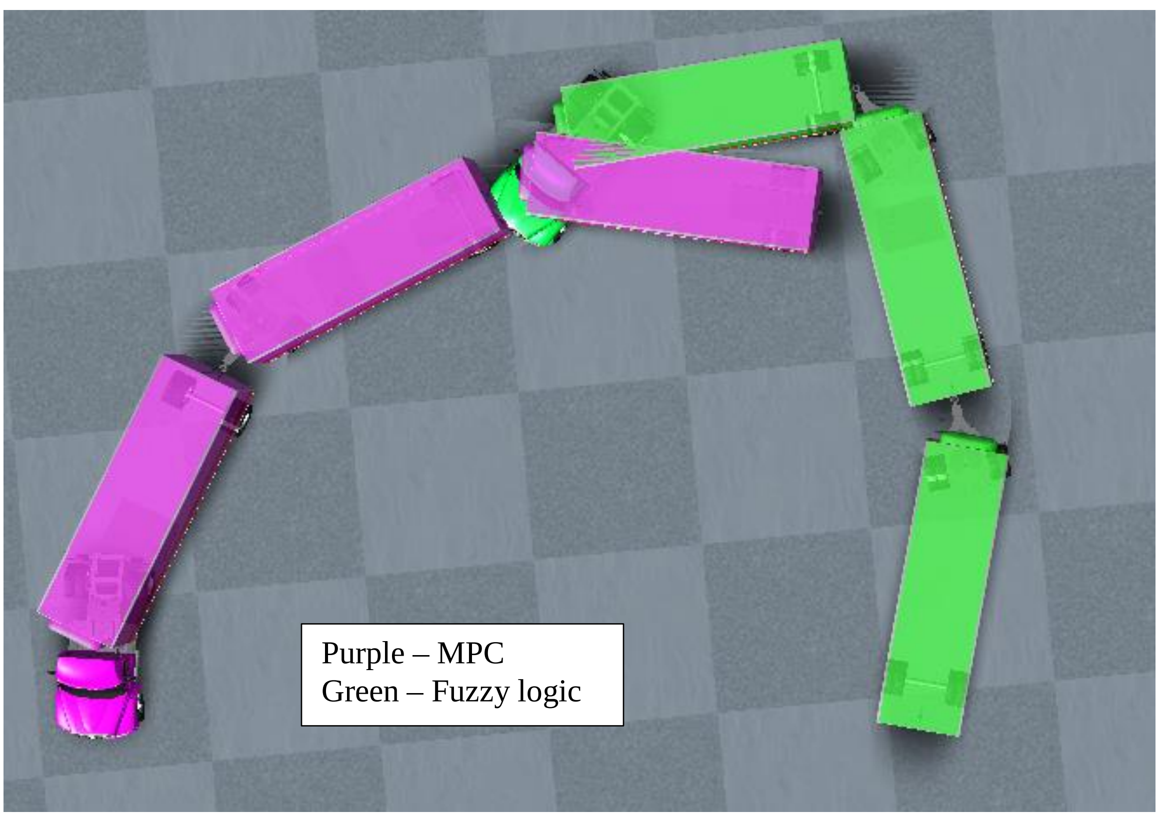

Figure 8-7: Illustration, MPC - Fuzzy Comparison, Unloaded Ramp Steer, mu = 0.25

8.2.2. Unloaded Vehicle Step Steer on Ice

While the case study in Section 8.2.1 demonstrated the value of the MPC's predictive capability, the case here shows a potential weakness in the MPC predictive capability. The unloaded vehicle step steer on ice is an interesting case study as the free response of the vehicle is stable. The vehicle may slide, but all states remain well within safe bounds. Since there is no "reference" path to indicate that the vehicle needs corrective action, the controller should just let the vehicle proceed. The fuzzy logic controller (green truck in Figure 8-8) does just that (blue truck is uncontrolled). However, the MPC controller intervenes and slows the vehicle (pink truck) at the cost of more side slip (Figure 8-9). Now the MPC vehicle never violates the side slip bounds of 5.7 degrees (Table 6-1) so the solution is still a "safe" condition. But the MPC activated when the free response vehicle was never in danger.

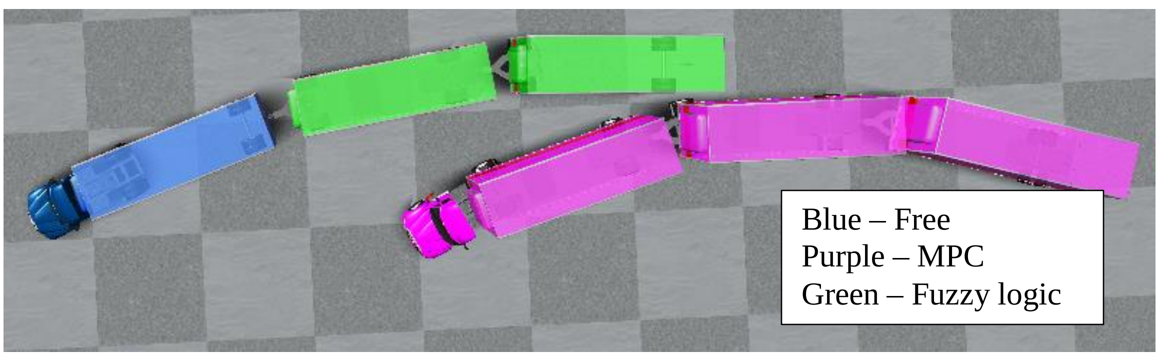

Figure 8-8: Illustration, MPC - Fuzzy Comparison, Unloaded Step Steer, mu = 0.25

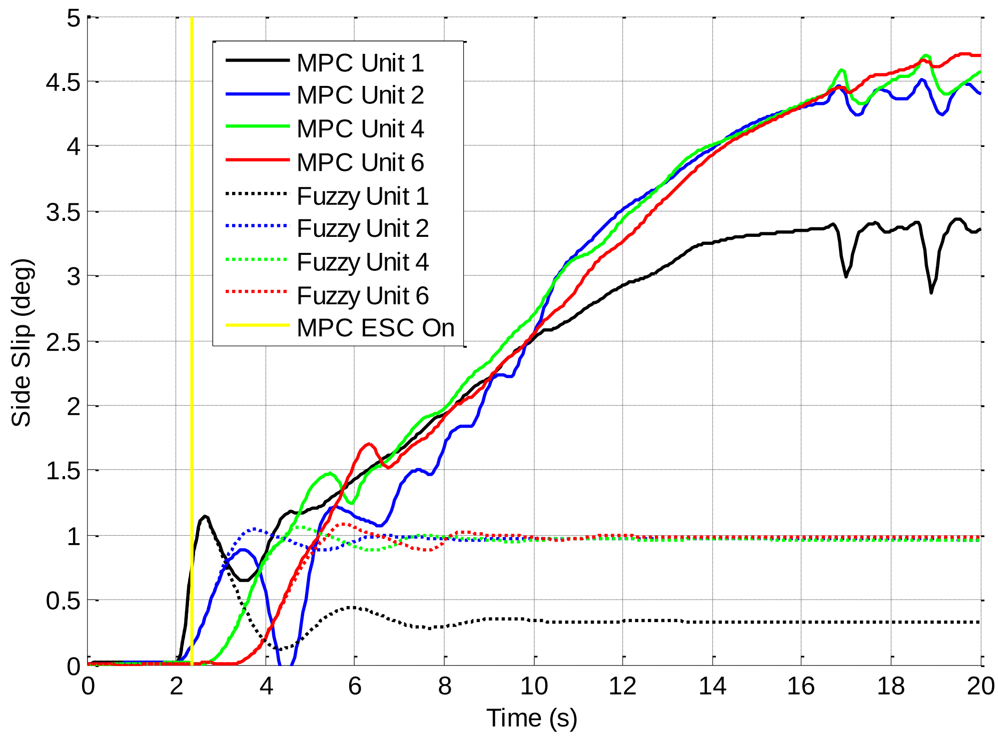

Figure 8-9: Side Slip, MPC - Fuzzy Comparison, Unloaded Step Steer, mu = 0.25

The explanation as to why this non-obvious MPC activation occurs is as follows: The predictive response of the MPC is based on the current vehicle's states and the LTI model. However, the LTI model does not contain any information on road surface; it only contains information on cornering stiffness. Thus the predicted roll response was significantly higher than the actual roll of the vehicle as the prediction did not account for tire saturation effects. This higher roll prediction was what triggered the MPC to activate the brakes. The result was that the MPC erred on the side of over application of stability control. Whether this is desirable or not is a point of debate.

8.2.3. Unloaded Vehicle Double Lane Change on Wet Asphalt

Wet asphalt can be a tricky surface to manage as both yaw and roll issues are likely to occur (Section 2.1.2) and correcting one stability risk can cause a second risk (Sections 2.2.2 and A.2.4). In this case the open loop vehicle was susceptible to third trailer roll (Figure 8-10). The controllers recognized this risk and reacted but the MPC reacted sooner (prediction capability) and less aggressively (Figure 8-11). The result of the delayed and more aggressive brake command from the fuzzy logic controller (Figure 8-12) was a reduced efficiency in resisting roll (Figure 8-10) and an increase in trailer three side slip (Figure 8-13, Figure 8-14) as the sudden brake (longitudinal force) limited the tire's lateral force potential.

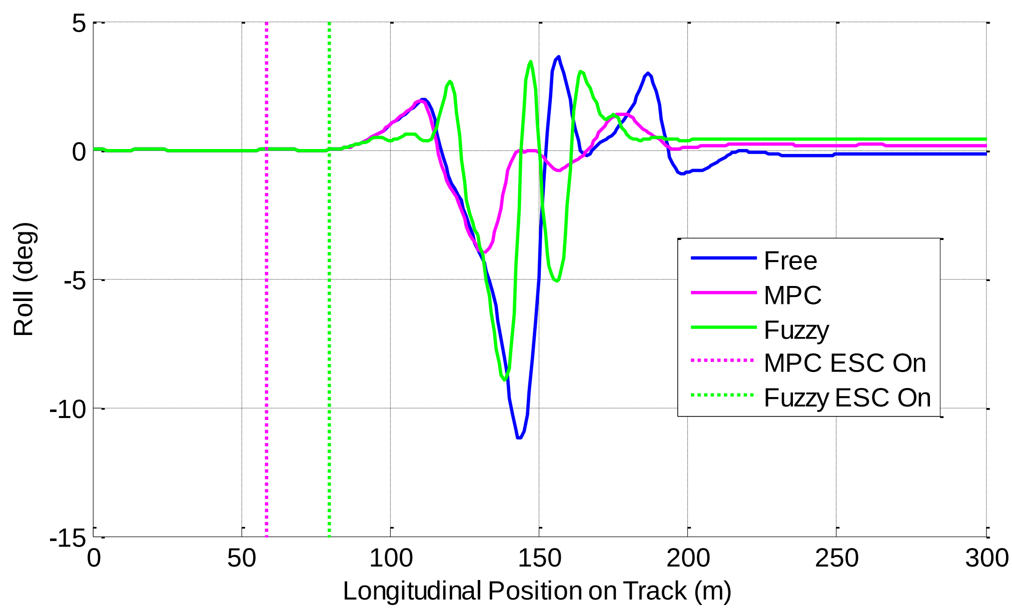

Figure 8-10: Trailer 3 Roll, MPC - Fuzzy Comparison, Unloaded Double Lane Change, mu = 0.6

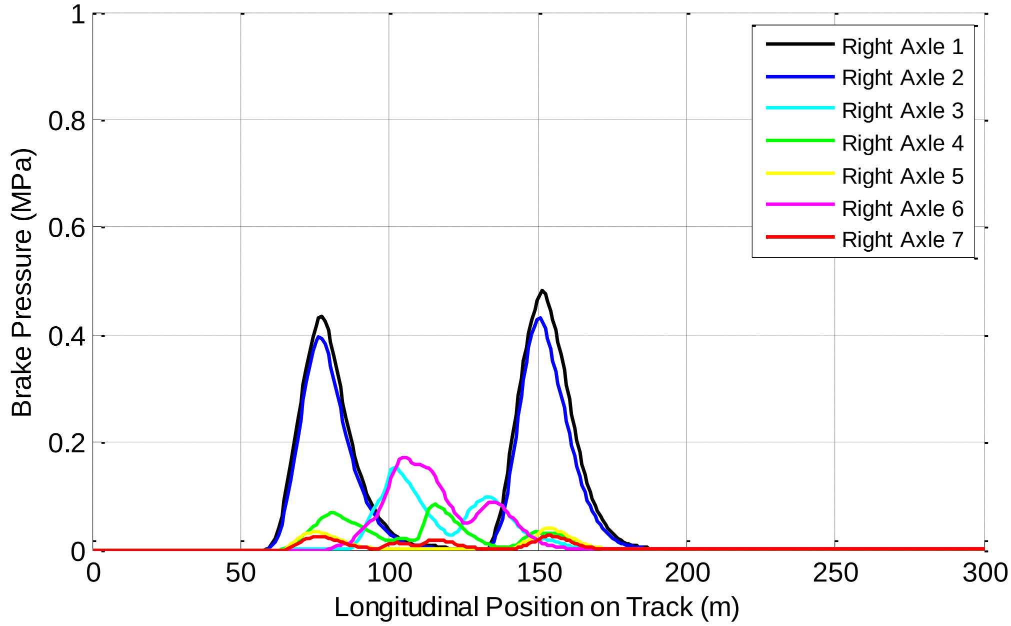

Figure 8-11: Brake Pressure, MPC, Unloaded Double Lane Change, mu = 0.6

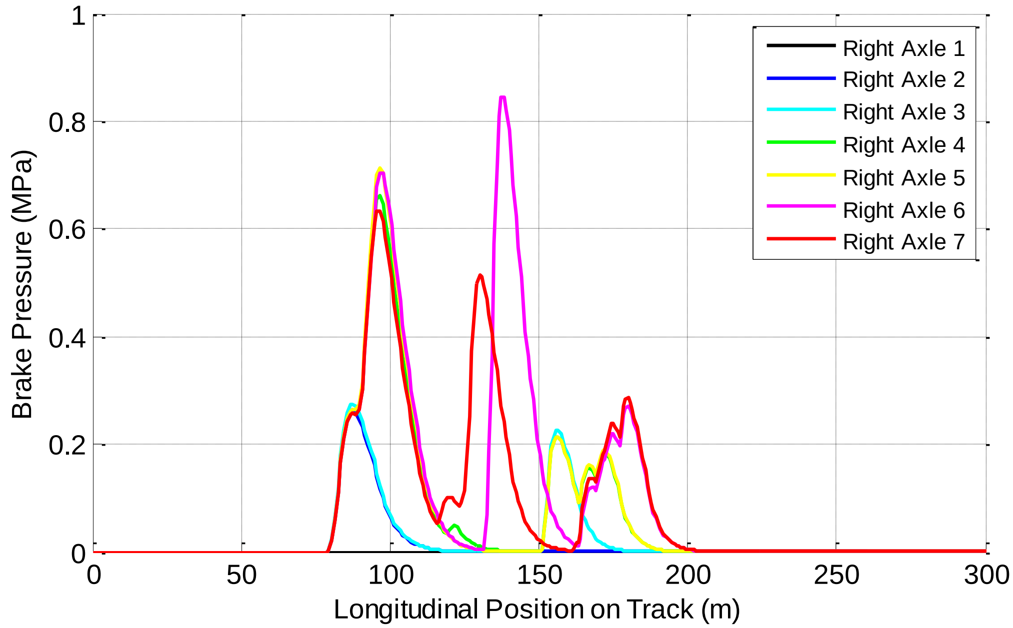

Figure 8-12: Brake Pressure, Fuzzy, Unloaded Double Lane Change, mu = 0.6

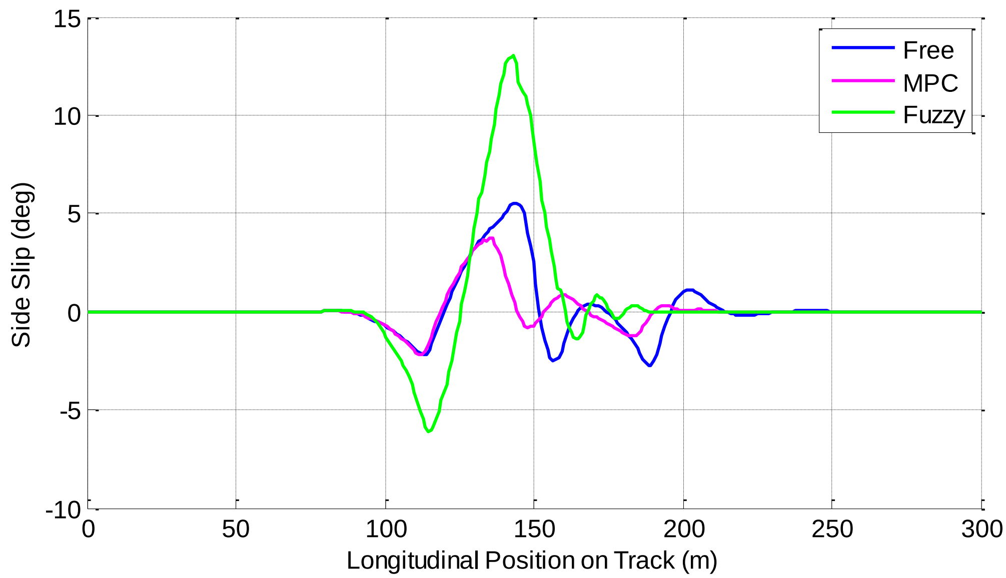

Figure 8-13: Trailer 3 Side Slip, MPC - Fuzzy Comparison, Unloaded Double Lane Change, mu = 0.6

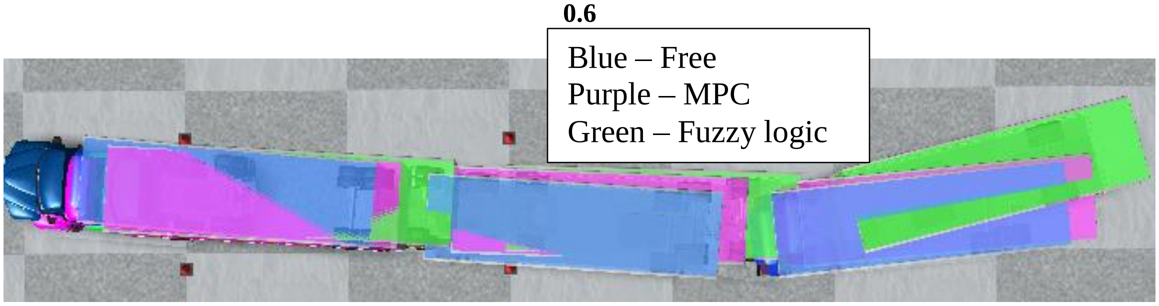

Figure 8-14: Illustration, MPC - Fuzzy Comparison, Unloaded Double Lane Change, mu = 0.6

8.2.4. Loaded Vehicle Double Lane Change on Wet Asphalt

Adding a payload to the above double lane change on wet asphalt case increased the roll risk (Figure 8-15 and Figure 8-16) as one would expect. As the fundamental controller strategies had not changed, the MPC controller was again able to react sooner and with less brake demand (Figure 8-16 or Figure 8-17 vs. Figure 8-18). It also resulted in better roll dynamics relative to the fuzzy logic controller. Note: To gage how aggressive the fuzzy logic brake demand was, it is helpful to observe how quickly the vehicle's speed reduced when the controller activated (Figure 8-19).

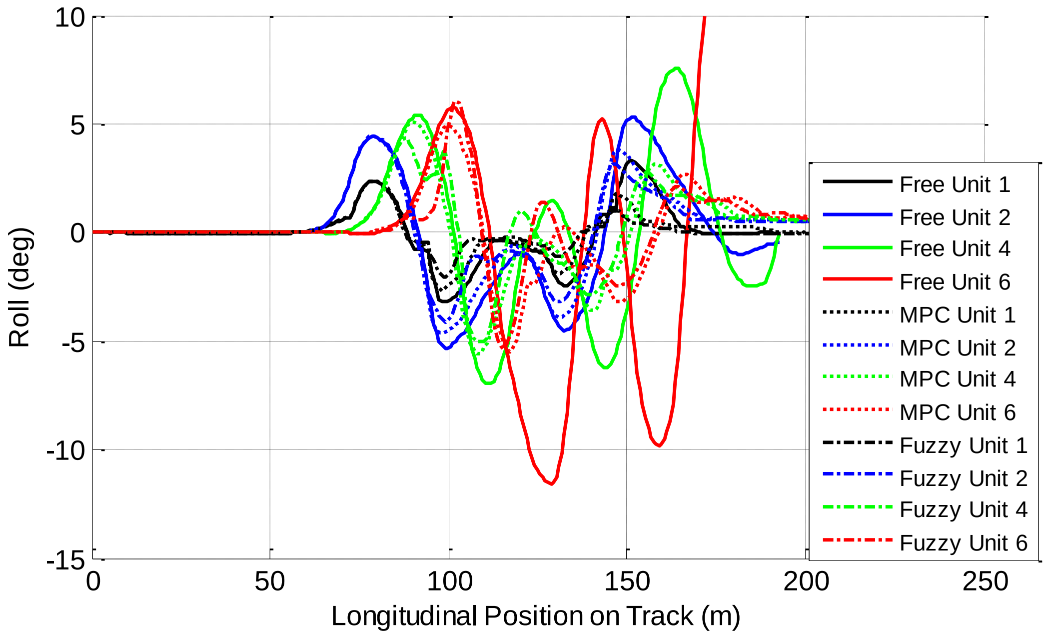

Figure 8-15: Roll Angle, MPC - Fuzzy Comparison, Loaded Double Lane Change, mu = 0.6

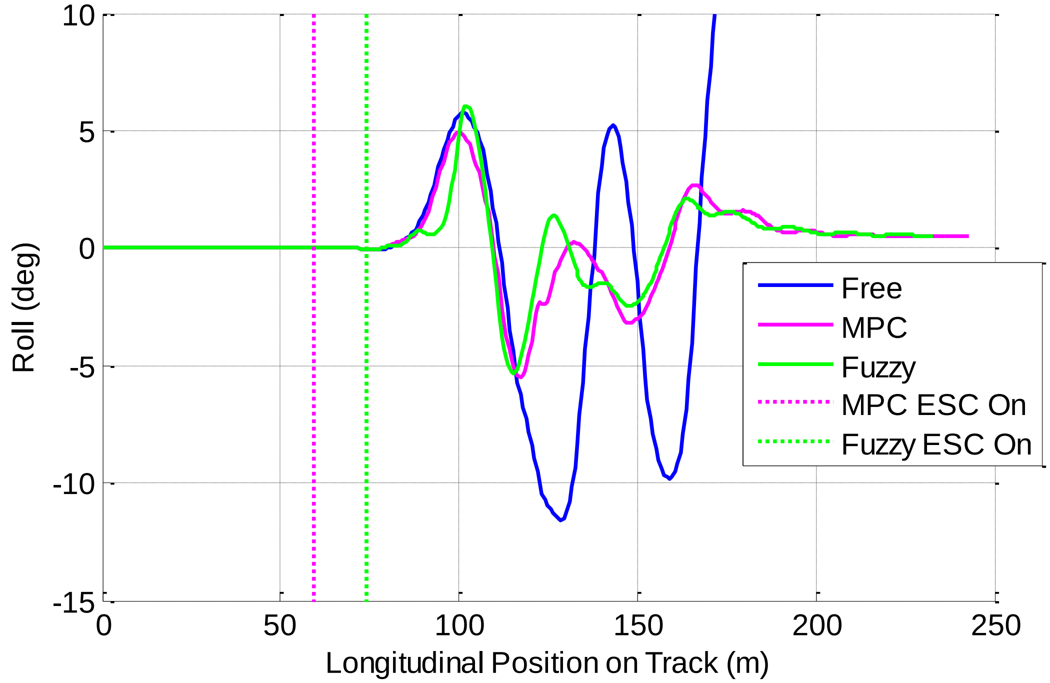

Figure 8-16: Trailer 3 Roll, MPC - Fuzzy Comparison, Loaded Double Lane Change, mu = 0.6

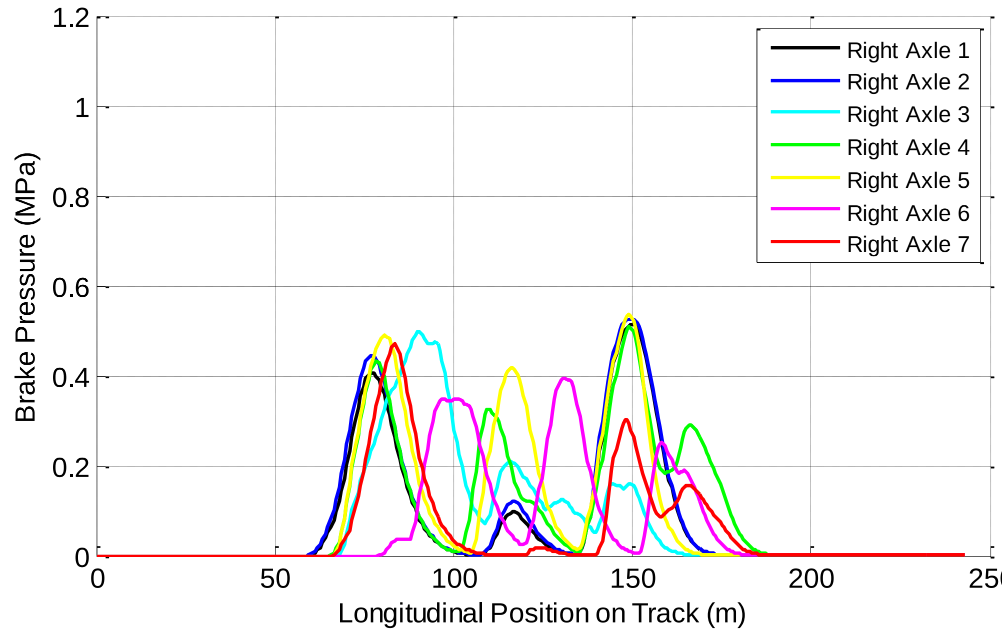

Figure 8-17: Brake Pressure, MPC, Loaded Double Lane Change, mu = 0.6

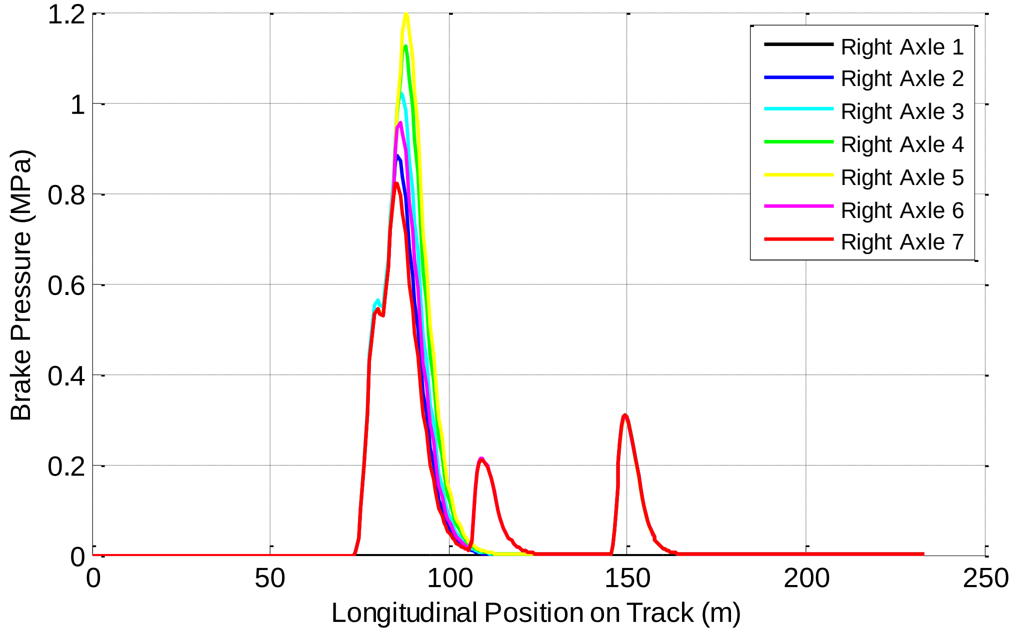

Figure 8-18: Brake Pressure, Fuzzy, Loaded Double Lane Change, mu = 0.6

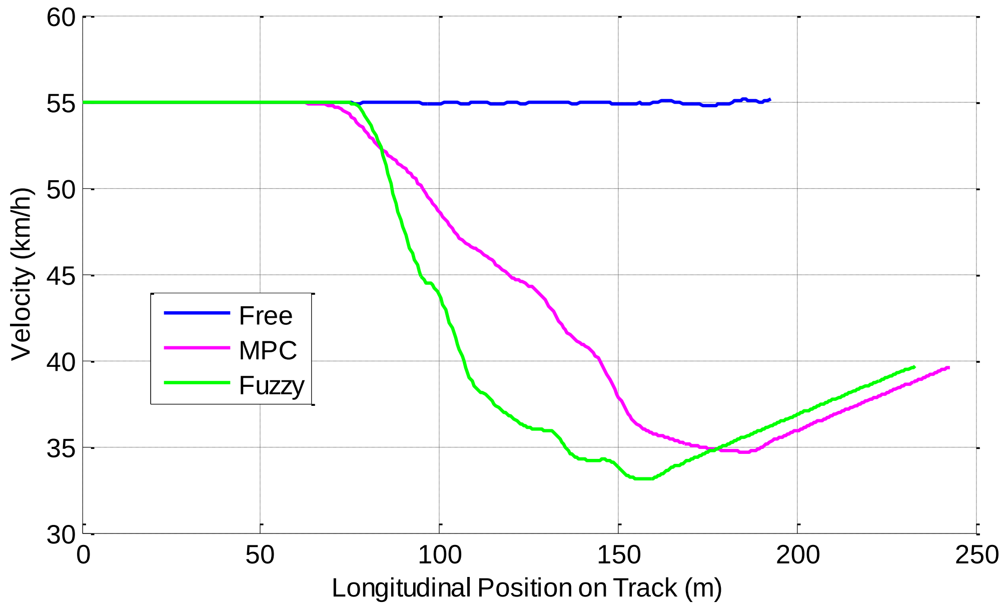

Figure 8-19: Velocity vs. Station, MPC - Fuzzy Comparison, Loaded Double Lane Change, mu = 0.6

8.2.5. Loaded Vehicle Step Steer on Ice

The model predictive controller was not always the winner in head to head analysis cases. For instance, the MPC does not monitor or control for trailer offset (lateral path deviation). Thus the MPC had no idea that trailers one and two were colliding in the loaded step steer test on ice (Figure 8-20). As the side slip for each unit was within bounds (Figure 8-21) up until the point the trailers contacted and displaced the first trailer, the MPC thought all was well. While the MPC did a better job of modulating the brakes for optimal stability (Figure 8-22 vs. Figure 8-23), it was blind to the real risk. Now, to be fair, the fuzzy logic controller is also blind to this unit-to-unit contact risk, but its controller strategy is simpler and fixed so there is reasonable confidence that this type of issue is very unlikely to occur.

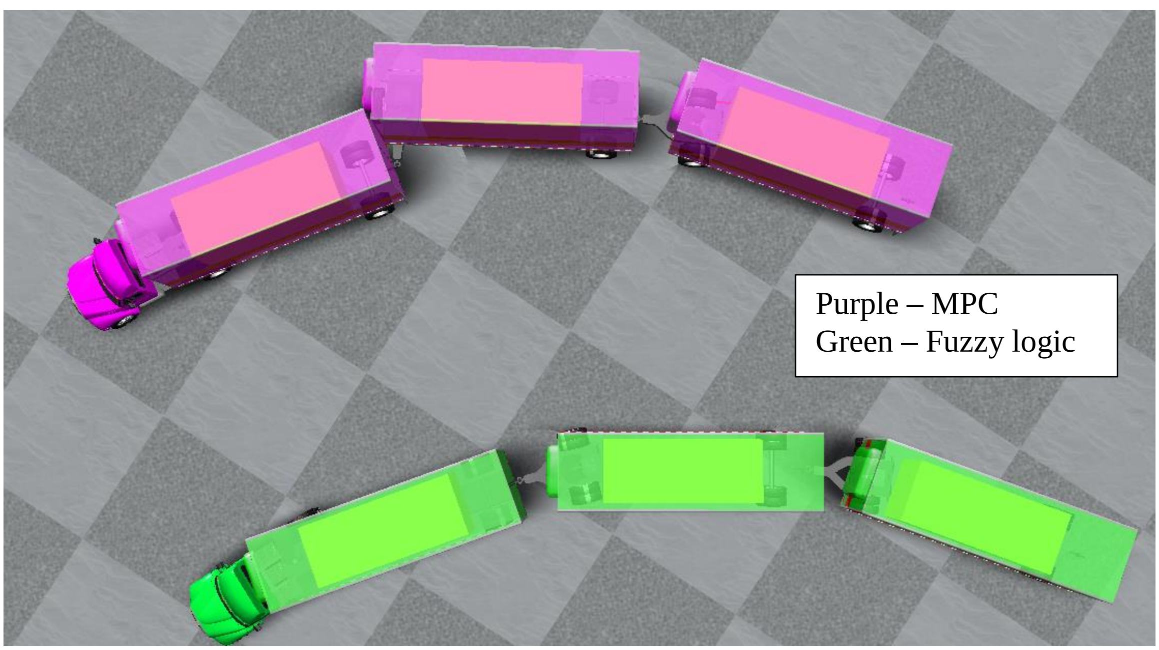

Figure 8-20: Illustration, MPC - Fuzzy Comparison, Loaded Step Steer, mu = 0.25

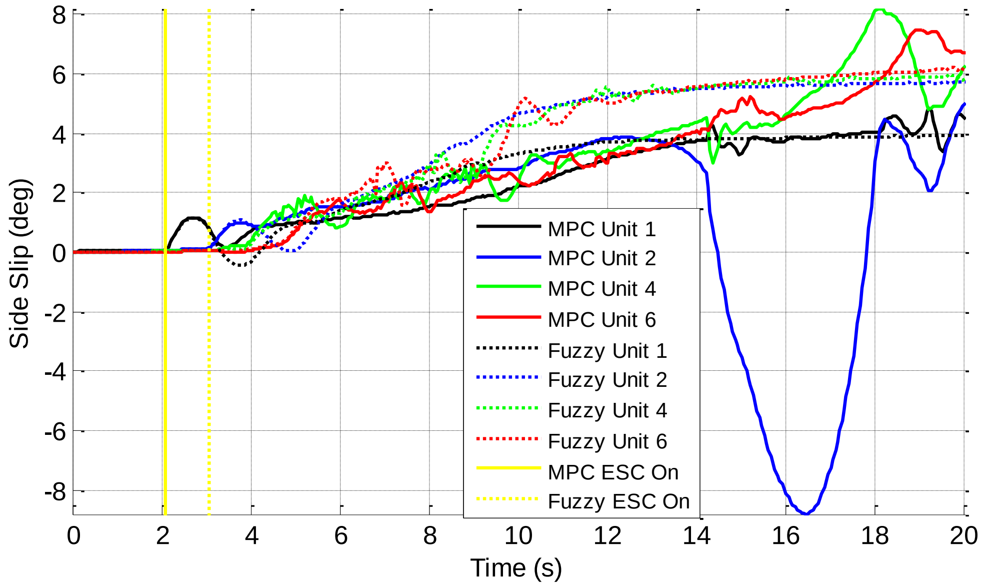

Figure 8-21: Side Slip, MPC - Fuzzy Comparison, Loaded Step Steer, mu = 0.25

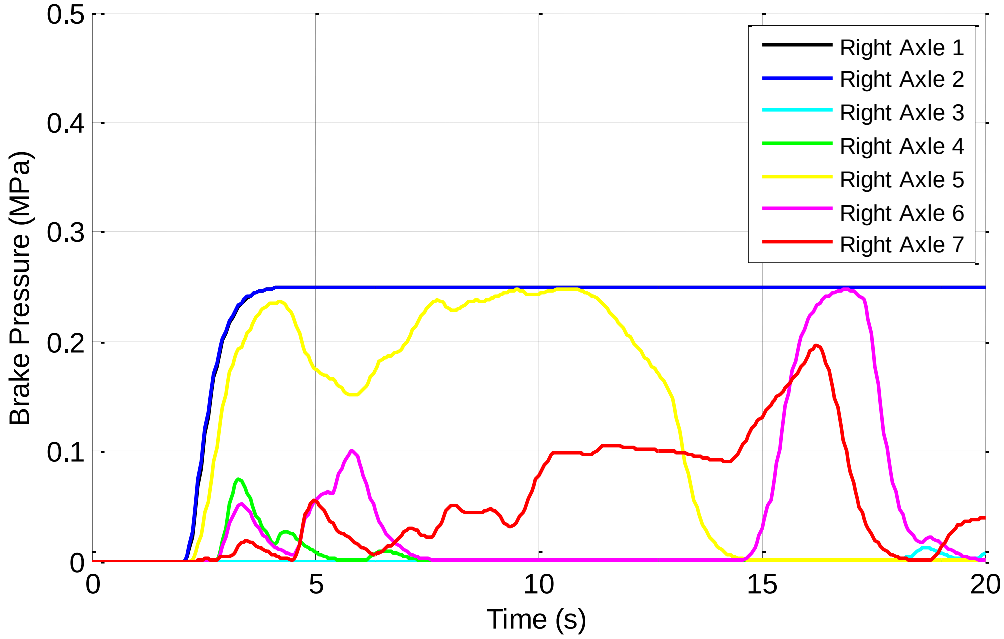

Figure 8-22: Brake Pressure, MPC, Loaded Step Steer, mu = 0.25

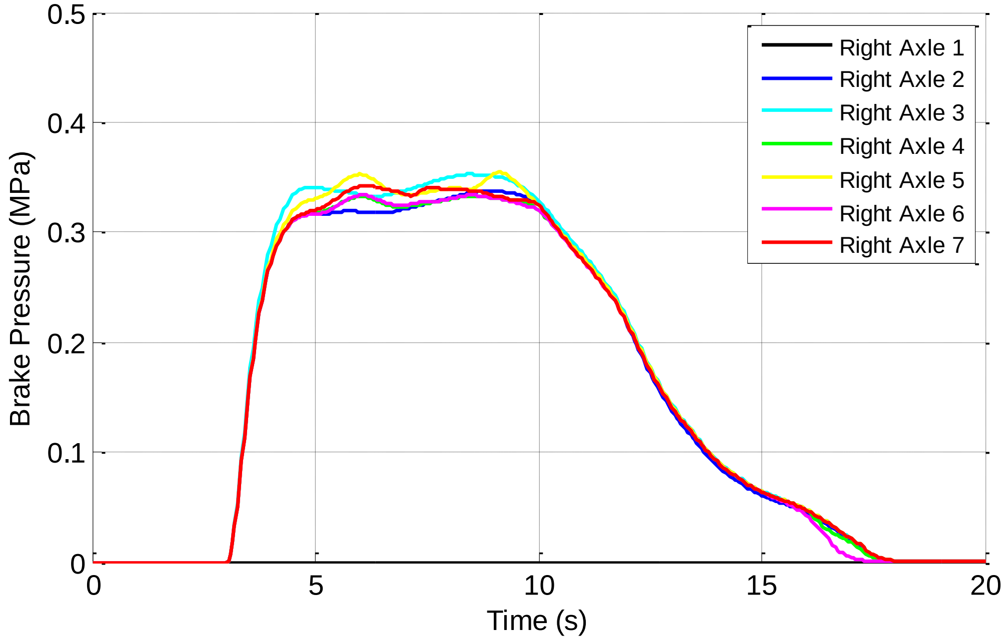

Figure 8-23: Brake Pressure, Fuzzy, Loaded Step Steer, mu = 0.25

8.2.6. Empty Vehicle Step Steer Dry

One would normally think that an unloaded vehicle on dry asphalt would not have a significant roll risk with a low CG height and plenty of traction. However, if you get a commercial vehicle going fast enough, you can overturn it with relative ease (Figure 8-24). Reviewing the controller responses for trailer 3 (unit 6) roll (Figure 8-25) showed that both controllers quickly saw the potential problem and addressed it though the MPC again reacted more quickly.

This case is of interest here as it highlights a consequence of the fuzzy logic controller's aggressive brake response (Figure 8-27 vs. Figure 8-26). With a low mass and high brake demand, the trailers began to hop and this can be seen in the roll (Figure 8-25) and side slip (Figure 8-28). The controller attempted to regulate the brake pressure

(Figure 8-27) but was unable to mitigate the effect. While this effect does not pose a stability risk, it would be unwelcome by the driver.

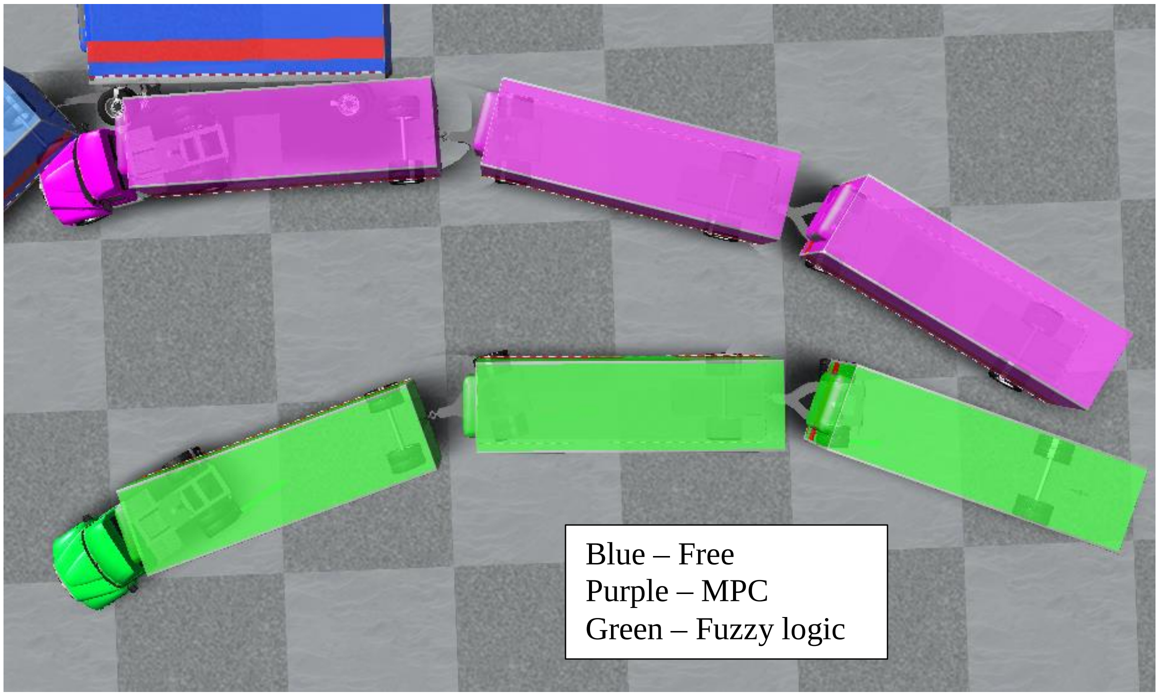

Figure 8-24: Illustration, MPC - Fuzzy Comparison, Unloaded Step Steer, mu = 0.85

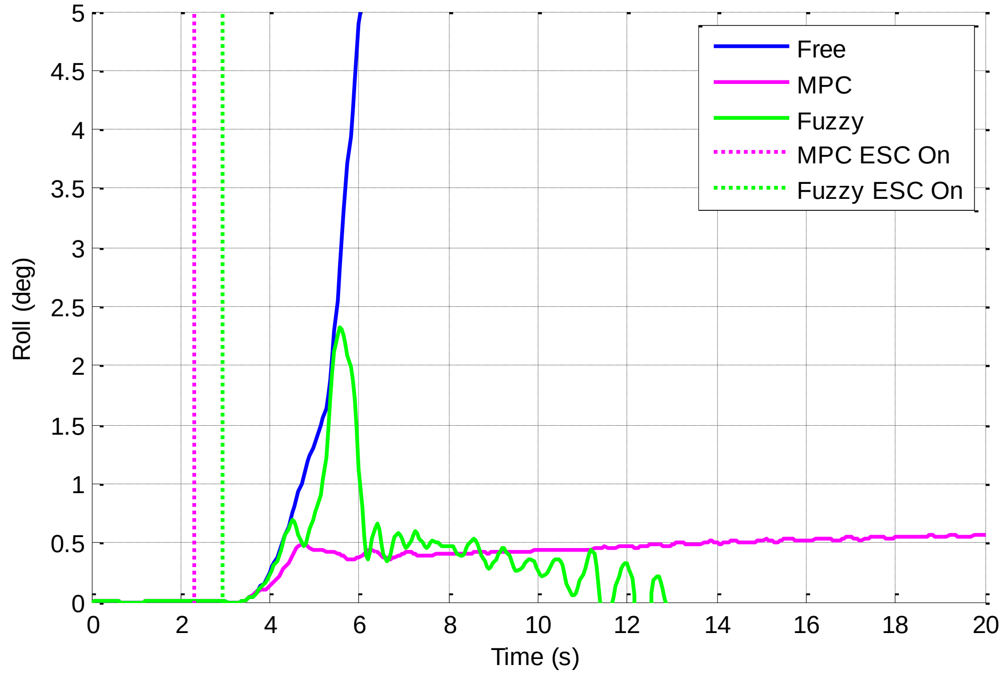

Figure 8-25: Trailer 3 Roll, MPC - Fuzzy Comparison, Unloaded Step Steer, mu = 0.85

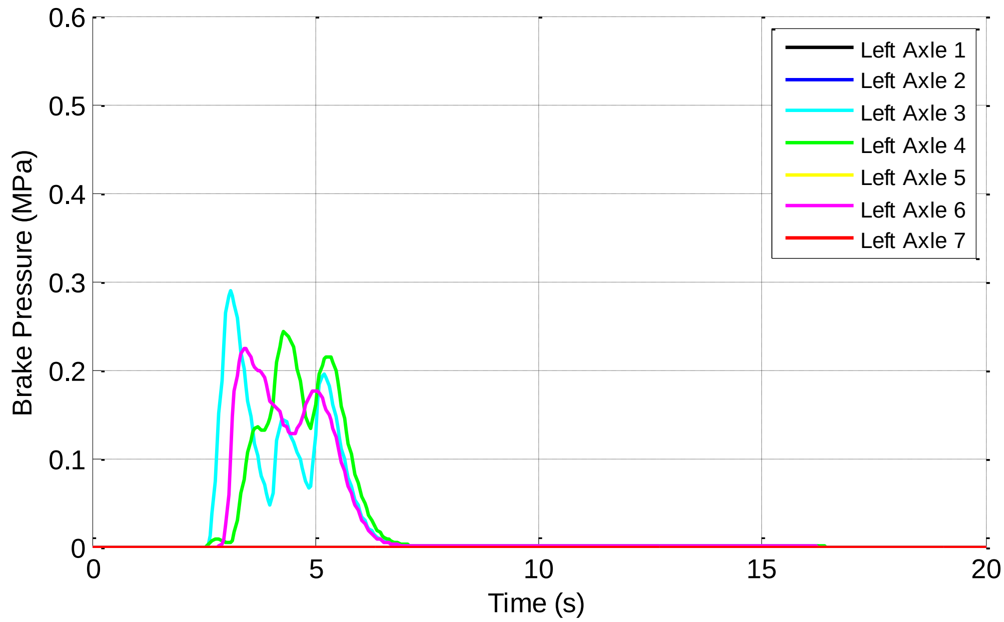

Figure 8-26: Brake Pressure, MPC, Unloaded Step Steer, mu = 0.85

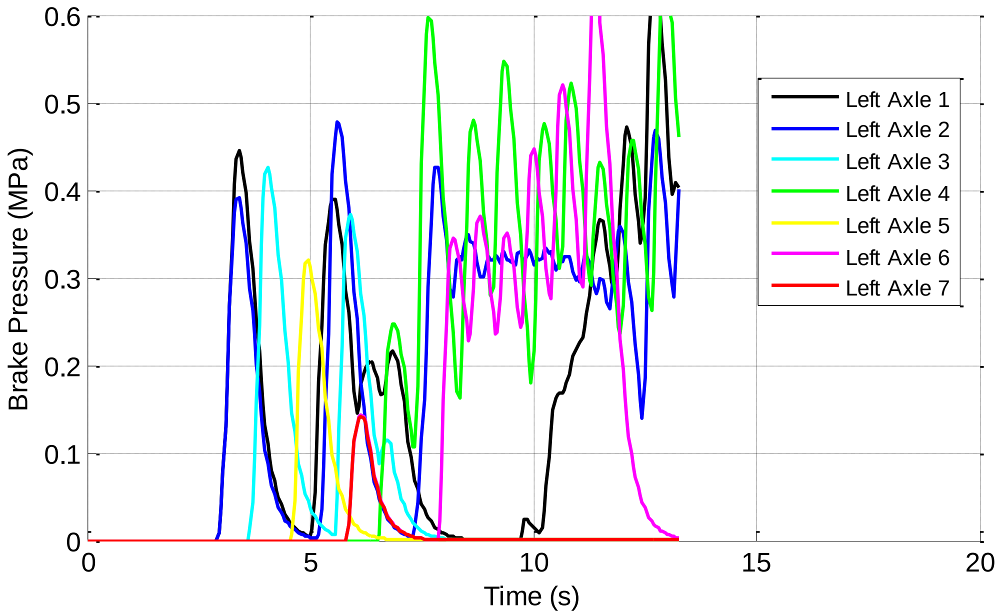

Figure 8-27: Brake Pressure, Fuzzy, Unloaded Step Steer, mu = 0.85

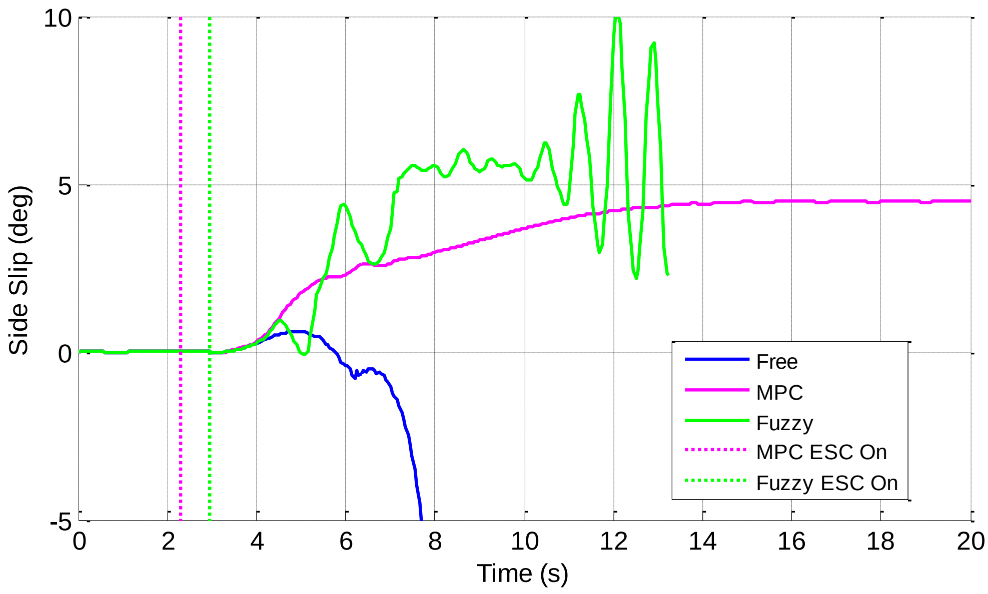

Figure 8-28: Trailer 3 Side Slip, MPC - Fuzzy Comparison, Unloaded Step Steer, mu = 0.85

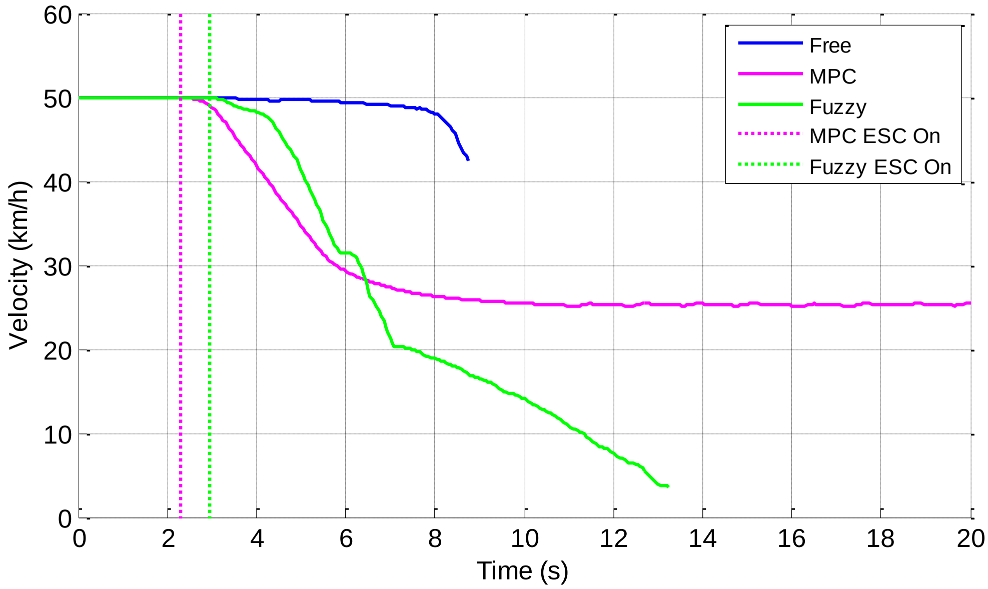

Figure 8-29: Velocity, MPC - Fuzzy Comparison, Unloaded Step Steer, mu = 0.85

8.3. Controller Cost

For a controller to be effective, it must be computationally efficient to provide useful corrective action in time to affect the system. The computational cost of the controllers can be divided into a cost to define the vehicle and a cost to define corrective actions. The following section breaks down the cost for each system.

8.3.1. Model Cost

As implemented here, the MPC strategy required that a linear model be generated at each time step and checked for observability and controllability. While this was a very quick operation, it was an additional task in the solution process that had to be repeated. Note: one could argue that the observability and controllability tasks were unnecessary at each time step (just needed when the model was derived to prove controllability and observability). In this case, the tests were executed, along with a positive eigenvalue test, as MPC can generate poor commands when observability or controllability is deficient and it is difficult to know if the corrective actions are deficient by inspection.

In contrast, the fuzzy logic controller had no development cost. It simply looked at the current states and applied logic based decisions. The only “model” cost was in defining the number of units, scaling the input / output memberships and replicating rules. As this was a onetime cost at startup, it was not considered to be relevant.

8.3.2. Computational Cost

While every effort has been made to make the MPC approach as fast as possible, the fuzzy logic controller was still faster. The MPC approach had to build the quadratic cost function and solve the quadratic system (Equation 8-1) at every time step.

$$J = \min_{U}\left(\frac{1}{2} * U' * G * U + U' * F * x(0)\right) \tag{8-1}$$

The fuzzy logic controller was much simpler having three parts:

- A linear scaling on input members
- A set of logic rules
- A centroid assessment of area

The difficulty was in determining how much faster the fuzzy logic would be as the solvers needed to be tested on dedicated hardware which was unavailable at the time. Therefore, it can be reasonably concluded that the MPC will be a bit more expensive, but it is not possible to quantify the difference.

8.3.3. Required Sensors / Hardware

The final cost for the controllers was in the hardware needed to implement them on a vehicle. As both the MPC and fuzzy logic controllers needed the same sensors for vehicle state evaluation and brake actuation relays for control, that part of the cost was the same. However, the MPC system also needed a few cheap air pressure sensors (total vehicle cost of approximately $400) (Newmatics Inc., 2013). The MPC system also needed more static vehicle parameters loaded into the unit controllers such as unloaded CG height, track width, etc. While these parameters are not a system cost, they were a minor additional installation cost.

8.4. General Performance

Based on the performances shown for the MPC (Section 6 and Appendix J) and the performances shown for the fuzzy logic controller (Section 7 and Appendix K), the MPC strategy had an advantage in overall stability. However, the fuzzy logic controller was not significantly worse and there were no test cases found that the MPC could correct but the fuzzy logic could not correct. The difference was in observed state magnitudes, brake demand magnitudes, and system response times.

8.4.1. Robustness

As was noted in Section 6.1.1, MPC can have difficulty when the linearized system becomes unstable (i.e. the vehicle is already crashing). While this is an unlikely situation as the goal of the controller is to prevent instability, it can happen. As the fuzzy logic controller does not require a LTI model, it does not suffer from this limitation. Note:

one can make the argument that this is a moot point because if the vehicle system ever becomes so unstable that the MPC cannot determine a viable corrective action then the system is by definition beyond the corrective potential of the brakes and neither controller is going to be able to save the vehicle.

8.4.2. “System” Stability Optimization

While the MPC strategy is not an infinite horizon type solution (LQR), it does look far enough into the future to accurately gage the impending stability needs. The horizon distance is a balance between being able to see potentially pending issues and the quality of the future estimations (Section 6.4.2). After all, the driver may well be changing the steering wheel angle at some point in time which degrades the feed forward assumption. Additionally, the further out in time the prediction gets, the less important the inputs are as the effect is mostly on the predicted control response that is never used. Only the first time step control action is used on the real vehicle and then the optimization is repeated again. So in practical terms, the MPC strategy is the optimal solution for the current time which is nearly the same as the global optimal solution.

The fuzzy logic controller makes no attempt to generate an optimal solution. While the selection of good rules can improve the vehicle’s stability, it is not an optimal response. Even if one could write a set of optimal rules, they would only be optimal for a set maneuver or instability type as differing maneuvers would want differing relative (tractor and trailer) responses.

CHAPTER NINE

CONCLUSIONS

While there were many interesting and useful results generated in this work, a few items stood out as being of particular importance. These were the major contributions to vehicle modeling, state and parameter estimation, model predictive controller development, and fuzzy logic controller development.

9.1. Summary of Work

The stated objective of this work was to develop modular multi-unit vehicle controllers that treated the vehicle as a system. I.e. the controllers stabilized the vehicle system as opposed to stabilizing the vehicle units. To meet that objective, several other advancements to the current state of the art were needed. These advancements included the development of simplified linear time invariant models, development of new parameter assessment methods, implementation of state estimation techniques that do not require physical models, and the development of new controller strategies. The result was the development of two scalable controllers that can be easily implemented on multiple unit vehicles.

9.1.1. Linear Model Development

The linear time invariant model developed here can reduce any multiple unit vehicle down to four states per tractor or trailer. This was accomplished by realizing that the fifth wheel can be effectively treated as a pin joint (no moments) and that the dolly states can be dropped without negatively affecting the performance of the model. Finally, as the only use of the LTI model was as a future prediction tool and not as a reference, the refinement of the data parameters needed by the model was substantially lower.

9.1.2. State and Parameter Data

One of the most enduring and difficult aspects encountered in developing vehicle control strategies is the interdependence of state estimation and parameter estimation. The work here breaks this interdependence by obtaining all state information from direct measurement or direct measurement and the use of kinematic models with Kalman filters. Additionally, all parameters save tire cornering stiffness are directly measured or estimated based on measurements alone. As the LTI model really only needs the ratio of tire cornering stiffness to mass, the use of a physical model to determine tire cornering stiffness is quite acceptable and does not pose a problem.

9.1.3. Model Predictive Control

The model predictive controller presented here is a significant departure from prior work and offers some unique and powerful features. First, the controller does not use a reference vehicle nor does it have an output cost. Second, the model's speed and quality both increase as the step size increases (within reason). Third, the model has proven to be very robust even when the quality of the vehicle parameter data used in the LTI model was deliberately reduced.

All of the test cases presented here used the same set of bounds, step size, and horizon. No scaling for load, speed, road surface, etc. was needed regardless of the vehicle combination (load arrangements) or maneuver. The model even worked when the axle roll stiffness was not updated with payload (Section 3.2.3). Parameter evaluations showed that the controller behavior was consistent even when the bounds were varied by ±25%. Finally, all indications are that a fixed step size of 1 second and a fixed horizon of 5 seconds will manage any vehicle arrangement.

9.1.4. Fuzzy Logic Control

The proposed fuzzy logic controller is so simple that there are virtually no set-up requirements needed to implement it on a vehicle. It requires no knowledge of the vehicle (mass, CG, inertia, tire cornering stiffness, etc.) and no knowledge of the driver's behavior. All that is needed is the number of units in the vehicle (not counting dollies) and estimates of the states of the vehicle (side slip, yaw rate, roll angle for each unit).

The input membership sets for the controller are all identical in structure with only the bounds changing based on the state that is being monitored (scaling for acceptable behavior limits). The output membership sets are all identical. Finally, the rules are scalable and only require a loop to add additional units to the controller.

9.2. Contributions to Body of Knowledge

It has been long observed that stability control of multiple unit vehicles is a big challenge; particularly on low friction surfaces (MacAdam, 1982; MacAdam et al., 2000; Sampson, 2000). This work presents two computationally fast, scalable, and simple to implement controllers that meet the challenge of managing multiple unit vehicles as a system. Moreover, the controllers require minimal or no information on the vehicle itself (mass, CG location, etc.) and the state information can be obtained through readily available and relatively cheap sensors.

9.3. Future Work

The controller models developed here have proven to be robust and simple to implement. The most significant issue affecting the performance was actually the anti-lock brake controller as wheel control has a larger effect on handling performance than the selection of bounds or other controller parameters (Section 6.6). Thus investigations into the capabilities of electronic air disk brakes would be quite useful.

As for the controllers themselves, the selection of the ideal set of bounds (fuzzy logic) and the selection of ideal bounds, time step, and horizon (MPC) could be explored in more depth. The limiting factor at the moment was access to accurate models for many vehicle types and / or access to test data on various vehicle types and loading arrangements. Should such data become available, the analysis would also require a good deal of statistical modeling to extract trends and causal effects.

As part of this work, studies were executed on the traditional factors that affect controller performance. Items such as the effect of state estimation quality, sampling rates, controller step size, and sensor noise were proven to have minimal effect on the performance of the controllers. Thus these are not likely areas for significantly improving the controllers. However, there is one major weakness in the model predictive controller that might be addressed: The MPC uses a feed forward of the driver's steering demand with the steer angle fixed over the horizon. However, the driver may in fact be changing the steering over the horizon. It is proposed that game theory might be useful to estimate the driver's behavior and thus improve the feed forward estimate and, as a result, the controller's response.

APPENDICES

APPENDIX A
OVERVIEW OF THE COMMERCIAL VEHICLE INDUSTRY AND ESC

Over the last 60 years, the heavy truck industry has matured into a very efficient and effective goods transportation enterprise. As is the case with most industries, the initial developments in the heavy trucking industry dealt primarily with operational limitations (payload limitations, human limitations, etc.) and equipment cost. Later developments were mostly focused on improving efficiencies and ergonomics (allowing the human to be more productive). In keeping with usual technology development trends, the last two decades have demonstrated a move towards improving vehicle safety in addition to improving operational efficiency. This interest in safety has also been increasing due to rising injury and disability costs as well as governmental regulations and mandates. Examples of recent safety related activities include the mandate by the US government to have anti-lock brakes on all tractors and trailer made after March 1, 1997 (NHTSA, 2009) as well as the reduction of maximum stopping distances (60 mph to 0 mph) for class 8 vehicles from 335 feet to 250 feet in 2011 (NHTSA, 2009) and the more recent proposal for adding tractor only ESC to class 8 vehicles (NHTSA, 2012).

Based in part on the undisputable results of electronic stability controls (ESC) in reducing passenger car accident rates, injuries, and deaths, there is now interest by the US government in ESC systems for commercial vehicles as well (NHTSA, 2011; NHTSA, 2012). Additionally, other markets (Europe) have already begun the transition to ESC for all commercial vehicles increasing the probability that similar legislation will be forthcoming in the US. Thus there is now significant interest within the commercial vehicle industry for evaluation of ESC capabilities, costs, benefits, and limitations. It is with these facts in mind that the current research on commercial vehicle stability is being conducted.

A.1. Commercial Vehicle Design

Before evaluating the stability of commercial vehicles it is useful to have a good understanding of the design and operation of these vehicles. Understanding how these vehicles are constructed, used, and operated will make understanding their stability limitations easier. With a better understanding of the limitations of the vehicles, the analysis and modeling of the vehicles will be more productive and permit better insights into how to improve their stability.

It is also important to keep in mind that the person paying for a tractor or trailer is very seldom the operator of the vehicle. So as long as the owner can find an operator for hire willing to drive the vehicle, the owner only cares about the cost of the vehicle and its suitability / legality for usage. As a result, the vehicle design becomes a direct outcome of the cost to manufacture and operate the vehicle within the constraints imposed by the government to register the vehicle for use on public roads.

A.1.1. Economics of Commercial Vehicles

The commercial trucking industry transports approximately 70% of all freight in the US (Gerdes, 2002), (Windsor, 2011). Between the years of 1987 and 2007 there was a

58% increase in registered large trucks and a 70% increase in miles traveled by large trucks. From 1997 to 2007 there was a 27% increase in registered large trucks and a 19% increase in miles traveled by large trucks (Federal Motor Carrier Safety Administration, 2009). While the recent economic downturn has slowed the trucking industry growth, all indications are that the trucking industry will again be growing at the same rates with the recovery of the economy.

The average tractor semi-trailer travels six times the miles per year as a typical passenger car (C. Chen & Tomizuka, 2000). Commercial vehicle usage (miles per year) is also increasing at approximately 3.5% per year compared to 2.5% for passenger car usage (Woodrooffe et al., 2009). Additionally a tractor and semitrailer gets an average 7 miles per gallon (Woodrooffe et al., 2009) assuming the vehicle is loaded to the current maximum load of 80,000 lb. gross vehicle weight (GVW). Based on these facts it is easy to see why fuel costs are the biggest expense a trucking fleet incurs and why there is interest in increasing the efficiency of the vehicles by the owners and the government.

A.1.2. Regulatory Restrictions

There are essentially three types of regulations imposed on commercial vehicles. These are:

- Infrastructure requirements (bridge loads, vehicle widths, lengths, etc.)
- Safe operation restrictions (brake standards, fail safes, etc.)
- Road sharing requirements (under ride protection, mirrors, etc.)

Most of the regulatory requirements applied to commercial vehicles can be categorized as one of these three types of regulations. Further, it is the first two that restrict the profitability of commercial vehicles the most severely.

Of these safety regulations, the following are the most important from a design point of view:

- Requirement (FMVSS 121) that the vehicle be able to stop from 60 mph in 250 feet or less (Esber et al., 2007).
- Requirement (FMVSS 121) that all units (tractor or trailer) be equipped with an antilock brake system (NHTSA, 2009)
- Requirement (STAA 1982) that all vehicles be 102" or less in width (FHWA, 2004)*
- Maximum gross vehicle weight of 80,000 lb. (STAA 1982)* (Woodrooffe et al., 2009)

Asterisks indicate exemptions for "grandfather" rule exemptions in individual states.

The commercial vehicle industry is exceedingly slow to change due to regulatory burdens as well as resistance from owners to spend capital on anything not proven in the field to increase profits. Thus technologies that may offer both improved safety and improved economics are often not pursued by the industry. Examples of new technologies that are being limited by regulatory requirements or lack of proven cost savings include:

- Air disk brakes. These are considered as being too expensive (NHTSA, 2009)

- Electronic Braking ECE R13. The common perception is that EBS will not meet regulatory requirements in FMVSS 121 (Esber et al., 2007), (NHTSA, 2009)
- Full vehicle stability. The current standard tractor to trailer electrical connector is a 7-pin design. There are no open pins for conveyance of any additional data thus any stability improvements will need to incorporate additional data transfer methodologies.

Note: Not all regulatory changes are seen as being restrictive toward commercial trucking. The 1982 Surface Transportation Assistance Act opened the use of doubles significantly. Between 1982 and 1985, double use increase 50%. By 1990, double use had increase and additional 40% (Rempel, 2001).

Table A-1. Test Standards for Air Brake Systems

SAE Standard No.	Standard Title
J294	Service Brake Structural Integrity Test Procedure-Vehicles Over 4500 kg (10,000 lb.) GVWR (gross vehicle weight rating)
J1505	Brake Force Distribution Test Procedure-Trucks and Buses
J1854	Brake Force Distribution Performance Guide-Truck and Bus
J1859	Test Procedures for Determining Air Brake Valve Input-Output Characteristics
J1911	Test Procedure for Air Reservoir Capacity--Highway Type Vehicles
J2115	Air Brake Performance and Wear Test Code Commercial Vehicle Inertia Dynamometer
J2318	Air Brake Actuator Test Performance Requirements - Truck and Bus

A.1.3. Heavy Vehicle Design Constraints

The first, and possibly the most critical, observation regarding the design of tractors and semi-trailers has to do with the many constraints placed on the design of the vehicles.

For trailers these design constraints include dock heights of shipping and receiving centers, flat trailer flooring needs for drive on / drive off of loading equipment, clearance of relatively tall tires required for load carrying capacity, dump valve heights for tankers, and more. Tractor design limitations include physical constraints such as the size and weight of engines strong enough to pull the heavy loads, attachment requirements for trailer connections, chassis flexibility requirements to maintain drive traction over uneven ground, plus the common manufacturing and usage constraints such as component packaging and driver needs (Arant, 2010).

Additional overall design constraints are imposed on tractors and trailers such as weight, width, length, height, and more by local and national regulations. Moreover, many of these governmental regulations are based on protection of the road infrastructure and traffic considerations (Fancher & Mathew, 1989), (Gerdes, 2002) rather than improving the safety of the vehicles. With the majority of the parameters governing the design of commercial vehicles concentrated on issues other than stability, it is not surprising that the result is a vehicle with relatively low stability levels (Arant, 2010).

A.1.4. Commercial Vehicle Articulation

One of the most significant issues with operating a large vehicle is off tracking of the rear of the vehicle. Off tracking is the phenomenon where the rear axles track a different path around a turn from the steer axles. This error (distance between path arcs) is proportional to the square of the vehicle's wheel base and the vehicle's speed (Fancher & Winkler, 2007). For low speeds and long wheelbases, the error can be quite large and can lead to maneuverability issues. To resolve this problem, commercial vehicles are often broken into smaller segments with articulation points connecting the segments. This permits a longer overall vehicle while minimizing the off tracking issues. But the articulation points also reduce the overall vehicle stability as additional degrees of freedom are introduced with each articulation point.

In the US, there are generally three types of articulated commercial vehicle designs used for transporting goods. The most common vehicle design is the typical tractor and semitrailer. Here the semi-trailer could be a dry van (box), flatbed, refrigerated, tanker, or other trailer design. In addition to the conventional tractor semi-trailer are doubles (tractor and two trailers) and triples (tractor and three trailers). Doubles are permitted on most US interstates but triples are mainly restricted the western US. For the reader's reference, a conventional tractor and semitrailer (left) and a triple (right) are shown below in Figure A-1. An illustration of common commercial vehicle types operating in the US is also presented in (Figure A-2) (Rempel, 2001).

Figure A-1: Tractor Semitrailer and Tractor Triple (ATA, 2011)

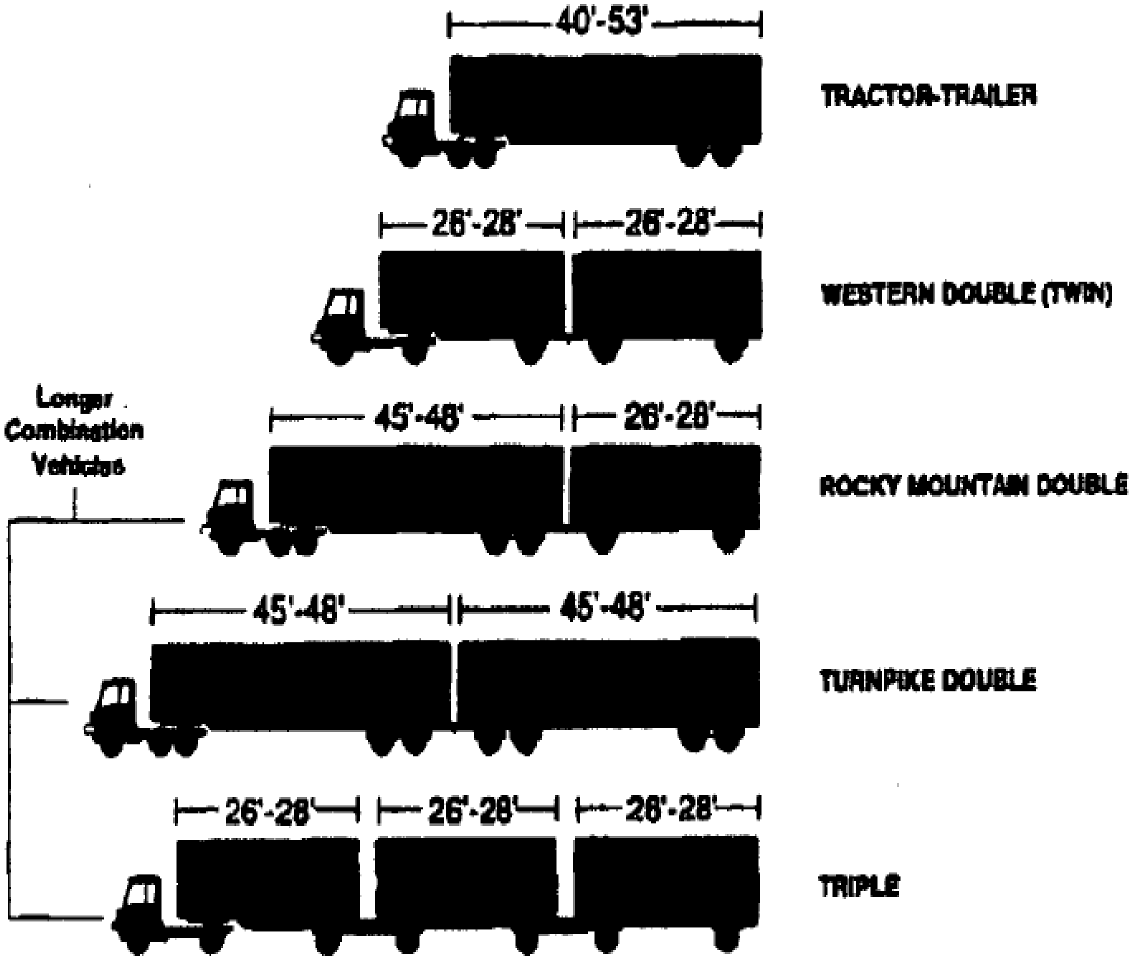

Figure A-2: Common Commercial Vehicle Arrangements in the US (Rempel, 2001)

To understand how the trailers are connected, the fifth wheel (left illustration in Figure A-3) and the pintle hook (right illustration in Figure A-3) must be explained. The fifth wheel is attached to the back of the tractor (Figure A-4) or to a dolly and the kingpin is attached to the trailer (Figure A-4). The notch in the kingpin locks into pawls in the fifth wheel preventing it from coming out during operation (Figure A-5). In theory, the kingpin connection provides two degrees of freedom (pitch and yaw), however, in practice, it also permits roll due to compliance issues as shown in Figure A-6.

The pintle hook is used with an A type dolly (Figure A-7) such that the dolly is connected to the rear of a trailer (Figure A-4). The dolly has a fifth wheel on it which then connects to the kingpin of a second trailer. This arrangement introduces an additional three degrees of freedom (roll, pitch, and yaw) at the pintle location. The result is less off tracking of the vehicle (Figure A-8).

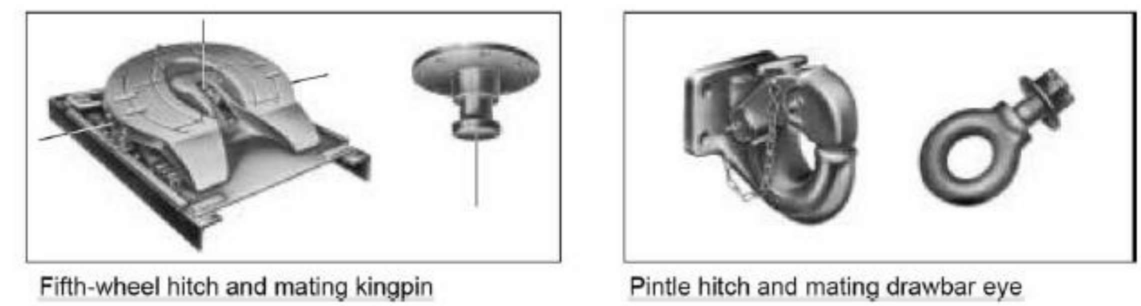

Figure A-3: Fifth Wheel and Pintle Hook Connections (Fancher & Winkler, 2007)

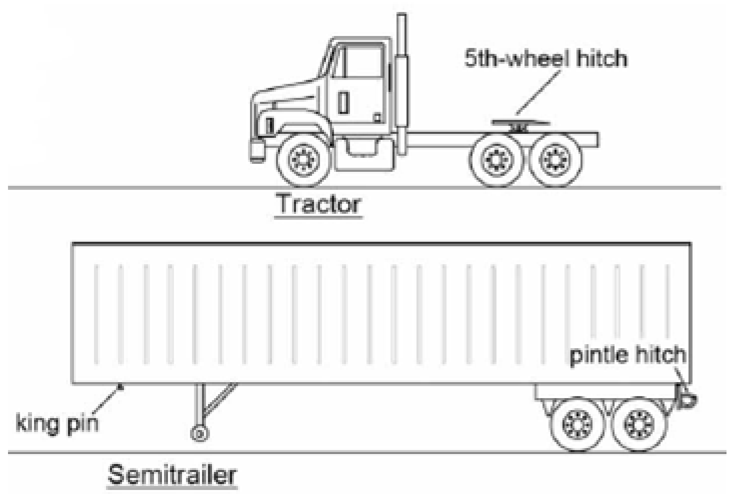

Figure A-4: Tractor and Semi-Trailer (Fancher & Winkler, 2007)

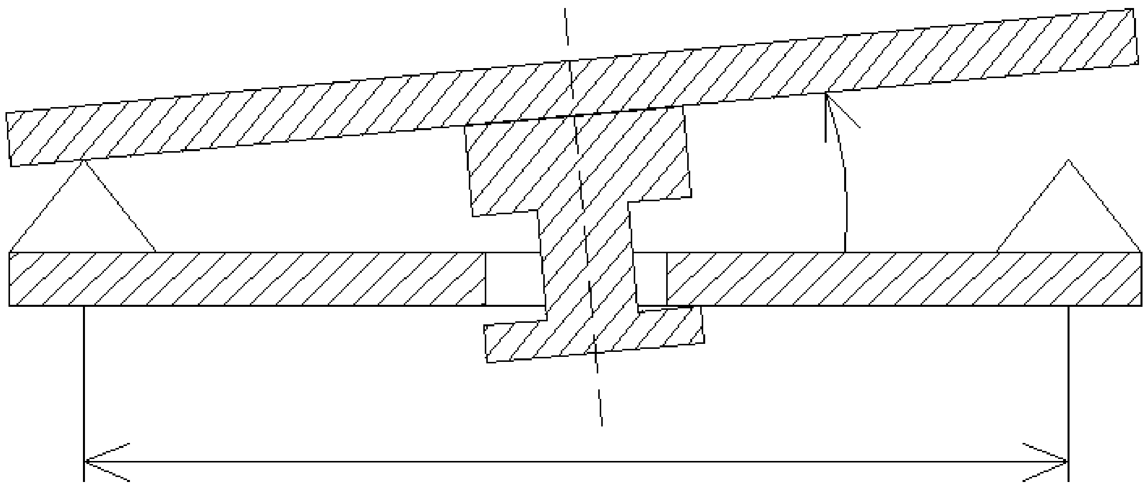

Figure A-5: Fifth Wheel Cross Section (Lawson, 2004)

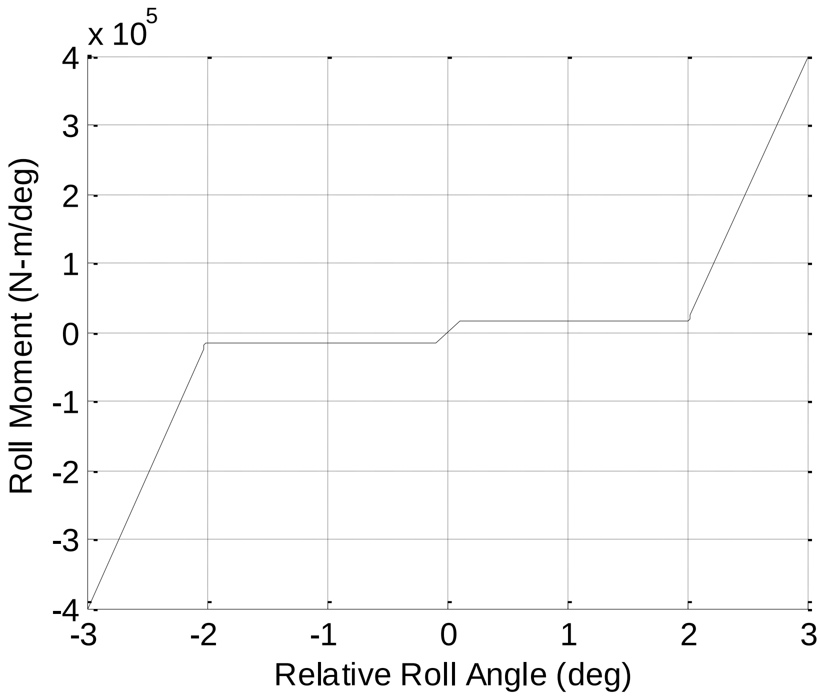

Figure A-6: Typical Fifth Wheel Roll Moment (Arant, 2010)

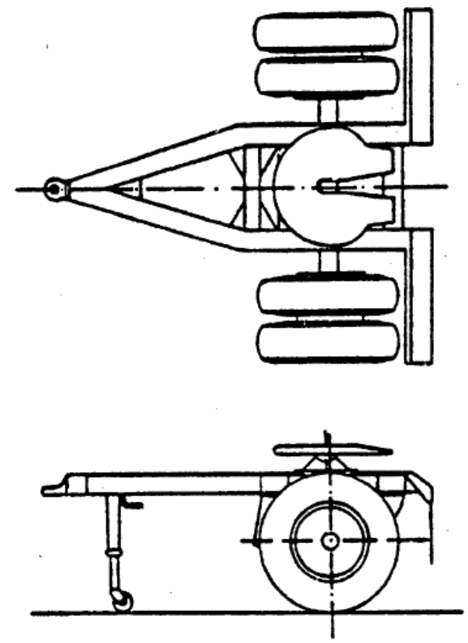

Figure A-7: A-Train Dolly (Rempel, 2001)

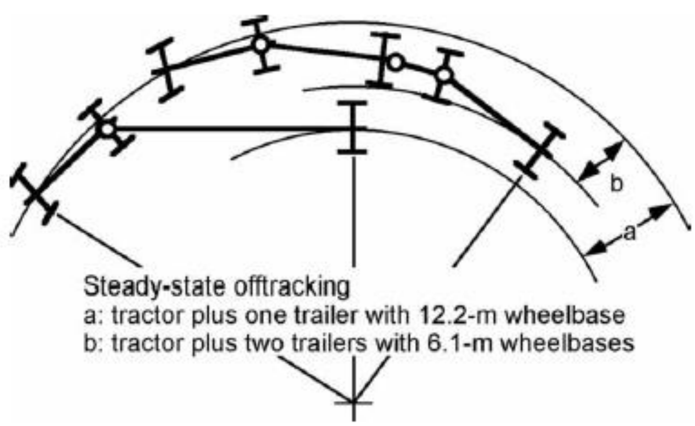

Figure A-8: Articulation and Off Tracking (Fancher & Winkler, 2007)

Note: There are other dolly types ("B" and "C") which eliminate roll and yaw degrees of freedom at the pintle hook. But as these types are not commonly used in the US and are, dynamically speaking, subsets of the "A" type, these are not presented here for reasons of brevity. "A" type dollies are the least stable and thus the most interesting to study here.

A.1.5. Increasing Capacity of Commercial Vehicles

Most trucking operations operate on very small profit margins (Freightliner LLC, 2007), so increases in cost as documented in section A.1.1 have major consequences to the industry's financial results. As a result the industry is actively lobbying congress to reduce restrictions on the size, weight, and number of units comprising a commercial vehicle (ATA, 2011). While the request is being based on fuel consumption (more cargo per gallon of diesel) and traffic congestion (fewer trucks on the road), there are other factors at play. The second and third largest expenses for a trucking company are drivers followed by tires. Fewer trucks hauling more goods mean fewer drivers and fewer tires wearing out. Though tire wear will increase and fuel economy will decrease with added mass, the effects are more than offset by the reduction in the number of vehicle units.

Aiding the industry's request are statistics developed by governmental agencies such as the Federal Highway Administration. The FHWA found that allowing doubles and triples to operate nationwide would result in a 25% reduction in miles travelled by commercial trucks (ATA, 2011). They also concluded that allowing heaver trucks (96,000 lb. vs. 80,000 lb.) would reduce miles travelled by 11% (ATA, 2011). This research was confirmed by the U.S. Department of Transportation which found that permitting heavier trucks to operate in the US would reduce shipping costs by 7% and longer combination vehicles (LCV) would reduce shipping costs by 11% (ATA, 2011). Note: LCV are defined as double or triple trucks.

As one would anticipate, there are other groups opposed to any increase in truck sizes or weights. Many of these groups site safety as a concern under the presumption that a heavier or longer vehicle will necessarily be a less safe vehicle. At the same time, the US government is interested in increasing the safety of commercial vehicles (NHTSA, 2011; NHTSA, 2012). Thus it seems quite plausible that should there be a change in the usage restrictions of commercial vehicles, such a change would also include new or modified safety mandates.

A.2. Commercial Vehicle Safety and Stability

In section A.1.2 many of the constraints that dictate commercial vehicle design were reviewed where it was noted that some of these constraints are not helpful for enhancing vehicle stability. Given this situation, the logical response would be to document the actual safety performance of commercial trucks and then to assess how safety could be improved while respecting the existing functional requirements of the vehicles. While certainly not an exhaustive review of commercial vehicle safety, the following evaluation of the performance of commercial trucks is intended to provide an accurate understanding of the stability properties of these vehicles and to identify any areas where improvements might be achievable.

A.2.1. Accident Statistics

For the last 20 years, the federal government and some states have been keeping records on accidents in order to identify trends and develop responses to reduce those accidents. These databases have been very valuable in determining the true safety performance of commercial vehicles operating within the US. Analysis of the databases indicates that, in general, safety has improved over time, but there is still potential for more improvement.

Over the last 20 years, the number of accident fatalities for both cars and trucks has dropped considerably (Figure A-9). Similar results have been documented for serious injuries as well (Figure A-15). But while these trends are encouraging, these results do not tell the whole story as what is really needed is an understanding of what happened to cause the accident and if the accident could be prevented. To answer that question, the conditions under which the accidents occurred need to be investigated.

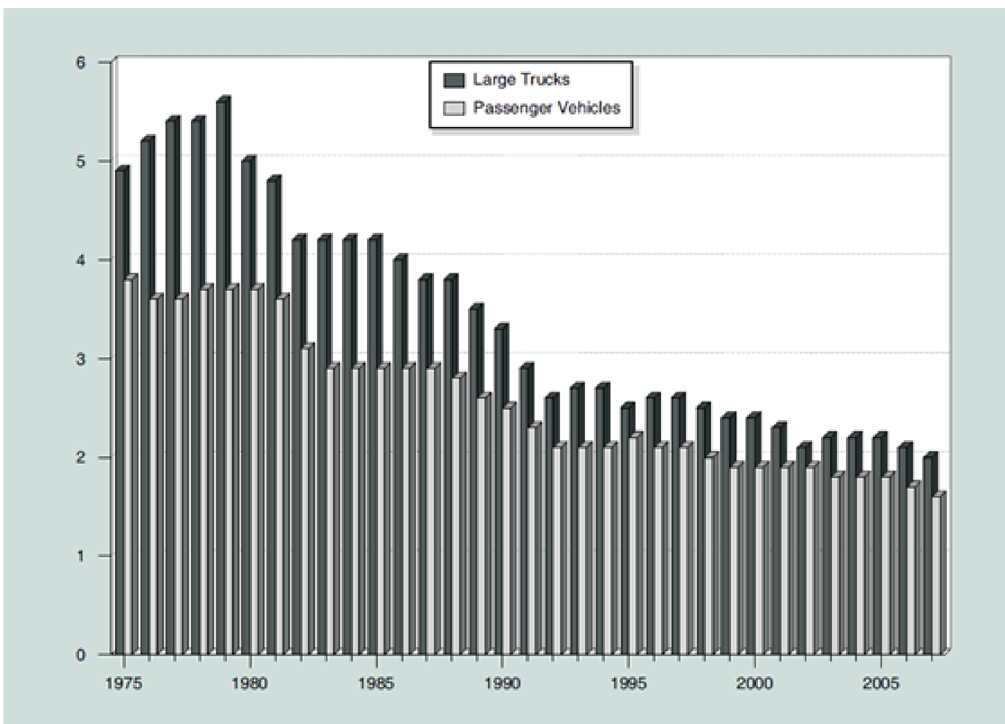

Figure A-9: Fatalities per 100 Million Miles (Federal Motor Carrier Safety Administration, 2009)

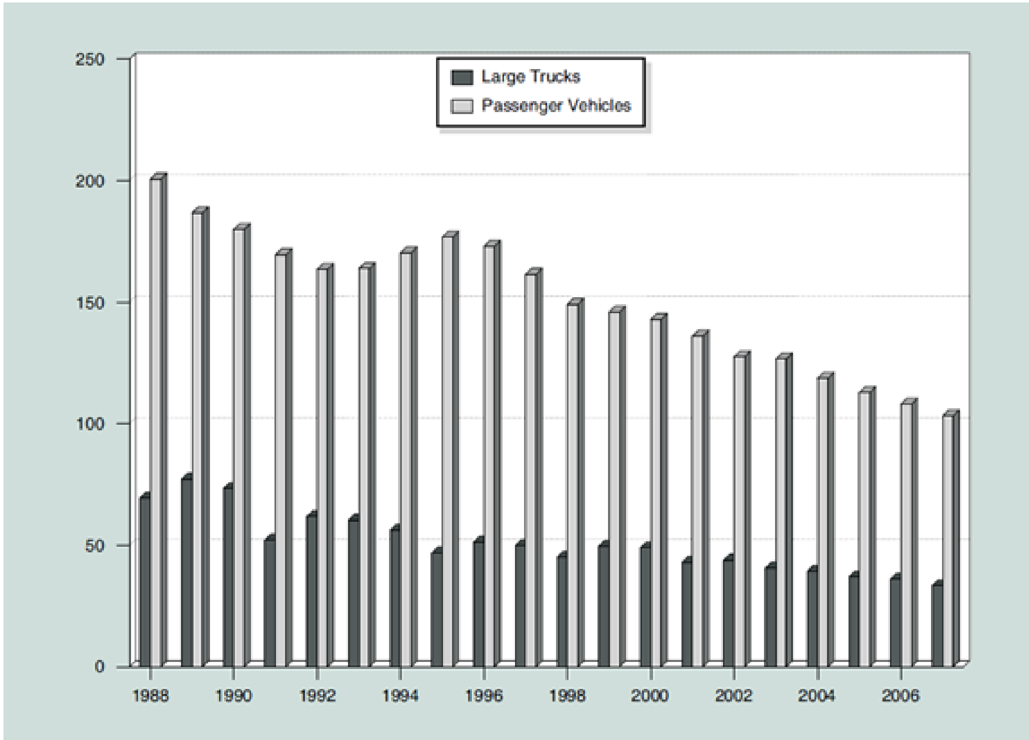

Figure A-10: Injuries per 100 Million Miles (Federal Motor Carrier Safety Administration, 2009)

In terms of overall safety, passenger cars account for the majority of vehicle related fatalities in the US (Figure A-11), but they also account for about 90% of the total miles driven in the US (NHTSA, 2011). So judging solely on the number of accidents is not an accurate method for evaluation of vehicle safety. The better index to use in assessing accident risk is the frequency of accidents and the severity of the accidents. Though trucks account for 7% of all miles traveled, they make up 12% of all fatalities (Kharrazi & Thomson, 2008a). Additionally, commercial vehicle accidents do tend to be more severe with 0.7% of commercial vehicle accidents being fatal compared to 0.2% for cars and 0.3% for SUVs (Blower & Kostyniuk, 2007).

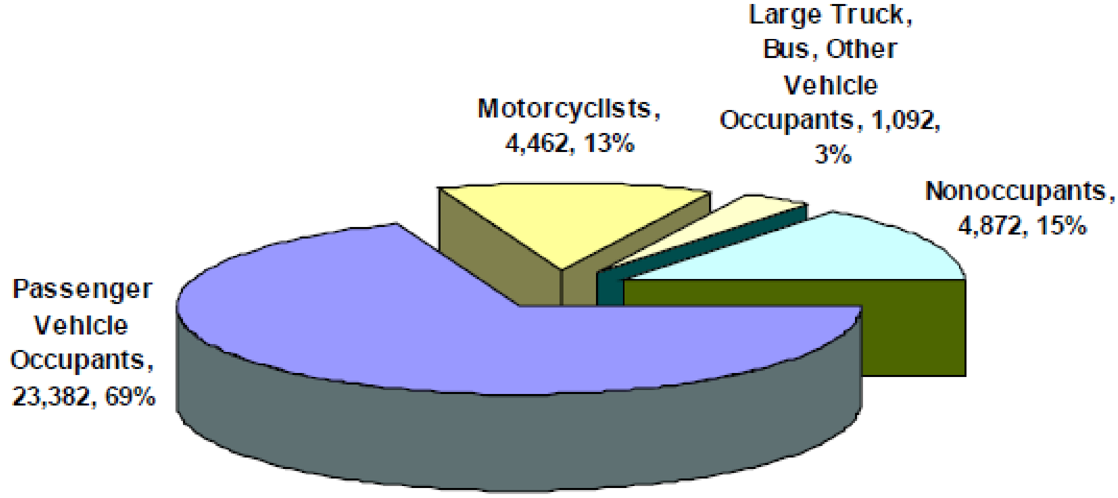

Figure A-11: Fatalities by Vehicle Type (NHTSA, 2011)

When the commercial vehicle crashes are separated out, it can be seen that the majority of truck accidents are with conventional tractor semi-trailer vehicles (Figure A-12). This indicates that enhancing stability of articulated vehicles could significantly affect the overall safety record of commercial vehicles. Note: Tractors with multiple trailers and bobtails have low numbers as there are comparatively few of them on the road.

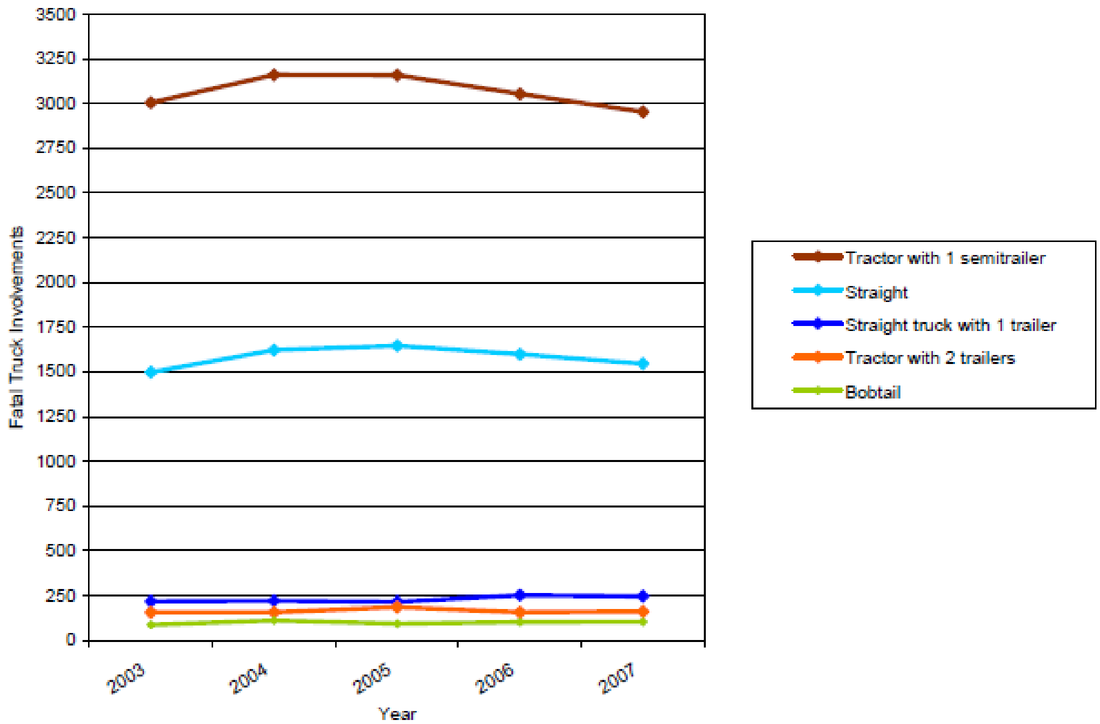

Figure A-12: Fatal Truck Crashes by Vehicle Type (Jarossi, Matteson, & Woodrooffe, 2010)

The next question to be resolved is where these accidents occur. Multiple organizations have researched this point and the conclusions of the different organizations all indicate that the interstates are not the major safety concern. The Federal Motor Carrier Safety Administration (FMCSA) found that just over three-fifths (62%) of all fatal crashes involving large trucks occurred on rural roads, and one-fourth (25%) occurred on Interstate highways (Federal Motor Carrier Safety Administration, 2009). Matteson and Blower found that 33% of fatal tractor semi-trailer accidents occur on interstate highways, 27.6% on U.S. highways, 27.3% on state highways, and the remainder on secondary roads (US highways and state highways representing the rural roads in the FMCSA study) (Matteson, Blower, & Woodrooffe, 2004).

If most accidents are not occurring on major interstates, then what are the conditions under which the accidents are occurring? Bexwada and Dissanayake determined that most fatal accidents occurred when the vehicle was traveling between 40 and 70 mph (Figure A-13) indicating that speed was a factor in accidents but not the only significant factor. Kharrazi and Thompson found that in most cases, the road was dry as well (Figure A-14) indicating that poor road conditions were not to blame for many accidents. Matteson and Blower also found similar accident distributions with regard to weather conditions (Matteson et al., 2004) as did the US DOT (U.S. Department of Transportation, 2003)**.**

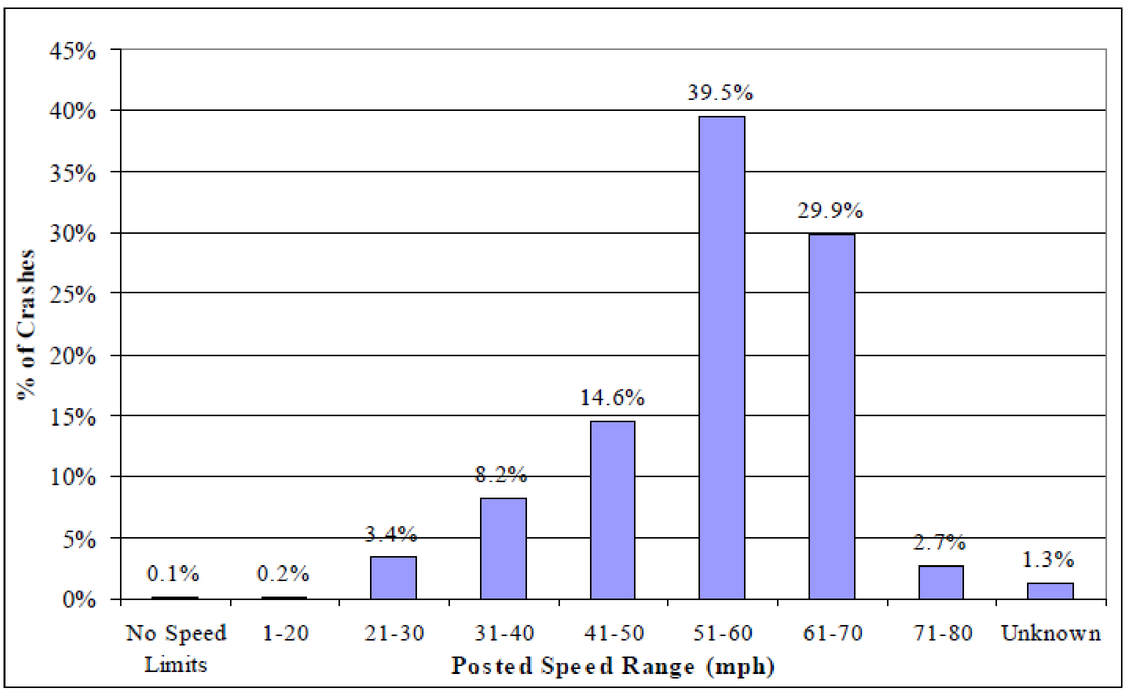

Figure A-13: Vehicle Speed at Time of Fatal Accident (Bezwada & Dissanayake, 2009)

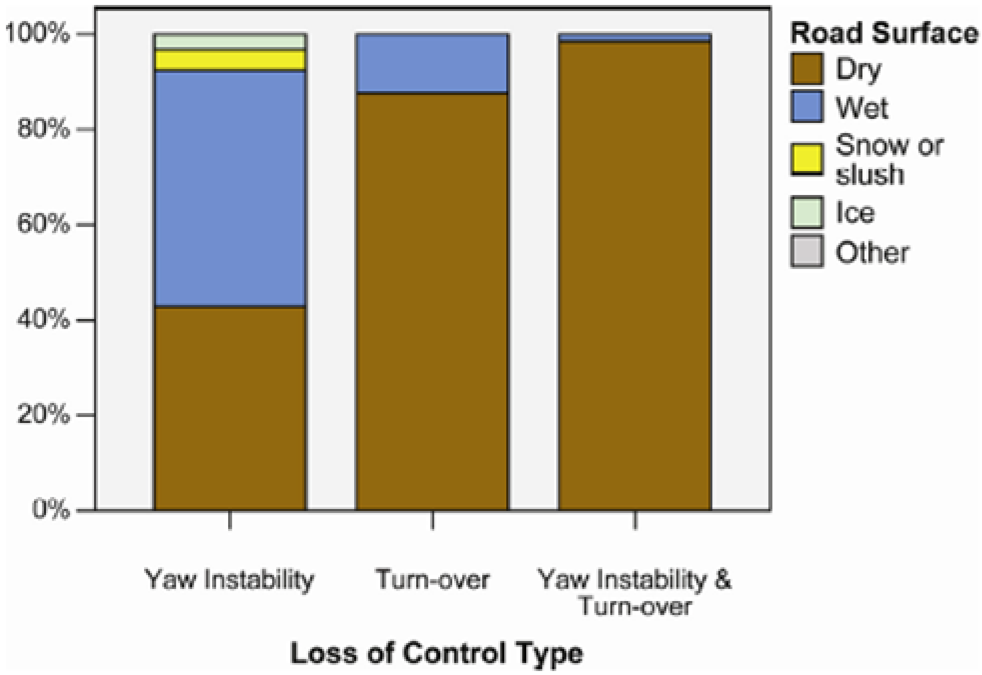

Figure A-14: Road Surface Condition and Accident Type (Kharrazi & Thomson, 2008b)

Battelle Memorial Institute conducted a detailed review of tanker accidents in 2007 that broke the accident recorded down further into where on the road the accidents occurred. While the data was limited to tankers, the results are still relevant as tractor tankers are not that different in mass, size, and geometry from typical tractor and semi-trailer vehicles. Their results indicate that most accidents occur on rural undivided highways and most accidents are not near an intersection or exit (Table A-2).

Table A-2: Tanker Accident Location (Pape et al., 2007)

Location of Accident	Total Rollovers	Percent of All Rollovers
Close to Interchange	11	4.6%
Not at Interchange	45	19.0%
On or Off Ramp	17	7.2%
Total Divided Highway	74	31.2%
Close to Intersection	82	34.6%
Not at Intersection	81	34.2%
Not on Roadway	0	0%
Railroad Grade Crossing	0	0%
Total Undivided Highway	163	68.8%
Total	237	100.0%

This result is supported by an independent review of the US Large Truck Crash Causation Study (LTCCS) where 43% of accidents occurred when the vehicle was traveling straight down the road, 37% when turning right, 21% turning left (Starnes, 2006). Note: on ramps and off ramps are right handed leading to a slight bias to the right in the crash data.

In terms of cost, commercial vehicle accidents are also quite expensive. Blower and Kostyniuk found that the average cost of a fatal accident was $2.7M per individual killed and $50k per individual injured (Blower & Kostyniuk, 2007). The Federal Motor Carrier Safety Administration (FMCSA) found that the average commercial vehicle fatal accident was $6.3M where there is usually more than one person killed or injured in an accident (Table A-3). FMCSA analysis of injury causing accidents also agreed with other similar studies (Table A-4) showing that commercial vehicle accidents are usually quite costly.

Table A-3: Cost of Fatal Crashes by Type (FMCSA, 2008)

Type of Truck Involved	Cost of Fatal Crash
Straight truck, no trailer	$6,314,659
Straight truck with trailer	$6,349,486
Bobtail	$6,394,300
Truck-tractor, 1 trailer	$7,633,600
Truck-tractor, 2 or 3 trailers	$6,667,552
Unknown medium/heavy truck	$6,319,226
All medium/heavy trucks	$7,200,310

Table A-4: Cost of Injury Causing Crashes by Type (FMCSA, 2008)

Type of Truck Involved	Cost of Injury Crash
Straight truck, no trailer	$247,353
Straight truck with trailer	$293,922
Bobtail	$327,405
Truck-tractor, 1 trailer	$334,892
Truck-tractor, 2 or 3 trailers	$1,202,697
Unknown medium/heavy truck	$221,531
All medium/heavy trucks	$331,108

These studies indicate that any stability enhancing system will need to manage a variety of driving conditions (straight, turning, wet, dry) rather than one or two special conditions (ex. dry exit ramp). Further, the data indicates that both yaw and roll stability issues exist (Figure A-14). That means the final controller will have to be more complex and account for more vehicle states as well.

A.2.2. Roll Stability

Research by the University of Michigan Transportation Institute (UMTRI) has shown that although rollovers account for just 13% of truck accidents, they account for 50% of the fatalities (Woodrooffe et al., 2009). This statistic has been confirmed by others as well (Toth, Radja, Thiriez, & Carra, 2003). Thus rollovers are easily the most costly type of accident. To understand why rollovers are so deadly, one only needs to understand how little structural support is in the cab of a conventional tractor (Figure A-15) with the result that a rollover exposes the driver to significant bodily harm.

Figure A-15: Post Rollover Tractor (Evans, Batzer, & Andrews, 2005)

Because rollovers are so deadly, they have been the subject of research for quite some time. The evaluation of commercial vehicle roll stability is a well-researched topic with publications dating back to the early 1980's with much of that work done by the University of Michigan Transportation Research Institute (UMTRI). The UMTRI work documented the relationship between payload, center of gravity (CG) height and rollover risk (Ervin & Mathew, 1988), (Fancher & Mathew, 1989), the effect of compliances on roll stability (Winkler & Ervin, 1999), (Winkler, 2000), and suspension roll stiffness influences (Winkler, 1987). UMTRI also developed relationships between a vehicle's roll threshold and its probability of having an accident (Winkler & Zhang, 1995), (Winkler, 2000) as well as documenting typical commercial vehicle suspension properties (Winkler, Bogard, & Karamihas, 1995).

Static Stability Factor

In assessing a vehicle's roll stability, the most basic parameter is the Static Stability Factor (SSF). This is simply the ratio of the vehicle's wheel base to the CG height (Dahlberg, 2000), (Dahlberg & Stensson, 2006) as shown in Equation A-1. However, this parameter does not account for compliances in the vehicle which will act to reduce the effective wheel base of the vehicle as the vehicle rolls in a turn (Δy in Figure A-16). Correcting for the vehicle compliances gives Equation A-2.

$$SSF = \frac{Ay}{g} = \frac{T}{2 * h_{cg}} \qquad \textbf{A-1}$$

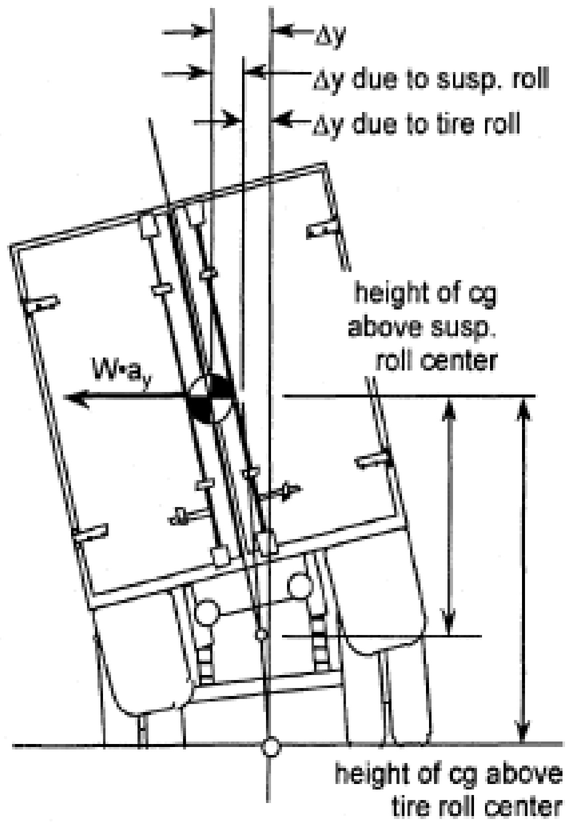

Figure A-16 Roll Displacements and Reactions (Winkler & Ervin, 1999)

$$SSF_{compliance} = \frac{\left(\frac{T}{2} - \Delta y\right)}{h_{cg}} \qquad \textbf{A-2}$$

Equation A-2 states that the highest possible lateral acceleration a vehicle may safely manage is equal to half of the wheel base minus any lateral offset of the CG divided by the CG height. So the higher the CG or the narrower the effective track, the less stable the vehicle is.

This cumulative compliance induced reduction in rollover threshold is significant as the resulting limit to vehicle stability begins to approach the field usage conditions of the vehicle. The AASHTO (American Association of State Highway and Transportation

Officials) guidelines for highway curve design result in lateral accelerations as high as 0.17g at the advised speed limits (Winkler, 2000). Furthermore, it has also been observed that drivers maneuver their vehicles at well over 0.2 g fairly regularly (Winkler, 2000). This means that in many cases the rollover margin of a typical tractor semi-trailer vehicle operating on the public road system is very small.

Roll Axis

For most tractor semi-trailer vehicles, the loaded CG height tends to increase along the vehicle length with the lowest CG height being at the steer axle and the highest CG height at the rear of the vehicle (Fu, 2002), (ISO 15037-2, 2002) , (Lawson, 2004). That is if one treated the vehicle as a series of longitudinal segments, the front segment would have the lowest CG height and the rear the highest CG height. The front axle load is dominated by the weight of the engine and transmission which makes the CG height of the front part of the vehicle fairly low. The drive axles are also of significant mass (with a low CG height) so that the total CG height of the rear of the tractor and front of the trailer is lowered. Finally, the trailer axles are typically lighter than the drive axles as there are no power transmission components so the CG height of the back part of the trailer is closer to the CG height of the cargo in or on the trailer. So, assuming a constant CG height of the cargo along the length of the trailer, the CG height tends to drift upward toward the rear of the vehicle.

This rise in CG height toward the rear of the vehicle would indicate that the rear of the trailer would typically have the lowest rollover threshold, followed by the drive axles, and then the steer axle. Helping to mitigate the lower rollover threshold of the drive and trailer axles, the roll stiffness of the suspensions also tends to increase from the steer axle toward the trailer axles (Winkler, 1987), (Winkler & Ervin, 1999), (Sampson & Cebon, 2001), (Winkler et al., 1995). The stiffer suspensions work to reduce the compliance (Δy term) in the roll stability limit equation (Equation A-2) (Arant, 2010).

Along with the suspension stiffness variations, the sprung mass rotation heights, or suspension roll centers, also typically increase in height above the ground from the front to the rear of the truck (Lawson, 2004), (ISO 15037-2, 2002),(Winkler et al., 1995). A higher roll center results in a reduction in the amount of rotation of the sprung mass thereby reducing the Δy term in the roll stability equation (Equation A-2). The roll center height of any given axle suspension is a design property of the vehicle and the variation in roll center heights comes from the fact that the front suspension is low (below the engine), the drive axle suspension is relatively low to fit under the fifth wheel, and the trailer suspension is under the trailer bed and above the axles (Arant, 2010).

Both the stiffer rear suspension rates and higher rear roll centers act to reduce the lateral deflection of the CG (Δy term) and thus increase the roll stability limit for the rearward axle groups. However, despite these improvements most tractor semi-trailers rollovers start at the rear of the vehicle and move forward to the steer axle (Macnabb, Brewer, Baerg, & Billing, 2002),(Winkler, 2000) as the higher rearward CG dominates the roll stability balance for most commercial vehicles (Arant, 2010).

Roll and Load Transfer

The only way that a vehicle can remain upright during a handling maneuver is for the vehicle to transfer vertical load from one wheel to the other generating a moment counter to the overturning moment (Equation A-3). Note: In this case, the vehicle compliances have been neglected as the goal is to develop a method to keep the vehicle below its roll threshold which will result in relatively small chassis roll angles and hence small Δy contributions. This simplification assumption is made for two reasons:

- Calculating chassis roll requires more precise information on the vehicle (suspension stiffness, roll center, etc.) than needed to assess rigid chassis behavior.
- Calculating chassis roll requires additional computational time when the goal is to have a fast estimator of roll potential.

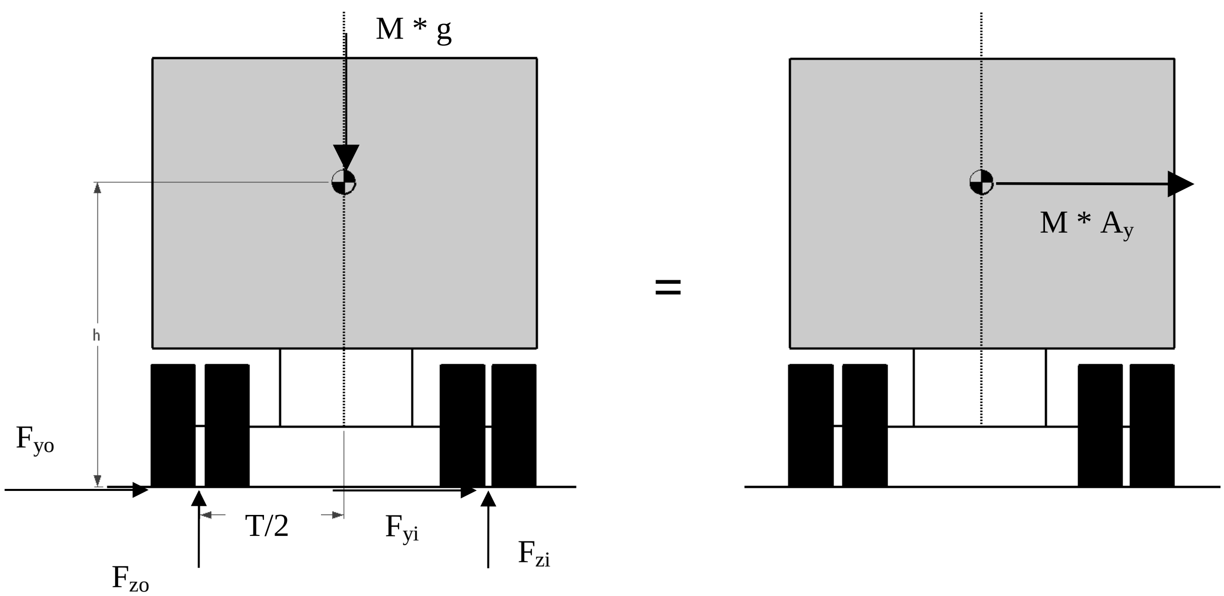

Figure A-17 Overturning Moment Diagram (Arant, 2010)

$$F_{zo} * \frac{T}{2} - F_{zi} * \frac{T}{2} = M * A_y * h_{cg} \quad \textbf{A-3}$$

Assuming that the vehicle can generate sufficient lateral forces to prevent it from sliding off the road (yaw divergence), the load transfer will build until the vertical load on the inner wheel reaches zero. At this point the vehicle is said to be at its stability limit even though it will not actually roll over until the CG location passes outside the wheel base or the roll inertia of the vehicle becomes greater than the stabilizing moment generated by the mass and half the track width.

The objective of any roll warning or roll mitigating controller is to anticipate roll instability and to intervene before instability is reached. If instability is detected, the controller will need to either reduce the lateral acceleration induced overturning moment or increase the potential restoring moment. However, as both corrective options are relatively slow to implement, the stability system will need to predict the roll state of the vehicle several seconds into the future. If additional information on commercial vehicle rollover is desired, it can be found in (Arant, 2010).

A.2.3. Yaw Stability

While roll stability is generally considered the bigger issue in commercial vehicle safety (Figure A-18), yaw instability is still a significant safety issue (Kharrazi & Thomson, 2008a) . Further, the types of maneuvers which result in yaw instability are more diverse than the maneuvers which generate roll instability (Figure A-19) (Kharrazi & Thomson, 2008a). Thus any attempt to manage yaw instability will have to manage a much larger set of driving situations as compared to roll instability.

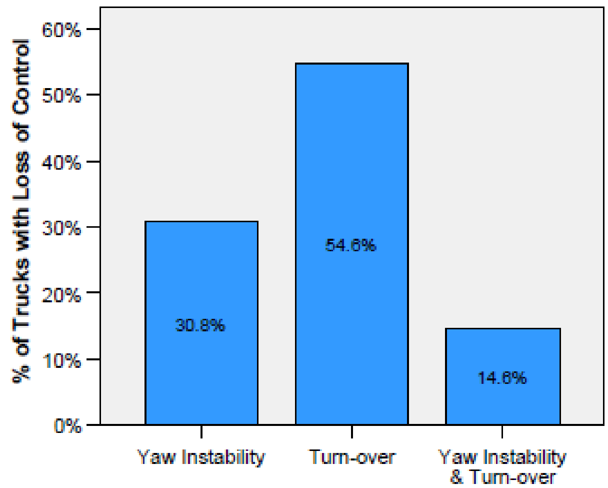

Figure A-18: Commercial Vehicle Accident Type (Kharrazi & Thomson, 2008a)

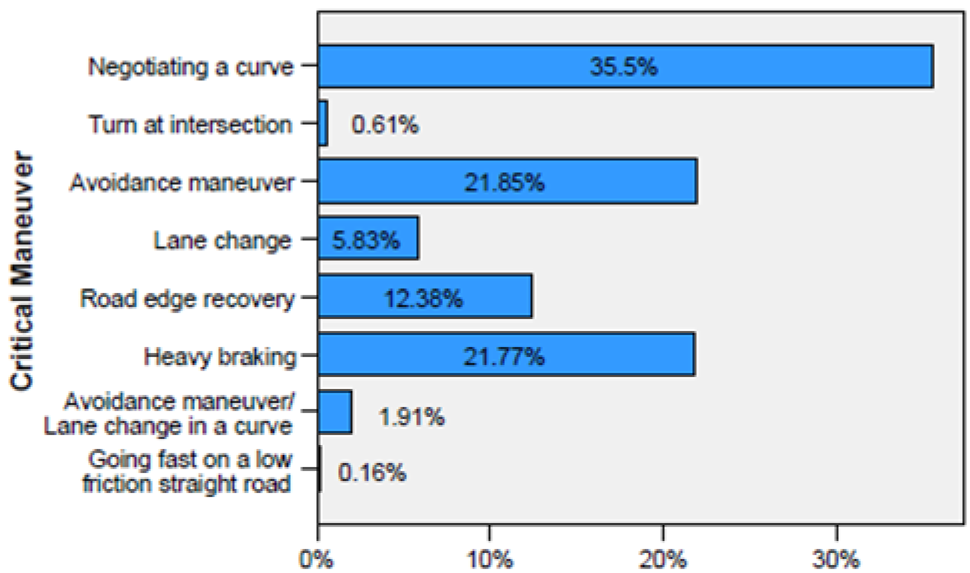

Figure A-19: Yaw Instability Accident Type (Kharrazi & Thomson, 2008a)

Yaw instability is also a more complex control problem than roll instability. While roll instability is primarily related to excessive lateral acceleration, yaw instability is a function of lateral acceleration and vehicle speed where instability can be observed in common commercial vehicles at lateral accelerations as low as 0.1 (Ma & Peng, 1999). Yaw instability can also be triggered by the vehicle's control system thorough poor activation of brakes. In particular, a jackknife event can be triggered if the trailer brakes do not match the drive axle brakes in declaration (Ma & Peng, 1999). This probably leads to an under representation of yaw instability accidents in the crash data analysis as drivers occasionally willingly choose to be involved in a rear-end collision through less than full brake activation rather than risk a jackknife accident (Palkovics & Fries, 2001)

Understeer and Oversteer

Yaw instability for a passenger car is manifested as either understeer or oversteer indicating which axle is saturating (Figure A-20). In the case of understeer, the vehicle has reached the limit of lateral force potential at the front axle and the vehicle slides head first off the road. In the case of oversteer, the rear axle has reached the limit of lateral force potential and the vehicle spins. All passenger car yaw stability systems place priority on avoiding oversteer accidents as these are the most dangerous.

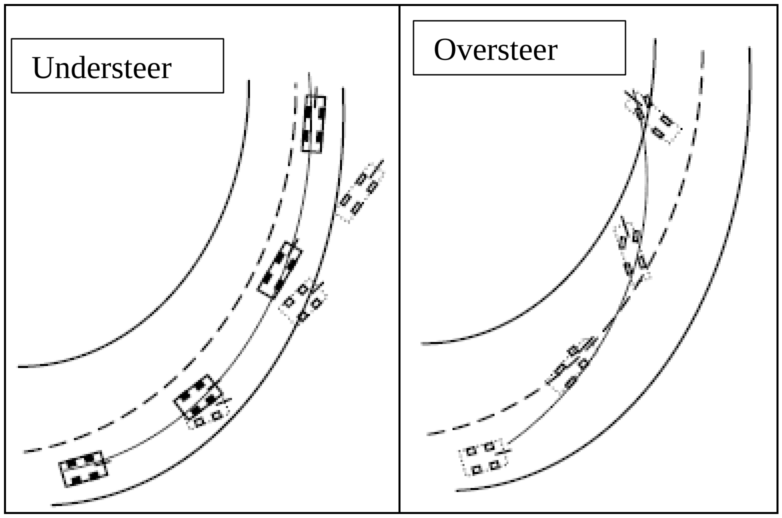

Figure A-20: Passenger Car Yaw Instability (Tekin & Unlusoy, 2010)

This steering behavior of the vehicle is often quantified as the understeer gradient which is a measure of the amount of understeer present in the vehicle per g of lateral acceleration (Equation A-4). It is usually denoted as degrees of road wheel steer per g of lateral acceleration.

$$Kus = \frac{M_f * g}{C_{\alpha f}} - \frac{M_r * g}{C_{\alpha r}} \qquad \textbf{A-4}$$

Here, M_f and M_r are the mass carried by each axle and $C_{\alpha f}$ and $C_{\alpha r}$ are lateral forces generated by the tires on an axle per degree of slip. Note that a positive gradient means that the vehicle is stable and understeering as the front axle has a lower lateral force to normal force ratio. This means that as lateral acceleration builds (through an increase in speed or a decrease in turning radius), the driver has to input an increasing amount of steering to keep the desired path (Equation A-5). Here δ_r is the road wheel steer angle (in radians), L is the vehicle wheel base, R is the turn radius, and g is gravity.

$$\delta_r = \frac{L}{R} + Kus * \frac{V}{R * g} \quad \textbf{A-5}$$

In cases where Kus is negative, the steering input goes down with increasing lateral acceleration (and may even become a negative steering input). This leads to an unstable vehicle that is difficult or even impossible to control. Therefore all stability systems act to make sure that Kus is always positive (though short negative spikes are occasionally used to induce vehicle yawing in emergency maneuvers).

Understeer and Oversteer for Articulated Vehicles

In commercial vehicles, yaw instability is more complicated as each unit of the vehicle can become unstable in yaw. Moreover, unlike single unit vehicles, the understeer gradient changes with speed and lateral acceleration. Thus the models are good for "fixed" lateral accelerations and need to be updated as the vehicle's lateral acceleration changes (Yu et al., 2008), (S. Zhou et al., 2008). For illustration, Figure A-21 shows a typical tractor response where the vehicle is initially understeering but transitions to oversteer. This is a typical loaded tractor and trailer behavior response.

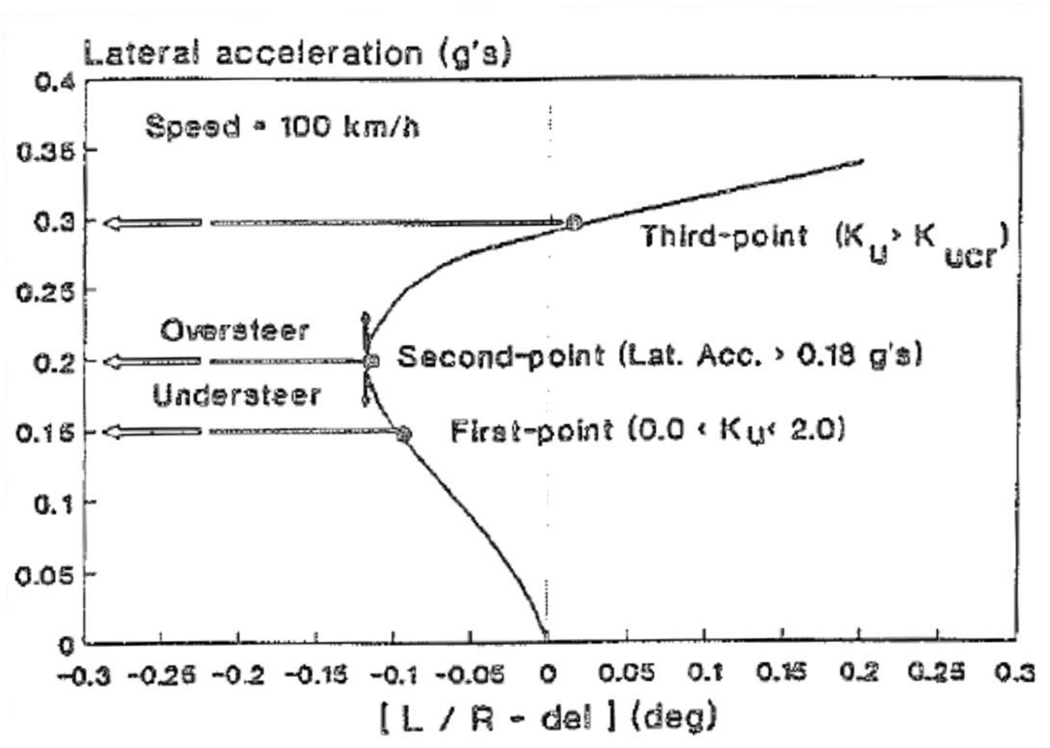

Figure A-21: Constant Radius Understeer Results (El-Gindy, 1995)

As each unit of a tractor and trailer can be understeering or oversteering, there are four stability combinations relating the behavior of a typical tractor and semi-trailer through the articulation of the vehicle (Equation A-8). Here Γ is the articulation angle, δ is the road wheel steering, $L_{tractor}$ is the tractor wheel base, $L_{trailer}$ is the trailer wheel base, $Kus_{tractor}$ is the tractor understeer gradient at the given conditions, $Kus_{trailer}$ is the trailer understeer gradient at the given conditions, V is the vehicle speed, and g is gravity.

$$\frac{\Gamma}{\delta} = \frac{\frac{L_{trailer}}{L_{tractor}} + Kus_{trailer} * \left(\frac{V}{\sqrt{L_{tractor} * g}}\right)^2}{1 + Kus_{tractor} * \left(\frac{V}{\sqrt{L_{tractor} * g}}\right)^2} \qquad \textbf{A-6}$$

$$Vcrit_{tractor} = \sqrt{\frac{L_{tractor} * g}{|Kus_{tractor}|}} \qquad \textbf{A-7}$$

$$Vcrit_{trailer} = \sqrt{\frac{L_{trailer} * g}{|Kus_{trailer}|}} \qquad \textbf{A-8}$$

- Tractor and trailer both understeer. Articulation angle gain (increase in articulation relative to steering input increase) will approach the ratio of the understeer gradients as speed increases (Equation A-6). Vehicle is stable.
- Tractor understeer and trailer oversteer. As $Kus_{trailer}$ is negative, the articulation gain is initially positive but becomes negative and the trailer swings out. This is an unstable arrangement at speed. However, at low speeds, the articulation gain is positive making the vehicle drivable.
- Tractor oversteer and trailer understeer. As speed increases toward the critical speed, the articulation gain approaches infinity. This results in a jackknife. System is unstable at speed.
- Tractor and trailer both oversteer. Depending on the if the ratio of the understeer gradients is greater or less than the ratio of the wheel bases, the articulation gain will drive to negative or positive infinity. This results in a jackknife or a swing out though the difference will be hard to tell from the driving perspective. The vehicle is unstable at speed.

Longer combination vehicles (LCV) have even more complicated stability interactions in yaw making them difficult to analyze analytically.

Correcting Yaw Instability

Yaw instability is correct through selective braking which generates countering yaw moments. An illustration of how a tractor and trailer will interact with and without stability is shown below in Figure A-22.

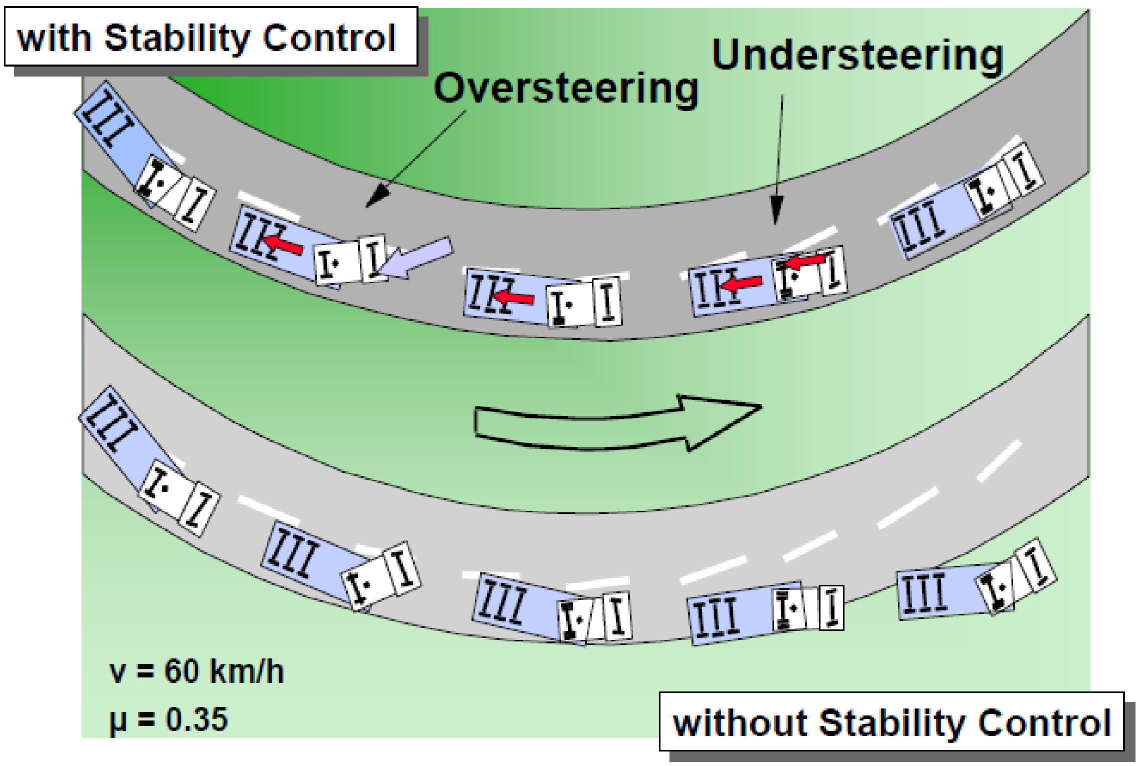

Figure A-22: Articulated Vehicle Stability Control Illustration (Freightliner LLC, 2007)

The goal of a typical stability system is to evaluate each unit of the vehicle to determine the desired vehicle response based on steering inputs and a simple model of the vehicle's dynamic behavior. The desired behavior model can be implemented as a set of state equations (state space model) or a set of transfer functions (Ghoneim et al., 2000). The ideal output of the controller is a neutral steering vehicle (S. Zhou et al., 2008) as that is how the driver intuitively expects the vehicle to behave. An example of a traditional yaw stability controller is shown below in Figure A-23.

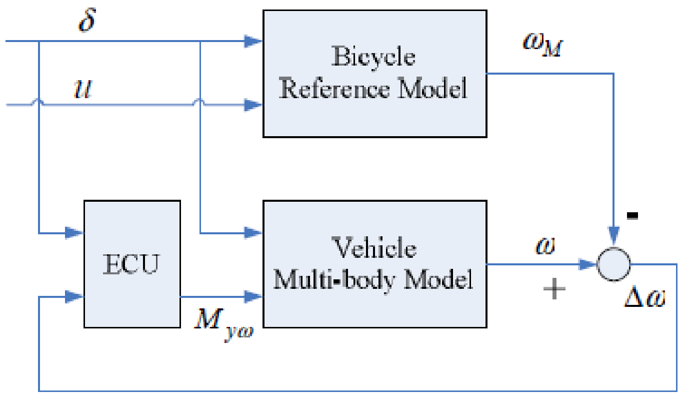

Figure A-23: Example Yaw Controller (S. Zhou et al., 2008)

A.2.4. Combined Roll and Yaw Stability

The major difficulty in developing a controller to manage both yaw and roll stability is that the stability demands for yaw and roll may conflict (S. Zhou et al., 2008). For example, if a vehicle is understeering and rolling over, the yaw controller will indicate that more yaw rate is needed to correct the understeer. But increased yaw rate means increased lateral acceleration which exacerbates the roll stability problem. Thus a priority or hierarchal control algorithm is needed to manage the inevitable trade-offs (Yoon, Kim, & Yi, 2007).

This is not a hypothetical problem as shown in Figure A-18 where 14% of fatal truck accidents involved both yaw and roll instability (Kharrazi & Thomson, 2008b). Further, MacAdam noted that in some cases it was not possible to decouple the yaw and roll stability requirements for a commercial truck, particularly when the CG was relatively high (MacAdam, 1982). Finally, large tire slip angles, which provide quick yaw corrections, also produce large lateral accelerations which reduce roll stability (MacAdam, 1982).

To visualize this interaction of yaw and roll, the reader is pointed to Figure A-24 where the overlap of yaw and roll stability is clearly observable. Note that a significant portion of the stability map indicates both yaw and roll stability risks. However, there have been successful controllers built to manage both yaw and roll stability with some providing improved overall stability with both yaw and roll control enabled (Figure A-25) (Chan, 2010), (Yoon, Cho, Yi, & Koo, 2009). An example response of such a controller is shown in Figure A-26 (B. Chen & Peng, 1999b).

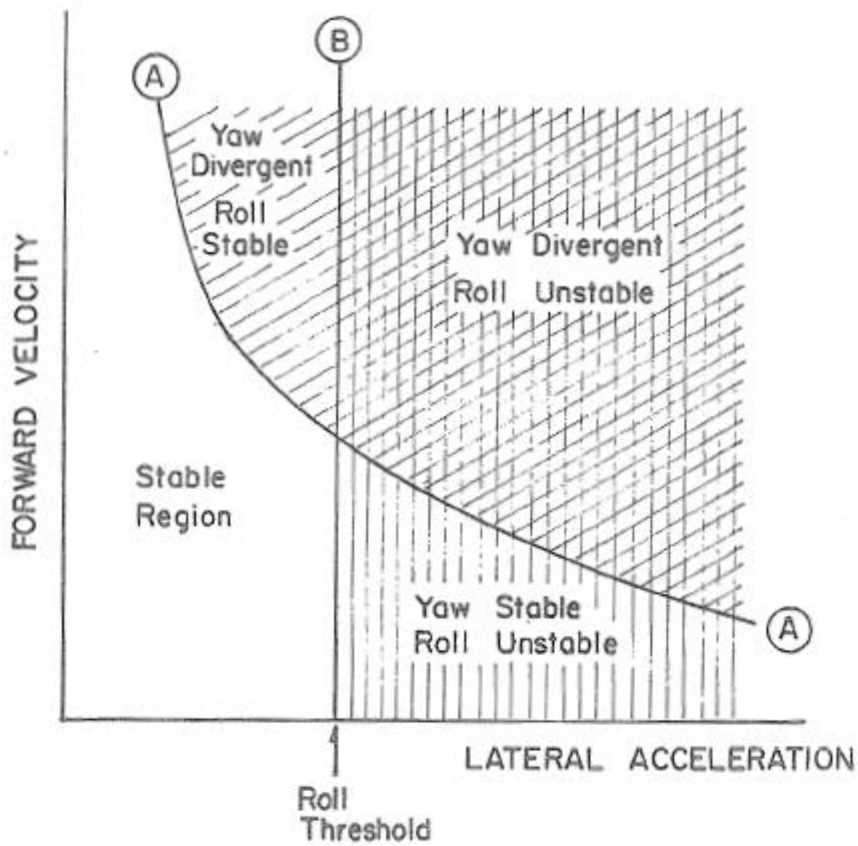

Figure A-24: Yaw and Roll Stability Regimes (MacAdam, 1982)

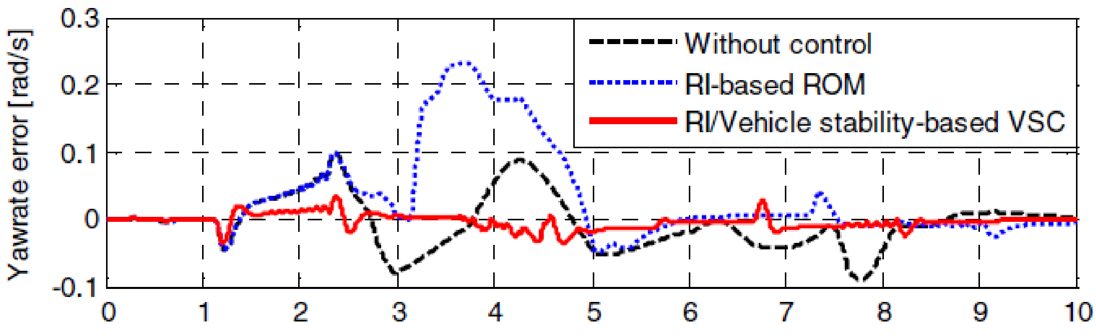

Figure A-25: Combined Yaw and Roll Controller for a Car (Yoon et al., 2009)

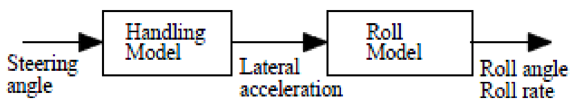

Figure A-26: Yaw and Roll Controller (B. Chen & Peng, 1999b)

To underscore the interaction of yaw and roll stability, the following excerpt on coupled yaw and roll is presented (Andersky & Conklin, 2008). Both Andersky and Conklin are with Bendix Commercial Vehicle Systems LLC, manufactures of commercial vehicle stability control systems.

> "By helping a vehicle maintain directional stability during both over-steer and under-steer situations, the driver's intended path continues to be followed, and loss-of-control situations are minimized. (Many rollovers are) the outcome of loss-of-control situations that begin when the driver maneuvers to avoid a situation – which, in turn, initiates directional instability – leading to the eventual lateral acceleration event culminating in the rollover." (Andersky & Conklin, 2008)

In a similar light, Woodriffe and Blower noted that adding yaw ESC improved roll stability and concluded that the added roll benefit came from the yaw controller activating before the roll controller producing a restorative response before the activation of the roll controller (Woodrooffe et al., 2010). Clearly there are solutions where the competing goals of yaw and roll control can be achieved, but the controller approach must be rather sophisticated.

A.2.5. Current Production Stability Systems

As noted directly above in section A.2.4, there are commercially available systems which manage heavy truck stability on the market today. In fact, some manufactures, such as Volvo, have adopted a progressive approach and now have ESC standard on all tractors. But while this is a very positive step towards improved commercial vehicle safety, there are some limitations to these commercially available systems. To better understand what improvements could be made, it is necessary to review how these systems operate.

All of the major brake control systems manufactures produce ESC systems with slight variations in performance between systems. The major system suppliers are Bendix (Holler & Macnamara, 2001), (Andersky & Conklin, 2008), Haldex (Kienhöfer, Miller, & Cebon, 2008), Wabco (Petersen, Neuhaus, Gläbe, Koschorek, & Reich, 1998), (Winkler, Sullivan, Bogard, Goodsell, & Hagan, 2002), Bosch (Liebemann, Schuh, Meder, & Nenninger, 2004), and Knoorr-Bremse (Palkovics, Semsey, & Gerum, 1999). Note some of these companies have collaborative agreements in certain economic zones and may not be truly independent entities. However, they are marketed individually

The first and most significant issue with existing ESC systems is that the available stability control systems are all single unit controllers. That is each unit can "see" just one unit of the vehicle and there is no communication of vehicle stability between units. Further, tractor based systems can activate the trailer brakes blindly (no feedback of activation) but trailer systems cannot activate the tractor brakes. The reasons for this lack of communication are three fold:

- There is no open channel for data communication between the trailer and the tractor. The sole electrical connector (7 – pin connector) does not have any free pins left.
- There is no standard for what to communicate and how. Given that trailers are switched frequently, there would need to be a standard communication that all manufacturers agreed to.
- While there are FMVSS 121 standards in place to ensure adequate brake performance, there is still a significant amount of variability between tractors and trailers with regard to brake performance. For that matter, there is significant variation within a vehicle unit as the brakes wear. Thus critical timing and control parameters would need to account for variances in brake responses.

The result is that each unit "sees" and responds to the stability issues of the unit to which it is mounted with no regard to other units (Holler & Macnamara, 2001).

Generally most tractor systems are full ESC systems with yaw and roll stability (similar to a car system) but with controllers optimized for trucks (CG height and mass). Further, the systems can estimate some trailer behavior (yaw) based on the difference between the ideal (modeled tractor dynamic behavior) and the actual behavior as the trailer acts on the tractor. These systems can also anticipate a roll problem for the trailer from measured lateral accelerations at the tractor though they cannot see the trailer behavior.

Trailer only systems are often roll control only as yaw instability calculations would require either the articulation angle be known or the target yaw rate be known. Both of these are difficult to determine in practice. When tractor and trailer ESC systems are paired together, the result is a more stable vehicle system (Arant et al., 2009), but further improvements could be made if information was shared about the dynamic state of each unit.

A.2.6. Multiple Unit Stability

As mentioned in section A.2.3, the control problem for ensuring stability increases in complexity and scope with the number of units in the vehicle (tractor / trailer(s)). In fact, for multiple unit vehicles, closed form solutions defining the vehicle's stability may not be possible. Therefore, different approaches to evaluating and managing stability are needed.

Perhaps the two biggest issues facing a multiple unit controller are state measurement / control actuation delays and system interactions where improving the stability of one unit may negatively affect the stability of an adjacent unit. To understand the data communication issue, it helps to understand that a triple can be over 110 feet from end to end. This is a significant transport distance. Further, as will be explained in section A.5.1, there are significant issues with the manner in which current brake systems communicate brake demand. The unit stability interaction issue is a bit easier to understand in light of the discussion in section A.2.4, just expanded to account for multiple unit interactions.

There has been little published research on stability control of long combination vehicles (doubles and triples) with the Rearward Amplification Suppression system (RAMS) (MacAdam et al., 2000) being one of the few major studies. In this study, a multi-unit system was evaluated to help mitigate rollover due to the natural tendency of trailing units to have amplified lateral accelerations relative to the tractor (whip effect) (Figure A-27). The research compared individual units (no networking between trailers) and interconnected unit responses.

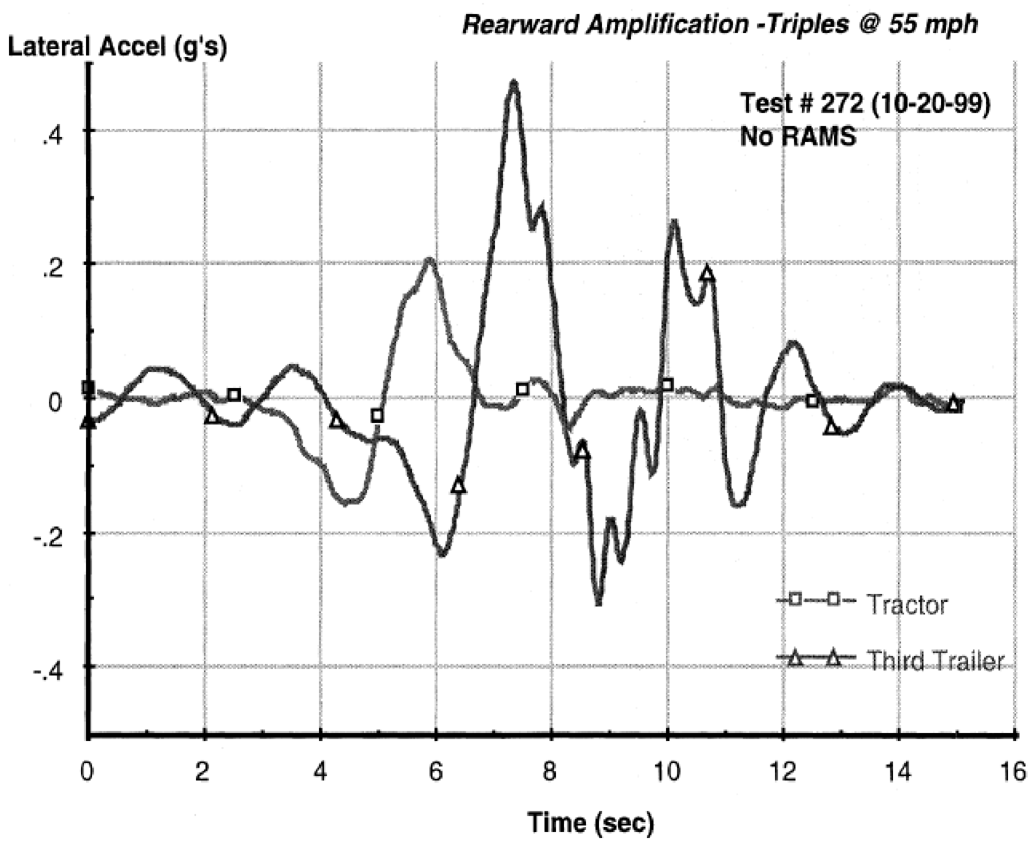

Figure A-27: RAMS Rearward Amplification (MacAdam et al., 2000)

The control response used diagonal braking to produce countering yaw moments on each trailer suppressing the build-up of lateral acceleration (Figure A-28, Figure A-29).

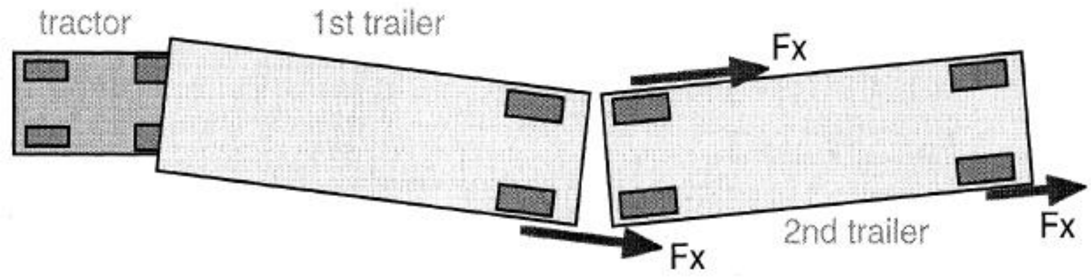

Figure A-28: RAMS Control Illustration (MacAdam et al., 2000)

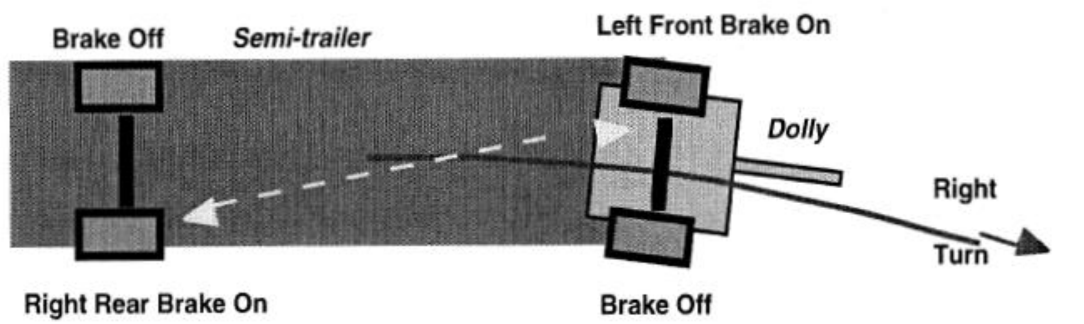

Figure A-29: RAMS Diagonal Brake Illustration (MacAdam et al., 2000)

The results were quite encouraging even though there was no communication between the trailers and each system was reacting to the yaw rate and lateral accelerations seen at that unit (Figure A-30). RAMS was able to reduce the third trailer lateral acceleration by approximately 0.1 g and the final roll angle by approximately 4 degrees (11 degree peak roll angle).

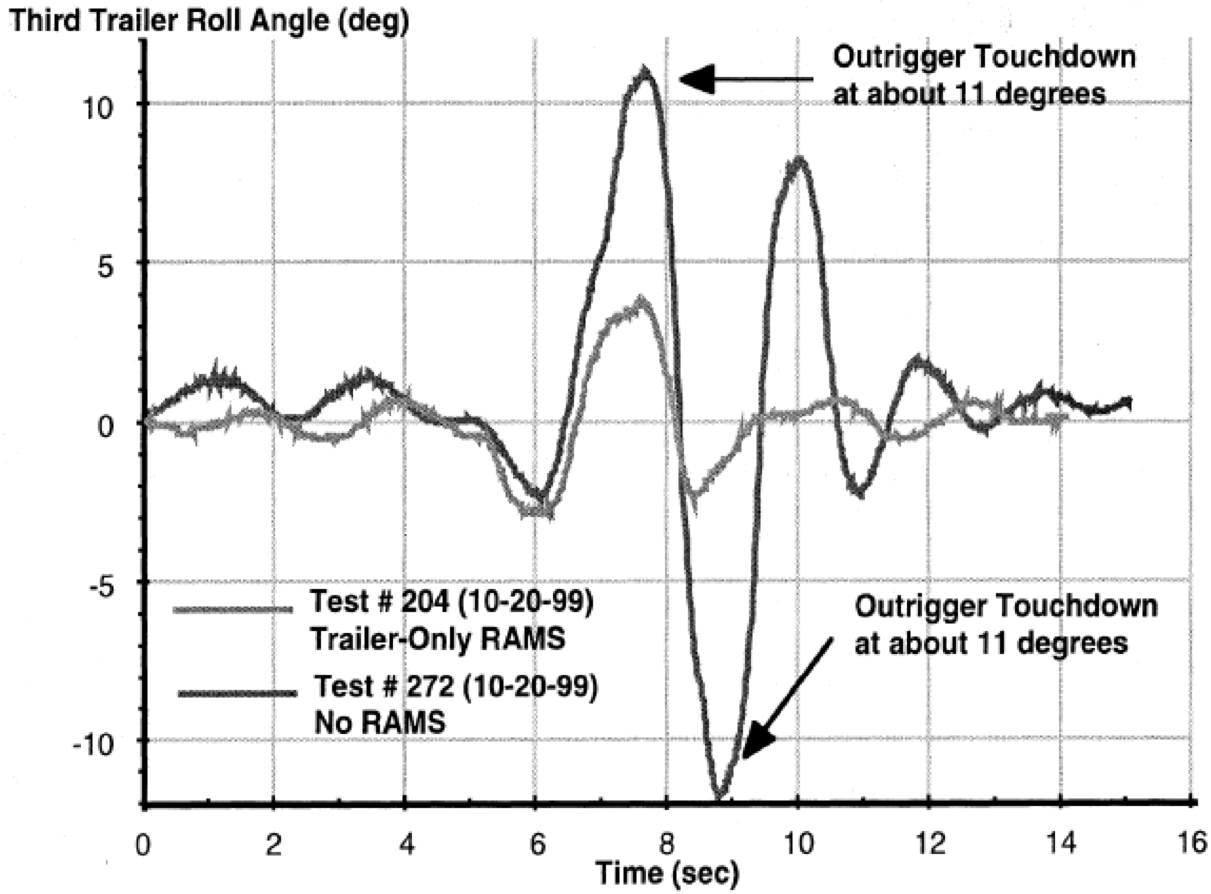

Figure A-30: RAMS Roll Suppression (MacAdam et al., 2000)

Several control strategies were investigated (both single unit and multi-unit control) (Figure A-31). As anticipated, the complete vehicle control strategies performed better. However, the research also uncovered the same difficulties in defining a standard for managing such communication of states and control commands.

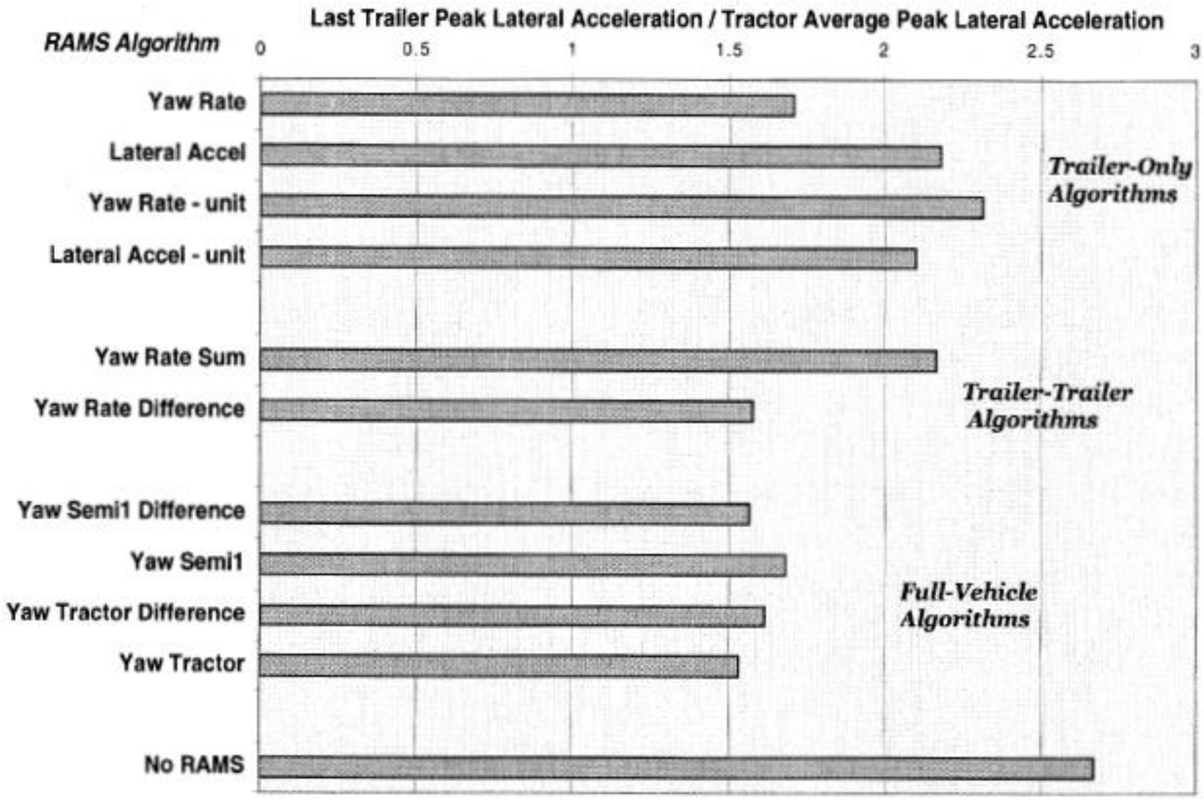

Figure A-31: RAMS Control Algorithms (MacAdam et al., 2000)

Finally, none of the control strategies were found to improve yaw stability on low mu surfaces (slick road). In fact, those full-vehicle RAMS algorithms that performed the best under dry and wet asphalt operating conditions, demonstrated the poorest performance under the very low friction test conditions (MacAdam et al., 2000).

A.2.7. Estimates on the Value of Commercial Vehicle Stability Control

Given that there are some stability control systems in the market, the logical question to ask would be how effective are they. Unfortunately, these systems are simply too new and have been phased in over the last 5 years to be accurately reflected in the crash databases (Woodrooffe et al., 2009), (J. Wang, 2011), (Pape et al., 2007), (Woodrooffe et al., 2010). It needs to be remembered that the databases are based on field crashes and if the percentage of vehicle with ESC is small, the database results will be much less accurate. The best data available on potential benefits of commercial vehicle ESC is from Wang (Table A-5) where RSC (roll only) offers an improvement of around 25% and full ESC (roll and yaw) offers an improvement of around 33% (J. Wang, 2011). To show the uncertainty in the analysis, Bendix estimates the safety improvements at 29% and 68% ((Andersky & Conklin, 2008)) while the Insurance Institute for Highway Safety estimates the improvements at 11% and 20% (Jermakian, 2010). And it is important to remember that these are tractor only control systems.

Table A-5: Estimated Commercial Vehicle ESC Benefit (J. Wang, 2011)

Effectiveness Rates for RSC and ESC by Target Crashes (Current NHTSA Estimates)

Technology	Target Crashes	Low	High
RSC	Rollover[1]	37	53
	LOC[2]	3	3
	Combined	21	30
ESC	Rollover[3]	40	56
	LOC[2]	14	14
	Combined	28	36

1. Based on the 2008 FMCSA study
2. Revised estimates from the 2009 UMTRI study
3. Based on the 2008 FMCSA study and the revised estimates from the 2009 UMTRI study

Table A-6: Estimated Commercial Vehicle ESC Benefit (Andersky & Conklin, 2008)

Stability-Related Cases: ESP Efficacy	130	
ESP would have been expected to mitigate the event	88	68%

Stability-Related Cases: RSP Efficacy	130	
RSP would have been expected to mitigate the event	38	29%

Given that ESC shows promise of improving safety, the next logical question is what is / would be the cost of an ESC system. To help answer that, the cost of passenger car ESC systems were evaluated as shown in Table A-7 (NHTSA, 2007). Knowing that a truck ESC system would need to monitor more wheels and be distributed over a larger area, it is estimated from the NHTSA data that a commercial vehicle system would cost about $500 per vehicle unit (tractor or trailer) above the current brake management system cost. Additionally, the systems will add about 2 kg above the existing ABS mandated equipment.

Table A-7: Estimated Cost of ESC components (Passenger Car) (NHTSA, 2007)

Incremental Cost and Weights for ABS and ESC

	ABS	ESC	ABS/ESC Combined
Costs	$368	$111	$479
Weights	4.85 kg. 10.7 lbs.	0.82 kg. 1.8 lbs.	5.67 kg. 12.5 lbs.

Given the high cost of accidents, the cost of and ESC system appears to be quite reasonable. Bendix estimates that one fatal accident could cover the cost of outfitting 3,000 tractors (Andersky & Conklin, 2008). But commercial transport companies are very slow to adopt new technologies and expect proven testing to show that they will save money by doing so. Freightliner observed that the DOT needs safety benefits data that demonstrate the reduction in crashes, fatalities, and injuries offered by these systems if they want the industry to support policy changes that encourage their adoption (Freightliner LLC, 2007). Short of a federal mandate to install ESC systems, it will take a thorough review of ESC technology cost, effectiveness (statistical analysis,) and operational / maintenance difficulties to convince most fleet owners to fully adopt ESC on all tractors and trailers.

A.3. Safety and Stability Enhancements

The above analysis of ESC capabilities and operation has been based on brake based ESC technology where the restorative actions are accomplished through brake activation. While the research presented here continues with brake based systems, it was deemed important that the reader understand the stability augmentation options and why brake based systems are used.

A.3.1. Warning Systems

The most basic of stability enhancement systems is a simple warning system where a light, buzzer, or other device is activated to warn the driver that a stability risk is present. Typically these are roll over risk only systems as it is simpler to estimate rollover (function of lateral acceleration) than yaw instability (function of lateral acceleration and velocity). Usually the warning activates at some percentage of the roll threshold, such as the 75% threshold noted in (Hyun & Langari, 2003), and the 60% metric in (El-Gindy, 1995). The most common warning metric is called the time to rollover (TTR) metric (B. Chen & Peng, 1999a). This metric "counts down" to the anticipated rollover based on current vehicle states. The typical maximum window of projection is 3 seconds. Note: TTR is also used by many ESC algorithms to determine when to intervene.

The actual calculation of rollover risk usually looks at the estimated load transfer from the inner wheel to the outer wheel, called the Lateral Load Transfer (LTR) (Changfu, Yu, Miao, & Zhang, 2010). This metric is relatively easy to project as the progression of lateral acceleration is simple to monitor and the vehicle's load transfer can be estimated using simple models (Tianjun & Changfu, 2009), (Tianjun & Changfu, 2010). However, other methods which use estimated roll angle and roll rate exist as well (Park et al., 2008).

Determining the effectiveness of these systems is a little difficult as the effectiveness depends on the driver recognizing and warning and acting appropriately. Both of these tasks can be problematic as the driver may not immediately recognize the warning or the driver may feel that the warning is pre-mature and ignore it. Still, Winkler and Sullivan estimated that warning only systems could potentially mitigate approximately 47% of all single truck rollovers (Winkler et al., 2002).

A.3.2. Active Suspensions

When a vehicle experiences a lateral acceleration, the compliances in the chassis result in the vehicle leaning out of the turn which reduces stability. This occurs because the roll center height is below the CG height so that the sprung mass rotates outward as it pivots about the roll axis. This sprung mass roll is then added to the roll generated at the ground plane due to tire deformation with load change. Both roll responses act in the negative direction for roll stability.

To counter this roll instability, several groups have investigated and tested so called active suspensions which either limit the outward roll of the vehicle or impose an inward roll (enhancing stability). Figure A-32 illustrates an active suspension where the chassis is tilted into a turn and Figure A-33 illustrates the mechanism of active hydraulic rams (Figure A-34 is a photograph of the actual device). Some of these systems have been quite effective at increasing roll stability (lateral acceleration potential). For instance, Sampson and Cebon found improvements of 26% for steady state turns (Figure A-35), 38% for steep steer inputs, and 48% for lane changes (Sampson & Cebon, 2003), (Sampson et al., 2000).

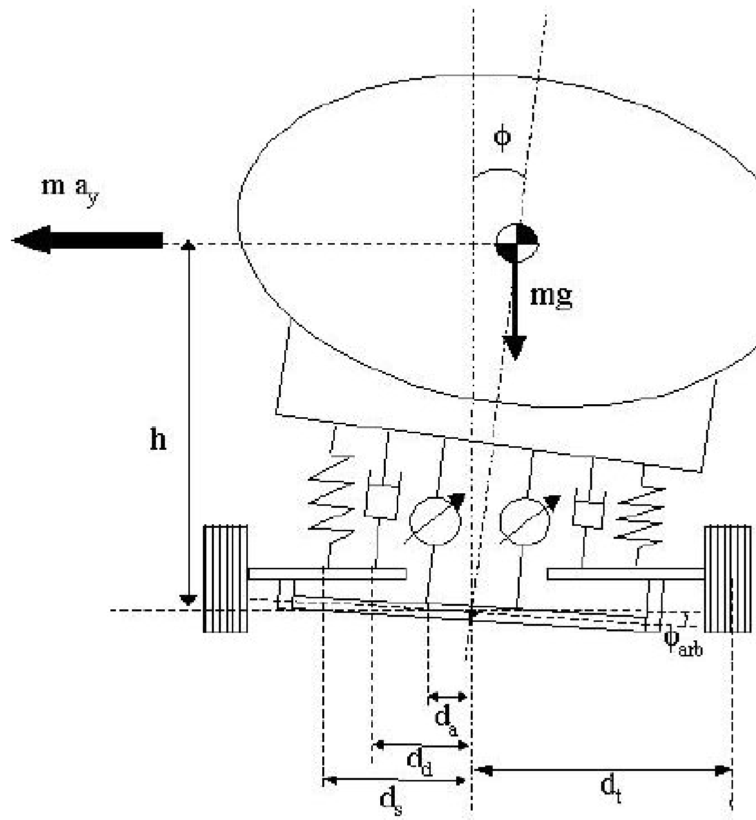

Figure A-32: Active Roll Suspension (Miege & Cebon, 2002)

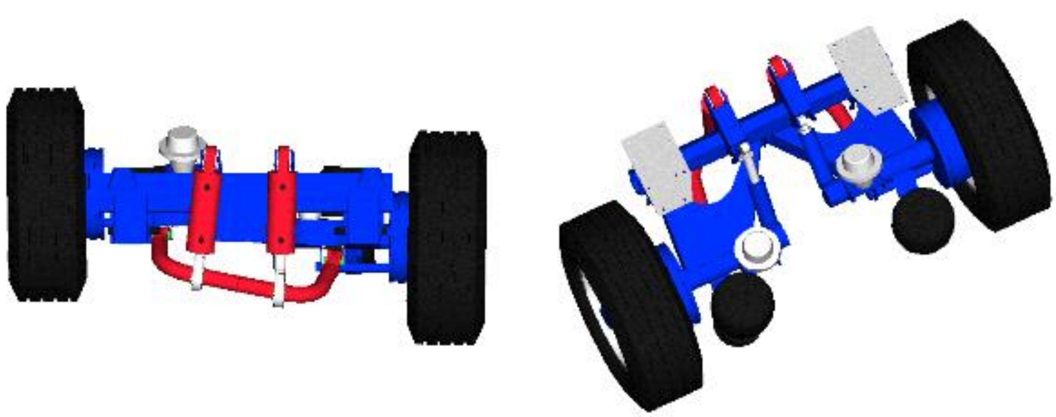

Figure A-33: Active Suspension Mechanism (Sampson et al., 2006)

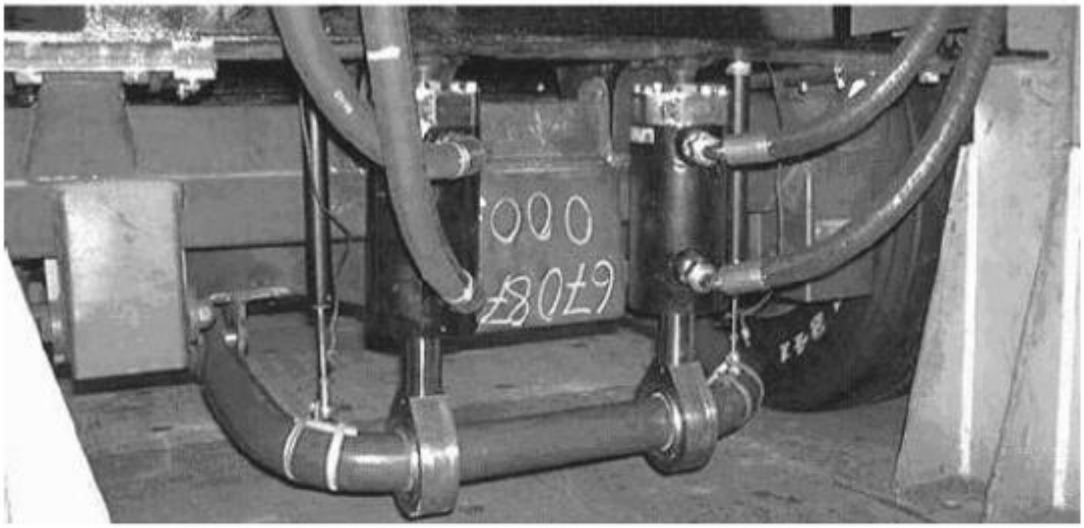

Figure A-34: Active Suspension (Stone & Cebon, 2008)

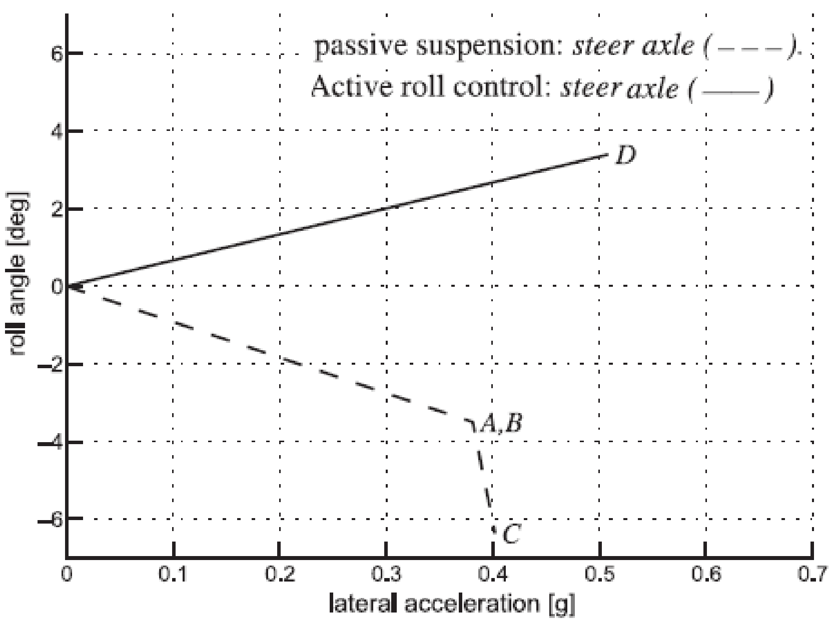

Figure A-35: Active Roll Control Response (Sampson & Cebon, 2003)

Unfortunately, these systems suffer from three major limitations. The first limitation is the cost where estimates range from $120,000 to $160,000 for a typical full vehicle system (Sampson, McKevitt, & Cebon, 1999). For reference, that value is on par with the price of a standard 6X4 tractor.

The second issue is that the active roll control response can lead to instability in controlling roll dynamics if the gains are too high (Sampson et al., 1999). While this is not an insurmountable problem, the potential to induce instability through active control is a serious issue and must be managed. To resolve this problem, slower acting suspensions (5 Hz range) are employed so that there is less feed-back gain instability but the system is less responsive in transient situations (Sampson, 2000)**.**

The third major issue with active suspensions is the power and force requirements needed to move an 80,000 lb. vehicle. Commercial vehicle active suspensions systems need 85 mm of travel and 6 degrees of rotation (Sampson et al., 2000). This constitutes the bulk of the suspension's free travel. Further, to move the vehicle, actuator forces of 137 kN (31k lb.) and pressures of 210 bar (3,100 psi) are needed (Sampson et al., 2000) generating roll moments of 64 kN-m (1.5 M ft.-lb.) (Sampson & Cebon, 2001). The average power requirement is 17 kW (23 hp) (Sampson & Cebon, 2003). These are serious demands and having an efficient and cheap power source on board is very unlikely. In fact, others have concluded that the insufficient response rates of these systems limit their effectiveness (Hac, 2002).

A.3.3. Active Steering

All modern steering systems use some form of a power assist to help the driver turn the wheel. Generally, these are either hydraulic pumps or electric motors. The idea behind active steering is to replace the "assistance" motor with a secondary steer input (Figure A-36). Thus "corrective" steering can be added to the vehicle by the controller (Figure A-37).

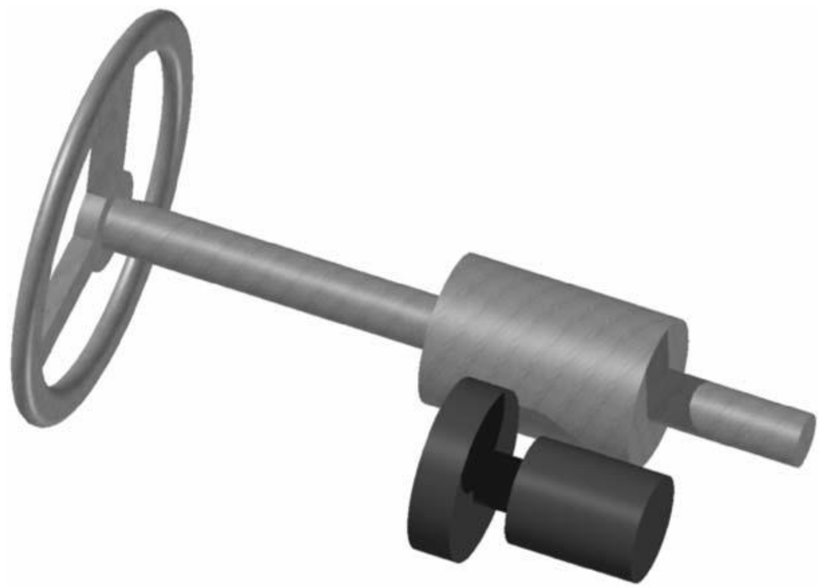

Figure A-36: Active Steering Illustration (Manning & Crolla, 2007)

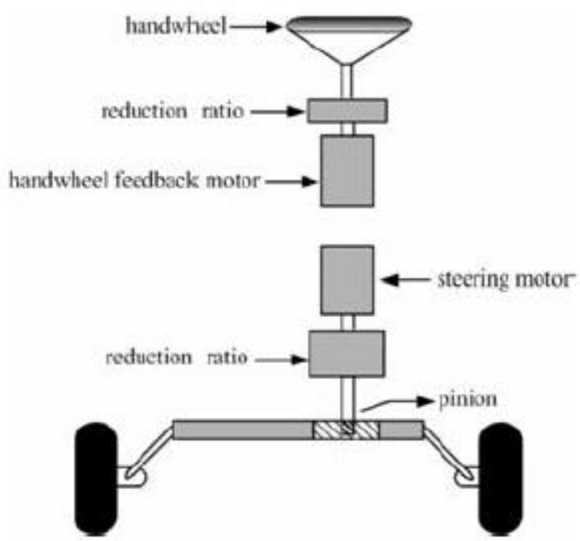

Figure A-37: Active Steering Schematic (Shun, 2007)

Successful systems have been developed and demonstrated for yaw control (Mammar & Koenig, 2002), (Chung, Kim, & Yang, 2010), (Yoon, Yim, Cho, Koo, & Yi, 2010), (Naraghi, Roshanbin, & Tavasoli, 2010), and roll control (Shim, Toomey, Ghike, & Sardar, 2008) though the latter three were active steering with brake control supplement.

The principle has a good deal of merit as the steering can be adjusted to counter unwanted brake moments or vice versa for the tractor. For example, Figure A-38 illustrates how active steering could “turn into” the yaw moment generated by having different braking forces on each side of the vehicle and Figure A-39 shows anticipated stopping performance improvements (Burgio & Zegelaar, 2006), (Chung et al., 2010), (Rieth & Schwarz, 2004). For these reasons, car manufactures have been actively researching this technology (Burgio & Zegelaar, 2006).

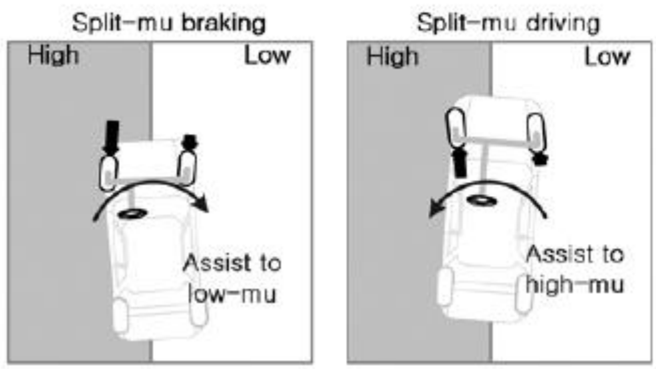

Figure A-38: Combined Steer and Brake Control (Chung et al., 2010)

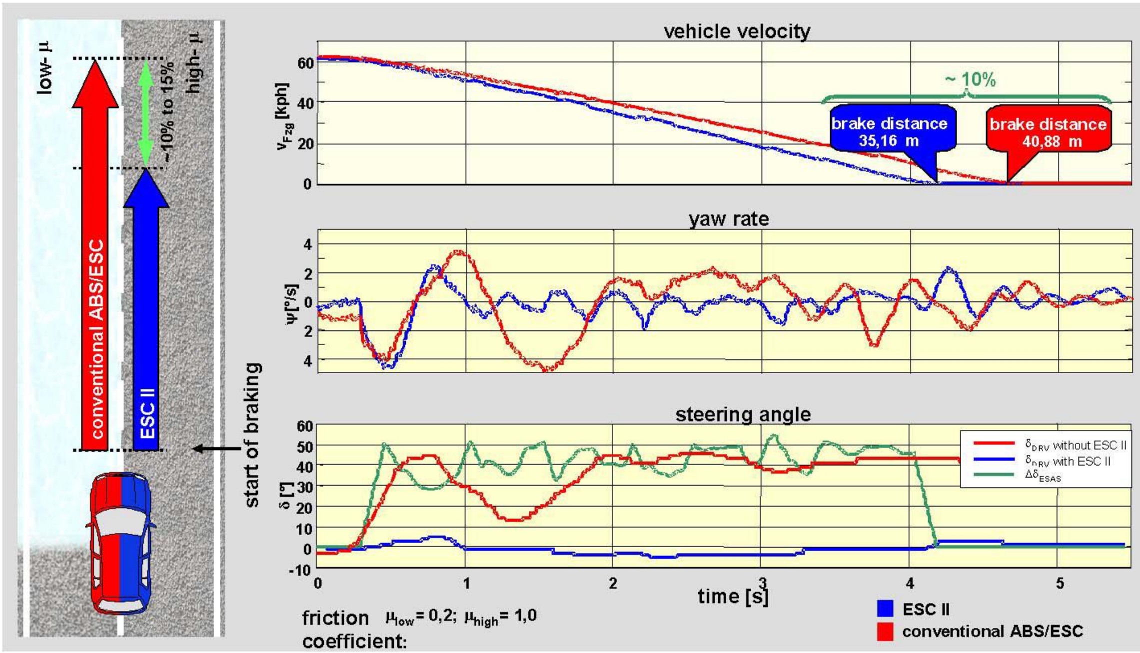

Figure A-39: Split mu Stopping Distance Reduction (Rieth & Schwarz, 2004)

However, while the systems do hold promise, there are three issues that are yet to be fully resolved. The first of these issues is liability if the driver has an accident. The question is who was "driving". While this same argument can be made about yaw corrective braking, it is a little more subtle and yaw braking cannot generate heading changes on the order that active steering can given that most cars have nearly 1,000 degrees of hand wheel (50 degrees of road wheel) steer angle.

The second issue is that the systems can become unstable in situations where there is a lag in system response to the control input. As an example, it was noted by Shun that the vehicle steering system exhibited chaos as steering speed increases on low mu roads (Shun, 2007). Again, this is not an insurmountable controls problem, but implementing an active steering, especially in parallel with a brake control system has to be done carefully to avoid system gains that are too high.

The final issue observed with active steering is that is really effective for the unit being steered. For trailers, which react to the heading of the tractor or tow dolly, the effect will be greatly reduced as the lead unit's yaw angle would have to be changed to affect the trailer.

A.3.4. Four Wheel Steer

Four wheel steer has been a cyclical technology over the last 30 years. Periodically, interest will grow in using the rear axle(s) to enhance controllability and then wane again due to the difficulties with such systems. While the technology has not been applied to class 8 tractors, it could conceivably be used though this is very unlikely.

While successful four wheel systems have been developed (Wu, 2001), four wheel steer can place too many simultaneous demands on the rear tires and hinder stability (Mokhiamar & Abe, 2002). Additionally, steering the rear wheels increases the vehicle's yaw rate significantly and non-linearly (Figure A-40). This makes predicting and controlling the desired yaw rate more complicated (Abe, 1999). Shen and Wang were able to develop systems where the yaw rate was controlled (Shen, Wang, Shi, & Premier, 2007), but Hac and Bodie noted that most drivers are only comfortable when a car is operating in a linear regime and sudden changes, such as sudden rear wheel steer, upset them and can result in poor control command decisions (Hac & Bodie, 2002).

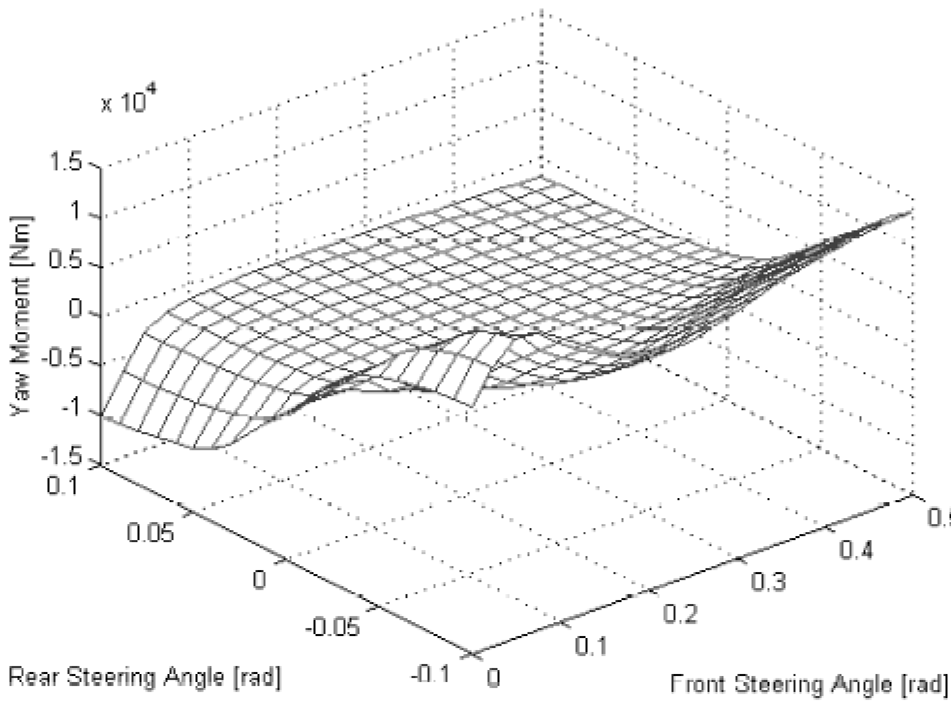

Figure A-40: Four Wheel Steer Yaw Moment (Hac & Bodie, 2002)

Four wheel steer systems are generally set-up to steer out of phase (opposite front and rear) at low speed to reduce turning radius and operate in phase (same steer direction) at higher speeds to enhance lateral motion. The problem with using out of phase low speed steering is that it would increase the likelihood of binding the trailer and tractor as the tractor pivoted in front of the trailer. At higher speeds, the trailer would have to yaw to maintain connection with a laterally translating tractor. The result would be that the trailer would drag on the tractor producing yaw in the tractor. This would increase the lateral acceleration seen by the tractor and possibly compromise stability.

Technical merits aside, rear wheel steering of tractors is not a likely technology option for class 8 tractors due to design and operational requirements. First, tractors have heavy solid axles that transmit large torques. Incorporating constant velocity (CV) joints into the axles would be complicated and most likely lead to fatigue failures due to torque cycling. Secondly, cost is the most important factor in selection of a tractor and development of a twin axle steer system will be quite complex and expensive.

A.3.5. Trailer Steer

While four wheel steering has been around for a few decades, trailer axle steering has been around for over 100 years. Examples of trailer steer include horse drawn wagons (Figure A-41) and early tractor drawn wagons (Figure A-42). Further, despite many advances in controls and vehicle dynamics modeling, human control of trailer steered vehicles is still the only practical production trailer steer option (Figure A-43). That fact alone indicates how difficult it is to develop a stable and robust controller for steerable trailer axles.

Figure A-41: 1903 Rear Steer Horse Drawn Fire Wagon (Hagy, 2011)

Figure A-42: 1916 Early Fire Wagon (Hagy, 2011)

Figure A-43: 2011 Fire Wagon (Pierce Manufacturing Inc, 2011)

Most steerable trailer designs are intended for low speed path flowing and not designed for higher speeds where yaw stability can be compromised (Odhams, Roebuck, Cebon, & Winkler, 2008). The objective is reduced off tracking and increased maneuverability in tight city streets rather than high speed dynamics. Active steering corrections during transient maneuvers at speed can cause large yaw accelerations and lead to rollovers (Odhams et al., 2008). Further, Odhams documented that the observed lateral acceleration is relatively linearly related to the rear steer rate (Figure A-44) though the slope of the curve is also a function of the trailer wheel base.

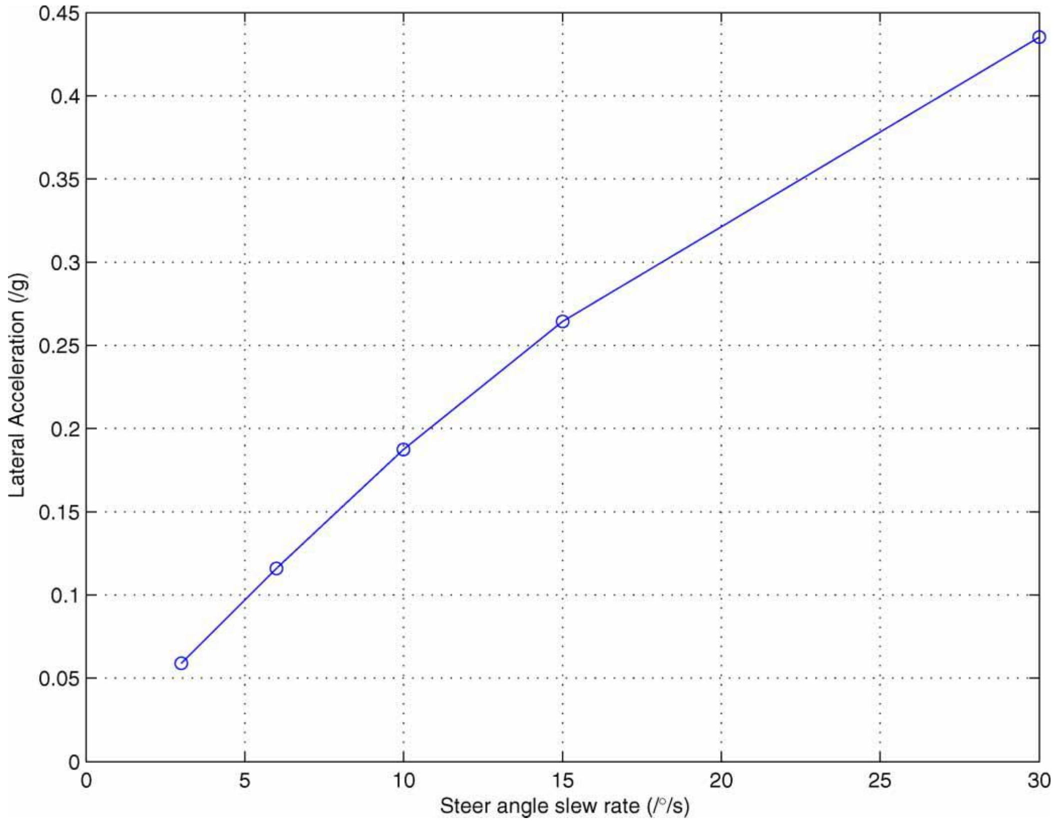

Figure A-44: Lateral Acceleration as a Function of Steer Rate (Odhams et al., 2008)

There have been a number of passive trailer steer systems developed where the axles are intended to "lock" at speed to maintain vehicle stability. However, most of these systems have negative effects on off tracking at speed and poor transient dynamics (Cheng & Cebon, 2011), (Lukowski, Lukowski, & Medeksza, 1998). To solve the high speed stability issues, Cheng and Cebon developed a control strategy to manage trailer steering using the fifth wheel as the preview distance and an optimal control strategy (Figure A-45) (Cheng & Cebon, 2011). The results indicated that tuning of the controller for better control of roll stability resulted in poorer off tracking results.

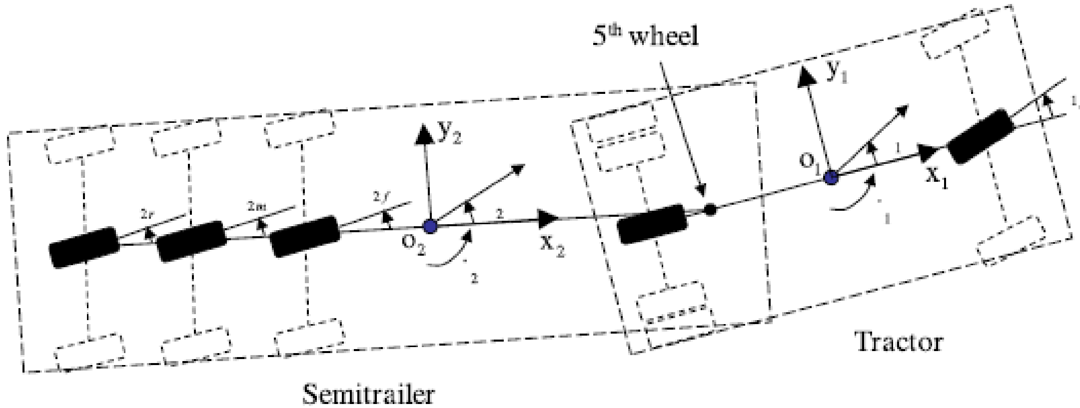

Figure A-45: Trailer Steer Diagram (Cheng & Cebon, 2011)

Steered trailer axle systems also require significant power; (32 kN – 7,200 lb.) for the Cheng and Cebon system. There is also no "safe" way to manage a failed trailer steer axle (Odhams et al., 2008) which mandates redundant controls for any steering trailer axle. Given that the best systems improve stability by only 20% (Cheng & Cebon, 2011) and the cost / complexity is relatively high, trailer steering is not seen as a practical solution to commercial vehicle stability needs.

A.3.6. Selective Brake Control

As noted before in section A.2.5, current production stability systems are all brake based systems. The principle is that the vehicle's path and accelerations can be manipulated by selectively applying brakes to introduce a yaw moment. Brake based controllers are a compromise solution where cost and complexity are weighed against the robustness and corrective action capabilities of the system.

As brakes are being used, it is not surprising that the vehicle's speed reduces somewhat when the system engages. However, Manning and Crolla found that despite the effect on speed control, brake based systems do offer the best compromise between controllability and driver intent (Manning & Crolla, 2007). Further Nantais found that while brake based system do result in the development of understeer, the effects are small enough and slow enough for the driver to compensate as needed (Nantais, 2006).

Brake based stability controls work by generating yaw moments as shown in Figure A-46 below. Here the oversteering of the vehicle is being corrected by introducing a moment counter to the vehicle's rotation.

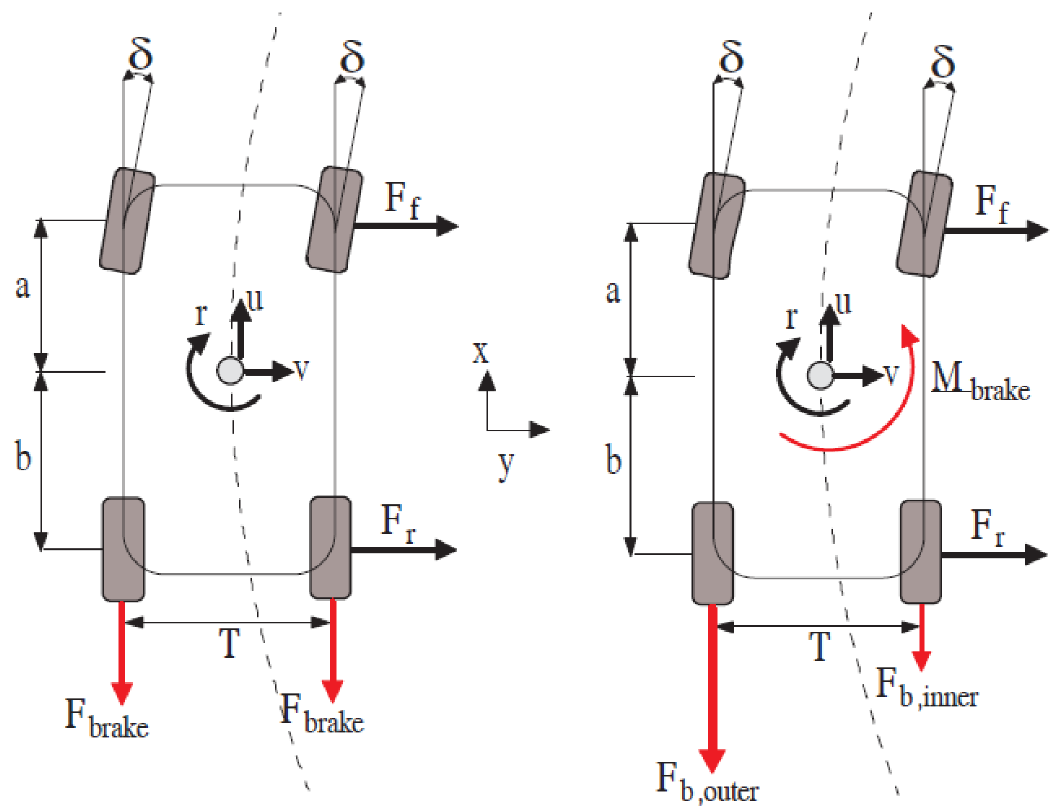

Figure A-46: Oversteer Correction (Nantais, 2006)

Roll control through braking is not so easy to understand on the surface however. To understand the relationship, it is easiest to start with the observation that the lateral acceleration the vehicle sees is a product of the vehicle's speed and the path radius (steady state model).

$$Ay = \frac{V^2}{R} \tag{A-9}$$

So to reduce the lateral acceleration, the vehicle's speed must decrease or the path radius must increase. By applying an understeer moment to the vehicle, the ESC system does both of these tasks (reduce speed and increase path radius) as the vehicle's yaw rate reduces and the path swings wide of the drivers intent. The only problem is that this is a relatively slow process so the system needs to intervene before rollover is imminent.

In the case of a tractor and trailer, there is an additional action that the ESC system can take to reduce rollover potential. As the trailer is always attached behind the tractor's longitudinal CG location, braking the tractor wheels will impart an understeering moment to the tractor (Figure A-47). The trailer brakes are also capable of removing significant kinetic energy from the vehicle thereby reducing the vehicle's speed.

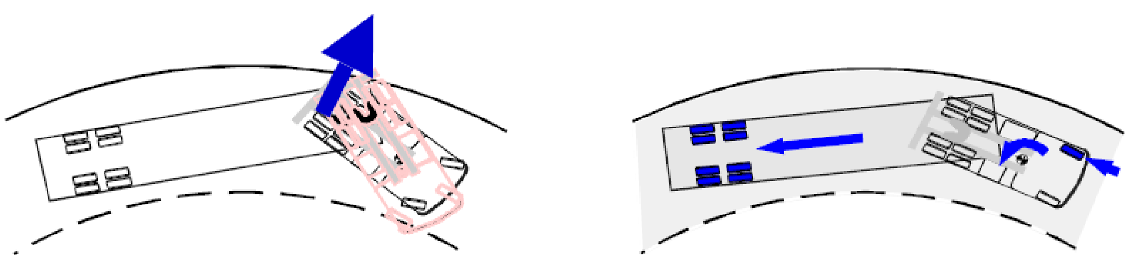

Figure A-47: Tractor and Trailer Yaw Control (Andersky & Conklin, 2008)

However, there if the tractor is understeering, then the only solution is to brake the inside rear tractor wheels much like would be done for a passenger car (Figure A-48).

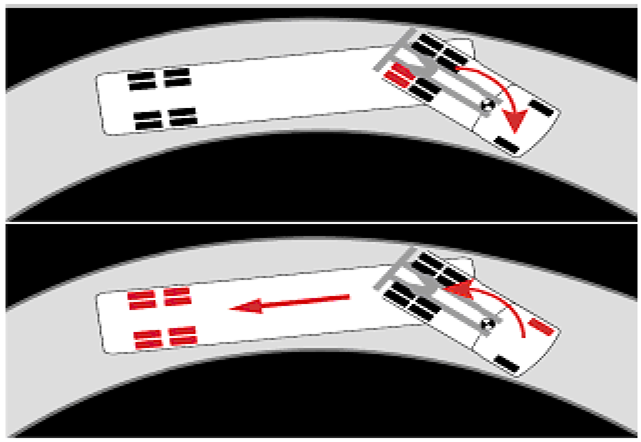

Figure A-48: Tractor Trailer Understeer and Oversteer Corrections (Goodarzi et al., 2009)

The last two points to keep in mind when using brakes for stability control are that vehicle speed also affects stability and steering response so the system becomes less stable as speed increases. This can be seen in the root locus plots developed by Yi for a tractor and semi-trailer (Figure A-49). The second observation is that the driver continues to want a linear feel to the vehicle and, as the slip angle increases, the restorative yaw moment potential drops (van Zanten, 2000). So the system needs to act prior to the vehicle developing a side slip angle sufficiently large to both dis-concern the driver and limit the control's effectiveness.

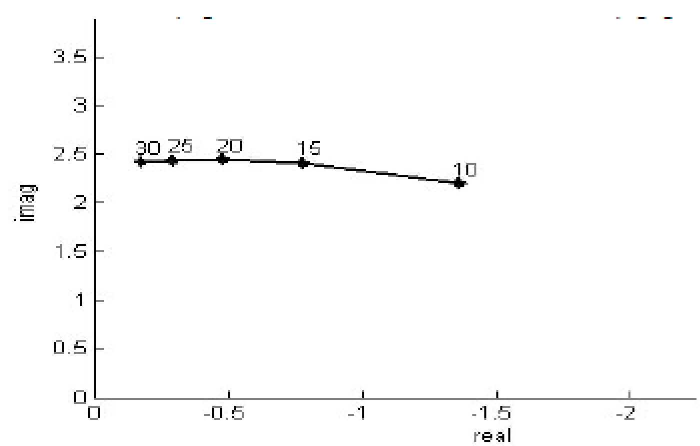

Figure A-49: Tractor Trailer Stability vs. Speed (Yi Feng-yan et al., 2010)

A.3.7. Thrust Vectoring

The last of the common stability control methods is thrust vectoring. Essentially, this is a bi-directional version of a brake based system where thrust as well as brake force can be directed. The same basic control strategies for yaw and roll control apply as well. There have been some successful systems built on this technology (Hancock, Williams, Fina, & Best, 2007), (Liebemann et al., 2004) focused on the passenger car domain.

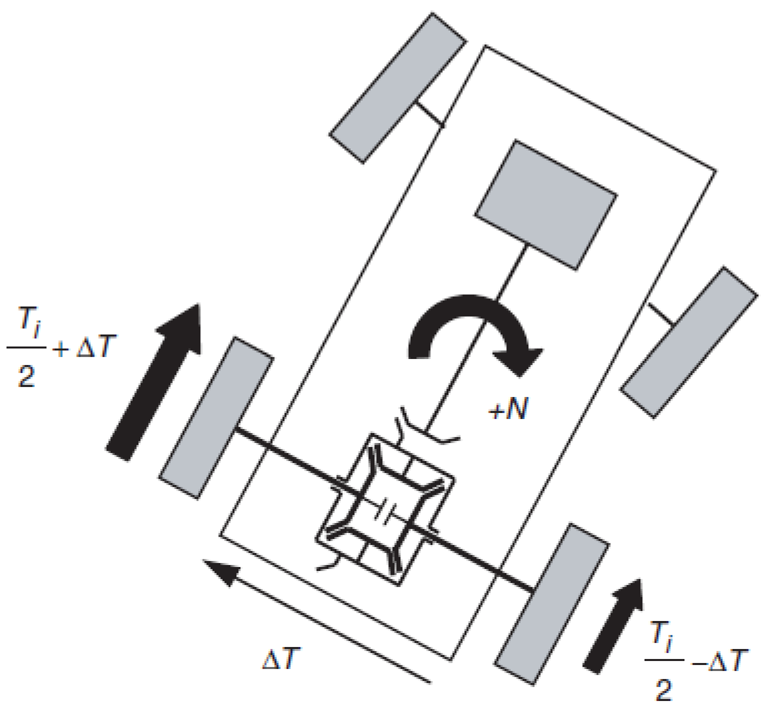

Figure A-50: Thrust Vector ESC (Hancock et al., 2007)

The vast majority of commercial tractors have open differential axles which prevent any form of thrust vectoring. Open differentials are used to eliminate tire scrub during in turns (each wheel rotates at the appropriate rate for the arc it is describing) and to prevent mismatched tire diameters (new tires on one side and used on the other) from "fighting" each other. Finally, trailers have no drive capability and thus no thrust vectoring ability. For these reasons, the research presented here does not use thrust vectoring of any kind.

A.4. Modeling Stability and Control Algorithm Development

There are four main tasks which need to be addressed in the development of a traditional ESC controller for a vehicle. The first task is to develop a simplified mathematical model of the vehicle to use as a "reference" vehicle. The second task is to develop the yaw control and roll control strategies. The third task is to identify the parameters to be measured. The fourth task is to convert the model in to a state space form or transfer function form for quick analysis so that the model can be used to control the actual vehicle.

While all of these tasks are important, perhaps the most important is for the resulting model to be efficient. In order for a controller to use the vehicle model in real time, the model must be significantly faster than the actual vehicle to give the controller time to evaluate the reference model and then act on the conclusions drawn from the results of the reference model. How fast the model needs to be is not universally agreed upon, however Chen recommends that the model be 60 times faster than real-time (B. Chen & Peng, 1999a).

A.4.1. Modeling the Vehicle

Many authors have evaluated the suitability of simplifying assumptions in the area of vehicle dynamics modeling. The general conclusion from this research is that linearizing the vehicle model is reasonable for sub-limit maneuvers (which is where we want to control the vehicle) (Eisele & Peng, 2000; Gao, Yu, Neubeck, & Wiedemann, 2010; Goodarzi et al., 2009; Hossein & Taheri, 2008; ISO 7401, 2003; Lawson, 2004; Minaker & Rieveley, 2010; Tianjun & Changfu, 2009; Yu et al., 2008). This is a fortunate result as rigorous stability proofs for fully non-linear articulated vehicles can be very difficult to develop (Antonov, Fehn, & Kugi, 2008). However, it should be noted that while the vehicle can be linearized and still maintain reasonable accuracy, the behavior may be non-linear due to non-linear input sources such as the tires which cannot be linearized (Gong & Ting, 2008; Kim, 2010; Ko & Lee, 2002; Lawson, 2004; Liang Chu, Yong Fang, Mingli Shang, Jianhua Guo, & Feikun Zhou, 2010) and some vehicle states, such as side slip, which depend on multiple vehicle parameters (Yu et al., 2008).

To illustrate the effect of linearizing the reference model, consider the study by Goodarzi where a full non-linear tractor and trailer model was evaluated at two speeds (15 m/s and 20 m/s) after which the model was linearized and re-evaluated (Figure A-51). The solid lines are the non-linear model results and the dashed lines are the linear model results.

	15 m/s	20 m/s
Yaw	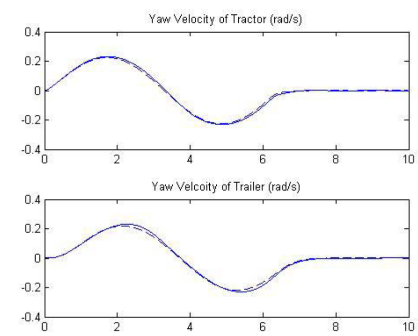	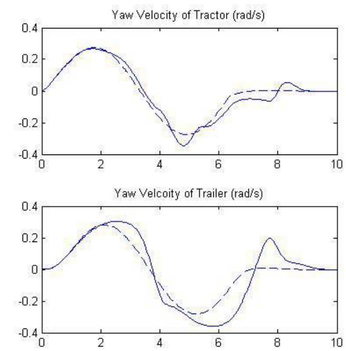
Roll	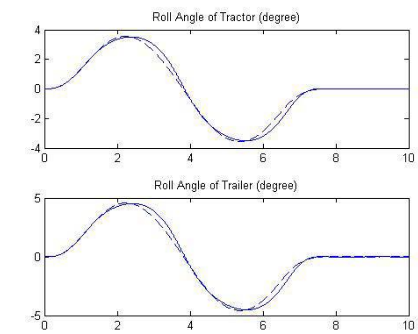	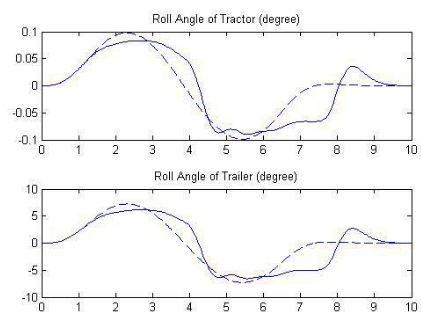

Figure A-51: Linear and Non-linear Vehicle Model Results (Goodarzi et al., 2009)

The results indicate that so long as the vehicle is operating in the linear domain (below the stability limit), the linear model is a very good approximation of the actual vehicle. Since the objective of the ESC system is to make sure the vehicle stays below the stability limit, the linear model should suffice.

For ESC development on a passenger car, the linearization of the vehicle would be sufficient. However, commercial vehicles are often quite torsionally flexible (Arant, 2010; Lawson, 2004; Park et al., 2008; Sampson & Cebon, 1998). The question then arises as to if the chassis torsional deformation significantly affects the model's results. Figure A-52 is a comparison of measured understeer of a tractor and flatbed trailer compared against two models (a rigid chassis model and a flexible chassis model). Similarly, Figure A-53 is a comparison of wheel load (up to rollover) for the same vehicle. As can be observed, the rigid and flexible chassis models are very similar up to half of the vehicle's roll threshold. Since it is desired to keep the vehicle well below the roll threshold, the rigid model, with its simpler and faster mathematical equations should suffice for the reference model. Note: The "stiff" chassis is actually the flexible model re-run with the torsional stiffness of the vehicle increased by three orders of magnitude. It should then match the rigid chassis.

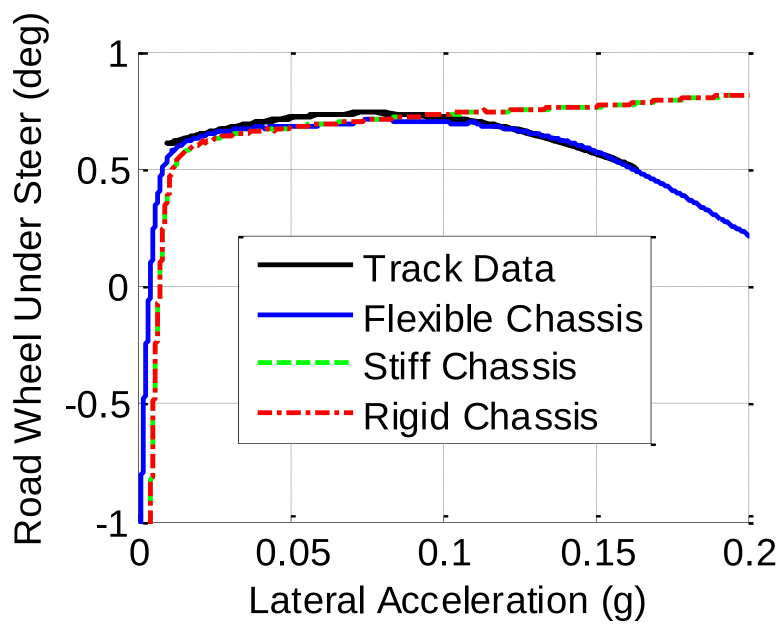

Figure A-52: Understeer Model and Test Data (Arant, 2010)

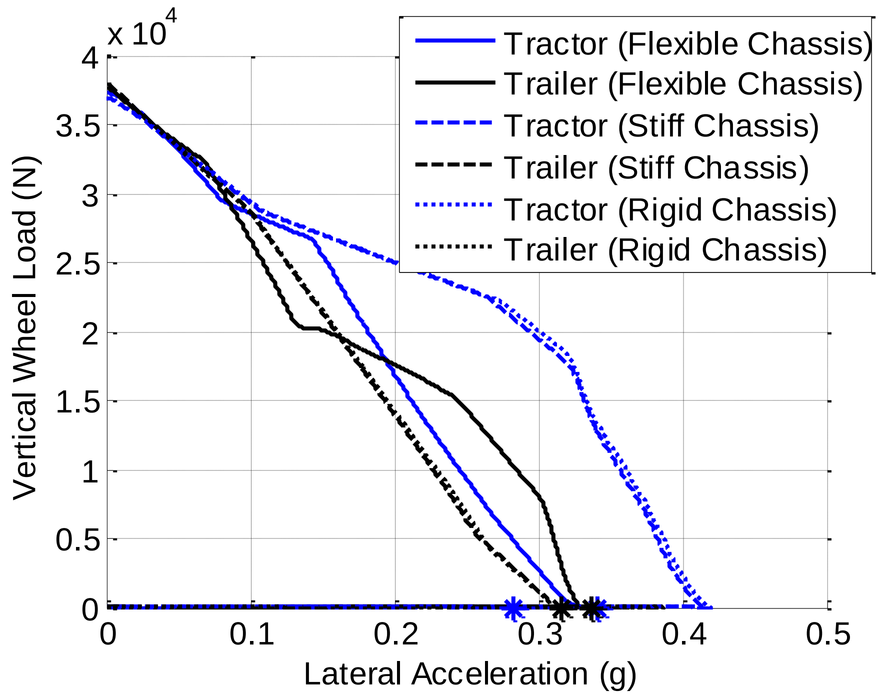

Figure A-53: Vertical Wheel Load Model and Test Data (Arant, 2010)

If the tractor and trailer is simplified as a linear system with a rigid chassis, then the model will become an eight degree of freedom model with six degrees of freedom for the tractor and two (yaw and roll) for the trailer. Of course, this also neglects wheel motions and their associated degrees of freedom. If pitch and vertical motion is neglected, the model can be further reduced to a 5 degree of freedom model. Such simplifications will allow the reference model to be significantly faster than real time enabling it to function in an ESC controller (Yu et al., 2008).

A.4.2. Multiple Axle Vehicles

In addition to articulated units, trucks frequently have tandem axles (Figure A-54). This complicates the dynamics modeling as the tandems affect the lateral force distribution. To resolve this problem, it is proposed to use an equivalent two axle model in the simulations. The procedure for defining the two axle vehicle is drawn from the UMTRI work with turning of tandem vehicles (Winkler, 1998). The resulting two axle vehicle is modeled with a slightly longer wheelbase and a higher rear cornering stiffness (Figure A-55).   The effective wheelbase increases based on the separation distance between the tandem axles and the total front and rear cornering stiffness (sum of all tires).

$$T = \frac{\sum_{i=1}^{N} \Delta_i^2}{\mathrm{N}} \tag{A-10}$$

$$l_e = l * \left(1 + \frac{T}{l^2} * \left(1 + \frac{C_{\alpha r}}{C_{\alpha f}}\right)\right) \tag{A-11}$$

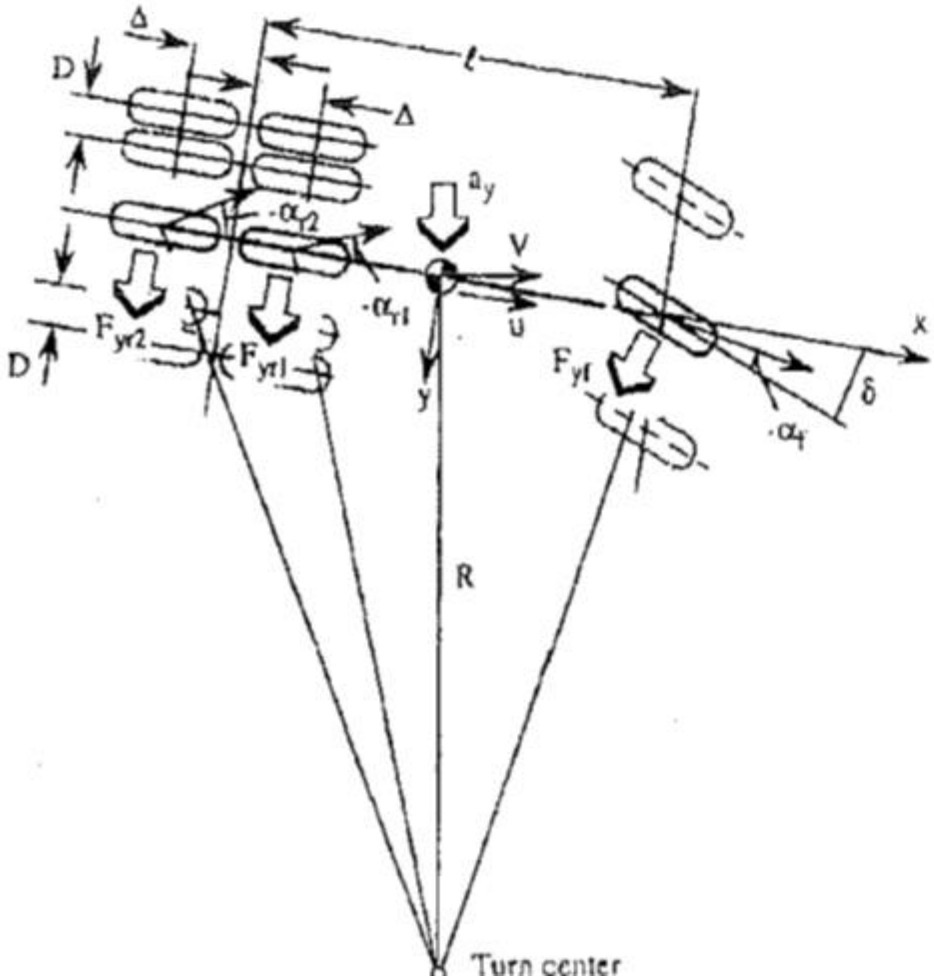

Figure A-54: Turning of Tandem Vehicles (Winkler, 1998)

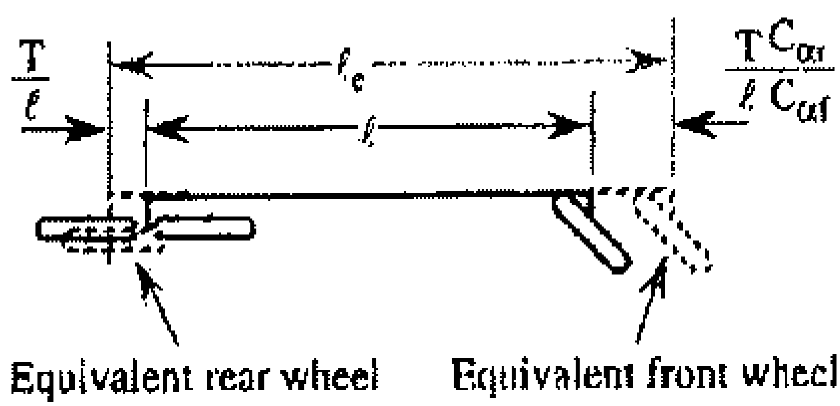

Figure A-55: Equivalent Two Axle Vehicle (Winkler, 1998)

A.4.3. Roll Stability

To best understand how to prevent a rollover of a tractor and semi-trailer, it helps to observe what really happens in a rollover. In 2009 UMTRI rolled a fully instrumented tractor and tanker over. Figure A-56 shows the measured vehicle speed, roll, and lateral accelerations. Note that the lateral acceleration reaches 0.6 g and holds while the trailer rolls. This is the limit of the tire lateral force. What this plot shows so well is that while the trailer rolled first, the tractor experienced the accelerations first. Thus there is a built-in warning of rollover risk which the control could use to implement corrective actions before the trailer begins to roll.

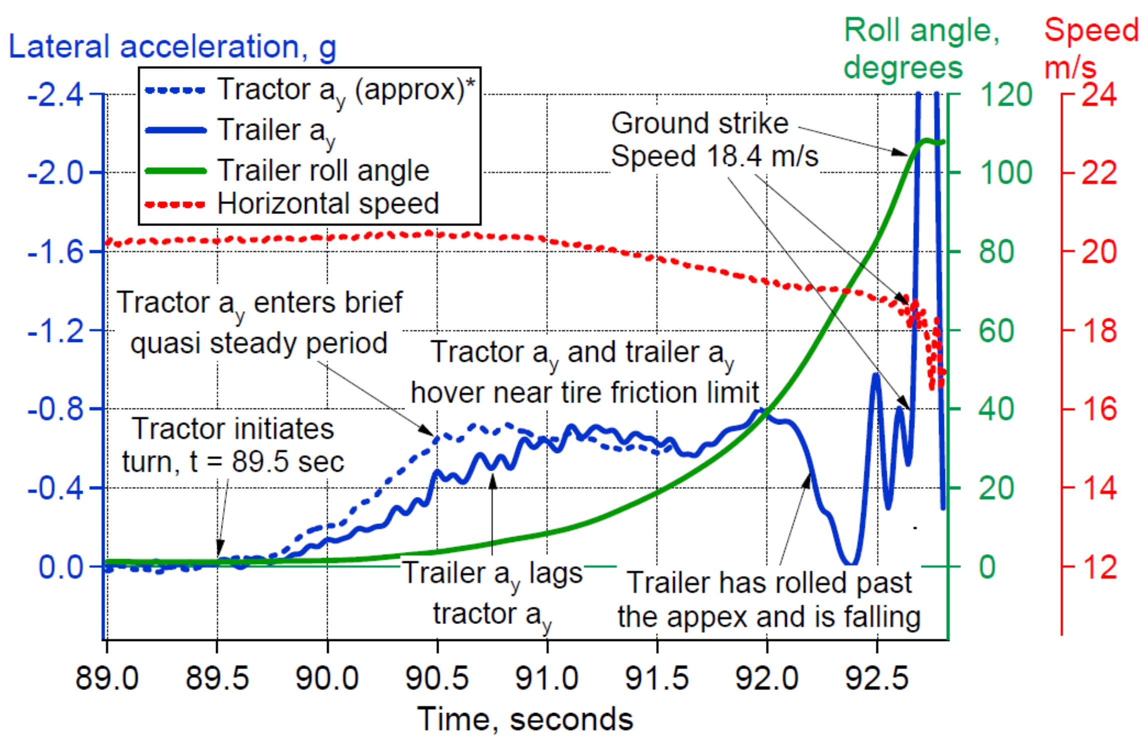

Figure A-56: Tanker Roll Test (Winkler, 2009)

There are basically three approaches used in the literature to gage impending rollover. The first is the lateral load transfer (LLT) described in section A.3.1 (Kamnik et al., 2003). The second method is by directly monitoring the lateral acceleration (Dahlberg & Stensson, 2006). The third is by monitoring the lateral kinetic energy (S. B. Choi, 2008). Of these, the third is the most accurate and realistic, but it is the most expensive computationally as both the roll angle and roll rate must be evaluated.

The vast majority of controller strategies for managing roll use either a PID (proportional integration derivative) scheme (L. K. Chen & Shieh, 2011), a PD (Chih-Keng Chen et al., 2010), a PI (Goodarzi et al., 2009), or a linear quadratic regulator approach (LQR) (Miege & Cebon, 2005; Tianjun et al., 2007; Tianjun et al., 2007; Tianjun & Zheng, 2008; Tianjun & Changfu, 2009; Tianjun & Changfu, 2009; Tianjun & Liyong, 2009). Of these, LQR is by far the most commonly implemented.

A.4.4. Yaw Stability

Generally, yaw stability analysis is more complicated than roll stability. This is due to the fact that, as noted in section A.2.3, yaw stability requires knowledge of more than just lateral acceleration. Further, some of the vehicle states required for evaluating yaw stability using traditional controller strategies are not directly observable. Additionally, yaw stability and yaw responsiveness (what the driver feels) is not the same thing and cannot always be improved at the same time (Bedner, Fulk, & Hac, 2007). These issues make yaw control a more challenging task.

A typical yaw controller has three parts: A top level instability monitoring routine, a second level corrective moment development routine, and a wheel management routine (Figure A-57). By splitting up the tasks, the control logic can be simplified and the behavior of the system easier to follow. Also, the top level controller is often of a PD (proportional derivative) design (Chih-Keng Chen et al., 2010) or a PID (proportional, integral, derivative) design (L. K. Chen & Shieh, 2011) although Lyapunov methods (Hossein & Taheri, 2008) are used as well as optimal control methods (Goodarzi et al., 2009).

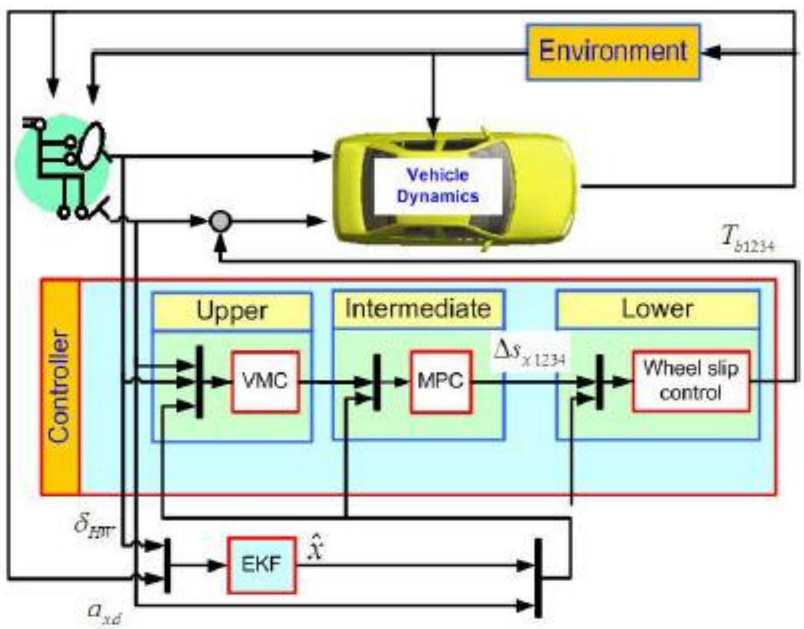

Figure A-57: Typical Yaw Controller Hierarchy (Chang & Gordon, 2009)

In addition to acting as the reference model for the controller, the linear yaw models are also used in root locus analyses to establish stability margins (Eisele & Peng, 2000), (Yi Feng-yan et al., 2010).

A.4.5. Combined Roll and Yaw Stability

In section A.2.4 it was noted that combining yaw and roll control can be difficult as the two stability demands can have competing objectives. To manage this issue several approaches have been proposed. Chen proposed a simple, but less effective, method where yaw was evaluated first, and then roll (B. Chen & Peng, 1999b). Goodarzi used an optimal control approach with both yaw and roll combined. The solution function contained the lateral velocity of the tractor, both roll angles, tractor yaw rate, and tractor heading. A PI controller was used for the sub-task of wheel control (Goodarzi et al., 2009). Tianjun developed a linear quadratic regulator (LQR) model using both yaw and roll states to solve for the needed control response (Tianjun et al., 2007). It is not clear which approach is best and what the limitations of each method are.

A.4.6. Common Assumptions

Anytime a complicated system such as a commercial vehicle is to be modeled, some simplifying assumptions must be made. While each of the modeling approaches reviewed was unique, there are a few common points that indicate a "preferred" solution method. These assumptions will be included in the research to be completed here.

- The vehicle may be linearized without significant error so long as the maneuvers are in the linear domain of the vehicle. As the controller's objective is to make sure the vehicle stays in the normal (linear) operational range, this is an acceptable simplification.
- Chassis torsional flexibility will be ignored. This is a follow-on to the linearization of the vehicle. For low lateral accelerations, there is little torsional deformation and little need to model torsion.
- The tires cannot be linearized as the tire response changes significantly and non-linearly with load. This will be reviewed in more detail in section A.5.2.

A.5. Significant Issues with Brake Based Stability Systems

With the decision to use a brake based ESC system, it becomes necessary to identify any limitations with this control approach that must be accounted for in the controller. To that end, there are three significant areas that should be managed. The first is that the tire is non-linear, the second is that the lateral acceleration can displays a bias or false state value (road profile), and the third is the potential for less than ideal control of the brakes. Through understanding of the affect and influence of each of these limitations, they can be accounted for and managed in the final ESC controller.

A.5.1. Pneumatic Brake Limitations

As with most of the design choices related to trucks, the selection of the braking system is a compromise between cost, usage requirements, and functionality. While passenger cars use an incompressible fluid to transport brake demands, trucks use air which is highly compressible. The reason is that a car's brakes are seldom, if ever, disconnected. But a commercial vehicle's brakes are disconnected every time a trailer is changed out. Using conventional brake fluid would require that the brakes be "bled" (purged of entrapped air) every time a trailer was connected or disconnected. Additionally, the environmental costs of leaking fluid from the connectors would be quite high. So to avoid these issues, trucks use compressed air to manage brakes.

Brake System Design

The brake system on most trucks consists of treadle valve (command vale) which is attached to the brake pedal. When the driver applies the brakes (opens the valve), a compressed air "signal" is sent to modulator valves at each axle which then actuate the brakes using compressed air in a local reservoir (Dunn, 2003). The amount of air supplied to the brakes (effectively the brake force) is also proportional to the command brake press from the treadle valve (Esber et al., 2007). The use of the reservoir and modulator valve may seem unnecessary until one considers that the driver command pressure does not have sufficient volume to actuate all of the brakes. Increasing the volume of air that the driver manages with the brake pedal would result in time delays (time constants) so large as to make the vehicle unsafe to drive.

Drum Brakes

Nearly all US commercial vehicles use drum brakes. This despite the fact that passenger cars are nearly exclusively disk brake and Europe has migrated its commercial vehicles to air disk brakes as well. The reasons for the continued use of air drum brakes in the US is due to the before mentioned resistance of the industry to change and the fact that air disk brakes would add $1,500 to the cost of current air drum brakes (NHTSA, 2009). Thus even though air disk brakes have quicker response times and do not suffer from heat fade as drum brakes do, there is no indication that the industry will convert in the near future.

A drum brake is comprised of an outer cast iron drum which rotates with the wheel. Inside the brake are shoes which are pressed against the inside of the drum (Figure A-58) generating friction and slowing the vehicle. The “Expander” in Figure A-58 is not what the actual actuator looks like, but is a simplified representation to make it easier to understand how the shoes are pressed against the drum. The actual mechanism (Figure A-59) is called an “S” cam and is designed to hold the brakes in the “on” position. When air pressure is supplied to the air chamber, the actuation spring force is overcome and the "S" cam rotates to release the brakes. Thus the default or fail safe state is for the brakes to be on.

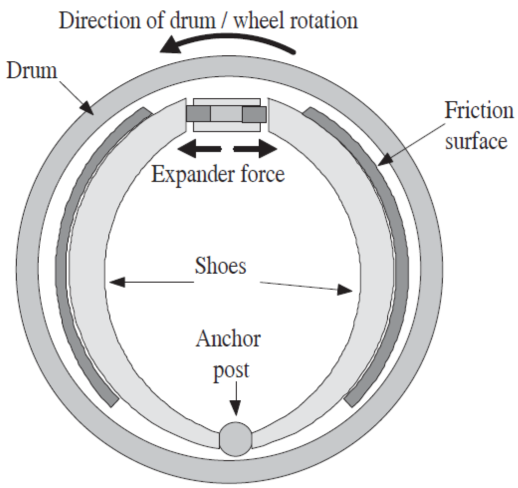

Figure A-58: Drum Brake Illustration (Nantais, 2006)

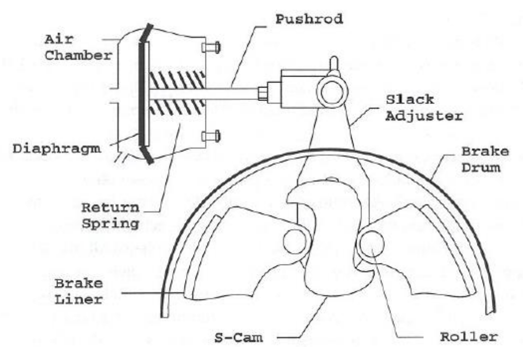

Figure A-59: Drum Brake Actuation (Dunn, 2003)

There are two significant weakness of this brake. The first is that as the brake heats up, the drum expands and limits brake torque. While this is great for thermal run-away protection, it leads to brake "failure" and run-away vehicles that cannot stop. Thus drivers have to be very careful of brake use especially on steep descents. The second problem is that the trailing shoe (left shoe in illustration) is "self-energizing" which means that the brake force generated by the shoe tends to drive the shoe into the drum. This makes releasing the shoe, and by extension controlling that release, difficult.

In 2011, the FMVSS 121 mandated that 60 mph to 0 mph stopping distances for commercial vehicles be changed from 335 feet to 250 feet (NHTSA, 2009). To meet this mandate, all manufactured adopted “enhanced” drum brakes, at a cost increase of $210 per tractor. The upgrades comprised the following changes (NHTSA, 2009):

- Front axle drums went from 15” diameter X 4” width to 16.5” X 7”
- Drive and trailer axles went from 16.5” X 5.5” to 16.5” X 8.675”

These are the largest drum brakes which can be fitted to a typical tractor and trailer.

Brake Delays

The selection of compressed air as the transmission medium for relaying brake commands to the modulator and then for the modulator to actuate the brakes results in two types of delays in the actuation of the brakes. The first is the transport delay as the pressure signal has to traverse a significant distance. This is essentially a volume change problem as the hose pressure changes with the change in inlet pressure. The second delay is in the actuation of the “S” cam where compressed air has to build on the diaphragm to release the brake or pressure has to be dumped to engage the brake. This constitutes a second time delay in the system. This system is thus often modeled as a first order system with a time delay (Kienhöfer et al., 2008) as shown in Equation A-14.

$$P_b = \frac{P_d}{1 + \tau s} * e^{-s*T_d} \qquad \textbf{A-12}$$

Here P_d is the demand pressure, P_b is the brake pressure, and T_d is the delay time for the valves.

Several people have modeled and measured this delay in brake actuation with reasonably similar results. Time delay between the treadle valve and the tractor modulator is 0.2 seconds with an additional 0.3 seconds to reach a trailer modulator (measured at 60 psi – partial brake). Full brake pressure (80 psi or higher) takes an additional 0.1 seconds (Bayan, Cornetto, Dunn, & Sauer, 2009). In a similar study, Dunn found pneumatic transport delay (treadle to modulator) can take 0.4 seconds or longer (Dunn, 2003). Finally, Kienhofer found delays between command and brake actuation of up to 0.4 seconds with charging time constants (command transport delay) of up to 0.1 second (Kienhöfer et al., 2008). As a result, several people have observed that it is very difficult to obtain optimal control with this type of brake system (Palkovics & Fries, 2001).

Anti-Lock Brake System Design

A second difference, the first being the brake command media, between cars and trucks is that it is common for each wheel in a car to be managed independently while in trucks, tandem axle sets are often managed as groups. For instance, Figure A-60 shows a 6s/4m tractor arrangement where "s" stands for sensor (i.e. the wheel is observed) and "m" stands for modulated (i.e. brake pressure is controlled). This means that each wheel is monitored for wheel lock, but the left and right sides of the drive axles are controlled as a group. Again, this is a cost / value issue where it is unlikely that just the front or rear wheels in a tandem set would lock so the system simplifies the control part of the system to four actuators.

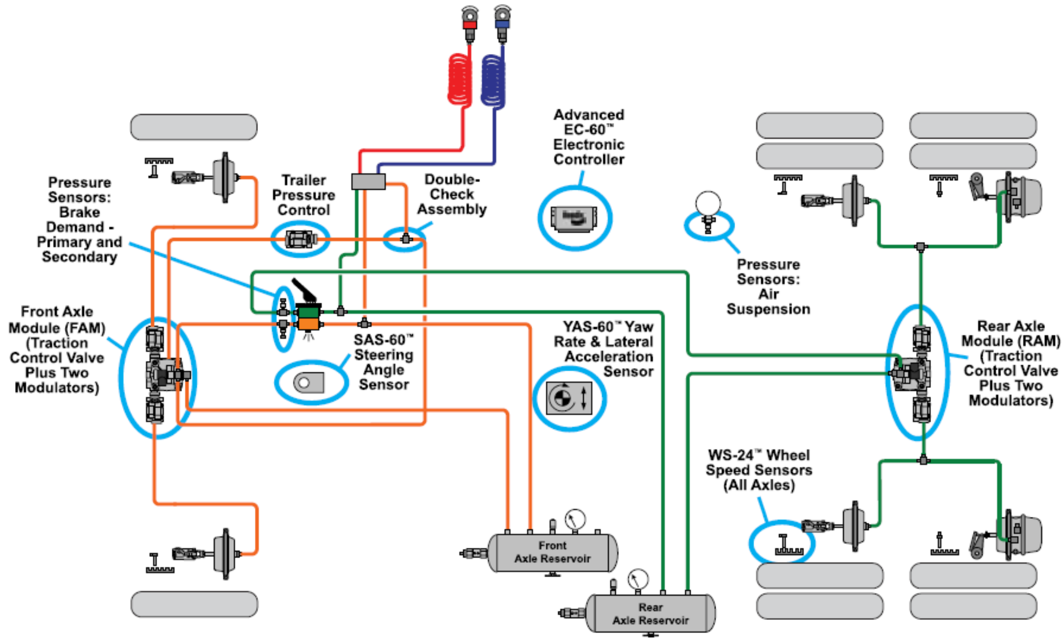

Figure A-60: Tractor Brake Control (Andersky & Conklin, 2008)

Figure A-61 shows an even simpler (and far more common) arrangement where only one axle of the tandem set is monitored. As it is not common for just one wheel on a tandem to lock, the system assumes that both wheels on a side of the truck are behaving in the same manner.

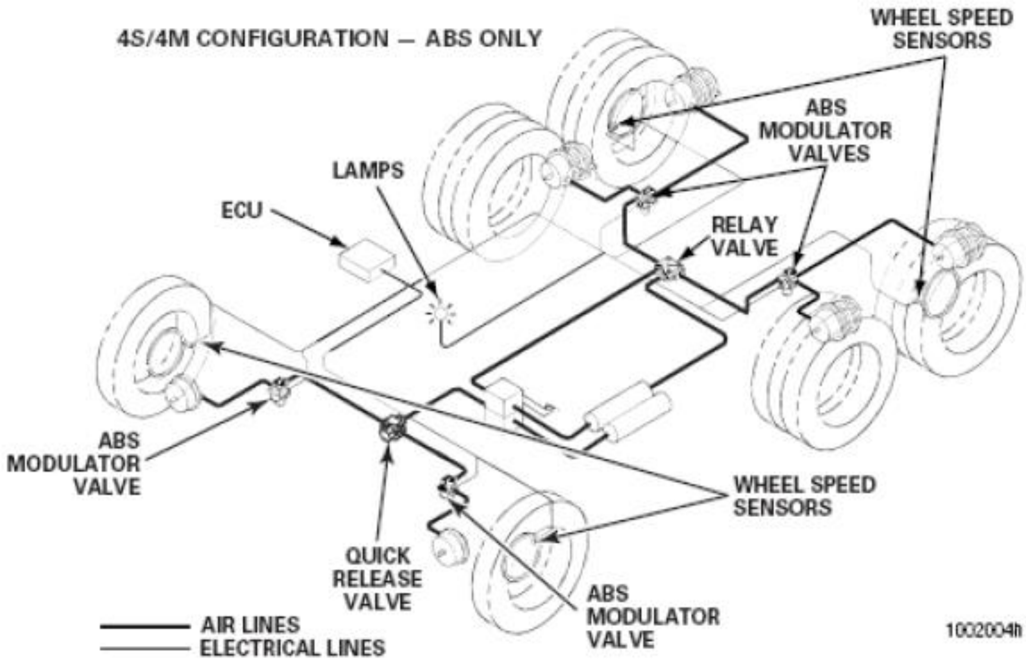

Figure A-61: Tractor 4S4M Control System (Chandrasekharan, 2007)

To evaluate if the lack of individual wheel monitoring and control affected braking performance, Shurtz and Guenther tested several brake arrangements (Shurtz, Guenther, Heydinger, & Zagorski, 2007). The results indicated that switching from 6S6M to a 4S4M system did not affect braking performance. However, it will affect tire life.

Table A-8: Stopping Distance (feet) as a Function of Brake Design (Shurtz et al., 2007)

Brake Design	GVW High mu	Curb High mu	GVW Low mu	Curb Low mu
6S6M	316	183	78	81
4S4M (1st and 2nd Axles)	321	185	77	85
4S4M (1st and 3rd Axles)	324	179	82	92

Anti-lock Brake System Response

Given the transport delays and compressible media limitations of a commercial air brake system, it is not possible to implement an ABS control system in the same manner as used in a passenger car. Car based systems are usually quite fast (on the order of 20Hz cycle times) and can control wheel slip quite well (targets are normally in the 10% to 30% slip ranges). Air brake systems have much less control and usually respond much slower with cycle times on the order of 1 Hz. They also typically result in less wheel control with the wheel operating from full lock to nearly complete release. For instance, Choi measured the pulse cycles to each of the four unique wheel actuators (tandems were tied together) for an ABS stop (S. Choi & Cho, 2001). The results show that there are brief spikes to full brake (85% peak system pressure) followed by no brake demand with a cycle time of approximately 0.75 seconds.

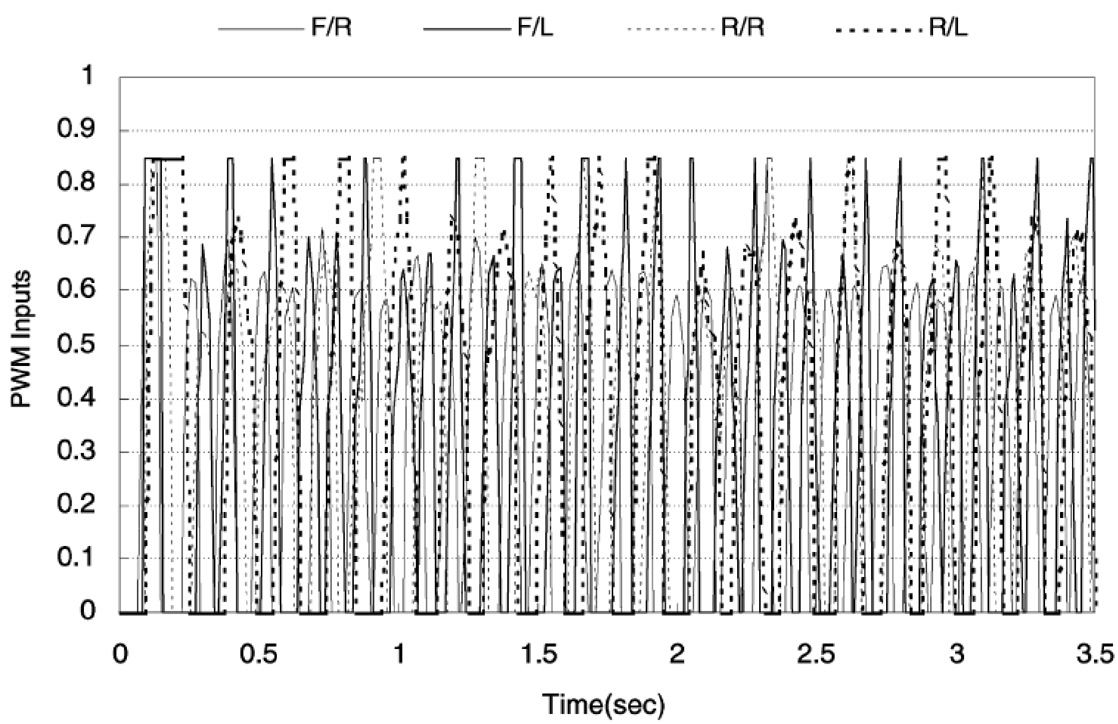

Figure A-62: Tractor ABS Modulation (S. Choi & Cho, 2001)

A similar study done by Kienhofer showed similar results with a cycle time of slightly more than 1 Hz (Kienhöfer et al., 2008). Note also that the wheel speed repeatedly goes to full lock before release.

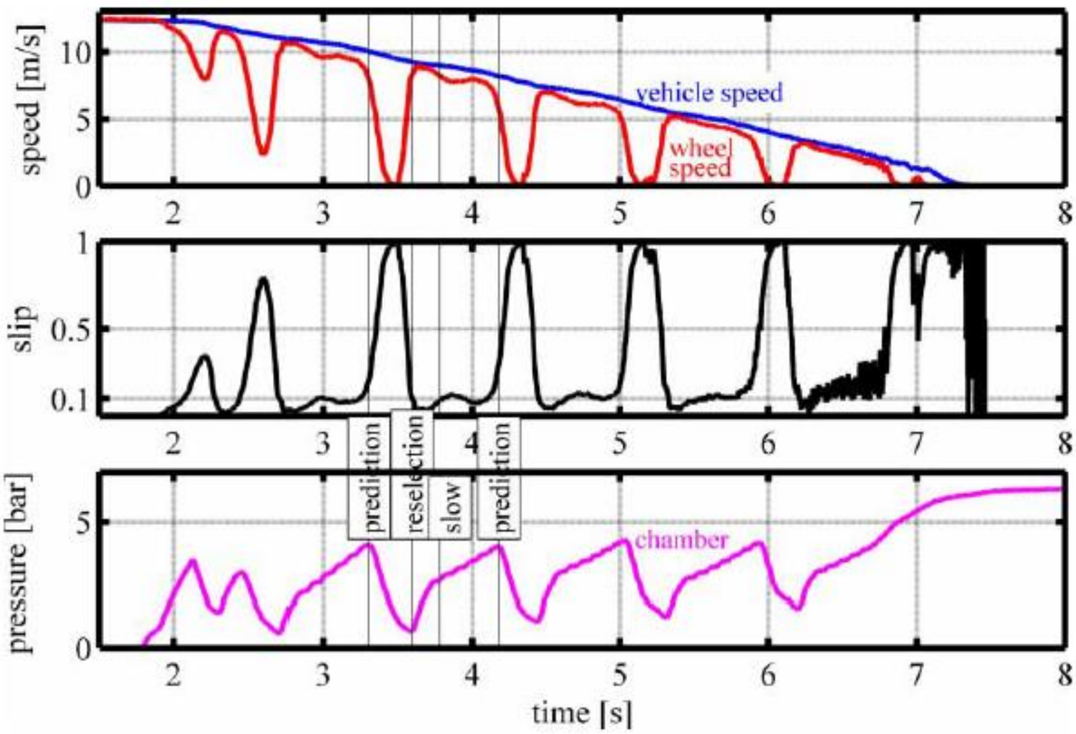

Figure A-63: Measured ABS Brake Cycle (Kienhöfer et al., 2008)

With such delays in ABS cycling and brake command, it may be difficult to develop sophisticated ESC systems as the foundation brake system may not be up to the challenge (Allen, 2010). Additionally, as conventional ESC systems cannot tell if a trailer has an operating ABS system, most current tractor ESC systems do not apply and hold pressure to the trailer but rather pulse the trailer brakes to simulate ABS (Chandrasekharan, 2007). This further reduces the effectiveness as potential braking capability is lost.

Electronic Brakes

In November 2007 the United Nations Economic Commission for Europe (UNECE) agreed to amend Regulation 13, requiring new trucks to be equipped with electronic stability control from 2010. ECE 13/11 requires nearly all commercial vehicles to be equipped with a stability control function including roll-over control and directional control (Wurster, Ortlechner, & Schick, 2010). This change was not easy to make and required many modifications to regulations and design practices. The largest of the changes was a switch from conventional air brakes to electronic air brakes (EBS).

EBS keeps compressed air as the brake application media but replaces the pneumatic control line with an electronic command. The driver's brake request is thus electronically measured and transmitted to the valve blocks, which connect the air reservoirs with the brake cylinders (Palkovics & Fries, 2001). With the change from pneumatic to electrical command, the cycle times were reduced and the ability to control and proportion braking improved (Esber et al., 2007). EBS is thus a much better platform on which to build an ESC system for a commercial vehicle (Petersen et al., 1998)

Unfortunately, it is the opinion of most experts that current US regulations, i.e. FMVSS 121, do not permit electronic brakes (Freightliner LLC, 2007), (NHTSA, 2009) as electronic brakes fail the redundant brake control requirement. The current rules have very explicit system failure criteria and there are simply too many potential failure modes for an electronic brake system. In fact one of the reasons for the revision of ECE R13 was to modify the fail safe criteria to permit electronic brakes (Palkovics & Fries, 2001). The modifications also provided for a second 7 pin connector between the tractor and the trailer to manage the trailer braking system and information communication (Freightliner LLC, 2007).

A.5.2. Tire and Wheel Modeling

As noted in section A.4.1, the tire cannot be linearized in an ESC model without the accuracy of the model degrading significantly; and since closed form solutions to tire behavior are very difficult to define (Gong & Ting, 2008), the only real option is to incorporate non-linear tire models into linear vehicle models through simplification of the physics. To help the reader understand the tire modeling approach, some background on tire functioning is included.

The tire essentially develops two forces as it rolls; a longitudinal force and a lateral force. While these responses are coupled, they can be solved for independently and then corrected based on the interaction of the longitudinal and lateral responses. For both the longitudinal and lateral behaviors, the basis for the tire models is derived from how the tire interacts with the ground under braking demands and steering demands. While the response of the tire does change with suspension changes such as camber (tire inclination) and toe, the suspension effects are generally much smaller than effects due to load change, steering inputs, and brake demands (Shim & Ghike, 2007). Thus the three inputs to the tire model are usually vertical load, steer, and wheel speed.

The tire generates forces between the vehicle and ground through a complex mix of static and sliding friction as parts of the tire remain planted on the road and parts slip along the surface of the road. Further, the nature of this contact force between the tire and road changes with the relative difference in tire circumferential speed and forward wheel speed (speed difference between the tire tread and the ground to which it comes into contact) and the angle between the tire heading and the vehicle path.

Lateral Traction

As a tire rolls, the blocks not contacting the ground act as free beams suspended from a rigid wall. However, one a tread block comes into contact with the ground, the free end of the block is no longer free but becomes fixed to the ground or slides along the ground depending on the local conditions. If there is a difference between the velocity vector of the tire and the tire's orientation (called a slip angle) then the tire develops a lateral force as the blocks experience a lateral deformation (Figure A-64).

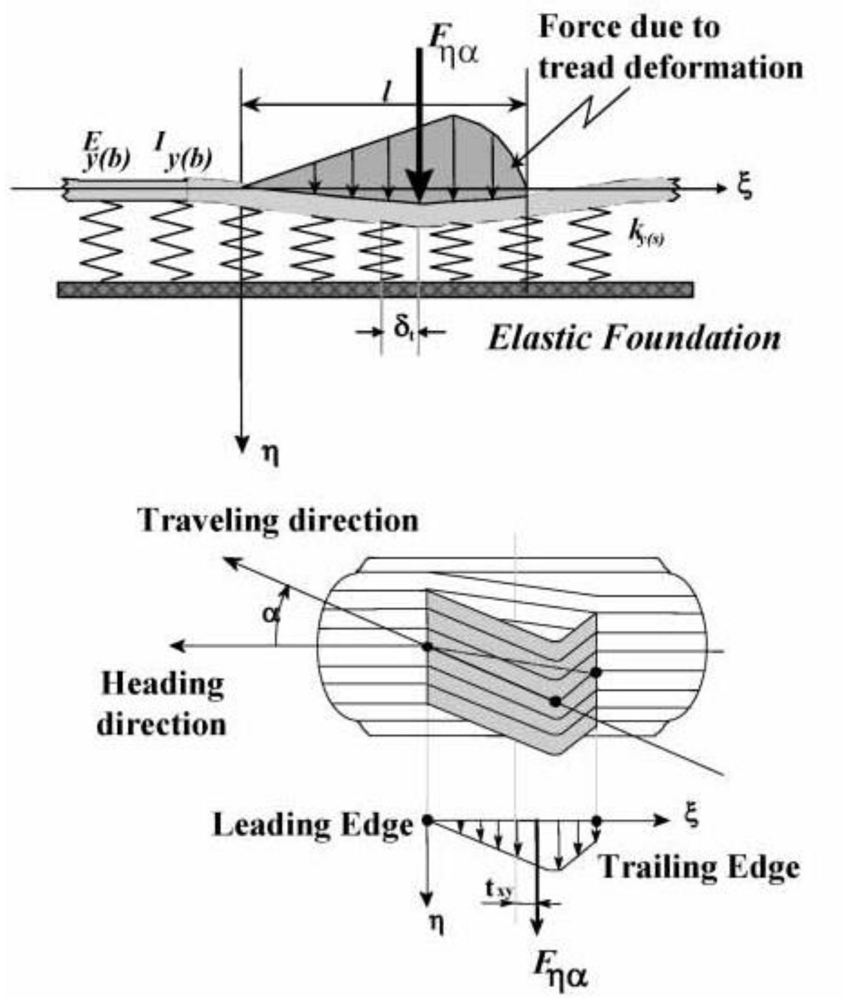

Figure A-64: Tire Lateral Force Development (Gim, Choi, & Kim, 2007)

As the tread block initially has no stress, the lateral force builds as the surface of the block, which is in contact with the road, is displace laterally relative to the tire carcass. This shear force continues to grow until the block slips and returns to its original state. The point at which it slips is dependent on the vertical load and the ground coefficient of friction. Note: The above explanation of lateral force is an oversimplification of the actual physics, but is accurate enough for the development of functional tire models.

As one would expect, the amount of lateral force generated by the tire increases as the slip angle increases (Equation A-13), but there is a limit to that increase after which the lateral force actually dissipates somewhat (seen in the data cloud in Figure A-65). Thus Equation A-13 cannot be used for simulating vehicle response in aggressive steering situations but it is reasonable for small slip angles. The linear constant in Equation A-13 is termed the tire's cornering stiffness and is defined as the initial slope in the tire's lateral force curve.

$$F_y = C_\alpha * \alpha \quad \textbf{A-13}$$

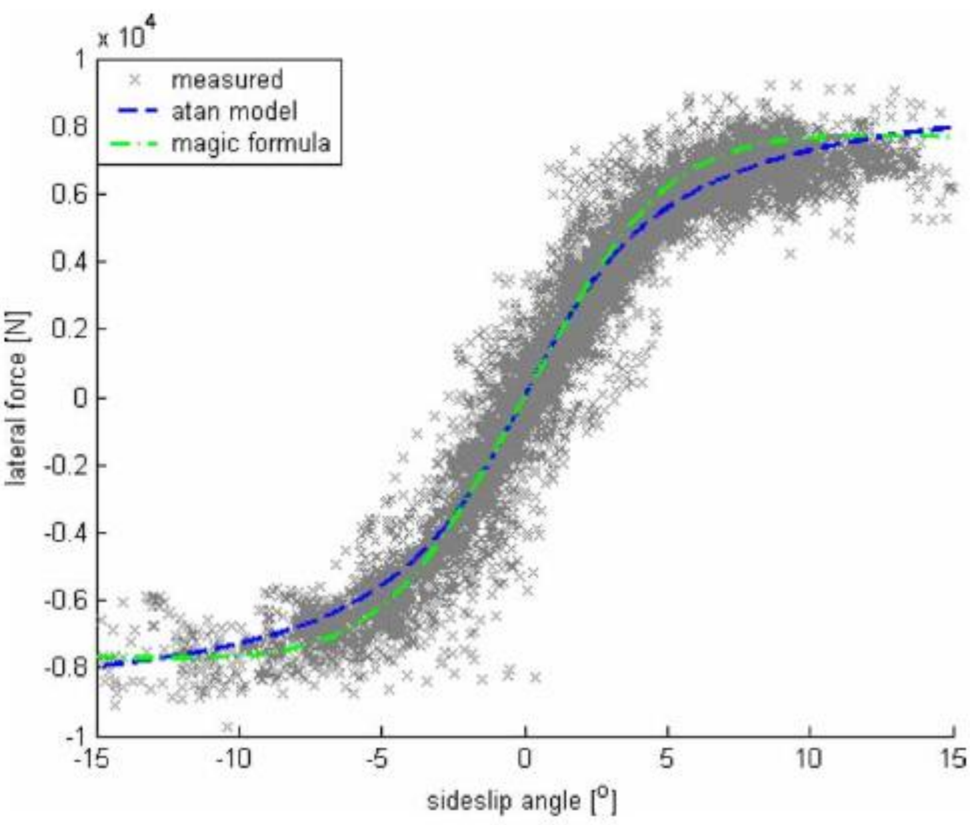

Figure A-65: Tire Lateral Response (Gao et al., 2010)

The peak in the lateral force development is part of the reason that the entire performance curve of a tire cannot be linearized successfully in vehicle simulations. Also, the tire response shown in Figure A-65 is only accurate for a given vertical load and road surface condition. As the vertical load increase, the lateral force generation increases as well, though not in a one to one manner (Figure A-66). To better understand how the vertical load and lateral force relate, consider Figure A-67 which plots the cornering stiffness against slip angle for multiple vertical loads. As load increases, the stiffness (and as a result the lateral force) increases, but it does so at a decreasing rate (Figure A-67).

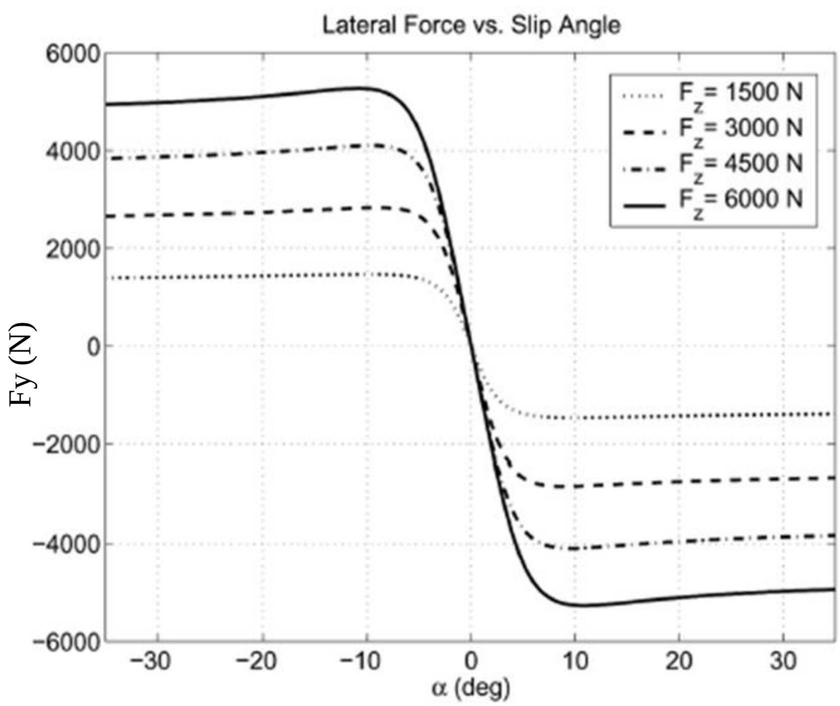

Figure A-66: Load Effect on Lateral Tire Response (Plumlee, Bevly, & Hodel, 2006)

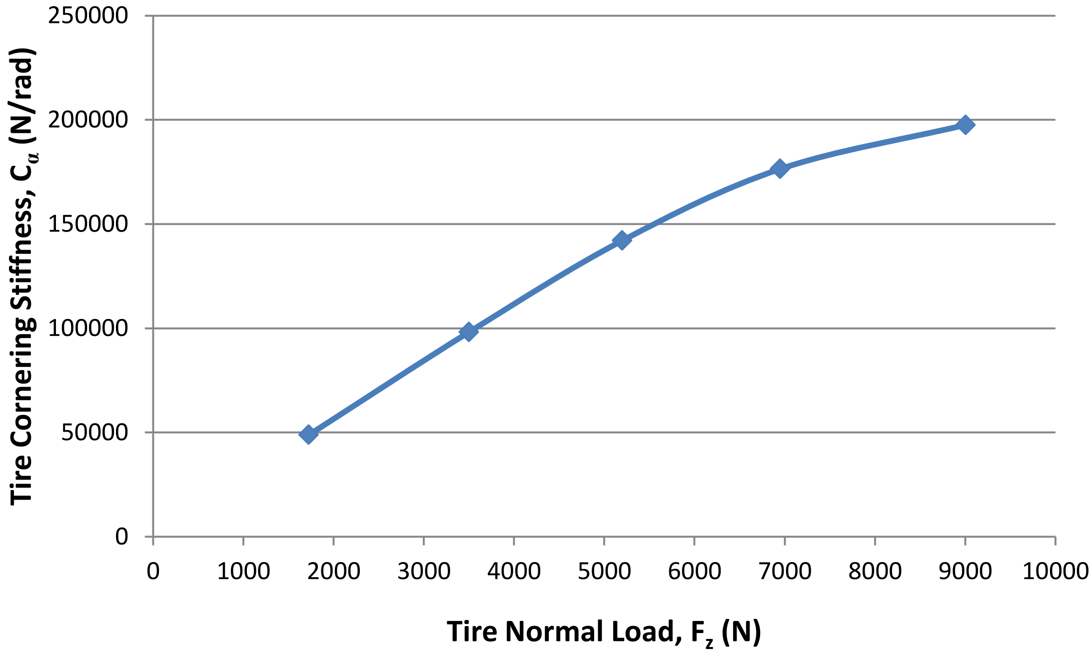

Figure A-67: Cornering Stiffness vs. Load (Limroth, 2009)

In Figure A-64 it can be observed that the peak lateral force occurs behind the center of the tire. This is intuitive as the lateral force is growing as the tread moves through the contact patch. This offset in lateral force also generates a moment about the vertical axis that tends to reduce the slip angle or re-align the tire with the wheel's trajectory. Thus the moment response (Figure A-68) is referred to as the tire's self-aligning moment. And like the lateral force response, it is also non-linear and dependent on the vertical load.

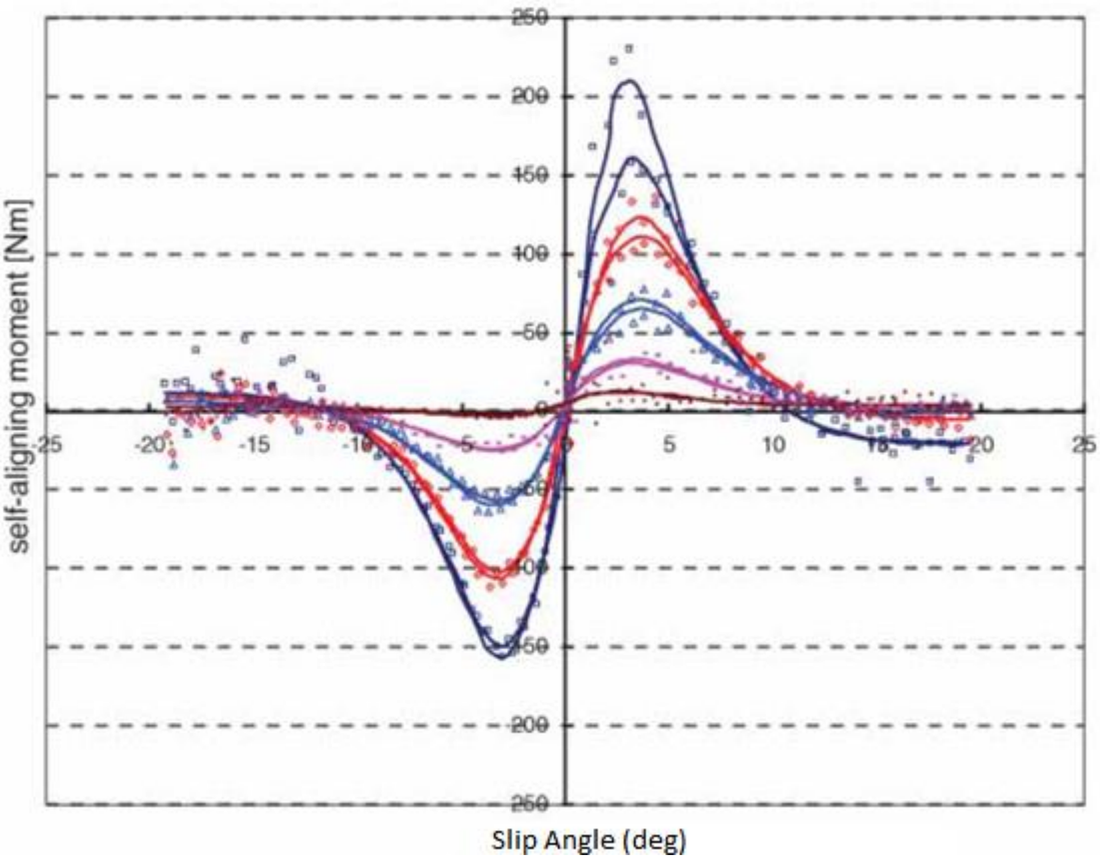

Figure A-68: Self Aligning Moment per Normal Load (Gim et al., 2007)

The last observation to make is that the lateral force developed by the tire is also dependent on the ground friction. As the road surface coefficient of friction drops, the lateral force (Figure A-66) and moment (Figure A-68) curves reduce as can be seen in Figure A-69. Fortunately, the shapes of the curves do not change significantly and the initial cornering stiffness about zero does not change significantly. Low road friction primarily shows itself by lowering the peak tactive potential in the non-linear segments of the curves. Thus any routine developed to evaluate the tire force curve at a given road mu will work for all road surfaces.

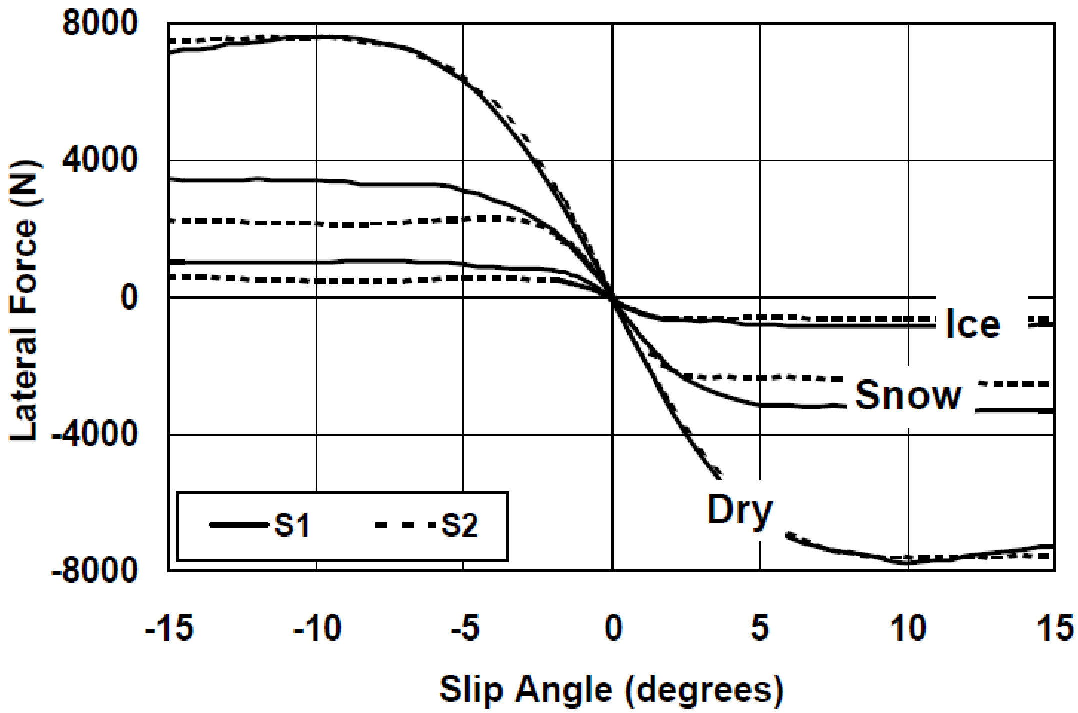

Figure A-69: Lateral Traction for Various Surfaces (Pottinger & McIntyre, 2000)

Longitudinal Traction

When a tire rolls along the road (Figure A-70), the normally curved circumference of the tire is forced to flatten along the road profile (Figure A-71). As the tire tread is attached to a stiff set of steel belts, it cannot simply buckle and fold. Additionally, the internal air pressure attempts to keep the tire in a round shape which also presses the tire against the road surface. The result is that a zone of vertical pressure develops between the tire and ground which is proportional to the tire's inflation pressure.

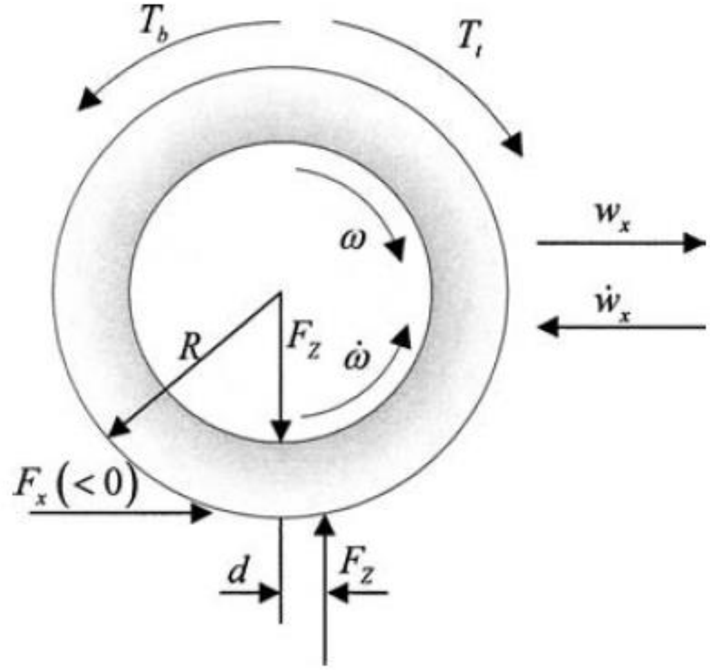

Figure A-70: Rolling Tire Diagram (Chun & Sunwoo, 2005)

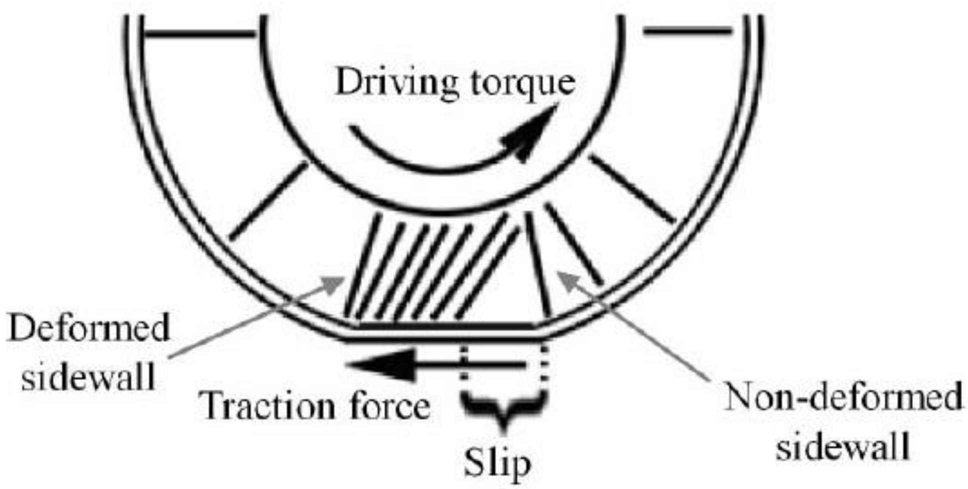

Figure A-71: Torque Transmission through the Tire (Nantais, 2006)

Note: While this is a simplification of the actual physics governing tire behavior, it is sufficient to help the reader understand the needs in modeling the tire's behavior without unnecessarily complicating the analysis.

As the vehicle drives down the road, torque generated by the engine and transmitted to the wheel is imparted to the tire at the tire / wheel interface. This torque is then transmitted through the tire via shear of the tire (again, a simplification but sufficient to understand the modeling requirements). As the tire is not under shear when it is not in contact with the ground, the actual longitudinal shear profile of a point on the tire grows as that point rolls through the contact patch until either the shear force increases beyond the tractive limits or the point exits the contact patch (Figure A-72). Either way, there is a portion of the tire contact that is static and a portion that is dynamics (relative slip between the tire and the ground). This type of model is commonly referred to as the brush model and is quite useful in modeling tire mechanics (Shraim et al., 2008), (M'Sirdi, Rabhi, Fridman, Davila, & Delanne, 2008).

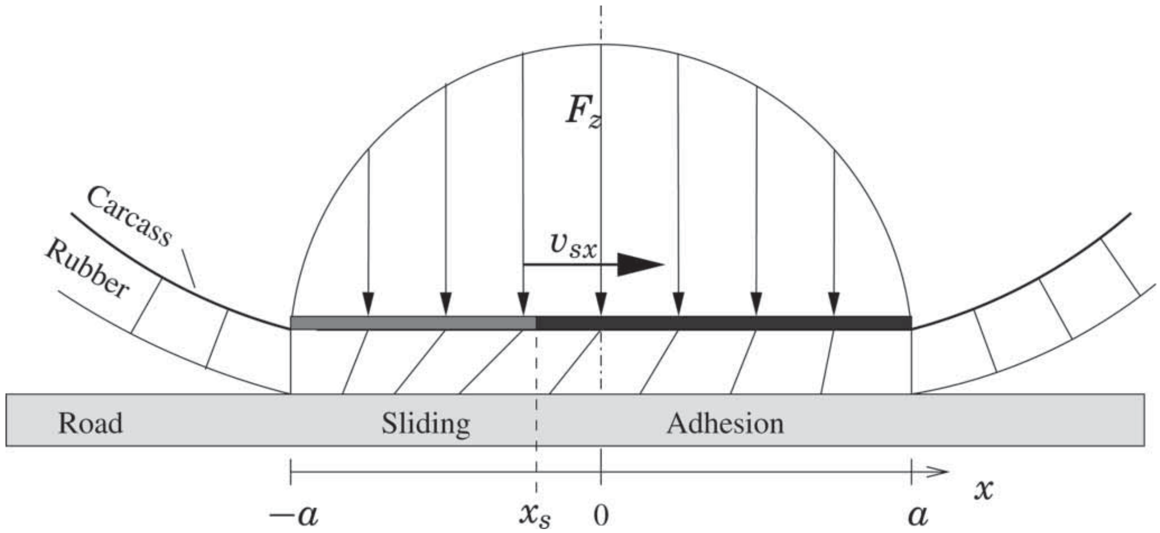

Figure A-72: Adhesion and Sliding (Svendenius & Gäfvert, 2006)

The relative slip between the tire and the ground means that the tire's rolling speed does not necessarily match the wheels forward velocity. When under driving torque (acceleration), it takes more revolutions of the tire to cover a given distance and when under braking the tire takes fewer revolutions to cover a given distance due to the continuously re-developed shear zone between the tire and ground. The amount of relative slip is defined as shown in Equation A-14 where ω is the wheel rotational speed, r is the distance from wheel center to the ground, and V is the wheel's forward speed. Positive slip indicates acceleration and negative slip indicates braking (though it is common to see the absolute value of slip used in brake response plots).

$$\lambda = \frac{\varpi * r - V}{V} \qquad \textbf{A-14}$$

The amount of braking force (or driving force) available is a product of the surface friction coefficient and the tire's normal force (Equation A-15). But the tire does not always use the available friction (simplification again) if the tractive demand is below the available tractive force.

$$Fx = \mu * Fz \quad \textbf{A-15}$$

When peak tractive force is required, it is best to operate the tire around a 10% to 20% slip ratio (Figure A-73). Operating the tire at slip levels above 20% should be avoided as the wheel tends to lock very quickly as the effective tractive force drops as wheel slip increases above 20%. This results in a negative force response for the tire.

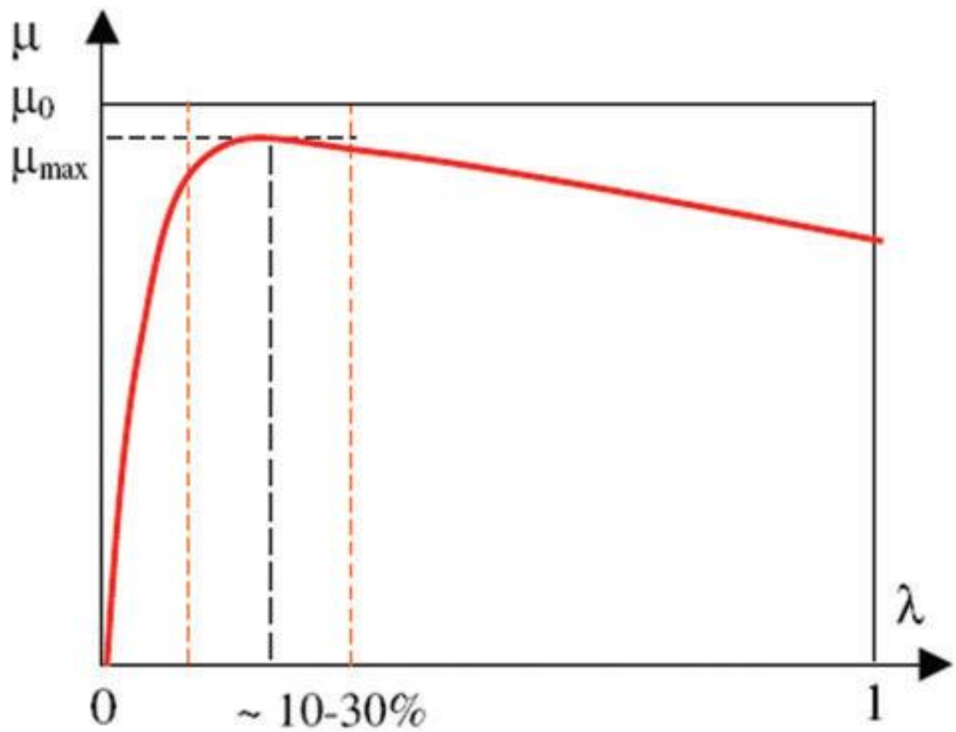

Figure A-73: Longitudinal Traction (Gong & Ting, 2008)

When the tire is rolling with no torque, there is no need for a large tractive force and thus the apparent road surface coefficient is very small. To make things more complicated, the peak road surface friction coefficient is not constant and changes with road conditions (Figure A-74). Thus one cannot know the maximum road surface friction coefficient until one actually needs to generate a force greater than the available traction will allow (Wakamatsu, Akuta, Ikegaya, & Asanuma, 1997). This can cause controllability problems when the surface traction drops quickly and the controller does not adapt (Ba, li, Kose, & Anlas, 2007; Liang Chu et al., 2010). Figure A-74 illustrates how the change in road friction affects tractive capabilities.

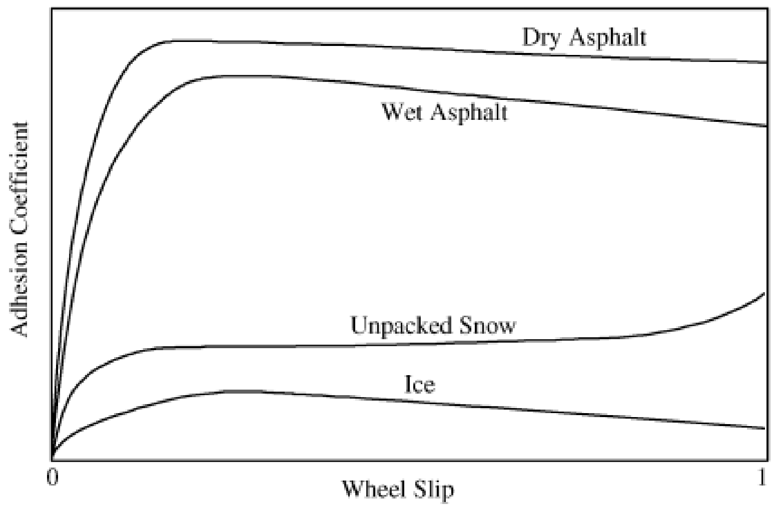

Figure A-74: Longitudinal Traction for Various Surfaces (S. Choi & Cho, 2001)

The most common method for managing longitudinal tire behavior in an ESC system is based on three observations from Figure A-74. The first is that the slope of the tractive force at zero wheel slip is nearly the same for all road surfaces. The second observation is that the shape of the tractive curve is the same for all surfaces (with the minor exception of complete wheel lock on snow) however, the peak magnitude is scaled. The third observation is that the amount of slip to reach the peak friction coefficient is nearly the same for all cases. Thus relatively simple controllers designed to keep the tire in a 10% to 20% slip window work quite effectively.

The goal of an anti-lock brake system (ABS) is to keep the tire operating near its peak tractive force when maximum braking is demanded. To do this, the brake pressure is regulated (applying and releasing pressure as needed) so that the wheel does not go into lock (stopped wheel) but continues to roll. This is done to ensure peak stopping, but more importantly, to ensure steer ability. For a hydraulic brake system, the slip ratio can usually be controlled quite well. However, for a traditional pneumatic brake system (commercial vehicle), the systems cannot generally control the wheel motion as well and the functional range is closer to 10% to 100% (see section A.5.1 for more information on this point).

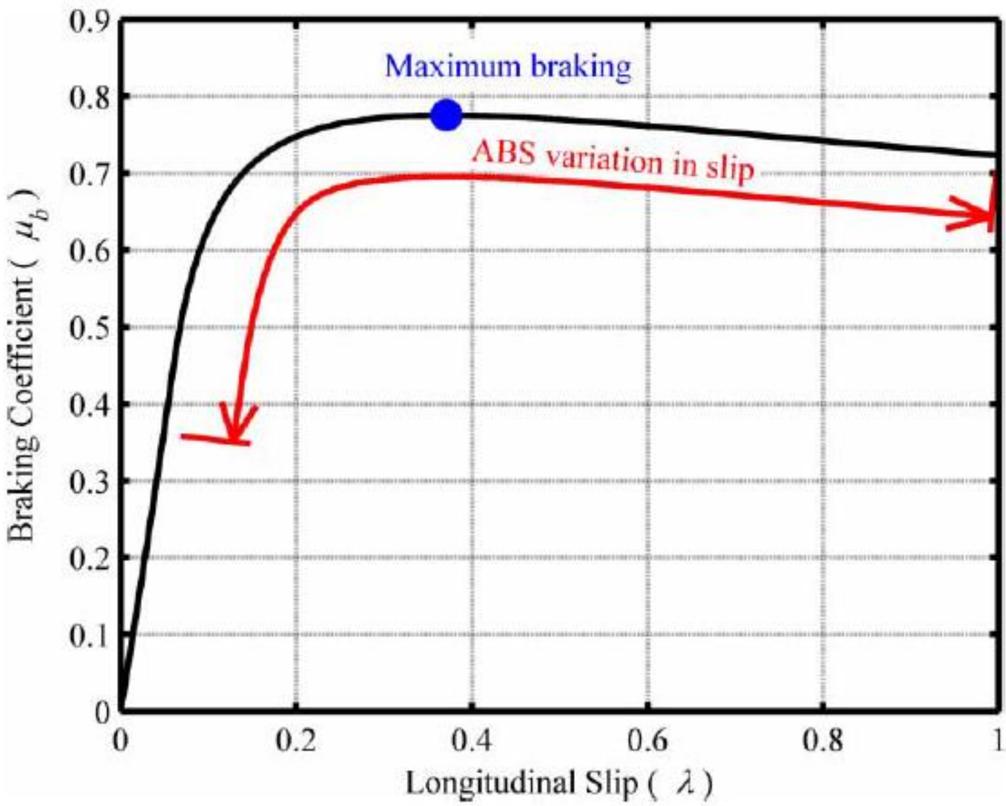

Figure A-75: Truck ABS Operational Zone (Kienhöfer et al., 2008)

Friction Ellipse

Since the tire is simply using friction to generate an in-plane force given a vertical load, there is a maximum tractive potential for any usage condition. That potential can be used for longitudinal force, lateral force, or a combination of the two. The maximum combination potential is usually referred to as the traction ellipse (Figure A-76). Most tires can generate slightly more force in the lateral direction than in the longitudinal direction (this is a complex issue and has to do with belt design, tread design, and carcass rigidity) but the difference is usually not that great. As a result, most models use a simple circle (ore ellipse) to describe the coupled traction behavior (Equation A-16).

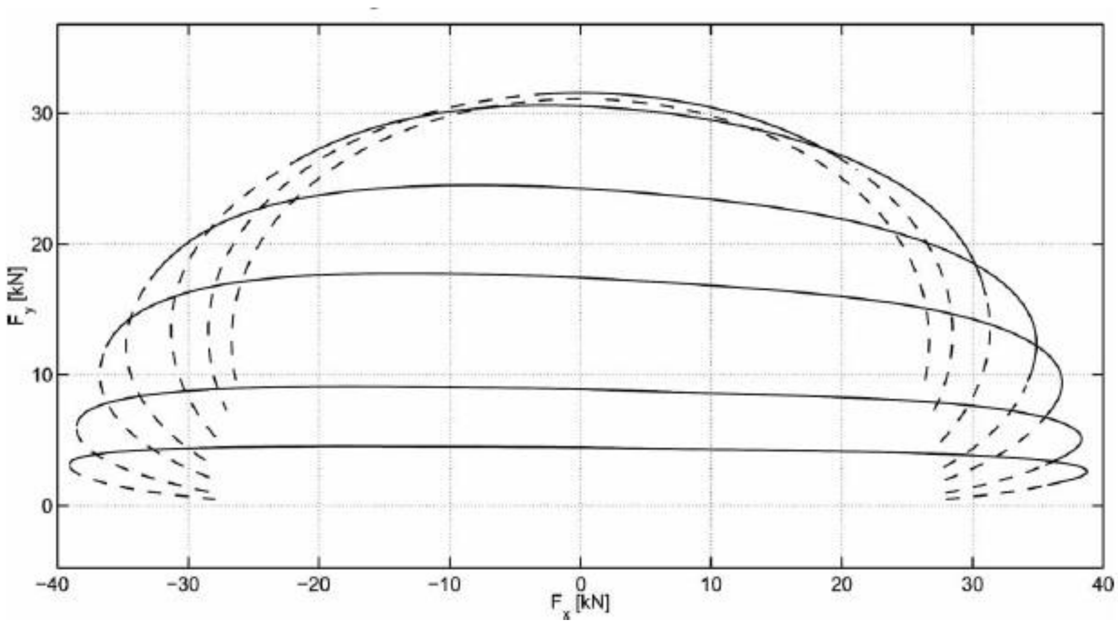

Figure A-76: Tire Friction Ellipse (Gäfvert & Svendenius, 2005)

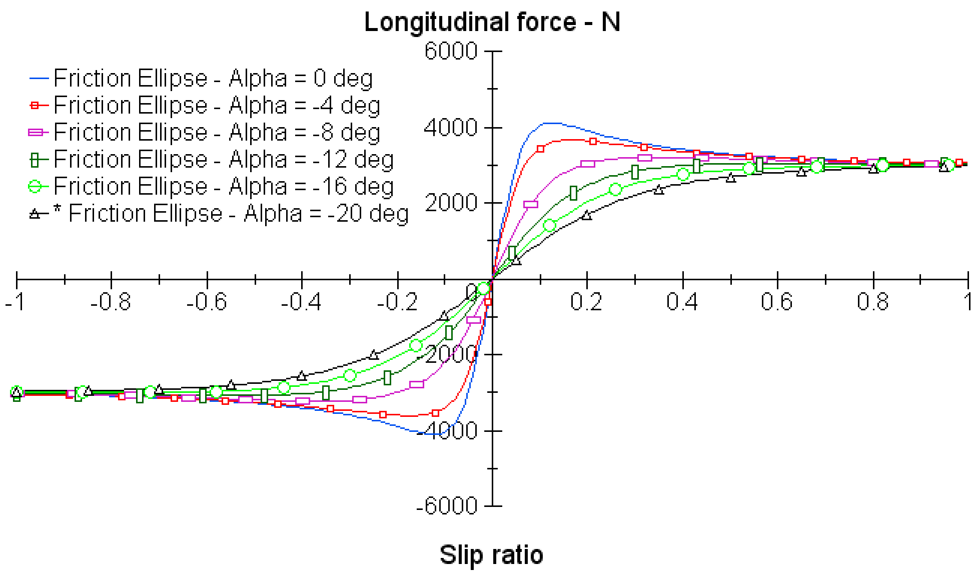

Figure A-77: Tractive Force Under Steer (Limroth, 2009)

$$\left(\frac{F_y}{F_y^*}\right)^2 + \left(\frac{F_x}{F_x^*}\right)^2 = 1 \qquad \textbf{A-16}$$

Relaxation Length

While the above analysis of tire performance has not explicitly stated that it was assuming a static or steady state operational condition it has none the less been treating the tire as operating in a steady state mode. Intuitively, this makes since as the shear layer in the tire does not spontaneously appear when the brakes are activated or the wheel heading changes. The shear layer has to build over time. For most tires, the shear layer develops fully after approximately two thirds of a revolution of the tire. During that time, the force build much like a first order system would respond (Figure A-78).

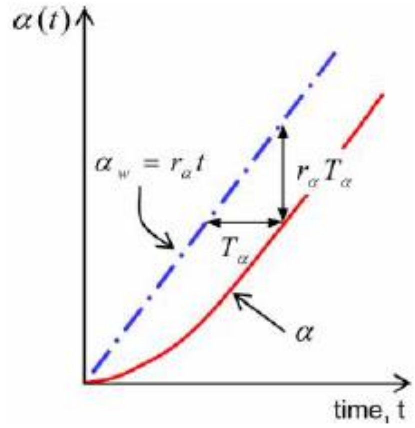

Figure A-78: Tire Relation Length to Step Input (Gim et al., 2007)

Several modeling experts have noted that correctly accounting for this relaxation length effect is important for accurate results from transient maneuvers (Gim et al., 2007; Kim, 2010; Svendenius & Gäfvert, 2006). Technically, to properly predict the tire's behavior, the distance it has rolled since the last change in heading or change in deceleration torque must be accounted for so that the estimated tractive force can be scaled as necessary. However, the relaxation length is often ignored as it cannot be incorporated into a linearized system easily.

A.5.3. Road Crown and Road Bank

As the vehicle's lateral acceleration is usually measured with an accelerometer mounted to the chassis, the controller will observe a false lateral acceleration level if the vehicle is not on a level surface (Hsu & Chen, 2010). This can lead to incorrect estimates of roll potential and to incorrect estimations of yaw rate. To address this problem, two different approaches have been used by other researches to correct the lateral acceleration.

The first method is a time averaging method where the steering input is monitored, the yaw rate is monitored, and the lateral acceleration is monitored. If the steering is straight or nearly straight and the vehicle is not yawing, then the lateral acceleration is due to road crown and can be subtracted out. The difficulty with this approach is that it does not update instantaneously when the road crown does change.

The second method uses additional data (e.g. GPS data) with a filter to evaluate the vehicle's true heading which then indicates if the observed acceleration should be canceled out or not (see sections A.6.3 and A.6.4 for information on filtering and GPS). The difficulties with this method are that the additional data may not always be available or is available at a much slower rate and the filtering usually introduces a delay in the correction. This approach is used in the work presented here.

Fortunately, road crowns in the US are typically quite small (below 3%) so the corrections are not usually large. The need to correct them actually has more to do with integration of the DC offset error when calculating yaw than it does on estimating lateral acceleration as the 3% error only produces a 0.03 g error in the measured lateral acceleration.

A.6. Sensors and Vehicle Observability

Once a vehicle model has been developed and a controller constructed, the simulation or validation process will need information on the vehicle it is attempting to control. The two types of data needed by the controller are vehicle parameter data (mass, length, tire properties, etc.) and vehicle states (lateral acceleration, side slip, yaw rate, etc.). The problem is that, with few exceptions, the needed information is variable with time. Thus methods to determine both the parameters and states are needed.

A.6.1. Measurement of Vehicle Parameters

When modeling passenger cars, it common to assume that the vehicle parameters are known as vehicle mass changes very little (Park et al., 2008). But this assumption is most definitely not true when dealing with commercial vehicles used to haul freight (L. K. Chen & Shieh, 2011; Du & Zhang, 2008; J. Wang & Hsieh, 2009). These parameters are not only difficult to obtain, but vital for accurate stability control when using traditional reference model controller architectures (Andersky & Conklin, 2008; Brown et al., 2009). Therefore methods to evaluate the vehicle's parameters are needed.

Measuring Mass

Traditionally, one of the more difficult parameters to measure has been vehicle mass and mass distribution. Usually mass has been measured through monitoring acceleration when the engine power is known (Nantais, 2006), (Huh et al., 2007), (Limroth, 2009) or through observed lateral accelerations and assumed tire cornering stiffness (Limroth, 2009), (Limroth, Kurfess, & Law, 2009). However, these methods become more complicated when the tractor can swap trailers (or the trailer swap tractors) as "knowing" the tire performance of all vehicle units and the engine performance from the trailer's perspective is difficult.

A second problem commonly encountered in estimating mass is accounting for road grade and road crown. Road grade results in a loss of gain of acceleration as potential energy is converted into kinetic energy. It also results in errors to the measured longitudinal acceleration. Meanwhile road crown results in errors to the measured lateral acceleration which will negatively affect the mass estimate. While these effects can be accounted for by using other sensors (GPS, yaw rate, etc.) the corrections usually require Kalman style filters which means a time averaging approach.

Fortunately the majority of US tractors and trailers have a readily available load indicator in the form of an air suspension. Most tractors and trailers produced today are equipped with air suspensions as air offers a superior ride and load leveling capabilities. The systems are set up to adjust the air pressure to maintain ride height and, in the process, identify the vertical load via the air pressure in the suspension. All that is needed is a constant to convert the air pressure to a force based on the fixed air bag surface area and this constant could be stored in the ESC controller / monitor attached to the vehicle unit. To avoid road noise in the mass estimate, the measurement could be highly damped (very large time constant) or designed to estimate and hold the current mass after each loading / unloading event (Figure A-79). A second benefit would be the determination of the longitudinal CG location of each vehicle unit.

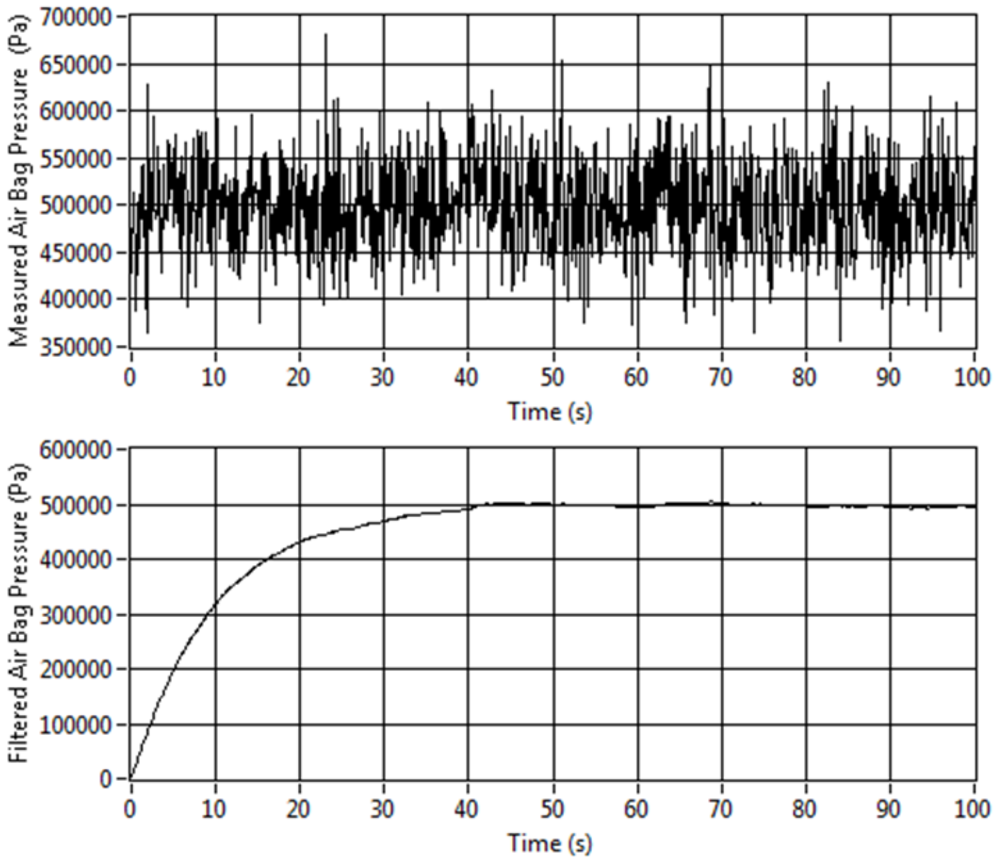

Figure A-79: Measured and First Order Filtered Air Bag Pressure

At this point, the knowledgeable commercial vehicle reader will likely point out that steer axles on tractors are usually leaf spring designs. That is true, but the typical US tractor sees very little static load change on the steer axle between a bobtail and a full GVW condition. Typically, the steer axle load range is between the high 10,000 lb. (bobtail) and high 11,000 lb. range GVW. This small change can be ignored and the steer axle treated as always loaded.

But what if it is desired to equip a spring loaded trailer or dolly with ESC? As there is no air suspension to measure, the best option would be to incorporate a simple and cheap linear potentiometer to measure suspension deflection. As the suspension stiffness is (relatively) constant, it would be easy to convert deflection into static load. It is recommended that the measurement be highly damped (very large time constant) to avoid noise in the measurement due to dynamic motion of the vehicle.

While this approach requires additional sensors to traditional mass estimation approaches, the sensors are warranted for two reasons: The first is that traditional approaches usually determine the relative ratios of the parameters such as mass and tire cornering stiffness ratio (Limroth, 2009) or mass and engine power ratio. To truly know mass, you must know another parameter which is difficult in this case. The second is that traditional ESC development was for vehicles with little change in mass and very little change in the CG position. This is most definitely not true for commercial vehicles. It is uncertain if estimation methods could manage all the extreme loading possibilities of a commercial vehicle particularly when more than one unit is present and they are interacting dynamically.

Measuring Mass Height (CG Height)

In the passenger car world, the general approach is to treat the vehicle CG height as fixed or to estimate the height from observed roll of the vehicle or pitch of the vehicle (Davis & Marting, 2002; Limroth, 2009). However, this is not as easy with a commercial vehicle. Using pitch to evaluate CG height is complicated by the fact that the trailer is acting on the tractor via the fifth wheel. Using roll to evaluate the CG height is complicated by the multiple compliances (suspension, fifth wheel, etc.) making it difficult to know the roll stiffness of the assembled vehicle.

Commercial vehicles do not typically have roll bars, but the suspensions themselves have significant roll stiffness. Most commercial vehicles have trailing arm suspensions similar to the one shown in Figure A-80. Inspection of the axle arrangement will show that the entire suspension is in effect a roll bar which can add significant roll stiffness to the vehicle. Further, the air bags add an additional transient roll moment due to differential loading (roll displacement). But the pneumatic roll moment does dissipate over time as the air bags are plumbed to a common air tank such that air can bleed from one side to the other mitigating the pneumatic roll moment. Never the less, reasonable estimates on roll stiffness are possible using simple tests such as static offset loading and parking the vehicle on an incline.

Figure A-80: Typical Commercial Vehicle Suspension Design (Hendrickson, 2011)

Measuring Chassis Length

Another important parameter for the ESC controller is chassis length. But given that trailers and tractors can be swapped so easily, knowing the length of each unit in a randomly configured vehicle poses a challenge. Again, there is a simple solution to this problem as well. Each vehicle unit will need to be equipped with a small ESC unit to measure and relay the sensor values and actuate the local brakes. After all, one would not want to have to re-wire every sensor when changing a trailer out so some sort of local unit communication device will be needed. This unit is fixed to the vehicle chassis (which has a fixed length) and can be programmed with a length constant when installed.

Measuring Tire Properties

As was discussed in section A.5.2, the tire is a very complicated structure and cannot be linearized in the modeling. That leaves a difficult problem in how to determine the tire properties for the given operational environment (load, road condition) (Cheng & Cebon, 2011). The solution is to recognize that the shape of a tire's lateral and longitudinal force curves does not change that significantly between surface conditions and load conditions (see section A.5.2 for more information). Thus what is needed is to use the known mass and the measured lateral acceleration to determine the tractive potential of the tire or the effective ground coefficient of friction. With that known, reasonable estimates of the tire force can be obtained given the load, torque, and the slip angle. Note: the secondary benefit of using this approach is that any errors in parameter estimation result in an error in the cornering stiffness estimation that cancels the error in the parameter estimation. What is desired and obtained here is, in effect, the ratio of cornering stiffness to the vehicle system mass / inertia (Limroth, 2009).

Several techniques exist to measure the tire's performance which account for measurement bias and error. Typical methods employ time based averaging of kinematic models or Kalman filters with secondary data sources such as GPS. A review of these techniques is included in the tire modeling discussion in section A.5.2.

Measuring Unit Inertia

As the load on a commercial vehicle changes, the vehicle's inertial properties will change as well. Fortunately, with the mass known, the vehicle's inertia can be evaluated fairly easily. In yaw, the inertia can be estimated by monitoring the yaw rate and lateral acceleration (Limroth, 2009). As the CG height cannot be easily identified, the overturning moment cannot be directly calculated. Thus the roll inertial of the vehicle can be defined only in terms of the lateral acceleration. However, the stability model needs to know the relationship between lateral acceleration and roll rate / roll angle, so this method will meet the modeling needs.

A.6.2. Measurement of Vehicle States

The identification of vehicle states can be generally broken into two categories: States that are directly observable, and states that are not directly observable. Directly observable states are ones for which sensors exist and are cheap enough to implement. Non-observable states are ones that are impractical to measure on the vehicle. Each of the major states to be measured is discussed below along with its observability.

Measuring Lateral Acceleration

As accelerometers are relatively inexpensive, obtaining a direct measurement of the vehicle's lateral acceleration is possible. But as noted in section A.5.3, road crown can introduce bias into the measurement. Lateral acceleration measurements can be compensated using GPS data (Section A.6.3) or by comparing the measured results against physical model based observers or estimation using kinematic model based observers (Limroth, 2009).

Measuring Roll Rate

Angular rate sensors are also relatively inexpensive thus measuring the roll rate is possible. However, the roll rate sensor can be noisy so integrating the signal to produce a roll angle can be problematic (Cheli, Sabbioni, Pesce, & Melzi, 2007). To correct for this, the roll rate can be compared to the observed or modeled lateral acceleration as the roll rate should be zero for a constant lateral acceleration. Alternately, GPS data could be used to correct any integration bias (Bevly, 2004). Depending on the quality of the measured signal, a corrective model, such as a Kalman filter, may be needed.

Measuring Lateral Velocity and Side Slip

Lateral velocity and side slip angle are often used interchangeably as the two are related kinematically (Equation A-17) where β is the side slip angle, V_y is the lateral velocity and V_x is the longitudinal velocity.

$$\beta = tan^{-1}\left(\frac{V_y}{V_x}\right) \quad \textbf{A-17}$$

While direct sensing of lateral velocity using cameras or GPS units has been demonstrated, these approaches generally suffer from low data throughput and are prohibitively expensive to implement (Limroth, 2009). Therefore, estimation methods are usually employed in practice.

As the side slip is the result of the non-linear responses of all tires, it is particularly sensitive to errors in tire estimations (Best et al., 2000), (Kim, 2010). Typical approaches use state space estimators based on physical models of the vehicle (such as Equation A-18) or kinematic models (such as Equation A-19) (Limroth, 2009).

$$\begin{bmatrix} \dot{v}_y \\ \dot{r} \end{bmatrix} = \begin{bmatrix} -\frac{C_1+C_2}{mv_x} & \frac{-aC_1+bC_2}{mv_x} - v_x \\ \frac{-aC_1+bC_2}{Jv_x} & -\frac{a^2C_1+b^2C_2}{Jv_x} \end{bmatrix} \begin{bmatrix} v_y \\ r \end{bmatrix} + \begin{bmatrix} \frac{C_1}{m} \\ \frac{aC_1}{J} \end{bmatrix} \delta \qquad \textbf{A-18}$$

$$A_y = \dot{V}_y + V_x * r \qquad \textbf{A-19}$$

The kinematic model has the advantage that it is accurate in the non-linear vehicle domain (no linearized terms) and it is easier and faster to solve, but it is subject to sensor bias errors (Cheli et al., 2007). The state space model simplifies the response and is less sensitive to sensor bias though it does need regular corrections to the tire cornering stiffness.

The last method for evaluating side slip is from GPS data. Here the vehicle's velocity vector is measured using GPS and compared to the gyro measurement (Equation A-20). The heading from the gyro is derived from integration of the yaw rate with Kalman or other filtering techniques used to remove bias and "zero" the integration error. The difference between the velocity vector and the vehicle axis (integrated yaw rate) is the side slip. As the GPS velocity error increases at lower speed (Doppler shift), the error is highest for low speed maneuvers (Figure A-81).

$$\beta = \psi_{Gyro} - \psi_{GPS} \qquad \textbf{A-20}$$

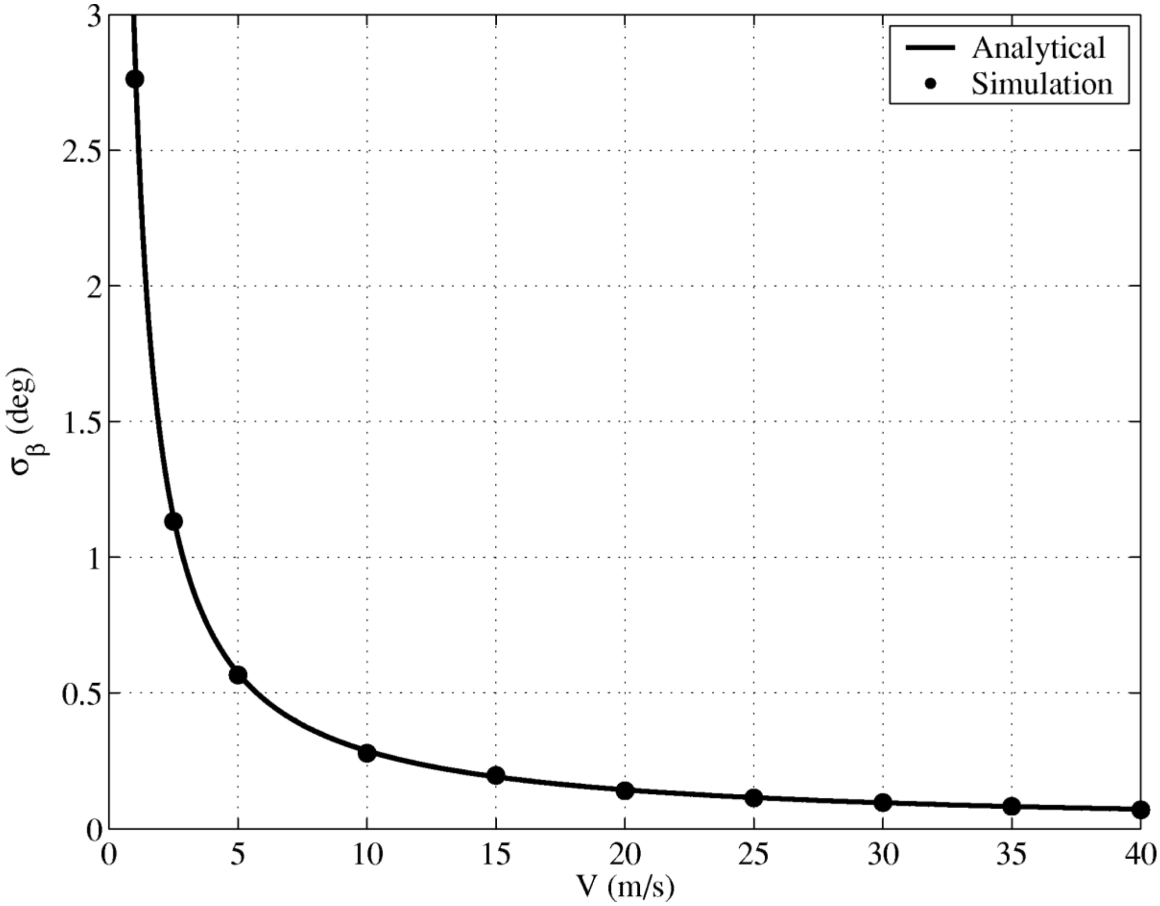

Figure A-81: Side Slip Error from GPS Measurement (Daily & Bevly, 2004)

In this work, kinematic model approaches using GPS and yaw rate sensors are used to evaluate side slip.

Measuring Yaw Rate

Like roll rate, sensors exist which can directly measure the heading change of the vehicle fairly cheaply. Further, the yaw moment is the difference between front and rear lateral forces and thus tire non-linarites do not affect the measurement as significantly as is the case for lateral acceleration (Kim, 2010).

General Comments on State Estimation

There are essentially three methodologies for acquiring the vehicle's dynamic states. These can be combined to improve state estimations in various ways but each permutation has its drawbacks. In Figure A-82, INS stands for inertial measurements and GNSS represents GPS (Global Navigation Satellite System). The following observations were made by (Tin Leung et al., 2011)

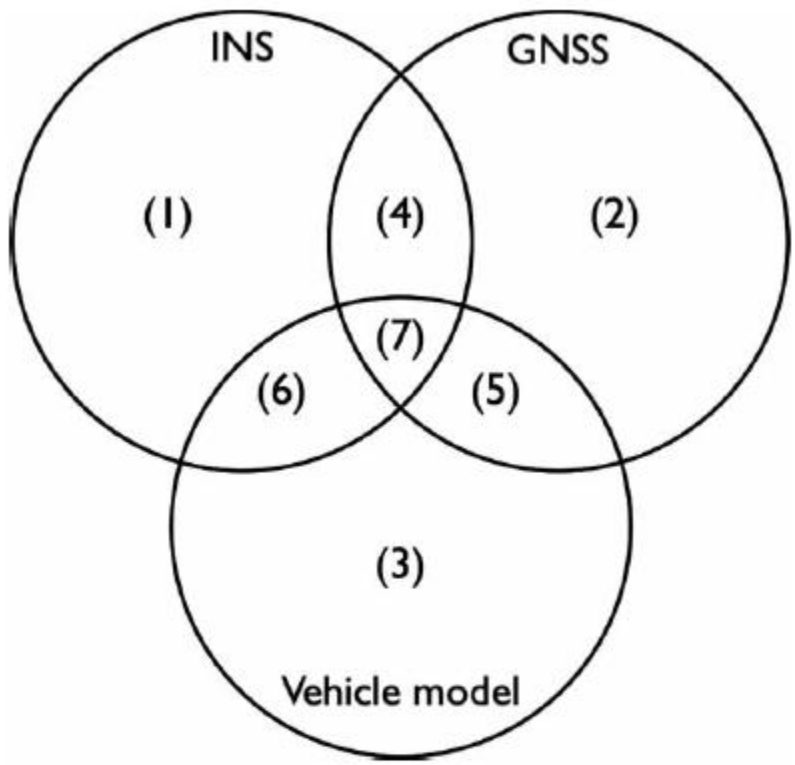

Figure A-82: Vehicle State Estimation Methods (Tin Leung et al., 2011)

- Inertial systems are fast and cheap. But bias errors lead to significant problems in integration of the signals.
- GPS is also (relatively) cheap and convenient to implement, but it has slow update rates (1 - 5 Hz) and occasionally drops out due to obstructions.

- Modeling the vehicle is fast (numerical issue) and simple to implement, but the models are usually linearized so limit behavior is not captured well.
- Using a kinematic model of the vehicle with a GPS correction for inertial drift is quite effective. However, the slow update rate of the GPS along with the intermittent drop-out of GPS means that filtering is required.
- Using a vehicle model and GPS allows for better limit behavior analysis (non-linear vehicle behavior). However, the GPS drop-outs result in the corrections for the non-linear vehicle behavior being inconsistent with time. The solution is to use the GPS to generate estimates of errors rather than correct the errors.
- Inertial measurements are effective at correcting modeled state errors due to incorrect parameter estimations. However, the results are sensitive to accurate tire response predictions.
- In this case, both the vehicle states and parameters can be evaluated continuously. This is obviously the optimal solution, but it is the most expensive and requires the most computational time to implement.

A.6.3. Sensors and Sensor Limits

With the discussion on measurement of parameters and states, it is logical to investigate what measurement devices exist and what their limitations are. To that end, a brief listing of measurement devices is included so the reader has some perspective on what is and is not possible to measure. Additionally, information on sampling frequency is included as well.

Inertial Measurement Units

The most basic vehicle sensor is the 3-axis gyro / accelerometer. While some manufactures simplify this to a 2 axis system (omitting pitch and vertical acceleration), the standard is still to measure all 6 degrees of freedom. Accuracies are in the rage of 0.06 m/s^2 and 0.2 deg/s (Bevly, 2004; Ryu & Gerdes, 2004) for accelerations and angular rates. Typically, the update rate is on the order of 100 Hz (Zhang Jin-zhu & Zhang Hong-tian, 2009). Costs range from $20 to $50 (Bevly, 2004).

Global Position Systems

While there is a broad range of GPS units in use, the most common, and cheapest, configuration is a single GPS receiver operating at 1 Hz. Position accuracies are on the order of 0.05 m, velocity accuracy is approximately 0.04 m/s (Figure A-83), and heading accuracy is on the order of 0.1 degree (Zhang Jin-zhu & Zhang Hong-tian, 2009). But it takes four or more satellites for the GPS to establish an accurate position (Tin Leung et al., 2011). Costs for single GPS units are on the order of $100 (Bevly, 2004).

In addition to the 1 Hz update rate, there is a 5 to 10 millisecond latency in calculating heading and speed. But the latency can be accounted for and the GPS data used to correct kinematic or state space model estimations (Figure A-84). Errors in velocity are also more significant at low speed as velocity is calculated using Doppler shifting of the satellite carrier wave (Figure A-81).

Finally, there are newer GPS systems which use two antennas (minimal cost increase) which can provide yaw and roll information (Bevly, 2004; Ryu & Gerdes, 2004). These systems operate at 5 Hz and are quite accurate. The work presented here uses this type of GPS system.

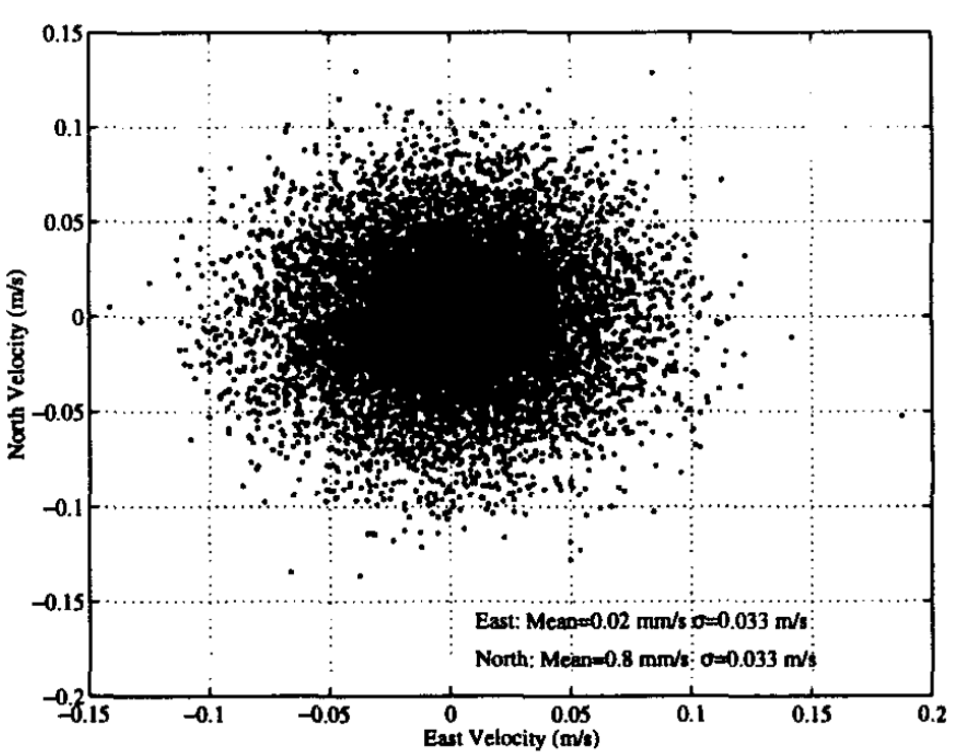

Figure A-83: Calculated Vehicle Velocity for Stationary GPS (Bevly, Gerdes, Wilson, & Gengsheng, 2000)

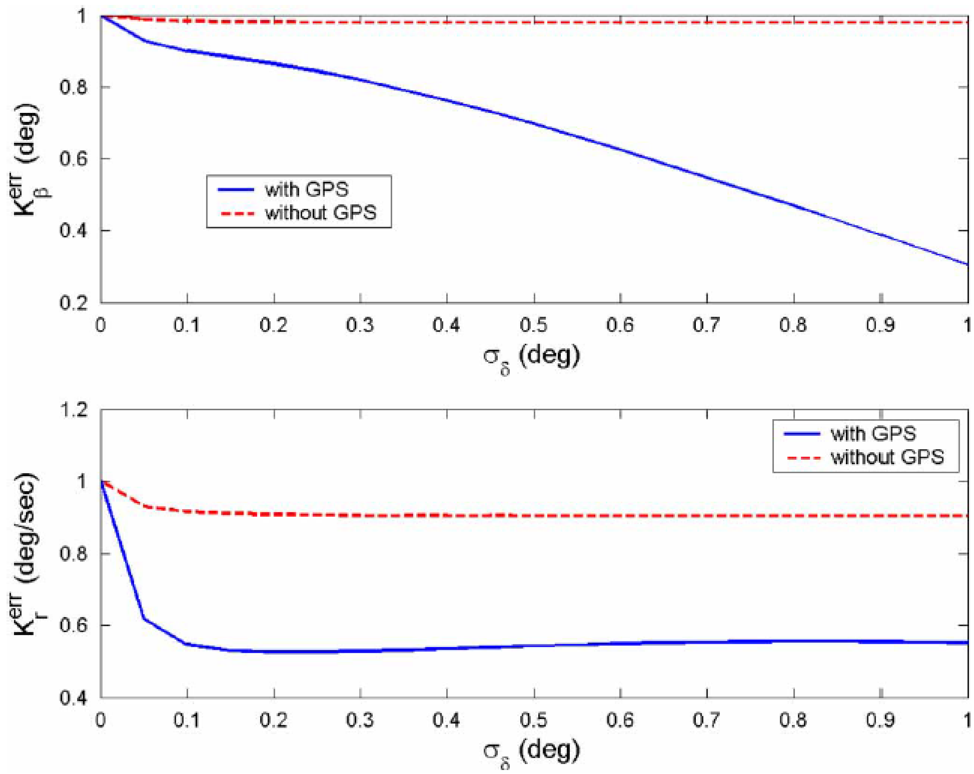

Figure A-84: GPS Corrected Side Slip Error (Anderson & Bevly, 2010)

Pressure Transducers

Pressure transducers for monitoring air suspensions or air brakes are on the order of $5 each. Accuracies are usually on the order of 1 psi for a 120 psi transducer. Frequency response is well over 100 Hz. The limitation is that they have low signal to noise ratios so filtering is required.

A.6.4. Kalman Filters

As a number of parameter and state estimations use Kalman filters, a short discussion on these filters is included along with a few observations on implementation.

Perhaps the best description of the filter and its use in vehicle dynamics modeling comes from Vehovens and Naab (Venhovens & Naab, 1999):

> "A Kalman filter is a stochastical state estimator. This means that the design engineer assumes that the plant to be observed (such as a car) is excited by noise that is characterized by stochastic quantities and that the sensors used are corrupted by stochastic noise as well. Essentially, the state estimator is driven by the same inputs as the plant with exception of the process noise. The principle of estimating the system states is based on a comparison of measured outputs y and estimated outputs y*. With a good state estimator, the difference e which is fed back into the Kalman filter will take care that the estimated states will follow the plant states." (Venhovens & Naab, 1999)

The reason that Kalman filters are so frequently used is that the modeling process used contains both a model of the vehicle or kinematic relationship and actual measured states from the vehicle so the error minimization can be completed efficiently. The only significant drawback to the Kalman filter is that low order filters must be used or the computational time grows too large (Best et al., 2000).

The extended Kalman filter (EKF) is an extension of a traditional Kalman filter designed to manage non-linear systems such as tires (Doumiati, Victorino, Lechner, Baffet, & Charara, 2010) or side slip (Song, Zweiri, Seneviratne, & Althoefer, 2008). In this approach, the state equations are linearized about the operating point, the model solved, and the state equations updated for the next time step (Wenzel et al., 2006), (Wenzel et al., 2007).

A.7. Summary

Modeling and controlling articulated commercial vehicles is a rather challenging task. To do so successfully, one must not only account for the extra degrees of freedom that arise with each additional unit to the vehicle, but manage added uncertainty in the vehicle parameter estimations (mass, inertia, CG location, etc.). Even after those challenges have been met, there are the added problems related to brake control and response time.

While the above material cannot cover all of the issues and concerns associated with developing and implementing commercial vehicle stability control systems, the material presented here is intended to provide the reader with a reasonable level of understanding of each of these issues as well as to document potential solutions and prior work. The issues raised in this review will be among the problems to be resolved during the development of a new commercial vehicle stability controller. When possible, the solution approach will use existing methodologies and market accepted equipment. But when changes are deemed necessary, the limitations of the current state of the art documented here will help justify any departures.

APPENDIX B

OBSERVATIONS ON COMMERCIAL VEHICLE STIFFNESS

Tractors generally have very low front axle CG heights due to the low engine and transmission placement. Further, the rear of the tractor is largely decoupled from the trailer in roll (see Section A.1.4) so the tractor usually has relatively small roll moments at both ends of the chassis. Thus, while tractor frames are usually quite flexible, the assumption that the tractor is rigid is not a significant issue so long as the vehicle remains in the nominal operational range (i.e. the trailer is not in danger of a rollover and has run through the fifth wheel lash).

Since the towing unit (tractor or dolly) is effectively decoupled in roll from the trailer except in extreme roll cases (refer to Section A.1.4 for background), nearly all of the restoring moment acting on the trailer comes through the rear suspension of the trailer. Any torsional deformation will result in the front rolling more than the rear and the true roll at the CG being slightly more than the rigid chassis calculated CG roll. But for low lateral acceleration cases, the torsional deformation will be low and the error small. A simple proof of this assumption can be seen on the public highways where trailer torsional deformation is not commonly seen. Again, for normal operational range cases, the rigid chassis assumption is not unreasonable, particularly if the objective is to keep the vehicle from operating in extreme roll angles or high lateral acceleration levels.

The dolly, by nature of its design, is the stiffest unit in the vehicle. Its short length (typically two to three meters in length) and ladder construction (Figure A-7) make the chassis quite stiff. Further, the nature of the connections between the dolly and trailers (Figure A-3) result in the dolly experiencing very low torsional moments for any usage case save an actual rollover event. Given this scenario, the assumption that the dolly is a rigid object is more than reasonable.

APPENDIX C

RIGID BODY EQUATIONS OF MOTION

For the work presented here, Newtonian methods were used to derive the combination vehicle's equations of motion. While energy methods (Lagrange for example) would have eliminated the observed issues related to the canceling of the internal reaction forces, they posed the problem of managing the relative movement of the individual unit coordinate systems. The need to manage relative movement of the unit coordinate systems resulted in complex energy functions and partial derivatives. Given that many of the internal forces could be dropped (Section D.2.5), which significantly simplified the cancelation process, a Newtonian approach was used. A second reason for using Newtonian methods was that it made it easier for the reader to follow the logic process in mathematically assembling the vehicle.

C.1. Single Unit Vehicle Motion

Before tackling the full vehicle, it helps to develop the basic equations of motion for a single chassis unit. Each unit of the vehicle can be initially treated as an independent rigid body moving relative to a fixed coordinate system defined as the inertial reference frame (R) and shown in Figure C-1. For the analysis case here, the rigid body can be assumed to have linear and angular velocities about all three axes.

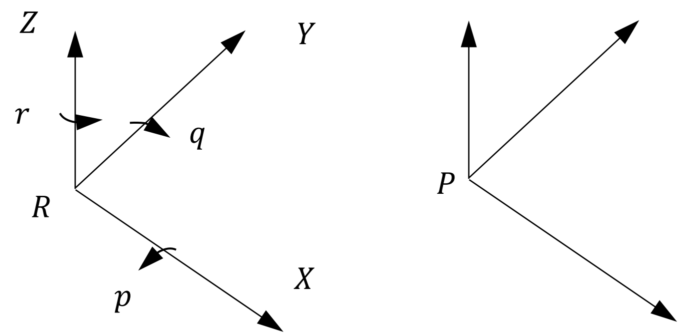

Figure C-1: Rigid Body Motion

In the analysis here, the linear velocities of the unit are defined as $\dot{x}$, $\dot{y}$, and $\dot{z}$ and the velocity of the unit origin (P) is $\dot{X}$, $\dot{Y}$, and $\dot{Z}$. The body velocity components are thus defined as Equations C-1 through C-3:

$$\dot{x} = \dot{X} - \dot{r} * y + \dot{q} * z \quad \textbf{C-1}$$

$$\dot{y} = \dot{Y} + \dot{r} * x - \dot{p} * z \quad \textbf{C-2}$$

$$\dot{z} = \dot{Z} - \dot{q} * x + \dot{p} * y \quad \textbf{C-3}$$

From the velocities, the accelerations can be obtained through differentiation with respect to time (Equations C-4 through C-6).

$$\ddot{x} = \ddot{X} - \dot{r} * \dot{y} + \dot{q} * \dot{z} - \ddot{r} * y + \ddot{q} * z \quad \textbf{C-4}$$

$$\ddot{y} = \ddot{Y} + \dot{r} * \dot{x} - \dot{p} * \dot{z} + \ddot{r} * x - \ddot{p} * z \quad \textbf{C-5}$$

$$\ddot{z} = \ddot{Z} - \dot{q} * \dot{x} + \dot{p} * \dot{y} - \ddot{q} * x + \ddot{p} * y \quad \textbf{C-6}$$

Substituting Equations C-1 through C-3 back into C-4 through C-6 gives Equations C-7 through C-9.

$$\ddot{x} = \ddot{X} - \dot{r} * (\dot{Y} + \dot{r} * x - \dot{p} * z) + \dot{q} * (\dot{Z} - \dot{q} * x + \dot{p} * y) - \ddot{r} * y + \ddot{q} * z \qquad \textbf{C-7}$$

$$\ddot{y} = \ddot{Y} + \dot{r} * (\dot{X} - \dot{r} * y + \dot{q} * z) - \dot{p} * (\dot{Z} - \dot{q} * x + \dot{p} * y) + \ddot{r} * x - \ddot{p} * z \qquad \textbf{C-8}$$

$$\ddot{z} = \ddot{Z} - \dot{q} * (\dot{X} - \dot{r} * y + \dot{q} * z) + \dot{p} * (\dot{Y} + \dot{r} * x - \dot{p} * z) - \ddot{q} * x + \ddot{p} * y \qquad \textbf{C-9}$$

Equations C-7 through C-9 then simplify to Equations C-10 through C-12. These equations define the acceleration of the rigid body in space.

$$\ddot{x} = \ddot{X} - \dot{r} * \dot{Y} + \dot{q} * \dot{Z} - x * (\dot{q}^2 + \dot{r}^2) + y * (\dot{p} * \dot{q} - \ddot{r}) + z * (\dot{p} * \dot{r} + \ddot{q}) \qquad \textbf{C-10}$$

$$\ddot{y} = \ddot{Y} - \dot{p} * \dot{Z} + \dot{r} * \dot{X} + x * (r * \dot{q} - \ddot{p}) - y * (\dot{p}^2 + \dot{r}^2) + z * (\dot{p} * \dot{q} + \ddot{r}) \qquad \textbf{C-11}$$

$$\ddot{z} = \ddot{Z} - \dot{q} * \dot{X} + \dot{p} * \dot{Y} + x * (\dot{p} * \dot{r} - \ddot{q}) + y * (\dot{q} * \dot{r} + \ddot{p}) - z * (\dot{p}^2 + \dot{q}^2) \qquad \textbf{C-12}$$

C.2. Rigid Body Equations of Motion

The rigid body accelerations are determined by the forces applied to the body as well as the mass and inertia of the body as shown in Equations C-13 through C-24.

$$\sum F_x = \sum m * \ddot{x} \qquad \textbf{C-13}$$

$$\sum F_y = \sum m * \ddot{y} \qquad \textbf{C-14}$$

$$\sum F_z = \sum m * \ddot{z} \qquad \textbf{C-15}$$

$$\sum M_x = \sum m * (y * \dot{z} - z * \dot{y}) \qquad \textbf{C-16}$$

$$\sum M_y = \sum m * (z * \dot{x} - x * \dot{z}) \qquad \textbf{C-17}$$

$$\sum M_z = \sum m * (x * \dot{y} - y * \dot{x}) \qquad \textbf{C-18}$$

$$I_{xx} = \sum m * (y^2 + z^2) \qquad \textbf{C-19}$$

$$I_{yy} = \sum m * (x^2 + z^2) \qquad \textbf{C-20}$$

$$I_{zz} = \sum m * (x^2 + y^2) \qquad \textbf{C-21}$$

$$I_{yz} = \sum m * y * z \tag{C-22}$$

$$I_{xz} = \sum m * x * z \tag{C-23}$$

$$I_{xy} = \sum m * x * y \tag{C-24}$$

Combining terns defines the equations of motion for the system (Equations C-25 through C-30). Note that the equations represent (in order of appearance) longitudinal, lateral, vertical, roll, pitch, and yaw motions.

$$\sum F_x = m * \left(\ddot{X} - \dot{r} * \dot{Y} + \dot{q} * \dot{Z}\right) \tag{C-25}$$

$$\sum F_y = m * \left(\ddot{Y} - \dot{p} * \dot{Z} + \dot{r} * \dot{X}\right) \tag{C-26}$$

$$\sum F_z = m * \left(\ddot{Z} - \dot{q} * \dot{X} + \dot{p} * \dot{Y}\right) \tag{C-27}$$

$$\sum M_x = I_{xx} * \ddot{p} - \left(I_{yy} - I_{zz}\right) * \dot{r} * \dot{q} + I_{yz} * (\dot{r}^2 - \dot{q}^2) - I_{xz} * (\dot{p} * \dot{q} + \ddot{r}) + I_{xy} * (\dot{p} * \dot{r} - \ddot{q}) \tag{C-28}$$

$$\sum M_y = I_{yy} * \ddot{q} - (I_{zz} - I_{xx}) * \dot{r} * \dot{p} + I_{xz} * (\dot{p}^2 - \dot{r}^2) - I_{xy} * (\dot{r} * \dot{q} + \ddot{p}) + I_{yz} * (\dot{p} * \dot{q} - \ddot{r}) \tag{C-29}$$

$$\sum M_z = I_{zz} * \ddot{r} - \left(I_{xx} - I_{yy}\right) * \dot{q} * \dot{p} + I_{xy} * (\dot{q}^2 - \dot{p}^2) - I_{yz} * (\dot{p} * \dot{r} + \ddot{q}) + I_{xz} * (\dot{q} * \dot{r} - \ddot{p}) \tag{C-30}$$

C.3. Simplification of the Equations of Motions

As the objective of the research here was to enhance handling stability of a vehicle, some simplifications to the above rigid body equations of motion were proposed. The simplifications are as follows: the vehicle does not pitch and the vertical forces remain constant with respect to the Y axis (i.e. there is no forward load transfer under braking - Equation C-31), the vehicle does not move vertically (Equation C-32), and the vehicle velocity remains constant over the analysis interval (deceleration forces are significantly less than lateral forces - Equation C-33).

$$\dot{q} = \ddot{q} = 0, \qquad M_y = 0 \tag{C-31}$$

$$\dot{Z} = \ddot{Z} = 0 \tag{C-32}$$

$$\ddot{X} = 0 \tag{C-33}$$

Additionally, the assumption that the vehicle was symmetric about the longitudinal axis meant that the inertia products about the symmetry axis could be treated as zero (Equation C-34).

$$I_{xy} = I_{yz} = 0 \tag{C-34}$$

With these simplifications, the rigid body equations of motion of interest were reduced as follows (Equations C-35 through C-40): Longitudinal acceleration has been defined to be zero so the product of yaw rate and lateral velocity was taken to be near zero (Equation C-35). The vehicle was at a constant height so the product of roll rate and lateral velocity was ignored (Equation C-37) (Static vertical force canceled with static weight). The vehicle did not pitch (no moment about the Y axis) so Equation C-39 was zero as well.

The three remaining equations governing the rigid body motion were the lateral force balance (Equation C-36), the roll moment balance (Equation C-38), and the yaw moment balance (Equation C-40). The analysis of each vehicle unit was derived from the basic rigid body motions defined here. Note: These equations do not account for sprung mass rotations about the vehicle roll axis. The effect of vehicle rotation about a point other than the CG location will be introduced later.

$$\sum F_x = m * (\dot{r} * \dot{Y}) \approx 0 \tag{C-35}$$

$$\sum F_y = m * (\ddot{Y} + \dot{r} * \dot{X}) \tag{C-36}$$

$$\sum F_z = m * (\dot{p} * \dot{Y}) \approx 0 \tag{C-37}$$

$$\sum M_x = I_{xx} * \ddot{p} - I_{xz} * \ddot{r} \tag{C-38}$$

$$\sum M_y = -(I_{zz} - I_{xx}) * \dot{r} * \dot{p} + I_{xz} * (\dot{p}^2 - \dot{r}^2) = 0 \tag{C-39}$$

$$\sum M_z = I_{zz} * \ddot{r} - I_{xz} * \ddot{p} \tag{C-40}$$

The objective of this analysis was to illustrate that the motion of any unit of the vehicle could be reduced to three equations with three unknown motion variables (four equations and unknowns if we include the axle motions). Each unit of the vehicle adds a set of three equations and unknowns to the total vehicle (Note: inclusion of roll and roll rate later will result in four unknowns and four first order equations per unit). Finally, as units are added, constraint equations will be needed to define the relative motion of the units (i.e. fifth wheel and pintle hook).

APPENDIX D

LINEAR MODEL DEVELOPMENT

In an effort to focus the overall flow of this document on the controller work, the development of the linear time invariant (LTI) model was relegated to the appendix here. This section deals with how the linear model was developed along with each vehicle unit's equations of motion. The final LTI model and the associated equations are presented in Section 4.2.

D.1. Modeling of the Vehicle Units

Before beginning to solve for the entire vehicle's motions to steering and brake inputs, it was necessary to develop the basic equations of motion for each unit of the vehicle. With the motions of each vehicle unit known, constraints could be added to generate the coupled vehicle's dynamic response. This section covers the development of the linearized vehicle model including the assumptions and equation development. In all cases, the ISO standard for vehicle coordinates was used. This system has the X axis along the vehicle centerline point forward, the Y axis to the left, and the Z axis upward.

D.1.1. Roll Free Body for each Unit

As each of the units is functionally equivalent in roll, the roll analysis is presented once for all of the vehicle units. As described in Section 3.2, the approach used in the development of the linear model was to account for the axle roll by proportionally increasing the distance between the sprung mass CG and the roll center height. This in turn permitted the removal the axle degree of freedom (axle roll) from the vehicle model.

In this model, each unit is essentially an inverted pendulum with a torsional spring at the base (Figure D-1). The restoring suspension moment counters the combined destabilizing moments generated by the lateral acceleration and the offset CG due to roll (Equation D-1). Note that the rotation of the sprung mass is not about its CG but about the suspension roll center.

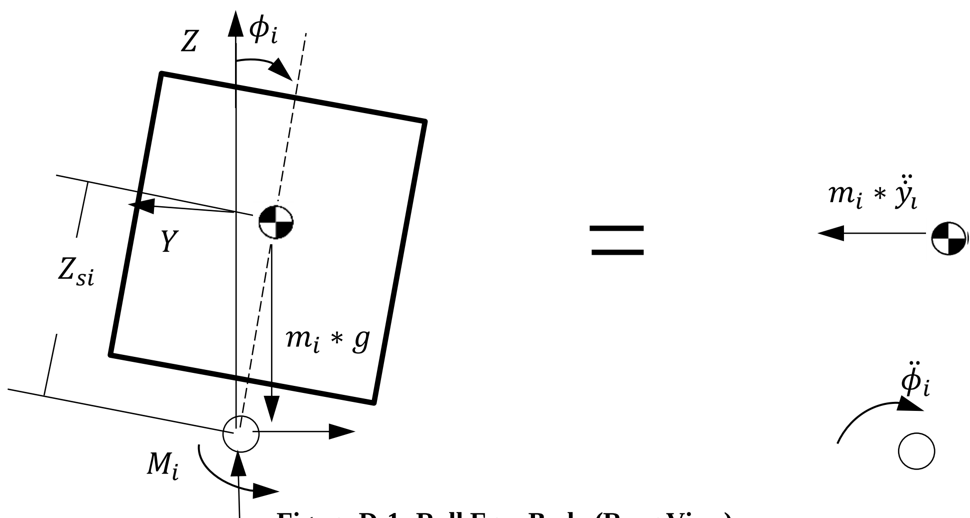

Figure D-1: Roll Free Body (Rear View)

$$(I_{ixx} + m_i * Z_i^2) * \ddot{\phi}_i = m_i * Z_i * \left(g * sin(\phi_i) + \ddot{y}_i * cos(\phi_i)\right) - M_i \qquad \textbf{D-1}$$

As discussed in Section 3.2.1, it is presumed that the fifth wheel constrains only linear motions (no moments). While not illustrated in this example, the lateral force at the fifth wheel does introduce a roll moment as the hitch is presumed to be a distance of f_i above the roll axis. This effect was also included in the final vehicle equations of motion (Section D.2).

D.1.2. Slip Angle Development for Tractor

As discussed in Section 3.3, the forces acting on the vehicle were presumed to be generated by the tires. As such, it was necessary to define the motion of each vehicle unit as well as the tire motions so that the relative differences could be obtained. As each unit type in the vehicle (tractor, trailer, and dolly) has some unique features, they are treated individually. To simplify the analysis for all vehicle units with tandem axles, each tandem set was treated as a single axle through the simplification approach documented in Section A.4.2. To make the modeling process easier to follow, each unit's velocities will be documented before the analysis of motion is presented.

The tractor is the most unique unit in the vehicle as there is only one (as opposed to multiple trailers and dollies), it is the only unit with two axles (the remaining units have a single axle and a hitch), and it is also the only unit for which the driver can directly control the heading through selection of the front axle slip angle. If the tractor is simplified using a bicycle model (Figure D-3), then the relative velocities of the tractor (at its CG) and the wheels can be determined given the instant center of rotation of the tractor. The difference between wheel velocity vectors and the chassis velocity vector at the wheel defines the wheel slip angle. In this model a_1 and b_1 denote the distance between the CG and the front and rear axles respectively. Note that the front axle (Equation D-2) includes a driver steering input (δ) while the rear axle (Equation D-3) does not. These resulting slip angles will determine the tire forces acting on the vehicle as shown in Equation 3-15 / Equation D-4.

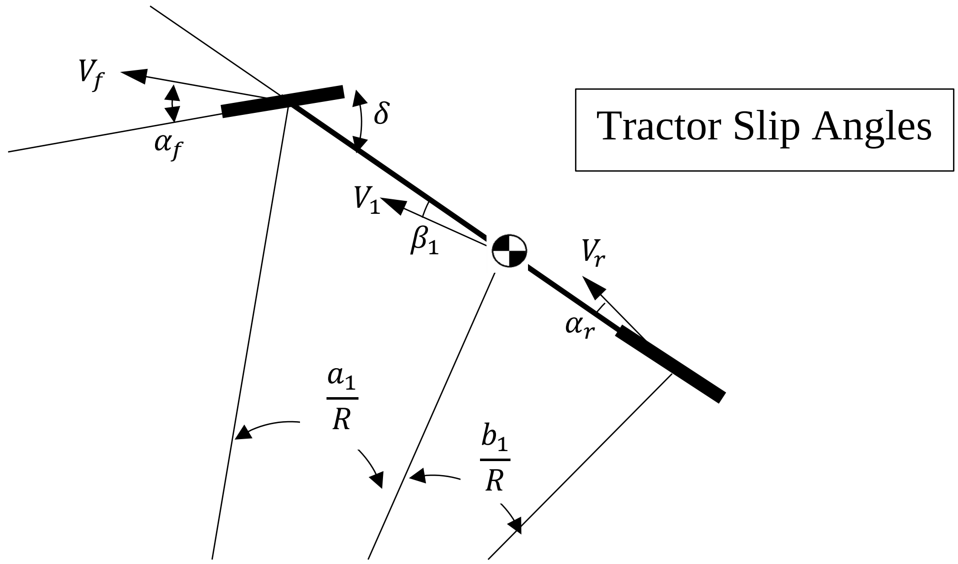

Figure D-2: Tractor Velocity Vectors and Angles

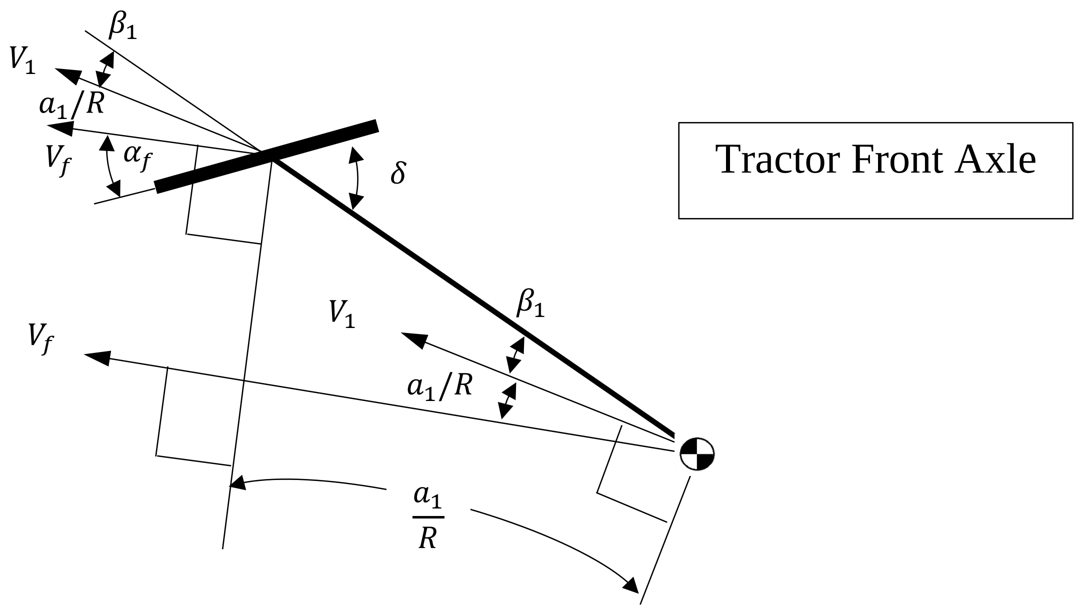

Figure D-3: Tractor Velocity Vectors and Angles Development (Front)

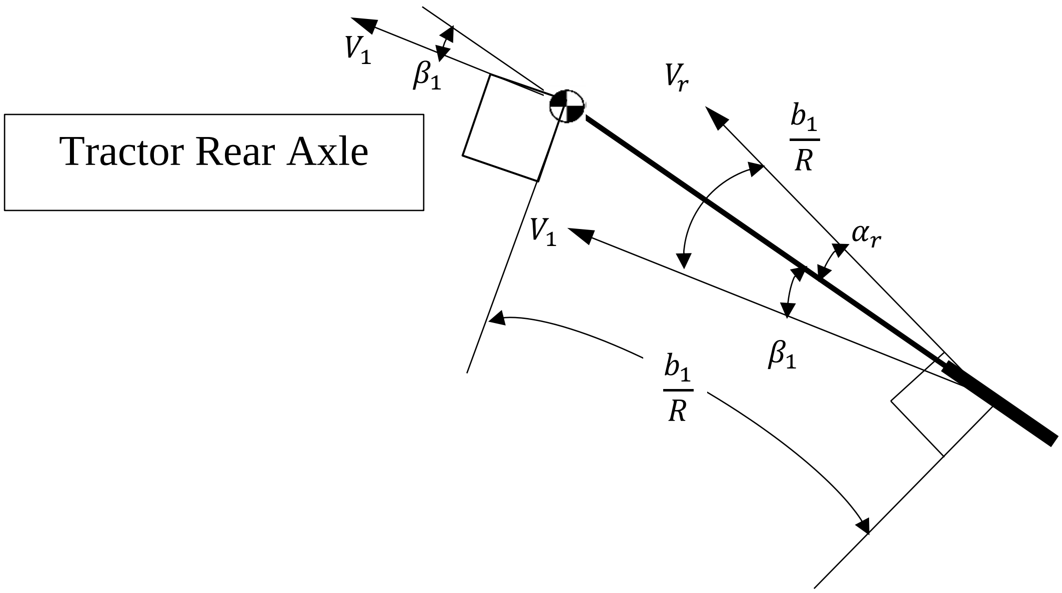

Figure D-4: Tractor Velocity Vectors and Angles Development (Rear)

$$\alpha_f = \delta - \frac{a_1}{R} - \beta_1 \quad \textbf{D-2}$$

$$\alpha_r = \frac{b_1}{R} - \beta_1 \quad \textbf{D-3}$$

$$F_y = C_\alpha * \alpha \quad \textbf{D-4}$$

D.1.3. Slip Angle Development for Trailer / Dolly

As the trailer and dolly both use a hitch for the forward support (Figure D-5), only the rear axle slip angels need to be defined. Not surprisingly, the resulting slip equation (Equation D-5) looks like the rear axle equation from the tractor (Equation D-3). As there is only one axle per dolly / trailer, the side slip angle will be denoted by use of the unit number in the subscript rather than "f" (front) or "r" (rear) as used with the tractor.

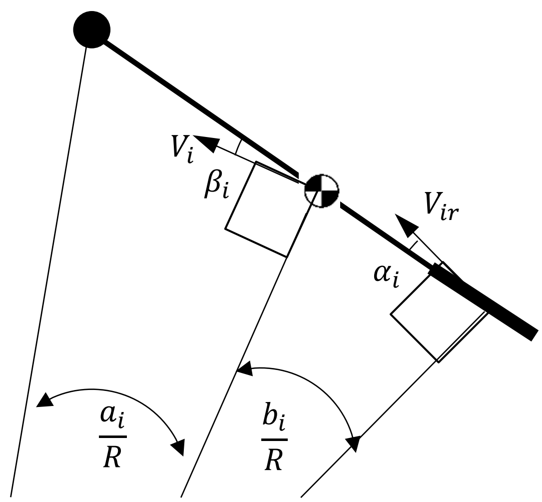

Figure D-5: Trailer / Dolly Velocity Vectors and Angles

$$\alpha_i = \frac{b_i}{R} - \beta_i \qquad \textbf{D-5}$$

D.1.4. Lateral Free Body of the Tractor

With the tire slip angles defined (Section D.1.2 and D.1.3) and the resulting tire forces defined (Section 3.3.1), the lateral dynamics of the vehicle units could be defined. This process began with the evaluation of the lateral forces and moments acting on each vehicle unit. In all cases, small angle assumptions were made as the steering and side slip angles of a vehicle are generally small when the vehicle is driven at any significant speed. Also, the small angle assumptions linearize the equations which permitted easier analysis. Note: This section is dealing with lateral motion only. The full vehicle motion (combined yaw and roll is documented in Section D.2).

The planar analysis of the tractor produced two equations, a lateral force equation and a moment (yaw) equation. These in-plane reactions are described in Equations D-6 and D-7. As before, a_1 and b_1 denote the axle to CG distances. Similarly, c_1 denotes the CG to fifth wheel distance. F_f and F_r are the tire forces while F_{12} denotes the tractor (unit 1) to first trailer (unit 2) reaction force.

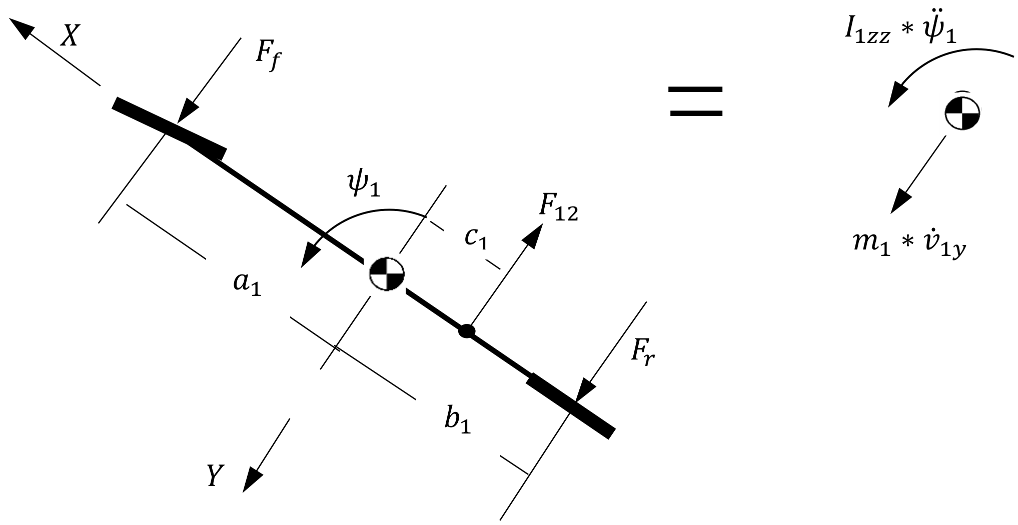

Figure D-6: Tractor Free Body

$$m_1 * \dot{v}_{1y} = F_f + F_r - F_{12} \quad \textbf{D-6}$$

$$I_{1zz} * \ddot{\psi}_1 = a_1 * F_f - b_1 * F_r + c_1 * F_{12} \quad \textbf{D-7}$$

D.1.5. Lateral Free Body of the Trailer

The trailer had similar lateral dynamics to the tractor save the replacement of the front axle with the fifth wheel hitch. It may also have a dolly attached to the rear. In all cases, c_i denotes the distance from the CG to the fifth wheel hitch and d_i denotes the distance from the CG to the dolly hitch where i represents the vehicle unit number. Reaction forces between units are again noted as F_{ij} where i and j are the unit numbers connected by the joint. Equations D-8 and D-9 denote a trailer's lateral dynamics.

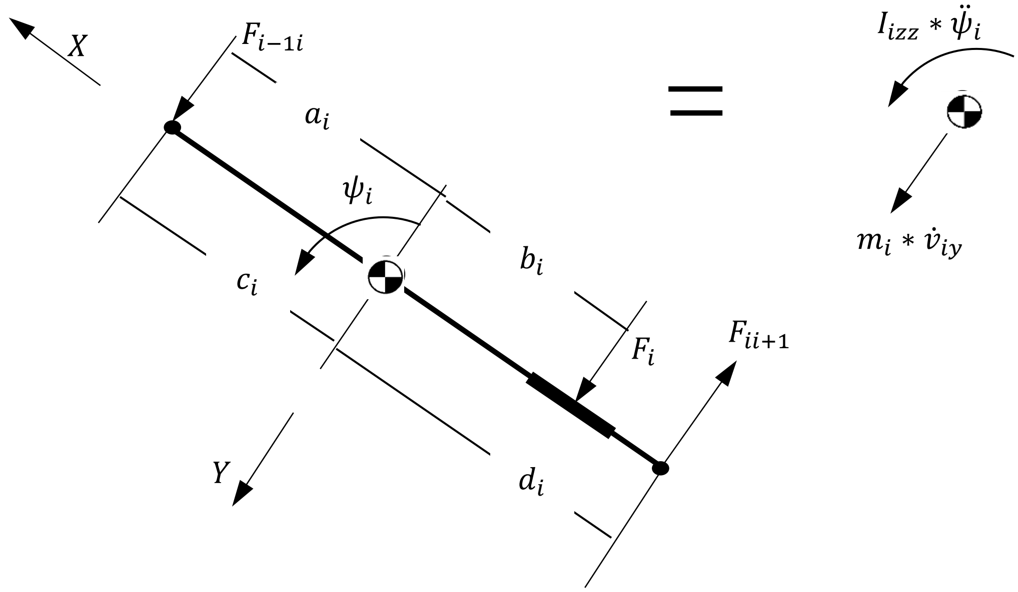

Figure D-7: Trailer Free Body

$$m_i * \dot{v}_{iy} = F_{i-1i} + F_i - F_{i+1i} \quad \textbf{D-8}$$

$$I_{izz} * \ddot{\psi}_i = c_i * F_{i-1i} - b_i * F_i + d_i * F_{ii+1} \quad \textbf{D-9}$$

D.1.6. Lateral Free Body of the Dolly

The lateral dynamics of the dolly (Figure D-8) were very similar to the trailer's except the locations of the hitch points (fifth wheel and dolly) are reversed (Equations D-10 and D-11).

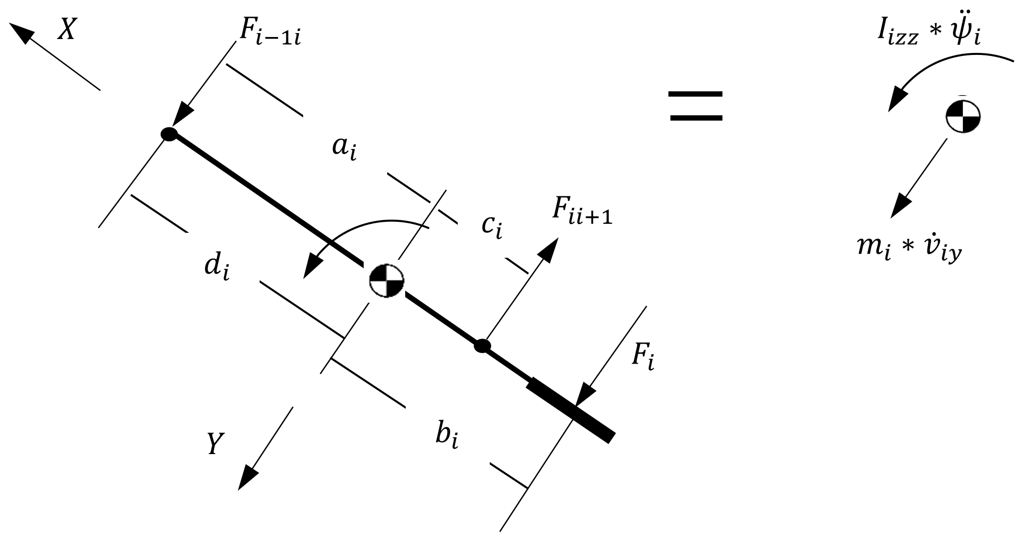

Figure D-8: Dolly Free Body

$$m_i * \dot{v}_{iy} = F_{i-1i} + F_i - F_{ii+1} \qquad \textbf{D-10}$$

$$I_{izz} * \ddot{\psi}_i = d_i * F_{i-1i} - b_i * F_i + c_i * F_{ii+1} \qquad \textbf{D-11}$$

D.1.7. Articulation Model

Based on the analysis of the vehicle in Sections A.1.4 and 3.2.1, the assumption was made that the hitches (fifth wheel and dolly) provide only linear constraints with unit to unit rotations in all three axes permitted. This means that the two connected units must have the same velocity at the hitch point (Figure D-9). This common velocity point defines the constraint needed to combine the equations of motion for each vehicle unit into a single set representing the entire vehicle.

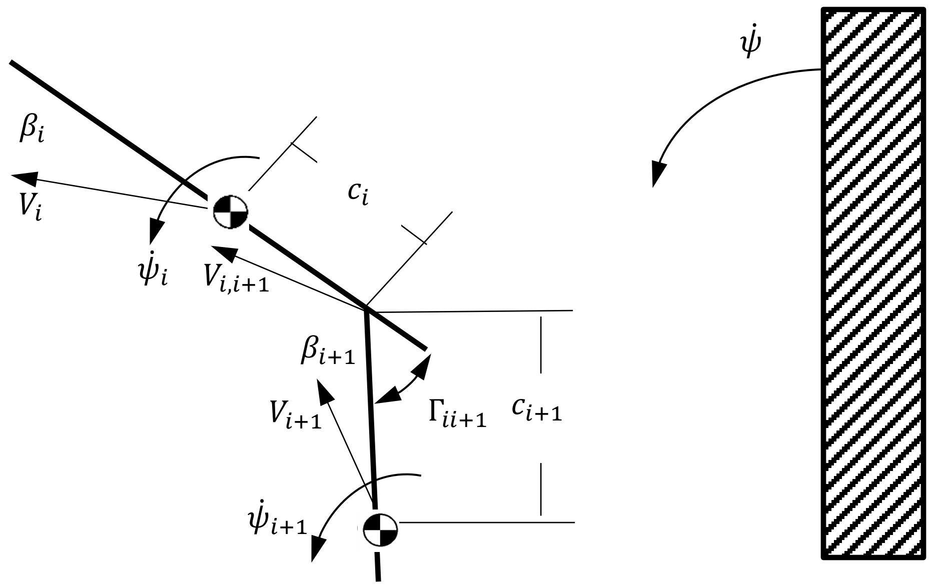

Figure D-9: Articulation Constraint

Knowing the relative angle between the two vehicle units (Equation D-12) and the lateral velocity of each unit at the hitch (Equation D-13) it was possible to define the relative lateral velocity of each unit (Equation D-14). Note: velocity defined lead unit coordinates. Again assuming small angles permitted the linearization of the constraint (Equation D-16). The known relationship between lateral velocity, longitudinal velocity, and side slip (Equation A-17) permitted writing the constraint in terms of yaw rate and side slip (Equation D-17). Finally, taking the time derivative resulted in a constraint equation that was a function of the model's state variables (Equation D-18). Note: Similar approaches were use used by other researchers and may be beneficial for review (Sampson, 2000; Tianjun et al., 2007).

$$\Gamma_{ii+1} = \psi_i - \psi_{i+1} \qquad \textbf{D-12}$$

$$Vy_{i,i+1} = Vy_i - c_i * \dot{\psi}_i = Vy_{i+1} + c_{i+1} * \dot{\psi}_{i+1} - \mathrm{U_i} * \sin(\Gamma_{\mathrm{ii+1}}) \qquad \textbf{D-13}$$

$$Vy_{i+1} = Vy_i - c_i * \dot{\psi}_i - c_{i+1} * \dot{\psi}_{i+1} + \mathrm{U_i} * \sin(\Gamma_{\mathrm{ii+1}}) \qquad \textbf{D-14}$$

$$Vy_{i+1} = Vy_i - c_i * \dot{\psi}_i - c_{i+1} * \dot{\psi}_{i+1} + \mathrm{U_i} * \Gamma_{\mathrm{ii+1}} \qquad \textbf{D-15}$$

$$Vy_{i+1} = Vy_i - c_i * \dot{\psi}_i - c_{i+1} * \dot{\psi}_{i+1} + \mathrm{U_i} * (\psi_i - \psi_{i+1}) \qquad \textbf{D-16}$$

$$\beta_{i+1} = \beta_i - \frac{c_i * \dot{\psi}_i}{\mathrm{U_i}} - \frac{c_{i+1} * \dot{\psi}_{i+1}}{\mathrm{U_{i+1}}} + \psi_i - \psi_{i+1} \qquad \textbf{D-17}$$

$$\dot{\beta}_{i+1} = \dot{\beta}_i - \frac{c_i * \ddot{\psi}_i}{\mathrm{U_i}} - \frac{c_{i+1} * \ddot{\psi}_{i+1}}{\mathrm{U_{i+1}}} + \dot{\psi}_i - \dot{\psi}_{i+1} \qquad \textbf{D-18}$$

D.2. Individual Vehicle Unit Equations of Motion

As noted at the outset of this section, the basics of the equations of motion development have been addressed for roll (Section D.1.1) and lateral dynamics (Sections D.1.4 through D.1.6). The separation of roll and yaw was intentional so that the interactions of the units could be better observed. Obviously, the roll and lateral motions are not decoupled in the actual vehicle leading to the need for a set of combined yaw and roll equations of motion for each vehicle unit. The material in this section will develop the full equations of motion for each vehicle unit and then generate the equations of motion for the combination vehicle.

D.2.1. States and Variable Relationships

As can be seen in the linearized system equations (Appendix D.1), there are many variables describing the motion of the vehicle units. For consistency and ease of use, all of the models developed in this work used the vehicle unit side slip (β), vehicle unit yaw rate$(\dot{\psi})$, vehicle unit roll rate $(\dot{\phi})$, and vehicle unit roll (ϕ) as the state variables. Thus each unit in the vehicle contributed four state variables to the combined vehicle. To convert all of the individual equations of motion into a form that used only the desired state variables, the following identities were used: Equation D-19 which relates lateral velocity, longitudinal velocity, and side slip and Equation D-20 which relates the longitudinal velocity and radius of curvature to yaw rate.

$$\beta = \tan^{-1}\left(\frac{V_y}{U}\right) \approx \frac{V_y}{U} \tag{D-19}$$

$$\dot{\psi} = \frac{\mathrm{U}}{\mathrm{R}} \tag{D-20}$$

D.2.2. Tractor EOM

In Appendix C the equations of motion for a rigid body in space were developed and then simplified for the case of a vehicle at constant velocity with no pitch. These simplifications resulted in three equations describing lateral (Y axis) forces (Equation D-21), moments about the yaw (Z) axis (Equation D-23), and moments about the roll (X) axis (Equation D-22). Note that the equations contain the coupled lateral and roll motions as the lateral CG shift due to roll was included in both the lateral equation (D-21) and the yaw equation (D-22) and the CG motion due to the lateral forces was included in the roll equation (D-23). The combined yaw and roll equations of motion for the tractor are thus given in Equations D-21 through D-23. M_f and M_r represent the potential brake moments from the stability control system.

$$m_1 * \left(\dot{v}_{1y} + \frac{U_1^2}{R_1} - Z_1 * \ddot{\phi}_1\right) = F_f + F_r - F_{12} \tag{D-21}$$

$$\begin{aligned} I_{1zz} * \ddot{\psi}_1 - I_{1xz} * \ddot{\phi}_1 + m_1 * Z_1 * U_1 * \dot{\phi}_1 \\ = a_1 * F_f - b_1 * F_r + c_1 * F_{12} + \mathrm{M_f} + \mathrm{M_r} \end{aligned} \tag{D-22}$$

$$(I_{1xx} + m_1 * Z_1^2) * \ddot{\phi}_1 - I_{1xz} * \ddot{\psi}_1$$

$$= m_1 * Z_1 * \left(g * \phi_1 + \dot{v}_{1y} + \frac{U_1^2}{R_1}\right) - \left(K_f + K_r\right) * \phi_1 - \left(L_f + L_r\right) \quad \textbf{D-23}$$

$$* \dot{\phi}_1 + \mathrm{k}_{12} * (\phi_2 - \phi_1) + \mathrm{F}_{12} * \mathrm{f}_1$$

With the development of the tractor's equations of motion, a couple of observations about the state equations could then be made:

- In Equation D-21, the lateral acceleration of the CG is a function of the lateral acceleration of the CG relative to the body centered reference $\left(\dot{v}_{1y}\right)$ plus the centripetal acceleration$\left(\frac{U_1^2}{R}\right)$ minus the roll acceleration about the roll axis$\left(-Z_1 * \ddot{\phi}_1\right)$. The roll motion is subtracted due to the definition of the right handed coordinate system (see Figure D-1 and Figure D-6).
- The product of inertia term $\left(I_{xz} * \ddot{\phi}_1\right)$ in Equation D-22 is negative as a result of the coordinate definition.
- The chassis roll about the roll axis (which is not at the CG location) introduces an additional term $(m_1 * Z_1 * U_1 * \dot{\phi}_1)$ in Equation D-22.
- In Equation D-23, the $I_{1xx} + m_1 * Z_1^2$ term accounts for the rotation about the suspension roll axis through use of the parallel axis theorem.

Breaking down these three equations into state variable form makes the implementation of the equations into the LTI model easier. This was accomplished by noting that the tire forces could be described using Equations 3-15, D-2, and D-3 as well as noting the state variable substitutions defined in Equations D-19 and D-20. For the lateral force equation, the process is documented in Equations D-24 through D-27.

$$m_1 * \left(\dot{v}_{1y} + U_1 * \dot{\psi}_1 - Z_1 * \ddot{\phi}_1\right) = C_{\alpha f} * \alpha_f + C_{\alpha r} * \alpha_r - F_{12} \quad \textbf{D-24}$$

$$m_1 * U_1 * \left(\dot{\beta}_1 + \dot{\psi}_1\right) - m_1 * Z_1 * \ddot{\phi}_1 = C_{\alpha f} * \left(\delta - \frac{a_1}{R_1} - \beta_1\right) + C_{\alpha r} * \left(\frac{b_1}{R_1} - \beta_1\right) - F_{12} \quad \textbf{D-25}$$

$$m_1 * U_1 * \left(\dot{\beta}_1 + \dot{\psi}_1\right) - m_1 * Z_1 * \ddot{\phi}_1 = -\left(C_{\alpha f} + C_{\alpha r}\right) * \beta_1 - \left(a_1 * C_{\alpha f} - b_1 * C_{\alpha r}\right) * \frac{1}{R_1} - F_{12} + C_{\alpha f} * \delta \quad \textbf{D-26}$$

$$m_1 * U_1 * \left(\dot{\beta}_1 + \dot{\psi}_1\right) - m_1 * Z_1 * \ddot{\phi}_1 = -\left(C_{\alpha f} + C_{\alpha r}\right) * \beta_1 - \left(a_1 * C_{\alpha f} - b_1 * C_{\alpha r}\right) * \frac{\dot{\psi}_1}{U_1} - F_{12} + C_{\alpha f} * \delta \quad \textbf{D-27}$$

The yaw moment equation was reduced in a similar manner (Equations D-28 through D-31).

$$I_{1zz} * \ddot{\psi}_1 - I_{1xz} * \ddot{\phi}_1 + m_1 * Z_1 * U_1 * \dot{\phi}_1 = a_1 * C_{\alpha f} * \alpha_f - b_1 * C_{\alpha r} * \alpha_r + c_1 * F_{12} + \mathrm{M_f} + \mathrm{M_r} \quad \textbf{D-28}$$

$$I_{1zz} * \ddot{\psi}_1 - I_{1xz} * \ddot{\phi}_1 + m_1 * Z_1 * U_1 * \dot{\phi}_1 = a_1 * C_{\alpha f} * \left(\delta - \frac{a_1}{R_1} - \beta_1\right) - b_1 * C_{\alpha r} * \left(\frac{b_1}{R_1} - \beta_1\right) + c_1 * F_{12} + \mathrm{M_f} + \mathrm{M_r} \quad \textbf{D-29}$$

$$I_{1zz} * \ddot{\psi}_1 - I_{1xz} * \ddot{\phi}_1 + m_1 * Z_1 * U_1 * \dot{\phi}_1$$

$$= -\left(a_1 * C_{\alpha f} - b_1 * C_{\alpha r}\right) * \beta_1 - \left(a_1^2 * C_{\alpha f} + b_1^2 * C_{\alpha r}\right) * \frac{1}{R} \quad \textbf{D-30}$$

$$+ c_1 * F_{12} + a_1 * C_{\alpha f} * \delta + \mathrm{M_f} + \mathrm{M_r}$$

$$I_{1zz} * \ddot{\psi}_1 - I_{1xz} * \ddot{\phi}_1 + m_1 * Z_1 * U_1 * \dot{\phi}_1$$

$$= -\left(a_1 * C_{\alpha f} - b_1 * C_{\alpha r}\right) * \beta_1 - \left(a_1^2 * C_{\alpha f} + b_1^2 * C_{\alpha r}\right) * \frac{\dot{\psi}}{U} \quad \textbf{D-31}$$

$$+ c_1 * F_{12} + a_1 * C_{\alpha f} * \delta + \mathrm{M_f} + \mathrm{M_r}$$

Finally, the roll moment equation was re-written as shown in Equation D-32.

$$(I_{1xx} + m_1 * Z_1^2) * \ddot{\phi}_1 - I_{1xz} * \ddot{\psi}_1$$

$$= m_1 * Z_1 * g * \phi_1 + m_1 * Z_1 * \mathrm{U}_1 * \left(\dot{\beta}_1 + \dot{\psi}_1\right) - \left(K_f + K_r\right) \quad \textbf{D-32}$$

$$* \, \phi_1 - \left(L_f + L_r\right) * \dot{\phi}_1 + \mathrm{k}_{12} * (\phi_2 - \phi_1) + \mathrm{F}_{12} * \mathrm{f}_1$$

Once the three equations for the tractor were written in terms of vehicle constants, inputs, and state variables (Equations D-33 through D-35), it became much easier to observe the four state variables$\left(\beta_1, \dot{\psi}_1, \dot{\phi}_1, \phi_1\right)$.

$$m_1 * U_1 * \left(\dot{\beta}_1 + \dot{\psi}_1\right) - m_1 * Z_1 * \ddot{\phi}_1$$

$$= -\left(C_{\alpha f} + C_{\alpha r}\right) * \beta_1 - \left(a_1 * C_{\alpha f} - b_1 * C_{\alpha r}\right) * \frac{\dot{\psi}_1}{U_1} - F_{12} \quad \textbf{D-33}$$

$$+ C_{\alpha f} * \delta$$

$$I_{1zz} * \ddot{\psi}_1 - I_{1xz} * \ddot{\phi}_1 + m_1 * Z_1 * U_1 * \dot{\phi}_1$$

$$= -\left(a_1 * C_{\alpha f} - b_1 * C_{\alpha r}\right) * \beta_1 - \frac{\left(a_1^2 * C_{\alpha f} + b_1^2 * C_{\alpha r}\right) * \dot{\psi}}{U_1} \quad \textbf{D-34}$$

$$+ c_1 * F_{12} + a_1 * C_{\alpha f} * \delta + \mathrm{M_f} + \mathrm{M_r}$$

$$(I_{1xx} + m_1 * Z_1^2) * \ddot{\phi}_1 - I_{1xz} * \ddot{\psi}_1$$

$$= m_1 * Z_1 * g * \phi_1 + m_1 * Z_1 * \mathrm{U}_1 * \left(\dot{\beta}_1 + \dot{\psi}_1\right) - \left(K_f + K_r \quad \textbf{D-35}\right.$$

$$* \, \phi_1 - \left(L_f + L_r\right) * \dot{\phi}_1 + \mathrm{k}_{12} * (\phi_2 - \phi_1) + \mathrm{F}_{12} * \mathrm{f}_1$$

Additionally, a few other observations could be made which explain the behavior of the vehicle.

- Vehicle side slip acts to stabilize the vehicle (Equation D-33).
- As the trailer is connected behind the tractor CG, the lateral force from the trailer acts to spin the tractor (Equation D-34).
- While the fifth wheel does not transmit a roll moment from the trailer to the tractor (see Section 3.2.1), the vertical offset of the fifth wheel from the roll axis does produce a roll moment (Equation D-35).
- In general, the only significant inputs acting to destabilize the tractor come from the trailer reaction force (F_{12}) or the driver input (δ).

D.2.3. Trailer EOM

The trailer dynamics were similar to the tractor's dynamics except for the lack of a front axle and the movement of the fifth wheel to the front. Equations D-36 through D-38 describe the trailer's dynamic behavior. Since there is more than one trailer, the subscript i is used to denote the trailer unit number. Note: When developing the tractor equations, it was noted that the fifth wheel height was above the roll axis. This height was denoted as f_i. In a similar manner, the height difference between the dolly pintle hook and the roll axis is denoted as g_i here. Again, M_i denotes the potential brake corrective moment generated by the stability control system.

$$m_i * \left(\dot{v}_{iy} + \frac{U_i^2}{R_i} - Z_i * \ddot{\phi}_i\right) = F_{i-1i} + F_i - F_{ii+1} \quad \textbf{D-36}$$

$$I_{izz} * \ddot{\psi}_i - I_{ixz} * \ddot{\phi}_i + m_i * Z_i * U_i * \dot{\phi}_i = c_i * F_{i-1i} - b_i * F_i + d_i * F_{ii+1} + \mathrm{M_i} \quad \textbf{D-37}$$

$$\begin{aligned}(I_{ixx} + m_i * Z_i^2) * \ddot{\phi}_i - I_{ixz} * \ddot{\psi}_i \\ = m_i * Z_i * \left(g * \phi_i + \dot{v}_{iy} + \frac{U_i^2}{R_i}\right) - K_i * \phi_i - L_i * \dot{\phi}_i - \mathrm{k_{i-1i}} \\ * (\phi_i - \phi_{i-1}) + \mathrm{k_{ii+1}} * (\phi_{i+1} - \phi_i) - \mathrm{F}_{i-1i} * \mathrm{f_i} + \mathrm{F_{ii+1}} * \mathrm{g_i}\end{aligned} \quad \textbf{D-38}$$

As was done for the tractor, the tire force can be broken down into cornering stiffness and slip angle (Equation 3-15). From there the slip angle could be reduced as described in Equation D-5. The equations could also be put in state variable form through the use of Equations D-19 and D-20. This process again permitted the equations to be written in the form of the desired state variables and the control inputs. For the lateral force balance, the simplification resulted in Equation D-39.

$$m_i * U_i * (\dot{\beta}_i + \dot{\psi}_i) - m_i * Z_i * \ddot{\phi}_i = F_{i-1i} - \beta_i * C_{\alpha i} + \frac{b_i * C_{\alpha i} * \dot{\psi}_i}{U_i} - F_{ii+1} \quad \textbf{D-39}$$

For the yaw balance, the transformation resulted in Equation D-40.

$$I_{izz} * \ddot{\psi}_i - I_{ixz} * \ddot{\phi}_i + m_i * Z_i * U_i * \dot{\phi}_i = c_i * F_{i-1i} + b_i * C_{\alpha i} * \beta_i - \frac{b_i^2 * C_{\alpha i} * \dot{\psi}_i}{U_i} + d_i * F_{ii+1} + \mathrm{M_i} \quad \textbf{D-40}$$

For the roll balance, the transformation resulted in Equation D-40.

$$\begin{aligned}(I_{ixx} + m_i * Z_i^2) * \ddot{\phi}_i - I_{ixz} * \ddot{\psi}_i &= m_i * Z_i * g * \phi_i + m_i * Z_i * \mathrm{U_i} * (\dot{\beta}_i + \dot{\psi}_i) - K_i * \phi_i - L_i * \dot{\phi}_i \\ &- \mathrm{k_{i-1i}} * (\phi_i - \phi_{i-1}) + \mathrm{k_{ii+1}} * (\phi_{i+1} - \phi_i) - \mathrm{F}_{i-1i} * \mathrm{f_i} + \mathrm{F_{ii+1}} \\ &* \mathrm{g_i}\end{aligned} \quad \textbf{D-41}$$

The resulting set of equations for the trailer was thus Equations D-39 through D-41.

D.2.4. Dolly EOM

The dolly equations of motion (Equations D-42 through D-44) were very similar to the trailer equations with the major difference being that the fifth wheel and pintle hook were reversed (pintle hook is now on the front and the fifth wheel in the rear).

$$m_i * \left(\dot{v}_{iy} + \frac{U_i^2}{R_i} - Z_i * \ddot{\phi}_i\right) = F_{i-1i} + F_i - F_{ii+1} \quad \textbf{D-42}$$

$$I_{izz} * \ddot{\psi}_i - I_{ixz} * \ddot{\phi}_i + m_i * Z_i * U_i * \dot{\phi}_i = d_i * F_{i-1i} - b_i * F_i + c_i * F_{ii+1} + \mathrm{M_i} \quad \textbf{D-43}$$

$$(I_{ixx} + m_i * Z_i^2) * \ddot{\phi}_i - I_{ixz} * \ddot{\psi}_i$$

$$= m_i * Z_i * \left(g * \phi_i + \dot{v}_{iy} + \frac{U_i^2}{R_i}\right) - K_i * \mathrm{\phi_i} - L_i * \dot{\phi}_i - \mathrm{k_{i-1i}} * (\phi_i - \phi_{i-1}) + \mathrm{k_{ii+1}} * (\phi_{i+1} - \phi_i) + \mathrm{F}_{ii+1} * \mathrm{f_i} - \mathrm{F_{i-1i}} * \mathrm{g_i} \quad \textbf{D-44}$$

Just as was done for the trailer, the dolly equations could be expressed in terms of the state variables and the control inputs through the substitution of the tire lateral force equation (Equation D-5) and the state identity equations (Equations D-19 and D-20). The resulting set of equations for the dolly are given in Equations D-45 through D-47.

$$m_i * U_i * \left(\dot{\beta}_i + \dot{\psi}_i\right) - m_i * Z_i * \ddot{\phi}_i = F_{i-1i} - \beta_i * C_{\alpha i} + \frac{b_i * C_{\alpha i} * \dot{\psi}_i}{U_i} - F_{ii+1} \quad \textbf{D-45}$$

$$I_{izz} * \ddot{\psi}_i - I_{ixz} * \ddot{\phi}_i + m_i * Z_i * U_i * \dot{\phi}_i = d_i * F_{i-1i} + b_i * C_{\alpha i} * \beta_i - \frac{b_i^2 * C_{\alpha i} * \dot{\psi}_i}{U_i} + c_i * F_{ii+1} + \mathrm{M_i} \quad \textbf{D-46}$$

$$(I_{ixx} + m_i * Z_i^2) * \ddot{\phi}_i - I_{ixz} * \ddot{\psi}_i$$

$$= m_i * Z_i * g * \phi_i + m_i * Z_i * \mathrm{U_i} * \left(\dot{\beta}_i + \dot{\psi}_i\right) - K_i * \mathrm{\phi_i} - L_i * \dot{\phi}_i - \mathrm{k_{i-1i}} * (\phi_i - \phi_{i-1}) + \mathrm{k_{ii+1}} * (\phi_{i+1} - \phi_i) + \mathrm{F}_{ii+1} * \mathrm{f_i} - \mathrm{F_{i-1i}} * \mathrm{g_i} \quad \textbf{D-47}$$

D.2.5. Unit to Unit Interaction Simplification

The final vehicle, a triple truck in this case, is comprised of six vehicle units and was assembled from the three unit types defined above. The units were constrained to operate as a system through pin connections, namely the fifth wheel and the dolly pintle hook connections. As the units were connected successively, the constraints were in series as well. The major difficult in developing the full vehicle equations of motion was thus in canceling out the internal reaction forces between the units.

As discussed in Sections A.1.4 and 3.2.1, fifth wheel and dolly connections can be modeled as spherical joints which meant that unit to unit moment transmission could be ignored for cases where the vehicle was operating in a stable manner. As such, all of the relative rotation stiffness terms in the equations of motion could be eliminated. This left only internal lateral forces connecting the vehicle units (model was constant velocity so no longitudinal forces were present). Additionally, the dolly connection height to the preceding trailer is generally very close to the roll axis height of the trailer and the dolly. This made it reasonable to drop dolly lateral force induced moment terns in the roll equations as well. Side note: even if the fifth wheel roll moments were kept, their extremely non-linear behaviors could not have been accurately captured with a conventional linear model.

Based on these simplifications, the equations of motion for the three unit types could be simplified as follows:

Tractor (Equations D-48 through D-50):

$$m_1 * U_1 * \left(\dot{\beta}_1 + \dot{\psi}_1\right) - m_1 * Z_1 * \ddot{\phi}_1 = -\left(C_{\alpha f} + C_{\alpha r}\right) * \beta_1 - \left(a_1 * C_{\alpha f} - b_1 * C_{\alpha r}\right) * \frac{\dot{\psi}_1}{U_1} - F_{12} + C_{\alpha f} * \delta \qquad \textbf{D-48}$$

$$I_{1zz} * \ddot{\psi}_1 - I_{1xz} * \ddot{\phi}_1 + m_1 * Z_1 * U_1 * \dot{\phi}_1$$

$$= -\left(a_1 * C_{\alpha f} - b_1 * C_{\alpha r}\right) * \beta_1 - \frac{\left(a_1^2 * C_{\alpha f} + b_1^2 * C_{\alpha r}\right) * \dot{\psi}_1}{U_1} + c_{:} \qquad \textbf{D-49}$$

$$* F_{12} + a_1 * C_{\alpha f} * \delta + \mathrm{M_f} + \mathrm{M_r}$$

$$(I_{1xx} + m_1 * Z_1^2) * \ddot{\phi}_1 - I_{1xz} * \ddot{\psi}_1$$

$$= m_1 * Z_1 * g * \phi_1 + m_1 * Z_1 * \mathrm{U}_1 * \left(\dot{\beta}_1 + \dot{\psi}_1\right) - \left(K_f + K_r\right) * \phi_{:} \qquad \textbf{D-50}$$

$$- \left(L_f + L_r\right) * \dot{\phi}_1 + \mathrm{F}_{12} * \mathrm{f}_1$$

Trailer (Equations D-51 through D-53):

$$m_i * U_i * \left(\dot{\beta}_\iota + \dot{\psi}_\iota\right) - m_i * Z_i * \ddot{\phi}_\iota = F_{i-1i} - \beta_i * C_{\alpha i} + \frac{b_i * C_{\alpha i} * \dot{\psi}_\iota}{U_i} - F_{ii+1} \qquad \textbf{D-51}$$

$$I_{izz} * \ddot{\psi}_i - I_{ixz} * \ddot{\phi}_i + m_i * Z_i * U_i * \dot{\phi}_\iota$$

$$= c_i * F_{i-1i} + b_i * C_{\alpha i} * \beta_i - \frac{b_i^2 * C_{\alpha i} * \dot{\psi}_\iota}{U_i} + d_i * F_{ii+1} + \mathrm{M_i} \qquad \textbf{D-52}$$

$$(I_{ixx} + m_i * Z_i^2) * \ddot{\phi}_i - I_{ixz} * \ddot{\psi}_i$$

$$= m_i * Z_i * g * \phi_i + m_i * Z_i * \mathrm{U_i} * \left(\dot{\beta}_i + \dot{\psi}_\iota\right) - K_i * \phi_\mathrm{i} - L_i * \dot{\phi}_\iota \qquad \textbf{D-53}$$

$$- \mathrm{F}_{i-1i} * \mathrm{f_i}$$

Dolly (Equations D-54 through D-56):

$$m_i * U_i * \left(\dot{\beta}_\iota + \dot{\psi}_\iota\right) - m_i * Z_i * \ddot{\phi}_\iota = F_{i-1i} - \beta_i * C_{\alpha i} + \frac{b_i * C_{\alpha i} * \dot{\psi}_\iota}{U_i} - F_{ii+1} \qquad \textbf{D-54}$$

$$I_{izz} * \ddot{\psi}_i - I_{ixz} * \ddot{\phi}_i + m_i * Z_i * U_i * \dot{\phi}_\iota$$

$$= d_i * F_{i-1i} + b_i * C_{\alpha i} * \beta_i - \frac{b_i^2 * C_{\alpha i} * \dot{\psi}_\iota}{U_i} + c_i * F_{ii+1} + \mathrm{M_i} \qquad \textbf{D-55}$$

$$(I_{ixx} + m_i * Z_i^2) * \ddot{\phi}_i - I_{ixz} * \ddot{\psi}_i$$
$$= m_i * Z_i * g * \phi_i + m_i * Z_i * \mathrm{U_i} * (\dot{\beta}_i + \dot{\psi}_i) - K_i * \phi_\mathrm{i} - L_i * \dot{\phi}_i \quad \textbf{D-56}$$
$$+ \mathrm{F}_{ii+1} * \mathrm{f_i}$$

The expansion of these equations to all six vehicle units can be found in Appendix D.3.

D.3. Vehicle Unit Expansion

If the reader is not familiar with the process of expanding equations of motion for multiple unit systems, then the following should aid in understanding how the final complete vehicle system was derived.

After the simplification of the equations of motion as discussed in Section D.2.5, the tractor equations reduced to Equations D-57 through D-59.

$$U_1 * m_1 * (\dot{\beta}_1 + \dot{\psi}_1) - Z_1 * \ddot{\phi}_1 * m_1$$
$$= C_{\alpha f} * \delta - \beta_1 * (C_{\alpha f} + C_{\alpha r}) - F_{12} \quad \textbf{D-57}$$
$$- \frac{\dot{\psi}_1 * (C_{\alpha f} * a_1 - C_{\alpha r} * b_1)}{U_1}$$

$$I_{1zz} * \ddot{\psi}_1 - I_{1xz} * \ddot{\phi}_1 + U_1 * Z_1 * \dot{\phi}_1 * m_1$$
$$= M_f + M_r + F_{12} * c_1 - \beta_1 * (C_{\alpha f} * a_1 - C_{\alpha r} * b_1) + C_{\alpha f} * \delta \quad \textbf{D-58}$$
$$* a_1 - \frac{\dot{\psi}_1 * (C_{\alpha f} * a_1^2 + C_{\alpha r} * b_1^2)}{U_1}$$

$$\ddot{\phi}_1 * (m_1 * Z_1^2 + I_{1xx}) - I_{1xz} * \ddot{\psi}_1$$
$$= F_{12} * f_1 - \phi_1 * (K_f + K_r) - \dot{\phi}_1 * (L_f + L_r) + U_1 * Z_1 * m_1 \quad \textbf{D-59}$$
$$* (\dot{\beta}_1 + \dot{\psi}_1) + \phi_1 * Z_1 * g * m_1$$

The first trailer's equations of motion reduced to D-60 through D-63. Note that an additional equation has been added to manage the kinematic constraint (Equation D-63). Similar constraints equations will appear for the remaining units.

$$U_2 * m_2 * (\dot{\beta}_2 + \dot{\psi}_2) - Z_2 * \ddot{\phi}_2 * m_2 = F_{12} - \beta_2 * C_{\alpha 2} + \frac{C_{\alpha 2} * b_2 * \dot{\psi}_2}{U_2} - \mathrm{F}_{23} \qquad \textbf{D-60}$$

$$\begin{aligned} &I_{2zz} * \ddot{\psi}_2 - I_{2xz} * \ddot{\phi}_2 + U_2 * Z_2 * \dot{\phi}_2 * m_2 \\ &\quad = M_2 + d_2 * F_{23} + F_{12} * c_2 + \beta_2 * C_{\alpha 2} * b_2 - \frac{C_{\alpha 2} * b_2^2 * \dot{\psi}_2}{U_2} \end{aligned} \qquad \textbf{D-61}$$

$$\begin{aligned} &\ddot{\phi}_2 * (m_2 * Z_2^2 + I_{2xx}) - I_{2xz} * \ddot{\psi}_2 \\ &\quad = Z_2 * m_2 * \left(\phi_2 * g + U_2 * (\dot{\beta}_2 + \dot{\psi}_2)\right) - L_2 * \dot{\phi}_2 - K_2 * \phi_2 \\ &\quad - F_{12} * f_2 \end{aligned} \qquad \textbf{D-62}$$

$$\dot{\beta}_2 = \dot{\beta}_1 + \dot{\psi}_1 - \dot{\psi}_2 - \frac{c_1 * dd\psi_1}{U_1} - \frac{c_2 * dd\psi_2}{U_2} \qquad \textbf{D-63}$$

The first dolly's equations of motion are reduced to D-64 through D-67.

$$U_3 * m_3 * (\dot{\beta}_3 + \dot{\psi}_3) - Z_3 * \ddot{\phi}_3 * m_3 = F_{23} + \frac{C_{\alpha 3} * b_3 * \dot{\psi}_3}{U_3} - \beta_3 * C_{\alpha 3} - F_{34} \qquad \textbf{D-64}$$

$$\begin{aligned} &I_{3zz} * \ddot{\psi}_3 - I_{3xz} * \ddot{\phi}_3 + U_3 * Z_3 * \dot{\phi}_3 * m_3 \\ &\quad = M_3 + d_3 * F_{23} + F_{34} * c_3 + \beta_3 * C_3 * b_3 - \frac{C_{\alpha 3} * b_3^2 * \dot{\psi}_3}{U_3} \end{aligned} \qquad \textbf{D-65}$$

$$\begin{aligned} &\ddot{\phi}_3 * (m_3 * Z_3^2 + I_{3xx}) - I_{3xz} * \ddot{\psi}_3 \\ &\quad = F_{34} * f_3 - L_3 * \dot{\phi}_3 - K_3 * \phi_3 + U_3 * Z_3 * m_3 * (\dot{\beta}_3 + \dot{\psi}_3) \\ &\quad + \phi_3 * Z_3 * g * m_3 \end{aligned} \qquad \textbf{D-66}$$

$$\dot{\beta}_3 = \dot{\beta}_2 + \dot{\psi}_2 - \dot{\psi}_3 - \frac{c_2 * \ddot{\psi}_2}{U_2} - \frac{c_3 * \ddot{\psi}_3}{U_3} \qquad \textbf{D-67}$$

The second trailer's equations of motion were identical to the first trailer's save the substitution of appropriate unit numbers (Equations D-68 through D-71).

$$U_4 * m_4 * \left(\dot{\beta}_4 + \dot{\psi}_4\right) - Z_4 * \ddot{\phi}_4 * m_4 = F_{34} - \beta_4 * C_{\alpha 4} + \frac{C_{\alpha 4} * b_4 * \dot{\psi}_4}{U_4} - F_{45} \qquad \textbf{D-68}$$

$$\begin{aligned} &I_{4zz} * \ddot{\psi}_4 - I_{4xz} * \ddot{\phi}_4 + U_4 * Z_4 * \dot{\phi}_4 * m_4 \\ &\qquad = M_4 + d_4 * F_{45} + F_{34} * c_4 + \beta_4 * C_{\alpha 4} * b_4 - \frac{C_{\alpha 4} * b_4^2 * \dot{\psi}_4}{U_4} \end{aligned} \qquad \textbf{D-69}$$

$$\begin{aligned} &\ddot{\phi}_4 * (m_4 * Z_4^2 + I_{4xx}) - I_{4xz} * \ddot{\psi}_4 \\ &\qquad = Z_4 * m_4 * \left(\phi_4 * g + U_4 * \left(\dot{\beta}_4 + \dot{\psi}_4\right)\right) - L_4 * \dot{\phi}_4 - K_4 * \phi_4 \\ &\qquad - F_{34} * f_4 \end{aligned} \qquad \textbf{D-70}$$

$$\dot{\beta}_4 = \dot{\beta}_3 + \dot{\psi}_3 - \dot{\psi}_4 - \frac{c_3 * \ddot{\psi}_3}{U_3} - \frac{c_4 * \ddot{\psi}_4}{U_4} \qquad \textbf{D-71}$$

The second dolly's equations of motion were identical to the first dolly's save the substitution of appropriate unit numbers (Equations D-72 through D-75).

$$U_5 * m_5 * \left(\dot{\beta}_5 + \dot{\psi}_5\right) - Z_5 * \ddot{\phi}_5 * m_5 = F_{46} + \frac{C_{\alpha 5} * b_5 * \dot{\psi}_5}{U_5} - \beta_5 * C_{\alpha 5} - F_{56} \qquad \textbf{D-72}$$

$$\begin{aligned} &I_{5zz} * \ddot{\psi}_5 - I_{5xz} * \ddot{\phi}_5 + U_5 * Z_5 * \dot{\phi}_5 * m_5 \\ &\qquad = M_5 + d_5 * F_{45} + F_{56} * c_5 + \beta_5 * C_{\alpha 5} * b_5 - \frac{C_{\alpha 5} * b_5^2 * \dot{\psi}_5}{U_5} \end{aligned} \qquad \textbf{D-73}$$

$$\ddot{\phi}_5 * (m_5 * Z_5^2 + I_{5xx}) - I_{5xz} * \ddot{\psi}_5$$

$$= F_{56} * f_5 - L_5 * \dot{\phi}_5 - K_5 * \phi_5 + U_5 * Z_5 * m_5 * \left(\dot{\beta}_5 + \dot{\psi}_5\right) \quad \textbf{D-74}$$

$$+ \phi_5 * Z_5 * g * m_5$$

$$\dot{\beta}_5 = \dot{\beta}_4 + \dot{\psi}_4 - \dot{\psi}_5 - \frac{c_4 * \ddot{\psi}_4}{U_4} - \frac{c_5 * \ddot{\psi}_5}{U_5} \quad \textbf{D-75}$$

Finally, the last trailer's equations of motion reduced to D-76 through D-79.

$$U_6 * m_6 * \left(\dot{\beta}_6 + \dot{\psi}_6\right) - Z_6 * \ddot{\phi}_6 * m_6 = F_{56} - \beta_6 * C_{\alpha 6} + \frac{C_{\alpha 6} * b_6 * \dot{\psi}_6}{U_6} \quad \textbf{D-76}$$

$$I_{6zz} * \ddot{\psi}_6 - I_{6xz} * \ddot{\phi}_6 + U_6 * Z_6 * \dot{\phi}_6 * m_6$$

$$= M_6 + F_{56} * c_6 + \beta_6 * C_{\alpha 6} * b_6 - \frac{C_{\alpha 6} * b_6^2 * \dot{\psi}_6}{U_6} \quad \textbf{D-77}$$

$$\ddot{\phi}_6 * (m_6 * Z_6^2 + I_{6x}) - I_{6xz} * \ddot{\psi}_6$$

$$= Z_6 * m_6 * \left(\phi_6 * g + U_6 * \left(\dot{\beta}_6 + \dot{\psi}_6\right)\right) - L_6 * \dot{\phi}_6 - K_6 * \phi_6 \quad \textbf{D-78}$$

$$- F_{56} * f_6$$

$$\dot{\beta}_6 = \dot{\beta}_5 + \dot{\psi}_5 - \dot{\psi}_6 - \frac{c_5 * \ddot{\psi}_5}{U_5} - \frac{c_6 * \ddot{\psi}_6}{U_6} \quad \textbf{D-79}$$

APPENDIX E

NOMINAL VEHICLE PARAMETERS

Table E-1: Vehicle Parameters

Parameter	Description	Value	Unit
m_1	Unit 1 mass	4457	kg
m_2, m_4, m_6	Units 2, 4, 6 mass	3000	kg
m_3, m_5	Units 3, 5 mass	500	kg
I_{1xx}	Unit 1 inertia	2300	Kg-m^2
$I_{2xx,}$ $I_{4xx,}$ I_{6xx}	Units 2, 4, 6 inertia	6000	Kg-m^2
$I_{3xx,}$ I_{5xx}	Units 3, 5 inertia	100	Kg-m^2
I_{1zz}	Unit 1 inertia	35000	Kg-m^2
$I_{2zz,}$ $I_{4zz,}$ I_{6zz}	Units 2, 4, 6 inertia	27000	Kg-m^2
$I_{3zz,}$ I_{5zz}	Units 3, 5 inertia	125	Kg-m^2
I_{1xz}	Unit 1 inertia	1600	Kg-m^2
$I_{2xz,}$ $I_{4xz,}$ I_{6xz}	Units 2, 4, 6 inertia	600	Kg-m^2
$I_{3xz,}$ I_{5xz}	Units 3, 5 inertia	100	Kg-m^2
K_f	Front roll stiffness	322000	N-m/rad
K_r	Rear roll stiffness	550000	N-m/rad
K_2, K_4, K_6	Trailer roll stiffness	677000	N-m/rad
K_3, K_5	Dolly roll stiffness	300000	N-m/rad
L_f, L_r, L_2, L_3, L_4, L_5, L_6	Roll Damping	100000	N-m-s/rad
WB_1	Tractor wheel base	3.5	m
WB_2, WB_4, WB_6	Trailer wheel base	6.7	m
WB_3, WB_5	Dolly wheel base	2.1	m
a_1	Tractor long. CG	1.53	m
a_2, a_4, a_6	Trailer long. CG	4.49	m
a_3, a_5	Dolly long. CG	1.7	m
fw_1	Tractor long. fifth wheel pos.	2.7	m
fw_3, fw_5	Dolly long. fifth wheel pos.	1.86	m
OL_2, OL_4, OL_6	Overall trailer length	7.5	m
f_1	Tractor fifth wheel to roll center	0.5	m
f_2, f_4, f_6	Trailer fifth wheel to roll center	0.2	m
f_3, f_5	Dolly fifth wheel to roll center	0.2	m
Z_1	Tractor CG to roll center height	0.727	m
Z_2, Z_4, Z_6	Trailer CG to roll center height	1.23	m
Z_3, Z_5	Dolly CG to roll center height	0.767	m
$C_{\alpha f}$	Steer axle cornering stiffness	221000	N/rad
$C_{\alpha r}$	Drive axle cornering stiffness	400000	N/rad
$C_{\alpha 2}$, $C_{\alpha 4}$, $C_{\alpha 6}$	Trailer cornering stiffness	800000	N/rad

Parameter	Description	Value	Unit
$C_{\alpha 3}$, $C_{\alpha 5}$	Dolly cornering stiffness	450000	N/rad

APPENDIX F

DOLLY TYPES

While there are many different dolly configurations used throughout the world to meet differing transportation needs, there are three general types that comprise the majority of dollies. These three types are designated as “A”, B”, and “C” and each contains a conventional fifth wheel that is used to connect to the following trailer. The difference in the dolly types is in how they attach to the lead trailer.

“A” type dollies (Figure E-1) use a pintle hook (Figure A-7) to connect to the preceding trailer. This connection decouples the leading trailer and the dolly in roll, pitch, and yaw. Only longitudinal, vertical, and lateral forces can be transmitted through the connection.

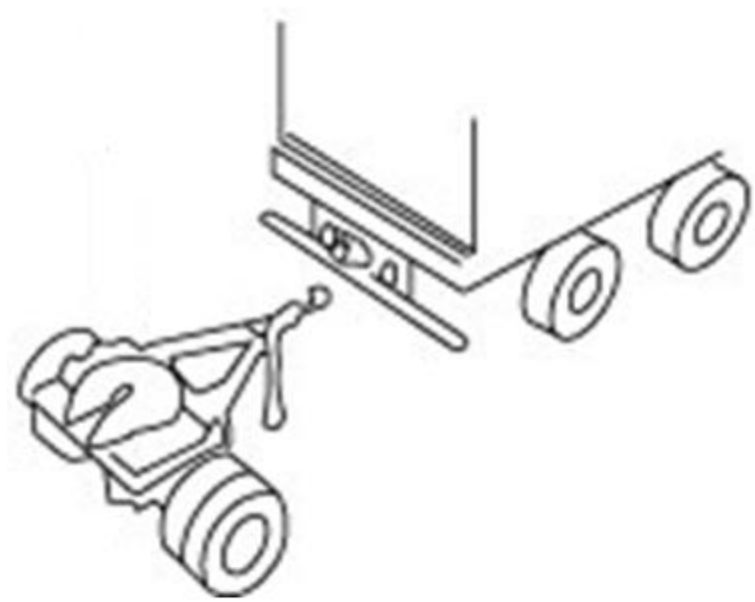

Figure E-1: "A" Type Dolly (Bennett & Norman, 2006)

"B" type dollies (Figure D- 2) are not actually dollies in the classical sense but are classified as such as they allow multiple trailer connections. The dolly is in fact an extension of the leading trailer's frame to which the trailing trailer connects via a fifth wheel. When modeling such a system, the dolly is not included as the trailers are directly connected to each other.

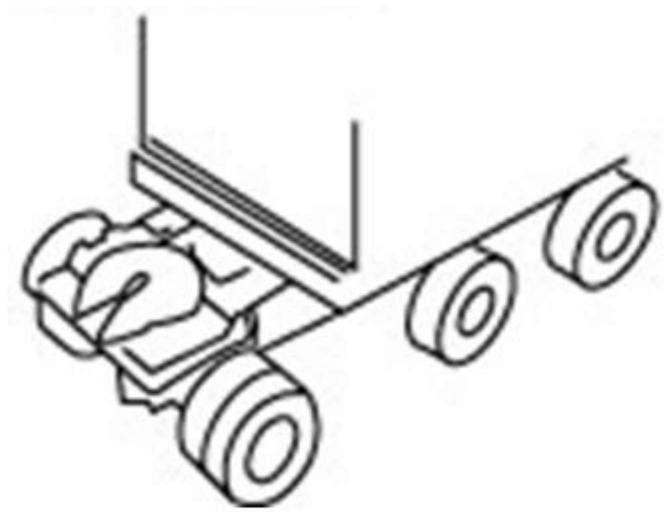

Figure D- 2: "B" Type Dolly (Bennett & Norman, 2006)

"C" type dollies (Figure D- 3) are similar to "A" type dollies except that there are two links connecting the dolly to the leading trailer. This prevents the dolly from rolling or yawing relative to the leading trailer like the "B" type while still allowing the dolly to pitch relative to the leading trailer. Of course, the trailing trailer can yaw and roll relative to the dolly. If pitch is not of concern, then this dolly type can also be dropped in the modeling analysis with the following trailer connected to the end of the lead trailer like a "B" dolly.

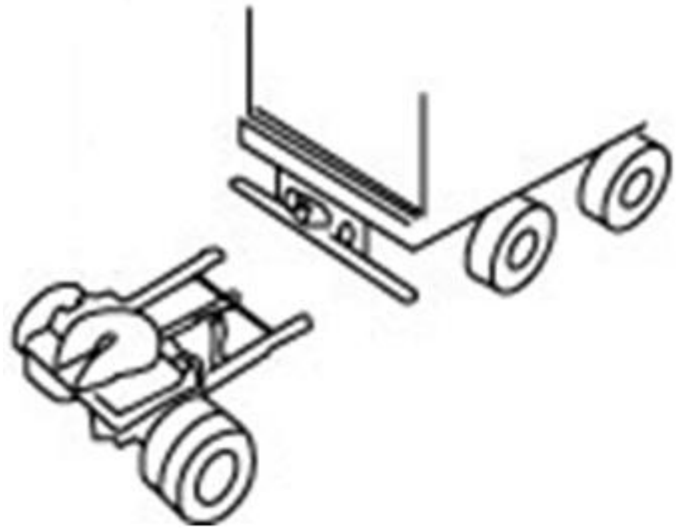

Figure D- 3: "C" Type Dolly (Bennett & Norman, 2006)

In the US, almost all multiple trailer vehicles use "A" type dollies which is why they were the dolly of choice in the modeling and control development here. Additionally, "A" type dollies have the most degrees of freedom which means that the work here can be easily simplified to simulate a "B" or "C" dolly type. To model a "C" type dolly, the dolly articulation equations (Equations D-67 and D-75) were altered to re-produce the leading trailer's side slip (Equations F-1 and F-2). To model a "B" type dolly, the dollies are simply deleted and the trailers are connected directly to each other.

$$\dot{\beta}_3 = \dot{\beta}_2 \quad \textbf{F-1}$$

$$\dot{\beta}_5 = \dot{\beta}_4 \quad \textbf{F-2}$$

Side Note: The keen observer might note that a "C" type dolly connection could produce a roll moment with the leading trailer. However, the two arms can scissor allowing a significant roll difference to exist between the leading trailer and the dolly. This precludes the possibility of significant roll moments save for cases where the lead trailer or the dolly is actually rolling over which would violate the linear model constraints.

APPENDIX G

LINEAR MODEL STATE SPACE FORMULATION

The following is the state space model for the linearized full vehicle model based on the development presented in Section 4.2.2. The mass (Equation G-5), and the stiffness (Equation G-6) matrices are both 24 by 24 (corresponding to the 24 state variables identified in Equation G-3). The input matrix (Equation G-7) is 24 by 8 corresponding to the 24 state variables and 8 inputs (Equation G-4).

$$M * \dot{x} = K * x + B_m * u \quad \textbf{G-1}$$

$$\dot{x} = M^{-1} * K * x + M^{-1} * B_m * u \quad \textbf{G-2}$$

$$x = \begin{bmatrix} \beta_1, \dot{\psi}_1, \dot{\phi}_1, \phi_1, \beta_2, \dot{\psi}_2, \dot{\phi}_2, \phi_2, \beta_3, \dot{\psi}_3, \dot{\phi}_3, \phi_3, \ldots \\ \beta_4, \dot{\psi}_4, \dot{\phi}_4, \phi_4, \beta_5, \dot{\psi}_5, \dot{\phi}_5, \phi_5, \beta_6, \dot{\psi}_6, \dot{\phi}_6, \phi_6 \end{bmatrix}^T \quad \textbf{G-3}$$

$$u = [\delta \quad M_f \quad M_r \quad M_2 \quad M_3 \quad M_4 \quad M_5 \quad M_6]^T \quad \textbf{G-4}$$

$$M = \begin{bmatrix} m_{1,1} & \cdots & m_{1,24} \\ \vdots & \ddots & \vdots \\ m_{24,1} & \cdots & m_{24,24} \end{bmatrix} \quad \textbf{G-5}$$

$$K = \begin{bmatrix} k_{1,1} & \cdots & k_{1,24} \\ \vdots & \ddots & \vdots \\ k_{24,1} & \cdots & k_{24,24} \end{bmatrix} \quad \textbf{G-6}$$

$$B_m = \begin{bmatrix} c_{1,1} & \cdots & c_{1,8} \\ \vdots & \ddots & \vdots \\ c_{24,1} & \cdots & c_{24,8} \end{bmatrix} \quad \textbf{G-7}$$

The terms comprising the state matrices are listed in Equations G-8 through G-10.

G.1. Mass Matrix

$$\begin{gathered} m_{1,1} = U_1 * m_1 \\ m_{1,2} = 0 \end{gathered} \quad \textbf{G-8}$$

$$m_{1,3} = -Z_1 * m_1$$
$$m_{1,4} = 0$$
$$m_{1,5} = 0$$
$$m_{1,6} = \frac{I_{2zz}}{c_2}$$
$$m_{1,7} = -\frac{I_{2xz}}{c_2}$$
$$m_{1,8} = 0$$
$$m_{1,9} = 0$$
$$m_{1,10} = -\frac{I_{3zz} * d_2}{c_2 * d_3}$$
$$m_{1,11} = \frac{I_{3xz} * d_2}{c_2 * d_3}$$
$$m_{1,12} = 0$$
$$m_{1,13} = 0$$
$$m_{1,14} = \frac{I_{4zz} * c_3 * d_2}{c_2 * c_4 * d_3}$$
$$m_{1,15} = -\frac{I_{4xz} * c_3 * d_2}{c_2 * c_4 * d_3}$$
$$m_{1,16} = 0$$
$$m_{1,17} = 0$$
$$m_{1,18} = -\frac{I_{5zz} * c_3 * d_2 * d_4}{c_2 * c_4 * d_3 * d_5}$$
$$m_{1,19} = \frac{I_{5xz} * c_3 * d_2 * d_4}{c_2 * c_4 * d_3 * d_5}$$
$$m_{1,20} = 0$$
$$m_{1,21} = 0$$
$$m_{1,22} = \frac{I_{6zz} * c_3 * c_5 * d_2 * d_4}{c_2 * c_4 * c_6 * d_3 * d_5}$$
$$m_{1,23} = -\frac{I_{6xz} * c_3 * c_5 * d_2 * d_4}{c_2 * c_4 * c_6 * d_3 * d_5}$$
$$m_{1,24} = 0$$
$$m_{2,1} = 0$$
$$m_{2,2} = I_{1zz}$$
$$m_{2,3} = -I_{1xz}$$
$$m_{2,4} = 0$$
$$m_{2,5} = 0$$
$$m_{2,6} = -\frac{I_{2zz} * c_1}{c_2}$$
$$m_{2,7} = \frac{I_{2xz} * c_1}{c_2}$$

$$m_{2,8} = 0$$
$$m_{2,9} = 0$$
$$m_{2,10} = \frac{I_{3zz} * c_1 * d_2}{c_2 * d_3}$$
$$m_{2,11} = -\frac{I_{3xz} * c_1 * d_2}{c_2 * d_3}$$
$$m_{2,12} = 0$$
$$m_{2,13} = 0$$
$$m_{2,14} = -\frac{I_{4zz} * c_1 * c_3 * d_2}{c_2 * c_4 * d_3}$$
$$m_{2,15} = \frac{I_{4xz} * c_1 * c_3 * d_2}{c_2 * c_4 * d_3}$$
$$m_{2,16} = 0$$
$$m_{2,17} = 0$$
$$m_{2,18} = \frac{I_{5zz} * c_1 * c_3 * d_2 * d_4}{c_2 * c_4 * d_3 * d_5}$$
$$m_{2,19} = -\frac{I_{5xz} * c_1 * c_3 * d_2 * d_4}{c_2 * c_4 * d_3 * d_5}$$
$$m_{2,20} = 0$$
$$m_{2,21} = 0$$
$$m_{2,22} = -\frac{I_{6zz} * c_1 * c_3 * c_5 * d_2 * d_4}{c_2 * c_4 * c_6 * d_3 * d_5}$$
$$m_{2,23} = \frac{I_{6xz} * c_1 * c_3 * c_5 * d_2 * d_4}{c_2 * c_4 * c_6 * d_3 * \quad {}_5}$$
$$m_{2,24} = 0$$
$$m_{3,1} = -U_1 * Z_1 * m_1$$
$$m_{3,2} = -I_{1xz}$$
$$m_{3,3} = I_{1xx} + Z_1^2 * m_1$$
$$m_{3,4} = 0$$
$$m_{3,5} = 0$$
$$m_{3,6} = -\frac{I_{2zz} * f_1}{c_2}$$
$$m_{3,7} = \frac{I_{2xz} * f_1}{c_2}$$
$$m_{3,8} = 0$$
$$m_{3,9} = 0$$
$$m_{3,10} = \frac{I_{3zz} * d_2 * f_1}{c_2 * d_3}$$
$$m_{3,11} = -\frac{I_{3xz} * d_2 * f_1}{c_2 * d_3}$$

$$m_{3,12} = 0$$
$$m_{3,13} = 0$$
$$m_{3,14} = -\frac{I_{4zz} * c_3 * d_2 * f_1}{c_2 * c_4 * d_3}$$
$$m_{3,15} = \frac{I_{4xz} * c_3 * d_2 * f_1}{c_2 * c_4 * d_3}$$
$$m_{3,16} = 0$$
$$m_{3,17} = 0$$
$$m_{3,18} = \frac{I_{5zz} * c_3 * d_2 * d_4 * f_1}{c_2 * c_4 * d_3 * d_5}$$
$$m_{3,19} = -\frac{I_{5xz} * c_3 * d_2 * d_4 * f_1}{c_2 * c_4 * d_3 * d_5}$$
$$m_{3,20} = 0$$
$$m_{3,21} = 0$$
$$m_{3,22} = -\frac{I_{6zz} * c_3 * c_5 * d_2 * d_4 * f_1}{c_2 * c_4 * c_6 * d_3 * d_5}$$
$$m_{3,23} = \frac{I_{6xz} * c_3 * c_5 * d_2 * d_4 * f_1}{c_2 * c_4 * c_6 * d_3 * d_5}$$
$$m_{3,24} = 0$$
$$m_{4,1} = 0$$
$$m_{4,2} = 0$$
$$m_{4,3} = 0$$
$$m_{4,4} = 1$$
$$m_{4,5} = 0$$
$$m_{4,6} = 0$$
$$m_{4,7} = 0$$
$$m_{4,8} = 0$$
$$m_{4,9} = 0$$
$$m_{4,10} = 0$$
$$m_{4,11} = 0$$
$$m_{4,12} = 0$$
$$m_{4,13} = 0$$
$$m_{4,14} = 0$$
$$m_{4,15} = 0$$
$$m_{4,16} = 0$$
$$m_{4,17} = 0$$
$$m_{4,18} = 0$$
$$m_{4,19} = 0$$
$$m_{4,20} = 0$$
$$m_{4,21} = 0$$

$$m_{4,22} = 0$$
$$m_{4,23} = 0$$
$$m_{4,24} = 0$$
$$m_{5,1} = 0$$
$$m_{5,2} = 0$$
$$m_{5,3} = 0$$
$$m_{5,4} = 0$$
$$m_{5,5} = U_2 * m_2$$
$$m_{5,6} = -\frac{I_{2zz}}{c_2}$$
$$m_{5,7} = \frac{I_{2xz}}{c_2} - Z_2 * m_2$$
$$m_{5,8} = 0$$
$$m_{5,9} = 0$$
$$m_{5,10} = \frac{I_{3zz}}{d_3} + \frac{I_{3zz} * d_2}{c_2 * d_3}$$
$$m_{5,11} = -\frac{I_{3xz}}{d_3} - \frac{I_{3xz} * d_2}{c_2 * d_3}$$
$$m_{5,12} = 0$$
$$m_{5,13} = 0$$
$$m_{5,14} = -\frac{I_{4zz} * c_3}{c_4 * d_3} - \frac{I_{4zz} * c_3 * d_2}{c_2 * c_4 * d_3}$$
$$m_{5,15} = \frac{I_{4xz} * c_3}{c_4 * d_3} + \frac{I_{4xz} * c_3 * d_2}{c_2 * c_4 * d_3}$$
$$m_{5,16} = 0$$
$$m_{5,17} = 0$$
$$m_{5,18} = \frac{I_{5zz} * c_3 * d_4}{c_4 * d_3 * d_5} + \frac{I_{5zz} * c_3 * d_2 * d_4}{c_2 * c_4 * d_3 * d_5}$$
$$m_{5,19} = -\frac{I_{5xz} * c_3 * d_4}{c_4 * d_3 * d_5} - \frac{I_{5xz} * c_3 * d_2 * d_4}{c_2 * c_4 * d_3 * d_5}$$
$$m_{5,20} = 0$$
$$m_{5,21} = 0$$
$$m_{5,22} = -\frac{I_{6zz} * c_3 * c_5 * d_4}{c_4 * c_6 * d_3 * d_5} - \frac{I_{6zz} * c_3 * c_5 * d_2 * d_4}{c_2 * c_4 * c_6 * d_3 * d_5}$$
$$m_{5,23} = \frac{I_{6xz} * c_3 * c_5 * d_4}{c_4 * c_6 * d_3 * d_5} + \frac{I_{6xz} * c_3 * c_5 * d_2 * d_4}{c_2 * c_4 * c_6 * d_3 * d_5}$$
$$m_{5,24} = 0$$
$$m_{6,1} = 0$$
$$m_{6,2} = 0$$
$$m_{6,3} = 0$$
$$m_{6,4} = 0$$

$$m_{6,5} = -U_2 * Z_2 * m_2$$
$$m_{6,6} = \frac{I_{2zz} * f_2}{c_2} - I_{2xz}$$
$$m_{6,7} = I_{2xx} + Z_2^2 * m_2 - \frac{I_{2xz} * f_2}{c_2}$$
$$m_{6,8} = 0$$
$$m_{6,9} = 0$$
$$m_{6,10} = -\frac{I_{3zz} * d_2 * f_2}{c_2 * d_3}$$
$$m_{6,11} = \frac{I_{3xz} * d_2 * f_2}{c_2 * d_3}$$
$$m_{6,12} = 0$$
$$m_{6,13} = 0$$
$$m_{6,14} = \frac{I_{4zz} * c_3 * d_2 * f_2}{c_2 * c_4 * d_3}$$
$$m_{6,15} = -\frac{I_{4xz} * c_3 * d_2 * f_2}{c_2 * c_4 * d_3}$$
$$m_{6,16} = 0$$
$$m_{6,17} = 0$$
$$m_{6,18} = -\frac{I_{5zz} * c_3 * d_2 * d_4 * f_2}{c_2 * c_4 * d_3 * d_5}$$
$$m_{6,19} = \frac{I_{5xz} * c_3 * d_2 * d_4 * f_2}{c_2 * c_4 * d_3 * d_5}$$
$$m_{6,20} = 0$$
$$m_{6,21} = 0$$
$$m_{6,22} = \frac{I_{6zz} * c_3 * c_5 * d_2 * d_4 * f_2}{c_2 * c_4 * c_6 * d_3 * d_5}$$
$$m_{6,23} = -\frac{I_{6xz} * c_3 * c_5 * d_2 * d_4 * f_2}{c_2 * c_4 * c_6 * d_3 * d_5}$$
$$m_{6,24} = 0$$
$$m_{7,1} = -1$$
$$m_{7,2} = \frac{c_1}{U_1}$$
$$m_{7,3} = 0$$
$$m_{7,4} = 0$$
$$m_{7,5} = 1$$
$$m_{7,6} = \frac{c_2}{U_2}$$
$$m_{7,7} = 0$$
$$m_{7,8} = 0$$
$$m_{7,9} = 0$$

$$m_{7,10} = 0$$
$$m_{7,11} = 0$$
$$m_{7,12} = 0$$
$$m_{7,13} = 0$$
$$m_{7,14} = 0$$
$$m_{7,15} = 0$$
$$m_{7,16} = 0$$
$$m_{7,17} = 0$$
$$m_{7,18} = 0$$
$$m_{7,19} = 0$$
$$m_{7,20} = 0$$
$$m_{7,21} = 0$$
$$m_{7,22} = 0$$
$$m_{7,23} = 0$$
$$m_{7,24} = 0$$
$$m_{8,1} = 0$$
$$m_{8,2} = 0$$
$$m_{8,3} = 0$$
$$m_{8,4} = 0$$
$$m_{8,5} = 0$$
$$m_{8,6} = 0$$
$$m_{8,7} = 0$$
$$m_{8,8} = 1$$
$$m_{8,9} = 0$$
$$m_{8,10} = 0$$
$$m_{8,11} = 0$$
$$m_{8,12} = 0$$
$$m_{8,13} = 0$$
$$m_{8,14} = 0$$
$$m_{8,15} = 0$$
$$m_{8,16} = 0$$
$$m_{8,17} = 0$$
$$m_{8,18} = 0$$
$$m_{8,19} = 0$$
$$m_{8,20} = 0$$
$$m_{8,21} = 0$$
$$m_{8,22} = 0$$
$$m_{8,23} = 0$$
$$m_{8,24} = 0$$
$$m_{9,1} = 0$$

$$m_{9,2} = 0$$
$$m_{9,3} = 0$$
$$m_{9,4} = 0$$
$$m_{9,5} = 0$$
$$m_{9,6} = 0$$
$$m_{9,7} = 0$$
$$m_{9,8} = 0$$
$$m_{9,9} = U_3 * m_3$$
$$m_{9,10} = -\frac{I_{3zz}}{d_3}$$
$$m_{9,11} = \frac{I_{3xz}}{d_3} - Z_3 * m_3$$
$$m_{9,12} = 0$$
$$m_{9,13} = 0$$
$$m_{9,14} = \frac{I_{4zz}}{c_4} + \frac{I_{4zz} * c_3}{c_4 * d_3}$$
$$m_{9,15} = -\frac{I_{4xz}}{c_4} - \frac{I_{4xz} * c_3}{c_4 * d_3}$$
$$m_{9,16} = 0$$
$$m_{9,17} = 0$$
$$m_{9,18} = -\frac{I_{5zz} * d_4}{c_4 * d_5} - \frac{I_{5zz} * c_3 * d_4}{c_4 * d_3 * d_5}$$
$$m_{9,19} = \frac{I_{5xz} * d_4}{c_4 * d_5} + \frac{I_{5xz} * c_3 * d_4}{c_4 * d_3 * d_5}$$
$$m_{9,20} = 0$$
$$m_{9,21} = 0$$
$$m_{9,22} = \frac{I_{6zz} * c_5 * d_4}{c_4 * c_6 * d_5} + \frac{I_{6zz} * c_3 * \quad {}_5 * d_4}{c_4 * c_6 * d_3 * d_5}$$
$$m_{9,23} = -\frac{I_{6xz} * c_5 * d_4}{c_4 * c_6 * d_5} - \frac{I_{6xz} * c_3 * c_5 * d_4}{c_4 * c_6 * d_3 * d_5}$$
$$m_{9,24} = 0$$
$$m_{10,1} = 0$$
$$m_{10,2} = 0$$
$$m_{10,3} = 0$$
$$m_{10,4} = 0$$
$$m_{10,5} = 0$$
$$m_{10,6} = 0$$
$$m_{10,7} = 0$$
$$m_{10,8} = 0$$
$$m_{10,9} = -U_3 * Z_3 * m_3$$

$$m_{10,10} = -I_{3xz}$$
$$m_{10,11} = I_{3xx} + Z_3^2 * m_3$$
$$m_{10,12} = 0$$
$$m_{10,13} = 0$$
$$m_{10,14} = -\frac{I_{4zz} * f_3}{c_4}$$
$$m_{10,15} = \frac{I_{4xz} * f_3}{c_4}$$
$$m_{10,16} = 0$$
$$m_{10,17} = 0$$
$$m_{10,18} = \frac{I_{5zz} * d_4 * f_3}{c_4 * d_5}$$
$$m_{10,19} = -\frac{I_{5xz} * d_4 * f_3}{c_4 * d_5}$$
$$m_{10,20} = 0$$
$$m_{10,21} = 0$$
$$m_{10,22} = -\frac{I_{6zz} * c_5 * d_4 * f_3}{c_4 * c_6 * d_5}$$
$$m_{10,23} = \frac{I_{6xz} * c_5 * d_4 * f_3}{c_4 * c_6 * d_5}$$
$$m_{10,24} = 0$$
$$m_{11,1} = 0$$
$$m_{11,2} = 0$$
$$m_{11,3} = 0$$
$$m_{11,4} = 0$$
$$m_{11,5} = -1$$
$$m_{11,6} = \frac{c_2}{U_2}$$
$$m_{11,7} = 0$$
$$m_{11,8} = 0$$
$$m_{11,9} = 1$$
$$m_{11,10} = \frac{c_3}{U_3}$$
$$m_{11,11} = 0$$
$$m_{11,12} = 0$$
$$m_{11,13} = 0$$
$$m_{11,14} = 0$$
$$m_{11,15} = 0$$
$$m_{11,16} = 0$$
$$m_{11,17} = 0$$
$$m_{11,18} = 0$$

$$m_{11,19} = 0$$
$$m_{11,20} = 0$$
$$m_{11,21} = 0$$
$$m_{11,22} = 0$$
$$m_{11,23} = 0$$
$$m_{11,24} = 0$$
$$m_{12,1} = 0$$
$$m_{12,2} = 0$$
$$m_{12,3} = 0$$
$$m_{12,4} = 0$$
$$m_{12,5} = 0$$
$$m_{12,6} = 0$$
$$m_{12,7} = 0$$
$$m_{12,8} = 0$$
$$m_{12,9} = 0$$
$$m_{12,10} = 0$$
$$m_{12,11} = 0$$
$$m_{12,12} = 1$$
$$m_{12,13} = 0$$
$$m_{12,14} = 0$$
$$m_{12,15} = 0$$
$$m_{12,16} = 0$$
$$m_{12,17} = 0$$
$$m_{12,18} = 0$$
$$m_{12,19} = 0$$
$$m_{12,20} = 0$$
$$m_{12,21} = 0$$
$$m_{12,22} = 0$$
$$m_{12,23} = 0$$
$$m_{12,24} = 0$$
$$m_{13,1} = 0$$
$$m_{13,2} = 0$$
$$m_{13,3} = 0$$
$$m_{13,4} = 0$$
$$m_{13,5} = 0$$
$$m_{13,6} = 0$$
$$m_{13,7} = 0$$
$$m_{13,8} = 0$$
$$m_{13,9} = 0$$
$$m_{13,10} = 0$$

$$m_{13,11} = 0$$
$$m_{13,12} = 0$$
$$m_{13,13} = U_4 * m_4$$
$$m_{13,14} = -\frac{I_{4zz}}{c_4}$$
$$m_{13,15} = \frac{I_{4xz}}{c_4} - Z_4 * m_4$$
$$m_{13,16} = 0$$
$$m_{13,17} = 0$$
$$m_{13,18} = \frac{I_{5zz}}{d_5} + \frac{I_{5zz} * d_4}{c_4 * d_5}$$
$$m_{13,19} = -\frac{I_{5xz}}{d_5} - \frac{I_{5xz} * d_4}{c_4 * d_5}$$
$$m_{13,20} = 0$$
$$m_{13,21} = 0$$
$$m_{13,22} = -\frac{I_{6zz} * c_5}{c_6 * d_5} - \frac{I_{6zz} * c_5 * d_4}{c_4 * c_6 * d_5}$$
$$m_{13,23} = \frac{I_{6xz} * c_5}{c_6 * d_5} + \frac{I_{6xz} * c_5 * d_4}{c_4 * c_6 * d_5}$$
$$m_{13,24} = 0$$
$$m_{14,1} = 0$$
$$m_{14,2} = 0$$
$$m_{14,3} = 0$$
$$m_{14,4} = 0$$
$$m_{14,5} = 0$$
$$m_{14,6} = 0$$
$$m_{14,7} = 0$$
$$m_{14,8} = 0$$
$$m_{14,9} = 0$$
$$m_{14,10} = 0$$
$$m_{14,11} = 0$$
$$m_{14,12} = 0$$
$$m_{14,13} = -U_4 * Z_4 * m_4$$
$$m_{14,14} = \frac{I_{4zz} * f_4}{c_4} - I_{4xz}$$
$$m_{14,15} = I_{4xx} + Z_4^2 * m_4 - \frac{I_{4xz} * f_4}{c_4}$$
$$m_{14,16} = 0$$
$$m_{14,17} = 0$$
$$m_{14,18} = -\frac{I_{5zz} * d_4 * f_4}{c_4 * d_5}$$

$$m_{14,19} = \frac{I_{5xz} * d_4 * f_4}{c_4 * d_5}$$
$$m_{14,20} = 0$$
$$m_{14,21} = 0$$
$$m_{14,22} = \frac{I_{6zz} * c_5 * d_4 * f_4}{c_4 * c_6 * d_5}$$
$$m_{14,23} = -\frac{I_{6xz} * c_5 * d_4 * f_4}{c_4 * c_6 * d_5}$$
$$m_{14,24} = 0$$
$$m_{15,1} = 0$$
$$m_{15,2} = 0$$
$$m_{15,3} = 0$$
$$m_{15,4} = 0$$
$$m_{15,5} = 0$$
$$m_{15,6} = 0$$
$$m_{15,7} = 0$$
$$m_{15,8} = 0$$
$$m_{15,9} = -1$$
$$m_{15,10} = \frac{c_3}{U_3}$$
$$m_{15,11} = 0$$
$$m_{15,12} = 0$$
$$m_{15,13} = 1$$
$$m_{15,14} = \frac{c_4}{U_4}$$
$$m_{15,15} = 0$$
$$m_{15,16} = 0$$
$$m_{15,17} = 0$$
$$m_{15,18} = 0$$
$$m_{15,19} = 0$$
$$m_{15,20} = 0$$
$$m_{15,21} = 0$$
$$m_{15,22} = 0$$
$$m_{15,23} = 0$$
$$m_{15,24} = 0$$
$$m_{16,1} = 0$$
$$m_{16,2} = 0$$
$$m_{16,3} = 0$$
$$m_{16,4} = 0$$
$$m_{16,5} = 0$$
$$m_{16,6} = 0$$

$$m_{16,7} = 0$$
$$m_{16,8} = 0$$
$$m_{16,9} = 0$$
$$m_{16,10} = 0$$
$$m_{16,11} = 0$$
$$m_{16,12} = 0$$
$$m_{16,13} = 0$$
$$m_{16,14} = 0$$
$$m_{16,15} = 0$$
$$m_{16,16} = 1$$
$$m_{16,17} = 0$$
$$m_{16,18} = 0$$
$$m_{16,19} = 0$$
$$m_{16,20} = 0$$
$$m_{16,21} = 0$$
$$m_{16,22} = 0$$
$$m_{16,23} = 0$$
$$m_{16,24} = 0$$
$$m_{17,1} = 0$$
$$m_{17,2} = 0$$
$$m_{17,3} = 0$$
$$m_{17,4} = 0$$
$$m_{17,5} = 0$$
$$m_{17,6} = 0$$
$$m_{17,7} = 0$$
$$m_{17,8} = 0$$
$$m_{17,9} = 0$$
$$m_{17,10} = 0$$
$$m_{17,11} = 0$$
$$m_{17,12} = 0$$
$$m_{17,13} = 0$$
$$m_{17,14} = 0$$
$$m_{17,15} = 0$$
$$m_{17,16} = 0$$
$$m_{17,17} = U_5 * m_5$$
$$m_{17,18} = -\frac{I_{5zz}}{d_5}$$
$$m_{17,19} = \frac{I_{5xz}}{d_5} - Z_5 * m_5$$
$$m_{17,20} = 0$$

$$m_{17,21} = 0$$
$$m_{17,22} = \frac{I_{6zz}}{c_6} + \frac{I_{6zz} * c_5}{c_6 * d_5}$$
$$m_{17,23} = -\frac{I_{6xz}}{c_6} - \frac{I_{6xz} * c_5}{c_6 * d_5}$$
$$m_{17,24} = 0$$
$$m_{18,1} = 0$$
$$m_{18,2} = 0$$
$$m_{18,3} = 0$$
$$m_{18,4} = 0$$
$$m_{18,5} = 0$$
$$m_{18,6} = 0$$
$$m_{18,7} = 0$$
$$m_{18,8} = 0$$
$$m_{18,9} = 0$$
$$m_{18,10} = 0$$
$$m_{18,11} = 0$$
$$m_{18,12} = 0$$
$$m_{18,13} = 0$$
$$m_{18,14} = 0$$
$$m_{18,15} = 0$$
$$m_{18,16} = 0$$
$$m_{18,17} = -U_5 * Z_5 * m_5$$
$$m_{18,18} = -I_{5xz}$$
$$m_{18,19} = I_{5xx} + Z_5^2 * m_5$$
$$m_{18,20} = 0$$
$$m_{18,21} = 0$$
$$m_{18,22} = -\frac{I_{6zz} * f_5}{c_6}$$
$$m_{18,23} = \frac{I_{6xz} * f_5}{c_6}$$
$$m_{18,24} = 0$$
$$m_{19,1} = 0$$
$$m_{19,2} = 0$$
$$m_{19,3} = 0$$
$$m_{19,4} = 0$$
$$m_{19,5} = 0$$
$$m_{19,6} = 0$$
$$m_{19,7} = 0$$
$$m_{19,8} = 0$$

$$m_{19,9} = 0$$
$$m_{19,10} = 0$$
$$m_{19,11} = 0$$
$$m_{19,12} = 0$$
$$m_{19,13} = -1$$
$$m_{19,14} = \frac{c_4}{U_4}$$
$$m_{19,15} = 0$$
$$m_{19,16} = 0$$
$$m_{19,17} = 1$$
$$m_{19,18} = \frac{c_5}{U_5}$$
$$m_{19,19} = 0$$
$$m_{19,20} = 0$$
$$m_{19,21} = 0$$
$$m_{19,22} = 0$$
$$m_{19,23} = 0$$
$$m_{19,24} = 0$$
$$m_{20,1} = 0$$
$$m_{20,2} = 0$$
$$m_{20,3} = 0$$
$$m_{20,4} = 0$$
$$m_{20,5} = 0$$
$$m_{20,6} = 0$$
$$m_{20,7} = 0$$
$$m_{20,8} = 0$$
$$m_{20,9} = 0$$
$$m_{20,10} = 0$$
$$m_{20,11} = 0$$
$$m_{20,12} = 0$$
$$m_{20,13} = 0$$
$$m_{20,14} = 0$$
$$m_{20,15} = 0$$
$$m_{20,16} = 0$$
$$m_{20,17} = 0$$
$$m_{20,18} = 0$$
$$m_{20,19} = 0$$
$$m_{20,20} = 1$$
$$m_{20,21} = 0$$
$$m_{20,22} = 0$$
$$m_{20,23} = 0$$

$$m_{20,24} = 0$$
$$m_{21,1} = 0$$
$$m_{21,2} = 0$$
$$m_{21,3} = 0$$
$$m_{21,4} = 0$$
$$m_{21,5} = 0$$
$$m_{21,6} = 0$$
$$m_{21,7} = 0$$
$$m_{21,8} = 0$$
$$m_{21,9} = 0$$
$$m_{21,10} = 0$$
$$m_{21,11} = 0$$
$$m_{21,12} = 0$$
$$m_{21,13} = 0$$
$$m_{21,14} = 0$$
$$m_{21,15} = 0$$
$$m_{21,16} = 0$$
$$m_{21,17} = 0$$
$$m_{21,18} = 0$$
$$m_{21,19} = 0$$
$$m_{21,20} = 0$$
$$m_{21,21} = U_6 * m_6$$
$$m_{21,22} = -\frac{I_{6zz}}{c_6}$$
$$m_{21,23} = \frac{I_{6xz}}{c_6} - Z_6 * m_6$$
$$m_{21,24} = 0$$
$$m_{22,1} = 0$$
$$m_{22,2} = 0$$
$$m_{22,3} = 0$$
$$m_{22,4} = 0$$
$$m_{22,5} = 0$$
$$m_{22,6} = 0$$
$$m_{22,7} = 0$$
$$m_{22,8} = 0$$
$$m_{22,9} = 0$$
$$m_{22,10} = 0$$
$$m_{22,11} = 0$$
$$m_{22,12} = 0$$
$$m_{22,13} = 0$$

$$m_{22,14} = 0$$
$$m_{22,15} = 0$$
$$m_{22,16} = 0$$
$$m_{22,17} = 0$$
$$m_{22,18} = 0$$
$$m_{22,19} = 0$$
$$m_{22,20} = 0$$
$$m_{22,21} = -U_6 * Z_6 * m_6$$
$$m_{22,22} = \frac{I_{6zz} * f_6}{c_6} - I_{6xz}$$
$$m_{22,23} = I_{6xx} + Z_6^2 * m_6 - \frac{I_{6xz} * f_6}{c_6}$$
$$m_{22,24} = 0$$
$$m_{23,1} = 0$$
$$m_{23,2} = 0$$
$$m_{23,3} = 0$$
$$m_{23,4} = 0$$
$$m_{23,5} = 0$$
$$m_{23,6} = 0$$
$$m_{23,7} = 0$$
$$m_{23,8} = 0$$
$$m_{23,9} = 0$$
$$m_{23,10} = 0$$
$$m_{23,11} = 0$$
$$m_{23,12} = 0$$
$$m_{23,13} = 0$$
$$m_{23,14} = 0$$
$$m_{23,15} = 0$$
$$m_{23,16} = 0$$
$$m_{23,17} = -1$$
$$m_{23,18} = \frac{c_5}{U_5}$$
$$m_{23,19} = 0$$
$$m_{23,20} = 0$$
$$m_{23,21} = 1$$
$$m_{23,22} = \frac{c_6}{U_6}$$
$$m_{23,23} = 0$$
$$m_{23,24} = 0$$
$$m_{24,1} = 0$$
$$m_{24,2} = 0$$

$$m_{24,3} = 0$$
$$m_{24,4} = 0$$
$$m_{24,5} = 0$$
$$m_{24,6} = 0$$
$$m_{24,7} = 0$$
$$m_{24,8} = 0$$
$$m_{24,9} = 0$$
$$m_{24,10} = 0$$
$$m_{24,11} = 0$$
$$m_{24,12} = 0$$
$$m_{24,13} = 0$$
$$m_{24,14} = 0$$
$$m_{24,15} = 0$$
$$m_{24,16} = 0$$
$$m_{24,17} = 0$$
$$m_{24,18} = 0$$
$$m_{24,19} = 0$$
$$m_{24,20} = 0$$
$$m_{24,21} = 0$$
$$m_{24,22} = 0$$
$$m_{24,23} = 0$$
$$m_{24,24} = 1$$

G.2. Stiffness Matrix

$$k_{1,1} = -C_{af} - C_{ar}$$
$$k_{1,2} = -U_1 * m_1 - \frac{C_{af} * a_1 - C_{ar} * b_1}{U_1}$$
$$k_{1,3} = 0$$
$$k_{1,4} = 0$$
$$k_{1,5} = \frac{C_{a2} * b_2}{c_2} \qquad \textbf{G-9}$$
$$k_{1,6} = -\frac{C_{a2} * b_2^2}{U_2 * c_2}$$
$$k_{1,7} = -\frac{U_2 * Z_2 * m_2}{c_2}$$
$$k_{1,8} = 0$$
$$k_{1,9} = -\frac{C_{a3} * b_3 * d_2}{c_2 * d_3}$$

$$k_{1,10} = \frac{C_{a3} * b_3^2 * d_2}{U_3 * c_2 * d_3}$$
$$k_{1,11} = \frac{U_3 * Z_3 * d_2 * m_3}{c_2 * d_3}$$
$$k_{1,12} = 0$$
$$k_{1,13} = \frac{C_{a4} * b_4 * c_3 * d_2}{c_2 * c_4 * d_3}$$
$$k_{1,14} = -\frac{C_{a4} * b_4^2 * c_3 * d_2}{U_4 * c_2 * c_4 * d_3}$$
$$k_{1,15} = -\frac{U_4 * Z_4 * c_3 * d_2 * m_4}{c_2 * c_4 * d_3}$$
$$k_{1,16} = 0$$
$$k_{1,17} = -\frac{C_{a2} * b_5 * c_3 * d_2 * d_4}{c_2 * c_4 * d_3 * d_5}$$
$$k_{1,18} = \frac{C_{a2} * b_5^2 * c_3 * d_2 * d_4}{U_5 * c_2 * c_4 * d_3 * d_5}$$
$$k_{1,19} = \frac{U_5 * Z_5 * c_3 * d_2 * d_4 * m_5}{c_2 * c_4 * d_3 * d_5}$$
$$k_{1,20} = 0$$
$$k_{1,21} = \frac{C_{a2} * b_6 * c_3 * c_5 * d_2 * d_4}{c_2 * c_4 * c_6 * d_3 * d_5}$$
$$k_{1,22} = -\frac{C_{a2} * b_6^2 * c_3 * c_5 * d_2 * d_4}{U_6 * c_2 * c_4 * c_6 * d_3 * d_5}$$
$$k_{1,23} = -\frac{U_6 * Z_6 * c_3 * c_5 * d_2 * d_4 * m_6}{c_2 * c_4 * c_6 * d_3 * d_5}$$
$$k_{1,24} = 0$$
$$k_{2,1} = C_a * b_1 - C_{af} * a_1$$
$$k_{2,2} = -\frac{C_{af} * a_1^2 + C_{ar} * b_1^2}{U_1}$$
$$k_{2,3} = -U_1 * Z_1 * m_1$$
$$k_{2,4} = 0$$
$$k_{2,5} = -\frac{C_{a2} * b_2 * c_1}{c_2}$$
$$k_{2,6} = \frac{C_{a2} * b_2^2 * c_1}{U_2 * c_2}$$
$$k_{2,7} = \frac{U_2 * Z_2 * c_1 * m_2}{c_2}$$
$$k_{2,8} = 0$$
$$k_{2,9} = \frac{C_{a3} * b_3 * c_1 * d_2}{c_2 * d_3}$$

$$k_{2,10} = -\frac{C_{a3} * b_3^2 * c_1 * d_2}{U_3 * c_2 * d_3}$$

$$k_{2,11} = -\frac{U_3 * Z_3 * c_1 * d_2 * m_3}{c_2 * d_3}$$

$$k_{2,12} = 0$$

$$k_{2,13} = -\frac{C_{a4} * b_4 * c_1 * c_3 * d_2}{c_2 * c_4 * d_3}$$

$$k_{2,14} = \frac{C_{a4} * b_4^2 * c_1 * c_3 * d_2}{U_4 * c_2 * c_4 * d_3}$$

$$k_{2,15} = \frac{U_4 * Z_4 * c_1 * c_3 * d_2 * m_4}{c_2 * c_4 * d_3}$$

$$k_{2,16} = 0$$

$$k_{2,17} = \frac{C_{a2} * b_5 * c_1 * c_3 * d_2 * d_4}{c_2 * c_4 * d_3 * d_5}$$

$$k_{2,18} = -\frac{C_{a2} * b_5^2 * c_1 * c_3 * d_2 * d_4}{U_5 * c_2 * c_4 * d_3 * d_5}$$

$$k_{2,19} = -\frac{U_5 * Z_5 * c_1 * c_3 * d_2 * d_4 * m_5}{c_2 * c_4 * d_3 * d_5}$$

$$k_{2,20} = 0$$

$$k_{2,21} = -\frac{C_{a2} * b_6 * c_1 * c_3 * c_5 * d_2 * d_4}{c_2 * c_4 * c_6 * d_3 * d_5}$$

$$k_{2,22} = \frac{C_{a2} * b_6^2 * c_1 * c_3 * c_5 * d_2 * d_4}{U_6 * c_2 * c_4 * c_6 * d_3 * d_5}$$

$$k_{2,23} = \frac{U_6 * Z_6 * c_1 * c_3 * c_5 * d_2 * d_4 * m_6}{c_2 * c_4 * c_6 * d_3 * \quad {}_5}$$

$$k_{2,24} = 0$$

$$k_{3,1} = 0$$

$$k_{3,2} = U_1 * Z_1 * m_1$$

$$k_{3,3} = -Lf - Lr$$

$$k_{3,4} = Z_1 * g * m_1 - Kr - Kf$$

$$k_{3,5} = -\frac{C_{a2} * b_2 * f_1}{c_2}$$

$$k_{3,6} = \frac{C_{a2} * b_2^2 * f_1}{U_2 * c_2}$$

$$k_{3,7} = \frac{U_2 * Z_2 * f_1 * m_2}{c_2}$$

$$k_{3,8} = 0$$

$$k_{3,9} = \frac{C_{a3} * b_3 * d_2 * f_1}{c_2 * d_3}$$

$$k_{3,10} = -\frac{C_{a3} * b_3^2 * d_2 * f_1}{U_3 * c_2 * d_3}$$
$$k_{3,11} = -\frac{U_3 * Z_3 * d_2 * f_1 * m_3}{c_2 * d_3}$$
$$k_{3,12} = 0$$
$$k_{3,13} = -\frac{C_{a4} * b_4 * c_3 * d_2 * f_1}{c_2 * c_4 * d_3}$$
$$k_{3,14} = \frac{C_{a4} * b_4^2 * c_3 * d_2 * f_1}{U_4 * c_2 * c_4 * d_3}$$
$$k_{3,15} = \frac{U_4 * Z_4 * c_3 * d_2 * f_1 * m_4}{c_2 * c_4 * d_3}$$
$$k_{3,16} = 0$$
$$k_{3,17} = \frac{C_{a2} * b_5 * c_3 * d_2 * d_4 * f_1}{c_2 * c_4 * d_3 * d_5}$$
$$k_{3,18} = -\frac{C_{a2} * b_5^2 * c_3 * d_2 * d_4 * f_1}{U_5 * c_2 * c_4 * d_3 * d_5}$$
$$k_{3,19} = -\frac{U_5 * Z_5 * c_3 * d_2 * d_4 * f_1 * m_5}{c_2 * c_4 * d_3 * d_5}$$
$$k_{3,20} = 0$$
$$k_{3,21} = -\frac{C_{a2} * b_6 * c_3 * c_5 * d_2 * d_4 * f_1}{c_2 * c_4 * c_6 * d_3 * d_5}$$
$$k_{3,22} = \frac{C_{a2} * b_6^2 * c_3 * c_5 * d_2 * d_4 * \quad {}_1}{U_6 * c_2 * c_4 * c_6 * d_3 * d_5}$$
$$k_{3,23} = \frac{U_6 * Z_6 * c_3 * c_5 * d_2 * d_4 * f_1 * m_6}{c_2 * c_4 * c_6 * d_3 * d_5}$$
$$k_{3,24} = 0$$
$$k_{4,1} = 0$$
$$k_{4,2} = 0$$
$$k_{4,3} = 1$$
$$k_{4,4} = 0$$
$$k_{4,5} = 0$$
$$k_{4,6} = 0$$
$$k_{4,7} = 0$$
$$k_{4,8} = 0$$
$$k_{4,9} = 0$$
$$k_{4,10} = 0$$
$$k_{4,11} = 0$$
$$k_{4,12} = 0$$
$$k_{4,13} = 0$$
$$k_{4,14} = 0$$

$$k_{4,15} = 0$$
$$k_{4,16} = 0$$
$$k_{4,17} = 0$$
$$k_{4,18} = 0$$
$$k_{4,19} = 0$$
$$k_{4,20} = 0$$
$$k_{4,21} = 0$$
$$k_{4,22} = 0$$
$$k_{4,23} = 0$$
$$k_{4,24} = 0$$
$$k_{5,1} = 0$$
$$k_{5,2} = 0$$
$$k_{5,3} = 0$$
$$k_{5,4} = 0$$
$$k_{5,5} = -C_{a2} - \frac{C_{a2} * b_2}{c_2}$$
$$k_{5,6} = \frac{C_{a2} * b_2}{U_2} - U_2 * m_2 + \frac{C_{a2} * b_2^2}{U_2 * c_2}$$
$$k_{5,7} = \frac{U_2 * Z_2 * m_2}{c_2}$$
$$k_{5,8} = 0$$
$$k_{5,9} = \frac{C_{a3} * b_3}{d_3} + \frac{C_{a3} * b_3 * d_2}{c_2 * d_3}$$
$$k_{5,10} = -\frac{C_{a3} * b_3^2}{U_3 * d_3} - \frac{C_{a3} * b_3^2 * d_2}{U_3 * c_2 * d_3}$$
$$k_{5,11} = -\frac{U_3 * Z_3 * m_3}{d_3} - \frac{U_3 * Z_3 * d_2 * m_3}{c_2 * d_3}$$
$$k_{5,12} = 0$$
$$k_{5,13} = -\frac{C_{a4} * b_4 * c_3}{c_4 * d_3} - \frac{C_{a4} * b_4 * c_3 * d_2}{c_2 * c_4 * d_3}$$
$$k_{5,14} = \frac{C_{a4} * b_4^2 * c_3}{U_4 * c_4 * d_3} + \frac{C_{a4} * b_4^2 * c_3 * d_2}{U_4 * c_2 * c_4 * d_3}$$
$$k_{5,15} = \frac{U_4 * Z_4 * c_3 * m_4}{c_4 * d_3} + \frac{U_4 * Z_4 * c_3 * d_2 * m_4}{c_2 * c_4 * d_3}$$
$$k_{5,16} = 0$$
$$k_{5,17} = \frac{C_{a2} * b_5 * c_3 * d_4}{c_4 * d_3 * d_5} + \frac{C_{a2} * b_5 * c_3 * d_2 * d_4}{c_2 * c_4 * d_3 * d_5}$$
$$k_{5,18} = -\frac{C_{a2} * b_5^2 * c_3 * d_4}{U_5 * c_4 * d_3 * d_5} - \frac{C_{a2} * b_5^2 * c_3 * d_2 * d_4}{U_5 * c_2 * c_4 * d_3 * d_5}$$

$$k_{5,19} = -\frac{U_5 * Z_5 * c_3 * d_4 * m_5}{c_4 * d_3 * d_5} - \frac{U_5 * Z_5 * c_3 * d_2 * d_4 * m_5}{c_2 * c_4 * d_3 * d_5}$$
$$k_{5,20} = 0$$
$$k_{5,21} = -\frac{C_{a2} * b_6 * c_3 * c_5 * d_4}{c_4 * c_6 * d_3 * d_5} - \frac{C_{a2} * b_6 * c_3 * c_5 * d_2 * d_4}{c_2 * c_4 * c_6 * d_3 * d_5}$$
$$k_{5,22} = \frac{C_{a2} * b_6^2 * c_3 * c_5 * d_4}{U_6 * c_4 * c_6 * d_3 * d_5} + \frac{C_{a2} * b_6^2 * c_3 * c_5 * d_2 * d_4}{U_6 * c_2 * c_4 * c_6 * d_3 * d_5}$$
$$k_{5,23} = \frac{U_6 * Z_6 * c_3 * c_5 * d_4 * m_6}{c_4 * c_6 * d_3 * d_5} + \frac{U_6 * Z_6 * c_3 * c_5 * d_2 * d_4 * m_6}{c_2 * c_4 * c_6 * d_3 * d_5}$$
$$k_{5,24} = 0$$
$$k_{6,1} = 0$$
$$k_{6,2} = 0$$
$$k_{6,3} = 0$$
$$k_{6,4} = 0$$
$$k_{6,5} = \frac{C_{a2} * b_2 * f_2}{c_2}$$
$$k_{6,6} = U_2 * Z_2 * m_2 - \frac{C_{a2} * b_2^2 * f_2}{U_2 * c_2}$$
$$k_{6,7} = -L2 - \frac{U_2 * Z_2 * f_2 * m_2}{c_2}$$
$$k_{6,8} = Z_2 * g * m_2 - K2$$
$$k_{6,9} = -\frac{C_{a3} * b_3 * d_2 * f_2}{c_2 * d_3}$$
$$k_{6,10} = \frac{C_{a3} * b_3^2 * d_2 * f_2}{U_3 * c_2 * d_3}$$
$$k_{6,11} = \frac{U_3 * Z_3 * d_2 * f_2 * m_3}{c_2 * d_3}$$
$$k_{6,12} = 0$$
$$k_{6,13} = \frac{C_{a4} * b_4 * c_3 * d_2 * f_2}{c_2 * c_4 * d_3}$$
$$k_{6,14} = -\frac{C_{a4} * b_4^2 * c_3 * d_2 * f_2}{U_4 * c_2 * c_4 * d_3}$$
$$k_{6,15} = -\frac{U_4 * Z_4 * c_3 * d_2 * f_2 * m_4}{c_2 * c_4 * d_3}$$
$$k_{6,16} = 0$$
$$k_{6,17} = -\frac{C_{a2} * b_5 * c_3 * d_2 * d_4 * f_2}{c_2 * c_4 * d_3 * d_5}$$
$$k_{6,18} = \frac{C_{a2} * b_5^2 * c_3 * d_2 * d_4 * f_2}{U_5 * c_2 * c_4 * d_3 * d_5}$$

$$k_{6,19} = \frac{U_5 * Z_5 * c_3 * d_2 * d_4 * f_2 * m_5}{c_2 * c_4 * d_3 * d_5}$$
$$k_{6,20} = 0$$
$$k_{6,21} = \frac{C_{a2} * b_6 * c_3 * c_5 * d_2 * d_4 * f_2}{c_2 * c_4 * c_6 * d_3 * d_5}$$
$$k_{6,22} = -\frac{C_{a2} * b_6^2 * c_3 * c_5 * d_2 * d_4 * f_2}{U_6 * c_2 * c_4 * c_6 * d_3 * d_5}$$
$$k_{6,23} = -\frac{U_6 * Z_6 * c_3 * c_5 * d_2 * d_4 * f_2 * m_6}{c_2 * c_4 * c_6 * d_3 * d_5}$$
$$k_{6,24} = 0$$
$$k_{7,1} = 0$$
$$k_{7,2} = 1$$
$$k_{7,3} = 0$$
$$k_{7,4} = 0$$
$$k_{7,5} = 0$$
$$k_{7,6} = -1$$
$$k_{7,7} = 0$$
$$k_{7,8} = 0$$
$$k_{7,9} = 0$$
$$k_{7,10} = 0$$
$$k_{7,11} = 0$$
$$k_{7,12} = 0$$
$$k_{7,13} = 0$$
$$k_{7,14} = 0$$
$$k_{7,15} = 0$$
$$k_{7,16} = 0$$
$$k_{7,17} = 0$$
$$k_{7,18} = 0$$
$$k_{7,19} = 0$$
$$k_{7,20} = 0$$
$$k_{7,21} = 0$$
$$k_{7,22} = 0$$
$$k_{7,23} = 0$$
$$k_{7,24} = 0$$
$$k_{8,1} = 0$$
$$k_{8,2} = 0$$
$$k_{8,3} = 0$$
$$k_{8,4} = 0$$
$$k_{8,5} = 0$$
$$k_{8,6} = 0$$

$$k_{8,7} = 1$$
$$k_{8,8} = 0$$
$$k_{8,9} = 0$$
$$k_{8,10} = 0$$
$$k_{8,11} = 0$$
$$k_{8,12} = 0$$
$$k_{8,13} = 0$$
$$k_{8,14} = 0$$
$$k_{8,15} = 0$$
$$k_{8,16} = 0$$
$$k_{8,17} = 0$$
$$k_{8,18} = 0$$
$$k_{8,19} = 0$$
$$k_{8,20} = 0$$
$$k_{8,21} = 0$$
$$k_{8,22} = 0$$
$$k_{8,23} = 0$$
$$k_{8,24} = 0$$
$$k_{9,1} = 0$$
$$k_{9,2} = 0$$
$$k_{9,3} = 0$$
$$k_{9,4} = 0$$
$$k_{9,5} = 0$$
$$k_{9,6} = 0$$
$$k_{9,7} = 0$$
$$k_{9,8} = 0$$
$$k_{9,9} = -C_{a3} - \frac{C_{a3} * b_3}{d_3}$$
$$k_{9,10} = \frac{C_{a3} * b_3}{U_3} - U_3 * m_3 + \frac{C_{a3} * b_3^2}{U_3 * d_3}$$
$$k_{9,11} = \frac{U_3 * Z_3 * m_3}{d_3}$$
$$k_{9,12} = 0$$
$$k_{9,13} = \frac{C_{a4} * b_4}{c_4} + \frac{C_{a4} * b_4 * c_3}{c_4 * d_3}$$
$$k_{9,14} = -\frac{C_{a4} * b_4^2}{U_4 * c_4} - \frac{C_{a4} * b_4^2 * c_3}{U_4 * c_4 * d_3}$$
$$k_{9,15} = -\frac{U_4 * Z_4 * m_4}{c_4} - \frac{U_4 * Z_4 * c_3 * m_4}{c_4 * d_3}$$
$$k_{9,16} = 0$$

$$k_{9,17} = -\frac{C_{a2} * b_5 * d_4}{c_4 * d_5} - \frac{C_{a2} * b_5 * c_3 * d_4}{c_4 * d_3 * d_5}$$
$$k_{9,18} = \frac{C_{a2} * b_5^2 * d_4}{U_5 * c_4 * d_5} + \frac{C_{a2} * b_5^2 * c_3 * d_4}{U_5 * c_4 * d_3 * d_5}$$
$$k_{9,19} = \frac{U_5 * Z_5 * d_4 * m_5}{c_4 * d_5} + \frac{U_5 * Z_5 * c_3 * d_4 * m_5}{c_4 * d_3 * d_5}$$
$$k_{9,20} = 0$$
$$k_{9,21} = \frac{C_{a2} * b_6 * c_5 * d_4}{c_4 * c_6 * d_5} + \frac{C_{a2} * b_6 * c_3 * c_5 * d_4}{c_4 * c_6 * d_3 * d_5}$$
$$k_{9,22} = -\frac{C_{a2} * b_6^2 * c_5 * d_4}{U_6 * c_4 * c_6 * d_5} - \frac{C_{a2} * b_6^2 * c_3 * c_5 * d_4}{U_6 * c_4 * c_6 * d_3 * d_5}$$
$$k_{9,23} = -\frac{U_6 * Z_6 * c_5 * d_4 * m_6}{c_4 * c_6 * d_5} - \frac{U_6 * Z_6 * c_3 * c_5 * d_4 * m_6}{c_4 * c_6 * d_3 * d_5}$$
$$k_{9,24} = 0$$
$$k_{10,1} = 0$$
$$k_{10,2} = 0$$
$$k_{10,3} = 0$$
$$k_{10,4} = 0$$
$$k_{10,5} = 0$$
$$k_{10,6} = 0$$
$$k_{10,7} = 0$$
$$k_{10,8} = 0$$
$$k_{10,9} = 0$$
$$k_{10,10} = U_3 * Z_3 * m_3$$
$$k_{10,11} = -L3$$
$$k_{10,12} = Z_3 * g * m_3 - K3$$
$$k_{10,13} = -\frac{C_{a4} * \quad {}_4 * f_3}{c_4}$$
$$k_{10,14} = \frac{C_{a4} * b_4^2 * f_3}{U_4 * c_4}$$
$$k_{10,15} = \frac{U_4 * Z_4 * f_3 * m_4}{c_4}$$
$$k_{10,16} = 0$$
$$k_{10,17} = \frac{C_{a2} * b_5 * d_4 * f_3}{c_4 * d_5}$$
$$k_{10,18} = -\frac{C_{a2} * b_5^2 * d_4 * f_3}{U_5 * c_4 * d_5}$$
$$k_{10,19} = -\frac{U_5 * Z_5 * d_4 * f_3 * m_5}{c_4 * d_5}$$
$$k_{10,20} = 0$$

$$k_{10,21} = -\frac{C_{a2} * b_6 * c_5 * d_4 * f_3}{c_4 * c_6 * d_5}$$
$$k_{10,22} = \frac{C_{a2} * b_6^2 * c_5 * d_4 * f_3}{U_6 * c_4 * c_6 * d_5}$$
$$k_{10,23} = \frac{U_6 * Z_6 * c_5 * d_4 * f_3 * m_6}{c_4 * c_6 * d_5}$$
$$k_{10,24} = 0$$
$$k_{11,1} = 0$$
$$k_{11,2} = 0$$
$$k_{11,3} = 0$$
$$k_{11,4} = 0$$
$$k_{11,5} = 0$$
$$k_{11,6} = 1$$
$$k_{11,7} = 0$$
$$k_{11,8} = 0$$
$$k_{11,9} = 0$$
$$k_{11,10} = -1$$
$$k_{11,11} = 0$$
$$k_{11,12} = 0$$
$$k_{11,13} = 0$$
$$k_{11,14} = 0$$
$$k_{11,15} = 0$$
$$k_{11,16} = 0$$
$$k_{11,17} = 0$$
$$k_{11,18} = 0$$
$$k_{11,19} = 0$$
$$k_{11,20} = 0$$
$$k_{11,21} = 0$$
$$k_{11,22} = 0$$
$$k_{11,23} = 0$$
$$k_{11,24} = 0$$
$$k_{12,1} = 0$$
$$k_{12,2} = 0$$
$$k_{12,3} = 0$$
$$k_{12,4} = 0$$
$$k_{12,5} = 0$$
$$k_{12,6} = 0$$
$$k_{12,7} = 0$$
$$k_{12,8} = 0$$
$$k_{12,9} = 0$$

$$k_{12,10} = 0$$
$$k_{12,11} = 1$$
$$k_{12,12} = 0$$
$$k_{12,13} = 0$$
$$k_{12,14} = 0$$
$$k_{12,15} = 0$$
$$k_{12,16} = 0$$
$$k_{12,17} = 0$$
$$k_{12,18} = 0$$
$$k_{12,19} = 0$$
$$k_{12,20} = 0$$
$$k_{12,21} = 0$$
$$k_{12,22} = 0$$
$$k_{12,23} = 0$$
$$k_{12,24} = 0$$
$$k_{13,1} = 0$$
$$k_{13,2} = 0$$
$$k_{13,3} = 0$$
$$k_{13,4} = 0$$
$$k_{13,5} = 0$$
$$k_{13,6} = 0$$
$$k_{13,7} = 0$$
$$k_{13,8} = 0$$
$$k_{13,9} = 0$$
$$k_{13,10} = 0$$
$$k_{13,11} = 0$$
$$k_{13,12} = 0$$
$$k_{13,13} = -C_{a4} - \frac{C_{a4} * b_4}{c_4}$$
$$k_{13,14} = \frac{C_{a4} * b_4}{U_4} - U_4 * m_4 + \frac{C_{a4} * b_4^2}{U_4 * c_4}$$
$$k_{13,15} = \frac{U_4 * Z_4 * m_4}{c_4}$$
$$k_{13,16} = 0$$
$$k_{13,17} = \frac{C_{a2} * b_5}{d_5} + \frac{C_{a2} * b_5 * d_4}{c_4 * d_5}$$
$$k_{13,18} = -\frac{C_{a2} * b_5^2}{U_5 * d_5} - \frac{C_{a2} * b_5^2 * d_4}{U_5 * c_4 * d_5}$$
$$k_{13,19} = -\frac{U_5 * Z_5 * m_5}{d_5} - \frac{U_5 * Z_5 * d_4 * m_5}{c_4 * d_5}$$

$$k_{13,20} = 0$$
$$k_{13,21} = -\frac{C_{a2} * b_6 * c_5}{c_6 * d_5} - \frac{C_{a2} * b_6 * c_5 * d_4}{c_4 * c_6 * d_5}$$
$$k_{13,22} = \frac{C_{a2} * b_6^2 * c_5}{U_6 * c_6 * d_5} + \frac{C_{a2} * b_6^2 * c_5 * d_4}{U_6 * c_4 * c_6 * d_5}$$
$$k_{13,23} = \frac{U_6 * Z_6 * c_5 * m_6}{c_6 * d_5} + \frac{U_6 * Z_6 * c_5 * d_4 * m_6}{c_4 * c_6 * d_5}$$
$$k_{13,24} = 0$$
$$k_{14,1} = 0$$
$$k_{14,2} = 0$$
$$k_{14,3} = 0$$
$$k_{14,4} = 0$$
$$k_{14,5} = 0$$
$$k_{14,6} = 0$$
$$k_{14,7} = 0$$
$$k_{14,8} = 0$$
$$k_{14,9} = 0$$
$$k_{14,10} = 0$$
$$k_{14,11} = 0$$
$$k_{14,12} = 0$$
$$k_{14,13} = \frac{C_{a4} * b_4 * f_4}{c_4}$$
$$k_{14,14} = U_4 * Z_4 * m_4 - \frac{C_{a4} * b_4^2 * f_4}{U_4 * c_4}$$
$$k_{14,15} = -L4 - \frac{U_4 * Z_4 * f_4 * m_4}{c_4}$$
$$k_{14,16} = Z_4 * g * m_4 - K4$$
$$k_{14,17} = -\frac{C_{a2} * b_5 * d_4 * f_4}{c_4 * d_5}$$
$$k_{14,18} = \frac{C_{a2} * b_5^2 * d_4 * f_4}{U_5 * c_4 * d_5}$$
$$k_{14,19} = \frac{U_5 * Z_5 * d_4 * f_4 * m_5}{c_4 * d_5}$$
$$k_{14,20} = 0$$
$$k_{14,21} = \frac{C_{a2} * b_6 * c_5 * d_4 * f_4}{c_4 * c_6 * d_5}$$
$$k_{14,22} = -\frac{C_{a2} * b_6^2 * c_5 * d_4 * f_4}{U_6 * c_4 * c_6 * d_5}$$
$$k_{14,23} = -\frac{U_6 * Z_6 * c_5 * d_4 * f_4 * m_6}{c_4 * c_6 * d_5}$$

$$k_{14,24} = 0$$
$$k_{15,1} = 0$$
$$k_{15,2} = 0$$
$$k_{15,3} = 0$$
$$k_{15,4} = 0$$
$$k_{15,5} = 0$$
$$k_{15,6} = 0$$
$$k_{15,7} = 0$$
$$k_{15,8} = 0$$
$$k_{15,9} = 0$$
$$k_{15,10} = 1$$
$$k_{15,11} = 0$$
$$k_{15,12} = 0$$
$$k_{15,13} = 0$$
$$k_{15,14} = -1$$
$$k_{15,15} = 0$$
$$k_{15,16} = 0$$
$$k_{15,17} = 0$$
$$k_{15,18} = 0$$
$$k_{15,19} = 0$$
$$k_{15,20} = 0$$
$$k_{15,21} = 0$$
$$k_{15,22} = 0$$
$$k_{15,23} = 0$$
$$k_{15,24} = 0$$
$$k_{16,1} = 0$$
$$k_{16,2} = 0$$
$$k_{16,3} = 0$$
$$k_{16,4} = 0$$
$$k_{16,5} = 0$$
$$k_{16,6} = 0$$
$$k_{16,7} = 0$$
$$k_{16,8} = 0$$
$$k_{16,9} = 0$$
$$k_{16,10} = 0$$
$$k_{16,11} = 0$$
$$k_{16,12} = 0$$
$$k_{16,13} = 0$$
$$k_{16,14} = 0$$
$$k_{16,15} = 1$$

$$k_{16,16} = 0$$
$$k_{16,17} = 0$$
$$k_{16,18} = 0$$
$$k_{16,19} = 0$$
$$k_{16,20} = 0$$
$$k_{16,21} = 0$$
$$k_{16,22} = 0$$
$$k_{16,23} = 0$$
$$k_{16,24} = 0$$
$$k_{17,1} = 0$$
$$k_{17,2} = 0$$
$$k_{17,3} = 0$$
$$k_{17,4} = 0$$
$$k_{17,5} = 0$$
$$k_{17,6} = 0$$
$$k_{17,7} = 0$$
$$k_{17,8} = 0$$
$$k_{17,9} = 0$$
$$k_{17,10} = 0$$
$$k_{17,11} = 0$$
$$k_{17,12} = 0$$
$$k_{17,13} = 0$$
$$k_{17,14} = 0$$
$$k_{17,15} = 0$$
$$k_{17,16} = 0$$
$$k_{17,17} = -C_{a2} - \frac{C_{a2} * b_5}{d_5}$$
$$k_{17,18} = \frac{C_{a2} * b_5}{U_5} - U_5 * m_5 + \frac{C_{a2} * b_5^2}{U_5 * d_5}$$
$$_{17,19} = \frac{U_5 * Z_5 * m_5}{d_5}$$
$$k_{17,20} = 0$$
$$k_{17,21} = \frac{C_{a2} * b_6}{c_6} + \frac{C_{a2} * b_6 * c_5}{c_6 * d_5}$$
$$k_{17,22} = -\frac{C_{a2} * b_6^2}{U_6 * c_6} - \frac{C_{a2} * b_6^2 * c_5}{U_6 * c_6 * d_5}$$
$$k_{17,23} = -\frac{U_6 * Z_6 * m_6}{c_6} - \frac{U_6 * Z_6 * c_5 * m_6}{c_6 * d_5}$$
$$k_{17,24} = 0$$
$$k_{18,1} = 0$$

$$k_{18,2} = 0$$
$$k_{18,3} = 0$$
$$k_{18,4} = 0$$
$$k_{18,5} = 0$$
$$k_{18,6} = 0$$
$$k_{18,7} = 0$$
$$k_{18,8} = 0$$
$$k_{18,9} = 0$$
$$k_{18,10} = 0$$
$$k_{18,11} = 0$$
$$k_{18,12} = 0$$
$$k_{18,13} = 0$$
$$k_{18,14} = 0$$
$$k_{18,15} = 0$$
$$k_{18,16} = 0$$
$$k_{18,17} = 0$$
$$k_{18,18} = U_5 * Z_5 * m_5$$
$$k_{18,19} = -L5$$
$$k_{18,20} = Z_5 * g * m_5 - K5$$
$$k_{18,21} = -\frac{C_{a2} * b_6 * f_5}{c_6}$$
$$k_{18,22} = \frac{C_{a2} * b_6^2 * f_5}{U_6 * c_6}$$
$$k_{18,23} = \frac{U_6 * Z_6 * f_5 * m_6}{c_6}$$
$$k_{18,24} = 0$$
$$k_{19,1} = 0$$
$$k_{19,2} = 0$$
$$k_{19,3} = 0$$
$$k_{19,4} = 0$$
$$k_{19,5} = 0$$
$$k_{19,6} = 0$$
$$k_{19,7} = 0$$
$$k_{19,8} = 0$$
$$k_{19,9} = 0$$
$$k_{19,10} = 0$$
$$k_{19,11} = 0$$
$$k_{19,12} = 0$$
$$k_{19,13} = 0$$
$$k_{19,14} = 1$$

$$k_{19,15} = 0$$
$$k_{19,16} = 0$$
$$k_{19,17} = 0$$
$$k_{19,18} = -1$$
$$k_{19,19} = 0$$
$$k_{19,20} = 0$$
$$k_{19,21} = 0$$
$$k_{19,22} = 0$$
$$k_{19,23} = 0$$
$$k_{19,24} = 0$$
$$k_{20,1} = 0$$
$$k_{20,2} = 0$$
$$k_{20,3} = 0$$
$$k_{20,4} = 0$$
$$k_{20,5} = 0$$
$$k_{20,6} = 0$$
$$k_{20,7} = 0$$
$$k_{20,8} = 0$$
$$k_{20,9} = 0$$
$$k_{20,10} = 0$$
$$k_{20,11} = 0$$
$$k_{20,12} = 0$$
$$k_{20,13} = 0$$
$$k_{20,14} = 0$$
$$k_{20,15} = 0$$
$$k_{20,16} = 0$$
$$k_{20,17} = 0$$
$$k_{20,18} = 0$$
$$k_{20,19} = 1$$
$$k_{20,20} = 0$$
$$k_{20,21} = 0$$
$$k_{20,22} = 0$$
$$k_{20,23} = 0$$
$$k_{20,24} = 0$$
$$k_{21,1} = 0$$
$$k_{21,2} = 0$$
$$k_{21,3} = 0$$
$$k_{21,4} = 0$$
$$k_{21,5} = 0$$
$$k_{21,6} = 0$$

$$k_{21,7} = 0$$
$$k_{21,8} = 0$$
$$k_{21,9} = 0$$
$$k_{21,10} = 0$$
$$k_{21,11} = 0$$
$$k_{21,12} = 0$$
$$k_{21,13} = 0$$
$$k_{21,14} = 0$$
$$k_{21,15} = 0$$
$$k_{21,16} = 0$$
$$k_{21,17} = 0$$
$$k_{21,18} = 0$$
$$k_{21,19} = 0$$
$$k_{21,20} = 0$$
$$k_{21,21} = -C_{a2} - \frac{C_{a2} * b_6}{c_6}$$
$$k_{21,22} = \frac{C_{a2} * b_6}{U_6} - U_6 * m_6 + \frac{C_{a2} * b_6^2}{U_6 * c_6}$$
$$k_{21,23} = \frac{U_6 * Z_6 * m_6}{c_6}$$
$$k_{21,24} = 0$$
$$k_{22,1} = 0$$
$$k_{22,2} = 0$$
$$k_{22,3} = 0$$
$$k_{22,4} = 0$$
$$k_{22,5} = 0$$
$$k_{22,6} = 0$$
$$k_{22,7} = 0$$
$$k_{22,8} = 0$$
$$k_{22,9} = 0$$
$$k_{22,10} = 0$$
$$k_{22,11} = 0$$
$$k_{22,12} = 0$$
$$k_{22,13} = 0$$
$$k_{22,14} = 0$$
$$k_{22,15} = 0$$
$$k_{22,16} = 0$$
$$k_{22,17} = 0$$
$$k_{22,18} = 0$$
$$k_{22,19} = 0$$

$$k_{22,20} = 0$$
$$k_{22,21} = \frac{C_{a2} * b_6 * f_6}{c_6}$$
$$k_{22,22} = U_6 * Z_6 * m_6 - \frac{C_{a2} * b_6^2 * f_6}{U_6 * c_6}$$
$$k_{22,23} = -L6 - \frac{U_6 * Z_6 * f_6 * m_6}{c_6}$$
$$k_{22,24} = Z_6 * g * m_6 - K6$$
$$k_{23,1} = 0$$
$$k_{23,2} = 0$$
$$k_{23,3} = 0$$
$$k_{23,4} = 0$$
$$k_{23,5} = 0$$
$$k_{23,6} = 0$$
$$k_{23,7} = 0$$
$$k_{23,8} = 0$$
$$k_{23,9} = 0$$
$$k_{23,10} = 0$$
$$k_{23,11} = 0$$
$$k_{23,12} = 0$$
$$k_{23,13} = 0$$
$$k_{23,14} = 0$$
$$k_{23,15} = 0$$
$$k_{23,16} = 0$$
$$k_{23,17} = 0$$
$$k_{23,18} = 1$$
$$k_{23,19} = 0$$
$$k_{23,20} = 0$$
$$k_{23,21} = 0$$
$$k_{23,22} = -1$$
$$k_{23,23} = 0$$
$$k_{23,24} = 0$$
$$k_{24,1} = 0$$
$$k_{24,2} = 0$$
$$k_{24,3} = 0$$
$$k_{24,4} = 0$$
$$k_{24,5} = 0$$
$$k_{24,6} = 0$$
$$k_{24,7} = 0$$
$$k_{24,8} = 0$$

$$k_{24,9} = 0$$
$$k_{24,10} = 0$$
$$k_{24,11} = 0$$
$$k_{24,12} = 0$$
$$k_{24,13} = 0$$
$$k_{24,14} = 0$$
$$k_{24,15} = 0$$
$$k_{24,16} = 0$$
$$k_{24,17} = 0$$
$$k_{24,18} = 0$$
$$k_{24,19} = 0$$
$$k_{24,20} = 0$$
$$k_{24,21} = 0$$
$$k_{24,22} = 0$$
$$k_{24,23} = 1$$
$$k_{24,24} = 0$$

G.3. Control Matrix

$$c_{1,1} = C_{af}$$
$$c_{1,2} = 0$$
$$c_{1,3} = 0$$
$$c_{1,4} = \frac{1}{c_2}$$
$$c_{1,5} = -\frac{d_2}{c_2 * d_3}$$
$$c_{1,6} = \frac{c_3 * d_2}{c_2 * c_4 * d_3}$$
$$c_{1,7} = -\frac{c_3 * d_2 * d_4}{c_2 * c_4 * d_3 * d_5}$$
$$c_{1,8} = \frac{c_3 * c_5 * d_2 * d_4}{c_2 * c_4 * c_6 * d_3 * d_5}$$
$$c_{2,1} = C_{af} * a_1$$
$$c_{2,2} = 1$$
$$c_{2,3} = 1$$
$$c_{2,4} = -\frac{c_1}{c_2}$$
$$c_{2,5} = \frac{c_1 * d_2}{c_2 * d_3}$$

G-10

$$c_{2,6} = -\frac{c_1 * c_3 * d_2}{c_2 * c_4 * d_3}$$
$$c_{2,7} = \frac{c_1 * c_3 * d_2 * d_4}{c_2 * c_4 * d_3 * d_5}$$
$$c_{2,8} = -\frac{c_1 * c_3 * c_5 * d_2 * d_4}{c_2 * c_4 * c_6 * d_3 * d_5}$$
$$c_{3,1} = 0$$
$$c_{3,2} = 0$$
$$c_{3,3} = 0$$
$$c_{3,4} = -\frac{f_1}{c_2}$$
$$c_{3,5} = \frac{d_2 * f_1}{c_2 * d_3}$$
$$c_{3,6} = -\frac{c_3 * d_2 * f_1}{c_2 * c_4 * d_3}$$
$$c_{3,7} = \frac{c_3 * d_2 * d_4 * f_1}{c_2 * c_4 * d_3 * d_5}$$
$$c_{3,8} = -\frac{c_3 * c_5 * d_2 * d_4 * f_1}{c_2 * c_4 * c_6 * d_3 * d_5}$$
$$c_{4,1} = 0$$
$$c_{4,2} = 0$$
$$c_{4,3} = 0$$
$$c_{4,4} = 0$$
$$c_{4,5} = 0$$
$$c_{4,6} = 0$$
$$c_{4,7} = 0$$
$$c_{4,8} = 0$$
$$c_{5,1} = 0$$
$$c_{5,2} = 0$$
$$c_{5,3} = 0$$
$$c_{5,4} = -\frac{1}{c_2}$$
$$c_{5,5} = \frac{1}{d_3} + \frac{d_2}{c_2 * d_3}$$
$$c_{5,6} = -\frac{c_3}{c_4 * d_3} - \frac{c_3 * d_2}{c_2 * c_4 * d_3}$$
$$c_{5,7} = \frac{c_3 * d_4}{c_4 * d_3 * d_5} + \frac{c_3 * d_2 * d_4}{c_2 * c_4 * d_3 * d_5}$$
$$c_{5,8} = -\frac{c_3 * c_5 * d_4}{c_4 * c_6 * d_3 * d_5} - \frac{c_3 * c_5 * d_2 * d_4}{c_2 * c_4 * c_6 * d_3 * d_5}$$
$$c_{6,1} = 0$$

$$c_{6,2} = 0$$
$$c_{6,3} = 0$$
$$c_{6,4} = \frac{f_2}{c_2}$$
$$c_{6,5} = -\frac{d_2 * f_2}{c_2 * d_3}$$
$$c_{6,6} = \frac{c_3 * d_2 * f_2}{c_2 * c_4 * d_3}$$
$$c_{6,7} = -\frac{c_3 * d_2 * d_4 * f_2}{c_2 * c_4 * d_3 * d_5}$$
$$c_{6,8} = \frac{c_3 * c_5 * d_2 * d_4 * f_2}{c_2 * c_4 * c_6 * d_3 * d_5}$$
$$c_{7,1} = 0$$
$$c_{7,2} = 0$$
$$c_{7,3} = 0$$
$$c_{7,4} = 0$$
$$c_{7,5} = 0$$
$$c_{7,6} = 0$$
$$c_{7,7} = 0$$
$$c_{7,8} = 0$$
$$c_{8,1} = 0$$
$$c_{8,2} = 0$$
$$c_{8,3} = 0$$
$$c_{8,4} = 0$$
$$c_{8,5} = 0$$
$$c_{8,6} = 0$$
$$c_{8,7} = 0$$
$$c_{8,8} = 0$$
$$c_{9,1} = 0$$
$$c_{9,2} = 0$$
$$c_{9,3} = 0$$
$$c_{9,4} = 0$$
$$c_{9,5} = -\frac{1}{d_3}$$
$$c_{9,6} = \frac{1}{c_4} + \frac{c_3}{c_4 * d_3}$$
$$c_{9,7} = -\frac{d_4}{c_4 * d_5} - \frac{c_3 * d_4}{c_4 * d_3 * d_5}$$
$$c_{9,8} = \frac{c_5 * d_4}{c_4 * c_6 * d_5} + \frac{c_3 * c_5 * d_4}{c_4 * c_6 * d_3 * d_5}$$

$$c_{10,1} = 0$$
$$c_{10,2} = 0$$
$$c_{10,3} = 0$$
$$c_{10,4} = 0$$
$$c_{10,5} = 0$$
$$c_{10,6} = -\frac{f_3}{c_4}$$
$$c_{10,7} = \frac{d_4 * f_3}{c_4 * d_5}$$
$$c_{10,8} = -\frac{c_5 * d_4 * f_3}{c_4 * c_6 * d_5}$$
$$c_{11,1} = 0$$
$$c_{11,2} = 0$$
$$c_{11,3} = 0$$
$$c_{11,4} = 0$$
$$c_{11,5} = 0$$
$$c_{11,6} = 0$$
$$c_{11,7} = 0$$
$$c_{11,8} = 0$$
$$c_{12,1} = 0$$
$$c_{12,2} = 0$$
$$c_{12,3} = 0$$
$$c_{12,4} = 0$$
$$c_{12,5} = 0$$
$$c_{12,6} = 0$$
$$c_{12,7} = 0$$
$$c_{12,8} = 0$$
$$c_{13,1} = 0$$
$$c_{13,2} = 0$$
$$c_{13,3} = 0$$
$$c_{13,4} = 0$$
$$c_{13,5} = 0$$
$$c_{13,6} = -\frac{1}{c_4}$$
$$c_{13,7} = \frac{1}{d_5} + \frac{d_4}{c_4 * d_5}$$
$$c_{13,8} = -\frac{c_5}{c_6 * d_5} - \frac{c_5 * d_4}{c_4 * c_6 * d_5}$$
$$c_{14,1} = 0$$
$$c_{14,2} = 0$$

$$c_{14,3} = 0$$
$$c_{14,4} = 0$$
$$c_{14,5} = 0$$
$$c_{14,6} = \frac{f_4}{c_4}$$
$$c_{14,7} = -\frac{d_4 * f_4}{c_4 * d_5}$$
$$c_{14,8} = \frac{c_5 * d_4 * f_4}{c_4 * c_6 * d_5}$$
$$c_{15,1} = 0$$
$$c_{15,2} = 0$$
$$c_{15,3} = 0$$
$$c_{15,4} = 0$$
$$c_{15,5} = 0$$
$$c_{15,6} = 0$$
$$c_{15,7} = 0$$
$$c_{15,8} = 0$$
$$c_{16,1} = 0$$
$$c_{16,2} = 0$$
$$c_{16,3} = 0$$
$$c_{16,4} = 0$$
$$c_{16,5} = 0$$
$$c_{16,6} = 0$$
$$c_{16,7} = 0$$
$$c_{16,8} = 0$$
$$c_{17,1} = 0$$
$$c_{17,2} = 0$$
$$c_{17,3} = 0$$
$$c_{17,4} = 0$$
$$c_{17,5} = 0$$
$$c_{17,6} = 0$$
$$c_{17,7} = -\frac{1}{d_5}$$
$$c_{17,8} = \frac{1}{c_6} + \frac{c_5}{c_6 * d_5}$$
$$c_{18,1} = 0$$
$$c_{18,2} = 0$$
$$c_{18,3} = 0$$
$$c_{18,4} = 0$$
$$c_{18,5} = 0$$

$$c_{18,6} = 0$$
$$c_{18,7} = 0$$
$$c_{18,8} = -\frac{f_5}{c_6}$$
$$c_{19,1} = 0$$
$$c_{19,2} = 0$$
$$c_{19,3} = 0$$
$$c_{19,4} = 0$$
$$c_{19,5} = 0$$
$$c_{19,6} = 0$$
$$c_{19,7} = 0$$
$$c_{19,8} = 0$$
$$c_{20,1} = 0$$
$$c_{20,2} = 0$$
$$c_{20,3} = 0$$
$$c_{20,4} = 0$$
$$c_{20,5} = 0$$
$$c_{20,6} = 0$$
$$c_{20,7} = 0$$
$$c_{20,8} = 0$$
$$c_{21,1} = 0$$
$$c_{21,2} = 0$$
$$c_{21,3} = 0$$
$$c_{21,4} = 0$$
$$c_{21,5} = 0$$
$$c_{21,6} = 0$$
$$c_{21,7} = 0$$
$$c_{21,8} = -\frac{1}{c_6}$$
$$c_{22,1} = 0$$
$$c_{22,2} = 0$$
$$c_{22,3} = 0$$
$$c_{22,4} = 0$$
$$c_{22,5} = 0$$
$$c_{22,6} = 0$$
$$c_{22,7} = 0$$
$$c_{22,8} = \frac{f_6}{c_6}$$
$$c_{23,1} = 0$$
$$c_{23,2} = 0$$

$$c_{23,3} = 0$$
$$c_{23,4} = 0$$
$$c_{23,5} = 0$$
$$c_{23,6} = 0$$
$$c_{23,7} = 0$$
$$c_{23,8} = 0$$
$$c_{24,1} = 0$$
$$c_{24,2} = 0$$
$$c_{24,3} = 0$$
$$c_{24,4} = 0$$
$$c_{24,5} = 0$$
$$c_{24,6} = 0$$
$$c_{24,7} = 0$$
$$c_{24,8} = 0$$

APPENDIX H

KALMAN FILTERING OF STATES

The basic premise behind the state estimation method used in this work was to break the historical interdependence between parameter estimation and state determination (Section 2.3). To that end, direct measurements using inertial measurement units (IMU) and global position systems (GPS) were combined using Kalman filtering techniques and kinematic models to determine the vehicle states. The Kalman filtering process use in this work is a combination of techniques proposed by Ryu (Ryu & Gerdes, 2004) and Bevly (Bevly, 2004) with the data on sensor noise / bias / etc. from Ryu and Bevly as well (Bevly, 2004; Bevly et al., 2006; Ryu & Gerdes, 2004).

H.1. General Kalman Filter Model

The basic idea used for all state estimations is to take the imu data (accelerations and rotational rates) and integrate them to get angular motions and velocities. These integrations are very sensitive to bias so the GPS data is used (when available) to correct the integration. Through this method, accurate state data could be determined as well as the identification of any bias (road crown for example).

H.1.1. Sensor data

The basic sensor data available had the following Gaussian noise levels inherent in the measurements (Table H-1). Again, as this research was limited by a lack of hardware to test, the data here was drawn from published work by Ryu and Bevly (Bevly, 2004; Bevly et al., 2006; Ryu & Gerdes, 2004).

Table H-1: Sensor Gaussian Noise

Measurement	Gaussian Noise
Ax, Ay	0.006 m/s
Yaw rate, Rollrate	0.0052 rad/s
Vx, Vy	0.02 m/s
Heading, Yaw	0.00087 rad
Grade slope	0.0017 rad
Markov Time Constant	100 s

H.1.2. General Kalman Model

For each state evaluation below, the particular data sets required for that filter will be provided. However, the generalized Kalman filter is presented here for all cases. The same Kalman arrangement was used for all state estimations.

The basic model of the system was a LTI system with Gaussian process noise (B_w) and measurement noise (v) (Equations H-1 and H-2). A and B are the traditional LTI state and input matrices with one exception. There are two variants of the A and B_w matrices to account for the implementation of the GPS signal. Normally, the traditional form is used but when the GPS is active, the time constant effect from the GPS data latency is included. In all cases, the matrices will be derived with the GPS effects. To get the normal form, set all $-\frac{1}{\tau_b}$ terms to zero. Note: This general process was derived from the work by Bevly (Bevly, 2004).

$$\dot{x} = A * x + B * u + B_w * w \qquad \textbf{H-1}$$

$$y = C * x + v \qquad \textbf{H-2}$$

The process noise vector (w) with covariance (Q_c) (Equation H-3) was derived from the sensor noise and is the same size as A since it represents the process noise in the system. The measurement noise covariance (R_v – Equation H-4) was derived from the GPS noise and is the same size as C since reflects noise in the observation. Note: R_v was also used to update the system to remove bias. Together these captured the Gaussian noise affecting the state estimation.

$$E[w^2] = Q_c = \begin{bmatrix} R_v & 0 \\ 0 & \sigma \end{bmatrix} \quad \textbf{H-3}$$

$$R_v = T_s * \sigma \quad \textbf{H-4}$$

The process began with the determination of the matrices. For this example, the yaw calculation is illustrated. The state equation (Equation H-1) became Equation H-5 and the output equation (Equation H-2) became Equation H-6. The parameters were as follows:

- ψ_i is the integrated imu yaw angle
- b_r is the yaw rate bias
- g_r is the measured yaw rate
- T_s is the sample time
- σ_g is the gyro sensor noise (Gaussian)
- σ_b is the gyro bias noise (Gaussian)

$$\begin{bmatrix} \dot{\psi}_i \\ \dot{b}_r \end{bmatrix} = \begin{bmatrix} 0 & -1 \\ 0 & -\frac{1}{\tau_b} \end{bmatrix} * \begin{bmatrix} \psi_i \\ b_r \end{bmatrix} + \begin{bmatrix} 1 \\ 0 \end{bmatrix} * [g_r] + \begin{bmatrix} 1 & 0 \\ 0 & -\frac{1}{\tau_b} \end{bmatrix} * \begin{bmatrix} T_s * \sigma_g^2 & 0 \\ 0 & \sigma_b^2 \end{bmatrix} \quad \textbf{H-5}$$

$$\psi_{GPS} = [1 \quad 0] * \begin{bmatrix} \psi_i \\ g_b \end{bmatrix} + \begin{bmatrix} \frac{\sigma_{GPS}^2}{V} \end{bmatrix} \quad \textbf{H-6}$$

Once Equations H-5 and H-6 were converted to discrete form, the process solution process could begin. As there are many good descriptions on Kalman filter design, only the steps of the process are presented here (Bennett & Norman, 2006; Bevly, 2004; Kalman, 1960; Venhovens & Naab, 1999; Wenzel et al., 2006; Wenzel et al., 2007). At each time step, the states (desired measurements and bias) were updated using standard discrete time step methods. When the GPS was available, the error between the estimated yaw and measured yaw was evaluated (Equation H-7) and used to calculate the Kalman gain (K) (Equation H-10). The states were then corrected (Equation H-11) and the Kalman gain updated (Equation H-12). Note P is the state estimation covariance matrix and is usually zeros initially.

$$V = Y_m - Y_{GPS} \quad \textbf{H-7}$$

$$P = A * P * A' + Q_c \quad \textbf{H-8}$$

$$S = C * P * C' + R_v \quad \textbf{H-9}$$

$$K = P * \frac{C'}{S} \quad \textbf{H-10}$$

$$X = X + (K * V)' \quad \textbf{H-11}$$

$$P = (I - K * C) * P \quad \textbf{H-12}$$

H.2. Measurement Sequence

The first step in the solution process was the collection of imu data as show in Figure H-1 and Figure H-2.

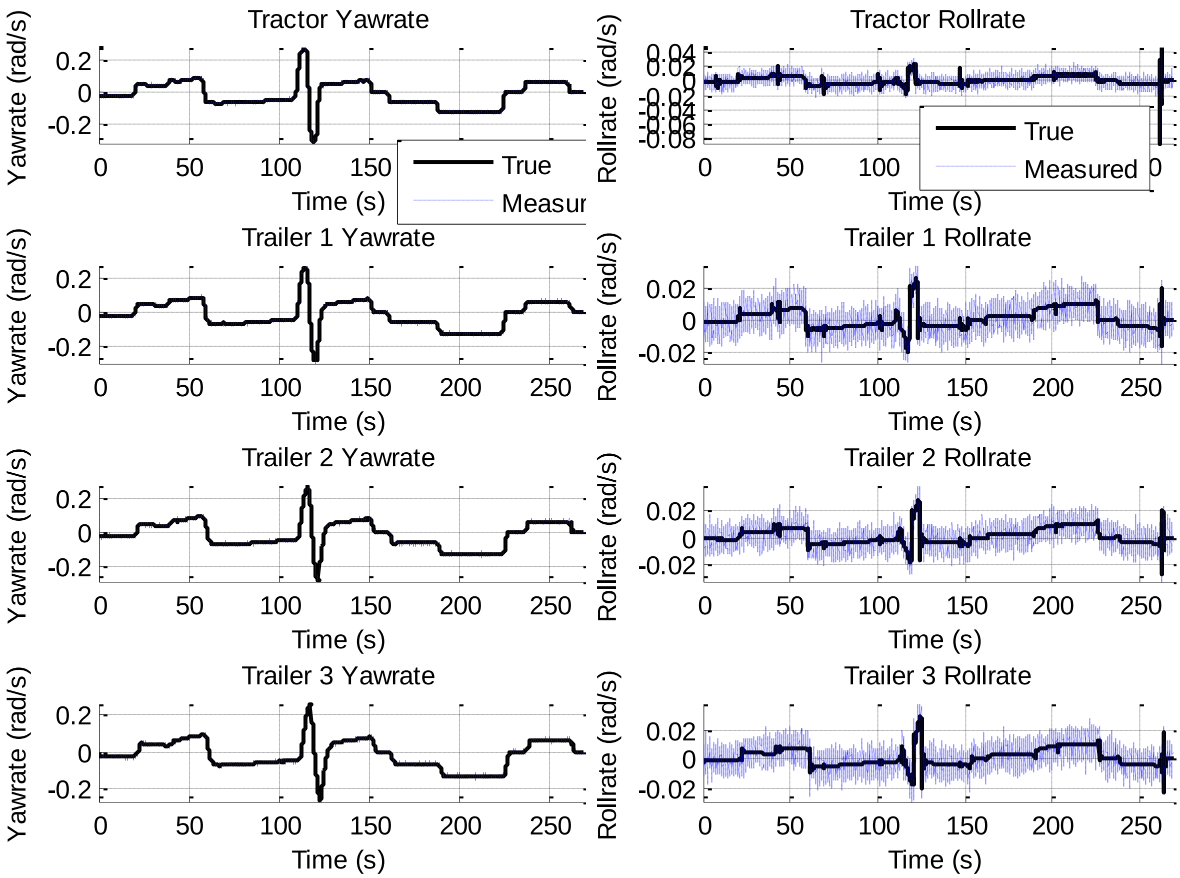

Figure H-1: IMU Data (Yaw Rate and Rollrate)

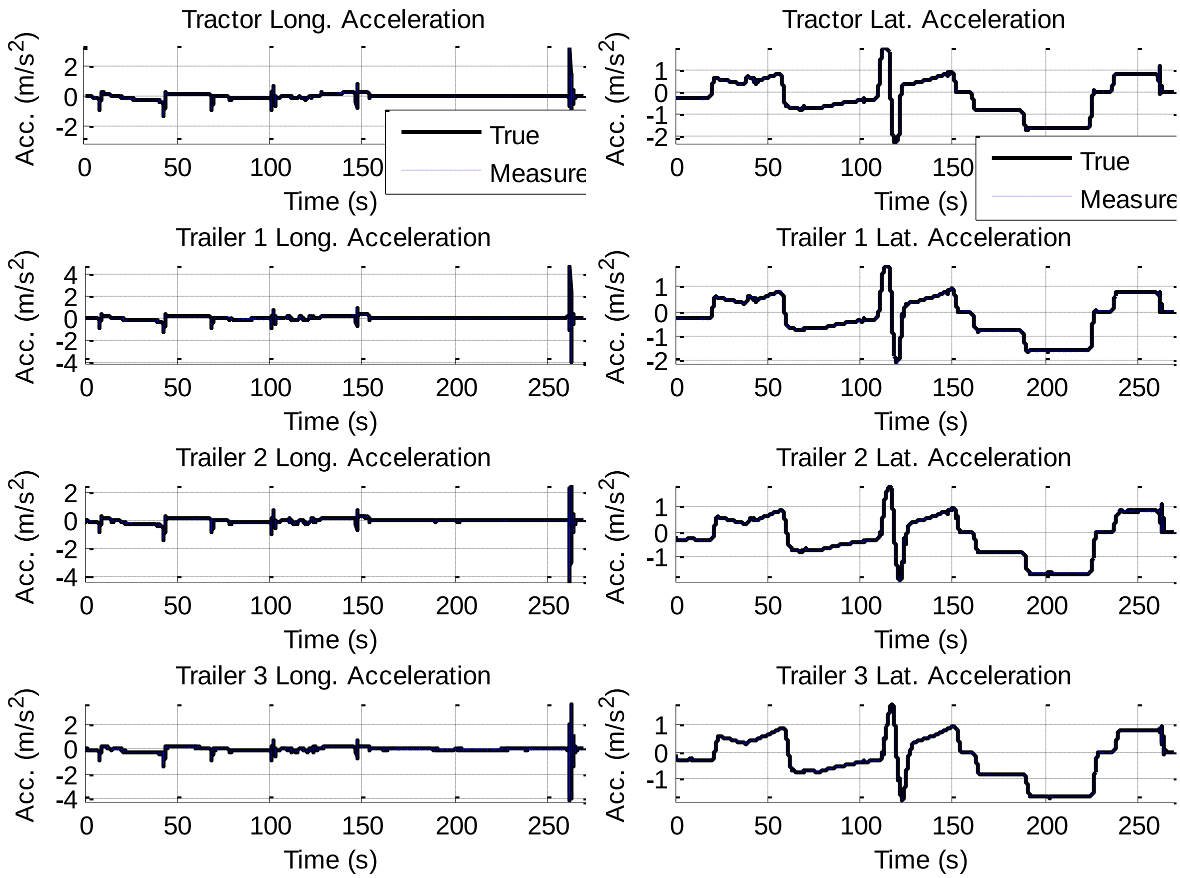

Figure H-2: IMU Data (Ax and Ay)

Using the measured GPS X velocity, the longitudinal acceleration was improved and the bias (generally from sensor mounting) removed (Bevly, 2004).

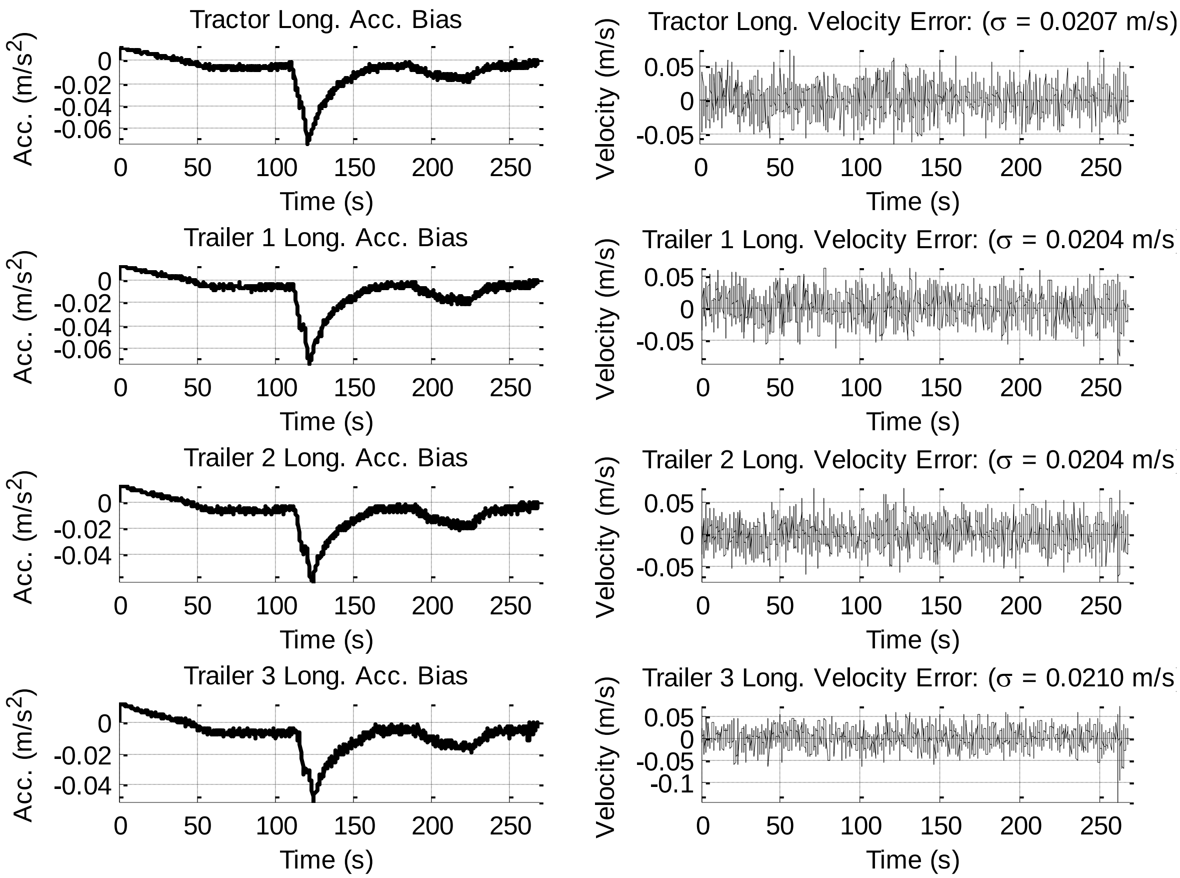

Figure H-3: Longitudinal Acceleration Kalman Filter

The next Kalman filter updated the heading and yaw rate bias using a standard yawrate integration to get yaw approach (Figure H-4, Figure H-5) (Bevly, 2004).

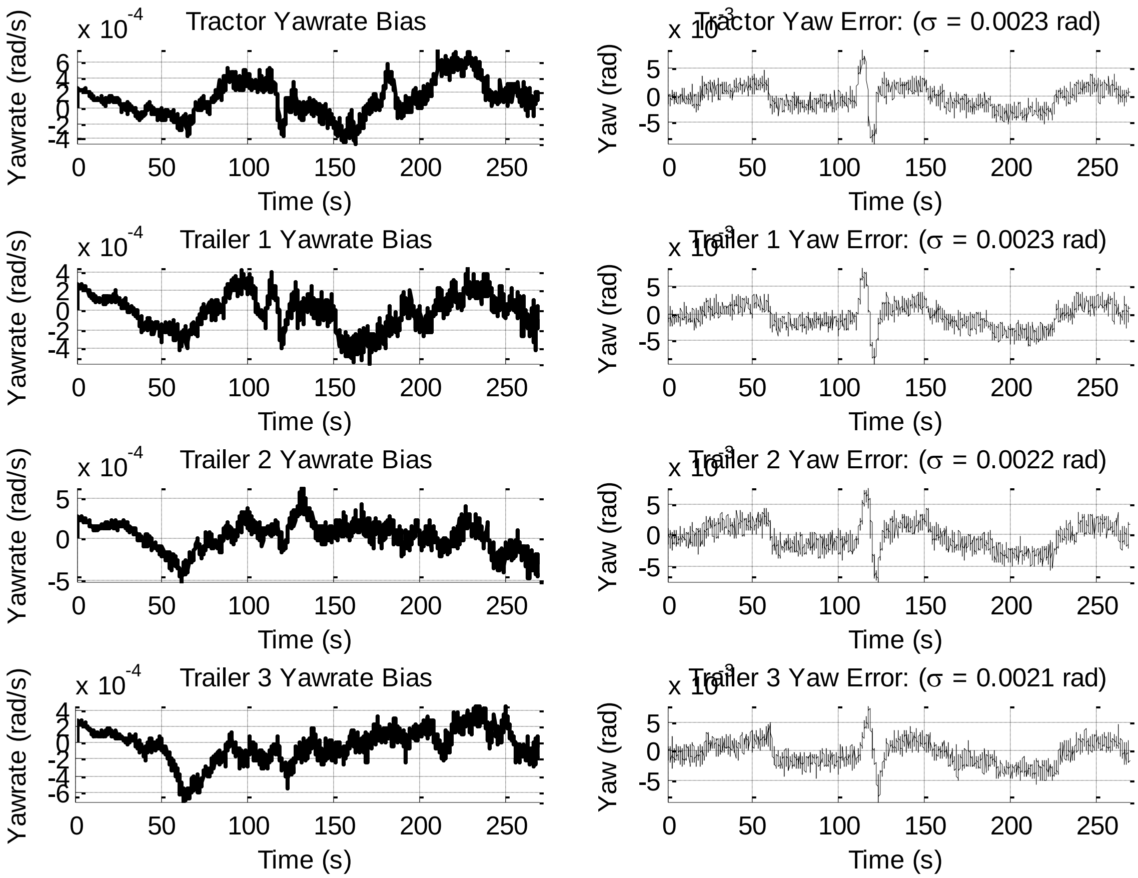

Figure H-4: Yaw Kalman Filter

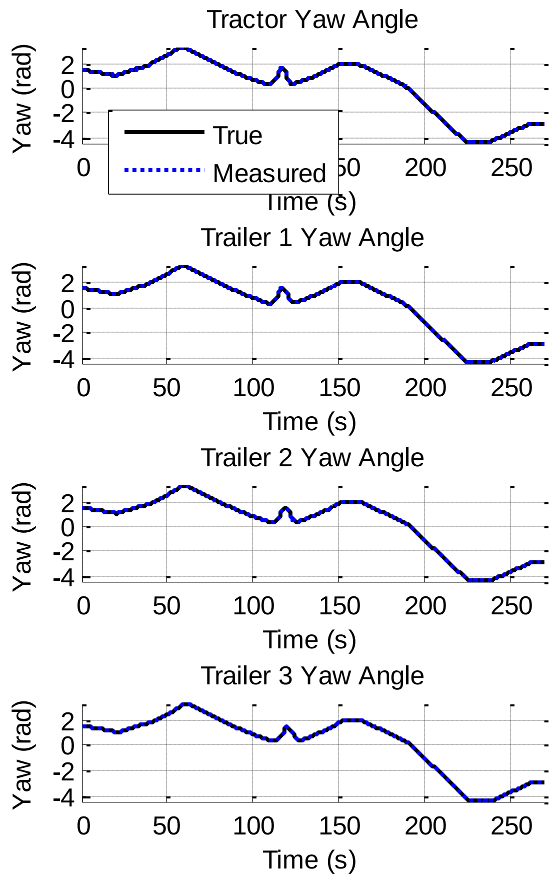

Figure H-5: Yaw Angle

This was followed by a longitudinal velocity update which improved the velocity estimation (Figure H-6) and determined the vehicle's pitch and road grade for later use (Figure H-7) (Bevly, 2004).

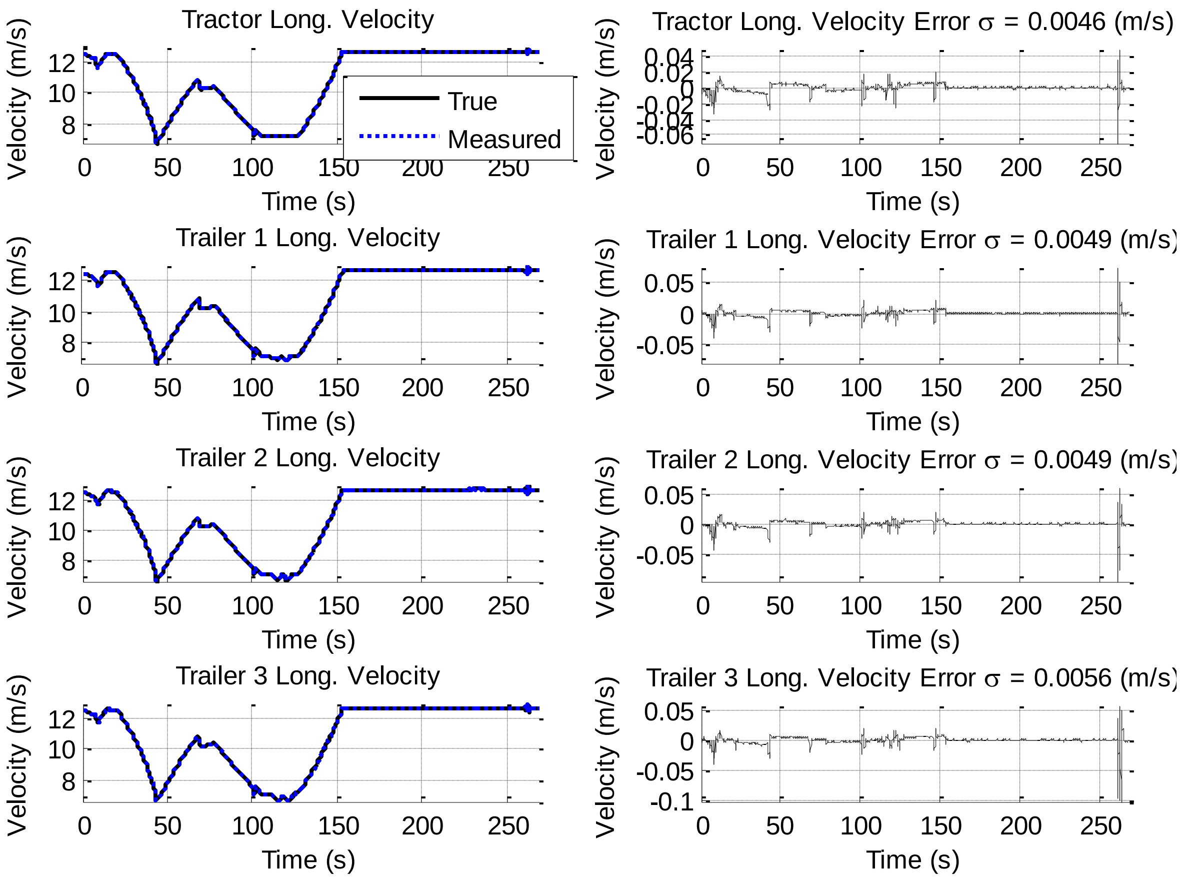

Figure H-6: Longitudinal Velocity Kalman Filter (Velocity and Error)

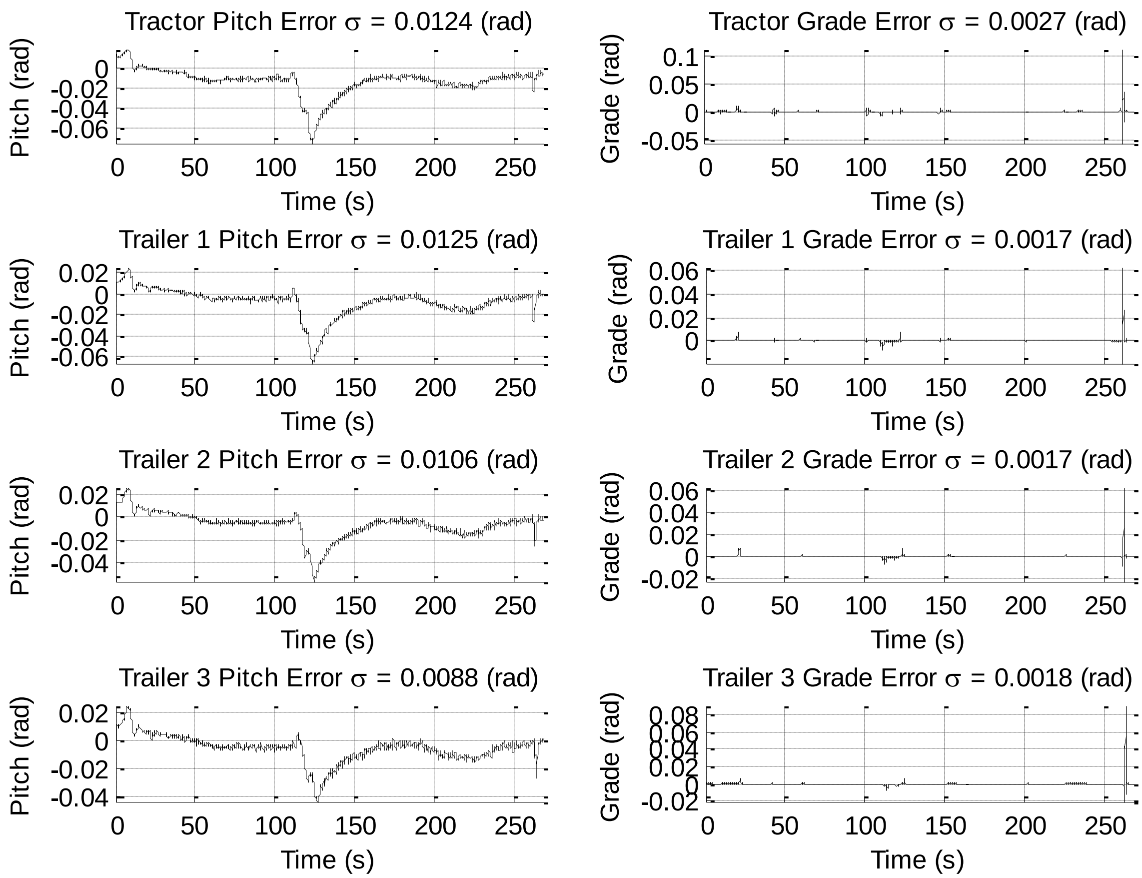

Figure H-7: Longitudinal Kalman Filter - Pitch and Grade Error

Using the IMU yaw rate, the GPS velocity information (Vx), and pitch information, the lateral acceleration bias was identified (Figure H-8) (Bevly, 2004).

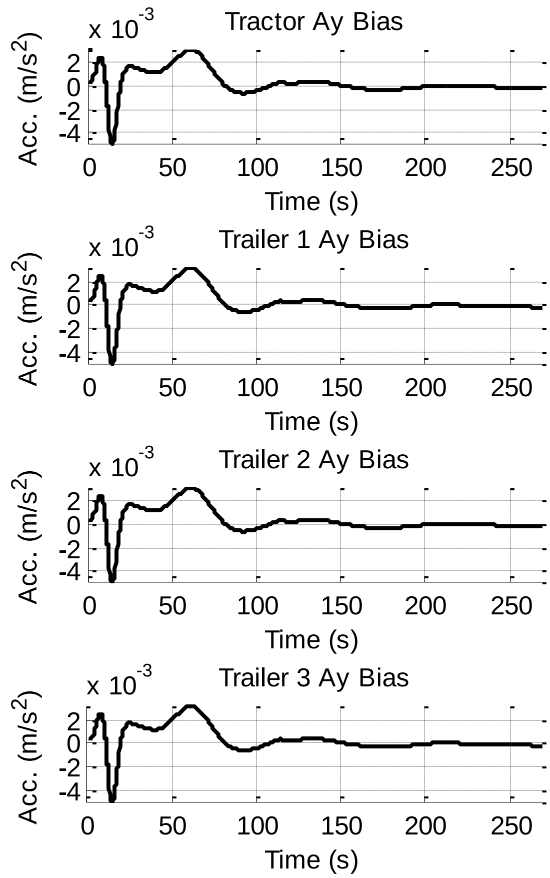

Figure H-8: Kalman Ay Bias

Next the lateral velocity (Figure H-9) and roll angle (Figure H-10) were evaluated (Bevly, 2004). Note that this lateral velocity filter (Figure H-9) significantly improves upon the prior lateral velocity estimation from the GPS alone (Table H-1).

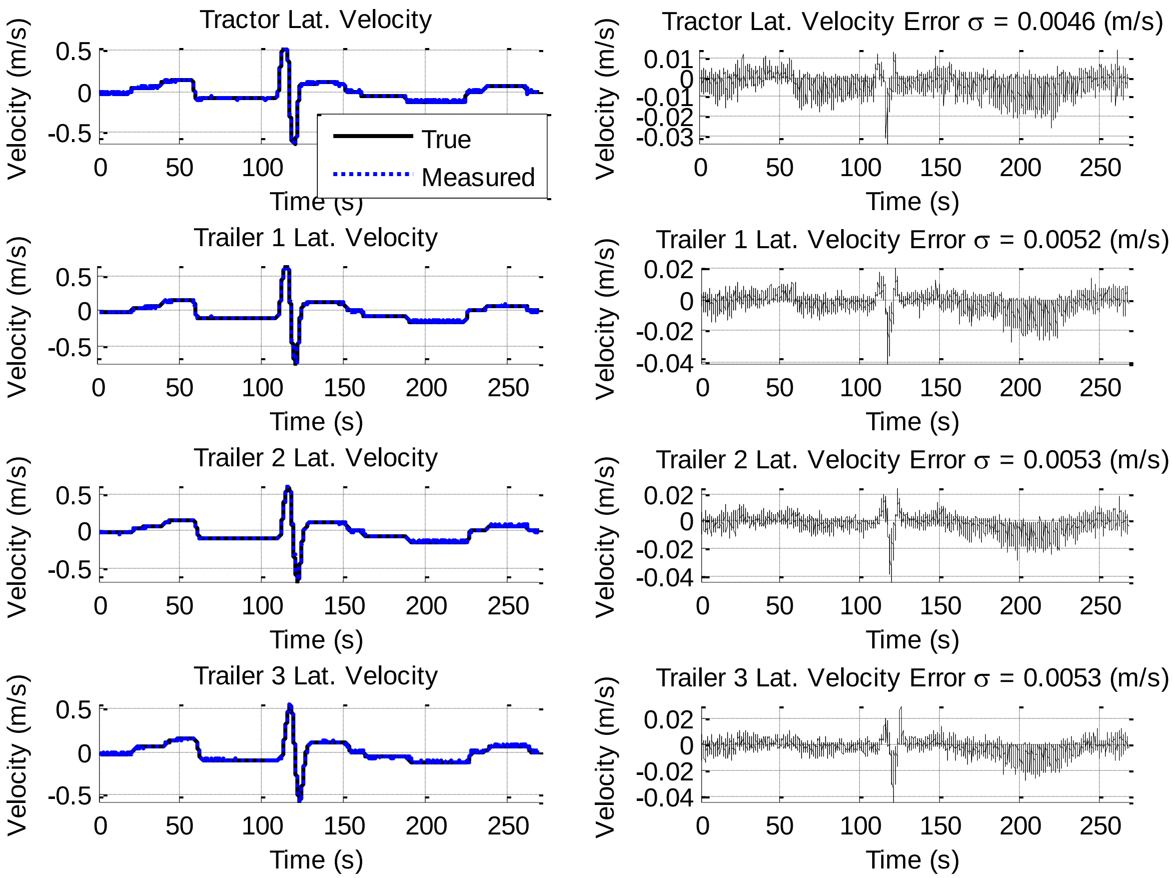

Figure H-9: Kalman Lateral Velocity

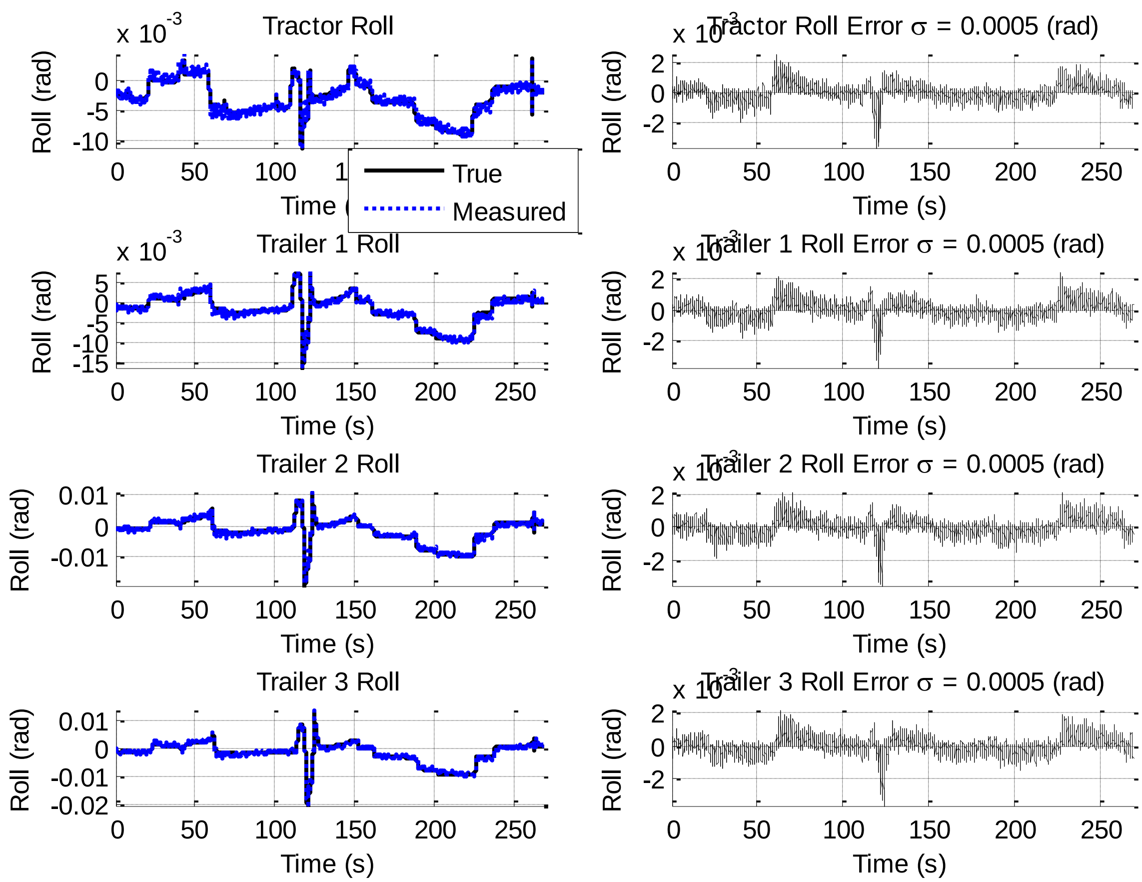

Figure H-10: Kalman Roll Angle

Finally with the longitudinal and lateral velocities known, the unit side slips were evaluated as well (Figure H-11).

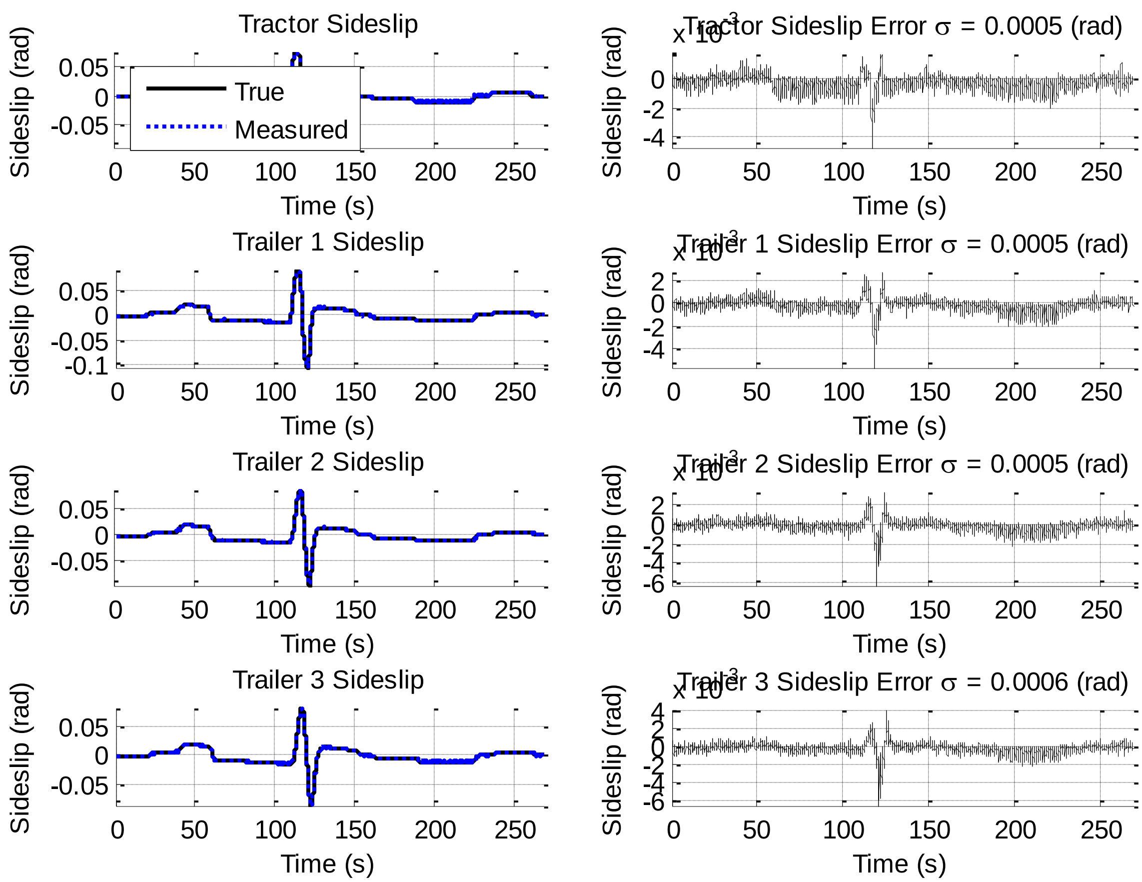

Figure H-11: Side Slip Evaluation

H.3. Final State Error Assessment

The magnitudes of the state errors were dependent on three main parameters: The IMU noise / accuracy, the GPS noise / accuracy, and the GPS update rate. The first two causal relationships are fairly obvious. The GPS cycle rate effect is due to the fact that the more often the GPS re-aligns the integration data, the faster the measurement drift is removed.

H.3.1. State Errors

After the above filtering of the IMU and GPS data, the resulting vehicle state information has significantly lower noise levels (Table H-2).

Table H-2: Effective State Gaussian Levels

Measurement	Gaussian Noise (SI)	Gaussian Noise (Common)
Side slip	0.0005 rad	0.028 deg
Yaw rate	0.005 rad/s	0.28 deg/s
Rollrate	0.005 rad/s	0.28 deg/s
Roll	0.0005 rad	0.028 deg
Yaw	0.002 rad	0.11 deg
Ay	0.006 m/s^2	0.0006 g
Vx	0.005 m/s	0.018 km/h
Vy	0.005 m/s	0.018 km/h
Pitch	0.010 rad	0.57 deg
Grade	0.002 rad	0.11 deg

H.3.2. Sensitivity of Errors to Sensor Accuracy

To gage the sensitivity of the state estimations relative to the Gaussian noise level for each sensor, a permutation table was developed where each sensor's noise level was doubled independently of the other sensors. Column 1 in Table H-3 represents the nominal state estimation results. Column 2 is the estimated state noise when the lateral acceleration noise was doubled. Column 3 is the estimated state noise when the yaw rate and roll rate sensor noise was doubled. Column 4 is the estimated state noise when the GPS velocity noise was doubled. Finally, Column 5 is the estimated state noise when the GPS heading angle noise was doubled.

As the GPS data is used to "zero" the integration of the IMU and the Kalman filter acts as a low pass filter to minimize the noise effect on the integration, doubling the noise in the GPS sensor (Columns 4 and 5) had minimal effect on the final state estimations. As the lateral acceleration was only used to evaluate roll bias through use of a Kalman filter, it too had a minimal effect on the final state estimations. The conclusion is that if it is desired to improve the state estimations, the rotational measurements (yaw rate and roll rate) would be the measurements to address.

Table H-3: Gaussian Noise Permutation Table

Measurement	Gaussian Noise (SI)	Gaussian Noise (SI)	Gaussian Noise (SI)	Gaussian Noise (SI)	Gaussian Noise (SI)
Side slip (rad/s)	0.0005	0.0005	0.0007	0.0005	0.0005
Yaw rate (rad/s)	0.005	0.005	0.010	0.005	0.005
Rollrate (rad/s)	0.005	0.005	0.010	0.005	0.005
Roll (rad)	0.0005	0.0005	0.0007	0.00052	0.0005
Yaw (rad)	0.0022	0.0022	0.0022	0.0022	0.0024
Ay (m/s^2)	0.006	0.012	0.006	0.006	0.006
Vx (m/s)	0.005	0.005	0.005	0.005	0.005
Vy (m/s)	0.005	0.005	0.007	0.005	0.005
Pitch (rad)	0.010	0.010	0.007	0.01	0.01
Grade (rad)	0.002	0.003	0.002	0.002	0.002

H.3.3. Sensitivity of Errors to GPS Update Rate

Finally, the sensitivity of the GPS update rate on state Gaussian noise can be observed in Figure H-12. Note that the states directly measured by the IMU (yaw rate, roll rate, and Ay) are not affected by the GPS update rate. However, yaw, Vx, Vy, side slip, and roll are significantly affected. For GPS update rates above 5 Hz. the additional benefit is minimal making it difficult to justify the expense of high update rate systems. The flat line indicating no improvement in noise level past 40 Hz. is due to the fact that the IMU sample rate was only 40 Hz.

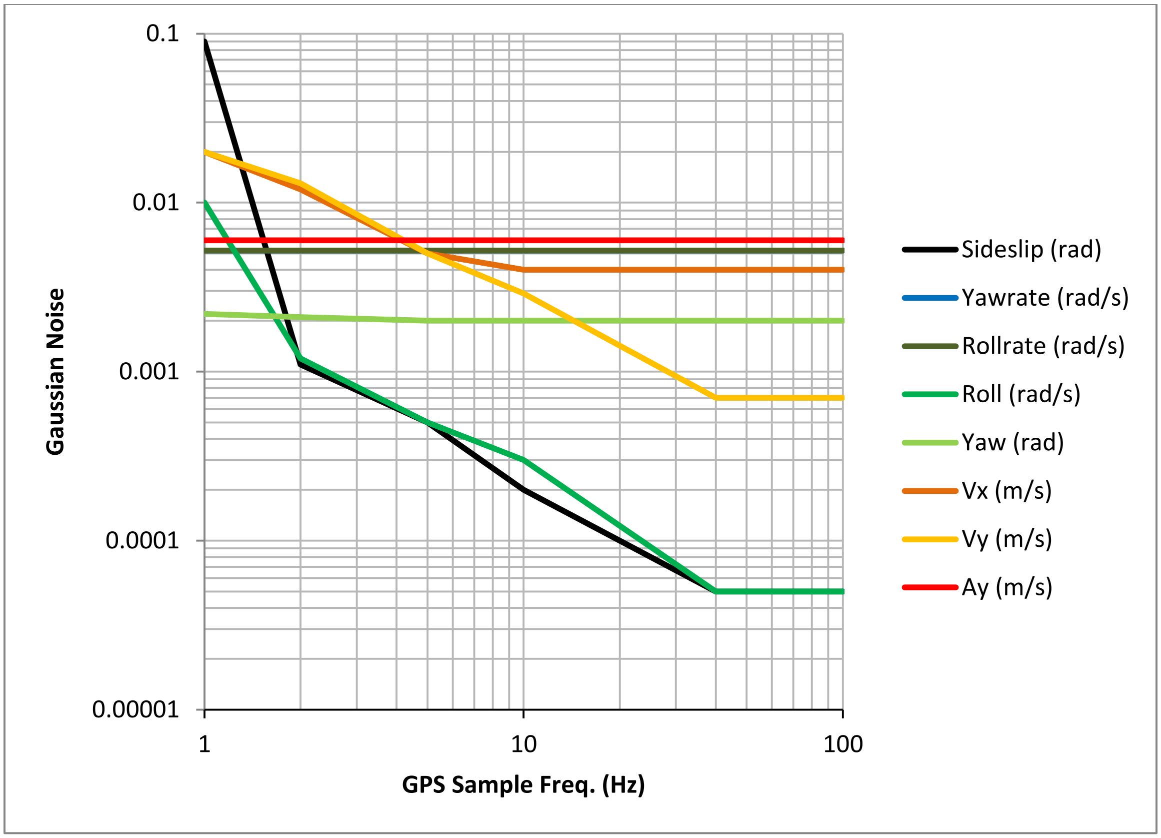

Figure H-12: Gaussian Noise vs. GPS Update Rate

APPENDIX I

CONTROLLABILITY AND OBSERVABILITY OF LINEAR TIME INVARIANT MODELS

For a controller to be able to stabilize a linear time invariant system, the controller must be able to see the needed states and affect the control inputs. In this case, B represents the input matrix (Equation I-1) and C defines the observable outputs (Equation I-2). The following are the requirements for determining observability and controllability and are referenced from Ogata (Ogata, 2002).

$$\dot{x} = A * x + B * u \qquad \textbf{I-1}$$

$$y = C * x + D * u \qquad \textbf{I-2}$$

I.1. Observability

A LTI system is said to be completely observable if every state (x) can be observed from the outputs (y). For a system described by Equation I-1 and I-2, the states are defined as Equation I-3 and the outputs as Equation I-4.

$$x(t) = e^{At} * x(0) + \int_0^t e^{A(t-\tau)} * B * u(\tau)\, d\tau \qquad \textbf{I-3}$$

$$y(t) = C * e^{At} * x(0) + \int_0^t e^{A(t-\tau)} * B * u(\tau)\, d\tau + D * u \qquad \textbf{I-4}$$

Since A, B, C, and D are known and u(t) is the desired input, only the part show in Equation I-5 is unknown.

$$y(t) = C * e^{At} * x(0) \qquad \textbf{I-5}$$

$$e^{At} = \sum_{k=0}^{n-1} \alpha_k(t) * A^k \qquad \textbf{I-6}$$

$$y(t) = \sum_{k=0}^{n-1} \alpha_k(t) * C * A^k * x(0) \qquad \textbf{I-7}$$

For the system to be complete observable, Q_o in Equation I-8 must be full rank (rank equal to the number of states). Note: Q_o is the expansion of Equation I-7 in matrix form.

$$Q_o = \begin{bmatrix} C \\ C * A \\ C * A^2 \\ \cdots \\ C * A^{n-1} \end{bmatrix} \qquad \textbf{I-8}$$

I.2. Controllability

The general solution to Equation I-1 is Equation I-9 where x(0) can be defined as Equation I-10.

$$x(t) = e^{At} * x(0) + \int_0^t e^{A(t-\tau)} * B * u(\tau)\, d\tau \qquad \textbf{I-9}$$

$$x(0) = -\sum_{k=0}^{n-1} A^k * B * \int_0^t a_k\,(\tau) * u(\tau)\, d\tau \qquad \textbf{I-10}$$

Substituting this definition into Equation I-11 produces Equation I-12.

$$\beta(t) = \int_0^t a_k\,(\tau) * u(\tau)\, d\tau \qquad \textbf{I-11}$$

$$x(0) = -\sum_{k=0}^{n-1} A^k * B * \beta(t) \qquad \textbf{I-12}$$

For the system to be completely controllable, the rank of Q_c in Equation I-13 must be equal to the number of states in A or full rank. Note Equation I-13 is the matrix expansion of Equation I-12.

$$Q_c = [B \quad A * B \quad A^2 * B \quad \ldots \quad A^{n-1} * B] \qquad \textbf{I-13}$$

APPENDIX J

MODEL PREDICTIVE CONTROLLER PERFORMANCE

Given the number of cases studies evaluated in this research, it was impossible to include them all in the formal dissertation. So that the reader could have some idea as to the overall performance of the model predictive controller, the cases are presented here in brief. These results are not all inclusive for obvious reasons but do show pertinent system responses. The two basic maneuvers used to evaluate the controllers were the step steer and double lane change. These were evaluated in loaded and unloaded configurations with dry roads (mu = 0.85), wet roads (mu = 0.6), and ice roads (mu = 0.25). For reference, the MPC bounds are listed in Table J-1

Table J-1: MPC Bounds

Measurement	Bound (SI)	Bound (Common)
Side slip	0.1 rad	5.7 deg
Yaw rate	0.3 rad/s	17 deg/s
Rollrate	0.05 rad/s	2.8 deg/s
Roll	0.03 rad	1.7 deg

J.1. Step Steer

The step steer maneuver was simply a 180º steering wheel input over 2/3 second. The initial vehicle speed depended on the load and the road surface.

J.1.1. Unloaded Mu = 0.25

The effect of the controller on the unloaded vehicle was to slow the vehicle and tighten the radius (Figure J- 1 where blue is the free response and pink is the MPC). In this case the open loop vehicle was stable (albeit sliding) as can be seen in the side slip figure (Figure J- 2). The MPC increased side slip, but it still remained within bounds.

What was surprising was that the controller activated when the base vehicle was stable and did not need assistance. To understand why the controller activated one must recognize that the model predictive controller has no idea what the road friction level is as friction is not a parameter in the LTI model. Thus it assumed that the step input would produce a large roll and acted before the roll actually developed. Once it was clear that roll was not an issue, the controller released the brakes (Figure J- 3) save for the tractor as the initial brake application had reduced the path radius and the controller was now managing yaw divergence. Note that the brake pressures are quite small indicating minor corrective actions.

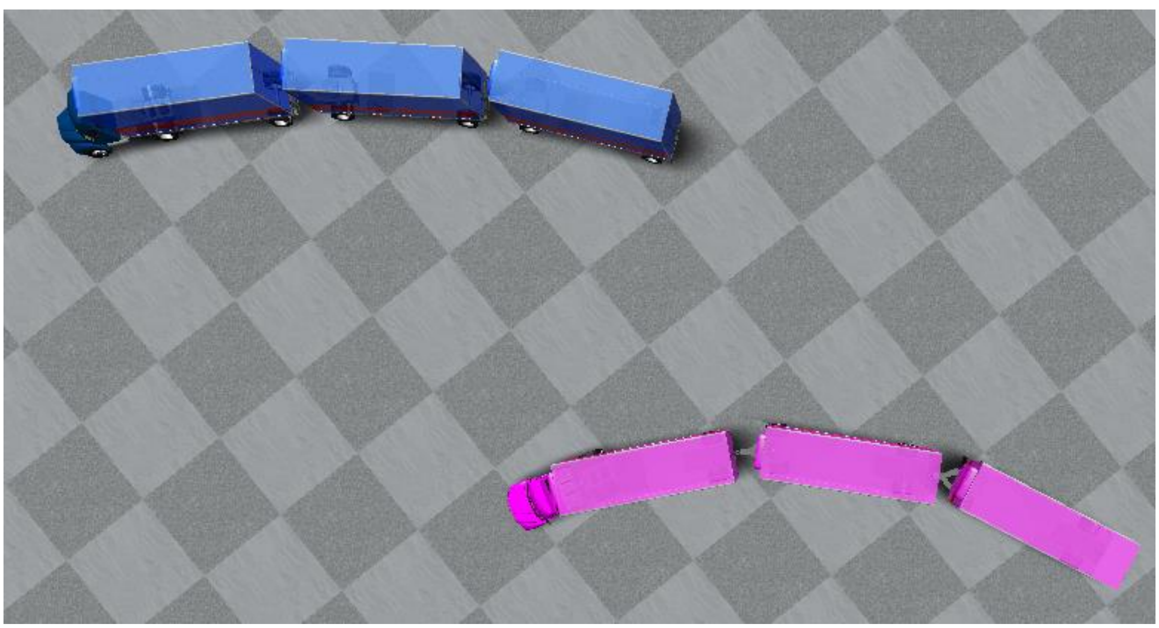

Figure J- 1: Illustration, MPC Unloaded Vehicle, Step Steer, mu = 0.25

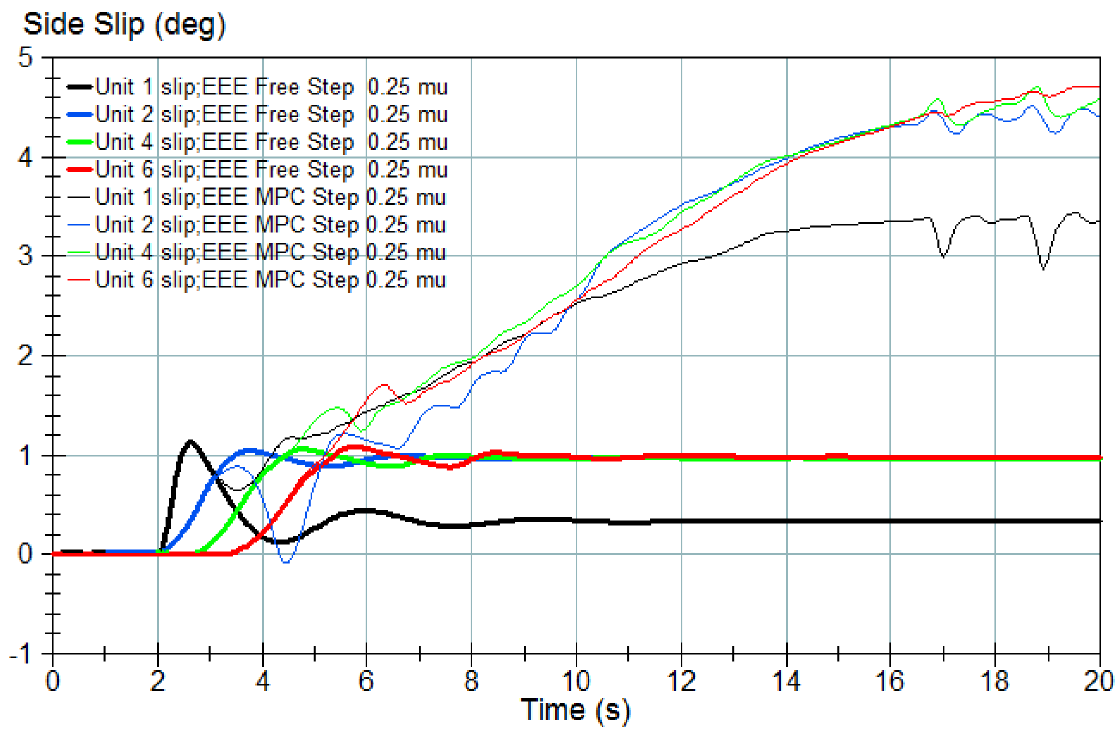

Figure J- 2: Side Slip, MPC Unloaded Vehicle, Step Steer, mu = 0.25

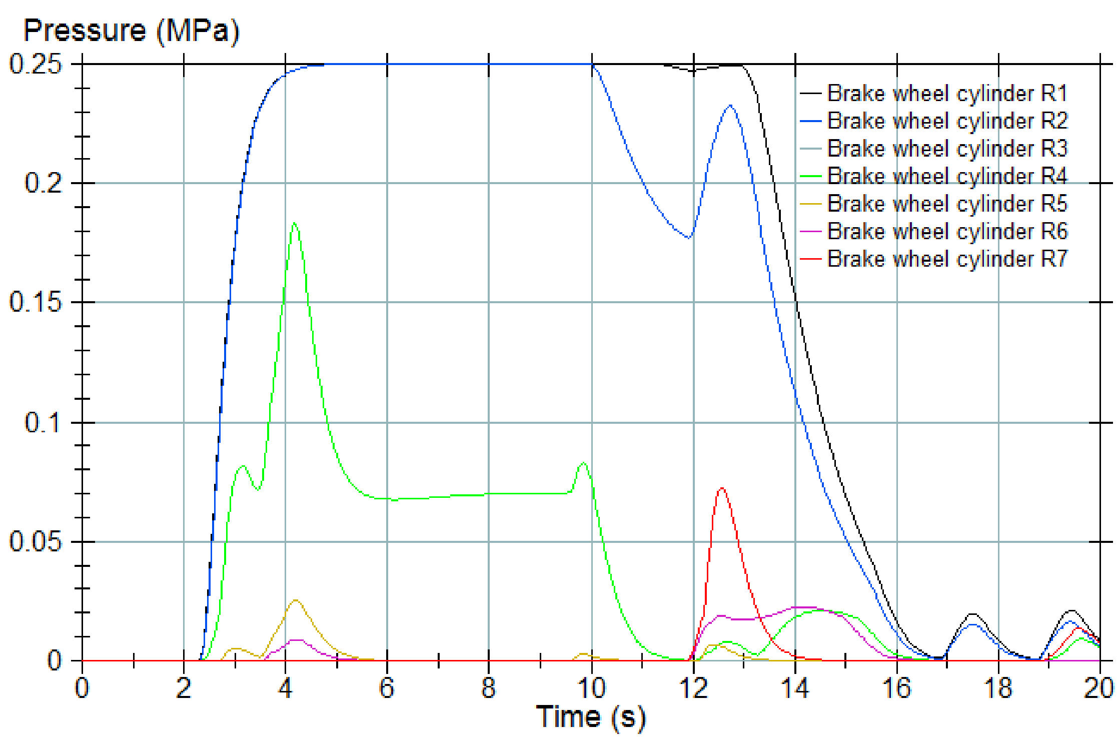

Figure J- 3: Brakes, MPC Unloaded Vehicle, Step Steer, mu = 0.25

J.1.2. Unloaded Mu = 0.6

For the wet unloaded step steer case, the risk was obviously rollover (Figure J- 4). The controller activated the right brakes to reduce yaw rate and Ay (Figure J- 6) and modulated the left brakes to maintain side slip (Figure J- 5). Note: “EEE” refers to Empty, Empty, Empty for the trailer configuration. “Free” is the uncontrolled vehicle response and “MPC” is the MPC response.

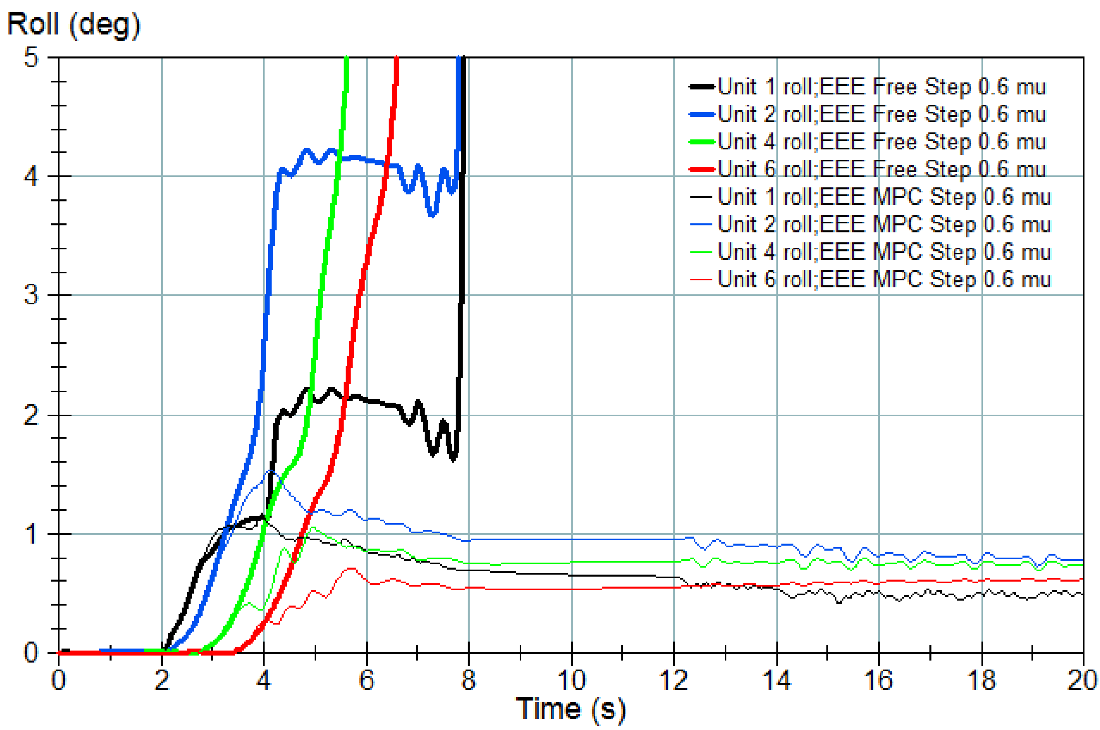

Figure J- 4: Roll, MPC Unloaded Vehicle, Step Steer, mu = 0.6

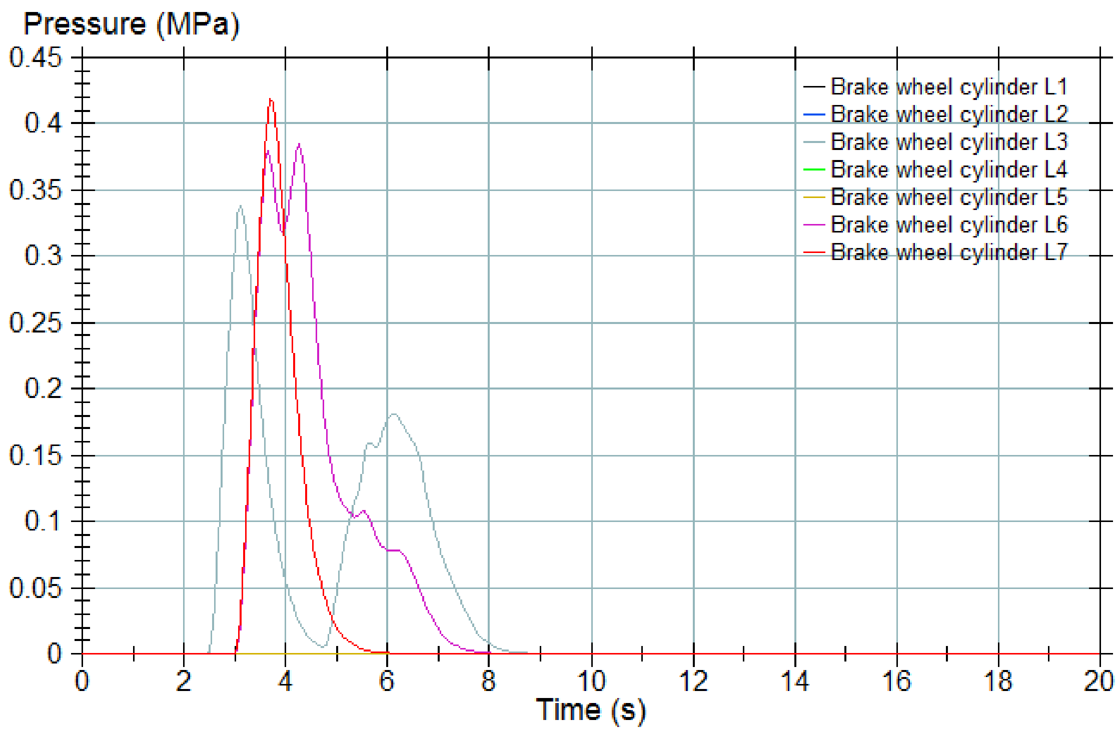

Figure J- 5: Left Brake, MPC Unloaded Vehicle, Step Steer, mu = 0.6

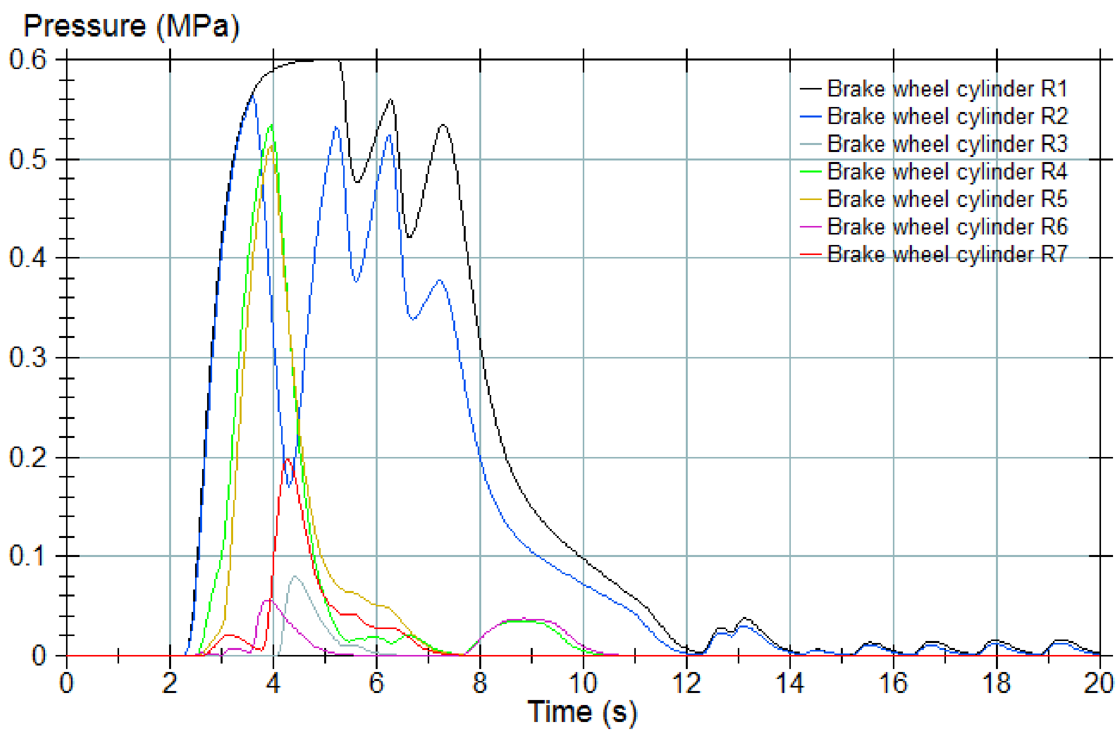

Figure J- 6: Right Brake, MPC Unloaded Vehicle, Step Steer, mu = 0.6

J.1.3. Unloaded Mu = 0.85

Not surprisingly, the dry unloaded step steer was also a roll reduction event with the controller activating to prevent rollover (Figure J- 7) by activating the right brakes (Figure J- 9) to reduce yaw rate (Figure J- 8). The small "blips" in brake pressure past 12 seconds (Figure J- 9) are where the controller releases (system is now stable), the tractor engine engages, the vehicle is again predicted to exceed a stability bound, and the controller re-engages. In practice, the vehicle would not see this small cycle in brake demand due to air valve crack pressures (minimum demand to open the valve).

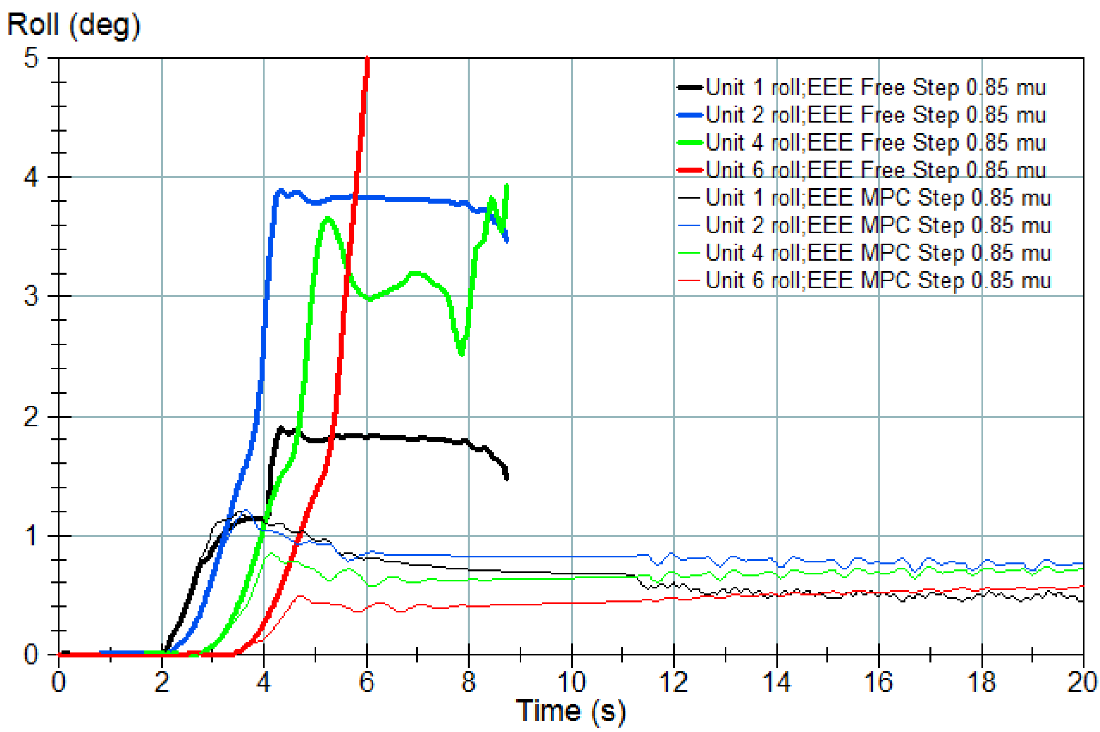

Figure J- 7: Roll, MPC Unloaded Vehicle, Step Steer, mu = 0.85

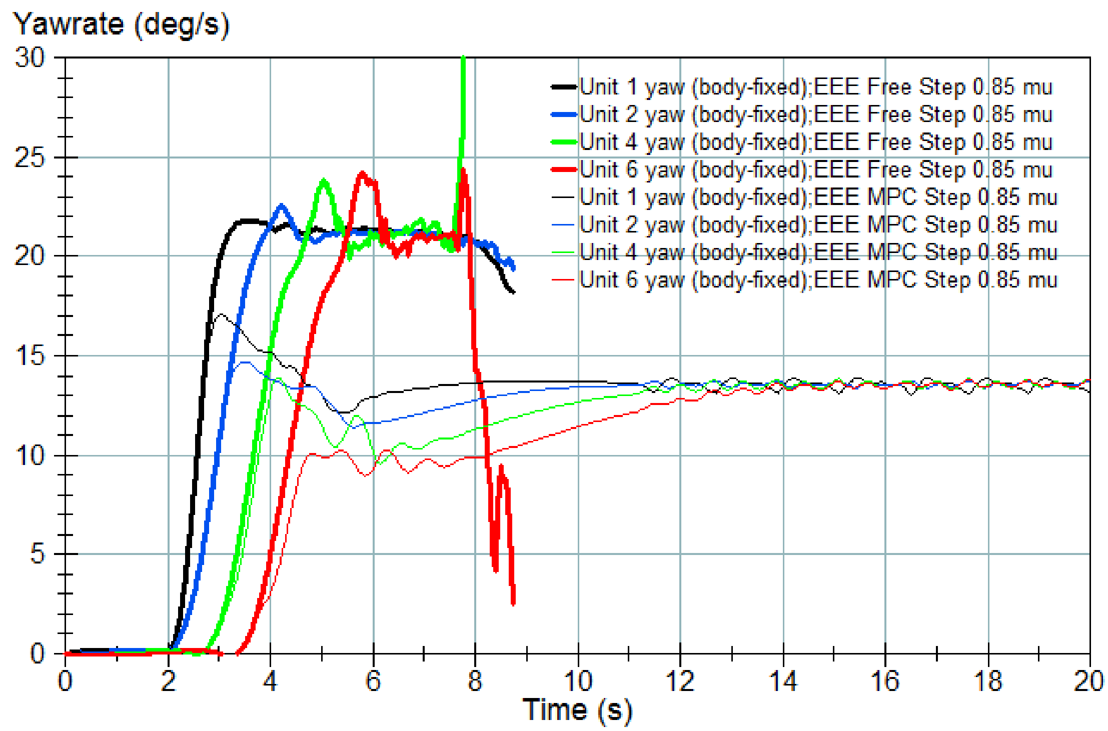

Figure J- 8: Yaw Rate, MPC Unloaded Vehicle, Step Steer, mu = 0.85

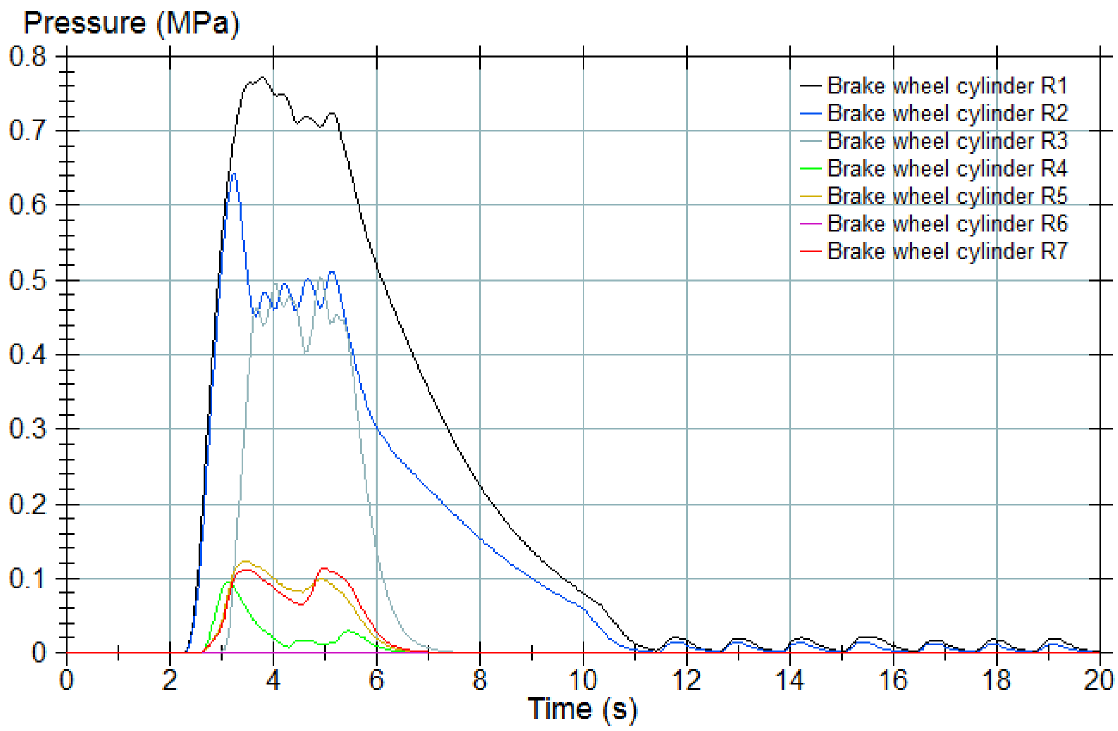

Figure J- 9: Right Brake, MPC Unloaded Vehicle, Step Steer, mu = 0.85

J.1.4. Loaded Mu = 0.25

The loaded vehicle step steer on ice was sensitive to jackknifing (yaw divergence) as seen in Figure J- 10. The MPC primarily acted here to reduce side slip (Figure J- 11) though it had some difficulty controlling the first trailer (unit 2) initially. Additionally, the controller also improved the yaw rate performance in the process (Figure J- 12).

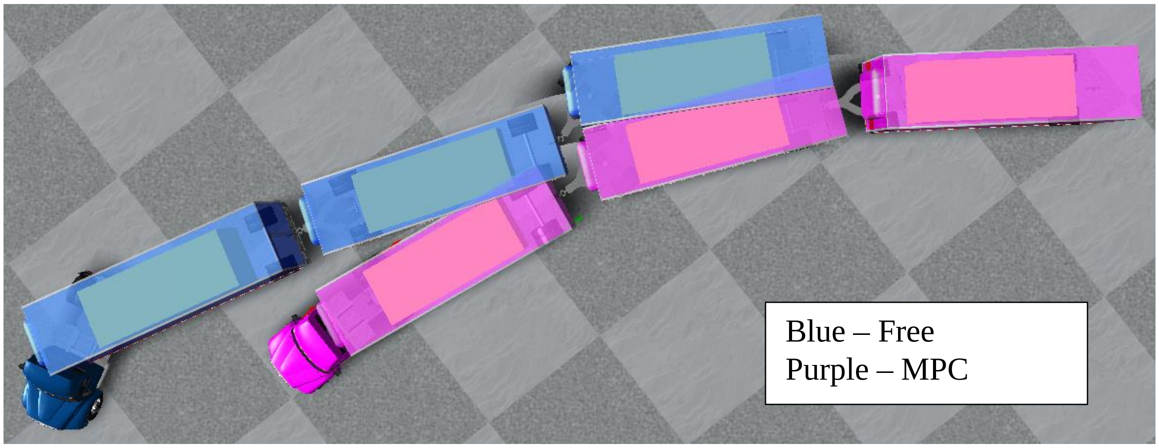

Figure J- 10: Illustration, MPC Loaded Vehicle, Step Steer, mu = 0.25

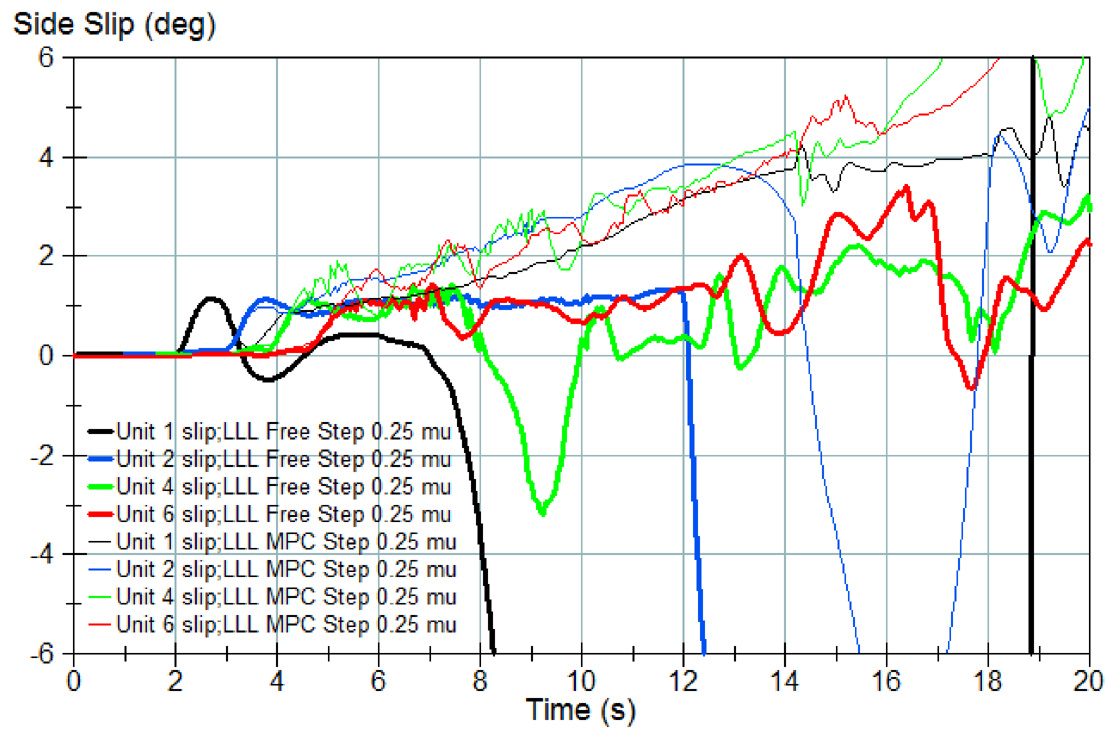

Figure J- 11: Side Slip, MPC Loaded Vehicle, Step Steer, mu = 0.25

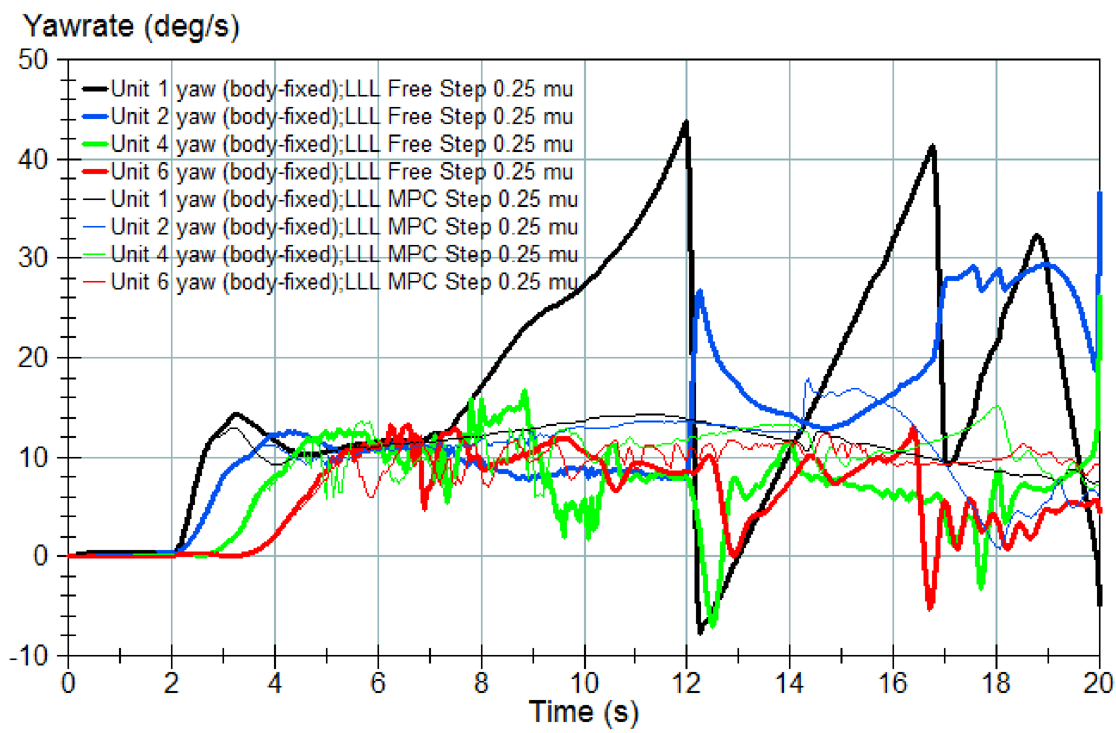

Figure J- 12: Yaw Rate, MPC Loaded Vehicle, Step Steer, mu = 0.25

J.1.5. Loaded Mu = 0.6

With the transition of mu from 0.25 to 0.6, the loaded vehicle step steer maneuver became roll unstable (Figure J- 13). The MPC response lowered the yaw rate (Figure J-14) at the cost of side slip (Figure J- 15) until both states were nearly within bounds. The side slip was slightly out of bounds but the total cost was lower than the cost of a rollover (side slip bound was 5.7 degrees).

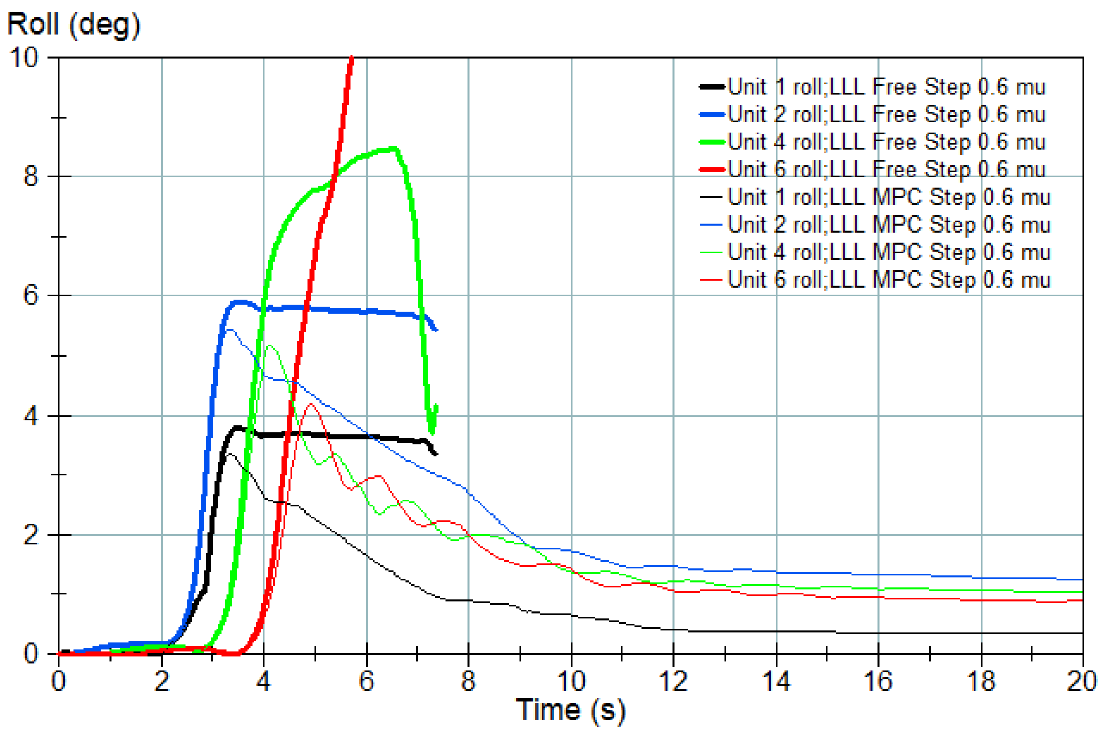

Figure J- 13: Roll, MPC Loaded Vehicle, Step Steer, mu = 0.6

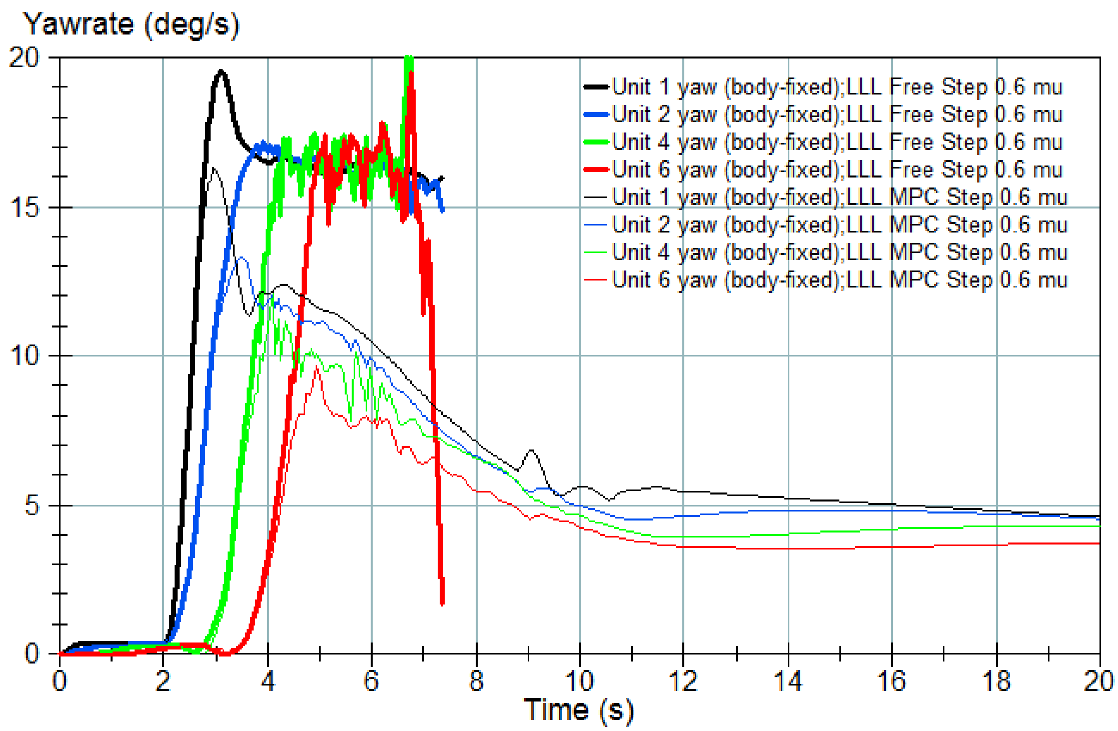

Figure J- 14: Yaw Rate, MPC Loaded Vehicle, Step Steer, mu = 0.6

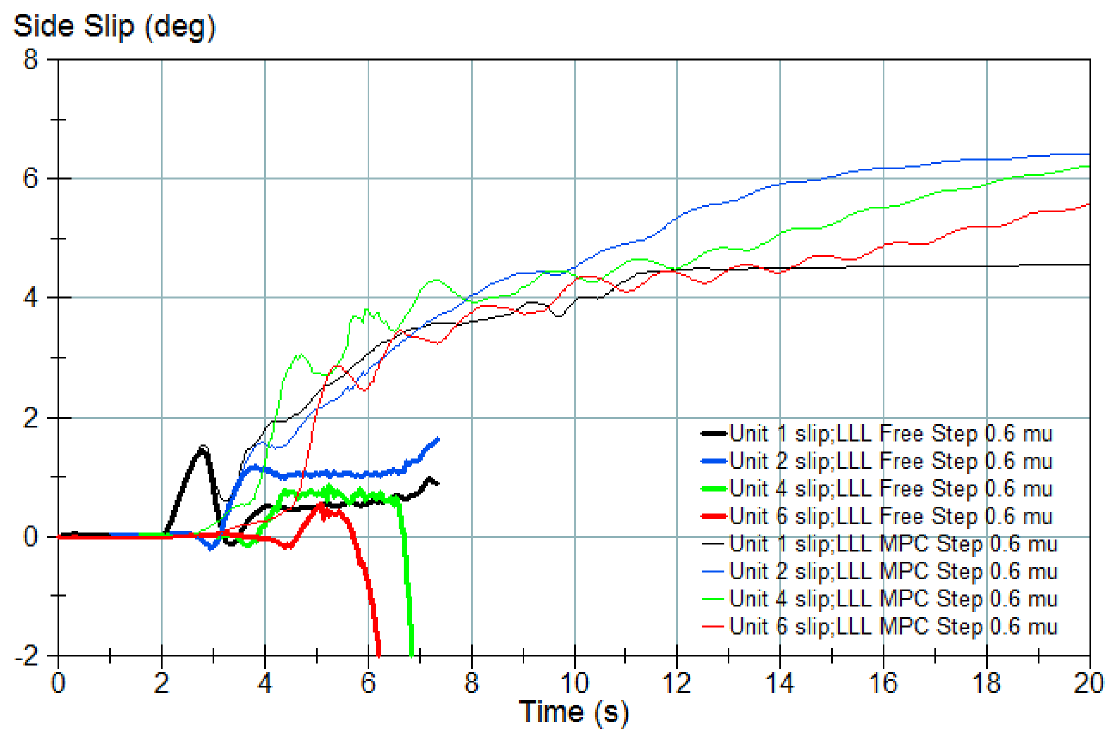

Figure J- 15: Side Slip, MPC Loaded Vehicle, Step Steer, mu = 0.6

J.1.6. Loaded Mu = 0.85

The dry loaded step steer case was essentially a repeat of the wet case above with the roll threat (Figure J- 16) being controlled through yaw rate reduction (Figure J- 17). In this case, the vehicle could be stabilized quickly and the brakes released (Figure J- 18) as there was sufficient traction to slow the vehicle without increasing yaw instability (side slip).

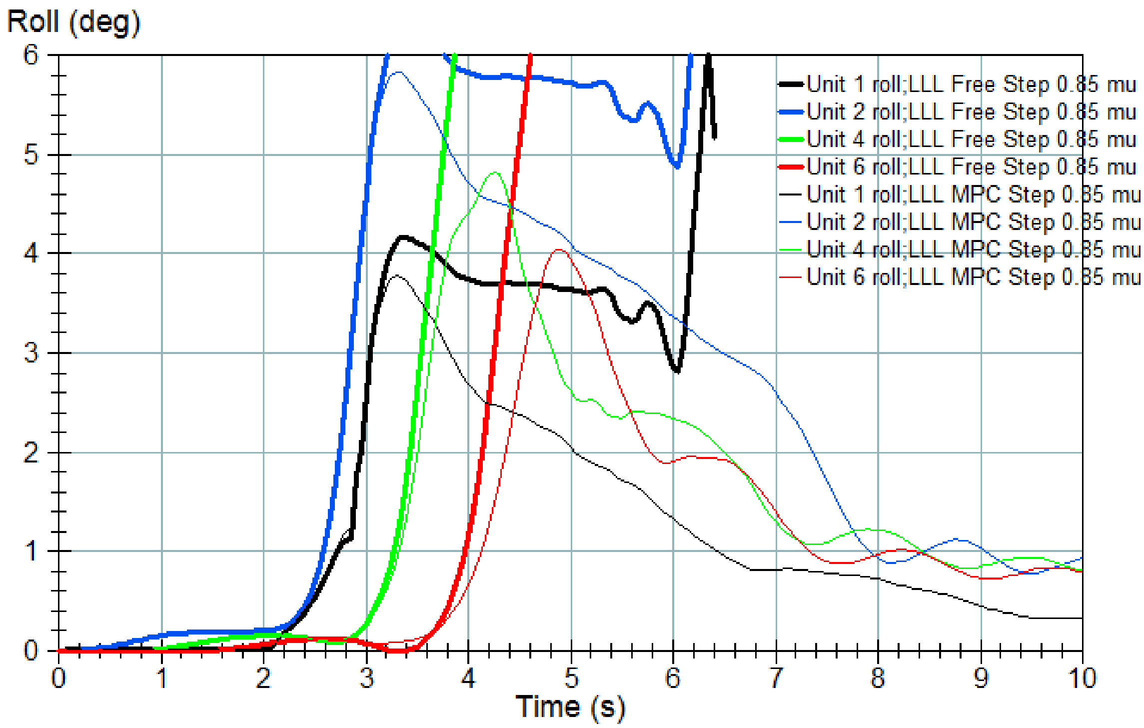

Figure J- 16: Roll, MPC Loaded Vehicle, Step Steer, mu = 0.85

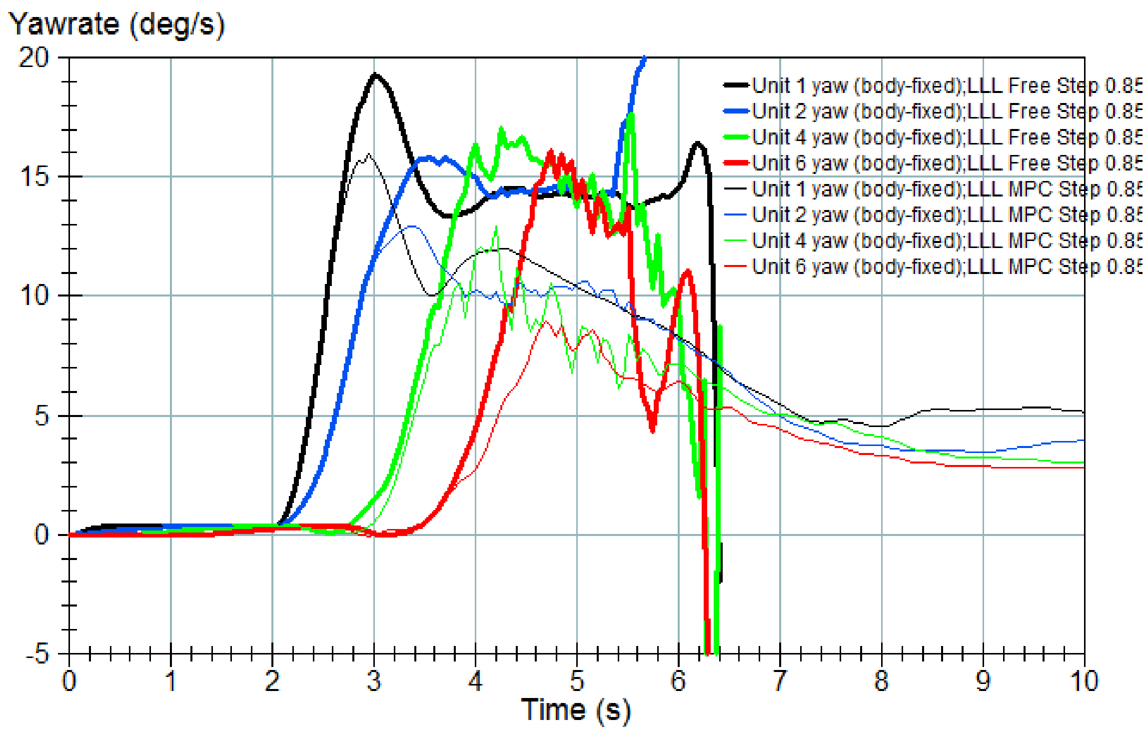

Figure J- 17: Yaw Rate, MPC Loaded Vehicle, Step Steer, mu = 0.85

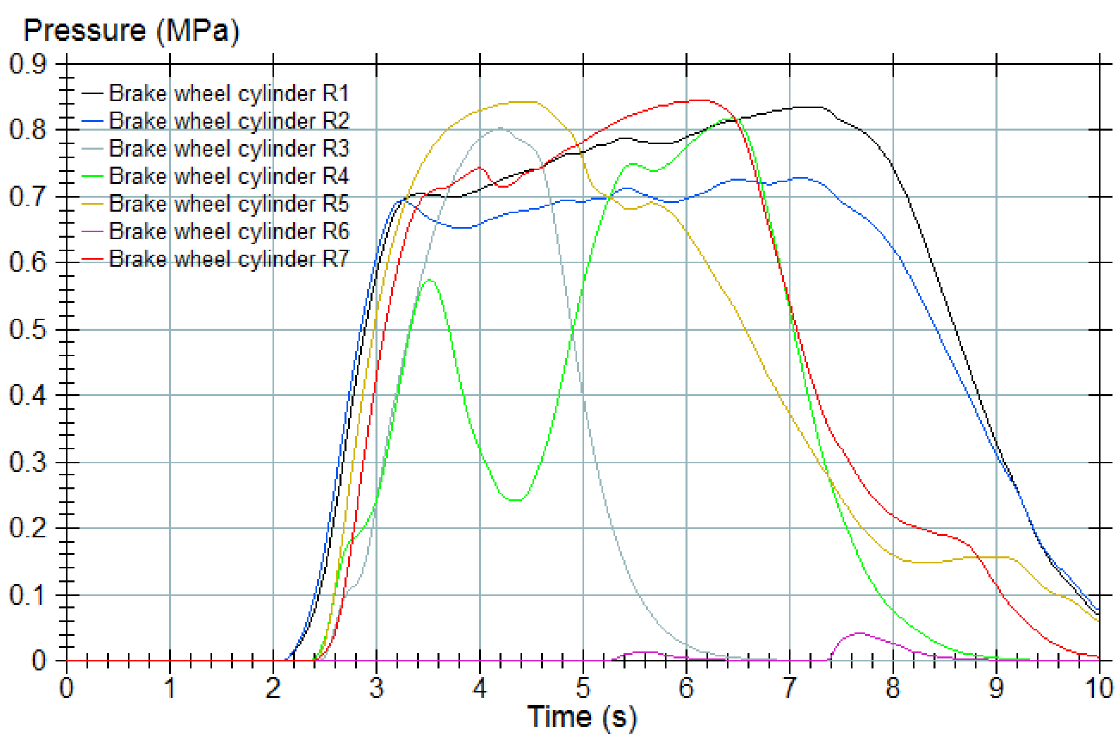

Figure J- 18: Brakes, MPC Loaded Vehicle, Step Steer, mu = 0.85

J.2. Double Lane Change

In addition to the step steer maneuver, each of the vehicle combination cases was also evaluated using the ISO double lane change. Given the multiple course corrections, this test was particularly demanding on the last trailer.

J.2.1. Unloaded Mu = 0.25

Not surprisingly, the unloaded vehicle on an icy lane change suffered from yaw divergence issues (Figure J- 19). However, this case study does highlight one weakness in the MPC controller (Figure J- 20). The controller only looks at the states of the tractor and trailers and, in this case, the side slips (Figure J- 19) and yaw rates (Figure J- 21) looked good. As the dollies are not monitored and the track of the trailers is not monitored, the controller had no idea that the 3rd trailer was off tracking as this is technically not a stability risk. Never the less, most drivers would much prefer not to see this event in a rear view mirror. However, this behavior is only seen on extremely low mu surfaces and drivers seldom achieve the speeds needed to see this effect on ice.

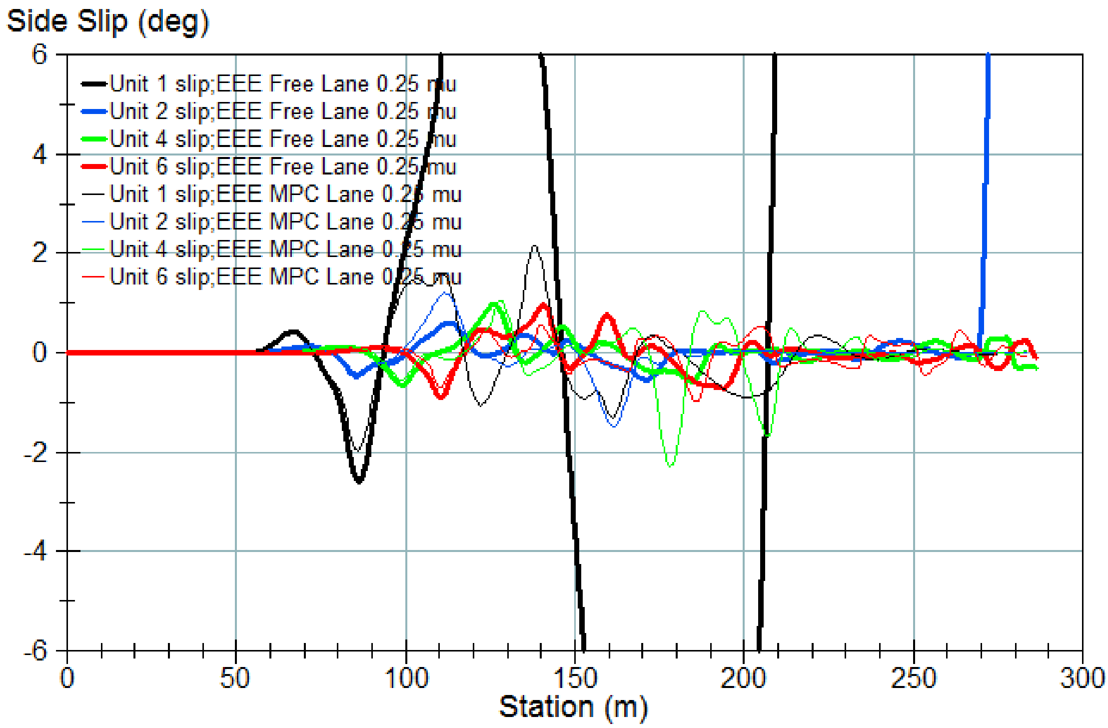

Figure J- 19: Side Slip, MPC Unloaded Vehicle, Lane Change, mu = 0.25

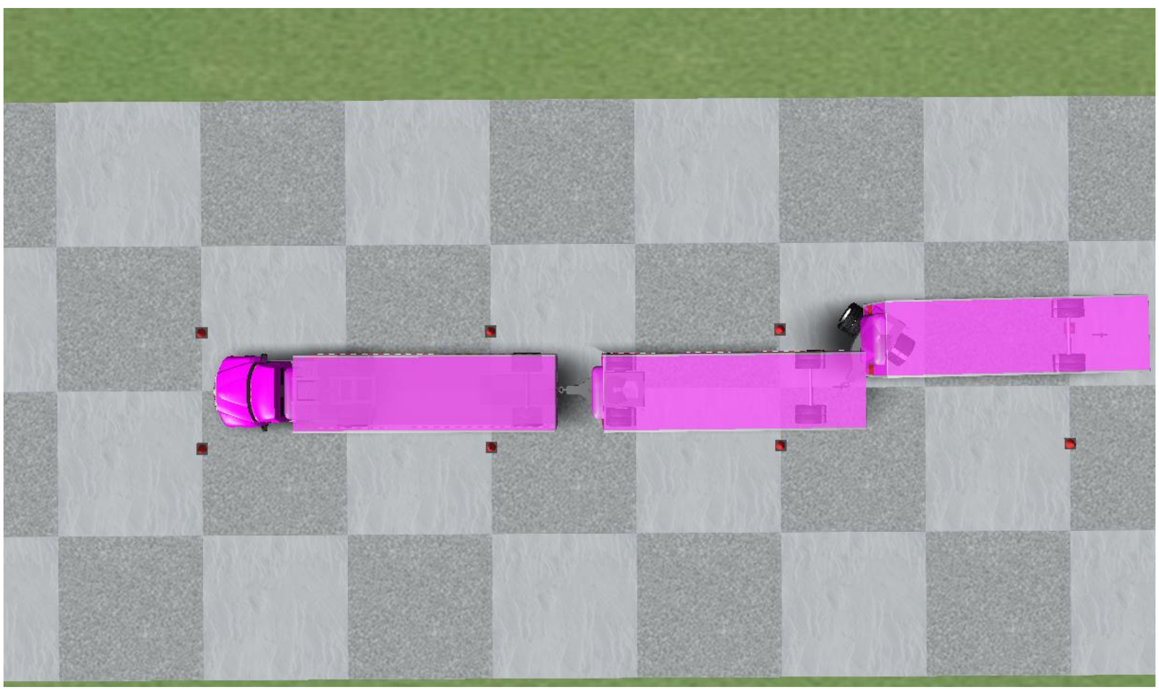

Figure J- 20: Illustration, MPC Unloaded Vehicle, Lane Change, mu = 0.25

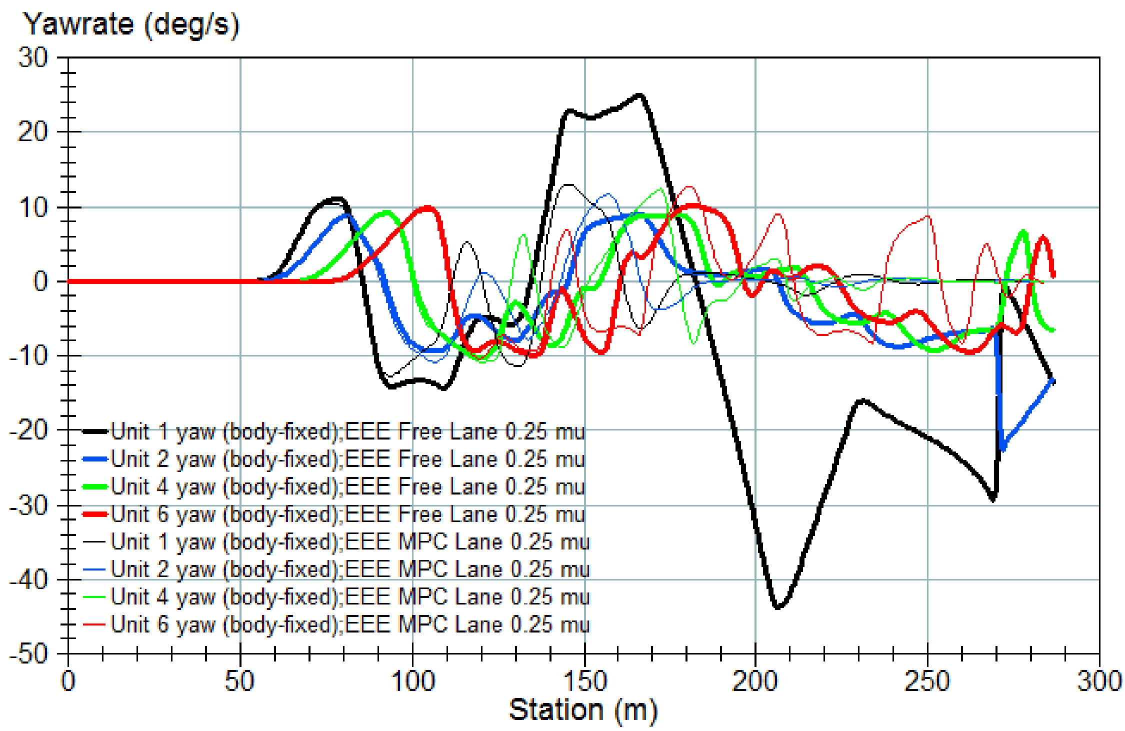

Figure J- 21: Yaw Rate, MPC Unloaded Vehicle, Lane Change, mu = 0.25

J.2.2. Unloaded Mu = 0.6

As the traction level increased, the empty double lane change became a combined yaw and roll stability risk (Figure J- 22). The controller had to dampen roll (Figure J- 23) while not reducing lateral traction potential and exasperating the side slip deviation (Figure J- 24). As can be seen, the controller was successful in this effort.

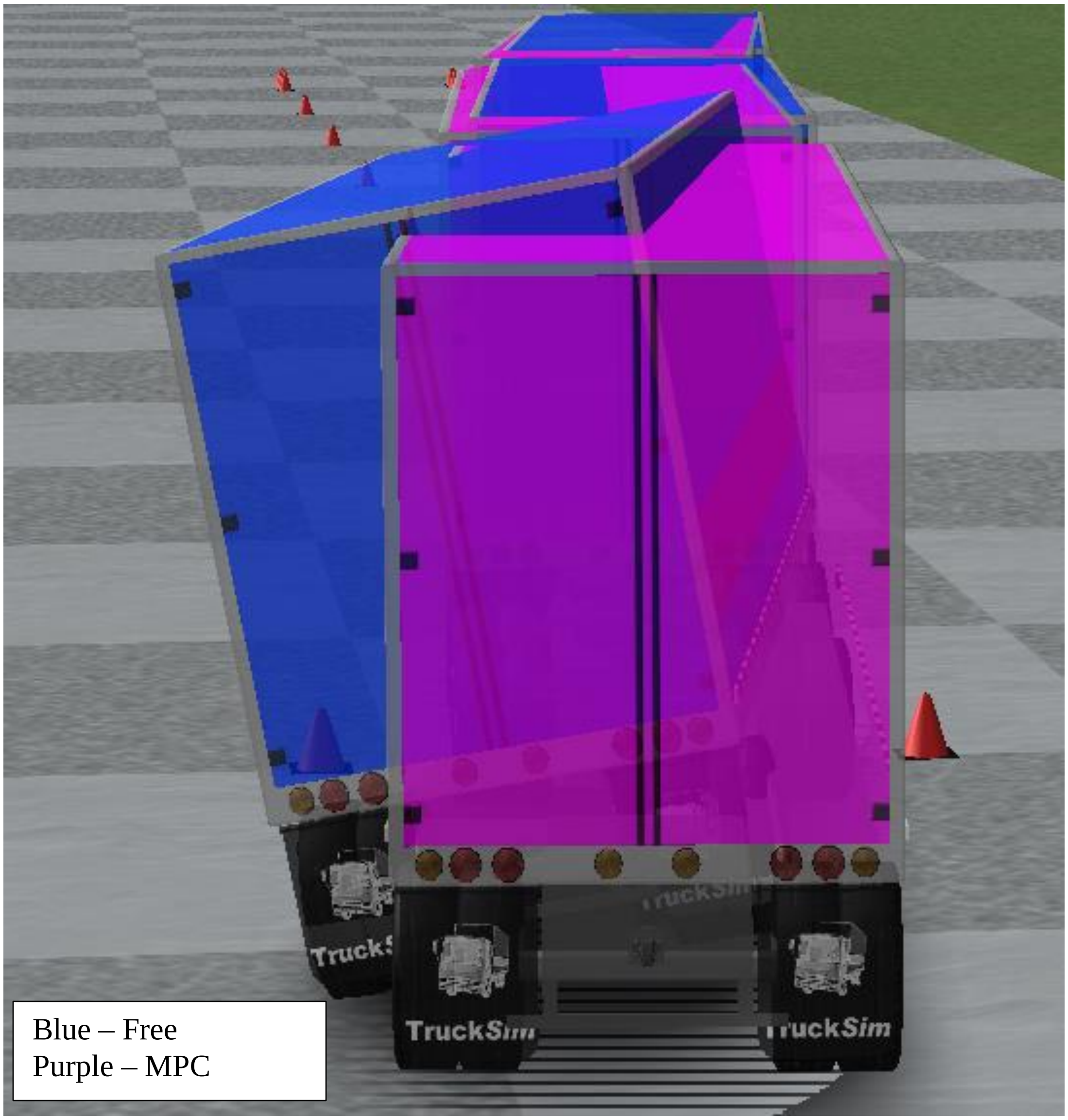

Figure J- 22: Illustration, MPC Unloaded Vehicle, Lane Change, mu = 0.6

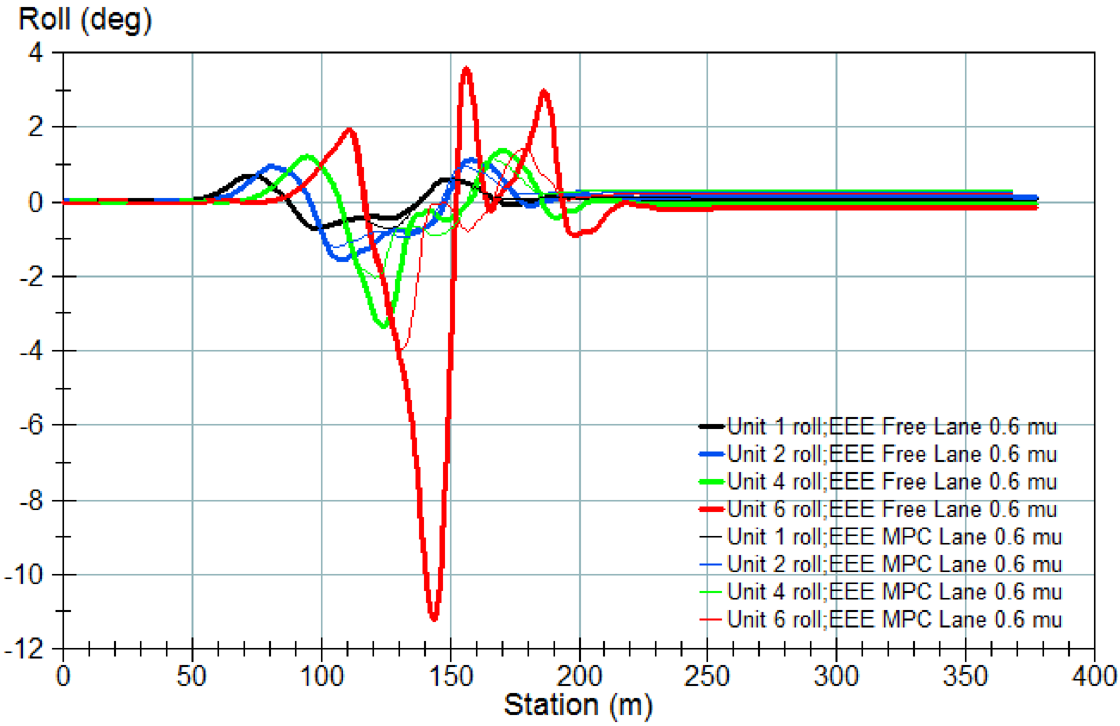

Figure J- 23: Roll, MPC Unloaded Vehicle, Lane Change, mu = 0.6

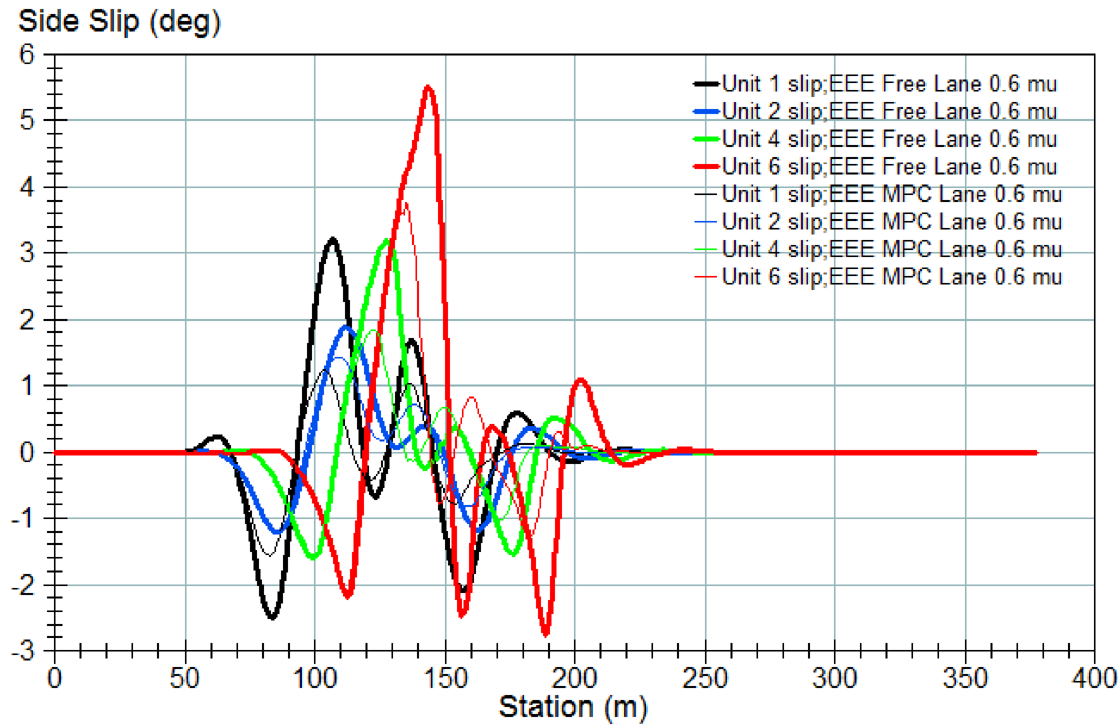

Figure J- 24: Side Slip, MPC Unloaded Vehicle, Lane Change, mu = 0.6

J.2.3. Unloaded Mu = 0.85

The dry road unloaded lane change had the same issues as the wet case (Figure J-25) with the controller balancing roll risk (Figure J- 26) and side slip risk (Figure J- 27). This event shows the power of the predictive capability as there would be little chance of correcting this issue if the controller only saw the current state of the vehicle. The controller succeeded as it began corrective actions at the start of the maneuver (Figure J-28) thus slowing the vehicle as well as placing the trailers in a better dynamic position prior to entering the first turn.

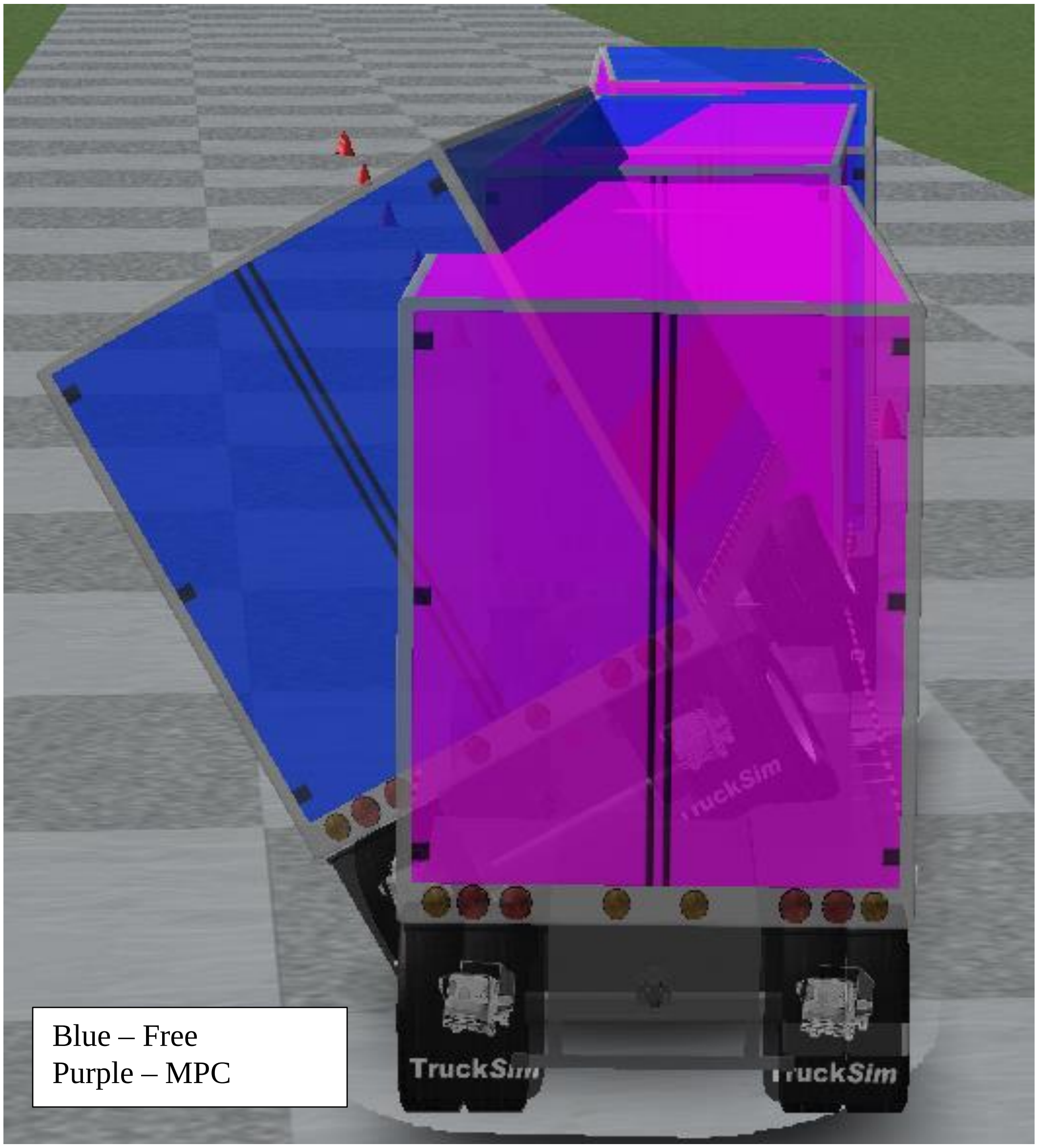

Figure J- 25: Illustration, MPC Unloaded Vehicle, Lane Change, mu = 0.85

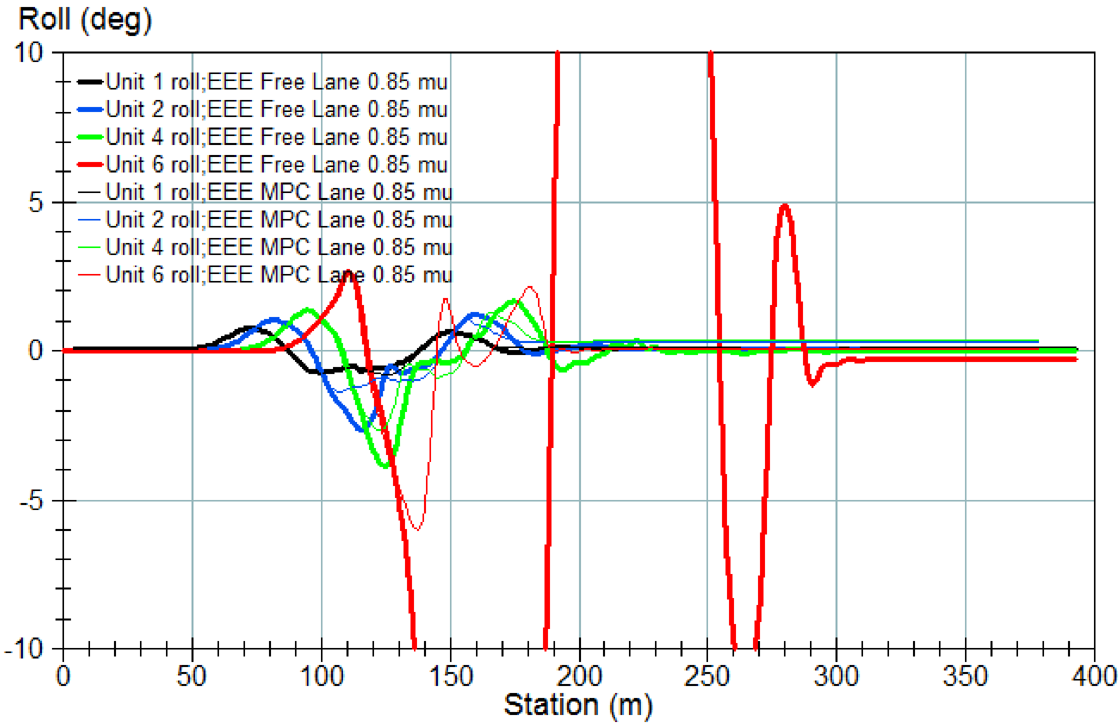

Figure J- 26: Roll, MPC Unloaded Vehicle, Lane Change, mu = 0.85

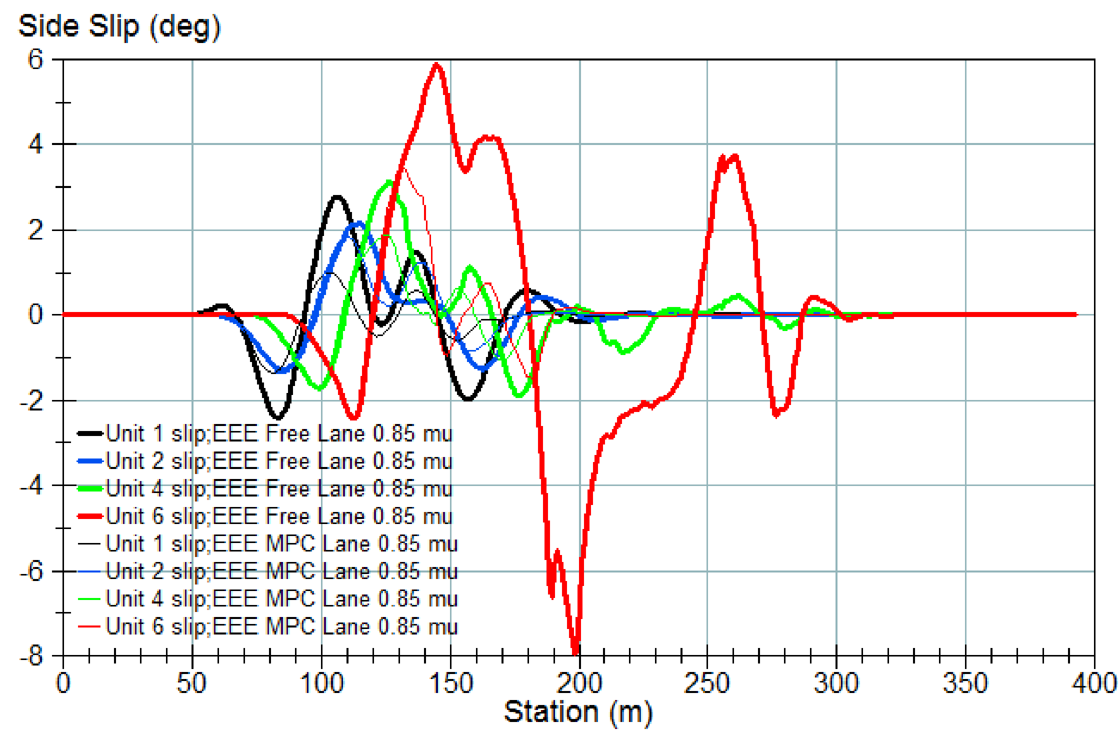

Figure J- 27: Side Slip, MPC Unloaded Vehicle, Lane Change, mu = 0.85

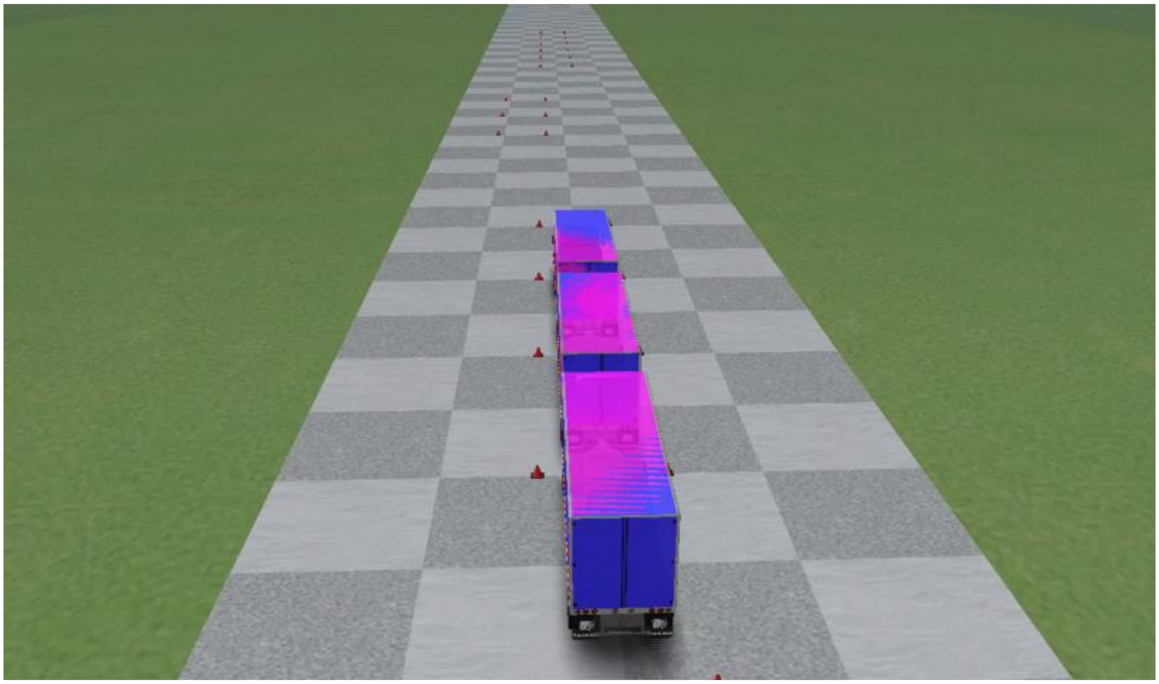

Figure J- 28: ESC Activation, MPC Unloaded Vehicle, Lane Change, mu = 0.85

J.2.4. Loaded Mu = 0.25

The effect of the controller on the loaded vehicle executing a double lane change on ice was as expected. The controller significantly reduced the vehicle side slip (Figure J-29) by modulating the left (Figure J- 30) and right (Figure J- 31) brakes. Note the trailer brake pressure modulations between the 150 and 200 meter marks. This is where the system was damping the rear amplification effect noted in Section 4.3.5.

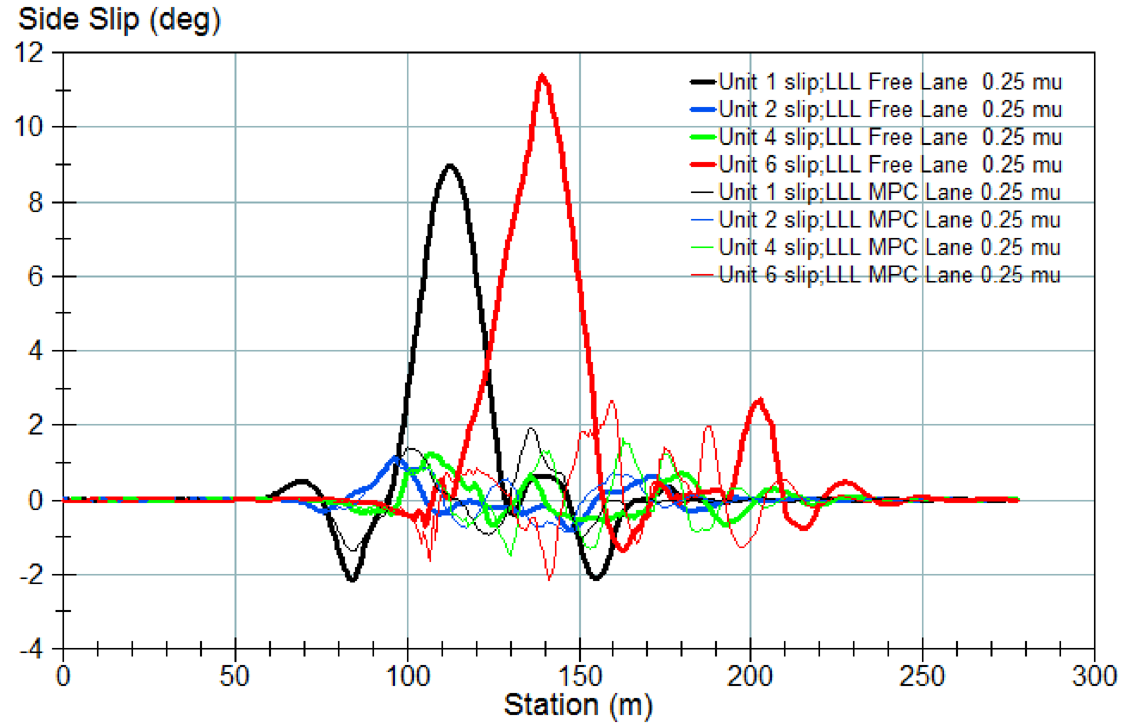

Figure J- 29: Side Slip, MPC Loaded Vehicle, Lane Change, mu = 0.25

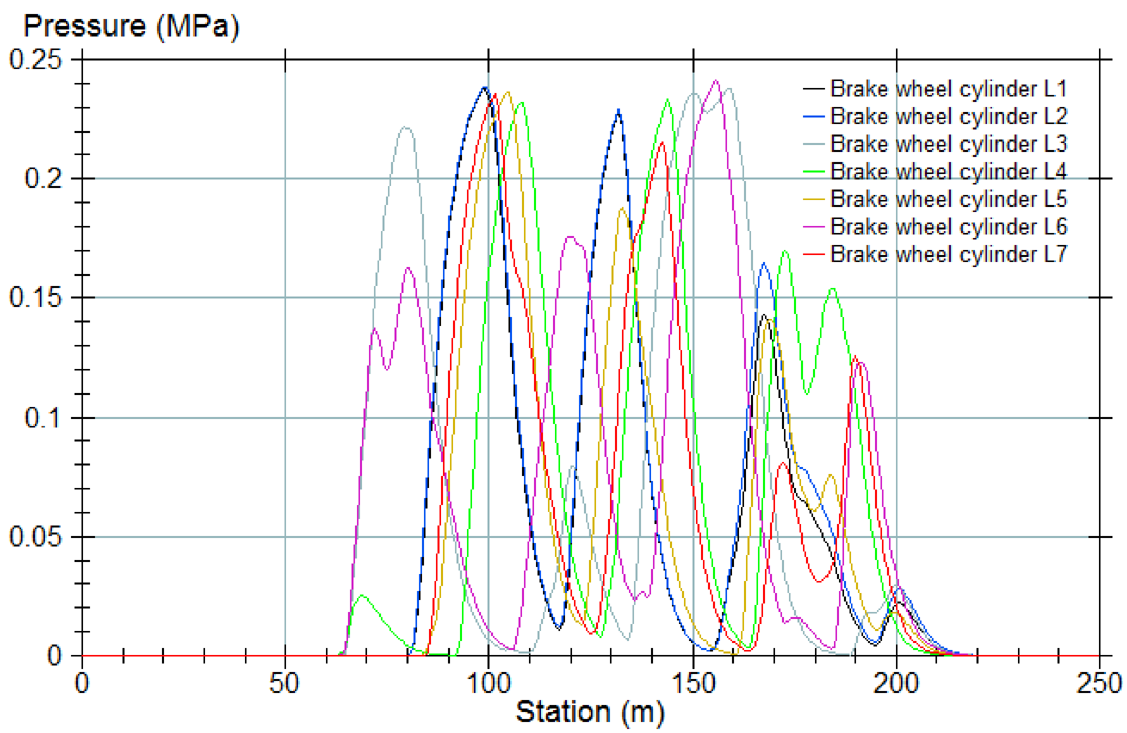

Figure J- 30: Left Brake, MPC Loaded Vehicle, Lane Change, mu = 0.25

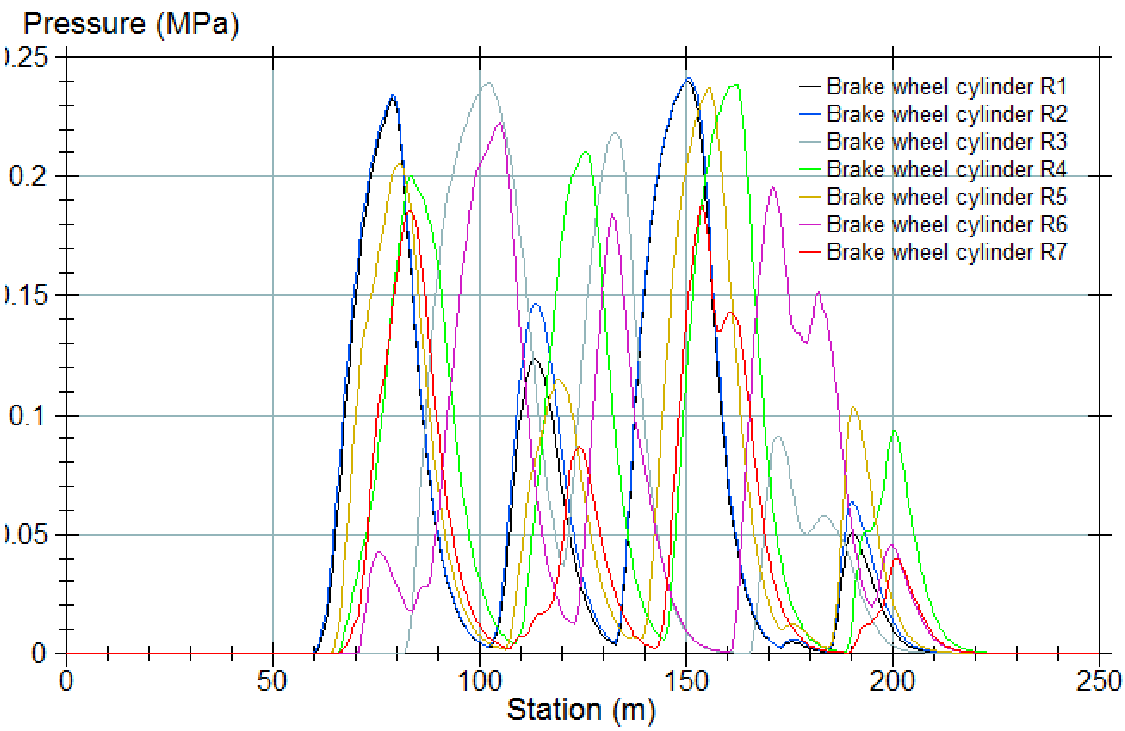

Figure J- 31: Right Brake, MPC Loaded Vehicle, Lane Change, mu = 0.25

J.2.5. Loaded Mu = 0.6

As was the case with the prior wet road simulations, the loaded vehicle was sensitive to both yaw (Figure J- 32) and roll (Figure J- 33) deviations at the same time. The controller predicted that all units would have a roll risk and applied the brakes to all units at nearly the same time (Figure J- 34). Additionally, the controller modulated the brakes to control side slip as it reacted to the roll threat.

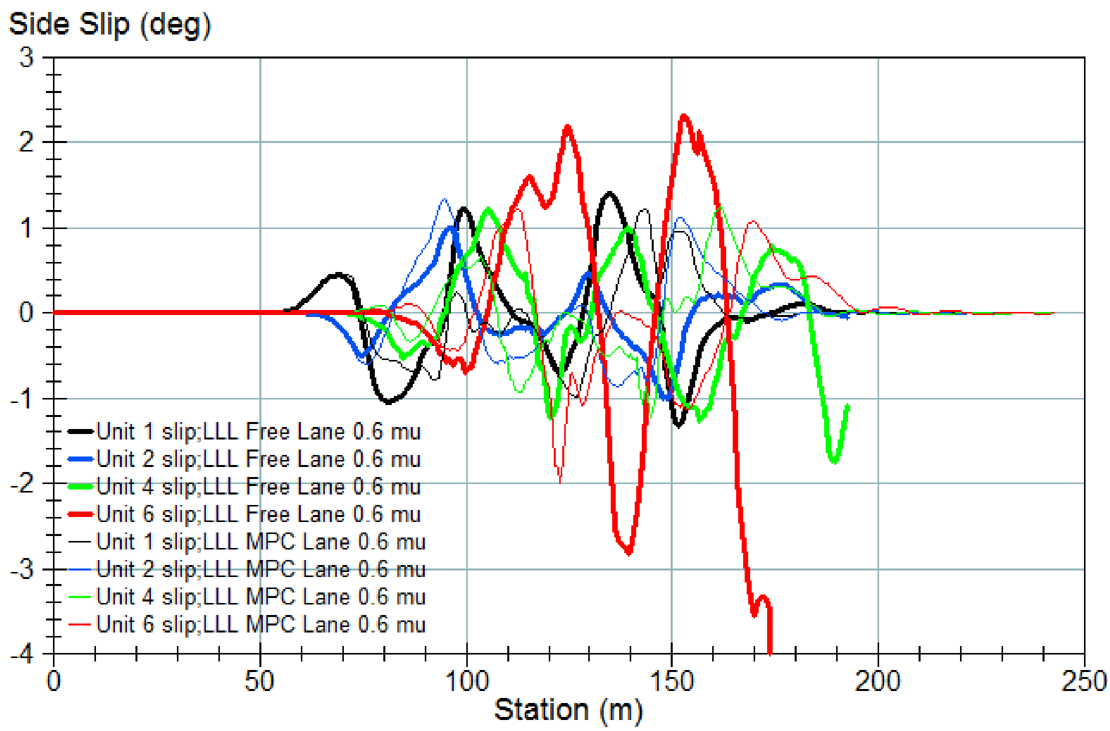

Figure J- 32: Side Slip, MPC Loaded Vehicle, Lane Change, mu = 0.6

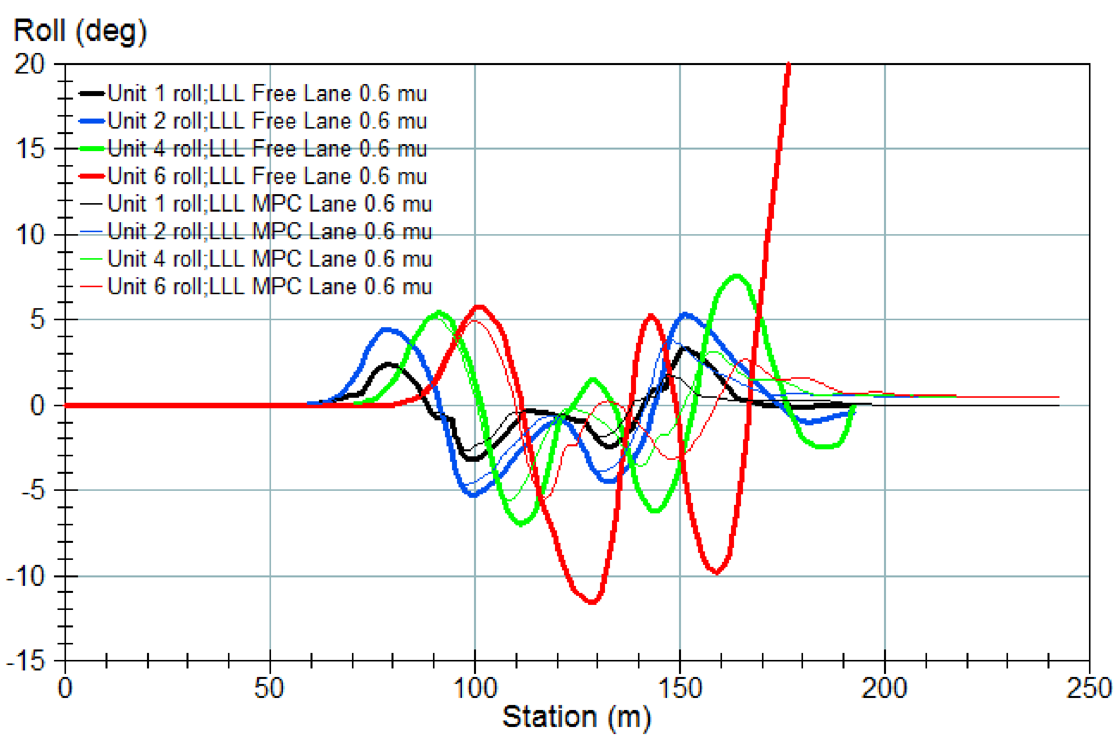

Figure J- 33: Roll, MPC Loaded Vehicle, Lane Change, mu = 0.6

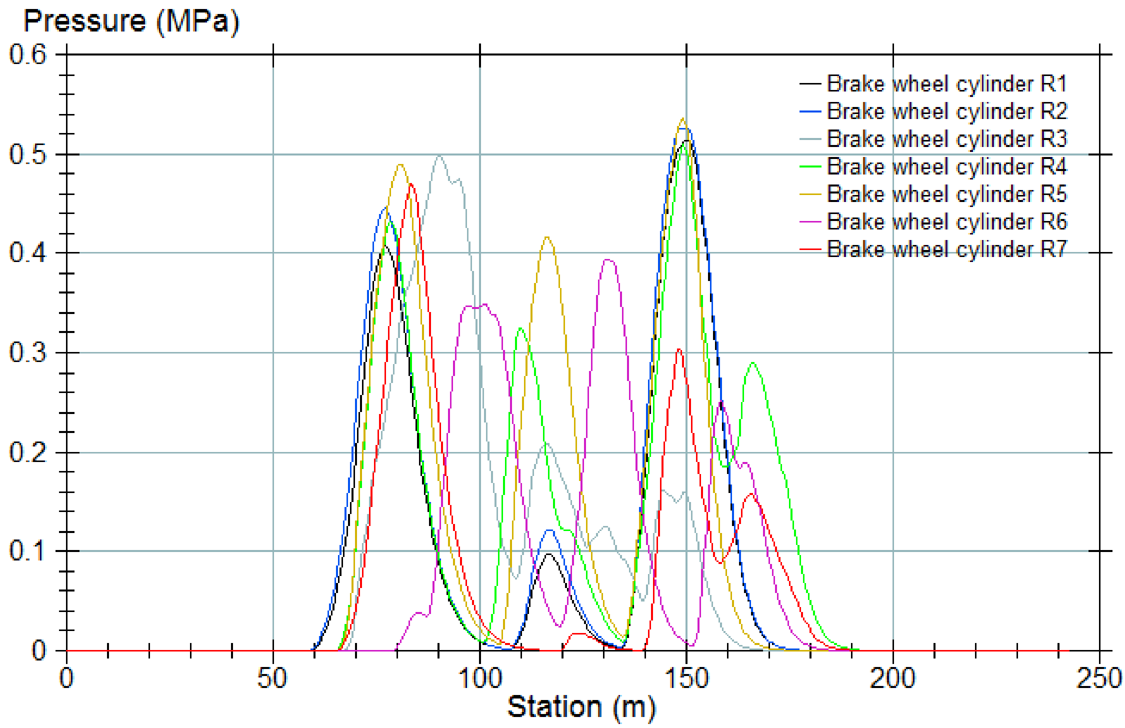

Figure J- 34: Right Brake, MPC Loaded Vehicle, Lane Change, mu = 0.6

J.2.6. Loaded Mu = 0.85

For the dry road loaded lane change case, the stability risk was in roll as expected (Figure J- 35). While the controller was successful in maintain stability, it was so aggressive in braking (Figure J- 36) that the vehicle slowed dramatically (Figure J- 37). This indicates that the controller may be a little too aggressive as the vehicle should certainly be able to manage this maneuver at 35 km/hour without stability control.

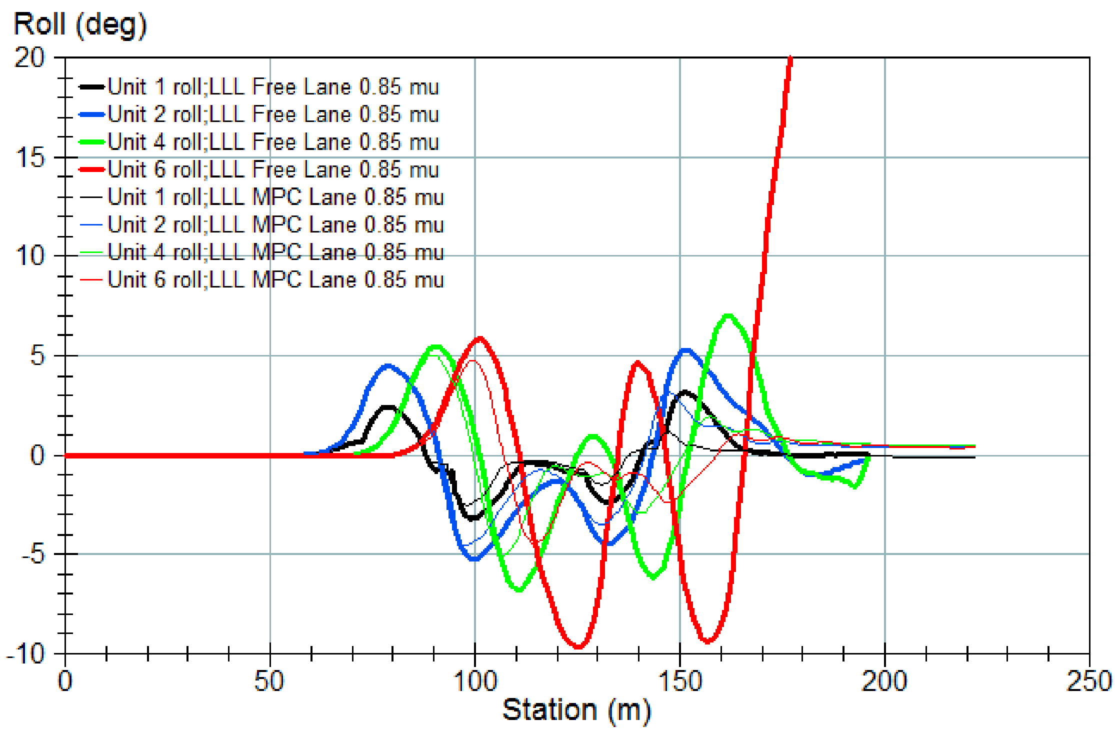

Figure J- 35: Roll, MPC Loaded Vehicle, Lane Change, mu = 0.85

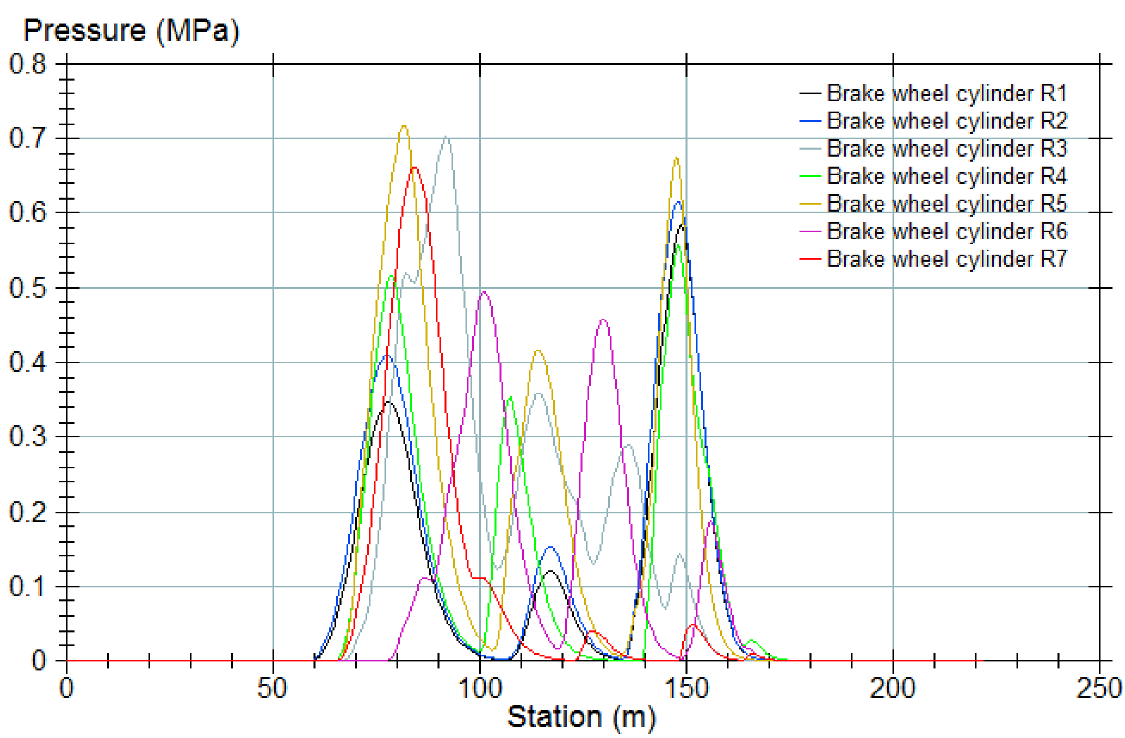

Figure J- 36: Right Brake, MPC Loaded Vehicle, Lane Change, mu = 0.85

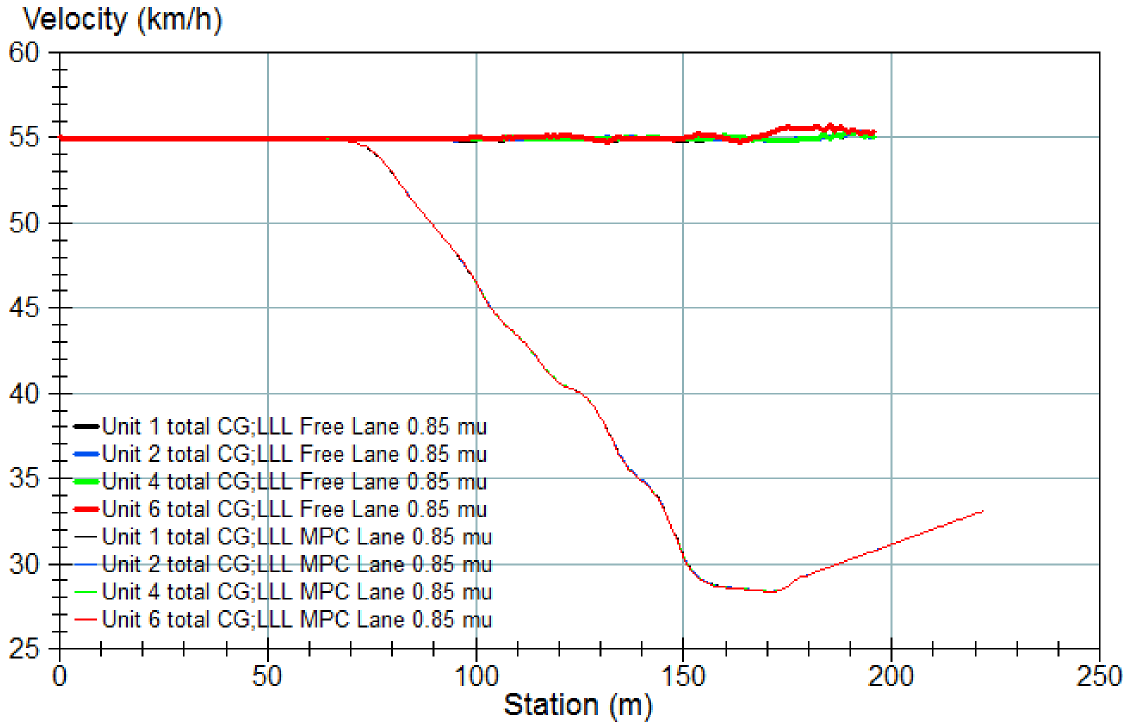

Figure J- 37: Velocity, MPC Loaded Vehicle, Lane Change, mu = 0.85

APPENDIX K

FUZZY LOGIC CONTROLLER PERFORMANCE

Just as the model predictive controller was evaluated using multiple cases, the fuzzy logic controller was evaluated using the same cases. The results of those case studies are presented here for review. For reference, the controller boundary limits are listed in Table K-1.

Table K-1: Fuzzy Logic Bounds

Measurement	Bound (SI)	Limit(SI)	Bound (CES)	Limit (CES)
Side slip	0.075 rad	0.15 rad	4.3 deg	8.6 deg
Yaw rate	0.3 rad/s	0.6 rad/s	17 deg/s	34 deg/s
Roll	0.05 rad	0.075 rad	2.9 deg	4.3 deg

K.1. Step Steer

The step steer maneuver was simply a 180º steering wheel input over 2/3 second. The vehicle speed depended on the load and the road surface.

K.1.1. Unloaded Mu = 0.25

As the model predictive controller was developed before the fuzzy logic controller, the vehicle target speeds were set to show the MPC response. In the case of the unloaded step steer on ice (Figure K- 1), this produced an interesting result as the fuzzy logic controller did not activate at all as can be observed in the brake responses for the left (Figure K- 2) and right (Figure K- 3) sides. As the vehicle never violated a boundary, the controller never actuated. This behavior is in complete agreement with the general theory on the controller's design.

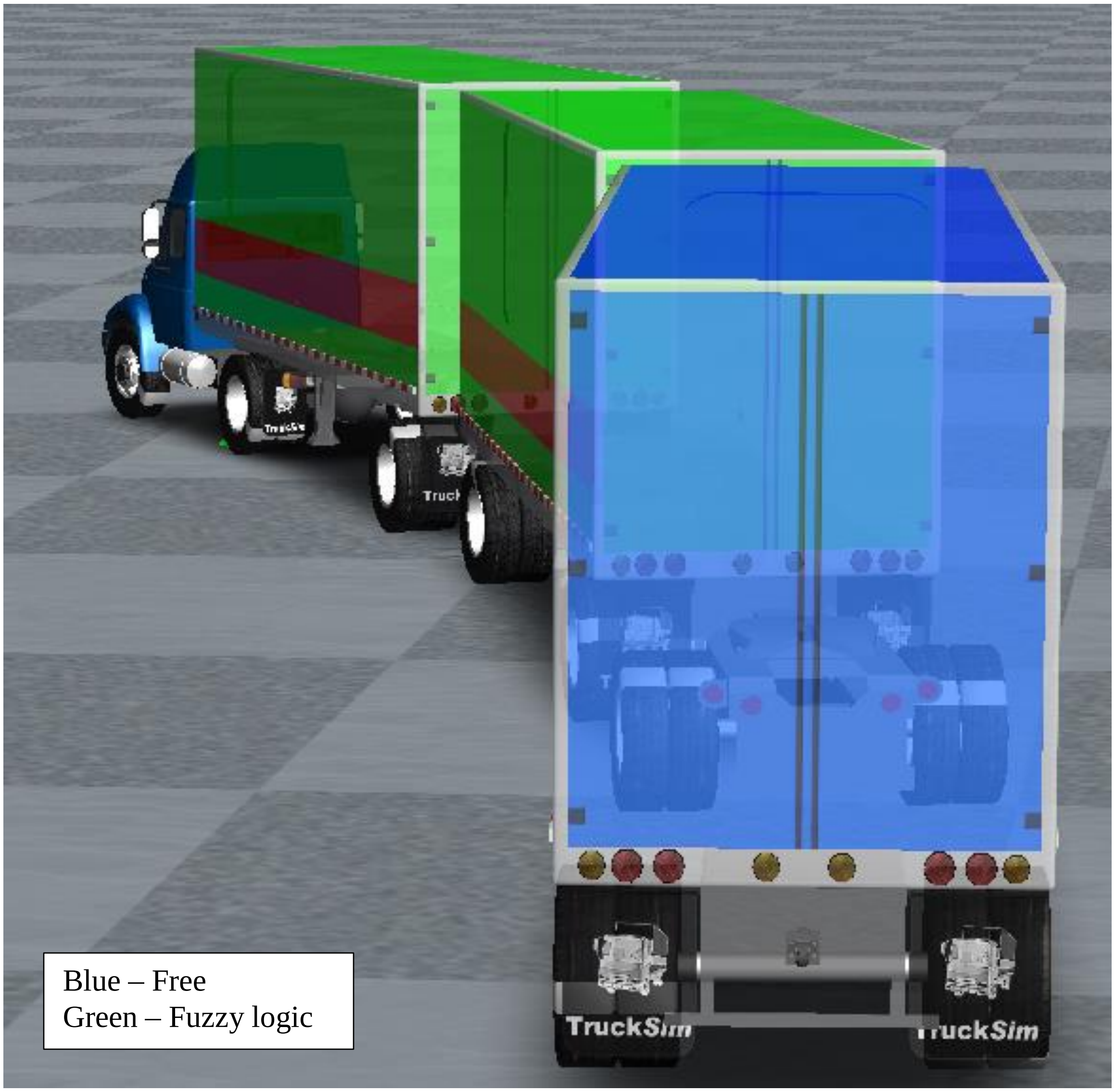

Figure K- 1: Illustration, Fuzzy Unloaded Vehicle, Step Steer, mu = 0.25

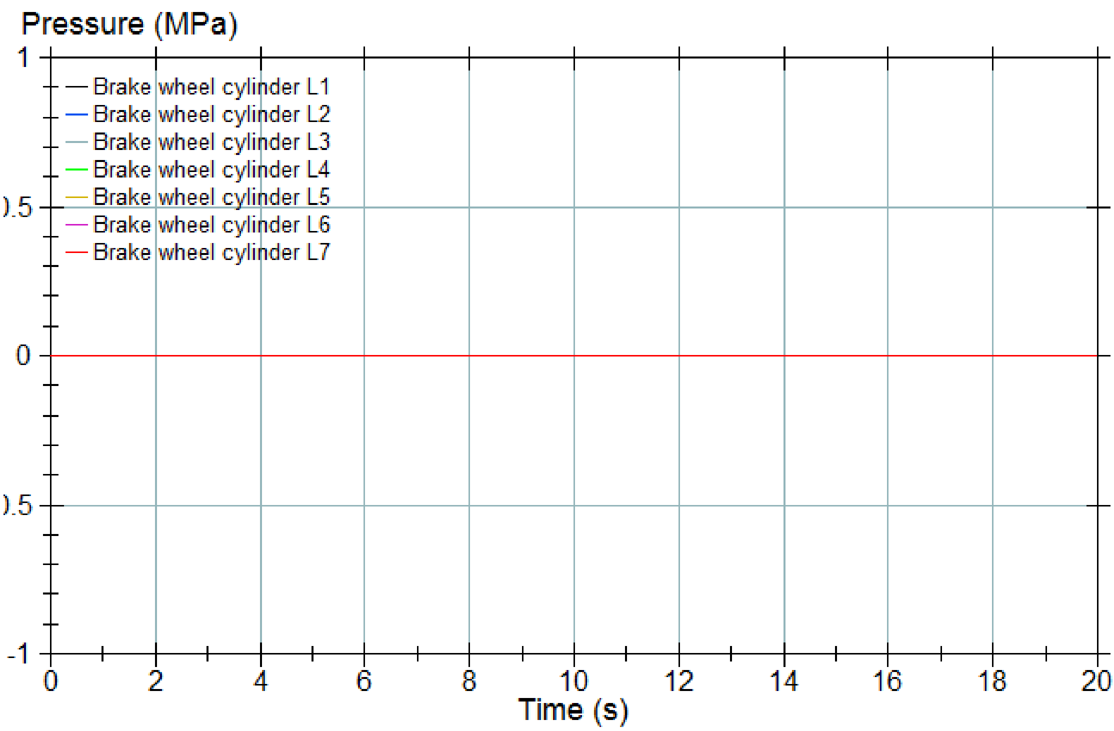

Figure K- 2: Left Brake, Fuzzy Unloaded Vehicle, Step Steer, mu = 0.25

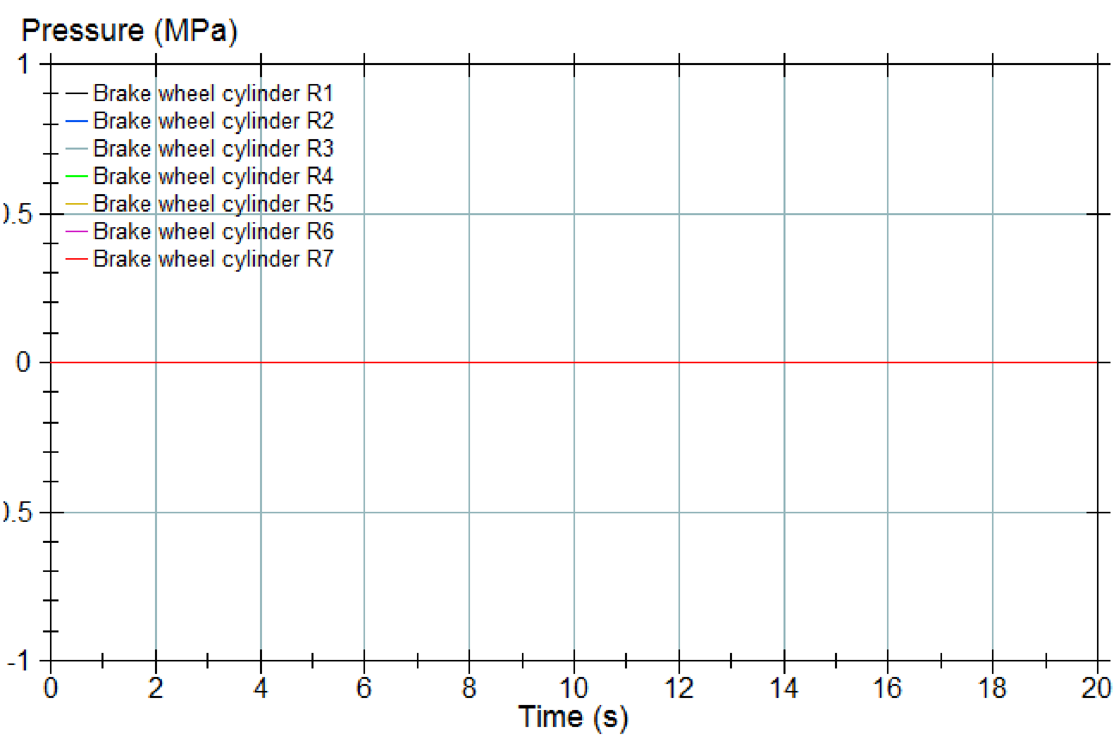

Figure K- 3: Right Brake, Fuzzy Unloaded Vehicle, Step Steer, mu = 0.25

K.1.2. Unloaded Mu = 0.6

When the road friction for the unloaded step steer maneuver was increased to 0.6 (wet), the vehicle became roll unstable (Figure K- 4). The controller responded by applying the brakes as expected (Figure K- 5, Figure K- 6). Note the minimal left brake (Figure K- 5) implementation to stabilize the vehicle in side slip.

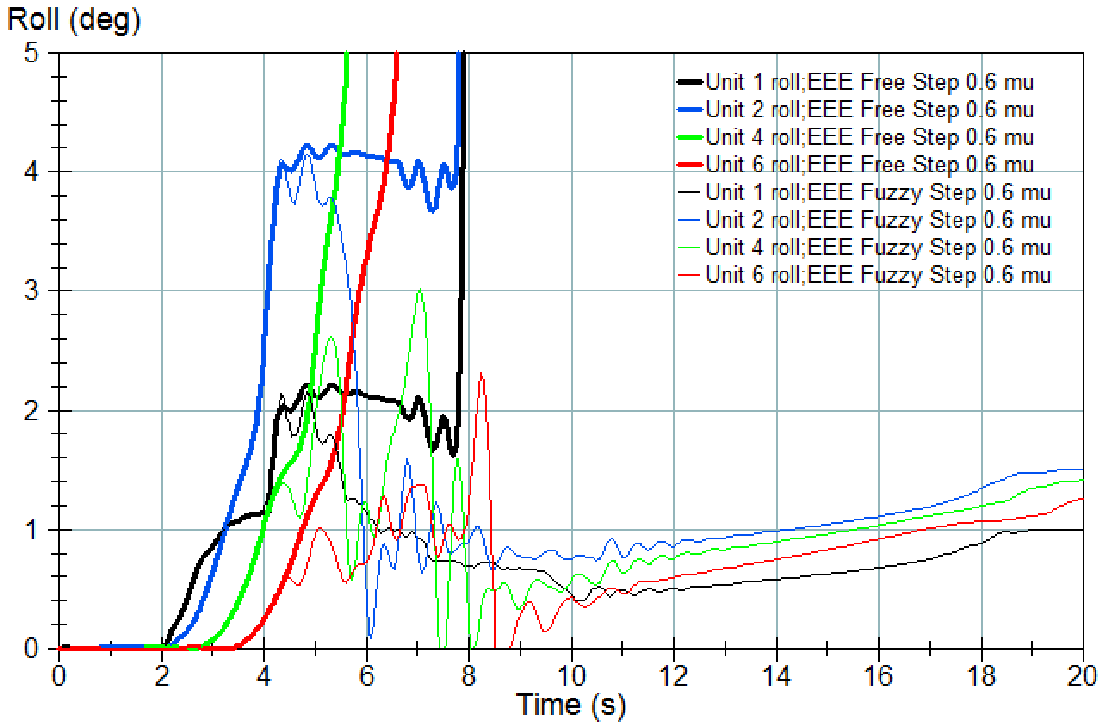

Figure K- 4: Roll, Fuzzy Unloaded Vehicle, Step Steer, mu = 0.6

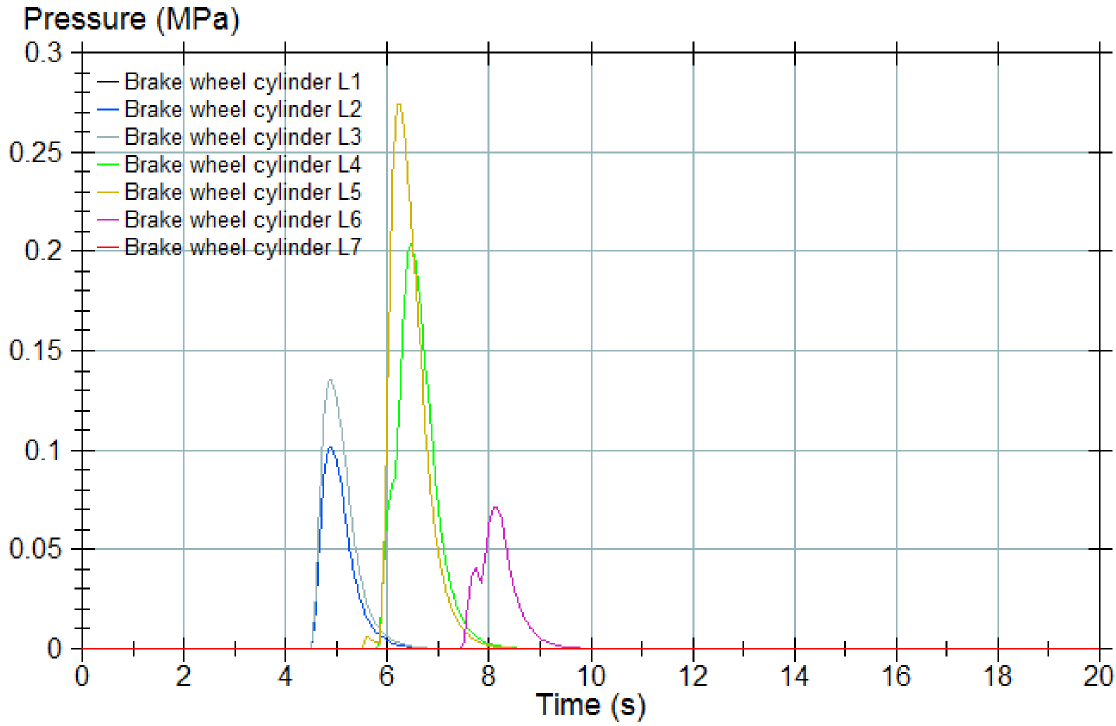

Figure K- 5: Left Brake, Fuzzy Unloaded Vehicle, Step Steer, mu = 0.6

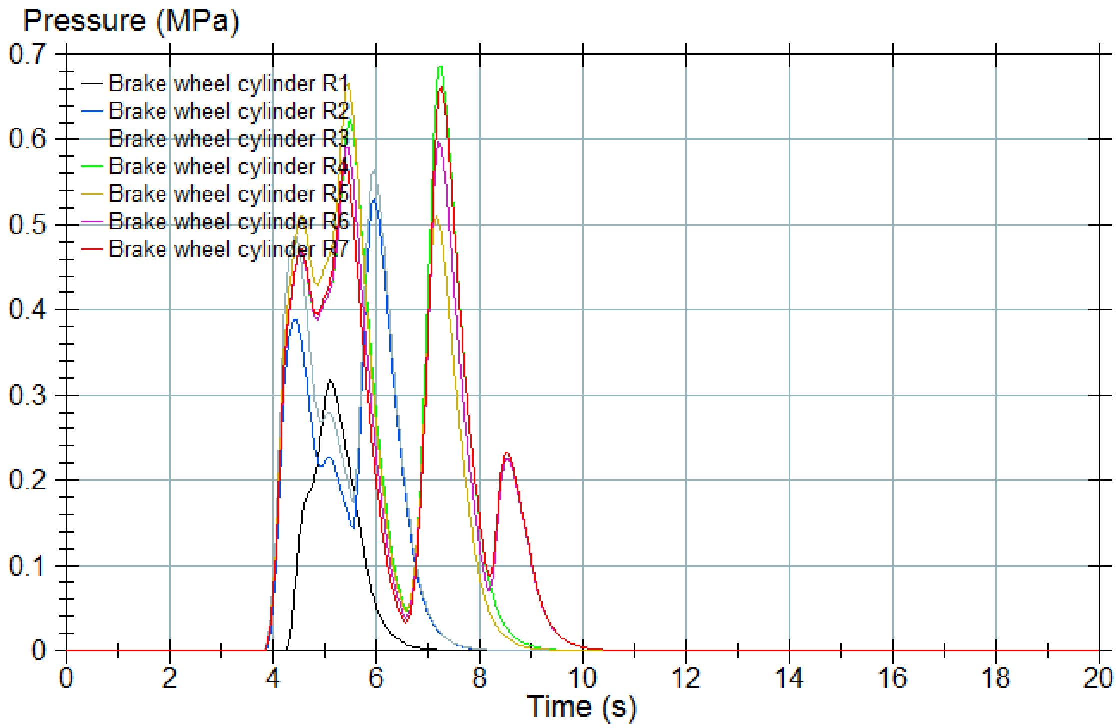

Figure K- 6: Right Brake, Fuzzy Unloaded Vehicle, Step Steer, mu = 0.6

K.1.3. Unloaded Mu = 0.85

As expected, the unloaded vehicle was even more sensitive to roll (Figure K- 7) as the mu increased to 0.85. The controller also could apply greater braking forces (the ABS controller limited pressure on lower mu surfaces). Note that the left side brakes (Figure K- 8) are now nearly as strong as the right side (Figure K- 9). This was to mitigate brake induced side slip, but the result of this frequent and aggressive left side braking was a severe shaking of the vehicle past 7 seconds as seen in Figure K- 7 .

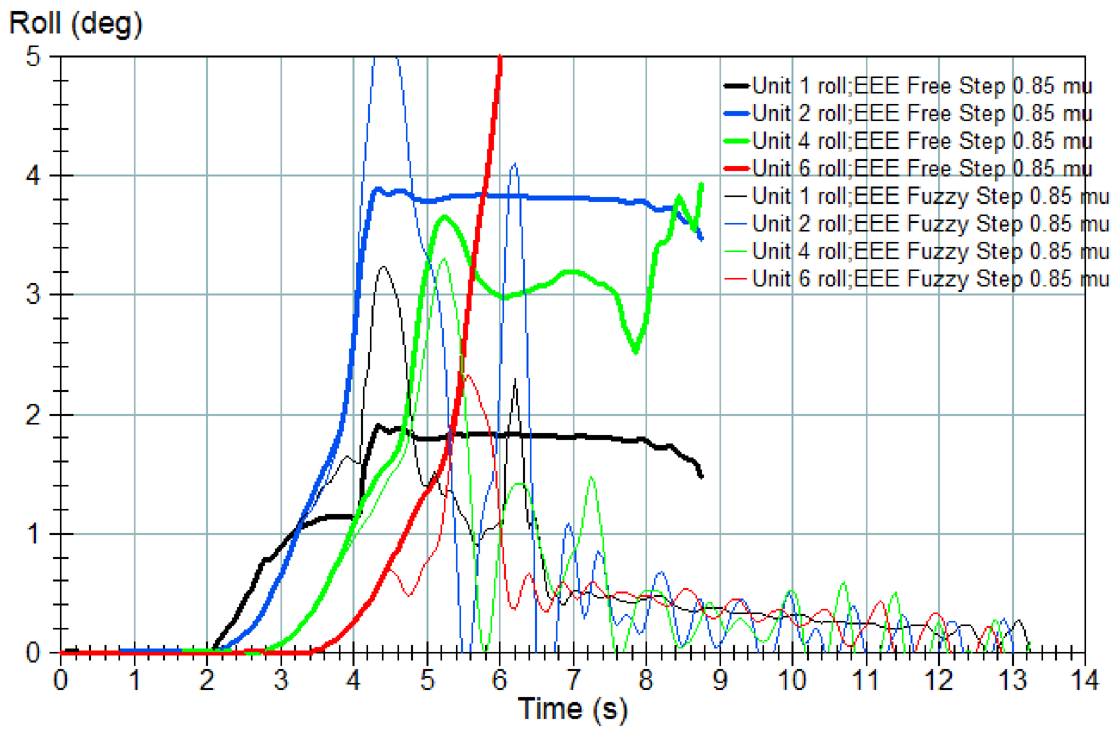

Figure K- 7: Roll, Fuzzy Unloaded Vehicle, Step Steer, mu = 0.85

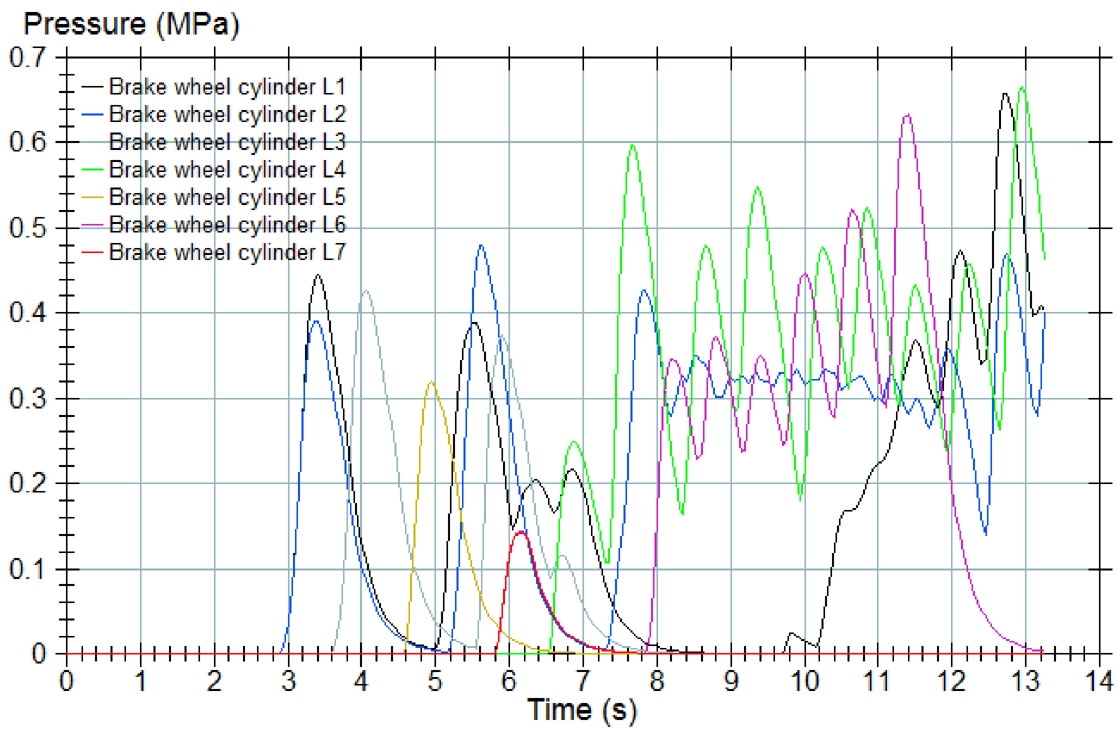

Figure K- 8: Left Brake, Fuzzy Unloaded Vehicle, Step Steer, mu = 0.85

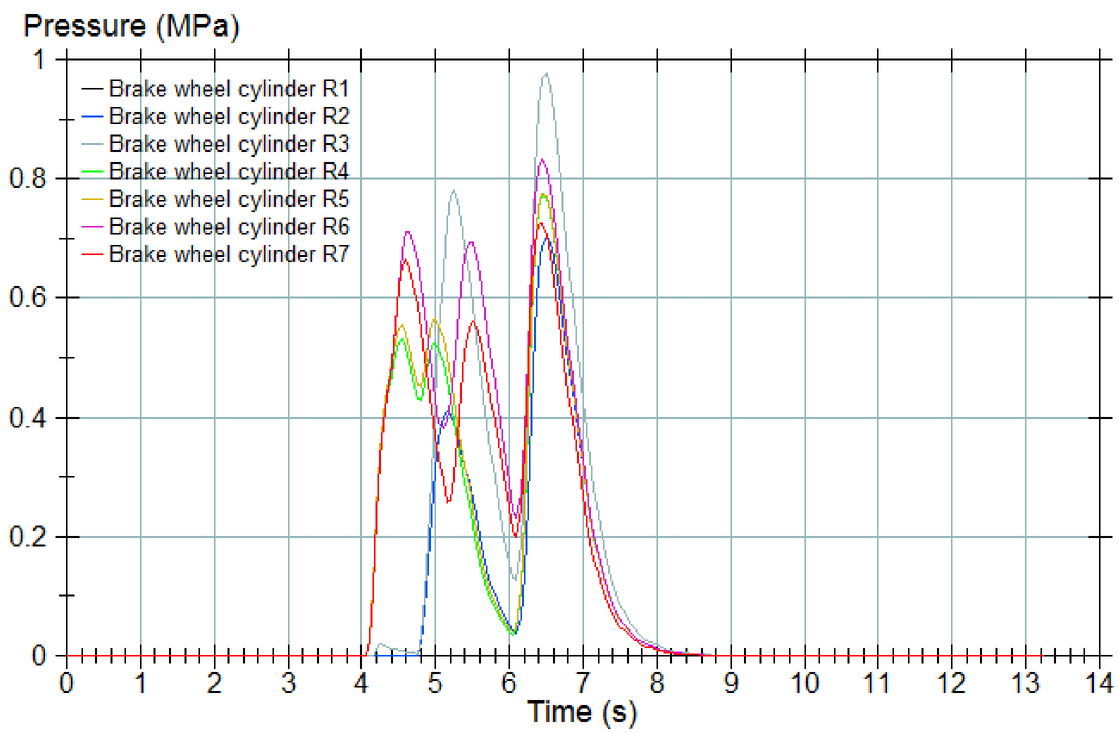

Figure K- 9: Right Brake, Fuzzy Unloaded Vehicle, Step Steer, mu = 0.85

K.1.4. Loaded Mu = 0.25

The loaded vehicle exhibited roll (Figure K- 11) and yaw (Figure K- 10) instability during the step steer maneuver on ice. While the open loop vehicle did not rollover, the resultant roll angles did exceed the stability bounds. The brake response (Figure K- 12) succeeded in stabilizing the vehicle in yaw (the most important requirement) as well as reducing the roll angle of the vehicle.

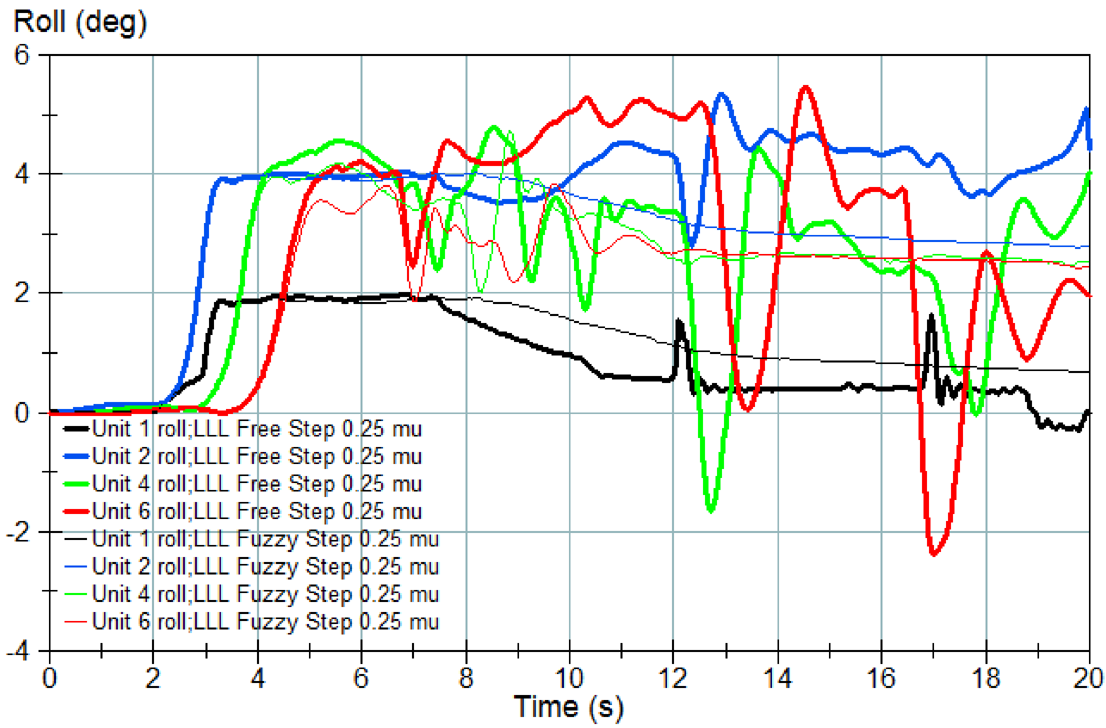

Figure K- 10: Roll, Fuzzy Loaded Vehicle, Step Steer, mu = 0.25

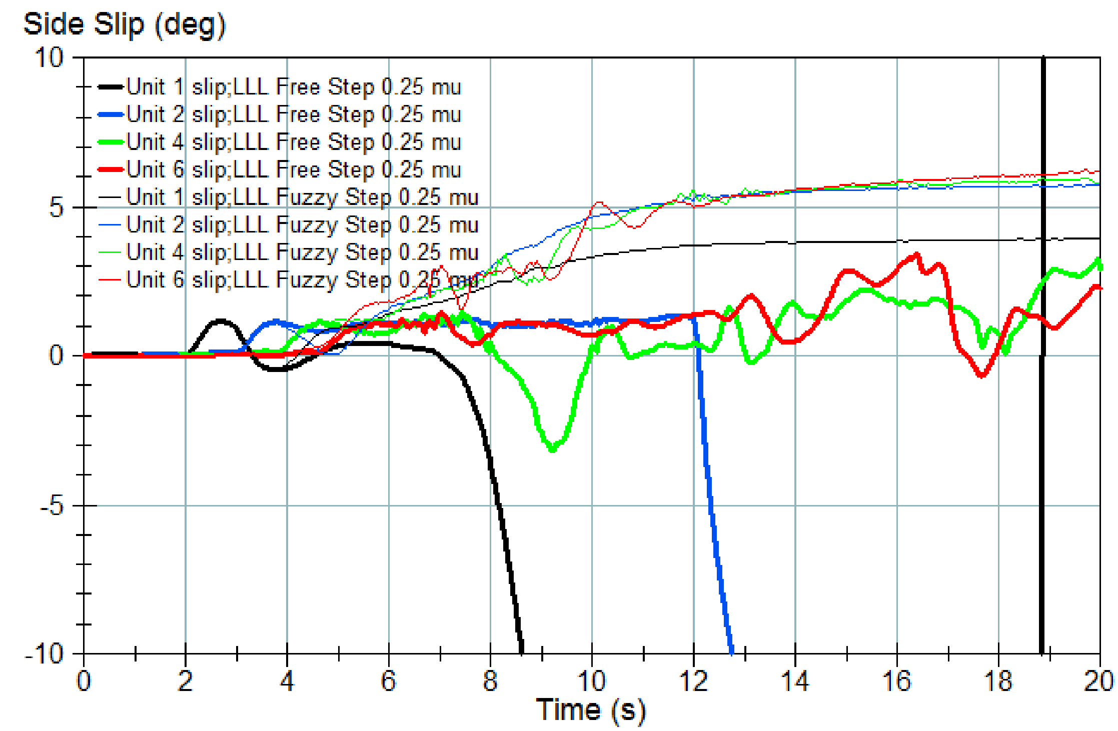

Figure K- 11: Side Slip, Fuzzy Loaded Vehicle, Step Steer, mu = 0.25

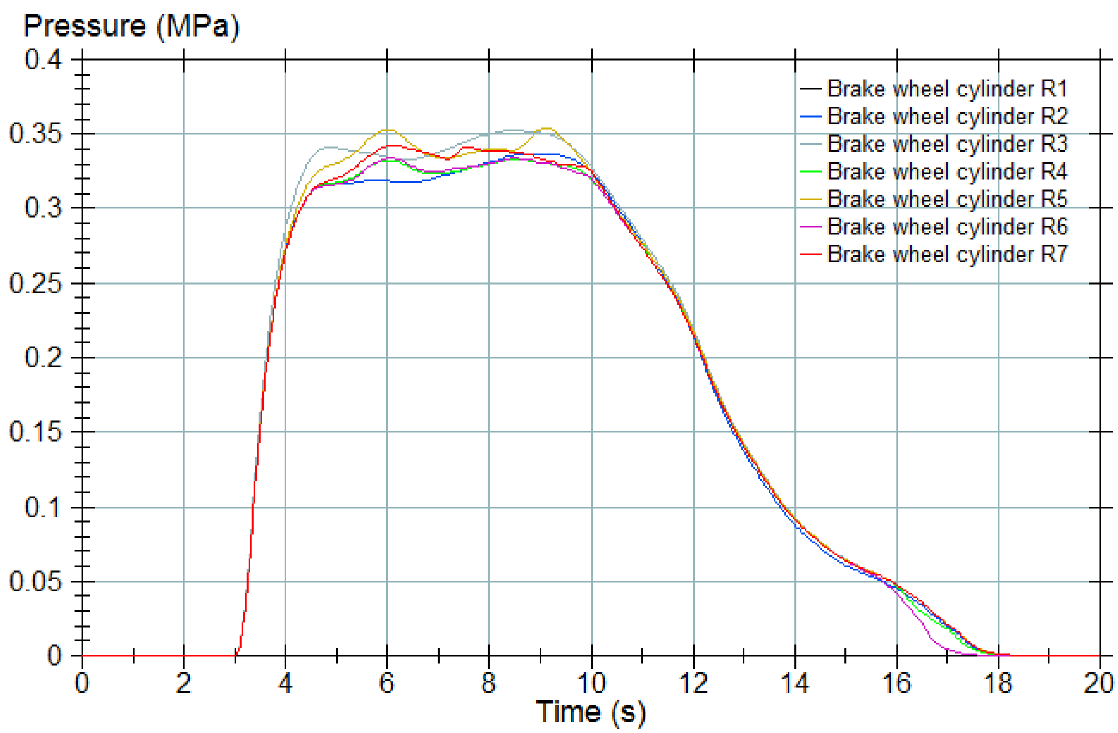

Figure K- 12: Brake, Fuzzy Loaded Vehicle, Step Steer, mu = 0.25

K.1.5. Loaded Mu = 0.6

With increasing road friction level, the loaded vehicle exhibited roll instability during the step steer event (Figure K- 13) and the fuzzy logic controller activated the brakes (Figure K- 15) to reduce the yaw rate (Figure K- 14) and thus lower the lateral acceleration. Note that the steer axle brakes (R1) were released fairly quickly as the tractor is not generally a roll risk.

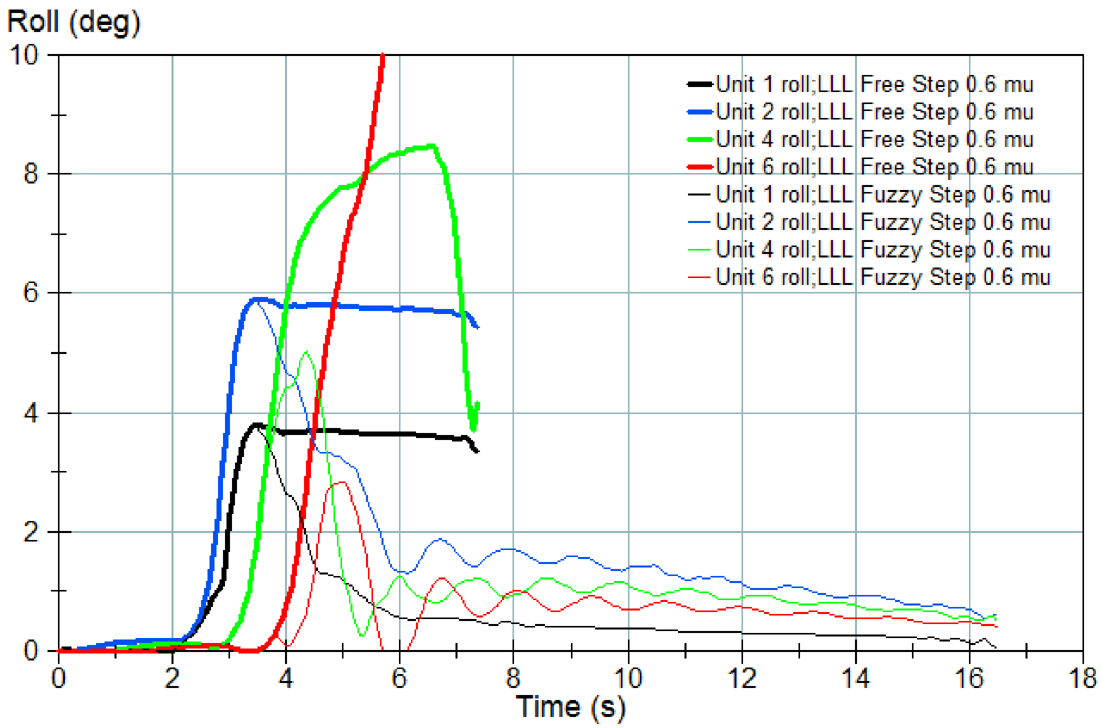

Figure K- 13: Roll, Fuzzy Loaded Vehicle, Step Steer, mu = 0.6

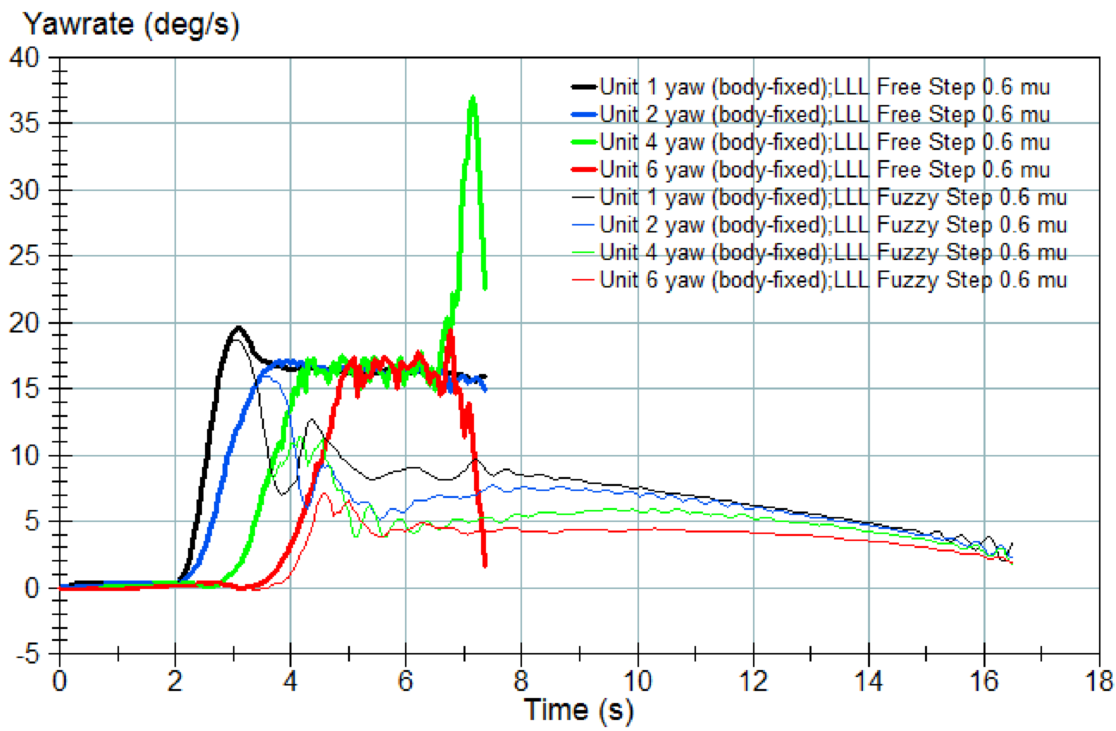

Figure K- 14: Yaw Rate, Fuzzy Loaded Vehicle, Step Steer, mu = 0.6

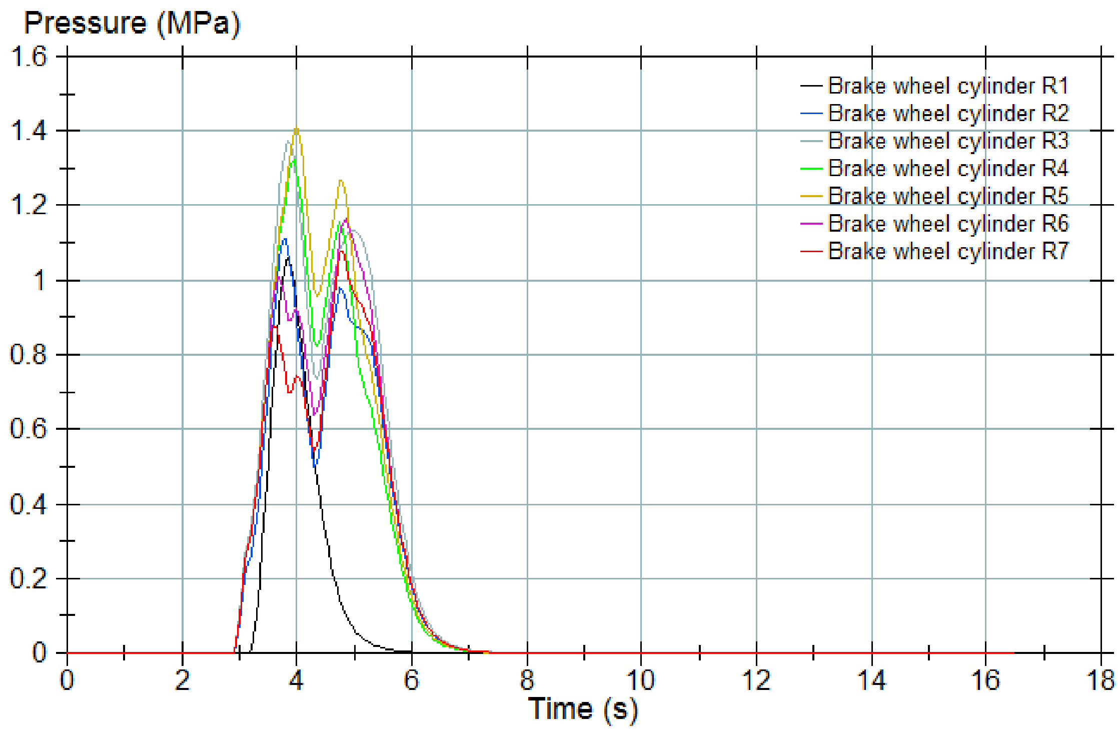

Figure K- 15: Right Brake, Fuzzy Loaded Vehicle, Step Steer, mu = 0.6

K.1.6. Loaded Mu = 0.85

The dry loaded step steer exhibited significantly more roll risk than the wet case as expected (Figure K- 16). The fuzzy logic controller also activated brakes on all units of the vehicle (predictive capability) as expected (Figure K- 17). Of course, with high traction limits and high brake pressures, the result was also a drastic reduction in vehicle speed (Figure K- 18).

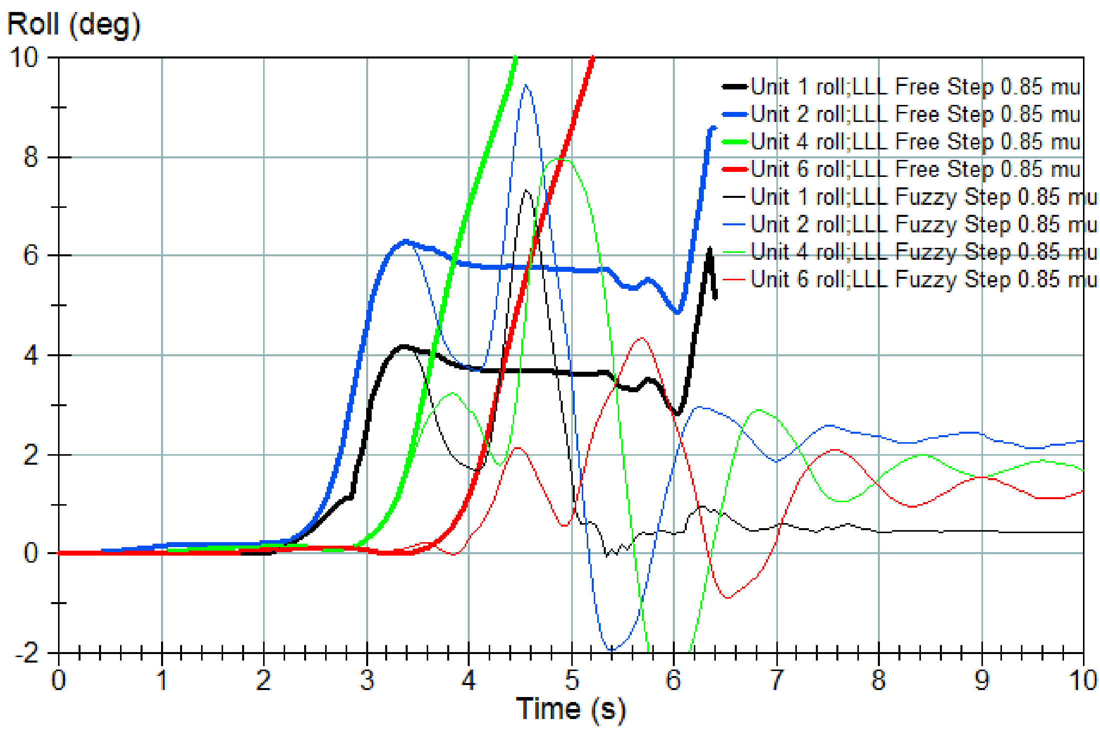

Figure K- 16: Roll, Fuzzy Loaded Vehicle, Step Steer, mu = 0.85

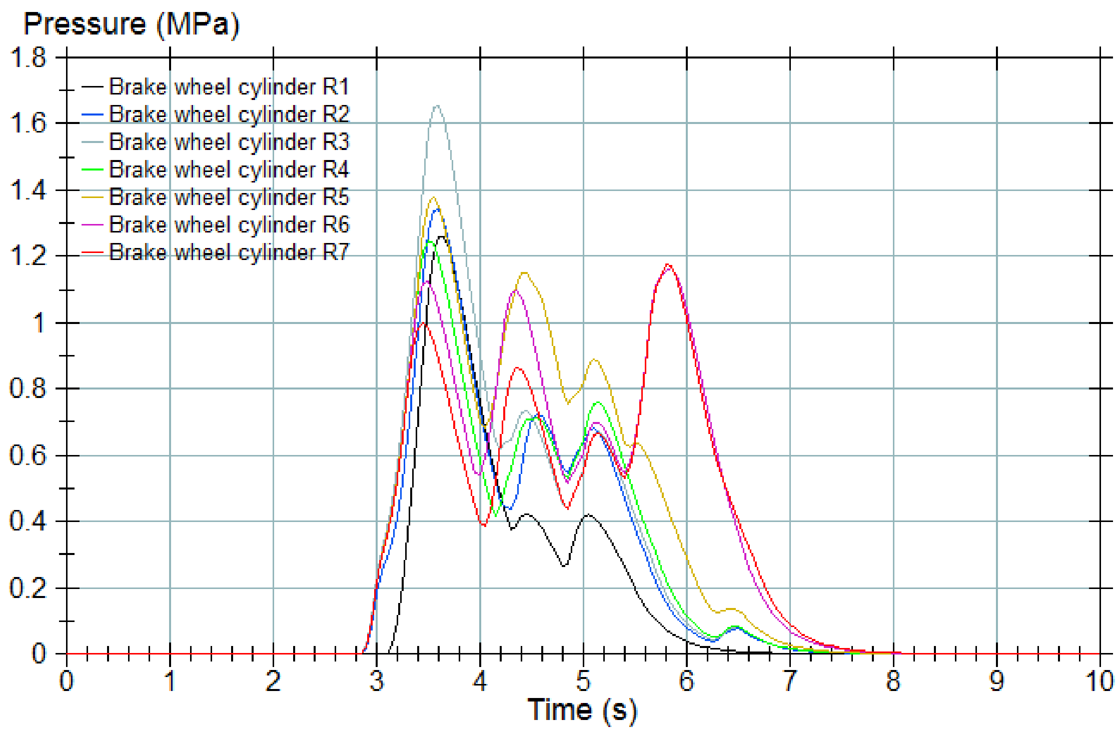

Figure K- 17: Brakes, Fuzzy Loaded Vehicle, Step Steer, mu = 0.85

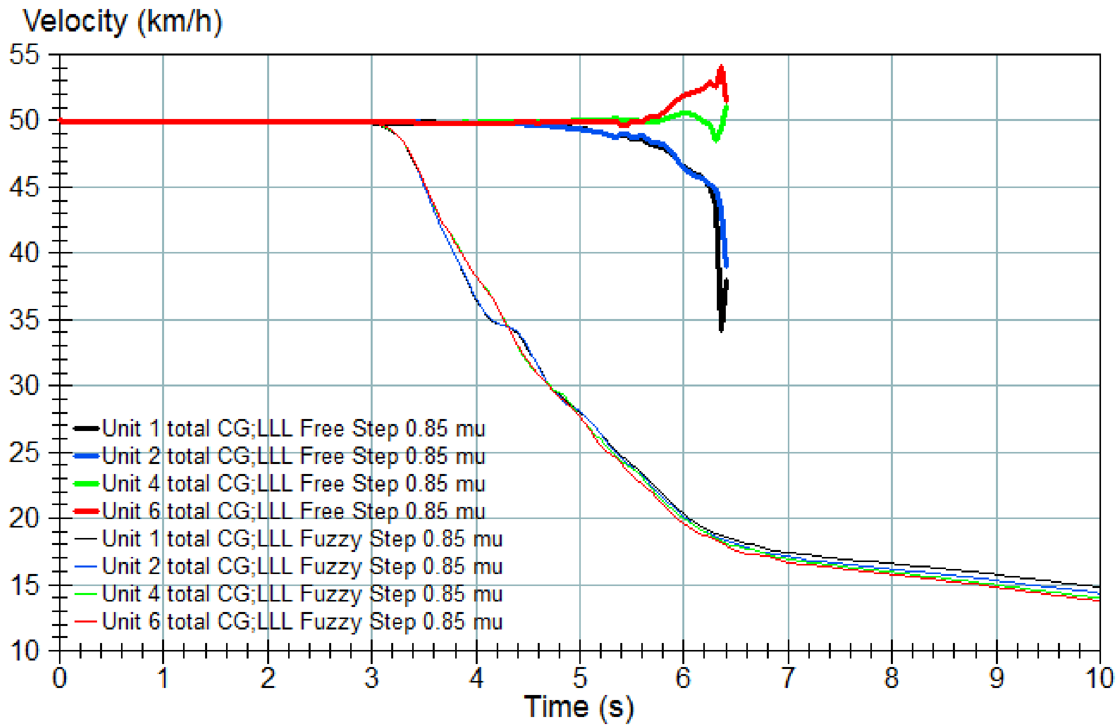

Figure K- 18: Velocity, Fuzzy Loaded Vehicle, Step Steer, mu = 0.85

K.2. Double Lane Change

In addition to the step steer maneuver, each of the vehicle combination cases was also evaluated using the ISO double lane change. Given the multiple course corrections, this test was particularly demanding on the last trailer.

K.2.1. Unloaded Mu = 0.25

The unloaded double lane change on ice proved to be a very interesting case as it showed just how little control was needed to correct some instability events. In this case, the vehicle was susceptible to side slip and jackknife (Figure K- 19). To stabilize the vehicle, the fuzzy logic controller had to apply a very short brake moment to the steer axle to get the vehicle to stabilize at the first gate (Figure K- 20) and a short brake moment on the steer axle to stabilize the vehicle at the second gate (Figure K- 21). The controller simply had to get the tractor's path under control and the trailers followed.

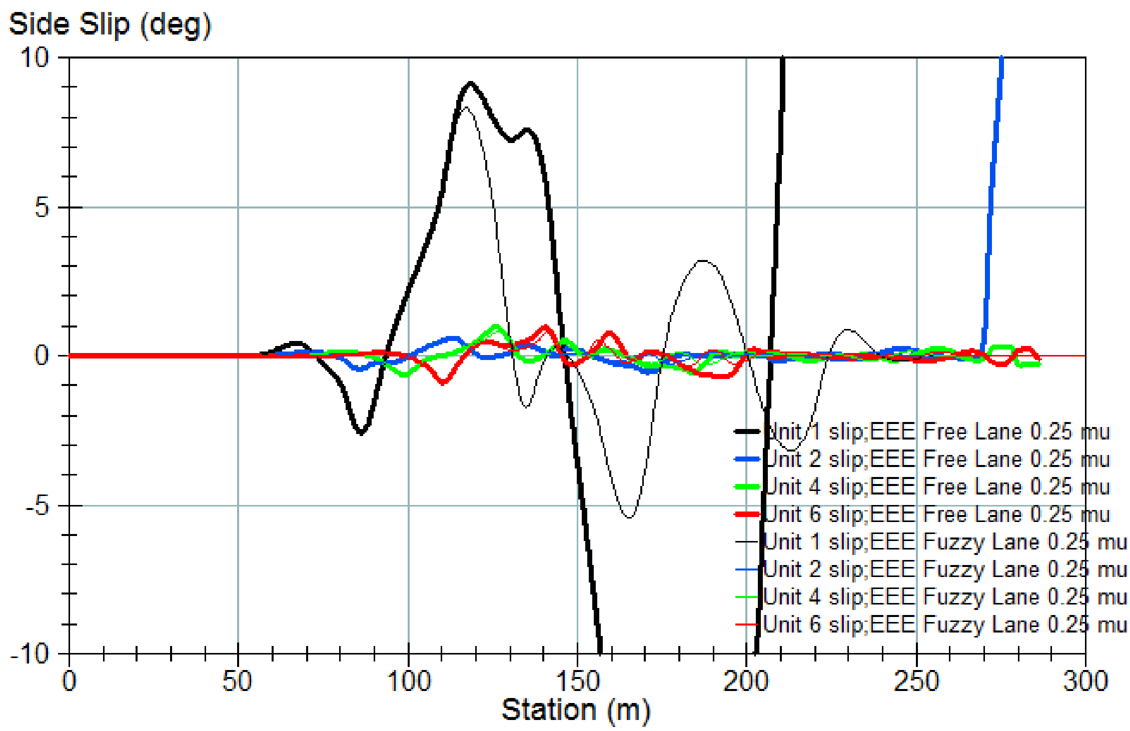

Figure K- 19: Side Slip, Fuzzy Unloaded Vehicle, Lane Change, mu = 0.25

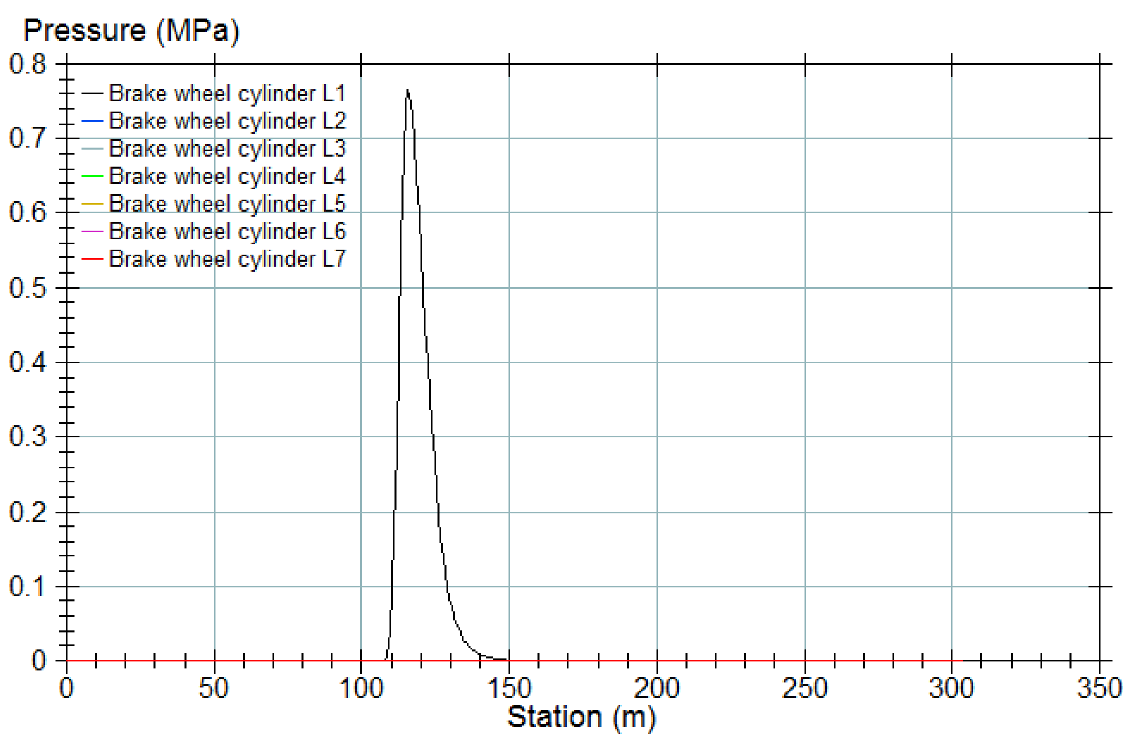

Figure K- 20: Left Brake, Fuzzy Unloaded Vehicle, Lane Change, mu = 0.25

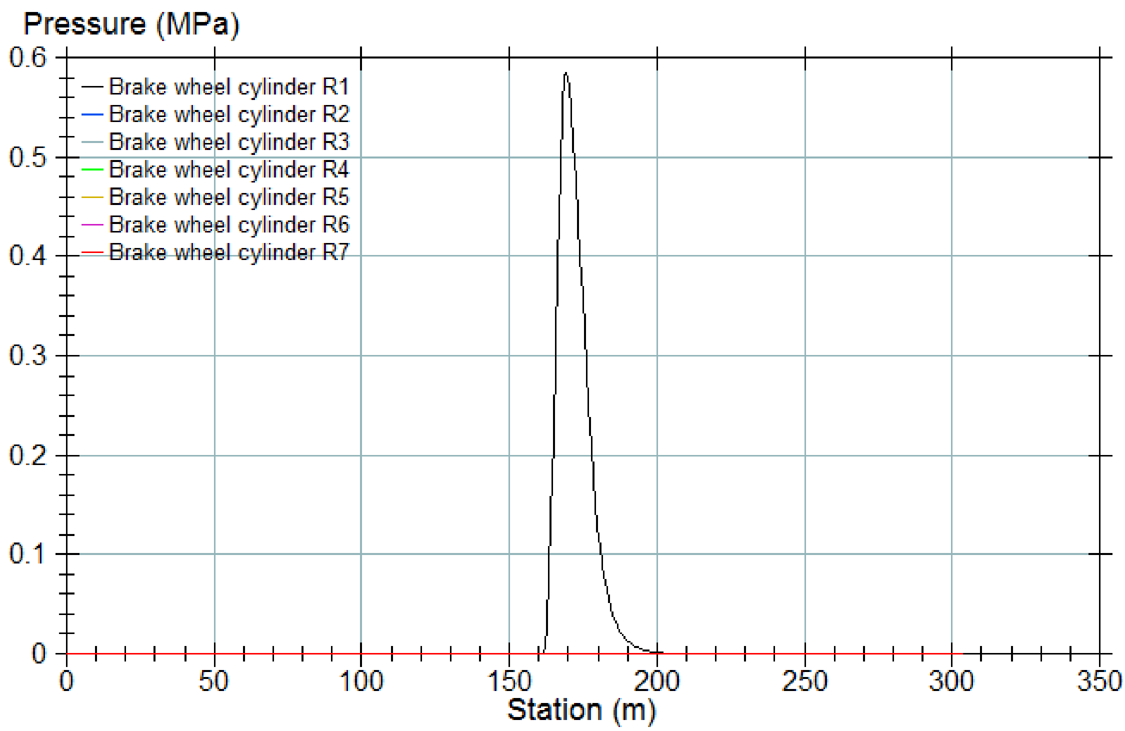

Figure K- 21: Right Brake, Fuzzy Unloaded Vehicle, Lane Change, mu = 0.25

K.2.2. Unloaded Mu = 0.6

As the traction level increased for the unloaded lane change, the yaw unstable vehicle above became more roll unstable as expected. As roll stability (Figure K- 22) was the biggest threat (had the largest membership value), the corrective action was dominated by the need to reduce the roll angle. This resulted in side slip (Figure K- 23) and yaw rate (Figure K- 24) increasing rather than decreasing relative to the uncontrolled vehicle. However, the yaw rate remained within the set bounds and the error in side slip was not nearly as significant as the error in roll.

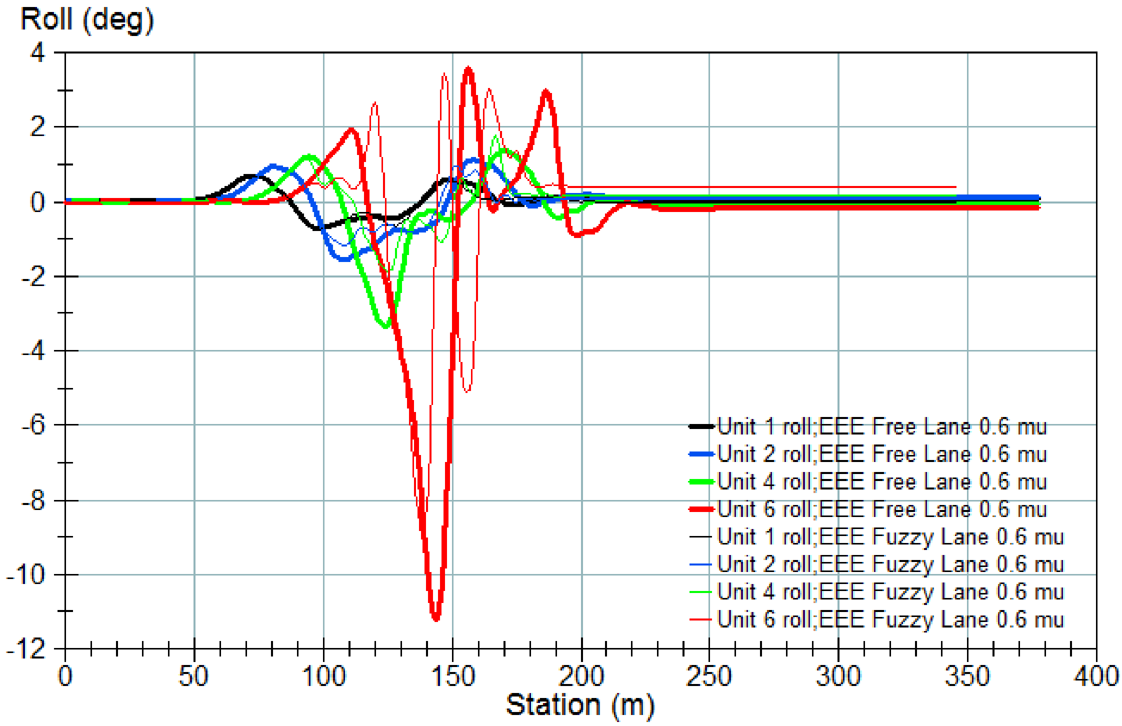

Figure K- 22: Roll, Fuzzy Unloaded Vehicle, Lane Change, mu = 0.6

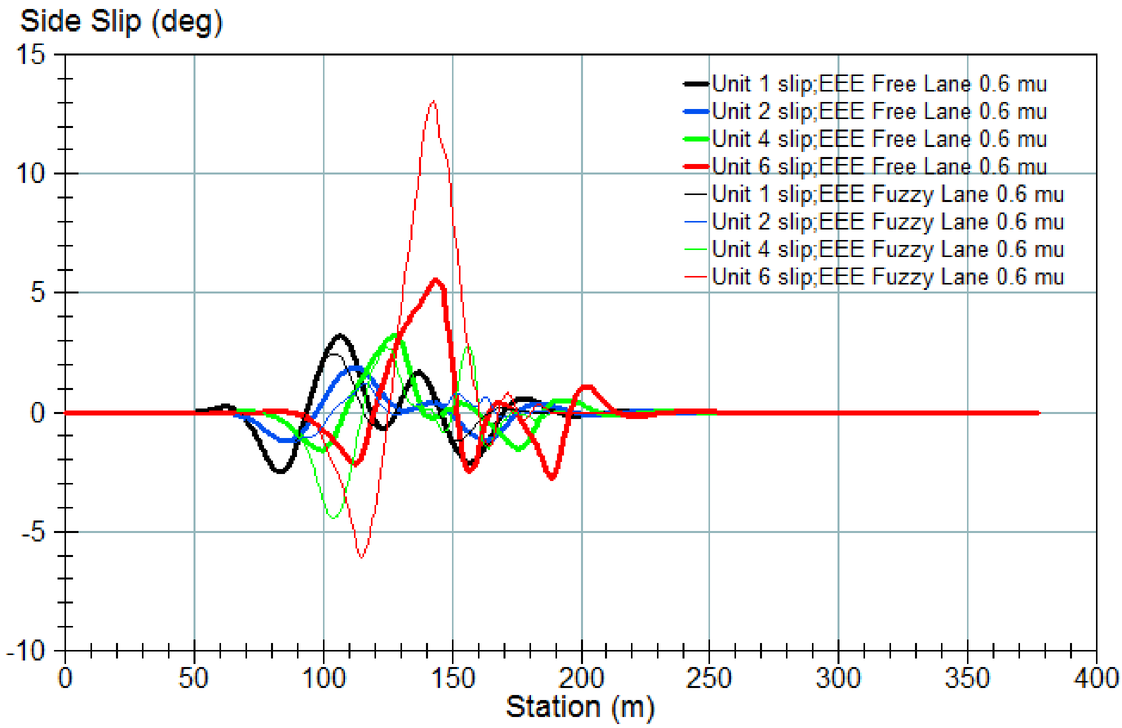

Figure K- 23: Side Slip, Fuzzy Unloaded Vehicle, Lane Change, mu = 0.6

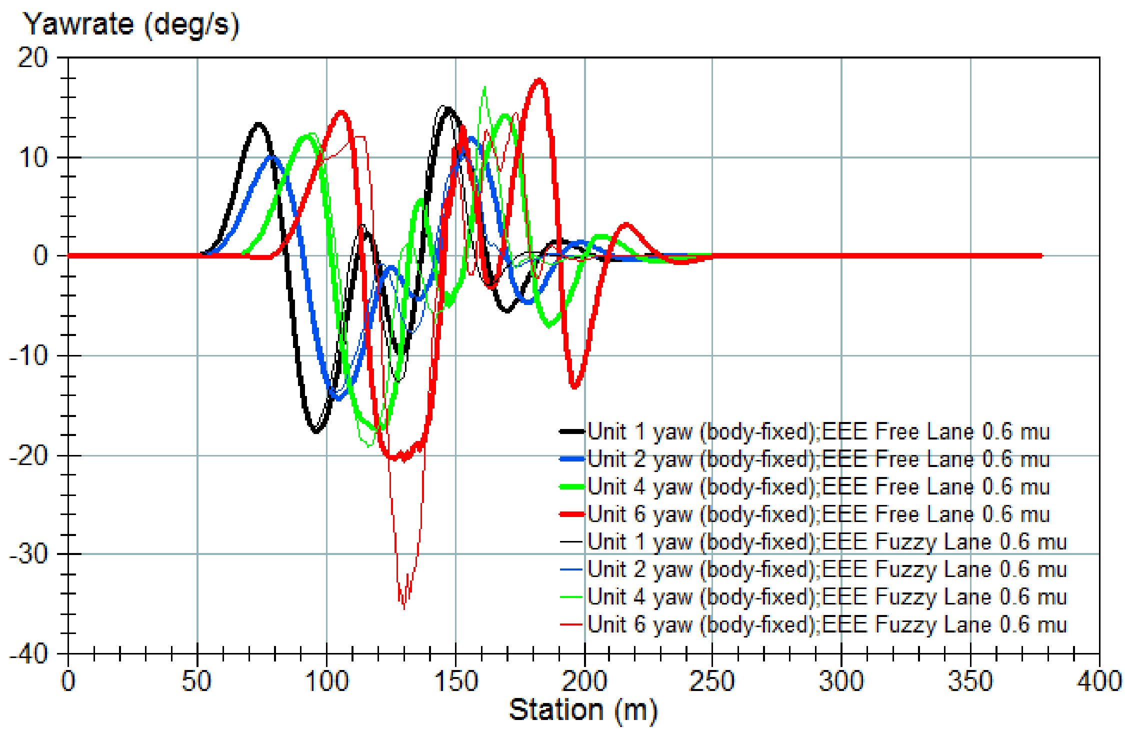

Figure K- 24: Yaw Rate, Fuzzy Unloaded Vehicle, Lane Change, mu = 0.6

K.2.3. Unloaded Mu = 0.85

Finally, the dry unloaded lane change indicated severe roll instability (Figure K- 25) where the fuzzy logic controller was not able to reduce the roll risk to acceptable levels (Figure K- 26) thought it was a significant improvement. While the controller did activate all brakes as soon as the problem was detected (Figure K- 27), there simply was not enough time to prevent the controlled vehicle from experiencing wheel lift.

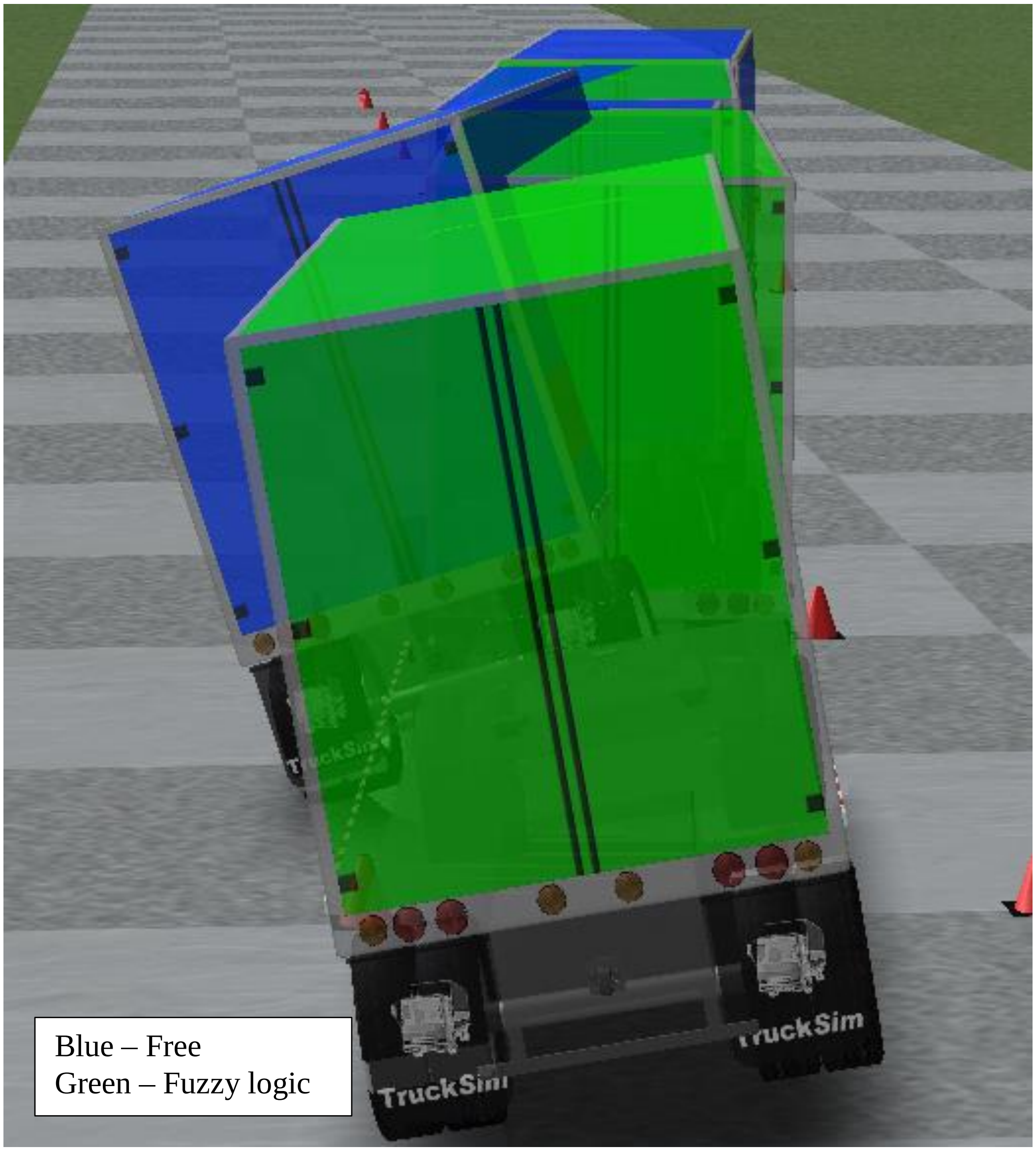

Figure K- 25: Illustration, Fuzzy Unloaded Vehicle, Lane Change, mu = 0.85

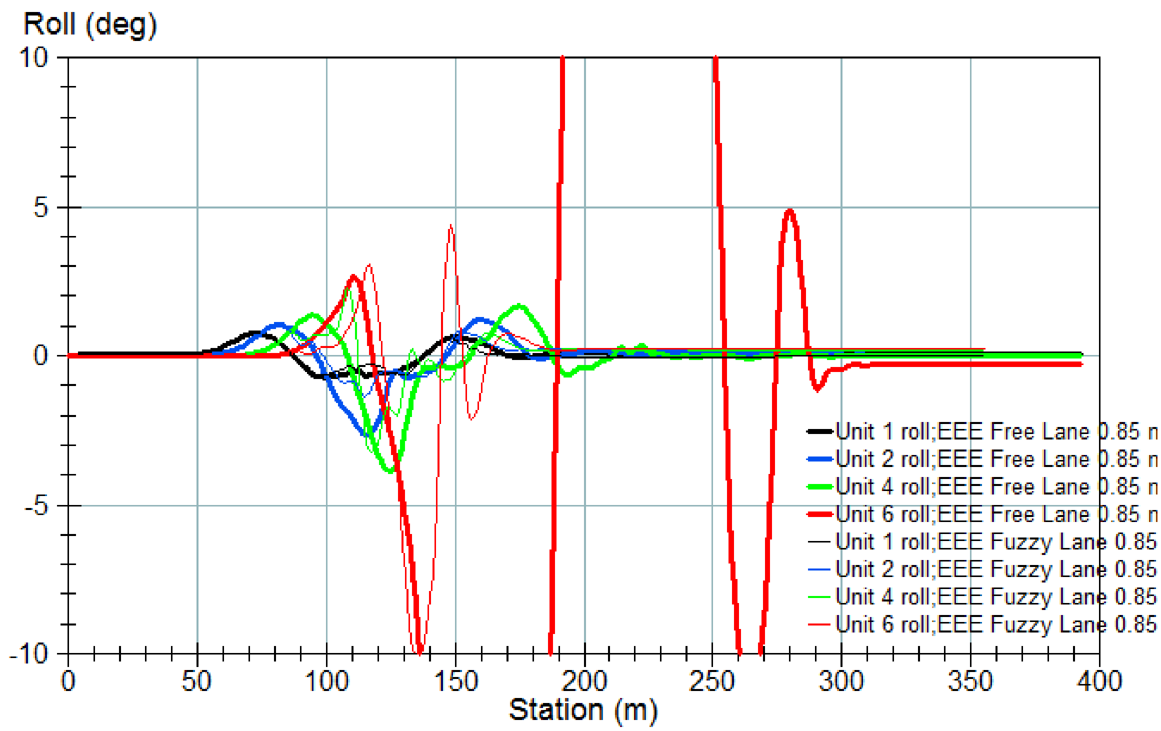

Figure K- 26: Roll, Fuzzy Unloaded Vehicle, Lane Change, mu = 0.85

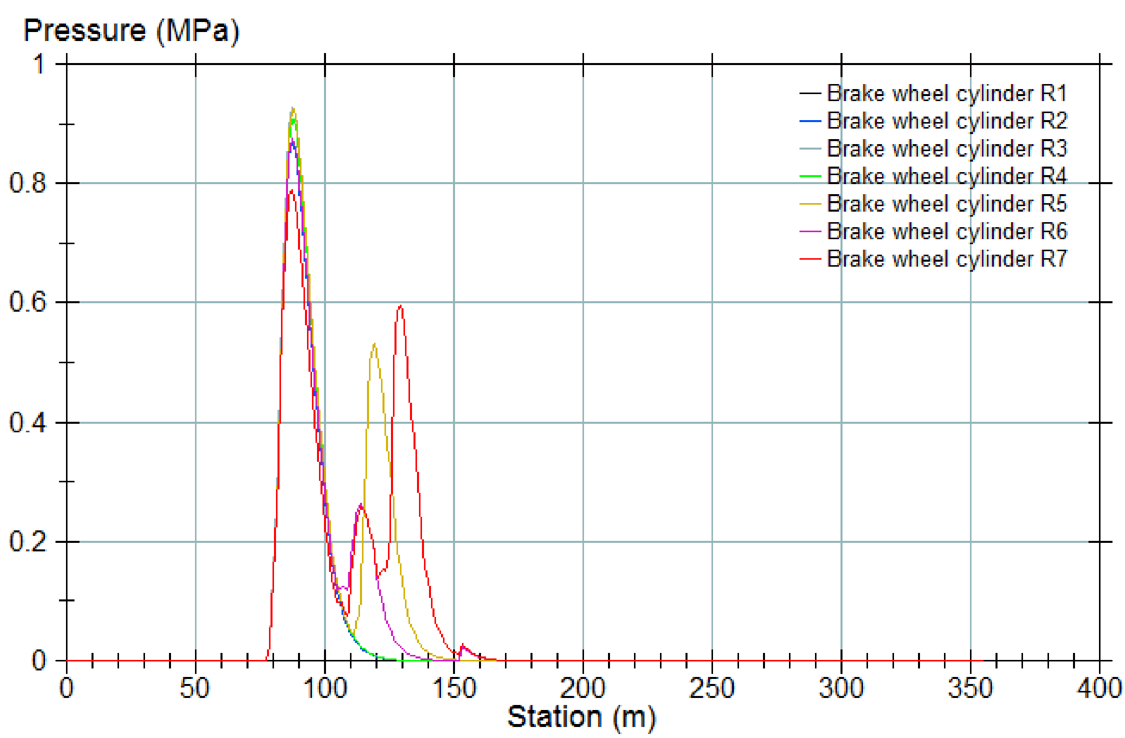

Figure K- 27: Brake, Fuzzy Unloaded Vehicle, Lane Change, mu = 0.85

K.2.4. Loaded Mu = 0.25

As it has been noted many times before that the vehicle seldom sees a rollover risk when operating on ice (lack of lateral force development), it was not surprising that the fuzzy logic controller demand for the loaded lane change maneuver was for side slip reduction (Figure K- 28). As the side slip bound was 4.3 degrees, the controller managed to bring the vehicle within bounds except for one deviation by the second trailer (unit 4).

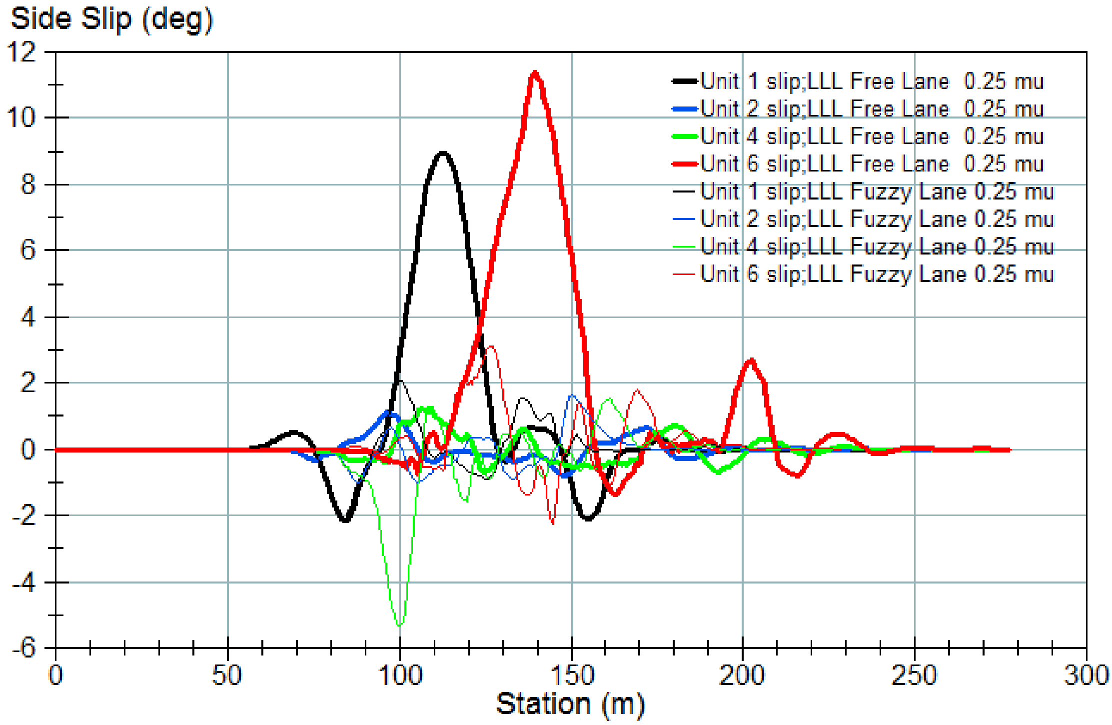

Figure K- 28: Side Slip, Fuzzy Loaded Vehicle, Lane Change, mu = 0.25

The brake controls (Figure K- 29 and Figure K- 30) were also pretty much as expected with the controller acting to turn the vehicle into and then out of the first gate followed by a mirrored response when transitioning back (second gate). Note again that the controller activated all trailer brakes at the start of the event (predictive rules) but then relaxed the lead axle braking as more steering demand was needed (traction ellipse optimization).

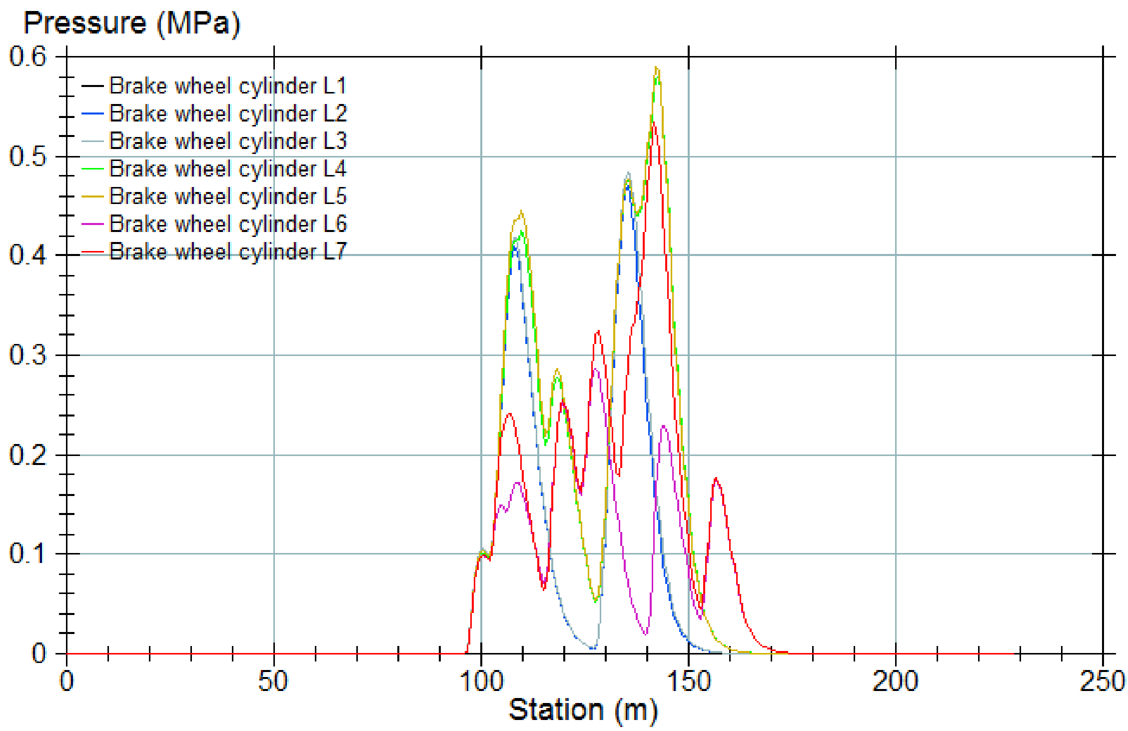

Figure K- 29: Left Brake, Fuzzy Loaded Vehicle, Lane Change, mu = 0.25

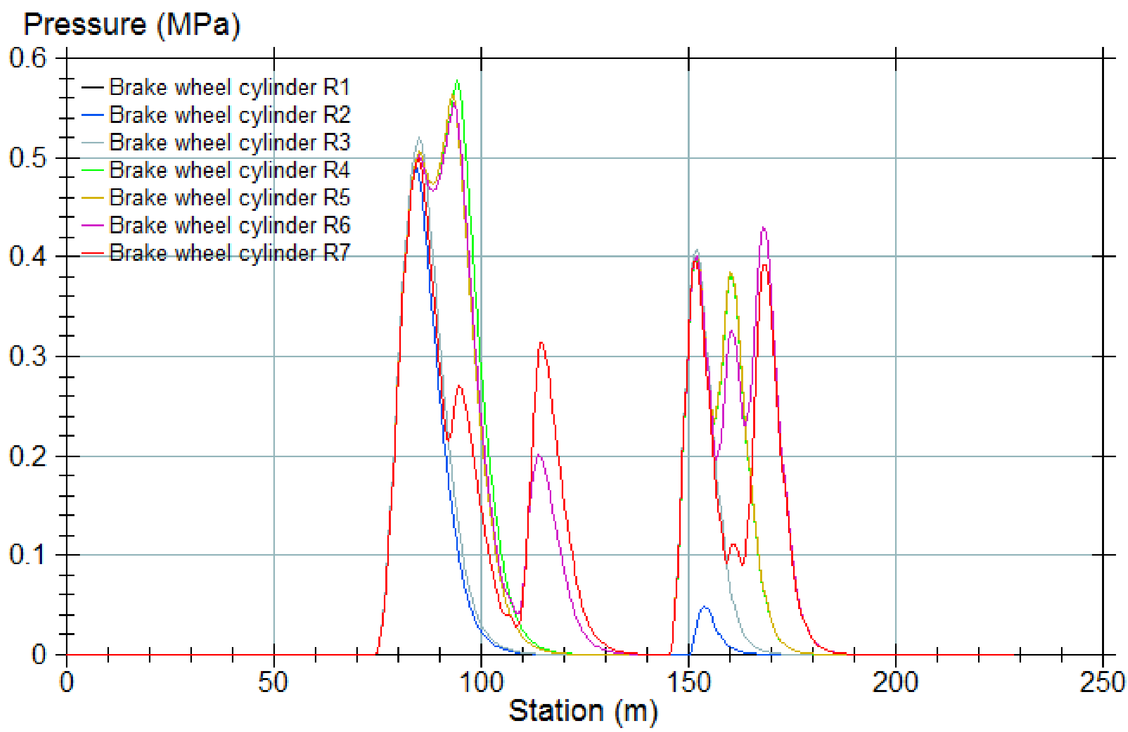

Figure K- 30: Right Brake, Fuzzy Loaded Vehicle, Lane Change, mu = 0.25

K.2.5. Loaded Mu = 0.6

Once again, the increase in road traction transitioned the loaded lane change vehicle from yaw to roll instability (Figure K- 31). The fuzzy logic controller activated to resist rollover on both the left hand part of the maneuver and the returning right hand part of the maneuver as can be seen in the shift of brake response between the left (Figure K- 32) and right (Figure K- 33) sides of the vehicle. The less aggressive right hand turn response was due to the fact that the preceding brake correction significantly slowed the vehicle.

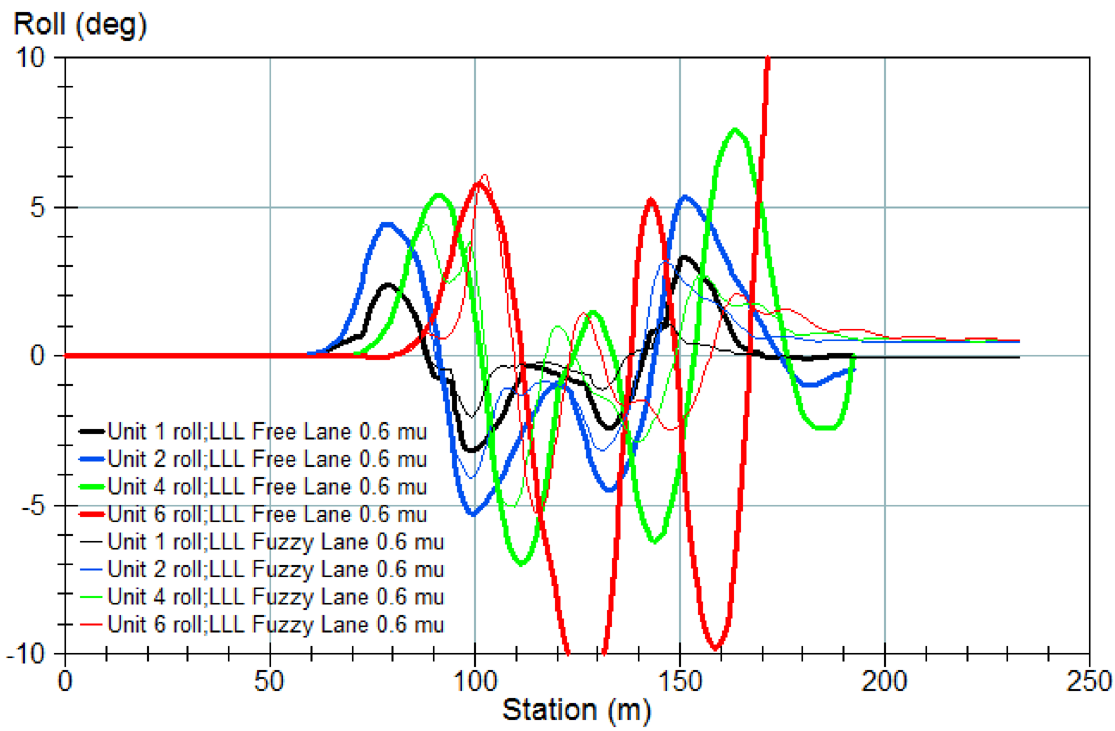

Figure K- 31: Roll, Fuzzy Loaded Vehicle, Lane Change, mu = 0.6

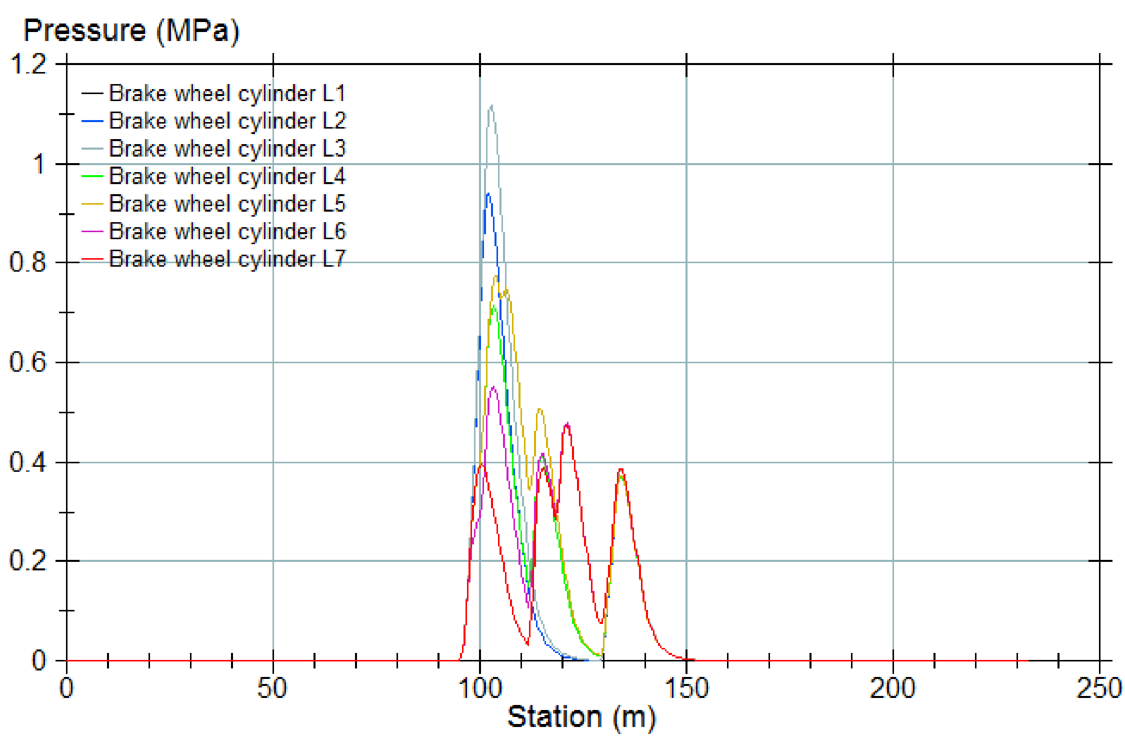

Figure K- 32: Left Brake, Fuzzy Loaded Vehicle, Lane Change, mu = 0.6

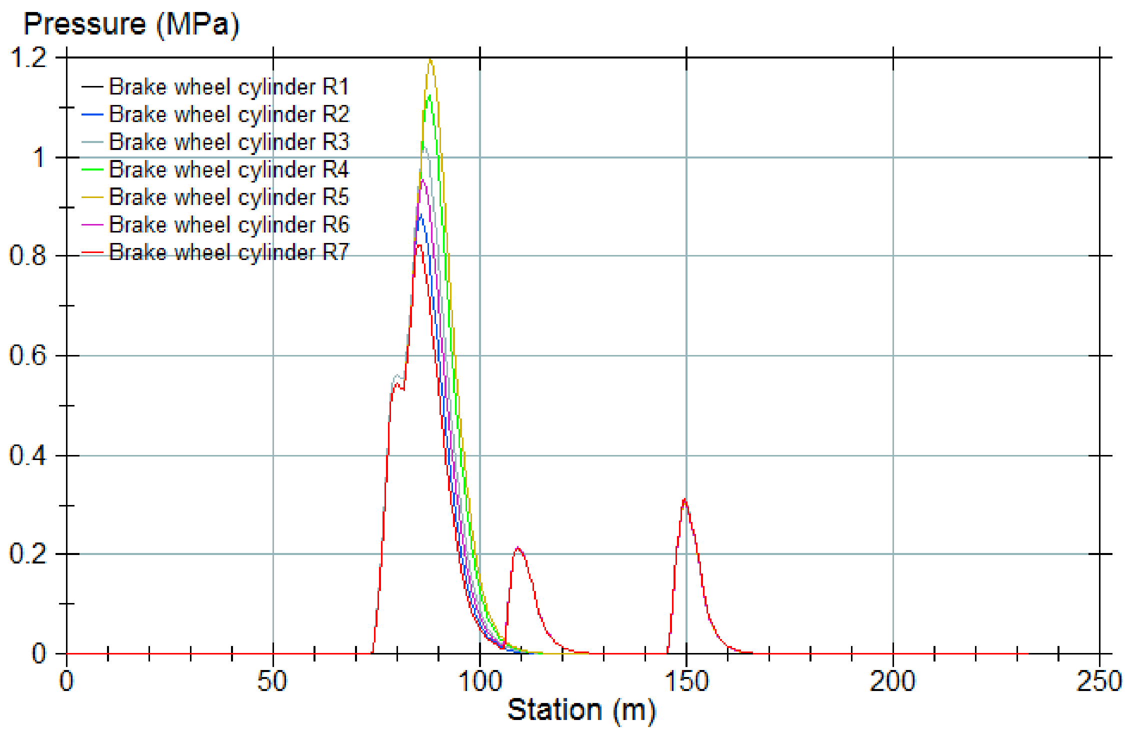

Figure K- 33: Right Brake, Fuzzy Loaded Vehicle, Lane Change, mu = 0.6

K.2.6. Loaded Mu = 0.85

The last test case was the loaded vehicle on a dry lane change. This was again a roll risk case (Figure K- 34) where the controller was able to stabilize the vehicle. However, the third trailer still rolled more than the 2.9 degree boundary limit (100 meter mark). The dry pavement permitted a much higher braking force (brake pressure) (Figure K- 35). This large deceleration force also slowed the vehicle and thus reduced the yaw rate of the vehicle as well (Figure K- 36).

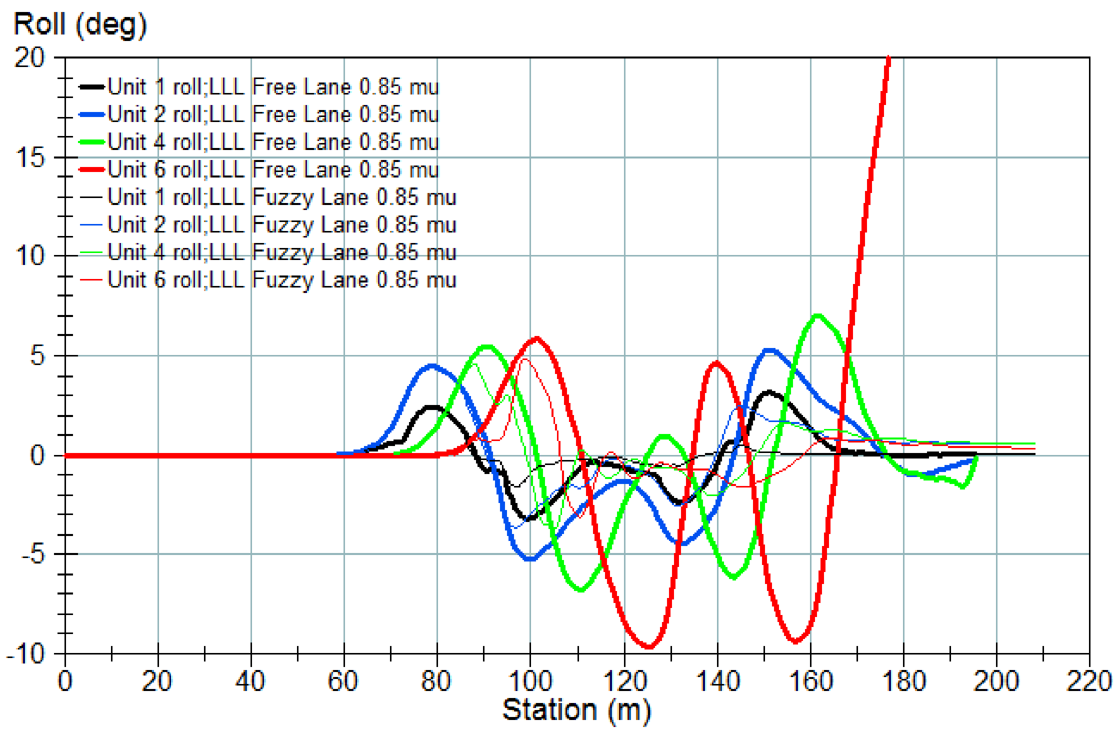

Figure K- 34: Roll, Fuzzy Loaded Vehicle, Lane Change, mu = 0.85

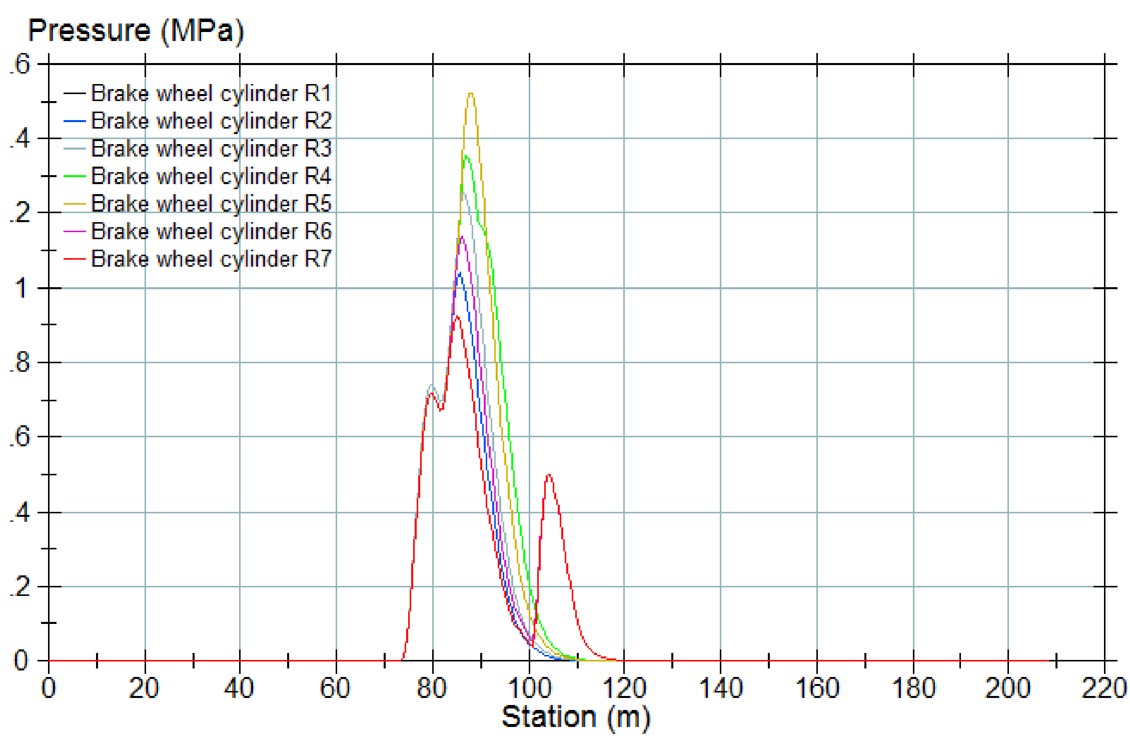

Figure K- 35: Brake, Fuzzy Loaded Vehicle, Lane Change, mu = 0.85

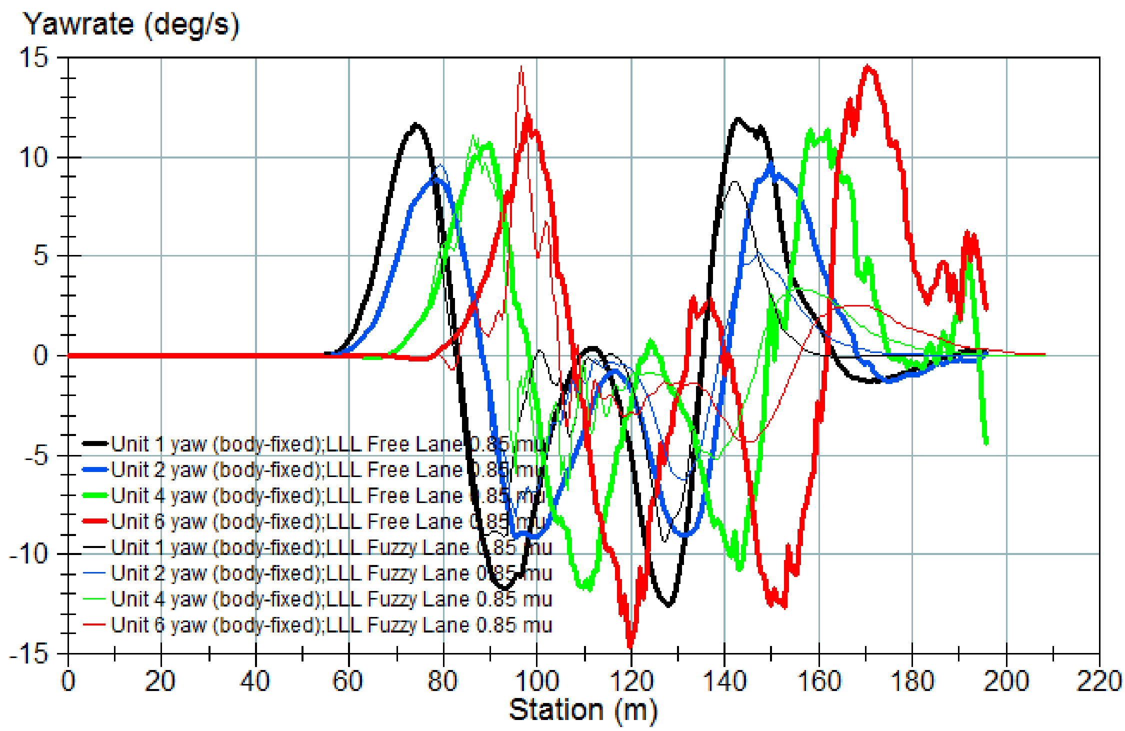

Figure K- 36: Yaw Rate, Fuzzy Loaded Vehicle, Lane Change, mu = 0.85

REFERENCES

Abe, M. (1999). Vehicle dynamics and control for improving handling and active safety: From four-wheel steering to direct yaw moment control. *Proceedings of the Institution of Mechanical Engineers, Part K: Journal of Multi-Body Dynamics, 213*

Allen, K. (2010). *The effectiveness of ABS in heavy truck tractors and trailers.* (No. DOT HS 811 339).National Highway Traffic Safety Administration.

Andersky, F., & Conklin, R. (2008). *Road map for the future* Bendix Commercial Vehicle Systems LLC. Retrieved from http://www.bendix.com/media/documents/products_1/BW2719-Road_Map_for_the_Future.pdf

Anderson, R., & Bevly, D. M. (2010). Using GPS with a model-based estimator to estimate critical vehicle states. *Vehicle System Dynamics, 48*(12), 1413-1438.

Antonov, S., Fehn, A., & Kugi, A. (2008). A new flatness-based control of lateral vehicle dynamics. *Vehicle System Dynamics, 46*(9), 780-801.

Anwar, S. (2005). Generalized predictive control of yaw dynamics of a hybrid brake-by-wire equipped vehicle. *Mechatronics, 15*(9), 1089-1108. doi: 10.1016/j.mechatronics.2005.06.006

Arant, M. (2010). *Assessing the effect of chassis torsional stiffness on the accuracy of heavy vehicle understeer and rollover modeling.* (Masters, Clemson University).

Arant, M., Pape, D., Nelson, S., Franzese, O., Knee, H. E., Hathaway, R., . . . Upul, A. (2009). *U19: Heavy truck rollover characterization (phase-B) final report.* (No. DTRT06G-0043).National Transportation Research Center Incorporated. Retrieved from http://tris.trb.org/view.aspx?id=908531

ATA. (2011). *More productive trucks: Delivering america safer, cleaner, and cheaper* American Trucking Association.

Ba, S. C., li, l., Kose, I. E., & Anlas, G. (2007). Robust control of anti-lock brake system. *Vehicle System Dynamics, 45*(3), 217-232.

Bahaghighat, M. K., Kharrazi, S., Lidberg, M., Falcone, P., & Schofield, B. (2010). Predictive yaw and lateral control in long heavy vehicles combinations. Paper presented at the *Decision and Control (CDC), 2010 49th IEEE Conference on,* 6403-6408.

Bayan, F. P., Cornetto, A. D., Dunn, A. L., & Sauer, E. (2009). Brake timing measurements for a tractor-semitrailer under emergency braking. *Society of Automotive Engineers International, 2009-01-2918*

Bedner, E., Fulk, D., & Hac, A. (2007). Exploring the trade-off of handling stability and responsiveness with advanced control systems. *Society of Automotive Engineers International, 2007-01-0812*

Bennett, & Norman. (2006). *Heavy-duty truck trailers* Thomason Delmar Learning.

Best, M. C., Gordon, T., & Dixon, P. J. (2000). An extended adaptive kalman filter for real-time state estimation of vehicle handling dynamics. *Vehicle System Dynamics, 34*(1), 57-75.

Bevly, D. M. (2004). Global positioning system (GPS): A low-cost velocity sensor for correcting inertial sensor errors on ground vehicles. *Journal of Dynamic Systems, Measurement, and Control, 126*(2), 255-264. doi: 10.1115/1.1766027

Bevly, D. M., Gerdes, J. C., Wilson, C., & Gengsheng, Z. (2000). The use of GPS based velocity measurements for improved vehicle state estimation. Paper presented at the *American Control Conference, 2000. Proceedings of the 2000, , 4* 2538-2542 vol.4.

Bevly, D. M., Ryu, J., & Gerdes, J. C. (2006). Integrating INS sensors with GPS measurements for continuous estimation of vehicle sideslip, roll, and tire cornering stiffness. *IEEE Transactions on Intelligent Transportation Systems, 7*(4), 483-93. Retrieved from http://dx.doi.org/10.1109/TITS.2006.883110

Bezwada, N., & Dissanayake, S. (2009). Characteristics of fatal truck crashes in the united states. Paper presented at the Ames, Iowa.

Blower, D., & Kostyniuk, L. P. (2007). *Strategies to reduce CMV-involved crashes, fatalities and injuries in michigan.* (No. UMTRI-2007-26).University of Michigan, Ann Arbor, Transportation Research Institute.

Boada, B. (2006). Integrated control of front-wheel steering and front braking forces on the basis of fuzzy logic. *Proceedings of the Institution of Mechanical Engineers.Part D, Journal of Automobile Engineering, 220*(3), 253-67.

Brown, T., Schwarz, C., Moeckli, J., & Marshall, D. (2009). *Heavy truck ESC effectiveness study using NADS.* (No. DOT HS 811 233).U.S. Department of Transportation National Highway Traffic Safety Administration.

Burgio, G., & Zegelaar, P. (2006). Integrated vehicle control using steering and brakes. *International Journal of Control, 79*(5), 534-541.

Chan, B. (2010). Evaluation of full and partial stability systems on tractor semi trailer using hardware-in-the-loop simulation. *Society of Automotive Engineers International, 2010-01-1902*

Chandrasekharan, S. (2007). *Development of a tractor-semitrailer roll stability controller model.* (Master of Science, Ohio State University).

Chang, S., & Gordon, T. (2009). Improvement of vehicle dynamics using model-based predictive control. *Society of Automotive Engineers International, 2009-01-0427*

Changfu, Z., Yu, Z., Miao, Q., & Zhang, B. (2010). Research on rollover warning algorithm of heavy commercial vehicle based on prediction model. *International Conference on Computer, Mechatronics, Control and Electronic Engineering,*

Cheli, F., Sabbioni, E., Pesce, M., & Melzi, S. (2007). A methodology for vehicle sideslip angle identification: Comparison with experimental data. *Vehicle System Dynamics, 45*(6), 549—563.

Chen, B., & Peng, H. (1999a). A real-time rollover threat index for sports utility vehicles. Paper presented at the

Chen, B., & Peng, H. (1999b). Rollover warning of articulated vehicles based on a time-to-rollover metric. Paper presented at the Knoxville, TN.

Chen, C., & Tomizuka, M. (2000). Lateral control of commercial heavy vehicles. *Vehicle System Dynamics, 33*(6), 391-420.

Chen, L. K., & Shieh, Y. A. (2011). Jackknife prevention for articulated vehicles using model reference adaptive control. *Proceedings of the Institution of Mechanical Engineers, Part D: Journal of Automobile Engineering, 225*(1), 28-42. Retrieved from http://dx.doi.org/10.1243/09544070JAUTO1513

Cheng, C., & Cebon, D. (2011). Parameter and state estimation for articulated heavy vehicles. *Vehicle System Dynamics, 49*(1), 399-418.

Chih-Keng Chen, Trung-Kien Dao, & Hai-Ping Lin. (2010). A compensated yaw-moment-based vehicle stability controller. *International Journal of Vehicle Design, 53*(3), 220-38.

Choi, S. B. (2008). Practical vehicle rollover avoidance control using energy method. *Vehicle System Dynamics, 46*(4), 323-337.

Choi, S., & Cho, D. (2001). Design of nonlinear sliding mode controller with pulse width modulation for vehicular slip ratio control. *Vehicle System Dynamics, 36*(1), 57-72.

Chun, K., & Sunwoo, M. (2005). Wheel slip tracking using moving sliding surface. Paper presented at the , *219*(1) 31-41. Retrieved from http://dx.doi.org/10.1243/095440705X6497

Chung, T., Kim, D., & Yang, S. (2010). Alternative approach to design ESC and MDPS integrated control system. *Society of Automotive Engineers International, 2010-01-0101*

Coleman, T. F., & Li, Y. (1996). A reflective newton method for minimizing a quadratic function subject to bounds on some of the variables. *SIAM Journal on Optimization, 6*(4), 1040-58.

Dahlberg, E. (2000). A method determining the dynamic rollover threshold of commercial vehicles. *Society of Automotive Engineers International,* (2000-01-3492)

Dahlberg, E., & Stensson, A. (2006). The dynamic rollover threshold - a heavy truck sensitivity study. *International Journal of Vehicle Design, 40*(1-3), 228-50. Retrieved from http://dx.doi.org/10.1504/IJVD.2006.008463

Daily, R., & Bevly, D. M. (2004). The use of GPS for vehicle stability control systems. *Industrial Electronics, IEEE Transactions on, 51*(2), 270-277.

Davis , M., & Marting, P. (2002). Predicting vehicle rollover propensity. *SAE Technical Paper Series,* (2002-01-3106)

Deng, W., & Zhang, H. (2006). RLS-based online estimation on vehicle linear sideslip. Paper presented at the *2006 American Control Conference,* 6 pp.

Doumiati, M., Victorino, A., Lechner, D., Baffet, G., & Charara, A. (2010). Observers for vehicle tyre/road forces estimation: Experimental validation. *Vehicle System Dynamics, 48*(11), 1345-1378.

Du, H., & Zhang, N. (2008). Robust stability control of vehicle rollover subject to actuator time delay. *Proceedings of the Institution of Mechanical Engineers.Part I: Journal of Systems and Control Engineering, 222*(3), 163-174. Retrieved from http://dx.doi.org/10.1243/09596518JSCE471

Dunn, A. L. (2003). *Jackknife stability of articulated tractor semitrailer vehicles with high-output brakes and jackknife detection on low coefficient surfaces.* (Doctor of Philosophy, Ohio State University).

Eisele, D. E., & Peng, H. (2000). Vehicle dynamics control with rollover prevention for articulated heavy trucks. *International Symposium on Advanced Vehicle Control, 5th International Symposium on Advanced Vehicle Control*

El-Gindy, M. (1995). An overview of performance measures for heavy commercial vehicles in north america. *International Journal of Vehicle Design, 16*(4/5)

Ervin, R. D., & Mathew, A. (1988). *Reducing the risk of spillage in the transportation of chemical wastes by truck.* (No. UMTRI-88-28). University of Michigan: University of Michigan Transportation Research Institute.

Esber, P., Shaffer, S., Pape, D., Gordon, T., Winkler, C. B., & Landes, R. (2007). *Engineering assessment of current and future vehicle technologies: FMVSS no. 121; air brake systems.* (No. DTNH22-02-D-02104).National Highway Traffic Safety Administration.

Evans, J., Batzer, S., & Andrews, S. (2005). *Evaluation of heavy truck rollover accidents.* (No. 05-0140).National Highway Traffic Safety Administration.

Falcone, P., Tseng, E. H., Borrelli, F., Asgari, J., & Hrovat, D. (2008). MPC-based yaw and lateral stabilisation via active front steering and braking. *Vehicle System Dynamics, 46*(1), 611-628. doi: 10.1080/00423110802018297

Fancher, P. S., & Mathew, A. (1989). Performance factors for heavy trucks. *Automotive Engineering,* , 21-24.

Fancher, P. S., & Winkler, C. B. (2007). Directional performance issues in evaluation and design of articulated heavy vehicles. *Vehicle System Dynamics, 45*(7), 607-647.

Federal Motor Carrier Safety Administration. (2009). *Large truck and bus crash facts 2007.* (No. FMCSA-RRA-09-029).Analysis Division Federal Motor Carrier Safety Administration.

FHWA. (2004). *Federal size regulations for commercial motor vehicles.* (No. FHWA-HOP-04-022).U.S.Department of Transportation Federal Highway Administration. Retrieved from http://ops.fhwa.dot.gov/freight/publications/size_regs_final_rpt/size_regs_final_rpt.pdf

FMCSA. (2008). *Current FMCSA crash cost figures.* ().Analysis Division Federal Motor Carrier Safety Administration. Retrieved from http://mcsac.fmcsa.dot.gov/documents/Dec09/FMCSACrashCostCalculationsDec08.pdf

Franklin, G. F., & Powell, D. J. (Eds.). (1994). *Feedback control of dynamic systems* [null] (3rd ed.). USA: Addison-Wesley Publishing Company.

Freightliner LLC. (2007). *Electronically controlled braking systems (ECBS) intelligent vehicle initiative field operational test.* (No. DTFH61-02-X-00096).U.S. Department of Transportation Federal Highway Administration.

Fu, T. -. (2002). Analysis of a truck suspension database. *International Journal of Heavy Vehicle Systems, 9*(4), 281-297.

Gäfvert, M., & Svendenius, J. (2005). A novel semi-empirical tyre model for combined slips. *Vehicle System Dynamics, 43*(5), 351-384.

Gao, X., Yu, Z., Neubeck, J., & Wiedemann, J. (2010). Sideslip angle estimation based on input-output linearization with tire-road friction adaptation. *Vehicle System Dynamics, 48*(2), 217-234.

Garcia, N., & Acha, E. (2008). Transmission line model with frequency dependency and propagation effects: A model order reduction and state-space approach. Paper presented at the *IEEE Power and Energy Society 2008 General Meeting: Conversion and Delivery of Electrical Energy in the 21st Century, PES, July 20, 2008 - July 24,* doi: 10.1109/PES.2008.4596875

Gerdes, J. C. (2002). *Safety performance and robustness of heavy vehicle AVCS.* (). Stanford University: Dept. of Mechanical Engineering – Design Division.

Ghoneim, Y. A., Lin, W. C., Sidlosky, D. M., Chen, H. H., Chin, Y., & Tedrake, M. J. (2000). Integrated chassis control system to enhance vehicle stability. *International Journal of Vehicle Design, 23*(1), 124-144.

Gim, G., Choi, Y., & Kim, S. (2007). A semi-physical tire model for a vehicle dynamics analysis of handling and braking. *Vehicle System Dynamics, 45*(1), 169-190.

Gong, S., & Ting, K. (2008). A novel wheel/tyre dynamics model and derivation of a generalized friction law. *Proceedings of the Institution of Mechanical Engineers, Part D: Journal of Automobile Engineering, 222*(2), 173-189. Retrieved from http://dx.doi.org/10.1243/09544070JAUTO417

Goodarzi, A., Ghajar, M., Baghestani, A., & Esmailzadeh, E. (2009). Integrated yaw and roll moments control for articulated vehicles. *Society of Automotive Engineers International, 2009-01-2874*

Gould, N., & Toint, P. L. (2004). Preprocessing for quadratic programming. *Mathematical Programming, 100*(1), 95-132. doi: 10.1007/s10107-003-0487-2

Hac, A. (2002). Influence of active chassis systems on vehicle propensity to maneuver-induced rollovers. *SAE Technical Paper Series,* (2002-01-0967)

Hac, A., & Bodie, M. O. (2002). Improvements in vehicle handling through integrated control of chassis systems. *International Journal of Vehicle Design, 29*(1-2), 23-50.

Hagy, S. (2011). Tiller history. Retrieved, 2011, from http://www.cfdhistory.com/htmls/tillers.html

Hancock, M. J., Williams, R. A., Fina, E., & Best, M. C. (2007). Yaw motion control via active differentials. Paper presented at the *, 29*(2) 137-157. Retrieved from http://dx.doi.org/10.1177/0142331207069489

Hendrickson. (2011). *INTRAAX® AAT 23K / 25K / 30K* Hendrickson. Retrieved from http://www.hendrickson-intl.com/pdfs/trailer_PDFs/L1153.pdf

Holler, G., & Macnamara, J. (2001). Roll over prevention based on state-of-the-art ABS systems. *Society of Automotive Engineers International, 2001-01-2727*

Hossein, S. T., & Taheri, S. (2008). Yaw stability control of tractor semi-trailers. *Society of Automotive Engineers International, 2008-01-2595*

Hsu, L., & Chen, T. (2010). Estimating road angles with the knowledge of the vehicle yaw angle. *Journal of Dynamic Systems, Measurement and Control, Transactions of the ASME, 132*(3), 1-9. Retrieved from http://dx.doi.org/10.1115/1.4001330

Huh, K., Lim, S., Jung, J., Hong, D., Han, S., Han, S., . . . Yun, J. M. (2007). Vehicle mass estimator for adaptive roll stability control. *Society of Automotive Engineers International, 2007-01-0820*

Hyun, D., & Langari, R. (2003). Modeling to predict rollover threat of tractor-semitrailers. *Vehicle System Dynamics, 39*(6), 401-414.

ISO 15037-2. (2002). *Vehicle dynamic test methods – Part2: General conditions for heavy vehicles and buses* International Standard Organization.

ISO 7401. (2003). *Road vehicles – lateral transient response test methods – open loop test methods test method* International Standard Organization.

Jarossi, L., Matteson, A., & Woodrooffe, J. (2010). *Trucks involved in fatal accidents factbook 2007.* (No. UMTRI-2010-4).University of Michigan, Ann Arbor, Transportation Research Institute. Retrieved from http://hdl.handle.net/2027.42/65063

Jermakian, J. S. (2010). *Crash avoidance potential of four large truck technologies.* ().Insurance Institute for Highway Safety.

Kalman, R. E. (1960). New approach to linear filtering and prediction problems. *American Society of Mechanical Engineers -- Transactions -- Journal of Basic Engineering Series D, 82*(1), 35-45.

Kamnik, R., Boettiger, F., & Hunt, K. (2003). Roll dynamics and lateral load transfer estimation in articulated heavy freight vehicles. *Proceedings of the Institution of Mechanical Engineers, Part D: Journal of Automobile Engineering, 217*(11), 985-997. Retrieved from http://dx.doi.org/10.1243/095440703770383884

Kharrazi, S., & Thomson, R. (2008a). Analysis of heavy truck accidents with regard to yaw and roll instability - using LTCCS database. Paper presented at the Paris France.

Kharrazi, S., & Thomson, R. (2008b). Study of heavy truck accidents with focus on maneuvers causing loss of control. *International Journal of Vehicle Safety, 3*(1), 32-44. Retrieved from http://dx.doi.org/10.1504/IJVS.2008.020077

Kienhöfer, F. W., Miller, J. I., & Cebon, D. (2008). Design concept for an alternative heavy vehicle ABS system. *Vehicle System Dynamics, 46*(1), 571-583.

Kim, J. (2010). Effect of vehicle model on the estimation of lateral vehicle dynamics. *International Journal of Automotive Technology, 11*(3), 331-337. Retrieved from http://dx.doi.org/10.1007/s12239-010-0041-1

Ko, Y. E., & Lee, J. M. (2002). Estimation of the stability region of a vehicle in plane motion using a topological approach. *International Journal of Vehicle Design, 30*(3), 181-192. Retrieved from http://dx.doi.org/10.1504/IJVD.2002.002032

LaClair, T., Knee, H. E., Franzese, O., Arant, M., Hathaway, R., Keil, M., & Pape, D. (2010). *U24 heavy truck rollover (phase C).* (No. DTRT06G-0043).National Transportation Research Center Incorporated. Retrieved from http://www.ntrci.org/library/U24_Heavy_Truck_Rollover_Phase_C_FINAL_1288900197.pdf

Lawson, R. (2004). *Optimization to reduce rollover propensity of tractor semi-trailers during steady state cornering.* (Masters Mechanical Engineering, Clemson University). (TR-04-104-ME-MMs)

Lee, J., & Yoo, W. (2009). An improved model-based predictive control of vehicle trajectory by using nonlinear function. *Journal of Mechanical Science and Technology, 23*(4), 918-922. doi: 10.1007/s12206-009-0312-9

Liang Chu, Yong Fang, Mingli Shang, Jianhua Guo, & Feikun Zhou. (2010). Estimation of articulation angle for tractor semi-trailer based on state observer. Paper presented at the *Measuring Technology and Mechatronics Automation (ICMTMA), 2010 International Conference on, , 2* 158-163.

Liebemann, E. K., Schuh, J., Meder, K., & Nenninger, G. (2004). Safety and performance enhancement: The bosch electronic stability control (ESP). *Society of Automotive Engineers International, 2004-21-0060*

Limroth, J. (2009). *Real-time vehicle parameter estimation and adaptive stability control.* (Doctorate, Clemson University). Retrieved from http://etd.lib.clemson.edu/documents/1263410198/. ((OCoLC)516352764).

Limroth, J., Kurfess, T., & Law, E. H. (2009). *U13: Co-simulation of heavy truck tire dynamics and electronic stability control systems (phase A).* (). University Transportation Center 2360 Cherahala Blvd. Knoxville, TN 37932: National Transportation Research Center, Inc.

Lukowski, S. A., Lukowski, S. A., & Medeksza, L. A. (1998). The influence of steered axles on the stability and followability of articulated vehicle system. *Society of Automotive Engineers International, 981483*

Ma, W., & Peng, H. (1999). Worst-case vehicle evaluation methodology - examples on truck Rollover/Jackknifing and active yaw control systems. *Vehicle System Dynamics, 32*(4), 389-408.

MacAdam, C. C. (1982). A computer-based study of the Yaw/Roll stability of heavy trucks characterized by high centers of gravity. *SAE Technical Paper Series, 821260*

MacAdam, C. C., Hagan, M., Fancher, P. S., Winkler, C. B., Ervin, R. D., Zhou, J., & Bogard, S. (2000). *Rearward amplification suppression (RAMS).* (No. UMTRI-2000-47). University of Michigan: University of Michigan Transportation Research Institute.

Macnabb, M., Brewer, E., Baerg, R., & Billing, J. (2002). Static and dynamic roll stability of various commercial vehicles. *SAE Technical Paper Series,* (2002-01-3075)

Mammar, S., & Koenig, D. (2002). Vehicle handling improvement by active steering. *Vehicle System Dynamics, 38*(3), 211-242.

Manning, W. J., & Crolla, D. A. (2007). A review of yaw rate and sideslip controllers for passenger vehicles. *Transactions of the Institute of Measurement and Control, 29*(2), 117-35. Retrieved from http://dx.doi.org/10.1177/0142331207072989

Matteson, A., Blower, D., & Woodrooffe, J. (2004). *Trucks involved in fatal accidents factbook 2002.* (No. UMTRI 2004-34).Center for National Truck and Bus Statistics, University of Michigan Transportation Research Institute.

Miege, A. J. P., & Cebon, D. (2002). Design and implementation of an active roll control system for heavy vehicles. *International Symposium on Advanced Vehicle Control,*

Miege, A. J. P., & Cebon, D. (2005). Optimal roll control of an articulated vehicle: Theory and model validation. *Vehicle System Dynamics, 43*(12), 867-893.

Minaker, B. P., & Rieveley, R. J. (2010). Automatic generation of the non-holonomic equations of motion for vehicle stability analysis. *Vehicle System Dynamics, 48*(9), 1043-1063.

Mokhiamar, O., & Abe, M. (2002). Active wheel steering and yaw moment control combination to maximize stability as well as vehicle responsiveness during quick lane change for active vehicle handling safety. *Proceedings of the Institution of Mechanical Engineers, Part D: Journal of Automobile Engineering, 216*(2), 115-124. Retrieved from http://dx.doi.org/10.1243/0954407021528968

M'Sirdi, N. K., Rabhi, A., Fridman, L., Davila, J., & Delanne, Y. (2008). Second order sliding-mode observer for estimation of vehicle dynamic parameters. *International Journal of Vehicle Design, 48*(3-4), 190-207. Retrieved from http://dx.doi.org/10.1504/IJVD.2008.022576

Nantais, N. (2006). *Active brake proportioning and its effects on safety and performance.* (Master of Applied Science, University of Windsor).

Naraghi, M., Roshanbin, A., & Tavasoli, A. (2010). Vehicle stability enhancement - an adaptive optimal approach to the distribution of tyre forces. *Proceedings of the Institution of Mechanical Engineers, Part D (Journal of Automobile Engineering), 224*, 443-53. Retrieved from http://dx.doi.org/10.1243/09544070JAUTO1332

National Instruments Corporation. (2009). *PID and fuzzy logic toolkit.* (No. 372192D-01). Austin, Texas: National Instruments Corporation.

Newmatics Inc. (2013). Dakota digital air pressure gauge pressure sending unit 0-150 psi max. Retrieved, 2013, from http://www.newmaticsinc.com/Dakota_Digital_Sending_unit_p/100482.htm

NHTSA. (2007). *FMVSS no. 126 electronic stability control systems.* (No. NTHSA-2007).Office of Regulatory Analysis and Evaluation National Center for Statistics and Analysis.

NHTSA. (2009). Federal motor vehicle safety standards; air brake systems. *NHTSA–2009-0083, 49 CFR Part 571*,(RIN: 2127-AJ37)

NHTSA. (2010). *Federal motor carrier safety administration standard no. 121; air brake systems* (2010th ed.) Department Of Transportation.

NHTSA. (2011). *NHTSA vehicle safety and fuel economy rulemaking and research priority plan 2011-2013.* ().National Highway Traffic Safety Administration. Retrieved from http://www.nhtsa.gov/staticfiles/rulemaking/pdf/2011-2013_Vehicle_Safety-Fuel_Economy_Rulemaking-Research_Priority_Plan.pdf

NHTSA. (2012). *Federal motor vehicle safety standards; electronic stability control systems for heavy vehicles.* (No. 49 CFR Part 571).National Highway Traffic Safety Administration.

Odhams, A., Roebuck, R., Cebon, D., & Winkler, C. B. (2008). Dynamic safety of active trailer steering systems. *Proceedings of the Institution of Mechanical Engineers, Part K: Journal of Multi-Body Dynamics, 222*(4), 367-380. Retrieved from http://dx.doi.org/10.1243/14644193JMBD174

Ogata, K. (Ed.). (2002). *Moden control engineering* [null] (4th ed.). N.J., U.S.A.: Prentice Hall.

Palkovics, L., & Fries, A. (2001). Intelligent electronic systems in commercial vehicles for enhanced traffic safety. *Vehicle System Dynamics, 35*(4-5), 227-89. Retrieved from http://dx.doi.org/10.1076/vesd.35.4.227.2044

Palkovics, L., Semsey, Á., & Gerum, E. (1999). Roll-over prevention system for commercial vehicles – additional sensorless function of the electronic brake system. *Vehicle System Dynamics, 32*(4), 285-297.

Pape, D., Arant, M., Hall, D., Nelson, S., Petrolino, J., Franzese, O., . . . Pollock, P. (2008). *U02: Heavy truck rollover characterization (phase-A) final report.* (No. DTRT06G-0043).National Transportation Research Center Incorporated.

Pape, D., Harback, K., McMillan, N., Greenberg, A., Mayfield, H., & Chitwood, C. (2007). *Cargo tank roll stability study.* (No. GS23-F-0011L).Battelle Institute.

Park, J. I., Yoon, J. Y., Kim, D. S., & Yi, K. -. (2008). Roll state estimator for rollover mitigation control. *Proceedings of the Institution of Mechanical Engineers, Part D: Journal of Automobile Engineering, 222*(8), 1289-1311. Retrieved from http://dx.doi.org/10.1243/09544070JAUTO803

Petersen, E., Neuhaus, D., Gläbe, K., Koschorek, R., & Reich, T. (1998). Vehicle stability control for trucks and buses. *Society of Automotive Engineers International, 982782*

Pierce Manufacturing Inc. (2011). Pierce 100 foot tiller. Retrieved, 2011, from http://www.piercemfg.com/en/trucks/aerials/100-tiller/100-tiller.aspx

Plumlee, J. H., Bevly, D. M., & Hodel, A. S. (2006). Control allocation in ground vehicles. *International Journal of Vehicle Design, 42*(3-4), 215-43. Retrieved from http://dx.doi.org/10.1504/IJVD.2006.010431

Pottinger, M. G., & McIntyre, J. E. (2000). Truck tire force and moment in cornering – Braking – driving on ice, snow, and dry surfaces. *SAE Technical Paper Series,* (2000-01-3431)

Rempel, M. (2001). *Improving the dynamic performance of multiply-articulated vehicles.* (Masters of Science, University of British Columbia).

Rieth, P. E., & Schwarz, R. (2004). ESC II – ESC with active steering intervention. *Society of Automotive Engineers International, 2004-01-0260*

Ryu, J., & Gerdes, J. C. (2004). Integrating inertial sensors with global positioning system (GPS) for vehicle dynamics control. *Journal of Dynamic Systems, Measurement and Control, Transactions of the ASME, 126*(2), 243-254. doi: 10.1115/1.1766026

Samar, R., Postlethwaite, I., & Gu, D. (1995). Model reduction with balanced realizations. *International Journal of Control, 62*(1), 33-64.

Sampson, D. J. M. (2000). *Active roll control of articulated heavy vehicles.* (Doctor of Philosophy, University of Cambridge).

Sampson, D. J. M., & Cebon, D. (1998). An investigation of roll control system design for articulated heavy vehicles. *Proceedings of the International Symposium on Advanced Vehicle Control, Proc. 4th Int. Symp. AVEC '98*

Sampson, D. J. M., & Cebon, D. (2001). *Achievable roll stability of heavy road vehicles.* (). Cambridge UK: Cambridge University Engineering Department.

Sampson, D. J. M., & Cebon, D. (2003). Active roll control of single unit heavy road vehicles. *Vehicle System Dynamics, 40*(4), 229-270.

Sampson, D. J. M., Jeppesen, B. P., & Cebon, D. (2000). The development of an active roll control system for heavy vehicles. Paper presented at the Saskatoon, Canada.

Retrieved from http://citeseerx.ist.psu.edu/viewdoc/download?doi=10.1.1.125.2840&rep=rep1&type=pdf

Sampson, D. J. M., Jeppesen, B. P., & Cebon, D. (2006). *The development of an active roll control system for heavy vehicles.* (). Cambridge UK: Cambridge University Engineering Department.

Sampson, D. J. M., McKevitt, G., & Cebon, D. (1999). The development of an active roll control system for heavy vehicles. *Proceedings of the 16th IAVSD Symposium on the Dynamics of Vehicles on Roads and Tracks, 16*

Shen, S., Wang, J., Shi, P., & Premier, G. (2007). Nonlinear dynamics and stability analysis of vehicle plane motions. *Vehicle System Dynamics, 45*(1), 15-35.

Shim, T., & Ghike, C. (2007). Understanding the limitations of different vehicle models for roll dynamics studies. *Vehicle System Dynamics, 45*(3), 191-216.

Shim, T., Toomey, D., Ghike, C., & Sardar, H. M. (2008). Vehicle rollover recovery using active steering/wheel torque control. *International Journal of Vehicle Design, 46*(1), 51-71.

Shraim, H., Ouladsine, M., Fridman, L., & Romero, M. (2008). Vehicle parameter estimation and stability enhancement using sliding modes techniques. *International Journal of Vehicle Design, 48*(3-4), 230-54. Retrieved from http://dx.doi.org/10.1504/IJVD.2008.022578

Shun, C. C. (2007). Adoption of state feedback to control dynamics of a vehicle with a steer-by-wire system. *Proceedings of the Institution of Mechanical Engineers, Part D: Journal of Automobile Engineering, 221*(1), 1-12. Retrieved from http://dx.doi.org/10.1243/09544070JAUTO354

Shurtz, M. L., Guenther, D. A., Heydinger, G. J., & Zagorski, S. B. (2007). Refinements of a heavy truck ABS model. *Society of Automotive Engineers International, 2007-01-0839*

Solmaz, S., Akar, M., & Shorten, R. (2006). Online center of gravity estimation in automotive vehicles using multiple models and switching. Paper presented at the *9th International Conference on Control, Automation, Robotics and Vision, 2006, ICARCV '06, December 5, 2006 - December 8,* doi: 10.1109/ICARCV.2006.345080

Song, Z. -., Zweiri, Y. H., Seneviratne, L. D., & Althoefer, K. (2008). Non-linear observer for slip estimation of tracked vehicles. *Proceedings of the Institution of*

Mechanical Engineers, Part D: Journal of Automobile Engineering, 222(4), 515-533. Retrieved from http://dx.doi.org/10.1243/09544070JAUTO452

Starnes, M. (2006). *Large-truck crash causation study: An initial overview.* (No. DOT HS 810 646).NHTSA's National Center for Statistics and Analysis.

Stone, E. J., & Cebon, D. (2008). An experimental semi-active anti-roll system. *Proceedings of the Institution of Mechanical Engineers, Part D: Journal of Automobile Engineering, 222*(12), 2415-2433. Retrieved from http://dx.doi.org/10.1243/09544070JAUTO650

Svendenius, J., & Gäfvert, M. (2006). A semi-empirical dynamic tire model for combined-slip forces. *Vehicle System Dynamics, 44*(2), 189-208.

Tekin, G., & Unlusoy, Y. S. (2010). Design and simulation of an integrated active yaw control system for road vehicles. *International Journal of Vehicle Design, 52*(1-4), 5-19. Retrieved from http://dx.doi.org/10.1504/IJVD.2010.029632

Tianjun, Z., & Changfu, Z. (2009). Rollover prevention for heavy trucks using robust control. *International Colloquium on Computing, Communication, Control, and Management,*

Tianjun, Z., & Changfu, Z. (2010). A real-time rollover warning system for heavy duty vehicle. *International Conference on Challenges in Environmental Science and Computer Engineering,* doi: 10.1109

Tianjun, Z., Changfu, Z., Zheng, H., Tian, C., & Zheng, H. (2007). Yaw/Roll stability modeling and control of heavy tractor-SemiTrailer. *Society of Automotive Engineers International, 2007-01-3574*

Tianjun, Z., & Changfu, Z. (2009). Modeling and active safe control of heavy tractor semi-trailer. Paper presented at the *2009 2nd International Conference on Intelligent Computing Technology and Automation, ICICTA 2009, October 10, 2009 - October 11, , 2* 112-115. Retrieved from http://dx.doi.org/10.1109/ICICTA.2009.264

Tianjun, Z., & Liyong, J. (2009). Dynamic modeling and roll control of heavy tractor-semitrailer. Paper presented at the *2009 Pacific-Asia Conference on Circuits, Communications and Systems (PACCS 2009),* 508-11. Retrieved from http://dx.doi.org/10.1109/PACCS.2009.44

Tianjun, Z., & Zheng, H. (2008). Active roll control of heavy tractor-semitrailer based on adaptive gain scheduling control. Paper presented at the *2008 ISECS International Colloquium on Computing, Communication, Control, and Management (CCCM), , 2* 131-4. Retrieved from http://dx.doi.org/10.1109/CCCM.2008.123

Tin Leung, K., Whidborne James, F., Purdy, D., & Dunoyer, A. (2011). A review of ground vehicle dynamic state estimations utilizing GPS/INS. *Vehicle System Dynamics, 49*(1), 29-58.

Toth, G. R., Radja, G. A., Thiriez, K. K., & Carra, J. S. (2003). *Large truck crash causation study in the united states.* (No. 252).National Highway Traffic Safety Administration Publication.

U.S. Department of Transportation. (2003). *An analysis of fatal large truck crashes.* (No. DOT HS 809 569). National Highway Traffic Safety Administration: National Center for Statistics and Analysis.

van Zanten, A. T. (2000). Bosch ESP systems: 5 years of experience. *Society of Automotive Engineers International, 2000-01-1633*

Varga, A. (1991). Balancing free square-root algorithm for computing singular perturbation approximations. Paper presented at the *91CH3076-7),* 1062-5. doi: 10.1109/CDC.1991.261486

Venhovens, P. J. T., & Naab, K. (1999). Vehicle dynamics estimation using kalman filters. *Vehicle System Dynamics, 32*(2), 171-184.

Wakamatsu, K., Akuta, Y., Ikegaya, M., & Asanuma, N. (1997). Adaptive yaw rate feedback 4WS with tire/ road friction coefficient estimator. *Vehicle System Dynamics, 27*(5), 305-326. doi: 10.1080/00423119708969334

Wang, J. (2011). *Effectiveness of stability control systems for truck tractors.* (No. DOT HS 811 437).NHTSA's National Center for Statistics and Analysis.

Wang, J., & Hsieh, M. F. (2009). Vehicle yaw-inertia- and mass-independent adaptive steering control. *Proceedings of the Institution of Mechanical Engineers, Part D (Journal of Automobile Engineering), 223*, 1101-8. Retrieved from http://dx.doi.org/10.1243/09544070JAUTO1135

Wenzel, T. A., Burnham, K. J., Blundell, M. V., & Williams, R. A. (2006). Dual extended kalman filter for vehicle state and parameter estimation. *Vehicle System Dynamics, 44*(2), 153-171.

Wenzel, T. A., Burnham, K. J., Blundell, M. V., & Williams, R. A. (2007). Kalman filter as a virtual sensor: Applied to automotive stability systems. *Transactions of the Institute of Measurement and Control, 29*(2), 95-115. Retrieved from http://dx.doi.org/10.1177/0142331207072990

Windsor, B. (2011). *Improving and reforming our Nation's surface transportation programs* American Trucking Association. Retrieved from http://www.truckline.com/Newsroom/Testimony1/032911%20FINAL%20Windsor%20Written%20Testimony%20TI%20hearing.pdf

Winkler, C. B. (1987). *Experimental determination of the rollover threshold of four tractor-semitrailer combination vehicles.* (No. UMTRI-87-31). University of Michigan: University of Michigan Transportation Research Institute.

Winkler, C. B. (1998). Simplified analysis of the steady-state turning of complex vehicles. *Vehicle System Dynamics, 29*, 141-180.

Winkler, C. B. (2000). Rollover of heavy commercial vehicles. *UMTRI Research Review, 31*(4), 2.

Winkler, C. B. (2009). Full-scale rollover testing of commercial cargo-tank vehicles. Paper presented at the Leicestershire UK. 159-169.

Winkler, C. B., Bogard, S., & Karamihas, S. (1995). *Parameter measurements of a highway tractor and semitrailer.* (No. UMTRI-95-47). University of Michigan: University of Michigan Transportation Research Institute.

Winkler, C. B., & Ervin, R. D. (1999). *Rollover of heavy commercial vehicles.* (No. UMTRI-99- 19). University of Michigan: University of Michigan Transportation Research Institute.

Winkler, C. B., Fancher, P. S., & MacAdam, C. C. (1983). *Parametric analysis of heavy duty truck dynamic stability.* (No. UMTRI-83-13). University of Michigan: University of Michigan.

Winkler, C. B., Sullivan, J., Bogard, S., Goodsell, R., & Hagan, M. (2002). *Field operational test of the Freightliner/Meritor WABCO roll stability advisor & control at praxair.* (No. UMTRI-2002-24).University of Michigan, Ann Arbor, Transportation Research Institute. Retrieved from http://hdl.handle.net/2027.42/1502

Winkler, C. B., & Zhang, H. (1995). *Roll stability analysis of the TARVAN.* (No. UMTRI-95-24). University of Michigan: University of Michigan Transportation Research Institute.

Woodrooffe, J., Belzowski, B. M., Reece, J., & Sweatman, P. (2009). *Analysis of the potential benefits of larger trucks for U.S. businesses operating private fleets.* (No. UMTRI 2009-11).University of Michigan, Ann Arbor, Transportation Research Institute. Retrieved from http://hdl.handle.net/2027.42/65000

Woodrooffe, J., Blower, D., Gordon, T., Green, P., Liu, B., & Sweatman, P. (2009). *Safety benefits of stability control systems for tractor-semitrailers.* (No. DOT HS 811 205).U.S. Department of Transportation National Highway Traffic Safety Administration.

Woodrooffe, J., Blower, D., & Green, P. (2010). Analysis of stability control systems for tractor-semitrailers. *Heavy Vehicle Transport Technology, 11th Heavy Vehicle Transport Technology Symposium*

Wu, D. H. (2001). A theoretical study of the yaw/roll motions of a multiple steering articulated vehicle. *Proceedings of the Institution of Mechanical Engineers, Part D: Journal of Automobile Engineering, 215*(12), 1257-1265. Retrieved from http://dx.doi.org/10.1243/0954407011528798

Wurster, U., Ortlechner, M., & Schick, B. (2010). First ECE 13/11 homologation of electronic stability control (ESC) by vehicle dynamics simulation – challenges, innovations and benefits. Paper presented at the Loughborough, UK.

Xiao, H., Chen, W., Zhou, H., & Zu, J. W. (2011). Integrated control of active suspension system and electronic stability programme using hierarchical control strategy: Theory and experiment. *Vehicle System Dynamics, 49*(1), 381-397.

Yi Feng-yan, Xie Mei-zhi, & Wei Chao-yi. (2010). Stability simulation of operation for tractor-semitrailer based on root-locus method. Paper presented at the *Intelligent Systems and Applications (ISA), 2010 2nd International Workshop on,* 1-4.

Yoon, J., Cho, W., Yi, K., & Koo, B. (2009). Vehicle stability control scheme for rollover prevention and Maneuverability/Lateral stability improvement. *Society of Automotive Engineers International, 2009-01-0826*

Yoon, J., Kim, D., & Yi, K. (2007). Design of a rollover index-based vehicle stability control scheme. *Vehicle System Dynamics, 45*(5), 459-475.

Yoon, J., Yim, S., Cho, W., Koo, B., & Yi, K. (2010). Design of an unified chassis controller for rollover prevention, maneuverability and lateral stability. *Vehicle System Dynamics, 48*(11), 1247-1268.

Yu, H., Güvenç, L., & Özgüner, Ü. (2008). Heavy duty vehicle rollover detection and active roll control. *Vehicle System Dynamics, 46*(6), 451-470.

Zhang Jin-zhu, & Zhang Hong-tian. (2009). Vehicle dynamic stability control based on GPS. Paper presented at the *Information Engineering and Computer Science, 2009. ICIECS 2009. International Conference on,* 1-4.

Zhou, S., Guo, L., & Zhang, S. (2008). Vehicle yaw stability control and its integration with roll stability control. *Chinese Control and Decision Conference,*

Zhou, H., & Liu, Z. (2009). Design of vehicle yaw stability controller based on model predictive control. Paper presented at the *2009 IEEE Intelligent Vehicles Symposium (IV),* 802-7. Retrieved from http://dx.doi.org/10.1109/IVS.2009.5164381